

**MONOGRAPH SERIES ON NONTHERMAL PHENOMENA
IN STELLAR ATMOSPHERES**

**FGK STARS AND
T TAURI STARS**

**Lawrence E. Cram
Leonard V. Kuhi**

**Stuart Jordan, Solar Physics
Editor/Organizer and American Coordinator**

**Richard Thomas, Stellar/Solar
Editor/Organizer and European Coordinator**

**Leo Goldberg*
Senior Adviser to NASA**

**Jean-Claude Pecker
Senior Adviser to CNRS**



**Centre National de la
Recherche Scientifique
Paris, France**

1989



**National Aeronautics and
Space Administration
Scientific and Technical
Information Branch
Washington, D.C.**

FGK STARS AND T TAURI STARS

Library of Congress Cataloging-in-Publication Data

Cram, Lawrence E.

FGK stars and T Tauri stars / Lawrence E. Cram, Leonard V. Kuhi.

p. cm. -- (Monograph series on nonthermal phenomena in stellar atmospheres) (NASA SP ; 502)

Includes bibliographical references.

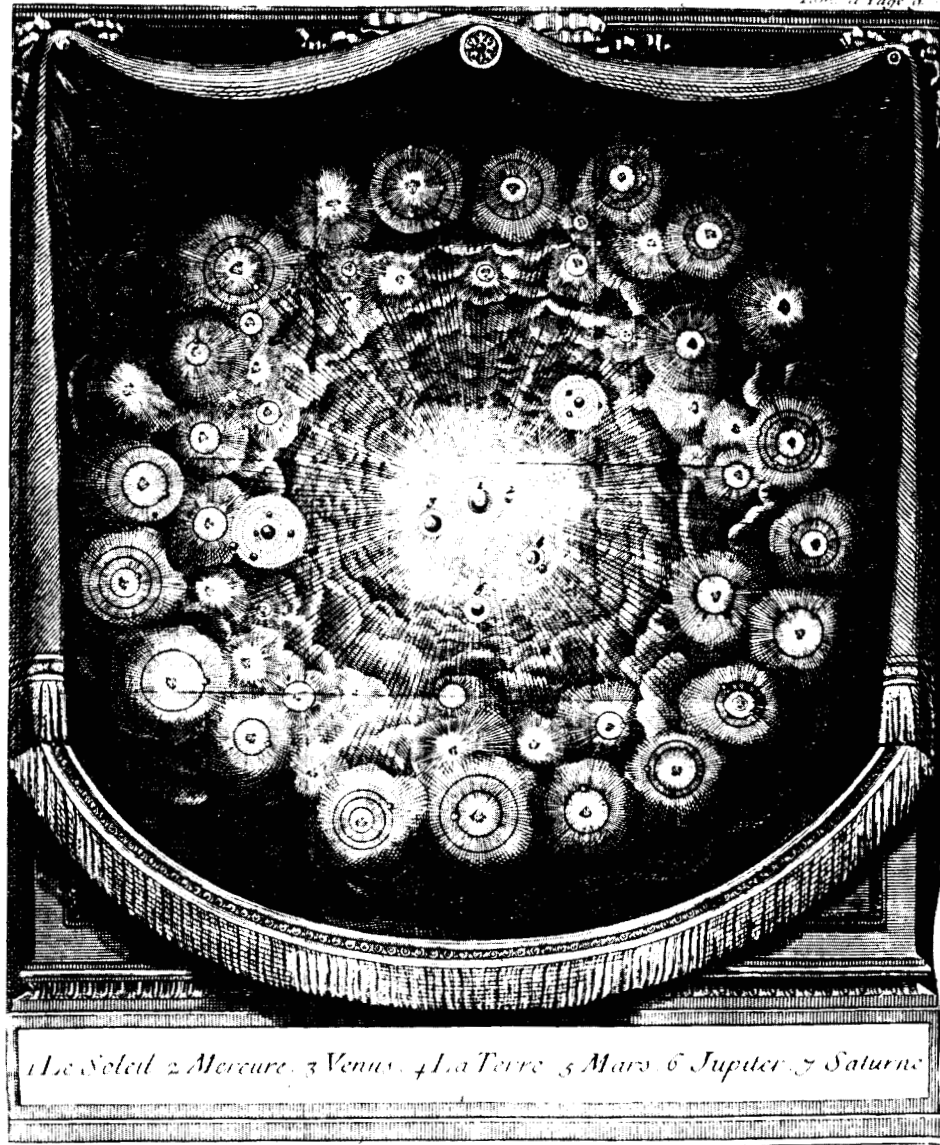
1. Cool stars. 2. T Tauri stars. I. Kuhi, Leonard V.

II. Title. III. Series. IV. Series: NASA SP ; 502.

QB843.C6C73 1989

523.8--dc20

89-600317
CIP



... Assurons-nous bien du fait, avant que de nous inquiéter de la cause. Il est vrai que cette méthode est bien lente pour la plupart des gens, qui courent naturellement à la cause, et passent par dessus la vérité du fait; mais enfin nous éviterons le ridicule d'avoir trouvé la cause de ce qui néest point.

...
...

... De grands physiciens ont fort bien trouvé pourquoi les lieux souterrains sont chauds en hiver, et froids en été; de plus grands physiciens ont trouve depuis peu que cela n'était pas.

—Fontenelle, *Histoire des Oracles*
Chapitre IV, pp. 20 et 23

DEDICATION

in grateful appreciation
we dedicate this series and these volumes

to *Cecilia Payne-Gaposchkin*, who, with Sergei, set the spirit of empirical-theoretical atmospheric modeling by observing:

“All true variable stars have variable atmospheres, but a variable atmosphere is probably the property of all stars, whether obviously variable in brightness or not [as witness the solar envelope]”;

and who, by her intimate knowledge of particular stars, pioneered in the recognition of the fundamental importance of “individuality of stellar atmospheric characteristics”

to *Daniel Chalonge*, who sought, by ingenious meticulous observations, to make quantitative the features of qualitative classical taxonomy, thereby laying the foundations of showing the inadequacy of its two-dimensional, single-region atmospheric, character;

and who always opposed the spirit of a distinguished theoretical colleague’s remark:

“Don’t show me those new observations of yours; they inhibit the range of my speculations.”

CONTENTS

| <u>Chapter</u> | <u>Page</u> |
|---|-------------|
| Perspective | ix |
| Résumé | lv |
| Summary | lix |
| | |
| 1 Introduction and Résumé | |
| <i>Lawrence E. Cram</i> | 1 |
| I. Introduction | 1 |
| II. Spectroscopic Taxonomy | 2 |
| III. Résumé of Volume | 3 |
| IV. Prospects | 5 |
| | |
| 2 Nonthermal Phenomena in the Photospheres of Cool Stars | |
| <i>David F. Gray</i> | 7 |
| I. Introduction | 7 |
| II. Spectral Lines: Fundamental Observations | 8 |
| III. Photospheric Turbulence | 10 |
| IV. Stellar Granulation | 17 |
| V. Rotation | 25 |
| VI. Starspots | 33 |
| VII. Magnetic Fields | 36 |
| VIII. Oscillations and Waves | 42 |
| IX. Comments | 44 |
| X. Appendix: Thermal Characteristics | 44 |
| | |
| 3 Observations of the Chromospheres, Coronae, and Winds of F, G, and K Stars | |
| <i>Dieter Reimers</i> | 53 |
| I. Overview: Evidence for and Incidence of Chromospheres, Coronae, and Winds in Cool Stars | 53 |
| II. Coronae of F to K Stars | 58 |
| III. Mass Loss | 63 |

| <u>Chapter</u> | <u>Page</u> |
|---|-------------|
| IV. Energy Losses by Radiation and Winds | 75 |
| V. Atmospheric Structure | 77 |
| VI. Linewidth-Luminosity Relations and Nonthermal Motions | 87 |
| VII. Stellar Activity in Cool Stars | 89 |
| 4 T Tauri Stars | |
| <i>L.V. Kuhi and L.E. Cram</i> | 99 |
| I. Taxonomy of T Tauri Stars and Related Objects | 99 |
| II. Broad-Band Photometric Observations | 102 |
| III. Line Spectrum | 114 |
| IV. The Interpretation of T Tauri Spectra | 129 |
| 5 Classical Theory of Stellar Atmospheres | |
| <i>Lawrence E. Cram</i> | 139 |
| I. Introduction | 139 |
| II. Historical Background | 140 |
| III. Radiation Transfer | 147 |
| IV. Classical Atmospheric Models | 156 |
| V. Applications and Limitations of Classical Models | 163 |
| VI. Semi-Empirical Constructs | 168 |
| 6 Dynamical Processes and the Origin of Atmospheric Structure in Cool Stars | |
| <i>Lawrence E. Cram</i> | 181 |
| I. Introduction | 181 |
| II. Spectroscopic Taxonomy and Atmospheric Structure | 182 |
| III. Basic Theory of Atmospheric Gasdynamics | 188 |
| IV. Subatmospheric Dynamics | 194 |
| V. Atmospheric Dynamics and Structure | 202 |
| 7 Theory of Magnetic Fields in Cool Stars | |
| <i>Cornelis Zwann and Lawrence E. Cram</i> | 215 |
| I. Introduction | 215 |
| II. Magnetic Fields in Stellar Interiors | 216 |
| III. Magnetic Fields in Stellar Atmospheres | 227 |
| IV. Evolutionary Aspects | 246 |
| V. Cool Stars and Stellar Systems: The Magnetic Connection | 250 |
| References | 253 |
| Subject Index | 291 |
| List of Contributing Authors | 297 |

PERSPECTIVE

A. OVERVIEW OF THE EVOLUTION IN OUR UNDERSTANDING OF THE THERMODYNAMIC ROLE, AND RESULTING STRUCTURAL PATTERNS, OF THE ATMOSPHERE IN THE STRUCTURE AND EVOLUTION OF A STAR — AS THESE ARE DELINEATED BY VOLUMES 1-7 OF THE MONOGRAPH SERIES, PLUS CURRENT WORK ON EPISODIC ENHANCEMENT OF MASS-OUTFLOW AND LUMINOSITY

The characterizing energy/mass loss plus the free-boundary of a thermodynamically open, self-gravitating, evolving, stellar concentration of mass/energy produces *an outermost transition-zone* (\equiv the atmosphere), from linear to nonlinear non-Equilibrium thermodynamic in modeling of: (i) energy/mass transfer; (ii) a regional-structural pattern. The observational/empirical associations between time-dependent (i) mass/energy fluxes, and (ii) regional-structure patterns guide, empirically, the integrated, whole-star, atmospheric, and local-environmental modeling.

1. GENERAL PERSPECTIVE ON SPECULATIVE-CLASSICAL THEORY VERSUS EMPIRICAL-MODELING OF ATMOSPHERIC STRUCTURE, CONSIDERING ADEQUATE THERMODYNAMICS, RADIATIVE PLUS NONRADIATIVE FLUXES, NONLINEARITY AND VARIABILITY, AS WELL AS LOWER VERSUS OUTER BOUNDARY CONDITIONS

This volume in the NASA-CNRS series *Nonthermal Phenomena in Stellar Atmospheres—i.e., Nonthermal Structure and Evolution of Stellar Atmospheres* — considers cool stars: those with visual-spectral types F-G-K, and visual-luminosity types ranging from subdwarfs, through main-sequence dwarfs, giants, and supergiants. Before we can recognize/delineate/model/theorize on *nonthermal* phenomena/structure, we must unambiguously understand *thermal*. The basic thermodynamics of this distinction are discussed elsewhere (in a companion to Volume 4 of this Series; unfortunately, to be published outside the Series). Here, in this Perspective Chapter of this Volume 7, I can only try to be very explicit on: (a) what states/phenomena/structures are *defined* as being thermal, and which as being nonthermal, by the characteristics that are included, or omitted, in their *speculative-theoretical* modeling; (b) which of these are *diagnosed/inferred* to be thermal, and which nonthermal, from *empirical-theoretical* analysis/modeling of observations; and (c) the observed relations of both thermal and nonthermal structural features to various stellar fluxes of matter and energy.

Use of the term speculative-theoretical, as opposed to empirical-theoretical, sounds, and is meant to be somewhat pejorative, at our epoch when such speculative-, as opposed to an empirical-approach is too often still retained. Yet we increasingly see how modern high-resolution observations — in the visual spectrum from ground-based telescopes, and in the X-ray and farUV spectra from space — so strongly contradict model predictions based on those classical theories which rest more on thermodynamic conjectures than on detailed observations (i.e., conjecture on *why* is X, before observational detailing *what* is X).

Classical theories resulted from combining: (α) superficial inferences from low-resolution visual-spectral observations of *normal*-star atmospheres; (β) an assumed irrelevance of *peculiar* star obser-

vations; (γ) an assumed applicability, to spectral diagnostics and atmospheric modeling, of that near-Equilibrium thermodynamics developed to describe systems with only small gradients in thermodynamic parameters; (δ) assumed absence of any nonradiative fluxes from stars. These speculative assumptions produced model atmospheres consisting of a single, thermal region, whose "temperature distribution" was fixed by the radiative flux. High-resolution (geometry, λ , t) study of the nearest star, our Sun, a "banal" member of this Volume's FGK class of stars, demonstrated, empirically, the errors in (α)-(δ) by delineating: an exo-photospheric multi-regional structure; its association with nonradiative fluxes (energy, mass), which evolved outward into strongly nonthermal phenomena; and many (solar, peculiar-star) similarities. These studies, and the preliminary non-Equilibrium-thermodynamic logic of their broad stellar applicability, led to "previewing" the modern continuing evolution in understanding the actual, not speculative, thermodynamic character of stars generally.

Many of the developments coming from the study of the Sun itself have been summarized in Volume 1 of this Series. Subsequent volumes have summarized such observational and thermodynamic evolution in the modeling of other stellar types, usually by comparison to these solar studies/results. These solar and stellar results also lay the basis for extending — via their empirical guidance — this preliminary non-Equilibrium thermodynamic diagnostics and modeling of such thermodynamically open, self-gravitating concentrations of mass and energy (CME).

The Sun is at once a "normal" star, because there are so many like it, and a "peculiar" star, because its increasingly detailed observational studies continually contradict the predictions from classical, thermodynamically naive theory devised to model such normal stars, but historically found inadequate for peculiar stars. In essence, less restrictive thermodynamic diagnostics of these higher-resolution solar observations exhibited the inadequacy of near-Equilibrium thermodynamics to describe low lying, outer atmospheric regions; they derived an outward increase in T_e instead of a decrease. So these studies put into focus the need for: (α) more careful attention to how, thermodynamically, we describe and model the transition regions — (i) between star and environment (atmosphere); (ii) between directly observable region (atmosphere) and main bulk of the star (the energy-producing regions of the deep interior, and the energy-transport-only regions of the subatmosphere) — and (β) higher resolution and broader- λ spectral observations and their thermodynamically better diagnostics. The "empirical-theoretical" requirement that any "improved thermodynamic" diagnostics and modeling represent better these "anomalous" observations guided the improvement's development, measured its degree of adequacy, and pointed where to go next.

Because of its proximity, studies of the Sun continue to provide primary guidance. Because of its relatively small radiative- and mass-fluxes, this solar guidance to the general thermodynamic characteristics of stars (the solar-stellar connection) requires broadening by that insight provided by "more peculiar" stars, which exhibit larger and more variable fluxes, and different atmospheric structural patterns (the stellar-solar connection). Because of the need for contrast between solar-similar and solar-different stars, a continuous intercomparison between Sun and stars — especially peculiar-star "cousins" — is invaluable. Because of their solar-similarity in electron temperature (a first-approximation measure of thermal state) at the base of the photosphere, the FGK stars provide an important pivot in detailing this stellar-solar connection, and "closing" on Volume 1: the Sun. This Perspective Chapter tries to abstract such comparisons between Sun, FGK stars generally, and their "cousins" across the HR diagram.

a. PERSPECTIVE ON THE NON-EQUILIBRIUM THERMODYNAMICS NEEDED FOR MODELING AND ITS IMPACT ON REGIONAL STRUCTURE OF A STAR

I have stressed the continuing development of a non-Equilibrium thermodynamics that is adequate to describe stellar structure — internal as well as atmospheric — and its relation to the various

thermodynamic fluxes. That thermal nonLTE developed for atmospheric diagnostics/modeling is hardly sufficient. I elaborate briefly. The only concentration of matter and energy (CME) sans structure is the conceptual one in strict Thermodynamic Equilibrium (TE). *Conceptual* because any attempt to measure it destroys the TE configuration of strict: (i) isolation from its environment; (ii) homogeneity \equiv without structure. So the TE configuration is defined by axiomatic (e.g., Carathéodory) construction, and is only related to observations by limiting inference as the conditions (i) and (ii) are more closely approached.

To construct a theory of, and to model, any nonTE configuration: the effects of any, even very small, departures from these two conditions must be investigated, observationally/experimentally as well as theoretically, not simply conjectured/axiomatized; because such a configuration can, at least in principle, be observed. Hence any speculative conjecture can be checked. We note the recent historic, “a priori speculative-theoretical” rejection (as having insignificant effect) of now accepted, solar-stellar-meteor observationally based, thermal, radiatively nonlinear, stellar-atmospheric, nonLTE “theory.” It was a first, empirical-theoretical, step, hardly a complete formulation of an unrestricted non-Equilibrium thermodynamics. Any such extension must be equally empirical-theoretical.

The obvious such effects of departure from the characteristics (isolation and homogeneity) of a TE configuration follow from simply removing those characteristics:

(a) replacing an homogeneous structure of the system by an inhomogeneous one, which may consist of a single region with gradients in those thermodynamic parameters necessary to describe the thermodynamic state at each point, or it may consist of a set of thermodynamically differing regions, each having such gradients in those thermodynamic parameters necessary for its local description. I emphasize: the details of the particular regional structure, and the choice of the state parameters, are not — if we would model real-world stars — free for speculation; they must agree with observations (cf., Volume 4).

(b) admitting any fluxes of matter and energy associated with the inhomogeneous structure. Again, the choice of such fluxes is not free for speculation; such speculative approach was the major error of classical modeling; cf., the Sun. The adopted set of fluxes must agree with observations — in addition to being compatible with the adopted thermodynamics (*inconsistency between the two aspects implies inadequacy of the adopted thermodynamics*). This point is well illustrated in the Volume 6 discussion of what fluxes are “present”/necessary in hot stars.

(c) destroying the system’s isolation by admitting interaction between it and its environment. As we see below, this interaction is, also, hardly free-for-speculation. Classically, modelers admitted only the interaction of the star’s radiative flux with its environment. Modern observations also demand the existence, and environmental interaction, of nonradiative fluxes of mass and energy from the star. Contemporary speculation suggests, for some stars (yesterday, the Sun; today, the CV, the T Tauri; tomorrow, ?), mass infall from a star or nebular companion. Thus the sign of the mass flux, its time dependence, and the problem of a local stellar environment — creating or created by the star, but interacting with it — are a priori unknown, and crucial in atmospheric modeling. The point has been exhaustively discussed in Volumes 2 and 4, and further developed, empirically-theoretically, for well observed Be stars by those volumes’ authors. An evolving insight into these stars may encompass Be-similar stars — among these the T Tauri, which are thus torn between outflow and inflow modeling. The point is critical in discussing/understanding/modeling the CV stars of Volume 8.

Which of (a)–(c) causes which, or whether all simply arise in association from something else, must be studied in each particular case — of course hoping to find observationally/thermodynamically-sustained generalizations. For an observed real-world CME, one first tries to establish the facts of

(a)–(c), then asks the cause. Of course, there may be nonTE effects other than (a)–(c) — which must also be delineated, once identified. To model a speculative-theoretical concept, one reverses the procedure — if one knows enough to model (a)–(c), self-consistently (we don't, yet) — then carefully compare it with observations.

Unfortunately, we yet know too little about general, unrestricted nonTE configurations to have confidence in “speculative-conceptual” thermodynamic modeling of stars, unguided by observation. So, we proceed observationally-theoretically. We seek: (I) how to model the variety of time-dependent atmospheric regions observationally discovered in the variety of stars across the HR plane plus their variety of thermal and nonthermal states; (II) the variety of fluxes, and their time-dependences, implied by the time-dependent characteristics of these atmospheric regions. This approach reflects our non-Equilibrium-thermodynamic immaturity for any wholly speculative approach (cf., Volumes 4 and 6, and Chapters 5 and 6 here).

For stars, the earliest modeled nonTE configuration was simply that arising from the inhomogeneous structure introduced by the CME's self-gravitation. Fluxes were neglected; any problem of maintaining isolation at the outer boundary was obviated by enveloping the star in a zero-pressure void: no ISM was allowed. Such an isolated star was invisible. So the obvious, gross stellar structure necessary to produce *radiative-flux*-observable objects, thus a first approximation to (a) above was, historically, 3-regional: (1) energy generating region; (2) region of only energy transport; (3) the outer-boundary \equiv atmosphere \equiv the immediate source of the observed radiative outflow. The then adopted modeling of region (3) via the linear nonE thermodynamics of the interior was thermodynamically inadmissible, as properly diagnosed observations showed. Excluding nonradiative fluxes requires theoretical consistency (it was not then explored) of both the thermodynamics and the model, and observational justification (pre-spatial visual-spectral observation of some stars implied mass and nonradiative energy fluxes). So, while a first-approximation modeling of a radiative flux from the star produces three distinct regions, the “theory's” basis hardly gives confidence in their reality/adequacy.

Regions of type (1) above are usually stellar-internal — either in the central core or in subatmospheric shells of various types — but mass-accretion models of some stars locate some of these regions in the atmospheres of such stars. The problems of both type (1) and type (2) regions focus on radiative versus mass transfer of that energy classically leaving region (3) as radiation — and, today, on both it and on (dissipative) transfer of the mass flux and its energy. Such energy transfer in regions (1) and (2) is usually discussed in terms of vaguely understood macroscopic “convection” and a “mixing-length” — developed by analogy with the kinetic LTE, as contrasted to radiative LTE — treatments of thermal convection and atomic mean-free-paths. Mass transfer is usually neglected: as being both small, and too newly discovered to be understood (the “accretion-disk,” hypothesized in mass-interchange theories, is even more vaguely discussed and then in terms of an hypothesized “super” {kinetic LTE} viscous-dissipation). One can hardly say that a thermodynamically satisfactory/complete description exists for either types (1) or (2) regions; whose existence is equally necessary for non-radiative fluxes to exist, but whose quasi-thermal structure, transport, and interface boundary conditions may well change with them. Regions (1) and (2) couple directly to the outer-boundary conditions only in the mass-interchange models. The boundary conditions between Regions (2) and (3) are, however, very important in describing the origin and propagation of the classically excluded non-radiative fluxes. I return to this point below, in this Perspective.

It is in the delineation of the type (3) regions, which are outer-atmospheric/transition-rather-than-boundary regions, that we have made the most solid progress in developing a sound stellar thermodynamics. Factually, this differential progress resulted because these type (3) regions are the only ones whose existence is directly observed and whose characteristics place constraints on: (i) actual regional structure; (ii) characteristics of the thermodynamic fluxes necessary to produce them; and

(iii) the kind of nonTE thermodynamics necessary to describe/model regions and fluxes; (iv) the locations/characteristics of the origins of the fluxes.

Thus, empirical-theoretical solar studies replaced the classical atmosphere's speculative single-region thermal photosphere by a quasi-thermal photosphere plus a chromosphere and corona — and the characteristics of these latter regions demanded the existence of those nonradiative fluxes of energy and matter speculatively suppressed by classical standard “theory.” The chromosphere plus lower corona demand a dissipative nonradiative energy flux; the upper/outer corona demands a mass outflow/flux. A self-consistent thermodynamics/diagnostics of the ensemble of high-resolution visual-spectral observations — continuum plus line — demanded the development of a *thermal* non-Equilibrium thermodynamics which considered the detailed, not simply averaged, energy distribution among the microscopic energy levels of the atoms, and their nonlinear coupling with the nonlinear monochromatic radiative transfer problem. This variety of nonTE thermodynamics was adequate to represent the (then observed) radiative spectrum of the chromosphere and low corona in the presence of those low-subthermal macroscopic velocities observationally characterizing these regions — where an “effective” thermal-HE gives an adequate description of the density distribution. But this variety becomes only an increasingly approximate representation in the outer corona, as the macroscopic gas velocity is (empirically observed to be) accelerated through the trans-thermal regime into the super- and ultra-thermic regimes (cf., Volumes 1 and 4).

These empirical-theoretical results are for a “banal” member of the cool FGK class of stars — which happens to be close enough that we can observe it in that detail necessary to establish the foregoing. But we find the same, when we turn to well observed members of the hot OB classes of stars. Even in the pre-space era, the stellar-solar connection of the Be — and Be-similar (like the T Tauri) — stars had suggested the variable presence of exo-photospheric, oscillating, “cool” regions, inferred to be produced by variable mass outflow from the star. Now, farUV data from space have shown that such stars also have chromospheres and expanding coronae; but that the “cool” regions are exo-coronal, and are the locus of a decelerated mass-outflow, associated with its variability. Thus nonradiative fluxes also exist in at least some hot stars, and for some of them are highly variable. Apparently this variability produces cool exo-coronal regions not found in the Sun — unless the planetary system be considered as such; and also their presence has not been established for all hot stars (cf., Volumes 2 and 4). For the viewpoint that many hot stars do not exhibit nonradiative energy fluxes/dissipation — and also the contrary viewpoint — cf., Volume 6.

Even more recent work shows the variability of Be — and possible of some Be-similar — stars to be patterned; apparently highly episodic; and that variations in the radiative flux of at least some of these stars are associated with such variations in the mass outflow (further studies by the authors of Volumes 2 and 4) The empirical similarity of Be — and possibly of other Be-similar — stars to the CV in this episodic variability of the fluxes, and of associated atmospheric structure, is becoming recognized by those who observe them simultaneously in the visual and the farUV via long-term programs (cf., the 1986 summary by the Be-volume author, Doazan). An empirical-theoretical modeler now begins to understand, phenomenologically, the confusion, in the early days of classification of some “peculiar” stars like P Cyg, ζ And, etc., between placing them in the novae, or Be, or symbiotic, classes. And because some of these stars are single, not binary, he begins to question why “binarity” is necessary -- rather than incidental — to producing such episodic mass and luminosity enhancements, contrary to the speculation of CV theoreticians. Again I stress Fontenelle's message in the volumes' frontispiece: *“be certain of what exists, before you try to explain why”* — but adding: “similarity in directly observed, associated, nonthermal phenomena in apparently different types of CME may imply similarity in underlying non-Equilibrium thermodynamic character — so supplement what is observed by exploring what nonTE character represents these observations before explaining why.”

Thus the necessity/utility of any modeling based on wholly speculative atmospheric structure and permitted set of fluxes, and of an equally speculative thermodynamics to produce them, is minimized for most stars sufficiently bright to be well observed across the spectrum. For such stars, we can in principle obtain an observationally well delineated atmospheric structural pattern — we require only access to simultaneous, long-time sequential, observations in the visual plus farUV. Such exist; via 2–3 meter ground-based telescopes plus the *IUE* (whose stellar-variability clone on an Explorer-type satellite is, incredibly, still overdue). Vital supplementary data on structural patterns/details come from extending the λ -coverage via observations: (a) in the X-Ray (survey results from *Einstein*, etc., amply confirm the general need to include dissipative nonradiative energy fluxes in modeling hot as well as cool stars, give valuable insight into variability in a given star and between similar stars, and suggest significant exo-coronal cool-envelope, X-ray opacity for Be-like stars; cf., Volume 4 and Chapter 4 here); (b) especially in the XUV for hot stars, of which a few preliminary observations — too long left unextended by Explorer-type satellites covering this λ -region — are tantalizing (e.g., Malina, Bowyer, and Basri; 1982); (c) in the farUV plus radio for delineating both the postcoronal/local-environmental cool envelopes as well as giving basic data on the coolest stars.

One requires, of course, telescope-allocation committees sufficiently versed in these stellar-atmosphere problems, and their implications on stellar interior plus evolutionary/cosmological problems, to allocate sufficient observing time — especially of the long-term, coordinated telescope, variety — to put into empirical focus the significance of patterned and episodic variable mass and luminosity fluxes. The problems there, as well as in the fund allocations for small-but-scientifically productive, versus grand-and-politically-productive, space- and ground-telescopes have been well caricatured by Dyson in his 1988 Wooster College Commencement Address (which should be required reading for working Indians as well as would-be tribal chiefs and federal reservation agents, of all countries).

To extend this data base to fainter stars requires larger telescopes of all λ -coverage, and more observing time. Given the problems in building the nearby Sun, and distant-but-bright star, stellar-solar data base, one can only be prepared to progress via what data become available — if one is not content to return to armchair speculation. Of course there is always the hope that our non-Equilibrium-thermodynamic insight into stellar-type CEM will mature sufficiently, via such solar-plus bright-star data, to convert a priori speculation into only extrapolative speculation from this beginning data-base.

Then given that we have at least some stars with observationally well defined atmospheric structural patterns, the current astrophysical-thermodynamic atmosphere/whole-star, empirical-theoretical focus is clear: the above points (i)–(iv), slightly reformulated: (A) relate such atmospheric patterns to the mass and energy fluxes equally arising in any *open* nonTE configuration — *effect* of the fluxes; (B) relate fluxes to subatmospheric structure and local environment — *origin* of the fluxes; (C) relate such origin to the thermodynamic character of the whole star — *basic nonTE thermodynamics of stellar-type CME*. Volumes 1–7 (Volume 8 remains to be assessed) collect and summarize the existing data base for (A), Volume 4, more explicitly so. Current interior modeling approximates (B) for radiative-flux; it has not yet matured to include nonradiative-fluxes. The omission is fundamental, re. whole-star modeling; I try to put it into perspective. I rest on these solar and stellar data of (A) for the foundation of such a perspective on (B)–(C).

To relate atmospheric structure to the effect of fluxes, and the origin of fluxes to the star's thermodynamic character, we first ask what fixes the existence and size of a flux: subatmospheric phenomena (thermal or nonthermal storage modes/gradients of thermodynamic state parameters); or atmospheric instability? In modeling an atmosphere: are the fluxes prescribed a priori, as being wholly fixed by subatmospheric conditions effectively uncoupled to atmospheric conditions, by giving their values at the base of the atmosphere (lower boundary conditions in the subatmosphere-atmosphere

transition-zone); or are these fluxes “speculated” to be predictable as part of an atmospheric modeling from outer-atmosphere boundary conditions not involving these fluxes? And is there a difference in the way radiative and nonradiative fluxes are prescribed, and/or determined in this modeling? We recall that under classical stellar modeling — of both interior and atmosphere (post-Eddington, initiated by Eddington) — only radiative fluxes exist, and are fixed by interior/subatmospheric conditions. So, the just stated questions did-not/do-not arise in such modeling. Introducing nonradiative fluxes — especially a mass-flux, and especially when we observe, in at least some stars, associated strong episodic increases in radiative- and mass-fluxes — we ask what changes in (interior, atmospheric) modeling of (origin,size) of all fluxes must be admitted. And we ask what this implies on stellar-structural thermodynamics generally. I do not pretend to answer these questions here, only to abstract some of that observational basis by which such answers must be guided, by contrast to current implicit/explicit “speculation.”

b. PERSPECTIVE ON FLUX ORIGINS AND THEIR ATMOSPHERIC STRUCTURAL EFFECTS

Under classical modeling, the star’s luminosity is produced by those thermal-nuclear reactions appropriate to Region-1 conditions; the radiative flux follows from this luminosity mixed with the T-gradient/radius structure (cf., Eddington). Thus the radiative flux originates, and its size is fixed, by conditions in the subatmosphere. Its existence and value are specified, a priori — in this classical atmospheric modeling, where a mass-flux is excluded — by the lower-atmospheric boundary-conditions (in the subatmosphere-to-atmosphere transition-zone). Even in pulsating stars, the “basic” luminosity, produced in the deep subatmosphere, is unaltered, according to its current modeling: the pulsation simply introduces time-dependent, upper-subatmospheric storage modes and flux phases. So subatmosphere-to-atmosphere, lower-boundary values of the radiative-flux are time-dependent; but the flux’s origin remains in the star’s subatmospheric structure.

These boundary conditions also represent the nonthermal pulsation velocity; and, under today’s thinking, possibly a time-dependent mass flux, associated with variable radiative flux, and differing from that of nonpulsating FGK supergiants. Because the modeling is speculatively ambiguous on the “adiabaticity” of the mass outflow, it is also ambiguous on whether one considers the (decreasingly opaque, thus decreasingly adiabatic) atmosphere as responding to an energy-instability, and so as “pulling-out” a mass flux from above.

Most current theoretical modeling of mass outflow rests on an equally conjectural thermodynamic basis, and equally seeks to theoretically specify the origin and size of the mass flux in parallel with specifying the atmospheric structure. Under such models/theories, the mass flux is not considered to be produced by the subatmospheric structure, in parallel with the radiative flux, nor to be specified a priori in atmospheric modeling by a lower-boundary condition in the subatmosphere-to-atmosphere transition-zone. This speculative modeling discords with observations of mass outflow, especially of its variability, but also simply of its evolution — in parallel with that of the radiative flux — from small-departure (linear, low subthermal), nonTE thermodynamic to large-departure (nonlinear, transthermal to super- and ultra-thermal). These conjectural theories fall into two broad types: a steady-state mass loss produced in single stars; and that conjectured to result by interaction between a star and its “local-environment” — star or nebula. I try to put these conjectural models into observational/thermodynamic perspective.

Such current speculative theories for mass loss by single stars, both solar-type coronal outflow, and hot-star radiation-driven winds, consider the existence and size of the mass flux as something which atmospheric models should predict. The existence and size of the mass fluxes are not specified as lower atmospheric boundary conditions. These theories, solar and hot-star alike, produce the mass

flux from exo-photospheric instability/outer-boundary conditions (cf., Volumes 1, 4, and 6). But these theories are steady-state; they exclude variability. So those stars with observed variable mass outflow — especially those with associated, episodic mass and luminosity enhancements — give a different perspective. Current modifications of those theories, which find them unstable, hence possibly with variable mass loss, have thus far produced only very short time-scales: much less than a day. While such short-time-scale variability has indeed been observed, it is random, with small amplitude. By contrast, that variability observed in such stars as the Be exhibits time-scales from days to decades — much too short to be linked to evolution, and much too long to be the variability produced by the cited instability found in hot-star theory. So applying such theories is questionable — observationally and thermodynamically — as discussed in Volumes 2, 4, and 6.

Those stars whose atmospheric structural patterns, and mass and energy fluxes, are imposed speculatively, and conjectured to originate by mass-transfer effects from something in the star's local environment to the star, give yet another kind of perspective. I abstract a perspective on them, as exhibiting an exception to objectives (A)–(B)'s logic of relating fluxes from the subatmosphere to the observationally delineated atmospheric structure. One must realize that none of these mass-accretion concepts are observationally based in any sense other than such stars not being objects quasi-isolated in space. They are either very near, or enveloped-in “nebulae;” or they are inferred to have a very close stellar companion (only a few are double-line spectroscopic binaries; cf., Volume 8; and Chapter 4 of this volume). The basic question is whether any binarity is incidental to, or causes, the prototype novae behavior that originally characterized such stars.

The dilemma is: spectroscopic observations show us mass outflow, but speculative theory — developed/proposed before space observations showed some mass outflow from all, and patterned/episodic mass outflow from some, stars — demands mass infall. So, theory beclouds observational diagnostics. I paraphrase one author of volume 8: “present CV focus lies on exploring gross concepts about the nature, dynamics, etc., of a CV system — which has nothing to do with spectrum computations.” That is; the focus of these mass-infall theories still lies on explaining *why* a conjectured model exists; not on asking *whether* the best, highest resolution, panspectral, modern observations show that the conjectured model actually exists, and is (non)-Equilibrium-thermodynamically coherent. Their modeling approach characterized classical standard stellar modeling, which produced models differing strongly from what observations, and self-consistent non-Equilibrium-thermodynamic diagnostics, tell us actually exist for real-word stars.

I briefly put the conjectures underlying these stars into this perspective. For the T Tauri stars, covering the FGK spectral range treated in this Volume 7, the conjectured existence of a mass infall arose from the conjectured identification of the T Tauri as being stars in an early, hence still contracting/accreting, stage of evolution. The source of the infalling mass is identified as the nebulosity usually, but not always, found near such stars. Unfortunately for such conjectures, mass-infall models do not well represent the strong and variable $H\alpha$ emission profiles characterizing such stars. Attempts to study, and model, such $H\alpha$ profiles generally finish by requiring an extended atmosphere exterior to, and cooler than, a deep lying chromosphere-corona — which latter are demanded by other spectroscopic observations (cf., Chapter 4 of this volume). Thus such a combination of visual and farUV spectral observations is essential for delineating atmospheric structure, and making any inference as to whether the mass flux is outward or inward from the star. A modeling discussion, or stellar-evolutionary inference, based on only one of these spectral regions is inadequate. Based on their compilation and diagnostics of the best existing observations — visual, farUV, and X-ray — the authors of Chapter 4 of this Volume 7 (who are also the volume's editors) conclude that the observations are best represented by a mass outflow, with no yet established relation to any still only conjectured, not observed, mass infall. Based on my own efforts at modeling T Tauri atmospheres, I accord.

But one must realize that while these T Tauri stars are Be-similar in diagnosed atmospheric structural pattern — chromosphere-corona, post-coronal cool H α emission envelope — we have nowhere near that quantity of visual plus farUV long term sequential observations which could let us decide whether or not they are indeed Be-similar in any variable mass outflow/flux aspects. We have a century of detailed visual-spectral observations of Be-stars, upon which associated visual plus farUV programs could be (and have been) carefully planned and executed for those stars whose historic, visual-spectral performance forecasts valuable results. (cf., Volume 2, and the 1986 summary of current such studies by its Be-author/“forecaster,” Doazan). Such is the basis for an empirical-theoretical program to delineate the actual time-dependent structure and flux production, and behavior/evolution, of stars as “quasi-isolated CEM,” open, thermodynamic systems — so that we learn how to formulate, and model, the applicable nonTE thermodynamics. Among the FGK stars, the T Tauri — and their possible “eventual-evolutionary-state successors,” the FU Orionis stars — seem the most promising for eventual such guidance (when NASA plus ESA plus USSR collaboration provides a variable-star-dedicated *IUE*-clone). With, possibly, added information from the pulsating members of the FGK class — whose radially pulsating examples are, unfortunately, not covered in the series, because of budgetary/time limitations imposed by our (long-suffering, from our insatiable demands) sponsors: NASA and CNRS.

The situation differs considerably, in considering current CV modeling — the original and outstanding example of mass interchange/transfer modeling. *For the T Tauri stars*, it was evolutionary arguments plus the nebulosity often associated with these stars which led to speculative mass infall. *For the CV stars*, it is their often/usual — but not always — inferred membership in a (single-line) binary system plus the (at that epoch) need for an energy source to produce that (one-time, for novae; episodic, for other CV) mass-outflow coupled with luminosity outburst which historically characterizes them. As the CV class was broadened from the novae and recurrent novae, the amplitude of the “outburst” required to put them in the novae-prototype, “lesser-breed”-diluted, maybe now Be-clarified, CV class of peculiar stars has decreased very considerably. Indeed, some dwarf-novae theoreticians have occasionally suggested that these types “need have” no mass loss — which, however, contradicts what is observed. Search for the outburst’s energy source, under the condition that it be associated with binarity, led to the basic speculation that mass transfer from a normal star to a degenerate companion is necessary to produce that quantity of energy. The observed universal presence of a mass outflow of some size, from all sufficiently observed stars (cf., later remarks on observed/inferred mass outflow velocities), and especially of episodic, associated enhancement of mass outflow and luminosity in some nonbinary stars, removes the need for an “enhancement” mechanism unique to the CV stars — we need such (several?) in a much broader range of stellar types.

Very current observations, and their diagnosis (Doazan and Thomas, 1988) suggest that also an energy source large enough to produce simultaneous mass outflow and luminosity enhancement may not be unique to such mass-transfer models. Preliminary empirical estimates of the total energy involved in “one complete episode of such enhancement,” for at least some Be-stars, suggest that it is comparable to that released during the whole of one nova outburst. Note that during this Be-episode, both mass and radiative fluxes oscillate about a secular rise (for just short of a decade, somewhat longer than the duration of even slow-novae “enhancement phases,” which also oscillate), ending with each significantly larger than its initial value (cf., Doazan’s 1988 description). Also like the novae, these Be-enhancements eventually decay; although other such “episodes” sometimes occur before, or after, return to “normal.” Detailed statistics are woefully lacking; even partially complete sequences of even visual-only observations resulted only rarely, obtained by observers with intuitive noses having long-term access to adequate telescopes, sans “committee” interference. The stellar-evolution implications are stimulating: either variability in production of luminosity and mass-outflow on time-scales much less than evolutionary; and/or the “Be/CV” configurations are only transient evolu-

tionary stages. I emphasize: some stars, occasionally, show luminosity and mass outflow increases/decreases of different sign; some, as here, of the same sign. Any complete model must be able to produce either, or both. A constant energy production, somehow variably partitioned between radiative and mass fluxes, is insufficient in the present case — just as for the novae/CV.

Thus, *I emphasize that these observations — not any “theory” or even physical picture — suggest that CV-like behavior exists in, and CV-like energies are produced by, some single stars.* We do not yet know how. Hopefully, a mixture of more observations, on a variety of stars — not just on CV and Be, but maybe also on T Tauri, FU Orionis-type, etc. — will give us insight. This recognition poses, today, an essential question, in terms of “concept-clarifying by observation not simply by speculation”: Do we continue to consider the CV as species quite alien — as being nonsingle stars — from other, single-star, examples of the kind of variable mass outflow they exhibit in common: episodic, associated, enhancement of mass outflow and luminosity? Or do we consider the CV, and these other single-star examples such as the Be, planetary nebulae, T Tauri, maybe FU Ori, as giving us a variety of complementary examples of the facts of stellar production of variable fluxes of all type — in which binarity has at most a second-order role? From such variety of examples, under this second alternative, it may ultimately be possible to infer the thermodynamic mechanism of such variable flux production — and its link to the (time-dependent — in less than thermal-nuclear, evolutionary time-scales) structure of the star as a whole, not just to that (time-dependent) atmospheric structure of the star which we observe. (We regard “time-independent stars” as either being not well observed, or as being only “small-amplitude peculiar — first-approximation normal.”) Also under the second alternative, one recognizes the interesting question of whether the associated episodic variability in mass outflow and luminosity implies variable energy production, by at least some types of stars — on time-scales much less than those of thermal-nuclear evolution. These possibilities raise broad thermodynamic questions on their implications on stellar structure, stellar evolution, and a “cosmology” based on a more detailed consideration of the thermodynamic structure/state of the “stars \equiv the particles” \equiv “the local (nonstatistical) thermodynamic state” of the Universe. It is much too easy to postulate particles, etc., whose thermodynamic structure/state has significant time dependence, and is nonlinearly non-Equilibrium *only* during a “birth-phase,” and is thereafter quiet, thermal, linearly non-Equilibrium.

Quite apart from “cosmological” questions, obtaining a more clear empirical-theoretical picture of the modeling distinction between variable/episodic mass outflow, and mass infall, as primary, gives us a better picture of the variety of possible relations between a stellar-type open system and its local environment. Apparently, *all* stars produce a mass outflow; *some* produce a variable outflow; for *some of these*, the variability is episodic. A question is whether, in some situations, a mass infall from the local environment — leading to a *surface* energy production which ejects mass from the “system” — effectively takes over from whatever is the single-star mechanism, which itself may be able to produce episodic variability, even sometimes of both mass outflow and luminosity. This conceptual situation differs from that of the pulsating FGK sg, where each source driving the mass outflow is subatmospheric. In the mass infall picture, the perturbing source is an atmosphere-level energy production, and mass ejection. So there are two distinct questions: the origin of the observationally-well-established, single-star mass outflow — constant, variable, or episodic; and whether there indeed exists, in the real-world, mass-infall-stimulated mass outflow — of the variety of types described by the observations of the CV variety of objects, and “evolving/blending” into the cited single-star range of phenomena (presumably as binarity effects disappear with increasing separation?). Resolving these questions should clarify what is meant by a star as a quasi-isolated object in terms of the characteristics of the fluxes it transfers to — or receives from — its environment.

It should clarify the basis for describing some stars as being in *early* stages of evolution because they lie *above* the main-sequence and are surrounded by nebulosity (T Tauri); while other stars are

in *late* stages of evolution because, while they also lie above the main-sequence, they are surrounded by time-dependent nebulosity/H α -emission envelopes (Be and some Be-similar); and some stars are also “assigned” to late stages of evolution, but because they lie *below* the main-sequence and are also enveloped by H α -emission-envelopes (subdwarf central stars of planetary nebulae, ranging from WR to Type-F in {uncertain} spectral type). All such characterizations of “evolutionary” state rest on (outdated?) “standard” concepts of “normal star” interiors and atmospheres — based on the cited quasi-thermal tripartite structure associated with only radiative fluxes and “small-departure” nonTE thermodynamics (to which limitation we return below). Such models/concepts/characterizations are increasingly “patched,” as the phenomena observed in peculiar stars, including the Sun, become increasingly accepted as nonpeculiar — except in size/degree. I suggest that a re-examination of whole-star modeling, from basic panspectral observations of all stellar types and unrestricted nonTE-thermodynamics, is a more coherent approach than such “patch-work” progress.

This distinction between empirical-theoretical modeling of “observationally-defined Be” and conceptual modeling of “conceptually-defined CV” serves as an illustrative transition to our focus on coherently understanding/formulating that thermodynamics necessary and sufficient to describe/represent/model the empirical relations between observed atmospheric structural patterns and observed/inferred fluxes — toward whose interpretation we need a clear understanding of the origin, and size, of these fluxes. Our repeated question, toward whose resolution we assemble, and diagnose, all data available to us, is: Are such origin and size determined only by the thermodynamic characteristics (or by the thermodynamic state under specified characteristics) of only the “internal” structure of the star (but admitting either thermal or/and nonthermal storage modes)? That is, can we treat the star as an effectively isolated CEM, in whose flux production we can ignore the effect of some “outer part” of the star — e.g., those regions containing only some small fraction of the total mass of the star, including the atmosphere? In this alternative *B1*, we would indeed specify the effect of the fluxes on atmospheric structure by the particular boundary conditions (values of the fluxes) at a lower boundary (subatmosphere to atmosphere transition). Or do the existence and size of some flux depend on the whole structure of the star, possibly also of its local environment? In this alternative *B2*, the amount of mass involved is not the sole factor; also the (nonTE) thermodynamic distribution of it and its energy states enter, through boundary conditions for flux-propagating (cf., below). Here, a determination of flux(es) and a star’s whole structure is a symbiotic problem: each depends on the other; they must be determined simultaneously. An outer boundary condition (atmosphere to environment), and possibly also another further out (local environment to ISM), are as important as the lower one.

Stellar modelers historically/speculatively adopt the first alternative for the radiative flux, and the second for nonradiative fluxes. But they (we) yet know too little about the broad nonTE thermodynamics of open systems, especially of the self-gravitating, free-boundary stellar type, to trust such a wholly speculative theoretical choice between *B1* and *B2*. Atmospheric modeling evolves by successive approximation to its thermodynamics, via successive extension of empirical-theoretical guidance by higher resolution/wider λ -range/time-dependent observation. Direct subatmospheric observation, except by inference from neutrinos and variability, is rare. I try to forecast the next approximation to whole-star modeling, by asking what gives thermodynamic self-consistency between subatmosphere and atmosphere.

c. PERSPECTIVE ON “EFFECTIVELY STEADY-STATE” WHOLE-STAR MODELING

The Emden-Eddington approach/approximations followed the above first alternative. Emden set aside the question of primary interest to us — the production of fluxes and their relation to structure — to focus on the linear-nonTE specification of deep-interior conditions; the outer regions of the star, its environment, fluxes, and energy production were neglected. This was a good approximation

for estimating thermal-hydrostatic conditions (density, temperature) for thermal energy-production in the deep interior. To introduce the primary observational quantity, the radiative-flux, set-aside by Emden, without being handicapped by the then lacking knowledge of the (nuclear-reaction) details of its production mechanism, Eddington set-aside the question of energy *production* to focus on energy *transport*. His explicit, critical-assumption, *CA1*, was that *all* energy-fluxes could be modeled in the “energy-transport” Region 2 of a single star’s tripartite structure, by adopting the linear-nonTE representation of fluxes being proportional to space gradients of those linear-nonTE state-parameters adopted in Emden’s assumed thermal, time-independent conditions. Eddington showed that, under the assumed stellar-interior, linear-nonTE, conditions, energy-transport by radiation is more efficient than by mass (thermal conduction or convection). His explicit critical-assumption, *CA2* — that *all* energy-transport is linear-nonTE radiative — replaced Emden’s polytropic representation of nonTE energy transfer, by radiative equilibrium, under linear nonTE for both matter and radiation. His assumption *CA3* further imposed, explicitly, that such conditions required the energy transported through Region 2, and ejected from Region 3, to equal that produced in Region 1; so ignorance of the details of the Region 1 energy production, if it involved only thermally controlled processes, would not inhibit modeling stars that satisfy these conditions.

This assumption, challenged by Jeans et al. who asserted that reliable modeling must incorporate the details of the energy-generation process in Region 1, is critical in the kind of nonTE picture one adopts for Region 1 (cf., below). But it is Eddington’s implicit critical assumption *CR4* — continuing Emden’s equally implicit assumption that conditions in the deep interior are time-independent, thermal, and linearly-nonTE, thus locally controlled — that chooses between Section 1.b alternatives, *B1* and *B2*, on luminosity/radiative-flux production, there “abstracted” as the basic modeling question. *CR4 implicitly chooses B1*. It was essentially unchallenged at that epoch as (apparently) offering the only way to avoid the too short time-scales of “change” in stellar luminosity produced by those other, then identified alternatives such as gravitational contraction, meteor infall, etc. It imposes that the single-star luminosity is independent of its environment, even of its atmosphere (\equiv transition zone from star to environment), even of any binarity. *The mode and rate of energy production in Region 1, which is (then thought to be) observed to leave the star only as a radiative flux, is implicitly assumed to depend only on local conditions/thermodynamic parameters CR4 \equiv B1.*

The validities of these four critical assumptions are linked mainly through their common assumptions that *the rate of energy production in Region 1 depends only on the thermal, linear-nonTE (hence local) state parameters of that region’s assumed thermodynamic characterization*; that the overlying regions are also linear-nonTE in structure and flux transport; and that *all* that energy leaves the star radiatively. In nonTE abstract: only a radiative-flux is assumed to be associated-with/produced-by the (very slowly, secularly evolving, stable) nuclear interaction that exo-thermically changes the nonLTE populations of the local mass (so also energy) states of the matter comprising Region 1.

Combined, the essential aspects of the “thermodynamic picture” modeled by these assumptions are: (i) the Region-1 energy-production rate’s independence of anything but that “effective-mass” assumed (by HE + RE) to produce the local values of the thermal, linear-nonTE state-parameters (temperature, density) for a given nuclear composition; (ii) the equality of energy-production rate to its linear-nonTE transport rate in Regions 2 and 3; (iii) hence, the radiative flux produced in Region 1 is related to atmosphere/subatmosphere structure via the (RE plus linear-nonTE) relation between flux and T-gradient. Any influence of lower (subatmosphere-to-atmosphere) and/or outer (atmosphere-to-environment) boundary conditions on the energy production, or a diversion from the star’s radiative flux, is (implicitly) assumed to be negligible.

Later evolution of such modeling to “detail” it by computing an actual thermal nuclear energy production in Region 1 does not change this basic thermodynamics. Eddington’s relaxation of linear-nonTE for Region 3 did, but incompletely. To infer total (bolometric) luminosity from that observed

in the accessible spectral regions (the visual at his epoch), he adopted in Region 3 a linear-nonTE for matter, and matter-radiation interaction, but removed it for the radiation field (such is thermodynamically inconsistent in any “boundary” region). But it maintains the assumed equality between “corrected-observed” radiative flux from Region 3, energy transported through Region 2, and energy produced in Region 1; there is no energy to a nonradiative flux from the star. Likewise his Cepheid modeling removed “thermal” in, and “zero radiative-flux phase-lag” between, Regions 2 and 3; but negligible pulsation amplitudes in Region 1 left its characteristics unchanged.

We note that none of the: high-resolution visual-spectral, X-ray, farUV, and farIR observations; diagnostics of these showing a nonlinear nonTE thermodynamic state in the outer atmospheres of all stars, and in the lower atmospheres of some stars; the existence of a significant mass flux from all well observed stars; and an evolutionary short, but pulsationally long, variability of luminosity, which is sometimes associated in phase with variability of the mass flux in some stars — *none of these agree with the basic thermodynamics of these Emden-Eddington models, nor with the so-called “standard theoretical” models whose basic thermodynamics rests on the Emden-Eddington approach.* Neither does any self-consistent nonTE thermodynamic theory of such open systems as stars.

In re-examining this Emden-Eddington approach to whole-star modeling of single/isolated stars, asking improvements based on both better nonTE-thermodynamic understanding and expanded observational knowledge, and trying to remedy these conflicts with observations, we recognize three aspects: (α) clarifying perspective on the thermodynamics of stellar structure and evolution, based on assuming that a star is a concentration of matter and energy in a parental ISM, which evolves because the concentration process is exo-thermic; (β) removing what was speculative imposition of oversimplified kinds of nonTE thermodynamics, in both their diagnostic and modeling uses; (γ) adding conceptually-new information on stellar regional structure and fluxes, and their association, especially on a ubiquitously-existing mass flux, and on the (sometimes associated) patterned variability of mass and radiative fluxes over time-scales up to several decades.

Then relative to Point (α), we should put into clear perspective the implications of Eddington’s assumption *CA3* — introduced to be able to ignore energy production and focus on energy propagation, and implicitly used to decouple the production of a mass flux from that of a radiative flux in the subatmosphere. The requirement that such energy production in Region 1, under such modeling, must precisely match radiative energy transport in Region 2, and radiative energy loss from Region 3, historically introduced confusion on what, basically, fixes the star’s luminosity and radiative flux. Note the “perspectives” by Schwarzschild (1958), and by Sears and Brownlee (1960), on Eddington’s abstract (1926): “the cause of a flow of radiation from a star to the ISM is the gradually increasing T from surface to center of a star.” Consider Schwarzschild: (a) “the luminosity of a star is not determined by the rate of energy generation by nuclear processes, but by the radiative-equilibrium condition — (attained) not by adjusting its luminosity (fixed by the linear-nonTE T-gradient) but by adjusting its nuclear sources (interaction rates) by contraction/expansion,” and (b) “(we can) derive *uniquely* the (star’s) internal structure from values of the mass, luminosity, radius, and composition of the outer-layers — because the constancy of stars (luminosity and structure) asserts that the stellar interior must be in perfect equilibrium.”

Sears and Brownlee: “There exists a T-gradient because there is a pressure gradient. The pressure gradient is fixed by hydrostatic equilibrium; i.e., $g > 0$ sets up a pressure gradient.”

To put this into perspective, we caricature/abstract the essential thermodynamics of the Emden-Eddington (and before them, Lane, Riter, Kelvin, et al.) approach as: (1) We observe stars because they produce a radiative flux to the ISM. (*Ibis*) Under linear-nonTE thermodynamics, a “local thermal energy partitioning” exists; a T measures it; and such radiative fluxes imply $T(\text{star center}) > T(\text{star surface}) > T(\text{ISM})$. (2) Astronomical and geological observations imply any secular change in such flux over times of $0(10^6 - 10^9 \text{ years})$ to be very small, or (relative to stellar-evolutionary times) of very

short-duration. (2bis) Under linear-nonTE, such small secular change in flux implies a near-Equilibrium $T(r)$ structure of the star, which some modelers impose as perfect Equilibrium. (3) Under thermal HE and their gravity, single stars have $P(\text{center}) > P(\text{surface}) > P(\text{ISM})$. To specify $P(r)$ requires $P(\rho)$ which, for a perfect gas, requires specifying energy exchange between adjacent “thermodynamic-elements.” (3bis) Emden by-passed the details by exploring stellar structure as a function of polytropic index: showing that an isothermal model has infinite mass and extent, so cannot represent any actual star; obtaining order-of-magnitude estimates for $P(\text{center})$, $\rho(\text{center})$, $T(\text{center})$ that allowed (eventual) identification of change in nonLTE nuclear mass states as a source of stellar energy-fluxes in a quasi-steady-state nonLTE configuration. (4) Eddington replaced the polytropic approach by literal linear-nonLTE, with the radiative flux proportional to the radial gradient of the radiative energy density $\sim T^4$. (4bis) He imposed that the total energy flux is, in his models, radiative, so that the only admissible energy-production mechanisms are those matching a radiative-equilibrium energy flux given by the r -gradient of T .

Even before questioning the thermodynamic reality of each step (the above point B), we see that the *sequence (1)–(4bis)* only establishes an association between, it does not establish any causal sequence of, radiative flux and structure $\equiv T(r)$ of the star. Indeed, without (4bis), it would only establish such association between energy flux (of whatever variety, so long as it depends only on the T -gradient) and structure. If we want, a priori, to assume that one of these quantities (radiative flux, structure) is fundamental, thus fixing the other, we can caricature/abstract the two extreme alternatives for modeling such assumption:

(a) *Emden-Eddington (E-E)* — structure of the star [$T(r)$] is fixed by thermal HE plus radiative energy-transfer independently of the source/size of the star’s energy-loss/radiative-flux; the energy-producing mechanism must “adjust” to match that radiative flux transmitted, as specified by $r^2 \text{grad} T^4 =$ “the fundamental” quantity of stellar-structure, in addition to self-gravity, under this (E-E) alternative. That quantity of energy which the (subatmospheric-atmospheric) Regions (2, 3) can transmit determines what energy the star must produce in Region 1, if the star is to maintain that “equilibrium which is conjectured from observations.” Stellar mass determines structure; structure determines luminosity — under (E-E).

Or, (b) *Essential-Jeans (E-J)* — local energy production/star’s luminosity are determined by conditions (nuclear reaction-rates) in Region 1, independently of the structure of, and energy-transport through, overlying regions; energy-transporting mechanisms in, and structure of, overlying regions must “adjust” to match the energy-loss size specified by the nuclear reaction rates changing the local nonLTE nuclear mass-state populations = “the fundamental” quantity of stellar structure and evolution, in addition to self-gravity, under this (E-J) alternative. *The quantity of energy which the star produces in Region 1 determines what energy Regions (1 and 2) must transmit, and what structure they must have, if the star is to maintain the “observed/inferred kind of equilibrium.”* Stellar mass determines energy production; energy production determines subatmospheric-atmospheric structure — under (E-J).

We note an essential thermodynamic difference between the two alternatives. Essentially, for Regions 2 and 3, the Emden-Eddington orientation rests on adopting the linear-nonTE description of structure and flux transport throughout the star, in terms of “a” local temperature, and its distribution $T(r)$, as being the basic parameter specifying the star’s structure. The Essential-Jeans orientation does not need such linearization in discussing steady-state modeling. The nuclear nonLTE reaction-rate computations need only a kinetic, not an equipartitioning T . One can adopt arbitrary nonTE alternatives in Regions 2 and 3 without changing Region 1 under this (caricatured) (E-J) alternative. As Eddington emphasized, (E-E) modeling rests on gross thermodynamics, via time-independent, thermal, linear nonTE description, and by minimizing that dependence on knowledge of detailed

microscopic processes/rates which permits exploration of time-dependent, nonthermal, nonlinear-nonTE. It asked what one could say about stellar structure/evolution from such a gross thermodynamic viewpoint, much as one proceeded in the early, pre-nonLTE, pre-nonradiative-flux, speculatively rather than observationally oriented, modeling of stellar atmospheres — asking into temperature and composition, rather than nonTE-thermodynamics and structure.

Schwarzschild's extensions of his above remark, (b), reflect the same linear-nonTE approach to the meaning of "equilibrium": (i) supplementing/replacing radiative transport by convective was discussed in terms of stability of the (fundamental) T-gradient basic in linear-nonTE, not in terms of the inadequacy of linearity by considering the amount of energy to be transported; (ii) the discussion during that epoch of the origin, not amplitude, of pulsational instability follows the same linearity; (iii) Schwarzschild estimates the consequences of violating a "strong" thermal hydrostatic equilibrium in terms of an added macroscopic force, not of an outward-evolving nonlinearity under, e.g., (microscopically-specified) radiative energy/momentum addition to a Region 1 initiated mass flux, such as observations during our epoch of mass outflow/flux exhibit (cf., below). This orientation leads him to suggest that such departure from HE would cause a star to collapse/explode in times of 0 (minutes), rather than produce the episodically enhanced/diminished radiative and mass fluxes observed in some stars, with time-scales of 0(hours to decades, or centuries); (iv) but his emphasis that a departure from RE over reasonably long times should not affect (these models') structure gives a more relaxed viewpoint on the implication of "perfect" equilibrium, and its perspective in modeling an observed variability not (thought to be) associated with a pulsation.

Indeed, Schwarzschild's (iv)th point implies the starting point of that reorientation which we have been following, and which I think marks the future: the question of whether the continually cited episodic variability implies a variability in stellar energy production, or simply in energy partition. Extensive studies of these alternatives for the variability attributed to stellar pulsation (cf., especially Ledoux's work) conclude it implies no variability in energy production, only in its storage. We find the same (cf., the cited summaries by Doazan and myself) for the behavior of the H α outer-atmospheric envelope/local environment of Be-stars, but not for the behavior of the whole-star radiative and mass fluxes.

The above caricature/abstract puts our above points (α)–(β) into perspective. Concerning Point (β), nonTE-thermodynamic inadequacy, I have stressed the dependence of the (E–E) modeling on the linear-nonTE assumption. In terms of relaxing it, I mentioned the (empirical-theoretical) outward evolution of nonTE representations, and their introducing confusion between the origin and outward evolution of fluxes. Concerning Point γ , observational guidance of improvement, I continually stress the impact of variability, especially of patterned episodic variety, on understanding the origin of fluxes. Concerning Point α , specifying a better — at least thermodynamically more consistent — picture of structure/evolution, I think one needs to put Points β and γ into the same caricature/abstract perspective as above, as a preliminary to such a caricature/abstract of Point α . I so illustrate Points β and γ , and conclude with a comment on Point α based on this.

As a Point β example of how linear-nonTE modeling leads to a quite erroneous picture of the actual situation, I choose meteor luminosity and "evolution," which occur as the meteor enters, and traverses, the Earth's atmosphere. The luminosity arises by converting a small solid surface into an extended gaseous one, by producing a mass flux from the solid surface via energy transfer to it at a rate too great for a linear modeling of heat conduction inward; the surface "explodes" backward/outward (CV mass-exchange model analogy, contrary to this Perspective's orientation? Be patient.) Meteors are very small objects, whose surface is "heated" by the ultrathermal impact of atmospheric atoms (in the meteor rest-frame). Under a linear-nonTE description of a speculative "thermal structure" of the meteor, as it enters the atmosphere, the energy "produced," from converting arriving-atom kinetic energy to thermal heat on impact, would be conducted inward. The meteor would radiate as

a solid body; feebly, from its very small surface. If this linear nonTE estimate — reached by computing a T-distribution to the interior of the meteor from a heat flux proportional to the T-gradient — did not equal the energy arriving, something should happen. The meteor cannot “adjust” its energy production by slowing down under a deceleration law based on matching heat conduction inward; it cannot arbitrarily adjust its T-gradient because $T(\text{mass, surface})$ would exceed solid-state binding energies. What happens is that both meteor and modeler discard linear nonTE. The meteor is observed to radiate a line spectrum characteristic of its constituents — they had no time to relax and/or conduct energy inward at this surface, because of the too large energy-production rate there: surface atoms “explode” to the gaseous phase, but not to an “explosive” outflow velocity — rather, their outflow velocity is very slow (relative to the meteor surface), quasi-“thermal” (“T” means what?).

So we adopted one variety of nonlinear-nonTE modeling: treating the thin surface layer, where the phase changes from solid to gas, as the highly nonTE reaction zone, whose detailed structure one ignores, considering it to be the “activated-complex” of (Eyring’s) absolute-rate theory of chemical reaction kinetics. The parameter is the energy-production rate given by meteor velocity and atmospheric density. This nonlinear-nonTE model predicts how the energy is partitioned into ablation (mass-loss) and radiation (line spectrum, from atom-atom interaction between atmospheric atoms and the moving gaseous envelope resulting from the phase change). Hence it predicts height of meteor appearance — and not badly — no comparison with the feeble solid-body radiation of linear theory, under which the meteor is essentially invisible.

The vagueness of *how* slow is the outflow, and what happens a short distance from the surface, is a weakness in the particular adopted chemical reaction-rate modeling — which simply gives the rate of a quasi-equilibrium phase change, not asking where the products go. High speed (μsec exposure) photographs of “simulated” (but much lower velocity) meteors show the ablated material simply following the flow lines of that part of the incident air-stream not “absorbed” into the meteor surface. The mass outflow expands, behind the meteor, into the large volume observed — producing, under impact with the atmospheric atoms, the observed line spectrum of meteor plus atmospheric atoms/molecules. So any “analogy” one might seek with the effect of the “surface reactions” hypothesized in mass-interchange CV modeling, would suggest that such reactions might provide a deep-atmosphere, low-velocity outflow: an enhanced value of that lower boundary value produced by modeling the mass outflow of normal stars under the assumption that it is determined by subatmospheric conditions. If correct, then the acceleration to the observed ultra-speed values would be a separate process — again as in normal stars; but of course possibly linked to the associated luminosity enhancement. So we would return to the same problem as in single stars: the outward evolution of the outflow velocity — to which we return below.

Here, our primary objective is to exhibit the effect of an actual nonlinearity on a picture based on linear modeling. In essence, it shows that the rate of energy production, relative to the rate at which linear-nonTE theory lets it be transported away, provides the critical “test” of the utility of linear-nonTE for modeling this particular phenomenon. Whether production equals transport does indeed “test” such model’s adequacy — but re. linearized-transport, not re. production, in this meteor example. Here, both observations and theory reject the adequacy, not the particular variety, of linear-nonTE. The basic question is not the stability of one variety of linear-nonTE transport versus that of another linear variety — the focus of (E-E) type modeling. Clearly, the meteor is only a specific example of the general problem of the effect of size of energy production on the kind of nonTE-character the medium must have to transport the energy away. It simply stimulates asking, in re-examining whole-star modeling, occasioned by “variability,” what is the basic problem: variety of linearity; or applicability of linearity — and if it is not applicable, with what do we replace it? The meteor example is illustrative: experiments/observations guided the replacement choice.

The meteor example also illustrates the interrelation between flux characteristics, kind of nonTE, and “whole-phenomenon structure,” For small enough energy-production/inward-energy-flux, the linear-nonTE description of a heat conduction into the solid meteor suffices; $T(\text{depth})$ describes the thermodynamic state of the 1-region (solid phase) meteor. The “atmosphere” arises outside the meteor as a mass inflow, and is not influenced by the meteor, except as the boundary for the aerodynamic flow pattern. For large energy production/flux, we adopt the cited variety of nonTE configurations: the four-regioned “phase-structure” (linear-TE solid, unspecified nonTE “reaction-zone,” unspecified-nonTE slowly moving vapor, blending into the atmospheric aerodynamic flow) results as an empirical-theoretical “construction.”

For meteors, we can reproduce all the above in the laboratory — of course, at velocities lower than the fastest meteors (Charters, Cook, Eyring, Mayfield, Rinehart, Thomas, Whipple, White; 1945–1955). Such astrobballistic studies were an early example of that laboratory astrophysics which provides an experimental complement to the stellar-observational data base in developing insight into nonlinear-nonTE. But we note that well before this nonlinear-nonTE formulation of the problem, the basic “gross model” was proposed, and explored, by Opik (1933); then by Whipple and the Harvard meteor program — basically, from the (linear-expected) solid-body radiation versus the observed (nonlinear expected) line spectrum. Such observationally anomalous thermodynamics resembles that found in early historical observations of “peculiar” stars — emission-lines, extended atmospheres, superionization — by Opik-kindred observers (Beals, McLaughlin, Secchi, Struve, Swings — Payne-Gaposchkin from the empirical-theoretical outlook), which underlies our modern “variegated-nonTE” examples/studies. Once stimulated, the nonlinear-nonTE outlook provides a marvelous umbrella — if we can predict/distinguish where differing degrees of nonlinearity will appear. As yet, such prediction usually lies beyond our experience; but our experience is evolving. In the cited examples, observations provided the stimulation/guide/distinction.

Thus far in this Perspective, contrasting with that of earlier volumes, we have focused on stellar *internal* structure, mainly motivated by trying to understand the origin of the patterned, medium-term (hours to decades/centuries) variability in both luminosity and mass flux which current farUV plus visual *atmospheric* observations delineate. We went back to Eddington, and others, to try to put the origin of the *luminosity* into perspective — the primeval choice between production and subatmospheric/atmospheric transmissivity as being basic in fixing the size of the radiative flux. When we ask about the origin of mass flux, the situation becomes even less clear: current “theory” oscillates between various alternatives on atmospheric instability as the origin; little attention lies on a production in parallel with that of the luminosity, in the interior. Yet, a naive approach might consider stellar evolution/structure as simply reflecting the thermodynamic behavior of an evolving concentration of that energy and mass “stored” in a “sufficiently massive local coagulation” of the ISM. Empirically, this evolving concentration of mass and energy, CME, continuously returns some of that energy and mass to its parental medium: the star is structured and evolves as an open thermodynamic system. We ask how, then why? The initial, ISM, state of this matter could hardly be TE, even if it might be more nearly homogeneous than after significant concentration. So the star’s differential local-nonTE configuration as a function of (radius, time) is symbiotically interlinked with the production and transmission of those (empirically) required energy and mass fluxes back to the parental ISM. Thermodynamically, such open-system characterization would seem to demand whole-system “participation” in producing all fluxes, and in determining its radially evolving nonTE structure. Our preceding discussion illustrates the danger of proceeding by speculative, a priori, imposition of origin of fluxes and nonTE character. So one best proceeds empirically-theoretically: as in the meteor, solar chromospheric T Tau, and Be studies. I return to the above aspect (α), “naive” evolving CME picture, after further illustrating aspect (β), improved nonTE representation/structure.

In the preceding, I have focused on a subatmospheric origin of fluxes, hence on specifying such a flux by the *lower* (subatmosphere-to-atmosphere) boundary condition. But we recognize that most of our empirical guidance to real-star, relative to speculative-star, structure comes from observations of the (classically anomalous) *upper* atmosphere. We largely infer lower atmospheric anomalies from how its structure evolves into the observed upper atmosphere configuration. Nonetheless, even the lower atmospheric regions differ significantly from their classical models. In Section B following, I abstract these differences for the FGK stars, in summarizing their features discussed in this Volume 7. One member of this class, the Sun, has been responsible for clarifying, via that high resolution permitted by its proximity, a variety of “classically anomalous” observations of other stars. So here, for illustration, as was the meteor example, I abstract the outward evolution of radiative and mass fluxes, re. their relation to the outward evolution of nonlinear-nonTE effects and regional structure, as guided by the solar case supplemented by studies of some bright “peculiar” stars.

A critical aspect in studying such outward evolution in nonTE description/character of a given flux, and its impact on regional-structure, is to distinguish these from the effects introduced by the “coming into observational/structural importance” of some other flux. In the early days of stellar application of the solar inspired nonLTE treatment of radiative flux, and its impact on photospheric regional structure, this “mixing” was often ignored. The solar-nonLTE treatment of the radiation field was developed in concert with the identification of the effect of nonradiative energy fluxes on chromospheric $T_e(r)$ and $\rho(r)$ — and eventually was “blended” into the outward evolving effects of the mass outflow/flux. Too often, early stellar nonLTE studies — and currently, nonLTE plus wind studies — ignored the evidence/presence of nonradiative energy fluxes, usually for modeling simplicity. This insularity obscures attempts to delineate the origin of such nonradiative fluxes. One confuses effects coming from outward evolution of one flux with those coming from interaction between several fluxes. Abstracting our conceptual evolution in treating the radiative energy flux in the atmosphere when a nonradiative energy flux is also present/evolving illustrates both nonlinear-nonTE evolution and flux-mixing confusion — and guides mass-flux evolution.

d. PERSPECTIVE ON LOWER ATMOSPHERIC nonTE FROM nonTE EVOLUTION OF RADIATIVE, NONRADIATIVE, AND MASS FLUXES IN THE UPPER ATMOSPHERE

The “classical” criterion for applying Equilibrium thermodynamics is energy-flux \ll local energy density. Such logic rests on the total energy of a (homogeneous) TE system being thermally partitioned over all energy-storage modes via one parameter T; $\text{grad}T = 0$ gives zero energy-flux. Linear-nonTE definition: Small flux implies small $\text{grad}T \equiv$ one “T” still exists but both inhomogeneity and $\text{grad}T$ are sufficiently small that local, microscopic, energy-state distribution functions are only small-perturbed by “thermal-mixing” with adjacent regions, which differ little in thermodynamic state. Small T-gradient $\equiv dT/T \ll 1$; so sufficiently large T implies that ΔT can be large. One neglects asking: how small is small, re. effects (cf., Table 1).

From such logic, *not asking how small is small*, grew that thermodynamics one applied to stellar structure: (1) adapting the foundations of TE thermodynamics of homogeneous systems to the inhomogeneous structure of actual stars (linear-nonTE); (2) adapting strongly nonLTE distribution functions of nuclear mass states to linear-nonTE; (3) adapting strongly nonLTE distribution functions of atomic energy states to linear-nonTE in regions where radiative flux \sim radiation density. On this basis, one obtained the above discussed tripartite stellar structure: energy-producing, energy-transporting, energy-ejecting regions. Eddington’s modification of strict linear-nonTE in Region-3, retaining it for velocity distributions and for internal energy states of atoms but not for photons, was thermodynamically inconsistent: it abandoned the equipartitioning basis of both TE and linear-nonTE thermodynamics, via one “T” for both particles and photons, without replacing it by time-

dependent microscopic rate processes. Observations reinforced such a critique of thermodynamic-consistency. The modified linearity represented neither the observed radiation spectrum, nor an observed substructure of Region 3, increasingly so as observational resolution increased, so especially for the Sun.

Early Region-3, atmospheric, modeling approximated the radiation continuum as produced by the TE-modeling of black-body emission from a photospheric surface at T_{eff} . Under linear-nonTE diagnostics, the approximation appeared reasonably good for the radiation spectrum and flux. *Quality of radiation* measures T_{eff} conditions; *quantity*, a lesser T , measured by the average of outgoing and ingoing intensity. One sees absorption lines because T decreases outward, being measured by radiative equilibrium with $T^4 \sim$ local radiation energy density, whose “reversing layer/upper photosphere” T -value corresponds to that lack of inward flowing radiation. There is no outward evolution in nonTE description; it is always linear-nonTE. On an equally gross basis, the situation worsens if one tries to model the mass flux as the outward component of a TE thermal-velocity distribution of particles whose kinetic energies exceed gravitational escape. Such predicted mass-loss values are many orders of magnitude smaller than the observed, equally for the “peculiar” stars showing a mass loss from visual-spectral observations, and for more normal stars showing it only in the farUV spectrum.

Solar observations guided the path to replace such a patchwork-modified linear-representation by a more-coherent nonlinear-nonTE representation of the radiation field/flux and of the substructure of Region 3. One abandoned “equipartitioning temperature”: as a parameter, and $f(T)$ microscopic distribution functions, introducing microscopic rate-process computations of such distribution functions in terms of “local” parameters which describe such rates: $T_e(r)$ to describe a (assumed to exist) TE-type, thermal velocity distribution for the electrons; $n(r)$ to give the local particle concentration; and $J_\nu(r)$, a photon distribution function resulting from solution of the (nonlinearly-nonTE) radiative-transfer problem over the atmosphere as a whole. T_e and $n(r)$ fix collision-rates; J_ν and $n(r)$, radiative-rates. Such nonLTE distribution functions partition $n(r)$ into atomic/molecular energy-state populations for prescribed (nonLTE) mass-state populations (abundances). Applying radiative equilibrium fixes T_e in the absence of dissipative nonradiative energy fluxes. If one permits those latter, some kind of transfer problem for such fluxes must be solved. Applying thermal hydrostatic equilibrium, assuming no mass fluxes nor “random turbulence,” fixes $n(r)$ [equivalently, $\rho(r)$]. This variety of (steady-state,thermal) nonlinear-nonTE was/is thermodynamically self-consistent to the validity of its explicitly stated assumptions: essentially, quasi-thermal thermodynamic state, and existence of a T_e . “Quasi-thermal” implies no velocities $\geq q/3$; q is the local one-dimensional thermal velocity. Such restriction implies no aerodynamic energy dissipation nor significant violation of HE.

The guiding role of solar observations was their variety suggesting $T_e > “T”$ in the outer solar atmosphere; demanding its effect on rate-process-determined, microscopic, energy-level populations; and their effect on the thermodynamics of the “source-function” of the radiative-transfer equation, and on its variation/distribution over the atmosphere, hence on those diagnostics of observed line plus continuum spectra which produce our empirical knowledge of stellar atmospheres. Self-consistent, nonTE thermodynamic, study of the latter, especially of high-resolution observations telling us what empirical relations we had to satisfy between I_ν and S_ν , produced the form: $S_\nu = \sigma \{ J_\nu + sB^* \}$ to replace $B_\nu(T_e)$. B^* can be (local) T_e independent; $\sigma \sim 1$, $s \ll 1$ for strong lines. So the local value of $S \sim$ the local value of J ; but the latter, coming from the solution of the radiative transfer problem over the (ν -visible) atmosphere, is not locally determined. Its local value, at some τ_1 , depends on the $\exp(-\tau)$, —weighted integration of the distribution of source(sB^*) and sink ($1-\sigma$) terms over all regions that are “visible” to it. Such regions, both stellar and local-environmental, are those contained within $|\tau-\tau_1| \leq 1$. Thus even an atmosphere homogeneous in (sB, σ) does not produce homogeneity in S ; rather, an outward decreasing S . Absorption lines do not imply an outward decrease in T_e , but in S . An iso- T_e atmospheric region does not imply iso- S . The T_e -dependence of S is via (s, B^*, σ) — via the relevant microscopic rate processes. Such T_e -dependence can be strong, as in the CaII and

the superionized lines in the farUV — or weak, as for H α . The flux is (symbiotically) fixed by grad S, not grade T $_e$; even an isothermal star produces a radiative flux. Emden-Eddington thermodynamics are oversimplified. One requires a whole-star/environment nonlinear-nonTE; not a local-linear-nonTE.

Such representation makes clear both the outward evolution of nonTE effects, and their effect on atmospheric structure, when only a radiative flux is present, or when both radiative, and nonradiative-dissipative, fluxes are present. With only a radiative flux, S $_{\nu}$ evolves from: B $_{\nu}$ (T $_e$) in the very deep atmosphere where the “environment” is opaque and I $_{\nu}$ is quasi-isotropic at all ν ; through a value of B*(T $_e$)*(s/[1- σ]) at greater heights; to a value $\sim B*s^{1/2}$ in surface regions quasi-homogeneous in [sB*, σ] — always with radiative equilibrium T $_e$ values. One obtains simply LTE and nonLTE photospheric regions. With nonRE-T $_e$, one adds a chromosphere. If one introduces a mass flux, which evolves outward as sketched below, one obtains some variety of corona. I emphasize that it is the kind of nonTE effects, which reflect both themselves and the kind of fluxes present — not the particular values of T $_e$, etc. — which relate atmospheric structure to fluxes and nonTE effects. So the problem is to specify which fluxes, in addition to the radiative, are present; to ask what kind of atmospheric structure they produce — and compare this with observations — and only then return to ask the (subatmospheric — or instability?) origin of both. Thus far, our insight has been wholly observational, and rests essentially on outer atmospheric observations/studies, where “outward evolution/amplification” makes their presence/effects unmistakable. Nonetheless, ambiguity remains, as illustrated for the mass flux in the following.

For the radiative-nonTE effects and outward evolution, we first gave (above) the “finished product,” then put it into the context of the (solar) observations that inspired it. Largely, these were solar-eclipse studies, where direct (limb) observations of the outer atmosphere are possible. Indications of observational-T $_e$ > theoretical-T, even in lower regions of the outer atmosphere; the outward enhancement of this; its complication by opacity effects, which also evolve outward; and the question of the relative importance of collisional and radiative rate processes had stimulated these efforts to obtain greater observational precision and more coherent nonTE theory. Stellar generalization of the thermal, radiative-flux-only aspects was essentially immediate; only in the nonradiative energy flux applications has there been inertia, largely in nonsolar astronomers.

But for mass fluxes, and the observational delineation of their associated outer-atmospheric velocities, it was visual-spectral observations of extreme peculiar stars — now complemented by farUV observations of them, and of “lesser-peculiar,” and increasingly of normal, stars — which give our present extensive (but yet inadequate in terms of variability) sets of observations. “Asymptotic” velocities of the solar wind come from particle collectors, not from direct, solar-atmospheric spectroscopic observations. And although (Parker’s) solar modeling of such aerodynamic mass outflow was the first, it is inadequate to represent the observed range of stellar observations, especially those of variability. So we have, as yet, no “finished-product” picture/model/concept/theory from whose even quasi-comprehensive perspective we might view the observed relations between mass flux, its outward nonlinear evolution, its effect on atmospheric structure, its time-dependence — toward identifying a “whole-star thermodynamic” origin.

So we focus first on abstracting what observational generalities one can identify; then present a perspective on modeling and implications on origin. So long as stars were “normally” modeled as closed thermodynamic systems, the observed/inferred, anomalously present, macroscopic velocity fields were generally modeled as low-subthermal, consequently, as having only minor effects on atmospheric structure — even less, on subatmospheric structure. When a nonradiative heating of the solar chromosphere was inferred, a subatmospheric production of highly subthermal acoustic fluxes was suggested as one possible origin. But these were not associated with mass-outflow; and the eventual shocks were small-amplitude, treated essentially linearly. Only the solar spicules were modeled as

(nonlinear) superthermic, but outwardly decelerated, mass outflow, with aerodynamic energy dissipation (cf., Volume 1 for summaries of these problems/discussions in the Sun).

However, historic visual-spectral observations of some peculiar stars, and current farUV spectral observations of all stars, show ultra-thermal velocities in the exo-photospheric transition between star and environment to be common. They are always accelerated from photospheric measured (usually unobserved) values. Sometimes they are observed to be eventually decelerated, especially in stars showing very extended (and variable), cool, exo-coronal envelopes, producing H α emission (like the Be stars, planetary nebulae, etc). In very low mass-flux stars like the Sun, where densities in the ultra-speed region are too low to permit direct spectroscopic observation, only indirect measures, from some variety of particle detectors, have provided information on the maximum outflow velocity reached. For the Sun, these values range between 400–800 km s⁻¹, thus are ultra, not simply super-, thermic, and variable. So we can only conclude that in other stars, also with much smaller mass fluxes than those from stars where the ultra-speed character is spectroscopically blatant, wholly spectroscopic evidence that maximum outflow velocities are only small, or not even superthermic, may be very misleading (cf., the discussion in Volume 4, particularly its Figure 3-13, which exhibits such evidence all across the HR diagram).

One should think carefully about this possible observational ambiguity when reading the discussion in Chapter 3 of the present volume on the evidence, from spectroscopic measurements, for differences in maximum velocities of winds between differing types of stars. Parts of that discussion compare maximum wind velocities of FGK stars with a value of some 500 km s⁻¹ for the Sun — without emphasizing that the former are spectroscopic, while the latter is from particle collectors and is variable. Moreover, referring to the above cited Volume 4, Figure 3-13, this 500 km s⁻¹ is completely anomalous, by more than a factor 2, relative to all other stars in that region of the HR diagram, from mid-B to the Sun. Such caution, and qualification, are especially necessary in inferring the characteristics of the wind from the K–M supergiant component of binaries where the other component is of type B. While most of the values cited in Chapter 3 lie near 100 km s⁻¹, a few values, variable, near 400 km s⁻¹, are found for absorption lines. Wind lines from single B stars are always in absorption (cf., the above-cited nonlinear-nonTE radiative transfer in an optically thick atmosphere), never in emission — which generally requires an atmosphere much more extended in the line than in the adjacent continuum. For cool stars like the Sun, the highly ionized lines are in emission — the regions of their formation being far removed from those where arises the adjacent continuum: there is no line-continuum coupling other than simple absorption. The authors do stress the variation of profile type with eclipse phase: being wholly in emission when the Be star is wholly eclipsed; and being a P Cyg mixture of emission and absorption at other epochs. Because such eclipsing systems give the best probes available of outer-atmospheric structure and inhomogeneity, their results are invaluable. The authors emphasize the complexity of diagnosing them.

I place great emphasis on this eventually ultrathermal character of the mass outflow; because it emphasizes that the “outer-boundary” nonlinearity of the mass flux is as important as that of the radiation flux in diagnosing, and modeling, atmospheric structure. The effect of mass outflow on atmospheric structure, by a momentum input perturbing HE, and on RE, by providing a source of nonradiative energy dissipation, is small for velocity $V \leq q/3$, as earlier mentioned. So an outward acceleration of V from the (usually, observationally) small subthermal values in the photosphere — the linear nonTE regime — through about $q/3$, where nonlinear effects begin, then through the (locally, very unstable, time-dependent) transthermal regime, into the superthermal, and eventually ultra-thermal, regimes does indeed represent a strong outward evolution of nonlinearity. When we add the observations of strong mass outflow/flux variability — noting that mass outflow and mass flux are not necessarily the same, especially if variable — we see that nonlinear evolution is a strong factor in fixing atmospheric structure.

We need to put two questions into clear focus:

(1) Given a mass flux, which aspects of its observed outward evolution (acceleration, deceleration, heating, cooling) come simply from the existence and outward-propagation of that flux alone — as in the outward evolution of the radiative-transfer source function, and of the (associated) populations of the (microscopic) atomic energy states under RE; and which aspects result from perturbations introduced by the parallel existence and propagation of other fluxes — as in the nonRE perturbations of the sink and source terms of the source function by a dissipative nonradiative energy flux? That is, how much of the outward evolution (acceleration) of the mass outflow, and its heating (controversial, for hot stars, among some astronomers — cf., Volume 6; not controversial for the FGK stars of this Volume 7), result from addition of energy and/or momentum to the flow because of the existence/evolving propagation of other fluxes? And for those stars where the outflow is eventually decelerated — and cooled: does the deceleration, and eventual cooling, arise from other-flux interaction, or simply from interaction with the ISM, independently of the existence of other fluxes? (cf., for these deceleration/cooling aspects, the cited summaries by Doazan, and Doazan and Thomas, of the results/inferences of the last decade's Be studies from combined IUE and ground-based time sequences of observations. And reflect on that Be and CV star similarity, re. episodic enhancement of mass outflow and luminosity, stressed in this Perspective.).

(2) What can we say about any coupling between outer and lower boundary/transition-region conditions relative to the origin of the mass flux from the star, under its thermodynamic characterization as an open, self-gravitating system? For the moment, we can only recognize that this characterization is empirical; we ask whether it is intrinsic to the picture of a star as a CME evolving from an ISM “fluctuation?” Once, astronomers thought such a picture could be satisfied by a structure/composition evolution which produced only a radiative flux — the star evolved as a closed system. They only debated whether the luminosity size could be represented by a boundary condition at the Region 1 to Region 2 transition (exo-thermic change in nonLTE mass-state populations in Region 1 fixes luminosity, independently of how the energy is transported/ejected in overlying regions — the radiative-flux determines, is not determined by, their (nonTE) structure). Alternatively, the size of the luminosity is fixed by how much radiation can be transported through the structure (both transport and structure now nonlinearly-nonTE) of Regions 2 and 3. (As above, we know something about nonlinearity in Region 3; not yet, in Region 2.).

(2bis) We now recognize the same dilemma in determining the size of the mass flux: Is it (somehow) fixed in (association with) the process of Region-1 change in nonLTE mass-state populations (maybe dropping the requirement/computational scheme that these reactions be wholly thermal); or is it fixed by how much mass (the conditions in) Regions 2 and 3 enable the star to transport/eject? (cf., the discussion in the Perspective of Volume 6.). Or, indeed, is the latter alternative more stringent: eject at large *super*-escape velocity, so that the asymptotic velocity is ultrathermal, following the above observational “facts/inferences?” Which of these is correct? Mass-flux evolution, or interacting/coupling with something else? And why?

That is, adopting as orientation the Essential-Jeans and Emden-Eddington types of alternatives: under (E-J), is the size of the mass flux determined simply by the quantity/quality of mass/energy concentrated into the star? Under this alternative, in modeling the (observed) atmosphere, one would impose the size of the mass flux as a lower-boundary (subatmosphere-to-atmosphere transition) condition. Or under (E-E), is the size of the mass flux imposed by the quantity of matter that the star's structure lets it eject, in parallel with the (E-E) approach to the size of the radiative flux being fixed by how much the subatmosphere/atmosphere $T(r)$ lets the star transmit/eject, ie, by the

quantity of matter which can be accelerated (by whatever mechanism) to escape (or super-escape) velocity? Under this alternative, exo-photospheric atmospheric structure and mass-flux size/velocity — as well as the origin of mass-flux — would be determined symbiotically. Because T_e (max) of the outflowing material is, for a wide variety of stars, $\gg T_{\text{eff}}$ (star), nonradiative energy fluxes must also be incorporated in such modeling and questions of origin.

In considering these two alternatives, one must recognize the observationally imposed requirement that the “successful” alternative must be able to produce that *patterned* variability, and its sometimes association with radiative-flux variability — on time-scales of hours to several decades — in at least a significant number/variety of stars. In using (E-J) and (E-E) alternatives as references, we must also realize that production/character of the radiative-flux must be reexamined in terms of that same patterned/associated variability. I stress that I hardly propose a resolution of these problems (in this Perspective Chapter or at this stage of these monographs): I simply try to put them into perspective.

A preliminary perspective comes from beginning at the bottom of the atmosphere and sketching, as for the radiative flux, the outward evolution of a small outflow velocity which may produce a mass flux from the star. I use a mixture of observations and thermodynamics, to identify where flux mixing enters. Then we note that any small-subthermal, radial mass outflow, of whatever origin, will, under radiative equilibrium, be amplified outward, to a value near the one-dimensional thermal velocity q corresponding to that local value of T_e determined by the solution (whether empirical or theoretical) of the (nonlinear-nonTE) radiative-transfer problem under RE. The “directionality” of the outflow is established by the (thermal) HE density gradient. Until the outward-accelerating, via mass-conservation, velocity V reaches $\sim q/3$, the outflow does not significantly perturb either RE or thermal-HE. For larger V , the outflow progressively perturbs both. When V reaches values near q , the outflow becomes unstable against producing acoustic radiation; thus (mechanically) dissipating the outflow (kinetic) energy (which is supplied by its radiatively maintained/controlled thermal energy) of any localized outflow originating in some low-atmosphere random perturbation (cf., Volume 4).

If the small-velocity outflow at the base of the atmosphere originates in some kind of steady-state subatmospheric “driving,” its outflow velocity is again bounded by the local thermal velocity, via the production of a decelerating (and compressing) shockwave when the flow-velocity exceeds q . Across the shock, the flow velocity falls to a subthermal value — dissipatively, not adiabatically, producing that irreversible “heating” which is the nonlinear characteristic of a shock wave compared to the (idealized) zero-amplitude acoustic wave; then the flow again accelerates, taking energy from its (radiatively controlled) thermal energy, still to conserve mass in this (imposed) steady-state mass outflow. This “shock-sequential” outflow persists until it reaches conditions where the acceleration can carry it through the “transthermal” region, quasi-linearly without a shock, to the superthermal. The sequence has been well observed in the laboratory since Prandtl’s (1904) studies, and also applied (Thomas, 1951) to solar phenomena.

So the basic physics of the subthermal — oscillating about the transthermal — part of the outward evolution of these two kinds of mass outflows (random origin; driven origin) is the same. This sub-transthermal part is the upward evolution, under mass conservation, of the small initial V , coupled with the (nonlinear-nonTE) T_e -gradient fixed by the (nonlinear-nonTE) upward evolution of the radiation field. The outflow energy comes from converting the (radiatively sustained) thermal energy into outflow-directed nonthermal, because of the (here, thermal-hydrostatic under gravity) pressure gradient. The sonic loci are the characteristics of the equations describing any eventual superthermal region of the outflow; their envelope is the shock; cf., the photographs in Volume 4. Replacing an RE- $T_e(r)$ by a nonRE- T_e only extends the transthermal region by increasing q , reflecting the (dissipative) upward evolution of the nonradiative flux. In either alternative, RE or nonRE, the outward-evolution of the mass outflow/flux is coupled to the outward evolution of the radiative and nonradiative

energy fluxes via their determination of $T_e(r)$, and its effect on the sub-transthermal regions of the mass outflow. Implicitly, I have assumed that the (details of the) energy flux determination of T_e is independent of the mass outflow; which is correct only for “sufficiently small” outflow velocity. So we see that the outward evolution of the several fluxes — and of the kind of nonTE, and of the variety/characteristics of the regional structure of the atmosphere — are generally (symbiotically) coupled. Considering the outward evolution of only (any) one of these hardly gives an adequate/complete picture.

The difference between the (considered) two alternative mass outflows lies in the character of the initial small-velocity outflow: its origin, size, and kind of “driving-from-below.” These, plus the coupling with the other fluxes, condition the mass outflow’s upward evolution. So, we see the essential role of the lower atmosphere boundary condition in influencing the outward evolution of upper-atmosphere phenomena — hence, on diagnosing the increasingly well observed latter to infer the less easily observed, re. mass outflow, former. The influence/role of the outer-boundary/transition-region is implicit, as requiring a nonlinearity by the structural nonhomogeneity of its existence. But my discussion adopts the (E–J) alternative; it does not consider the currently more popular picture that the mass outflow is “pulled-out” from above by these outer boundary conditions, to which the lower boundary must “adjust.” Effectively, this is the (E–E) alternative: atmospheric structure determines what it can transport, hence what the subatmosphere must feed into it, to produce the “observed stellar stability.”

One puts the (E–E) alternative in perspective by again focusing on the nonlinearity. Its effect/importance is trivially obvious in noting the dependence of the RE- $q(T_e)$ on such nonlinearity of the radiation-transfer solution in the “boundary value” which T_e would have in the absence of nonradiative heating. But it is more striking in asking the origin of the super- and ultra-thermal parts of the mass outflow. To have that outward evolution/acceleration of the mass flow, which is produced by mass conservation under a steady-state outflow, produce an expansion/acceleration instead of a compression/deceleration by a shock, requires a special atmospheric configuration. It must mimic an “equivalent perfect transonic nozzle.” If the only outward acceleration is the thermal-energy conversion, thermal density-gradient directing one, then the sub- to super-thermal velocity transition must occur where total outflow velocity of a (statistical) gas “particle” (macroscopic V plus one-dimensional microscopic thermal q) equals the local escape velocity. Under this condition, the transition is quasi-linear— “quasi;” because it involves no shock but is unstable. A very slightly differing configuration, which accelerates V to q at such an r that $T_e(r)$ has not risen enough to match $q(T_e) = V_{esc}(r)/2$, will simply produce a shock, and decelerate to subthermal, not accelerate to superthermal, the outflow — which will then repeat the acceleration/shock process at ever larger r until q rises, and V_{esc} decreases, to reach equality. The transonic regime is well recognized for such instability. Its description is usually (locally) time-dependent.

So we see how the (E–J) and (E–E) alternatives differ. If one assumes as in (E–J), that the subatmospheric regions of the star produce the mass outflow, we specify its size (via specifying V , because such low-subthermal outflow does not perturb $\rho[r]$) as a lower boundary condition. Thereafter, $V(r)$ evolves/accelerates outward, undergoing the “repetitive shock sequence” until it reaches $V = q = V_{esc}/2$: thereafter V expands super-thermally (maybe eventually ultra-thermally, depending on identifying an acceleration). The size of the mass-flux/lower-atmosphere V , “in collaboration” with the effects of ρ -gradient on V , and of the radiative and nonradiative energy fluxes on $T_e(r)$, determine the location and the “local structure” of the thermal-point/transonic-region, and the “intermediate boundary” conditions for the “beginning” part of the overlying (at least initially) superthermic-outflowing atmospheric regions. Any variability of such “lower-boundary-region specification” of mass flux strongly influences variability in whole-atmospheric structure, especially beginning with the

transonic region (cf., the cited Doazan., and Doazan-Thomas, Be-models — which are (this kind of) empirically based model).

On the contrary, if one assumes, as in (E-E), that the atmospheric structure fixes the origin/size of the mass flux, one very explicitly imposes (for this solar, FGK, cool-star-type picture): that the atmospheric structure ($T_e[r]$, $\rho[r]$, $g[r]$), above the lower-boundary, in the subthermal quasi-linear, but below the transthermal nonlinear, outflow regions determines the size of the mass outflow/flux. The distribution of these three quantities T_e , ρ , g fix the location, r , where the mass outflow must, for the first time, reach $V = q$, the thermal point. Thus they fix the value of $\rho V (= q)$ at that point — hence the value of the mass flux (assumed to be constant, because of time-independent outflow). The factor of three uncertainty in $\rho(r_{th})$, arising because it is only for $V \leq q/3$ that a static-atmosphere model is essentially unperturbed by the mass outflow, is clearly not critical to the picture. It simply means that the unperturbed regions do not extend precisely up to the thermal point, but only up to about a density scale-height below the thermal point, up to where $V \leq q/3$. *What is critical is the restriction of the mass flux to a size which does not produce a thermal point — $V \sim q$ — below the escape point — $q = V_{esc}/2$.* That is, the mass outflow is restricted to being subthermal and non-dissipative up to about a density scale-height below the escape point, and just reaching $V = q$ at the escape point. The particular value of the mass flux is fixed by these conditions. It is the largest mass flux which is “stably-compatible” with an effectively-static, unperturbed-by-nonthermal motions, “semi-lower” atmosphere extending nearly to the escape point. It differs from the classical standard thermal atmosphere by admitting dissipative nonradiative fluxes, but with the dissipation not arising in a mass outflow. It is the picture of a static chromosphere-corona as the outer atmosphere, of a star as a closed thermodynamic system — unperturbed by the existence of any mass outflow from an overlying region.

So this imposed (E-E) “quasi-linearity” introduces the *minimum* perturbation on closed-system models; it gives a *lower-limit* on the range of mass flux values which satisfy the (E-J) condition that they produce one or more thermal points at or below the critical point. Thus, by contrast, admitting a range of mass-flux values larger than this lower limiting one, the (E-J) model permits/introduces a perturbed atmospheric region well below the escape point — an extended transonic (unstable) region, whereas the (E-E) model does not. The (E-E)-type model restricts any change in atmospheric structure associated with a mass outflow to regions above a density scale-height below the escape point. The observational distinction between the two models is clear; obviously in regions below the escape point, and also in regions near the thermal point, which is now not “forced” to first occur at the escape point, and additionally, for sufficiently high-resolution observations/diagnostics, we should be able to delineate “probes” in the regions intermediate between the lower boundary and thermal point. Study of $T_e(r)$, especially *cooling* relative to RE predictions, may be one such probe.

Under the (E-J) outlook, such transonic instability, producing extended transonic regions, and their variability between differing, or the same, stars having apparently similar photospheres is viewed as “normal.” Local differences in values of the mass flux are viewed as “normal.” (E-J) modeling determines the location of the transthermal region, and of the thermal point, for a ($g[r]$, $T_e[r]$) — determined escape point and a (lower boundary prescribed) mass outflow — not the converse (cf., the comment on the location of the thermal point, and resulting atmospheric structure, as a function of mass-flux size for the WR stars, which have the largest yet observed mass flux, except for the novae and recurrent novae, in Section d. following). Such range of possible values for the mass flux, for a given escape point (even incorporating a variation in T_e), allows the currently observed variety of variability to be viewed as “normal.”

Evidently, we have not yet addressed the question as to *how* the star produces its mass outflow/flux, whether variable or not (and associated with variable luminosity, in some cases) Observationally, it does; and our models must reflect it. If the star produces a variable mass outflow, its

atmospheric configuration need not change in its basic thermodynamics — up through the escape point — following the above (E-J)-type modeling. It need change only in detail as to where the several (decelerating/heating) shocks occur below the escape point, and in the variability's effect on character/structure of post-escape-point regions (cf., the Be modeling cited, especially re. post-coronal and local-environmental regions).

Under (E-J), and “freedom to be nonlinear — i.e., permit shock waves to occur in the outflow,” there are a variety of mass-flux values that can satisfy the thermodynamic conditions. Under (E-E) imposed linearity — no shock waves, no dissipation permitted — there is a unique mass flux “permitted/imposed.” The latter is the original Parker picture, which is still retained re. this imposed-linearity. Under such picture, variability in mass outflow is difficult to incorporate, if one “believes” that a star has a unique luminosity and nonradiative energy flux. It is easier to simply re-examine the whole question of steady-state, in stellar structure and evolution. What steady-state means, and the kind/time-scale of variability which we must treat, are defined by the observations — not by a priori conjecture.

In the preceding, I have implicitly restricted attention to FGK-type atmospheric structure and mass outflow. The same (thermodynamic) kind of observational inferences, and thermodynamic-consistency arguments, can be made for (E-J) and (E-E) type origin/character of mass outflow for the hot stars. Again the critique is largely of minimum “perturbation” modeling, but noting that for the hot stars, “perturbation” mainly refers to nonRE heating, not mass outflow. For the Sun and most cool stars, there is no ambiguity on the presence of nonradiative heating: a 10^6 K solar corona sparked the cold-star, super-hot, outer atmosphere revolution. But only for cool supergiants do mass losses of size similar to those in hot stars exist; and for them, it is the large surface area, not high-speed outflow per unit area, which gives such values. As earlier mentioned, except for the Sun, it is the lack of observed 0 (10^3 km s⁻¹) velocities for stars cooler than late B which handicap panHR-diagram modeling of ultrathermal velocities. That they are observed for the Sun raises the question of observational incompleteness for nonsolar cool stars. The same question of incompleteness characterizes hot-star observations/diagnostics re. nonRE heating; cf., the Perspective of Volume 6. There is little point in repeating that discussion/critique here, because the thermodynamic point is, I trust, clear. The original choice between (E-E) and (E-J) alternatives for modeling stellar luminosity has been extended by modern observations to modeling stellar mass loss. Such extension strongly suggests that all stars require all fluxes to produce their open-system, often variably so, character. The problem is understanding/modeling the relative contributions to the origin and size of these fluxes made by: the energy production, from evolution in (nonLTE) mass states; and the energy and mass transport through the star.

Again the peculiar stars provide an example of the latter: flux-transport “conditioned” by atmospheric “opacity/transmissivity.” Those stars characterized by strong and variable H α emission lines — ranging from the Be to the planetary nebulae as the long-observed varieties, including the T Tauri as the more recently explored — exhibit a mass outflow which is decelerated, and sometimes stored, in the very outer atmospheric (local-environmental) regions, via the (transient) enhancement of the mass content of a cool envelope (possibly the predecessor of a planetary system). A mass outflow from the lower regions does not directly become a mass flux; the relation between the two shows strong phases, with time-scales from weeks to many decades. The mass outflow also shows strong variability; its combination with the deceleration/storage produces the variable mass content of the envelope. But the essential (observational) point is that we do indeed have evidence that *a combination of production and transport — neither of them alone* — underlies the observational behavior of at least some peculiar stars. And the thesis of the monograph series is that the high-resolution study of peculiar stars, made possible by the larger amplitude of “peculiar/anomalous (relative to speculative

theory)” phenomena in them, points the path to understanding “normal” stars, where such amplitudes are smaller, hence less readily observed.

The problem now, as earlier, is to develop a whole-star modeling symbiotically; between internal, atmospheric, local-environmental, thermodynamic structure on the one hand; and on the other, those evolutionary (spatial, from interior to boundary; and temporal, from ISM to end-product), microscopic mass-and energy-state populations that condition it. We note that at the epoch of Eddington’s work, the empirical mass-luminosity relation (i.e., the relation between total mass/energy of the CME and its exo- “thermal” flux of energy) provided a strong incentive to try to model such a relation, in which mass composition (chemical abundance, i.e., mass-state populations) was a parameter — even though the details of nuclear-energy production of that luminosity were then vague. The relation of structure to evolution was eventually identified as very-long-term secular, not short-term variable/oscillatory, changes in (nonLTE) mass-state populations.

At our epoch, modern observations suggest an extended such orientation: again seeking a relation between total mass/energy of the CME and its change/fluxes — but admitting a mass flux on the same “perturbative” (of a quasi-Equilibrium configuration) level as a (radiative) energy flux. An essential point is that the mass flux is not at all negligible relative to the radiative — so it is not at all a question of admitting the mass flux as a “minor” thermodynamic correction to a modeling based on only radiative energy flux (cf., Table 1). One could apply the same logic to that generally adopted at Emden’s epoch: as a first approximation, modeling a star while ignoring energy production and energy flux is not bad because its overall structure is largely fixed by its gravitational (energy) binding. At our epoch, two new (post-Emden) “thermodynamic/cosmological” facts have been added:

(1) As a star evolves, it produces a mass loss as well as radiative-energy loss.

(2) Both luminosity and mass loss are, for at least a variety of stars, variable over time-scales too long to represent simply “phase-storage” — as in the pulsating Cepheids — but too short to represent “simple, thermally controlled,” secular evolution in nuclear (nonLTE) mass-state populations. Moreover the amplitudes of such variability vary strongly: from one stellar type to another; within stellar types; at different epochs of one star.

(2)bis: Finally, while there is a strong observed association between size of mass flux and mass (or luminosity, as it is usually expressed) — we have even less idea on how to relate subatmospheric conditions in a star to any driving of the mass outflow. But the evidence for variability in both mass loss and luminosity — on time-scales too long to be pulsation, and too short to be standard nuclear-evolutionary — is strong, for a variety of stars. So the problem needs re-examination, free from the a priori judgement that the “(superficially) unchanging” appearance of stars implies “equilibrium.” On the contrary, the kind of “instability” associated with differing values of the mass flux for given “apparently-similar” photospheres, discussed above, identifies “instability” as basic in understanding that kind of structure and evolution associated with the presence of a mass, as well as a radiative, flux.

The implication of the preceding remarks on modeling stellar structure as it relates to evolution, or the converse, is clear, and implicitly mentioned throughout. One adopts mass loss as being as equally fundamental as radiative-energy loss to the evolution of some CME formed from the ISM. As before, one recognizes the basic evolutionary process to be that of the nonLTE states of mass population. In modeling, one should not try to minimize the implications/effects of mass loss relative to radiation loss. One should not, as in the above caricatured (E-E) approach, try to select models which produce minimal values of the mass flux. Rather, one should ask what sizes of mass loss are required to produce the other “anomalous” effects observed — as for the WR stars. It is useful to put the observed

range of sizes of the mass loss, their “maximum” velocities, and the energy loss from the star associated with them into perspective — to substantiate the above remarks that the mass flux is equally significant to the radiation flux, re. modeling/understanding stellar structure/evolution, for at least many stars.

I follow Schwarzschild’s presentation (1958) of a similar perspective for the situation when only a radiative flux was thought to be generally present, hence significant. We compare the energy and mass storage modes in a star; and the relative energetic sizes of the several fluxes. An aspect of such a comparison is to put into perspective whether stellar structure/evolution is necessarily “quiet” — i.e., thermal — except during certain “transition” epochs. The chief modeling question is how the star determines the size/outflow of its several fluxes, under the recognition that, for at least some stars, these can be significantly variable on time-scales of days to centuries. In essence, we need to re-examine the relative contributions of both the (E-J) and (E-E) outlooks to modeling.

We put all this into perspective by comparing the mass flux to the radiative flux in two ways:

First, we note the classical criterion for introducing a quasi-Equilibrium modeling: energy loss from, to energy content of, a system. For an open system, we should make the same comparison for mass loss and mass content. For the energy content of a star, we follow Schwarzschild (his Equations 5.4 through 5.7) to take the potential nuclear energy liberation as the star’s energy: $E^* = 0.07 \cdot 10^{20} M$ ergs. The star’s mass M is its mass content. I take the mass and radiative fluxes from the values in Table 3-11 of Volume 4 in this series, only slightly altered by data from succeeding volumes. We compare $F_{M(\text{gm/s})}/M$ to L/E^* , in Table 1 here. We see that the mass-loss perturbation exceeds the radiative perturbation for the WR and OB sg, and the M sg; but they are equal for the A sg and B-MS and for the Be stars during episodes of enhanced emission and mass outflow. For the Sun, the radiative perturbation is by far the larger. Mass-loss values are even more uncertain for the cooler MS, but they lie between the Sun and B-star values. But the essential point is that the mass loss indicates non-Equilibrium effects before the radiative loss does.

Table 1.
Crude Comparison of Energy and Mass Losses, to Energy and Mass Storage for Various Stellar Types

| Stellar Type | M units $2 \cdot 10^{33} \text{g}$ | ES units 10^{53}erg | \dot{M} units $6 \cdot 10^{20} \text{g/s}$ | V_{max} Obsv. units 10^3k/s | KE[\dot{M}] units 10^{40}erg/s | E[\dot{M}] units 10^{40}erg/s | L units 10^{40}erg/s | \dot{M}/M units $10^{-15}/\text{s}$ | L/ES units $10^{-15}/\text{s}$ |
|--------------|--|-------------------------------------|--|---|--|---|--------------------------------------|---|--------------------------------------|
| WR | 50-10 | 7-1.5 | 10-1 | 4-2 | $10^{-1}-10^{-3}$ | 5-1 | 0.4-0.08 | 60-30 | 6-8 |
| Osg | 30-10 | 5-1.5 | $1 \cdot 10^{-3}$ | 3-1 | $3 \cdot 10^{-3}-10^{-6}$ | 0.5-0.001 | 0.4-0.04 | 10-0.03 | 8-4 |
| Bsg | 20-10 | 3-1.5 | $1 \cdot 10^{-3}$ | 2-1 | $2 \cdot 10^{-3}-10^{-6}$ | 0.3-0.001 | 0.04- | 10-0.06 | 1- |
| Bd | 10-5 | 1.5-1. | $10^{-3}-10^{-6}$ | 2-1 | $10^{-6}-10^{-9}$ | $10^{-3}-10^{-6}$ | $4 \cdot 10^{-4}$ | $3 \cdot 10^{-2}-10^{-5}$ | $4 \cdot 10^{-2}$ |
| Be | 10-5 | 1.5-1 | $10^{-2}-10^{-6}$ | 2-0.5 | $10^{-5}-10^{-8}$ | $10^{-2}-10^{-6}$ | $10^{-3}-4 \cdot 10^{-4}$ | $3 \cdot 10^{-1}-10^{-5}$ | $6 \cdot 10^{-2}-10^{-2}$ |
| Asg | 25-5 | 4-1 | $10^{-2}-10^{-4}$ | 0.3 | 10^{-7} | $5 \cdot 10^{-3}$ | 10^{-2} | $10^{-1}-10^{-3}$ | $[2-0.4]10^{-1}$ |
| Ad | 2 | 0.3 | - | 0.3 | - | - | - | - | - |
| Sun | 1 | 0.15 | $3 \cdot 10^{-9}$ | 0.8 | 10^{-12} | 10^{-9} | $4 \cdot 10^{-7}$ | 10^{-6} | $3 \cdot 10^{-4}$ |
| Msg | 20-10 | 3-1.5 | $10 \cdot 10^{-3}$ | 0.3 | $10^{-4}-10^{-8}$ | $5 \cdot 10^{-4}$ | $0.4 \cdot 10^{-3}$ | 10^2-10^{-2} | $10 \cdot 10^{-1}$ |

Symbols: M = stellar mass, ES = energy stored, \dot{M} = mass-loss rate, V_{max} Obsv. = maximum *observed* wind velocity, KE[\dot{M}] = kinetic energy of mass outflow, E[\dot{M}] = total energy of mass outflow, L = stellar luminosity.

Second, we see this more explicitly by simply asking the relative energy carried away by mass and radiation fluxes. If we compute only the kinetic energy of the mass flux, we have the result already given in Volume 4, Table 3-11. Only for the WR — and of course for novae of various varieties — does the mass kinetic-energy approach the radiative energy. But if we compute the energy stored in the mass flux in the same way as that stored in the star — which obviously we should because we ask about the star's loss of its potential radiative energy — we see the underlying basis for the result above: the energy carried away by the mass flux generally exceeds that in the radiative flux, except for the Sun. Now, again, given the mass-flux uncertainties, one must be cautious with this result.

Nonetheless, it again makes the main point: in addition to being “spectacular” in its ultra-thermal velocities, the mass loss is an energetically important (in terms of stellar evolution as well as outer-atmospheric structure) quantity in modeling stars.

Thus, wholly from energy considerations, for all stars except the cool ones, it can hardly be argued that it is a good first approximation to neglect the mass flux relative to the radiative, in modeling the star as a whole. This thesis is strongly reinforced when one discusses the impact of the star's evolution on its environment — especially in creating those local environments associated with variable mass outflow; and, relative to the latter, via the T Tauri-solar association, to the formation of planetary systems. We turn to the T Tauri stars, in further developing this, but as part of the general summary of the FGK stars. The preceding has been a “thermodynamic perspective,” broadly across the HR diagram, as a kind of introduction to a specific perspective on this volume.

B. FGK PERSPECTIVE ON THE FOREGOING WHOLE-STAR MODELING OF SECTION A

From the preceding, we see the importance of synthesizing the modeling/theory/implications of the “nonclassical theoretical” structure/fluxes in the exo-photosphere with those in the low photosphere to see: (i) an overall picture of the structure of a stellar atmosphere; (ii) what is its relation to the fluxes of mass and energy existing in, and from, a star; and (iii) what is the relation of the atmospheric structure and fluxes to the structure of the local environment of the stars; (iv) how all these relate to, and how they are conditioned by, the subatmospheric/internal structure, and possibly nonthermal modes, of the star as a whole — which we cannot directly observe. One should try to synthesize that perspective on these questions gained from the FGK stars — recognizing that these stars, via their outstanding member, the Sun, plus judiciously adjoined fellow-peculiar stars, opened that “can of worms” which is nonclassical exo-photospheric structure, and extended it upwards and downwards. I try to abstract my own picture of what such a synthesis might be, beginning with the lowest photosphere, where those observable regions described by the classical-modeling approach should be the least perturbed; emphasizing the perturbation of a demand for realistic subatmosphere/atmosphere boundary conditions on that modeling.

Then we *assume* that the thermal state of the deepest directly observed part of these stars — the lowest atmospheric region, the photosphere — is characterized by a kinetic temperature of the electrons: $T_e(r)$. *It is assumed:* (α) that T_e is in equilibrium with the local, λ -integrated, radiation field; (β) that this λ -integrated radiation field is LTE-inferable from the observed visual-spectral radiation field plus an inferred photospheric radius. Such T_e , inferred for the FGK stars, range from ~ 9000 K for F0 stars to ~ 4000 K for K9 stars. These values refer to optical depth in τ (continuum) ~ 1 , depending on the T_e -gradient; so they characterize the lower photosphere. Thereabove, in those overlying photospheric layers where RE, under a Local Thermodynamic Equilibrium (LTE), remains applicable, T_e decreases outward until nonRE, or nonLTE (or strong change in dominating opacity source) — i.e., nonclassical atmospheric — regions occur. Such departure from classical atmospheric assumptions would define one variety of exo-photospheric regions. In such regions, T_e is neither wholly determined by, nor measured by, the radiation field alone.

But in the lower photospheres of these FGK stars: (i) a Planckian distribution of radiation in this T_e -range concentrates most of its energy in the visual spectrum; (ii) nonLTE effects in the visual continuum, in this lowest photosphere, are small for the atmospheric-opacity characteristics of FGK stars; (iii) nonRE effects are small. Thus the stated T_e -range so associated with these visual-spectral classes, inferred from the visual spectrum alone, should be reliable. Adjoining space-based luminosity measures in the farUV spectrum support this conclusion, by not forcing significant changes in the T_e values inferred from the visual spectrum alone — if one uses the same radius for the “effective emitting photosphere” in the visual and in the farUV.

Photospheric radii are inferred simultaneously with stellar masses from analysis of luminosity and radial-velocity variations in those eclipsing binaries that show the absorption-line spectra of both components: the so-called “double-line spectroscopic binaries.” (A set of emission lines, also showing periodic variation of the type associated with binarity, is sometimes also present — but it refers to other, nonphotospheric, behavior of the stellar atmosphere than that discussed here.) Existing values for photospheric-radii and stellar masses for FGK stars come, historically, from analyses of visual-spectral observations; so they indeed characterize the visual-spectral photospheric region of the preceding paragraph. Results of such analyses give the range, from F to K stars (Allen, 1955): $1.5\text{--}0.5R_\odot$ and $1.5\text{--}0.5M_\odot$ for main-sequence stars; $1.5\text{--}75R_\odot$ and $1.4\text{--}4M_\odot$ for giants; $50\text{--}500R_\odot$ and $10\text{--}15M_\odot$ for supergiants.

To the best of my knowledge, we have no directly inferred radii of the farUV continuum emitting/absorbing regions. Chapter 3 of this volume discusses those eclipsing systems consisting of a K–M type giant or supergiant, and a B main-sequence star — diagnosing both visual and farUV spectra. But the discussion focuses on the line spectrum and on the exo-photospheric regions of the cool star, and a bit on the mass outflow/wind of both stars — but not on the farUV continuum of either star. So we have no direct verification that visual and nonvisual contributions to the luminosity come from a same-size “effective” emitting disk; hence that they can be combined to produce, from the λ -integrated luminosity, an “effective” T_e which we can consider to thermally characterize a common photospheric region.

However, *for these FGK stars, especially those on the main sequence, the concept of a well defined stellar-photospheric radius, hence of a well determined T_e in the low photosphere, is made meaningful by the combination of: (i) a reasonably gray opacity (H^-) across the major contributing wavelengths in the visual plus IR plus farUV continua to the observed luminosity; with (ii) a sufficiently static kinetic state of the photosphere.* Point (i) ensures “seeing” to essentially the same atmospheric depth over a wide spectral range. Point (ii) produces an essentially exponential outward decrease of the density and opacity as that atmospheric height observed increases (under the thermal- T_e scale-height) — so that the local contribution to the emission/absorption decreases rapidly with height. Thus the geometrical extent of the effective emitting/absorbing region of continuum origin — especially of the visual continuum — is limited; its radius is well defined. Thus a T_e inferred from radially directed intensity observations is reasonably well determined near τ_c (radial) ~ 1 — for the FGK main-sequence stars.

If we combine this approach with limb-darkening measures, or with eclipse measures so that the optical path is tangential, the procedure works sufficiently well to provide T_e (τ or height) up to those heights where begin those nonclassical regions of nonRE and nonHE that invalidate the above listed assumptions. So there are two problems in inferring an extensive — from the low photosphere up through the nonclassical regions — height distribution of T_e , hence the height distribution of the local thermal state, from observations of the radiative continuum:

- (i) Such limb-darkening, or eclipse, observations that give information throughout the photosphere, and up some distance into the exo-photosphere, are directly possible only for the Sun — other-star

eclipse measures generally give only exo-photospheric information, and then of low resolution (e.g., as in Chapter 3). Hence, at present, we have as empirical guide to the transition between pseudo-classical photosphere and exo-photosphere only the Sun (*pseudo*-classical because even at the lowest depths there are nonclassical features; see below). So any nonsolar theoretical model which differs in gross thermodynamic structural pattern from the Sun, not just in particular values of the thermodynamic parameters, is wholly speculative until one has shown a sound thermodynamic basis for the difference. If, of course, sufficiently high-resolution observations show a nonsolar structural pattern — i.e., a difference in basic thermodynamic structure — the objective is to use this plus the Sun plus other observed differing patterns to construct a general thermodynamic scheme for atmospheric modeling which covers all patterns.

Chapter 3 discusses just such difference between the solar and some FGK (and M) giants/supergiants relating to the wind-size and “hotness” of the chromosphere-corona. But this is no basic thermodynamic difference, only a difference in values of some nonradiative fluxes and of the thermodynamic parameters which they affect. More basic are the differences with those speculative hot-star models which exclude nonradiative heating (cf., Volume 6). However, the well observed Be-stars differ from the Sun only in their post-coronal structure, and the much greater variability of atmospheric structure and nonradiative fluxes (cf., Volumes 2 and 4, and subsequent work by their authors). Before one tries to proceed too independently of solar and “peculiar” star guidance, one should remember that no theory predicted what the Sun, and other peculiar stars, exhibited until the wealth of high-resolution, detailed observations — especially in the farUV — showed that classical theory was inadequate even for “normal” stars.

(ii) Once in the exo-photosphere, one requires not just a diagnostics permitting nonLTE; but also one permitting nonRE and nonHE in the spectroscopic excitation and matter distribution. But while measurements of the radiative continuum alone may — under (non-Equilibrium) thermodynamically consistent diagnostics — imply departure from RE and HE; they do not suffice to specify, empirically, what are the nonRE and nonHE models. From the continuum alone we cannot infer these nonclassical effects — nor do we have, presently, any satisfactory whole-star theories for their modeling/origin.

In and above these nonclassical regions, except for solar eclipse — and to some degree occulting-disk observations — we have as yet no way to geometrically resolve/measure, directly, either the monochromatic radiative flux or the area producing it — thus to separate the thermal state of the atmosphere from any nonthermal, and/or nonradiative, effect on the distribution of emissivity.

Thermal nonLTE theory is sufficiently mature to be able to relate the distribution of source-sink terms of the source function, in thermal and quasi-thermal regions, to the emergent (observable) radiative flux, if we know: what those terms are, their distribution with opacity, and the distribution of opacity with geometry. At least the latter, usually also the former, require knowledge of nonRE and nonHE effects and their distribution — which existing theory cannot give, because it does not predict even the *existence* of nonradiative fluxes. Simply trying to invert the observed radiative-intensities to obtain source-sink terms and their distribution is difficult if one does not have the detail of solar eclipse observations, which is what has made the fine details of solar eclipse studies, and the gross details of those eclipsing-binary studies summarized in Chapter 3 of this volume, so invaluable. The usual alternative is to conjecture models of the nonradiative fluxes — often omitting some, selectively, because it is easier; then try to obtain a model of the nonRE and nonHE regions by iterating between model and selected observations — usually ignoring any variability. But each new set of observations, especially those delineating a time-dependence, exhibits how little rapport there is between such speculations and actual stars. The major progress has come from either such empirical analysis as that for the Sun from eclipse data, or, for stars, from seeking empirical associations between the various observable parameters characterizing the exo-photospheric regions.

The existence of these (nonRE, nonHE, nonthermal) exo-photospheric regions is associated with the outward amplification of the effects of nonradiative fluxes — whose existence is denied under classical thermal modeling — on thermal and nonthermal energy and mass distributions. A dissipative nonradiative energy flux perturbs T_e from its RE value; a sufficiently-high-velocity mass flux perturbs an exponential HE density distribution. In these “nonthermal” atmospheric regions, and above them: any sharp edge of a stellar-photospheric “disk,” any concept of a λ -independent radius of an LTE-thermally absorbing/emitting photosphere, any algorithm for inferring — unambiguously at each height in the atmosphere from a wholly thermal interpretation of observed radiative-flux height gradients — all of these become “fuzzy.” One questions if a meaningful determination of the local thermal state of the atmosphere can be made without a simultaneous determination of the local non-thermal state of the atmosphere — and conversely (cf., the Volume 6 discussion of this problem re. the thermal state of hot-star winds). We need to ask just where, in the atmosphere, that independent determination of thermal and nonthermal states used in the deep photosphere loses validity. We know it is invalid in the exo-photosphere, by definition of the exo-photosphere; but we ask if, even in the upper photosphere, the there-small effects of nonradiative fluxes perturb “classical” models and diagnostics of the local thermal state, and of the “standard” inferences of the character of nonthermal phenomena.

That is, in the lower parts of these exo-photospheric regions of FGK stars where the nonRE and nonHE regions begin, we delineate their mainly quasi-thermal characteristics — e.g., nonRE gradients of T_e — largely via nonLTE diagnostics of quasi-thermal monochromatic spectral features; and recognize that in these regions a value for T_e is no longer associated with values of the integrated radiative continuum alone. Nor can its value be determined from only measures of either integrated or monochromatic radiative continua alone. So we infer that the existence of these nonclassical regions arises from the presence and effects of nonradiative fluxes, whose perturbations on atmospheric structure become, observationally, significant only at these exo-photospheric heights; hence they must be modeled as varying significantly with radius. The first really detailed delineation of such height evolution of atmospheric structure was for the main-sequence Sun via study of its eclipses by the Moon (cf., Volumes 1 and 4). This Volume 7's Chapter 3 summarizes what smaller-star-eclipses of K g/sg atmospheres let us conclude on the radial structure of their exo-photospheres.

The same conclusion on radial structure for exo-photospheres results from study of where departures occur from thermal-HE density distributions — even using those T_e taken from the observationally inferred nonRE, not from theoretical RE, distributions — resulting from mass outflow. The observed/inferred outflow velocities demand accelerated outflow: for most stars, including the FGK, from the upper limit of low subthermal placed by photospheric observations up to the high ultrathermal values observed in the farUV. But WR stars, novae, and recurrent novae during “outburst,” possibly P Cyg and symbiotic stars at some epochs — all show large ultrathermal values in the lowest photospheric regions observed. Moreover, other stars than the cataclysmic show a mass outflow which is enhanced over its “normal” values at some epochs; and recent observations show a “more normal-star-like” mass outflow from cataclysmic stars during “quiet” epochs. Specific values of the maximum observed velocity vary between: (i) different stellar types; (ii) different stars within a given type; (iii) and for some types of stars (we do not yet know how many), the same star at different epochs. (cf., Volumes 2, 4, and 6; and Chapter 4 of this Volume.)

In addition to this evidence for a general outward-accelerated outflow, some stars show evidence of an eventual deceleration of the outflow. This is particularly observed among those stars exhibiting H α -type, low-ionization, emission envelopes — such as the T Tauri among the FGK; and the planetary-nebular, Be, cataclysmic, P Cyg, etc. outside the FGK type. But observations place such deceleration outside the lower exo-photospheric, nonradiatively heated regions. There appears to be some evidence for an additional, “second, pseudo-corona” arising from the shock-wave system produced by the

deceleration. And, like the acceleration in the lower exo-photospheric regions, there is evidence that such deceleration in the upper exo-photospheric regions is also time-dependent on the large time-scales found, empirically, for such changes. Indeed, decade-long (set by the existence of the IUE observatory), coordinated, simultaneous observations in the visual and farUV spectral regions show patterned variability in some kinds of stars; especially among these are the T Tauri-like Be-stars. Adjoining the knowledge resulting from a century of visual-spectral-only, Be-variability studies, one finds time-scales ranging from hours/days to several decades. All are much shorter than classical evolutionary time-scales, the only kind of variability permitted by classical models of both atmosphere and interior (cf., Volumes 2, 4, and 6; and subsequent work by the authors of these volumes).

The intrinsic brightness of these Be-stars makes their study much easier than that of other stars, especially the study of their variability. FarUV observations of Be-stars require exposures of a few seconds; of T Tauri stars, many hours. So in terms of *IUE* time allocation to study these variability problems, Be stars are the most “time/cost” effective. It is therefore not surprising that much of our “frontier” knowledge comes from Be studies. To establish a comparable level of empirical knowledge for the FGK class, using the T Tauri stars, we must simply follow the experience gained from the Be stars of the hot-star class. (cf., Volumes 2, 4, and 6; and Chapter 4 of this volume).

Thus observations show not only an r -dependent mass outflow, hence an r -sequence for any atmospheric structural pattern depending on the mass outflow, but they delineate also a t -dependence. And while there may be “stellar individuality” fluctuations in both r - and t -dependence, this dependence is, for the most part, patterned and systematic, and presumably reflects inherent structural differences between stars — even of the same spectral and luminosity class. Current practice is to classify stars according to their visual-spectral and visual-luminosity classes; seek a modeling theory that reproduces such “classical classification;” and interpret low-resolution observations of galactic star-clusters, and of distant galaxies themselves, in terms of distributions of stars of these several classes and how equally classical, internal-structural theory “predicts” they evolve. Voila, “cosmology!” These highly abstracted results on exo-photospheric structure and its variety show clearly the inadequacy of this visual-spectral-only classification scheme — and such “cosmology” based on it. An objective of the monograph series is simply to ask how to improve such atmospheric modeling and theory — and how to use it to improve internal-structural models and theory. The approach is necessarily empirical — since none of the above exo-photospheric structure, especially its time-dependence, is even hinted at by these classical models, even by their “neoclassical” nonLTE “refinement.”

Actually, such sets of exo-photospheric regions have been long observed, in a variety of stars, for more than a century, well-before the instability of such theoretically defined quasi-thermal photospheric regions was discussed [cf., the summary in Volume 4]. There are three notable examples of different types of such exo-photospheric structure among the FGK stars covered in this Volume 7, observed, at first, wholly in the visual spectrum: (i) comparatively high-resolution eclipse studies of a regional structure of the solar outer atmosphere; (ii) low-energy, emission-line (e.g., $H\alpha$) inferences of the existence of very extended atmospheres in a wide variety of stellar-types, including the T Tauri stars of this Volume, and (iii) binary-star eclipse observations of nonthermal phenomena in the upper-photosphere/chromosphere of the largest component — notable examples being some giants/supergiants of the FGK variety. Each of these three historical kinds of observational evidence that quasi-thermal, rather than strictly thermal, modeling of stellar photospheres is the more realistic is represented by stars of the FGK class, which are discussed in this volume: the Sun; T Tauri stars; and eclipsing systems such as 31 Cyg, consisting of a K giant and main-sequence B star.

The problem has long been simply how to replace the assumptions defining classical modeling of atmospheres — thermal, linear nonTE character — with something capable of reproducing/modeling such observations. A pragmatic approach, developed in the course of detailed solar-thermodynamic

studies, has been to simply diagnose/synthesize these observations to produce self-consistent distributions of [nonlinearly-nonTE, nonthermal] thermodynamic state parameters which are consistent with the observations. One asks what is this exo-photospheric structure, and what nonradiative fluxes exist and how do they evolve, and what changes in modeling the radiative flux are required to be consistent with the modeling of nonradiative fluxes — before asking what is the origin of the fluxes, and why do they exist. [cf., Chapter 6 of this volume, and Volume 4]. In Section A, we sketched the whole-star impact of such an approach. Here, in section B, we abstract what contribution the FGK stars have made to this, relative to the contents of this Volume 7. Roughly, we orient the Perspective around the three examples stated above: the Sun, especially via eclipse studies which give the best resolution of the upper-atmospheric regions; the T Tauri stars; and binary studies as “ersatz” solar-eclipse studies. But I emphasize: such insight does not come from studying the FGK stars wholly by themselves — rather, by also comparing their characteristics to those of other stars across the HR plane. Only in this way can we distinguish between different thermodynamic characteristics and simply differences in thermodynamic state.

So I repeat: this cool range of stellar types includes one star and one stellar class of particular interest to the Monograph Series in its search for common thermodynamic characteristics among a seeming diversity of individual stars: the Sun, and the T Tauri class of stars. These FGK stars also include, along with the solar, some of the best examples in the HR diagram of the invaluable contribution by eclipsing systems to the detailed delineation of atmospheric structure — in distinguishing between photospheric and exo-photospheric regions; and in seeking the distinction between nonradiative energy- and mass-flux perturbations of that wholly-radiative-flux-determined atmospheric structure represented by classical theoretical modeling. But the perspective they give comes in large measure by stressing the relation of each to the insight into stellar peculiarity coming from stars outside the strictly cool-star region.

Then essentially, the nonthermal aspects studied in this Volume 7 are those accompanying the outward propagation of nonradiative energy- and mass-fluxes, whose existence is anomalous under classical atmospheric theory, but whose observed presence and effects represent the strongest arguments against the broad applicability/utility of that classical theory (even its semi-classical modification that adds only nonLTE effects), and whose observed/inferred empirical characteristics provide the best guidance to constructing real-star models/theories to replace that classical theory. That theory was based on stars whose existence, and first-approximation classification, were shown by only visual-spectral radiative fluxes; but whose nonradiative-flux characteristics were defined speculatively — their direct observation, especially at high-resolution (λ , t , r), not having been possible, for guidance. And the “speculation” was based on thermodynamic insight too superficial to permit real-world diagnostic inference from only indirect observations. Especially the last decade of *IUE* farUV and X-ray observations gives an introduction to the earlier missing character of the nonradiative fluxes; and some details on the time-dependence of both radiative and nonradiative fluxes. These exhibit stellar atmospheres — and possibly interiors — as changing their structure on less than evolutionary times. Only based on such observations can we seek better models and theory — for the atmosphere, and for the whole star.

These nonradiative fluxes and their effects are not strikingly observationally obvious in the photospheres of “normal-stars” — like the solar; but the radially outward evolution of their character and effects produces the observed radial sequences of exo-photospheric regions, which are as anomalous as these fluxes themselves under classical/semi-classical modeling. The sequential thermodynamic characteristics of these sequential exo-photospheric regions were first, even if only partially, delineated in the Sun (a member of the FGK classes considered in this volume 7), initially by visual-spectral eclipse observations, later, by farUV plus X-ray observations made from space. “Partially” means that only some of the exo-photospheric regions identified in observing — not just speculating about — the whole

set of FGK stars plus other spectral-type stars across the HR diagram have been seen in the Sun. Fortunately, re. the breadth of FGK studies, the most notable of these “solar-missing” regions are prominent in the T Tauri class of stars — as well as in other, “similar” by having these regions, classes of stars occurring all across the HR diagram. So combining the “Sun-as-a-star,” observable under the highest resolution of any star, with the T Tauri as a class of stars characterized by the most prominent of those exo-photospheric regions missing in the Sun — with sister classes, some better observable than the T Tauri, all across the HR diagram, and with certain other “exceptional” FGK types (abstracted below), the FGK stellar-types — at least partially via this Volume 7 — should contribute strongly and broadly toward developing our insight into broad, “nonclassical” stellar structure.

We note that this volume does not consider the clearest examples of nonthermal photospheric structure among the FGK stars: those radially pulsating, such as the Cepheid (F-K) and W Virg (F-G) sg; and the RV Tauri (G-K), also sg and mainly radially pulsating, but with also some indication of nonradial modes. We had hoped to include a volume on pulsating-star atmospheric structural patterns; limits on our sponsors’ support do not permit it. Current developments in delineating that photospheric nonthermality stored in the variety of nonradial-pulsational modes discovered in the Sun are too briefly considered in Chapters 2 and 6 — supplementing their (circa 1981) extensive discussion in Volume 1.

However; *these nonthermal fluxes and their effects have been identified even in the photospheres of some peculiar stars.* They are observed as quasi-time-independent photospheric features of the exceptionally peculiar and exceptionally luminous Wolf-Rayet stars, which exhibit the highest yet observed quasi-steady-state mass-fluxes. Such effects are also observed as “episodic,” limited-duration events in the photospheres of the brightest (at maximum luminosity) — hence observable in greatest detail — subtypes of the cataclysmic stars, notably the novae and recurrent novae. These WR plus novae are the stellar types exhibiting, at a given epoch, the largest observed mass fluxes, whose size, apparently, determines at what distance above the deepest observable parts of the star — which is the low photosphere — this mass flux; and/or its effects, will be observable. By the presence of “superionized” lines — of even solar-coronal type in some novae — “dissipative” aspects of the “nonradiative energy-flux” character of these large mass fluxes have been inferred. This provides an extreme example of the general question of how closely associated are the nonradiative energy and mass fluxes, to which we return below.

We also note that the novae were originally distinguished from “normal” stars — centuries ago when only luminosity measurements were possible — by “outbursts” in their radiative flux. When reasonable-resolution spectroscopy became possible, mass-flow outbursts were observed to accompany these. The “normal, quiet” state of novae was “conjectured” — on the basis of only visual-spectral observations — to consist of a low-level radiative flux, and zero mass-flux. The “nova problem” was to find an energy-source capable of producing a strong increase in radiative, and initiating a large mass, flux. The Wolf-Rayet problem, by contrast, was to identify an energy source able to maintain steady-state, but also abnormally large radiative and mass fluxes. Modern farUV observations show some recurrent novae to produce ultra-speed, quasi-time-dependent, mass outflow at epochs well removed from those of any outbursts. The question is the relation of this steady-state mass outflow, anomalous under current speculative-theory, to whatever mechanism produces the outbursts — in both radiative- and mass-flux, steady-state levels.

The diagnostic problem of such direct observations resembles that of the indirect observations of the central stars of planetary nebulae. The PN themselves have long been recognized as the most extreme example of the exo-photospheric structure; indeed, they have often been classified as “phenomena of the interstellar medium.” Today, one would dispute between exo-photosphere and “local-environment,” and recognize their nearest “neighbors” as the Be and T Tauri stars. But the essential point re. the nova-problem is that the PN classical model is a one-time eruption-of/mass

ejection-from a cold giant star: something like a mass-loss of $0.25 M_{\odot}$ as contrasted to the 0.1 – $0.01 M_{\odot}$ associated with the nova “event.” In recent years, most well observed PN central stars show the same quasi-time-steady, ultra-speed mass outflow as do the above mentioned novae. Over the years, other stars showing intermediate-strength radiative- and mass-flux “episodic enhancements” have been observed in increasing detail, as observational resolution and spectral coverage increased: some symbiotic stars, some Be stars, some FU Orionis stars (believed to be related to the evolutionary phases of T Tauri stars).

Depending upon how “modelers” distinguish exo-photospheric regions from simply outer-photospheric, some of them argue that the nonthermal effects of the large-size mass fluxes found in hot O stars appear already in their upper photospheres, especially those of sg OB stars — but only as nondissipative, ultraspeed, mass outflow. The associated phenomena of superionization — historically interpreted in stars ranging from WR to the Sun as implying nonradiative heating — is suggested, in variants of such hot-star theory/models, to result from the large opacities accompanying the lower density gradients of such large mass outflow. They are to reflect only small density gradients, not nonradiative heating; the ultra-speed flow is postulated, by omitting dissipative terms in the equations assumed to describe the outflow, to be a nonradiative energy flux which does not perturb the atmosphere’s thermal state insofar as $T_e(r)$ describes it.

Thus such hot-star models, theories, and nonobservationally oriented theoreticians would identify OB hot stars — and presumably their extreme WR-cousins — as exhibiting the opposite nonthermal, non-Equilibrium-thermodynamic pole from the Sun — and its FGK cousins — of the effect of nonradiative fluxes on radiative-only atmospheric models. The first, and major, such effect discovered in the solar atmosphere was a nonradiative dissipative heating — sequentially upward from photospheric T_e to $\geq 1 \times 10^6$ K in a corona. A numerically small solar mass outflow was actually discovered before the identification of the corona as “super-hot” — in the particle streams producing the aurora; but its identification as an aerodynamic outflow, associated with the hot corona in its “equivalent-nozzle” aspects, came only later. The only as-yet-universally accepted hot-star effect of nonradiative fluxes is a numerically very large aerodynamic mass outflow — with the origin of the ubiquitously observed farUV and X-ray “superionization” still under debate. The modeling alternatives — to be decided by observations — are: either *some* coronal hot-atmospheric regions; or a super-opaque, photospherically hot, upper- and exo-photosphere (cf., Volume 6).

It is currently controversial whether such theories are thermodynamically inconsistent, and observationally incomplete, because of their exclusion of the observed variability of OB — especially of Be — mass outflow, and its association with observed variability of some exo-photospheric regions (Volumes 2, 4, and 6). In spite of their attempts to make more realistic their — as contrasted to classical-theory’s — thermodynamic basis (replacing a closed-system character for stars by one of an open system), such hot-star theoreticians exclude variability from their models/equations by considering only time-independent outflow. More pragmatic astronomers are currently exploring these questions by continuing *IUE* decade-long sequences of simultaneous observations in the farUV and visual spectral regions, which seek to further delineate any associated variability of mass outflow and atmospheric regions, in programs extending the Be work summarized in Volume 2 — organized by that volume’s Be editor/author.

But we also note that the FGK studies summarized in this Volume 7 pose the same problems of “mass-outflow with/without dissipative heating;” so these cool stars may also contribute to its broad thermodynamic resolution. On the one hand, we have just stressed the observed characteristic of the Sun and “stars like it” to have very hot coronae but numerically small mass outflow — with some OB-star theories saying these stars should show the reverse: large mass outflow, and negligible or nonexistent coronae. A number of FGK-studying astronomers find evidence that some GKM

giants and supergiants exhibit massive winds but only low-temperature upper-/exo-photospheric regions. [cf., Chapter 3]. Clearly, hot-star, cool-star collaboration on clarifying this problem would be useful.

1. BRIEF SOLAR PERSPECTIVE

Among the FGK stars the Sun is exceptional, because its proximity permits its high-resolution (in λ , t , geometry) study.

Although the whole of Volume 1 was devoted to its study, the Sun remains an implicit reference-focus in the present volume for delineating similarity and difference in atmospheric structures; and their subatmospheric implications, among stars of the “cool” type. The same applies in its comparison to the “hot” and colder stars. Historically, studies of the Sun have been frontier-stimulating because its proximity inspires attempts to quantitatively model its detailed structure, instead of only “describing gross structural features,” and then to test such modeling attempts for observational and thermodynamic consistency. For example, one used solar limb-darkening observations in the continuum as both a guide to, and a test of, the historical formulation of the classical RE, HE, LTE “standard-model” of photospheric thermal structure. One also used the λ -dependence of such solar-continuum observations to identify the importance of H^- as an opacity source. One used limb-darkening observations in the strong lines to explore pure absorption versus scattering — LTE versus a variety of nonLTE for the source function in the line-transfer problem. One used the observed height variation of the line and continuous spectrum at the solar limb, together with the simultaneous development of “modern” nonLTE theory, in an empirical-theoretical “iteration” to both develop a thermodynamically sound nonLTE diagnostics and infer the actual — not hypothetical — $T_e(r)$. And, as a by-product, this last kind of study produced a value for the solar LyC flux — a quantity lying outside the spectral region on whose observations the diagnostics/model was based, thus showing its thermodynamic soundness — that was orders-of-magnitude better in agreement with observations than was its predicted value on the basis of any other theory. Thus modeling of the solar atmosphere has steadily evolved toward an observationally — rather than a speculative-conceptually — guided approach, as higher resolution (λ , t , r) and broader spectral-coverage observations become available. This evolution simply reflects our still limited knowledge-of/intuition-on the thermodynamics of stellar structure. Basing modeling and theory on speculative concepts, rather than constructing a theory based on simply representing the results of empirical modeling, is presently a very dubious way to proceed — as it has been since the modeling sequence of epicycles to Brahe-Keppler-Newton produced both an empirical and a physical theory of planetary motion.

From this empirical-theoretical production of detailed models by direct analysis of spectroscopic observations, we discovered that the effects of a dissipative nonradiative energy flux — of unspecified origin — begin quite low in the solar atmosphere, i.e., the solar exo-photosphere begins at an $r/R_0 \lesssim 1.0007$. Presumably, therefore, one must not, in wholly theoretical modeling, prohibit — by speculatively characterizing/limiting nonradiative energy sources — similar departure from RE classical standard modeling to occur equally deeply in the atmospheres of other stars (or deeper or shallower, depending on size and character of the nonradiative flux and the atmosphere’s thermal state — neither of which we know, a priori). *All of these “exploitations” of the Sun were based on only visual-spectral observations — but on observations, not speculation, and represent successive approximations to exospheric atmospheric structure, following increasingly extensive observations.*

We must also note that this solar nonRE character is, empirically, so small in its lower-exo-photospheric effect as to cause the solar $T_e(r)$ to depart from T_{eff} (“effective” solar temperature — the visual radiative-energy-flux-based parameter of classical standard modeling) by $\lesssim 1000\text{--}1500$ K

over a height-range of some 3000 km, about 20–30 “classical” scale-heights, or over $\Delta\tau$ (visual) ~ 1 , or over $\Delta\tau$ (farUV) $> 10^6$. The *solar* nonRE effect is characterized by a relatively slow initial rise in T_e — even though the nonradiative-energy dissipation there is 10^4 times larger than in the outer-exo-photospheric corona. (We must realize that the rate of the nonRE rise in T_e depends upon both the amount of the nonradiative-energy dissipation and the thermal state of the upper photospheric region where such dissipation begins.) So small departure of T_e from T_{eff} is hardly evidence for absence of nonradiative energy flux/heating (cf., Volume 6 for hot-star discussion of opposing viewpoints).

Likewise, the small size of the solar nonradiative mass-flux, relative to that in other stars, can produce ambiguity in diagnosing both the presence of a nonradiative-energy flux, and the maximum size of mass-outflow velocity — in both Sun and “comparison” star. Such spectroscopic data as above, when combined with the radial variation of the electron-scattered continuum, lead to $n_e(r)$ — thence to $\rho(r)$. From these $T_e(r)$ and $\rho(r)$, we can separate the quasi-hydrostatic regions of density decrease from those associated with the mass flux (cf., Volume 4). We see that the small solar mass flux permits a large photospheric and exo-photospheric region satisfying HE — even at nonRE T_e , hence a large region with near exponential density decrease, hence a very large density decrease from photosphere to corona. This has two effects on exo-photospheric diagnostics: (a) too low densities to produce observable spectral features in those regions where $V(\text{outflow})$ lies in that 400–800 km s⁻¹ range diagnosed from particle collectors far from the Sun (not available for other stars); (b) low enough densities in the 10^6 K regions to produce the forbidden coronal lines occurring in the visual spectrum.

Thus the solar visual spectrum gives direct evidence of 10^6 K values for T_e — hence of a nonradiative-energy flux and its dissipation — because the small solar mass flux produces a low-density solar corona. Other stars, with sufficiently larger mass flux (a factor 10^3 – 10^4) will have too large densities in solar-type 10^6 K regions — if such exist — to produce the forbidden coronal lines. So XUV or X-ray observations are necessary to diagnose the presence/character of solar- T_e coronae in such stars. A similar argument applies even to a low-density corona if its size is significantly smaller than the solar (with Sun and star “projected” to the same distance). One needs low density and large volume for coronal regions, in order to detect them in the visual spectrum via the forbidden coronal lines.

Contrariwise, one needs large particle concentration in the regions of ultra-speed mass outflow to detect it, spectroscopically. So adding the solar farUV spectrum to its visual, even adding the XUV and the X-ray, does not provide that direct evidence found in many other stars of a mass outflow that reaches ultra-speeds in the exo-photosphere. As abstracted above, $n_e(r)$ plus $T_e(r)$ observations of the Sun show that a solar mass outflow exists, but not what is its maximum velocity. For the Sun, such ultra-speeds actually do exist — varying between 400–800 km s⁻¹ — but one requires particle collectors to directly detect them; and they occur only in very-low-particle-density regions.

Given the solar empirical result that there is no evidence for outflow deceleration until it collides with the planets — even though we yet have no theory for the complete acceleration mechanism (cf., Volume 1) — we would conjecture that such ultra-speed mass outflow also exists at sufficiently large r for other, “solar-similar,” very-small-mass-flux stars, even though we cannot observe it. So, as for the nonradiative-energy fluxes discussed above, any “theory” of stellar structure which one does construct cannot restrict/prohibit “solar-similar” stars from ultimately reaching ultra-thermal mass outflow, but simply at lower particle concentrations. By contrast, such ultra-speed velocities are well observed in the farUV spectrum of stars whose large mass flux shortens the regions of quasi-HE and exponential density decrease, hence gives large enough density to produce farUV-visible ions in those regions where the mass outflow reaches ultra-speeds ($0\{200\text{--}2000\}$ km s⁻¹). And in the extreme cases earlier cited of very large mass-fluxes (WR, CV, etc.) ultra-speed outflow is even observed in the photospheric — visual-region — spectrum, which is hardly produced in an HE photosphere.

Too often, superficial diagnostics have interpreted the absence of visual-spectral, forbidden, coronal lines to imply T_e values below the solar 10^6 K value, and the absence of ultra-speed spectral lines in the farUV — i.e., originating in the mid- or outer-exo-photosphere — to imply only low-velocity mass outflow (cf., Figure 3-33 of Volume 4). The resulting diagnostic implications — re. origin, prevalence, association with photospheric and exo-photospheric regional structure — can be quite misleading. All these results from studies of the Sun, and their comparison to the inferred “configuration” of other stars, exhibit the contrast between such spectroscopically-based, (non-Equilibrium) thermodynamically-consistent, diagnostic delineation of the actual characteristics of actually existing nonradiative fluxes and empirically inferred, associated atmospheric structure — and the variety of hypothetical fluxes and structures proposed in the literature. Hopefully the stellar-solar discussions in the present Volume 7 and the solar Volume 1 can put all this into focus for the FGK stars.

So the Sun gives us insight into the structural effects of: (i) a nonradiative-energy flux that is sufficiently large and dissipative to produce: a $T_e \sim 1\text{--}3 \cdot 10^6$ K in a coronal region extending over $r/R_\odot \sim 1.01\text{--}3$, and the thermodynamically-intermediate regions (where most of the energy is dissipated) lying between photosphere and corona; (ii) a weak mass-outflow, which suffices to significantly perturb a quasi-hydrostatic density distribution only for $r/R_\odot \geq 2$; (iii) an exo-photosphere “crowned” by a hot gas, which cools very slowly to $\sim 25,000$ K at $r/R_\odot \sim 200$, and apparently accelerates/expands freely until it decelerates by colliding with the “particles” of the planetary system. But just as solar observations do not give us direct spectroscopic observations of those ultra-thermal mass-outflow regions seen in a variety of other stars — those with much larger mass-fluxes — so there are a variety of other kinds of atmospheric regions not obviously directly observed in the Sun. And, as for the ultra-thermal velocity regions, we must ask whether not seeing such regions is because they do not exist, or because they occur at densities too low for spectroscopic detection. Fortunately for the breadth of FGK studies, the most notable of these “solar-missing” regions are prominent in the T Tauri class of stars — as well as in other, “similar” by having such regions, classes of stars. So combining the “Sun-as-a-star,” observable under the highest resolution of any star, with the T Tauri, as a class of stars characterized by the most prominent of those exo-photospheric regions missing in the Sun, and having sister classes — some better observable than the T Tauri because they are brighter — all across the HR diagram, and with other “exceptional” FGK types (abstracted below), we see enough variety of atmospheric structure to appreciate that study of the FGK stars should contribute strongly and broadly toward developing our insight into the range of “nonclassical” stellar structure. But I emphasize: such insight does not come from studying the FGK stars wholly by themselves — rather, by also comparing their characteristics to those of other stars across the HR plane.

By contrast to the preceding regions, characterized by their “at least eventual” ultra-thermal velocities, these most-prominent, apparently solar-absent regions are characterized by relatively small velocities, $25\text{--}100 \text{ km s}^{-1}$. While this fact has been long known, today’s interpretation that such velocities result from strong deceleration of a “closer-to-the-star,” high-velocity [ultra-thermal] mass outflow is relatively new. But again, the outstanding observational characterization of these regions is historically-well-known: it is that strong $H\alpha$ emission, whose presence, together with that of some other strong lines from low-ionization atomic species, characterize that “super-class” of stellar types to which the T Tauri stars belong. A major diagnostic approach to studying the “classical-theory-anomalous” exo-photosphere and the equally anomalous nonradiative fluxes producing them is the observational comparison of solar (and its FGK siblings) exo-photospheres to those of the T Tauri (and their exo-FGK cousins). Then we try to identify the differential characteristics of the nonradiative fluxes which produce these exo-photospheric differences — and model them. Based on a detailed study of one class of the T Tauri cousins — the hot and bright Be stars — the basic difference seems to be variability, indeed, patterned variability, and not just size, of the mass-flux.

2. BRIEF T TAURI PERSPECTIVE

The T Tauri class is frontier-stimulating because of its membership in a “super-class” of stars extending all across the HR diagram, characterized by the variable-presence/strength/profiles of such emission lines as hydrogen Balmer $H\alpha$ coming from low-ionization-level particles.

This super-class has member-types all across the HR diagram: Be, Herbig, Be, and Ae, a variety of cataclysmic-variable (CV) types, planetary-nebulae (PN), etc. Their most obvious common feature is the solar-missing region producing these low-ionization emission lines, which is (thermodynamically) most consistently identified as an exo-coronal, relatively low- T_e region — described alternatively as an $H\alpha$ envelope, or/and as a part of the “local-environment” of such stars. Among the T Tauri and Herbig stars, an important question is whether this cool region was primeval with the star or produced later by its mass flux. For the other stellar types, observations strongly support an origin of their usually time-variable envelope/local environment in a strongly variable mass outflow from the star — under widely differing time-scales. Such variability is the second common feature of this “super-class” of stellar type. Its detailed study requires long sequences of coordinated, pan-spectral observations — both for itself, and to inquire into any association with variability of the other stellar fluxes: radiative and nonradiative. While such association with luminosity outbursts is long known for the novae/recurrent-novae, only recently — from such panspectral time-sequential studies — is it becoming well established for other types within the super-class.

The T Tauri stars, and those like them, give us insight into a solar-structured, “hot,” lower exophotosphere — apparently with a greater rate of dissipative heating than the solar rate, but which is “crowned” by an extended cool post-corona, and cool local-environmental regions, rather than by the “hot,” very extended, solar-type crown. These stars also spark inquiry into the possibility of the cool, “solar-absent” region being associated, in its evolution, with the eventual production of a planetary system. Indeed, among the most important aspects of exo-photospheric regions for understanding atmospheric structure, and the role and character of those nonradiative fluxes which produce/maintain them, are just the existence and characteristics of these “solar-absent” regions characterizing the T Tauri and other stellar-types “like” them. Two of the most interesting of the problems concerning the origin, structure, and time-dependent behavior of these regions are: (a) the time-dependent behavior of their thermodynamic state; (b) their time-dependent geometrical structure.

a. THERMODYNAMIC STATE

In these regions arises that strong emission in hydrogen Balmer $H\alpha$ — together with that emission in certain lines from other low-ionization atomic species — which characterize that “super-class” of stellar types to which the T Tauri stars belong. As stated above, its presence is associated with variable mass outflow, whose study is the future focal point.

The T Tauri are but one type of star across the HR diagram which are characterized by such strong variable emission lines produced by lowly ionized ions. Among the “symbiotic” array of atmospheric regions of such stars we begin to recognize that region producing emission in $H\alpha$, etc., as more characteristic of a cool “local environment” of the star than an atmosphere-proper, although the distinction is a fine one. Combined farUV and visual-spectral observations begin to show us just how the several nonradiative fluxes from a star, especially when they are strongly variable, can produce such a “local-environment.” Such a scenario has been observationally delineated, and discussed in detail, for Be stars, in the cited volumes and subsequent work by their authors. It links to McLaughlin’s (1931) historic work on such low-ionization emission-line stars; caricatured/abstracted in his remark: “Be stars appear to be little planetary-nebulae,” when it is adjoined to very current,

high-resolution, farUV observations by the *IUE*. In place of the classical picture of the PN as the result of a one-episode low-velocity mass ejection during late stages of stellar evolution, these observations show a continuous mass outflow at $1\text{--}2000\text{ km s}^{-1}$. Observations interpreted as “proto-PN” have sometimes been reported; but the situation is currently ambiguous. The M-star volume discusses the “theoretical-parent” stars for the PN. But our projected volume in the series to cover the PN fell by the wayside from lack of the support to produce it.

Here, and as discussed in Volume 4, we can only emphasize that these high-resolution PN observations show a mass outflow from their central star which resembles an ever present high-velocity outflow from hot OB stars of all varieties. In view of the large proportion of such central stars which are early O and WR — although apparently of solar mass-size, and even though a few “cool” stars have been observed among them — this new result cannot be considered as anything but supportive of a coherent stellar thermodynamics based on mass outflow, especially variable such, as a “normal” stellar characteristic. The development of such a coherent thermodynamics is only beginning — guided by such observational results.

Then we note that a strong variability in such high-velocity mass outflow has been shown, in detail, to be associated with major structural variability of the Be star atmosphere (cf., Volumes 2 and 4, and subsequent work by these volumes’ authors). Indeed, so essential in studying these phenomena are high-resolution, farUV, spatial observations, coupled with simultaneous high-resolution observations in the visual, that one of the B-Be volume authors, Doazan, in collaboration with the ESA-Villafranca (via Barylak) and Trieste Observatory (Sedmak) data-analyzing facilities has undertaken — under ESA support — to produce an atlas of such Be spectra. In this atlas, all these observational results obtained since our NASA-CNRS-supported Volume 2 appeared are illustrated: for themselves, and as “similarity-indicators” of “episodic mass-outflow enhancement” in a variety of stars. For example, decade-long time-sequences of observations made simultaneously in the far-UV and visual, coupled with the century-long sequences of pre-space, visual-spectral-only observations, imply *bolometric* luminosity changes associated with these long-term, mass-outflow changes. The resemblance to the phenomena defining CV stars is remarkable, is elaborated in Section A of this Perspective Chapter, and raises questions on the possible relation to the T Tauri stars discussed in Chapter 4 of this volume, as mentioned above.

b. TIME-DEPENDENT GEOMETRICAL STRUCTURE

A major preoccupation among astronomers these days is the possible existence of exo-photospheric, probably exo-coronal, equatorial disks; their possible relation to the evolutionary development of planetary systems; and their possible significance in a variety of other problems. For such stars as the T Tauri — and their hot-star cousins, the Be — theoreticians focus on disks “cool” relative to adjoining atmospheric regions. These disks are conjectured to produce the Balmer emission lines, especially $H\alpha$. Such low-ionization emission lines are observed in a wide variety of stars across the HR diagram, and in some, have been known for a century. In the Be stars, the envelope producing them has always been recognized as “cold,” relative to B-star photospheric temperatures. In contrast, early observers suggested the $H\alpha$ regions of T Tauri stars were “hot chromosphere-like.” But other attributes of such T Tauri “chromospheres” suggested that they were higher density, i.e., lower lying, than their solar counterparts. Yet to produce the observed strength of $H\alpha$ in T Tauri stars, one requires the envelope to extend to several radii, as in the Be stars.

For some atmospheric modelers, modern farUV observations appear to resolve the dilemma, for both cool-star T Tauri, and hot-star Be, stars. One “diagnoses” the presence of both a low-lying, very hot relative to photospheric T_e of either type star, chromosphere-corona, and a very extended, exo-coronal envelope, which is cool relative to chromosphere-corona of both type stars, cool relative

to at least early-type Be-star photospheres, but hot relative to T Tauri photospheres. Current controversy centers on the degree of “diskness”: very thin geometrically, possibly optically thick at some λ — versus a more spheroidal configuration.

3. BRIEF, Be, WR, AND BINARY-STAR PERSPECTIVE

In the preceding, I stressed the *similarity* between the Sun and “H α emission-line” stars like the T Tauri and Be — in their each having chromospheres-coronae and ultra-speed mass outflow, although these regions occur in different [relative] locations; and the *nonsimilarity* in the T Tauri and Be having overlying, post-coronal cool [relative to corona] regions of much lesser [than underlying regions] velocity outflow. I also abstracted the evolution of the geometry of all this. Because of eclipse observations of the Sun, there is no question as to the radial sequence of regions; for stars in general there is usually ambiguity — largely because of conflict between a priori speculation of where [unpredicted by classical theory] such regions should be, not where the composite of visual plus nonvisual spectral data placed them for thermodynamic plus observational coherence. Thus, while the Sun and Be stars alike were discovered, in the 1860s to have greatly extended atmospheres; and both were originally modeled as cold extended atmospheres; only solar observations were sufficiently unambiguous to locate the chromosphere-corona as immediately post-photosphere. By contrast, because pre-space, pre-farUV Be-modeling placed the cool H α envelope immediately post-photosphere, most Be modelers kept it there when farUV data demanded adjoining coronal hot regions. Today, we recognize that the change in solar modeling, in going to T Tauri and Be stars, lies in adjoining an outer, postcoronal, cool H α envelope, with the deceleration of the ultra-thermal mass outflow occurring just below, or in the lower regions of, the H α envelope. Indeed, it is that decelerated flow which produces the envelope.

Presumably, this picture characterizes all the stellar types in that super-class to which Be and T Tauri stars belong — noting that the PN, symbiotic, P Cyg, and other CV stars all show the characteristics of this super-class. And the recent, IUE-sparked developments — taking account of the historical Be visual-spectral, long-time sequences of observations — suggest that many of the super-class types share the CV characteristics of patterned enhancement of luminosity and mass out-flow alike. The detailed structure of the decelerating, cooling, regions is not yet clear. There appears to be some evidence for an additional, “second, pseudo-corona” arising from the shock-wave system produced by the deceleration. And, like the acceleration in the lower exo-photospheric regions, there is evidence that such deceleration in the upper exo-photospheric regions is also t-dependent on the large time-scales found, empirically, for such changes. Indeed, decade-long (set by the existence of the IUE observatory), coordinated, simultaneous observations in the visual and farUV spectral regions show patterned variability in some kinds of stars, especially among these are the T Tauri-like Be-stars. Adjoining the knowledge resulting from a century of visual-spectral-only Be-variability studies, one finds time-scales ranging from hours/days to several decades. All are much shorter than classical evolutionary time-scales, the only kind of variability permitted by classical models of both atmosphere and interior (cf., Volumes 2, 4, and 6; and subsequent work by the authors of these volumes).

In section A, I stressed how essential it is to link the outer atmospheric studies to the boundary conditions in the low-photosphere. I stressed that the only star for which one had detailed observational knowledge is the Sun, and possibly some binaries, which one used to ‘mimic’ the solar eclipse studies. We see a combination of these aspects in considering the WR stars, and efforts to link their luminosity characteristics to their mass-outflow characteristics.

Study of stars with distinctly nonthermal photospheres provide a different aspect of insight into this problem of the lower boundary than do stars with only quasi-thermal photospheres. It may be that some aspects of the distinction between these two degrees of nonthermality simply reflect dif-

ferences in size of nonradiative fluxes. For example, we recognize that a change from HE to nonHE configuration arises when mass-outflow velocity reaches about $\frac{1}{3}$ the one-dimensional thermal velocity; so we expect a photosphere to become nonthermal for a mass outflow $\sim 10^{-4} M_{\odot} \text{ yr}^{-1}$ — which is the mass-outflow value observed for Wolf-Rayet stars, which are those stars exhibiting the largest quasi-steady mass outflow (cf., Volumes 4 and 6). Only some few other types of stars, and those generally have episodically enhanced mass outflow — such as some of the CV, possibly P Cyg, possibly FU Ori, possibly the central stars of planetary nebulae (of which some are WR-like) — appear to exhibit such nonHE photospheres; and then usually only transiently. Their study can certainly provide some empirical insight into the characteristics of both quasi-steady, and episodically enhanced, mass outflow — thence, eventually, into any relation that may exist between its origin and stellar structure.

Because of the extreme sensitivity of visual-spectral-inferred T_e to the bolometric correction for hot stars, an added complication in these discussions of WR stars lies in determining the “correct” radius to adopt in inferring radiative flux from luminosity. Does the farUV observed luminosity refer to the same “effective” radius — at all λ — as does the visual luminosity, especially if, as for these stars, the large mass outflow produces a density gradient enormously smaller than the exponential one of thermal-hydrostatic conditions? The same Volume 6 discussion of WR stars as above, and subsequent work by these same authors, demonstrate the effect of uncertainty in radius upon the “self-consistently-best” photospheric T_e . Its inferred values range from 20–100,000 K, depending upon the radius. For the WR, as for other stars, the radius is inferred from those eclipsing binary systems which have a WR star as one member. The system V444 Cyg has long been used for that purpose. One should read the analysis by Kopal and Shapley [1945] for an exhibition of the dependence of the solution for the radius upon what is “adopted” for the inclination of the orbit-plane; then note what such change in radius implies on T_{eff} [if this parameter has any meaning for such stars].

Finally, we note that observations of an eclipsing binary system in which the complete spectrum of each component can be observed — a “double-lined” eclipsing binary — and in which one component has an extended atmosphere much larger than the stellar disk of the other have long provided detailed information on any inhomogeneous structure of, and gradients of thermodynamic parameters within, that extended atmosphere. Eclipses by the opaque disk of the Moon (or its ersatz, a coronagraph) gave the first quantitative details of: an exo-photospheric structure for the Sun and stars like it; modern nonLTE (which couples radiative transfer to microscopic energy-level populations) effects on radiative diagnostics of the atmosphere, to obtain the distribution of its thermodynamic parameters; the radial distribution of a nonradiatively influenced T_e in the solar photosphere-chromosphere transition-region (Volumes 1 and 4). Two kinds of stellar eclipsing systems — (a) “all components hot” (O, WR, in Volumes 4 and 6); (b) “symbiotic” (the extended atmospheres of FGK cool giants or supergiants eclipsing the “search-light” of radiative and mass fluxes from hot OB dwarfs; Chapter 3 of this Volume 7) — have provided invaluable quantitative information on the distinction between stellar chromospheres, coronae, and simply an apparently “cool” mass outflow.

At the other extreme — turning from quantitative measures to qualitative speculation — the following Volume in this series — that on the cataclysmic variables — exhibits how a “concept” (mass interchange in a close binary) is used to replace missing observations (lack of a second spectrum in the “binary”), in order to “derive” the properties of a hypothetical “equatorial accretion disk.” The role and function of the disk is to replace the “classically modeled” stellar atmosphere in producing the radiation field at both “normal” and “eruptive” phases, and also to replace the star’s subatmosphere in producing the mass outflow at both normal and eruptive phases (cf., Volume 8). The concept of an accretion disk has more recently been applied to modeling the T Tauri stars discussed in Chapter 4 of the present volume. Unfortunately for “concept-hopping” the accretion disk does not reproduce the basic feature of T Tauri stars — the strong, and variable, $H\alpha$ emission.

REFERENCES

- Allen, C.W. 1955, *University of London*, the Athlone Press.
- Conti, P.S., Underhill, A.B. 1988, *O Stars and Wolf-Rayet Stars*, NASA/CNRS Series Vol. 6, NASA SP-497.
- Cook, A.F. 1954, *Astrophys. J.*, **120**, 572.
- Cook, M.A., Eyring, H., Thomas, R.N. 1951, *Astrophys. J.*, **113**, 475.
- Cram, L., Kuhl, L. 1989, *FGK Stars and T Tauri Stars*, NASA/CNRS Series Vol. 7, NASA SP.
- Doazan, V., 1987, Proceedings of IAU Coll. 92, *Physics of Be Stars*, A. Slettebak, T.P. Snow, eds., Cambridge Univ. Press, p. 384.
- Doazan, V., Thomas, R.N. 1988, *A Decade of Astronomy With the IUE*, Symposium Proceedings ESA SP-281, **2**, 121.
- Doazan, V., Thomas, R.N., Bourdonnau, B. 1988, *Astron. Astrophys.*, Vol. 205, p. L11.
- Dyson, F. 1988, *Commencement Address*, Wooster College (informally circulated).
- Eddington, A.S. 1930, *Internal Constitution of the Stars*, Cambridge Univ. Press.
- Emden, R. 1907, *Gaskugeln*, Teubner, Berlin 1907.
- Glasstone, S., Laidler, K.J., Eyring, H. 1941, *The Theory of Rate Processes*, McGraw-Hill Publishers.
- Hack, M. 1989, *Cataclysmic Variables and Related Objects*, NASA/CNRS Series Vol. 8, NASA SP.
- Jeans, J.H. 1917, *Mon. Not. Roy. Astron. Soc.*, Vol. 78, p. 36.
- Jeans, J.H. 1918, *Mon. Not. Roy. Astron. Soc.*, Vol. 79, p. 319.
- Johnson, H.R., Querci, F.R. 1986, *The M-Type Stars*, NASA/CNRS Series Vol. 5, NASA SP-492.
- Jordan, S.D. 1981, *The Sun as a Star*, NASA/CNRS Series Vol. 1, NASA SP-450.
- Kopal, Z., Shapley, M.B. 1946, *Astrophys. J.*, **104**, 160.
- Malina, R., Bowyer, S., Basri, G., *Astrophys. J.*, **262**, 717.
- McLaughlin, D.B. 1931, *Pub. Obs. Univ. Michigan*, **4**, 198.
- Opik, E. 1933, *Tartu Univ. Pub.*, **26**.
- Prandtl, L. 1904, *Phys. Zs.*, **5**, 599.
- Schwarzschild, M. 1958, *Structure and Evolution of the Stars*, Princeton Univ. Press.
- Sears, R.L., and Brownlee, R.R. 1965, *Aller Volume in Kuiper series, Stellar Structure*, L.H. Aller, and D.B. McLaughlin, (eds.) University of Chicago Press, Chicago, p. 575.
- Smith, N.J. 1954, *Astrophys. J.*, **119**, 438.
- Struve, O. 1942, *Astrophys. J.*, **95**, 134.
- Thomas, R.N. 1950, *Astrophys. J.*, **112**, 343.
- Thomas, R.N. 1952, *Astrophys. J.*, **116**, 203.
- Thomas, R.N. 1983, *Stellar Atmospheric Structural Patterns*, NASA/CNRS Series Vol. 4, NASA SP-471.

Thomas, R.N., Whipple, F.L. 1951, *Astrophys. J.*, **114**, 448.

Thomas, R.N., White, W.C. 1953, *Astrophys. J.*, **118**, 555.

Underhill, A., Doazan, V. 1982, *B Stars with and without Emission Lines*, NASA/CNRS Series Vol. 2, NASA SP-456.

Whipple, F.L. 1955, *Astrophys. J.*, **121**, 241.

White, W.C. 1955, *Astrophys. J.*, **121**, 271.

White, W.C. 1955, *Astrophys. J.*, **122**, 559.

Wolff, S.C. 1983, *The A-Type Stars; Problems and Perspectives*, NASA/CNRS Series Vol. 3., NASA SP-463.

Richard N. Thomas
Boulder, Paris 1989

RÉSUMÉ

Pendant toute la durée du vingtième siècle, l'astrophysique stellaire est restée un domaine extrêmement vigoureux de la recherche scientifique. Des progrès considérables ont été accomplis dans le domaine instrumental, et la qualité des données, tout comme leur quantité, a continué à se développer en une marche accélérée. Le résultat de ce développement, à première vue en tout cas, est une étonnante complexité de l'information disponible, ce qui lance un énorme défi à ceux qui tentent de comprendre les étoiles.

Une conséquence naturelle de cette complexité et une certaine tendance de l'astrophysique stellaire à se compartimenter en sous-disciplines et en spécialisations. En vérité, il ne serait pas possible de progresser dans ce domaine sans cette division fine, voire raffinée, du travail à laquelle nous assistons actuellement. Cependant, la compartimentation porte en elle sa punition, puisqu'elle a pour effet de camoufler les thèmes communs susceptibles de donner quelque unité à ces questions. Or, ces concepts unificateurs sont cruciaux dans la perspective du progrès scientifique, car ils permettent une organisation rationnelle de grandes quantités d'informations, et fournissent de ce fait les bases sur lesquelles pourront se développer les nouvelles voies de recherche.

L'un des buts de cette série de monographies est de fournir la possibilité d'explorer certains aspects des concepts unificateurs de l'astrophysique stellaire. Plus spécifiquement, l'attention du lecteur est attirée sur les phénomènes qui ont lieu dans les *atmosphères stellaires*, bien qu'il soit largement reconnu que les éléments courants du comportement des intérieurs stellaires doivent sous-tendre un grand nombre des structures dominantes dans les atmosphères.

Dans ce volume, l'attention est focalisée sur les étoiles de type spectral F, G, et K. Parmi les étoiles naines de ces catégories, l'on rencontre des étoiles très semblables au Soleil et elles nous offrent donc un moyen extrêmement utile d'appliquer nos connaissances relativement détaillées de la physique solaire à notre connaissance moins détaillée, mais beaucoup plus étendue, des étoiles, voire du reste de l'Univers. Mais l'on rencontre aussi parmi les étoiles F, G, et K des phénomènes qui semblent n'avoir que de très lointaines analogies sur le Soleil: l'existence de compagnons, la jeunesse de l'étoile, ou au contraire une évolution stellaire avancée, conduisent à mettre en évidence des caractéristiques fascinantes des atmosphères stellaires concernées; et l'élucidation des processus physiques de base responsables du comportement observé est une tâche difficile, qui est encore loin d'être accomplie.

D'une façon cohérente avec les objectifs de cette série des monographies, nous nous sommes concentrés dans ce volume sur des thèmes qui semblent nous offrir un chemin vers l'organisation rationnelle des données de l'observation. Actuellement, deux thèmes ont été particulièrement fructueux dans l'étude des étoiles F, G, et K, au cours des quelques décennies écoulées. Il s'agit des thèmes suivants:

- (1) L'existence de schémas structuraux communs à l'atmosphère d'étoiles qui apparaissent à première vue comme tout à fait différentes les unes des autres. Par exemple, une organisation radiale en photosphère, chromosphère, couronne et vent est très courante parmi les étoiles F, G, et K, et cela offre un paradigme d'une grande utilité en vue des recherches concernant tous les objets de cette catégorie.

- (2) L'importance cruciale de l'activité électrodynamique (magnétique) dans les atmosphères stellaires. Alors que les processus électrodynamiques ne sont sans doute pas importants au point de vue de *tous* les aspects des phénomènes observés dans les atmosphères des étoiles F, G, et K, l'insistance actuelle sur cette question a été très utile en ce qu'elle a permis de donner une certaine unité aux études de l'évolution et de la variabilité des atmosphères stellaires, tout comme les schémas structuraux décrits ci-dessus en (1). (Dans ce contexte, il est amusant de rappeler l'analogie, -attribuée à van de Hulst-, entre le "sexe" et les "champs magnétiques": dans le passé, on connaissait l'existence de l'un comme des autres, mais on évitait soigneusement d'en discuter; plus récemment, les deux sujets ont été promus avec vigueur, et proposés comme la clé de la solution de tous les problèmes; peut-être l'avenir verra l'un comme l'autre devenir un élément important, parmi d'autres, d'un ensemble plus vaste et même plus intéressant.)

Le lecteur trouvera que ces deux thèmes apparaissent au travers de nombre des observations présentées dans ce volume, et de nombre de leurs interprétations.

L'ouvrage est divisé en deux parties principales; les chapitres 2 à 4 concernent les données de l'observation, et les chapitres 5 à 7 l'interprétation et la théorie. Un résumé en est donné ci-après, chapitre par chapitre.

Le chapitre 2, par D.F. Gray, "*Phénomènes non-thermiques dans les photosphères des étoiles froides*" traite des observations de phénomènes hydrodynamiques et magnétiques dans les photosphères des étoiles F, G, et K de différentes classes de luminosité. L'information sur ces phénomènes est tirée principalement de l'analyse des raies spectrales, et le chapitre donne un résumé utile des techniques modernes (particulièrement l'application de l'analyse de Fourier) utilisées à l'extraction de l'information concernant les flux de masse et les champs magnétiques à partir des profils mesurés des raies spectrales.

Les résultats de ces recherches ont souvent été exprimés dans le passé dans le cadre des concepts vagues, mais profondément enracinés, de "micro-" et de "macro-turbulence". Ces phénomènes sont définis de façon opérationnelle à partir des spectres stellaires, et leur relation aux mouvements réels de la masse fluide est loin d'être claire. Quoiqu'il en soit, des tendances systématiques sont reconnues dans le comportement de la "macro-" et de la "micro-turbulence" en fonction de la température effective et de la gravité superficielle, et ces tendances *pourraient*, dans une étape ultérieure, fournir quelque idée de la variation des phénomènes de pénétration convective, des oscillations non-radiales, et de phénomènes similaires, d'une étoile à l'autre.

En sus de l'interprétation assez vague des spectres stellaires qu'offre le concept de "turbulence", il y a de nombreuses interprétations bien plus concrètes en termes de processus hydrodynamiques spécifiques. Gray donne un compte-rendu détaillé des résultats concernant la granulation (pénétration convective), la rotation, et les oscillations, fournissant ainsi une base solide au lecteur soucieux d'en tirer des comparaisons avec les études relatives au Soleil, et décrites dans notre volume (dans cette série) "The Sun as a star". De plus, les questions relatives aux taches stellaires et aux champs magnétiques sont également discutées, ce qui fournit une justification empirique au chapitre 7 ci-après. Le chapitre 2 se conclut par une série d'Appendices qui résument les caractéristiques essentielles des aspects dits "thermiques" (classiques) des étoiles F, G, et K.

On doit remarquer que le chapitre de Gray a été achevé presque quatre années avant la publication de l'ouvrage. Des progrès substantiels ont depuis lors marqué ce domaine de recherche, et la monographie récente de Gray donne une excellente vue d'ensemble de ces questions.

Le chapitre 3, dû à D. Reimers, "*Observations des chromosphères, des couronnes, et des vents des étoiles de type F, G, et K*" décrit les couches extérieures de l'atmosphère des étoiles décrites dans

le chapitre 2. Ce chapitre commence par un tour d'horizon très large du domaine étendu de caractéristiques spectrales utilisées pour étudier les chromosphères, les couronnes et les vents. Des descriptions plus fouillées de certains résultats spécifiques sont ensuite données, en y comprenant les couronnes d'étoiles simples (non binaires) et la question très vaste de la perte de masse et des vents dans les étoiles F, G, et K. Une attention considérable est apportée aux systèmes binaires à éclipses du type ζ Aur, où les circonstances autorisent une exploration détaillée de l'organisation de la matière dans l'atmosphère étendue de la composante géante froide.

Un aspect fascinant des chromosphères et des vents des étoiles froides est l'existence de relations de types divers entre les largeurs de raies et la luminosité. Certaines de ces relations reflètent plutôt des relations entre la vitesse réelle et la luminosité, mais la plupart sont probablement dues à des phénomènes complexes, capables néanmoins de donner des indications en vue d'une classification systématique des structures atmosphériques stellaires des différentes catégories d'étoiles F, G, et K. Le chapitre discute de diverses hypothèses relatives à ces relations empiriques, mais souligne aussi la nature fragmentaire de notre connaissance. Enfin, le chapitre 3 discute des phénomènes magnétiques dans les chromosphères et les couronnes des étoiles froides, fournissant ainsi de nouvelles bases empiriques au chapitre 7.

Le chapitre 4, par L. Kuhi et L. Cram, "*Etoiles T Tauri*", est, sous bien des aspects, parallèle aux chapitres 2 et 3; mais il démontre que les phénomènes non-thermiques ont lieu avec une fréquence plus grande dans les étoiles T Tauri. Les photosphères, chromosphères, couronnes, et vents sont présents dans les étoiles T Tauri, mais leurs caractéristiques permettent une séparation quantitative d'avec les étoiles F, G, K plus "normales", -et même peut-être une séparation qualitative (c'est-à-dire la mise en évidence d'un autre type de physique).

Le comportement assez bizarre des étoiles T Tauri est évidemment associé d'une certaine façon à leur caractère de jeunesse, attesté par diverses lignes de raisonnement, et d'arguments, décrits dans ce chapitre 4. Mais l'on ne trouve que fort peu de soutien empirique à la plupart des spéculations nombreuses qui se sont développées pour expliquer les mécanismes particuliers par lesquels la "jeunesse" conduit à un comportement si évidemment "non-thermique". Bien que nous disposions de données spectroscopiques et photométriques fort détaillées, avec une résolution temporelle utile, dans de nombreux cas, nous sommes loin d'une interprétation largement acceptée en termes d'une structure spécifique de l'atmosphère. Parmi les questions en suspens: Quelle est l'importance relative des chromosphères compactes et des atmosphères étendues dans la production des raies d'émission? Quelle est l'origine physique des excès d'UV et d'infrarouge? Et celle du "voilage" (anglais: veiling) du spectre optique? Quels sont les mécanismes de contrôle de la variabilité? Et, question peut-être encore plus fondamentale, quelle est l'interaction entre les processus d'accrétion et de perte de masse, et de quelle façon ceci est-il lié à la géométrie de l'atmosphère? Quelques-unes de ces questions sont examinées dans le chapitre 4; mais peu de conclusions définitives peuvent être tirées de cet examen.

Le chapitre 5, par L. Cram, "*Théorie classique des atmosphères stellaires*" est le premier chapitre de l'ouvrage consacré aux interprétations des données de l'observation. Le but primordial en est de suivre à la trace la genèse des structures de pensée qui ont abouti aux modèles stellaires "classiques", ou "thermiques". De tels modèles ont été étudiés de façon approfondie par les méthodes de la théorie, bien qu'il ait toujours été clairement reconnu qu'ils sont incapables de rendre compte de nombre des propriétés observées des étoiles. Il y a une sorte de mystère à constater que tant d'effort ait été dépensé pour améliorer les modèles classiques, face à tant de données posant question sur les effets non-thermiques.

Après avoir introduit une séquence de modèles classiques basés sur un traitement toujours plus fin des conditions de l'équilibre radiatif et de l'équilibre hydrostatique, le chapitre 5 présente une brève critique du modèle classique en le comparant avec les données de l'observation. On ne sera pas surpris de noter le caractère incomplet du modèle, que révèle cette comparaison. On rend compte

ensuite de quelques-uns des efforts les plus significatifs entrepris afin de modifier les modèles classiques par l'introduction de constructions semi-empiriques supplémentaires, bien mal comprises. L'auteur défend la thèse selon laquelle ces travaux n'ont pas en général porté de fruits, parce qu'on s'en est servi comme d'accessoires des modèles classiques, plutôt que comme de guides en vue de la construction de nouvelles générations de modèles non-thermiques.

Le chapitre 6, par L. Cram, "*Processus dynamiques et origine des structures atmosphériques*", part de la critique établie au chapitre 5 et aborde une modeste tentative pour donner quelque vue cohérente des phénomènes dynamiques dans les atmosphères stellaires. Après un examen systématique de quelques concepts de base de la dynamique des gaz, le chapitre passe en revue certains des processus dynamiques "*sous-atmosphériques*" dont on peut penser qu'ils jouent un rôle important dans les étoiles F, G, et K. Cet examen conduit à son tour à une discussion des phénomènes dans les atmosphères, et la possibilité est donc offerte de présenter une description cohérente des observations, en termes des processus physiques qui les sous-tendent.

Cependant, il n'existe à l'heure actuelle aucun modèle que l'on puisse considérer comme un lien satisfaisant entre la théorie et l'observation. Cette situation provient sans doute de ce que le domaine des comportements *théoriquement* possibles est illimité, alors que les observations sont rarement interprétées avec la rigueur d'ensemble dont on a besoin pour réduire le nombre de ces possibilités à un ensemble plus petit de processus plausibles. Dans ce but, le chapitre consacre une place considérable à une application de l'approche empirique-théorique, dont Thomas s'est fait l'avocat dans l'ouvrage "*Structures atmosphériques dans les étoiles*", publié dans la présente série de monographies. Bien qu'elle n'ait pas été entièrement couronnée de succès, l'exploration par Cram du travail de Thomas le conduit à mettre en lumière avec précision un certain nombre de questions importantes sur lesquelles la recherche à venir peut s'avérer très profitable.

Le chapitre 7, par C. Zwaan et L. Cram, "*Théorie des champs magnétiques dans les étoiles froides*", fournit une vue d'ensemble d'un aspect particulièrement important des étoiles F, G, et K. Nombre des données disponibles sur les phénomènes chromosphériques et coronaux dans ces étoiles (à l'exclusion des étoiles T Tauri), peuvent être codifiés et expliqués, -au moins dans une phase préliminaire, et qualitative, -comme résultant de processus électrodynamiques (champs magnétiques et phénomènes associés). De tels processus semblent se former au-dessous de l'atmosphère stellaire, mais ils exercent une influence très forte sur l'organisation spatio-temporelle de l'atmosphère. Une conséquence cruciale de l'activité électrodynamique est la présence de champs magnétiques hautement structurés, peut-être arrangés en "tubes de flux" ou en structures similaires. Nombre de données sur les chromosphères et les couronnes semblent exiger une interprétation en termes de couverture partielle de la "surface" stellaire par des tubes de flux, plutôt qu'en termes de différences dans les structures radiales au sein de régions homogènes dans les directions latérales (horizontales).

SUMMARY

Throughout the Twentieth Century, stellar astrophysics has remained an extremely vigorous area of scientific enquiry. Enormous advances have been made in the power of instrumentation, and the quality (and quantity) of data has continued to expand at an accelerated pace. The result — at least at first sight — is a bewildering complexity of information which poses an enormous challenge to those who seek to understand the stars.

A natural consequence of this complexity is the tendency to compartmentalize stellar astrophysics into subdisciplines and specializations. Indeed, it would not be possible to progress in the field without the refined division of labor which we see today. However, compartmentalization brings with it a penalty, since it tends to hide common themes which can provide unity to the subject. These unifying concepts are crucial to scientific progress, for they allow the orderly arrangement of large amounts of information, thereby providing a foundation from which new lines of investigation can be pursued.

One aim of this series of monographs is to provide an opportunity to explore aspects of the unifying concepts of stellar astrophysics. More specifically, attention is directed at the phenomena which occur in *stellar atmospheres*, although it is freely acknowledged that common elements in the behavior of stellar interiors must underlie many of the structural arrangements prevalent in atmospheres.

In this volume, attention is focused on stars having spectral type F, G, and K. Among the dwarf stars in these classes we find stars closely similar to the Sun, and these thus provide an extremely useful vehicle for transferring our relatively detailed knowledge of solar physics to our less detailed but far broader knowledge of stars and the rest of the Cosmos. But we also find among the F, G, and K stars phenomena which appear to have only the feeblest of analogies on the Sun: companionship, youth, and old age each lead to fascinating features in the atmospheres of stars, and the elucidation of the basic physical processes responsible for the observed behavior is a painstaking task which is far from complete.

Consistently with the objectives of the Series, we have concentrated in this volume on themes which seem to offer a path towards unity in the arrangement of observational material. At the present time there are two themes which have been particularly fruitful in the study of F, G, and K stars over the past few decades. They are:

- (1) The existence of common structural patterns in the atmospheres of stars which superficially appear to be quite different. For example, a radial arrangement into photosphere — chromosphere — corona — wind is very common among F, G, and K stars, and it provides an extremely useful paradigm for investigations of all objects in this class.
- (2) The crucial importance of electrodynamic (magnetic) activity in stellar atmospheres. While electrodynamic processes are probably not important in mediating *all* aspects of the phenomena observed in the atmospheres of F, G, and K stars, the current emphasis on this theme has

been very useful in giving unity to studies of the evolution and variability of stellar atmospheres, as well as the structural patterns described in (1) above. (In this context, it is amusing to recall the analogy attributed to van de Hulst between "sex" and "magnetic fields": in the past, both were known to exist but discussion of them was carefully avoided; more recently, both subjects have been vigorously promoted as providing the key to the solution of all problems; perhaps in the future both will come to be seen as an important part of a larger and even more interesting tapestry.)

The reader will find these two themes threading through much of the observation and interpretation presented in this volume.

The book is divided into two major parts, Chapters 2-4 dealing with observational material, and Chapters 5-7 dealing with interpretation and theory. A résumé of the individual chapters is given below:

Chapter 2, by D.F. Gray, "Nonthermal Phenomena in the Photospheres of Cool Stars" deals with observations of hydrodynamic and magnetic phenomena in the photospheres of F, G, and K stars in different luminosity classes. Information on these phenomena is obtained principally from the analysis of spectral lines, and the chapter gives a useful summary of modern techniques — particularly the application of Fourier analysis — for extracting information on fluid flows and magnetic fields from the measured line profiles.

The results of such investigations in the past have often been expressed in terms of the vague but deeply embedded concepts of macroturbulence and microturbulence. These phenomena are defined by the operations applied to stellar spectra, and their relation to actual fluid flows in the stellar atmosphere is quite unclear. Nevertheless, systematic trends are observed in the variation of macroturbulence and microturbulence with effective temperature and surface gravity, and these *may* ultimately provide insight into the variation of convective overshooting, nonradial oscillations and similar phenomena from star to star.

In addition to the rather vague interpretation of stellar spectra provided by the concept of "turbulence," there are several more concrete interpretations in terms of specific hydrodynamic processes. Gray provides an extensive account of results for granulation (penetrative convection), rotation, and oscillations, giving a sound basis for the reader who wishes to draw comparisons with solar studies reported in our companion volume "The Sun." Furthermore, the topics of starspots and magnetic fields are also discussed, providing an empirical foundation for Chapter 7. Chapter 2 concludes with a series of appendices which summarize the key characteristics of the "thermal" aspects of F, G, and K stars.

It should be noted that Gray's chapter was completed almost four years prior to publication. Substantial progress has occurred in this time, and Gray's recent monograph gives an excellent overview of this work.

Chapter 3, by D. Reimers, "Observations of Chromospheres, Coronae, and Winds in F, G, and K Stars" describes the outer atmospheric layers of the stars discussed in Chapter 2. The chapter begins with a comprehensive review of the broad range of spectroscopic features which are used to study chromospheres, coronae, and winds. More detailed descriptions of specific results are then presented, including the coronae of single stars and the very broad topic of mass loss and winds among the F, G, and K stars. Considerable attention is paid to eclipsing binary systems of the ζ Aur type, where the circumstances permit a detailed exploration of the arrangement of matter in the extended atmosphere of the cool-giant component.

A fascinating aspect of the chromospheres and winds of cool stars is the existence of linewidth-luminosity relations of various kinds. Some of these may reflect actual velocity-luminosity relations, but most are probably more complex phenomena which, nevertheless, must provide clues to the systematics of stellar atmospheric structure among different classes of F, G, and K stars. The chapter

discusses various conjectures pertaining to these relationships but also emphasizes the fragmentary nature of our knowledge. Finally, Chapter 3 discusses magnetic phenomena in the chromospheres and coronae of cool stars, providing further observational foundations for Chapter 7.

Chapter 4, by L. Kuhi and L. Cram, "T Tauri Stars" parallels in several respects the material in Chapters 2 and 3, but shows that nonthermal phenomena occur with much greater prominence in the T Tauri stars. Photospheres, chromospheres, coronae, and winds are apparently all present in T Tauri stars, but with characteristics which distinguish them quantitatively — and perhaps qualitatively — from the more "normal" F, G, and K stars.

The rather bizarre behavior of T Tauri stars is evidently related in some way to their youth, which is attested to by several lines of argument reviewed in the chapter. But there is only weak observational support for any of the many speculations which have been advanced to explain the specific mechanisms by which youth leads to such prominent nonthermal behavior. Although we have quite detailed spectroscopic and photometric data, with useful time resolution in many cases, we are far from a widely accepted interpretation in terms of a specific atmospheric structure. Unresolved questions include: What is the relative importance of compact chromospheres and extended atmospheres in producing emission lines? What is the physical origin of the UV and IR excesses, and the optical-spectrum veiling? What mechanisms control the variability? And, perhaps most fundamentally, what is the interplay between accretive processes and mass loss, and how is this related to the atmospheric geometry? Some of these questions are explored in Chapter 4, but few definitive conclusions can be drawn.

Chapter 5, by L. Cram, "Classical Theory of Stellar Atmospheres" is the first interpretational chapter in the volume. The first goal is to trace the genesis of the patterns of thought which describe "classical" or "thermal" stellar models. Such models have been thoroughly investigated by theoretical means, although it has always been recognized that they cannot account for many observed properties of stars. It is something of a mystery that so much effort has been expended refining the classical model in the face of the wealth of intriguing data on nonthermal effects.

After introducing a sequence of classical models based on progressively more refined treatments of the conditions of radiative hydrostatic equilibrium, Chapter 5 presents a brief critique of the classical model by contrasting it with observational data. Not surprisingly, the model is found to be incomplete. An account is then given of some of the more important attempts which have been made to modify the classical model by introducing additional, poorly understood, "semi-empirical constructs." It is argued that these have not usually been fruitful, because they have been used as props for the classical model rather than guideposts for new generations of nonthermal models.

Chapter 6, by L. Cram, "Dynamical Processes and the Origin of Atmospheric Structure" takes up the critique established in Chapter 5, and makes a modest attempt to provide some insight into dynamical processes in stellar atmospheres. After a survey of some basic concepts in gas dynamics, the chapter reviews some of the *subatmospheric* dynamical processes thought to be important in F, G, and K stars. These lead in turn to a discussion of phenomena in the atmospheres, and an opportunity is therefore available to present a coherent account of the observations in terms of underlying physical processes.

However, there are at present no models which could be regarded as successfully linking theory to observation. This presumably arises because the range of behavior which is *theoretically* possible is unlimited, while the observations are rarely interpreted with the comprehensive rigor needed to reduce these possibilities to a smaller set of plausible processes. In view of this, the chapter devotes considerable space to an application of the empirical-theoretical approach advocated by Thomas in the companion volume "Stellar Atmospheric Structural Patterns." While not entirely successful, our exploration of Thomas' work lets us bring into sharp focus a number of important questions where further research might be rewarded.

Chapter 7, by C. Zwaan and L. Cram, "Theory of Magnetic Fields in Cool Stars" provides an overview of a particularly important aspect of the F, G, and K stars. Much of the available data on chromospheric and coronal phenomena in these stars (excluding the T Tauri stars) can be codified and explained — at least in a preliminary, qualitative way — as the result of electrodynamic processes (magnetic fields and related phenomena). Such processes appear to originate beneath the stellar atmosphere, but they exert a strong influence on the organization of the atmosphere in space and time. A crucially important consequence of electrodynamic activity is the presence of highly structured magnetic fields, possibly arranged in "flux tubes" or similar structures. Much of the data on chromospheres and coronae appears to require an interpretation in terms of the fractional coverage of the star by flux tubes, rather than differences in radial structure within laterally homogeneous regions.

1

INTRODUCTION AND RESUME

Lawrence E. Cram

I. INTRODUCTION

This volume in the NASA-CNRS monograph series "Nonthermal Phenomena in Stellar Atmospheres" deals with cool stars, those with spectral type F, G or K. Such stars form an extremely diverse class of objects. The one property common to members of the class is that their visible spectrum indicates that the electron kinetic temperature in the deepest parts of the atmosphere lies within the range 4000 K - 9000 K. There are few, if any, other properties common to all members of the class. The pressure, chemical composition, and state of motion of the atmospheres of these stars vary greatly. There is abundant evidence for the existence of hot atmospheric regions (chromospheres or coronae) in F-G-K stars of all kinds, and the nature of such hot regions varies markedly within the group. Many F-G-K stars are losing mass, some at a rate sufficiently fast to influence the evolution of the star and the interstellar medium. It is the objective of this volume to assemble many of the available observations of the atmospheres of the members of this diverse set of objects, and to discuss the attempts which have been made to explain these observations.

The fact that the Sun is a dwarf G star makes the study of F-G-K stars additionally interesting. While it is becoming increasingly clear

that analogues of solar atmospheric structure may be found in stars of all kinds, it is likely that the closest similarities will be found in stars of similar spectral classification. By studying the similarities and differences between solar and stellar atmospheric structure, we can improve our understanding of such structure as a general property of stars. A companion volume in this series (Jordan, 1980) provides a comprehensive account of the solar atmosphere, and will be frequently referenced in the present discussion.

Studies of F-G-K stars are also of considerable interest in relation to the problem of stellar evolution. T Tauri stars and related types form a subset of the F-G-K class which is particularly important in understanding the early stages of stellar evolution, while many stars pass through cool giant and supergiant stages during the later phases of their evolution. We shall see that *for these stars there is still much to be learned about the relationship between the structure and evolution of their atmospheres and the structure and evolution of their interiors*, particularly in connection with the dynamical processes which occur in stars.

A great deal of observational and theoretical work remains to be done before we will be able to claim to understand stellar atmospheres. In

this volume we have attempted to describe systematically some of the observational foundations upon which such understanding must rest, and we have also explored some of the paths along which theoretical progress might be made. The main objective of the volume will be met if the reader is, on the one hand, stimulated by the need to explain the tremendous diversity of observed stellar atmospheric phenomena and, on the other, sobered by the inadequacy of our present understanding of these observations.

II. SPECTROSCOPIC TAXONOMY

One of the basic unifying concepts of astrophysics is the interpretation of the observed two-dimensional sequence of stellar spectral types in terms of differences in effective temperatures and surface gravities. However, there are many observed properties of stellar spectra which cannot be accommodated in this two-dimensional classification scheme. In particular, observations of infrared, ultraviolet and X-ray emissions from many stars imply that a much more complex taxonomy is required. Thus, much of the material presented in this volume cannot be explained in terms of the "classical" two-dimensional classification scheme, and hence it is necessary to discuss at this point the development of a more appropriate scheme.

It is convenient to divide the problem of stellar atmospheres into three subproblems:

- (a) the identification of spectral characters or features which appear to be useful as classification tools, and assignment of stars to taxons on the basis of these characters;
- (b) the empirical-theoretical interpretation of the observed nature of the spectral characters in terms of the structural properties of the atmospheres from which the spectra are emitted;

- (c) the development of theories of the physical processes which account for the inferred structural properties.

In broad terms, the first aspect is covered in this volume in Chapters 2, 3 and 4; the second in Chapter 5 and the early part of Chapter 6; and the third in the last part of Chapter 6 and in Chapter 7.

The task of providing a cohesive account of the great variety of observations available on diverse "types" of F-G-K stars can be assisted by introducing the concepts of *polythetic groups* and the *nexus of mechanisms*. The concept of polythetic groups can be defined as follows. Suppose we have identified a set $C = \{c_1, c_2, c_3, \dots\}$ of spectroscopic characters or features, and we have examined these features in a group $K = \{k_1, k_2, k_3, \dots\}$ of stars. The group K is said to be polythetic (with respect to C) if

- (a) each member of K possesses a large (but unspecified) number of the characters c_j , and
- (b) each character c_j is possessed by a large (but unspecified) number of the members of K .

The group is said to be *fully polythetic* if, in addition, no character C is possessed by all members of the group K . A *monothetic group* is one for which the group of characters is both necessary and sufficient to define membership of the group.

The available observations of stars indicate that the most useful systems of classification delineate polythetic groups. In the past there has been some tendency to adopt the view that "normal" stars form a monothetic group with respect to characters defining effective temperature, surface gravity, and chemical composition. However, the addition of recent observations of stellar X-ray and ultraviolet

emission to the previously available data on variability and emission lines has now clearly demonstrated the polythetic character of all kinds of subgroups of cool stars. For example, Chapter 4 shows that the F-G-K stars which have been variously called pre-main-sequence objects, nebular variables, the Orion population, or T Tauri stars form a polythetic group with respect to classification criteria such as IR, EUV, and X-ray intensity, line profile shapes, and patterns of variability.

Another useful concept involves the notion of the *nexus of physical mechanisms*, which may be defined as follows. Suppose that a set $P = \{p_1, p_2, p_3, \dots\}$ of physical processes is acting simultaneously in a stellar atmosphere. It may well be the case that a particular spectroscopic character, say c_k , is influenced by more than one process p_i . Moreover, different characters c_j may be influenced to different degrees by each one of the p_i . Consequently, it is the nexus of the mechanisms P which is responsible for the appearance of the characters C that are used to classify the group K .

The concept of polythetic groupings of stars with group membership defined by characters controlled by a nexus of mechanisms is closely related to the notion of “the population” now current in studies of biological taxonomy and evolution (Mayr, 1978). Before this concept was widely used, biological taxonomy was generally based on the idea of a “natural” or “prototypic” exemplar of each specified class, whose characters were “imperfectly” manifested by each member of the class. Now, however, many biological investigations circumvent the use of the (often fictitious) exemplar, and concentrate on the population itself. The population is regarded as an assembly of individuals which are similar to one another in many respects, but different in others. The central research problem is to account for the similarities and differences in terms of physical mechanisms (often through the nexus of molecular processes).

A similar approach is now sometimes used in the investigation of stars. In the past, the concept of “spectroscopic standard stars” has provided the exemplars, and many authors have tacitly assumed that these standards correspond closely (often exactly) to “classical” stellar model atmospheres. However, the availability of EUV, X-ray, and IR observations (combined with older data on variability and visible emission lines) has shown that a great variety of atmospheric structure is to be found in stars lying in a single classical taxon. As a result, many of the problems addressed in this volume are concerned with the desire to explain the similarities *and differences* among stars in quite narrowly defined spectroscopic classes. Having developed these basic concepts, we now provide a résumé of the remaining chapters.

III. RESUME OF VOLUME

Chapter 2: It has been known for many decades that photospheric absorption lines in stellar spectra are broadened beyond the widths that would be expected from thermal Doppler broadening alone. Chapter 2 provides a detailed account of the observed systematic properties of the extra broadening, which is interpreted in terms of various kinds of macroscopic flows in the stellar photosphere.

Some kinds of nonthermal Doppler broadening produce specific signatures in the resulting flux profiles emitted from a star. These include the symmetric signatures of microturbulence, macroturbulence and rotation, as well as the asymmetric signature produced by the cross-correlation of intensity and velocity fields in the presence of convection and waves. Chapter 2 describes these results in detail, and provides an extensive summary of the systematic variation of such properties with effective temperature, surface gravity, and age. These variations are very important, since they provide clues both to the origin of the photospheric effects in terms of internal structure and

to the consequences of the nonthermal phenomena on the outer atmosphere of the star.

Improvements in the sensitivity of modern stellar spectrographs have now made it possible to detect the Zeeman signature due to magnetic fields in the photospheric lines of cool stars. Chapter 2 reports the results of these studies, and summarizes the related observations of photometric variability induced by starspots. These observations provide much of the empirical knowledge underlying the theories discussed in Chapter 7. Chapter 2 concludes with a number of appendices, which summarize the basic astrophysical quantities associated with cool stars.

Chapter 3: Over the past decade, the successful flights of IRAS, IUE, and *Einstein* and have provided radically new information on the nature of the coronae, chromospheres and winds of cool stars. Chapter 3 provides a comprehensive account of these new data, integrated with old and contemporary data obtained from ground-based observatories. A remarkable aspect of this work has been the use of observations of eclipsing binary systems to probe in great detail the structure of the distended atmospheres of cool giant stars. One of the key results discussed in Chapter 3 is the existence of a dividing line in the Hertzsprung-Russell diagram, separating stars with "hot" outer atmospheres from those with "warm" outer atmospheres: this separation also corresponds to a substantial change in the character of the stellar wind, and poses a very significant challenge for theories of the atmospheres of cool stars.

The discussion of magnetically influenced phenomena opened up in Chapter 2 is continued in Chapter 3 through a survey of magnetic effects in the chromospheres and coronae of cool stars. Again, this material provides a foundation for Chapter 7.

Chapter 4: The spectacular and perplexing spectra of T Tauri stars provide evidence of ex-

tremely complex atmospheric structure in this class of cool stars. Chapter 4 summarizes the results of many investigations of these objects, and outlines a tentative explanation of the spectroscopic diversity in terms of a sequence of atmospheric phenomena which occur with different amplitudes in different stars and at different times. While many of the phenomena seen in T Tauri stars could be enhanced manifestations of chromospheres, coronae and winds similar to those described in Chapter 3, it appears that the presence of "pre-stellar" cloud material has a marked influence on certain features. Chapter 4 concludes with an outline of an empirical model which appears to unify many of the observed properties of T Tauri stars.

Chapter 5: There has been a substantial intellectual effort throughout the 20th Century to establish a sound theory of the structure of stellar atmospheres. Until recently, such theories were almost invariably based on the assumptions of radiative and hydrostatic equilibrium. Chapter 5 reviews the development of these theories, and summarizes the very valuable contribution they have made to the understanding of stellar photospheres.

However, there are several observed properties of the atmospheres of cool stars which do not agree with the predictions of the conventional theory; many of these have been discussed in Chapters 2-4. The limitations of the classical theory are summarized in Chapter 5, which also presents an account of some of the new concepts which have been developed as a first step to improving the classical model.

Chapter 6: It seems clear that the structure and the dynamical behavior of the atmospheres of most cool stars are controlled by phenomena which occur inside the star: rotation, convection, pulsation, and magnetic effects. If we are to understand stellar atmospheres, we must also investigate these internal dynamical processes. Chapter 6, therefore, provides a summary of the theory of several of these phenomena, and then attempts to show how they are linked to

observable manifestations in the atmosphere. While previous research has provided a great deal of valuable insight into the physical origins of the phenomena described in Chapters 2-4, it is clear from the material in this chapter that there are significant gaps remaining in our understanding of the physical processes which determine even the gross structure of the atmospheres of cool stars.

Chapter 7: The crucial importance of electrodynamic (or magnetogasdynamic) processes in understanding the behavior of the Sun has been recognized for many decades. It is now equally obvious that electrodynamic processes are important in a wide range of phenomena observed in other cool stars. Chapter 7 provides a short account of some of the basic theories related to the generation of magnetic fields in cool stars, particularly emphasizing the fact that observations show strongly inhomogeneous and markedly variable magnetic fields on the Sun and other cool stars. Inhomogeneity and variability appear to originate due to the fact that the magnetic fields of cool stars show a propensity to form flux tubes of various sizes. Thus, many of the theories described in Chapter 7 are, in essence, theories related to the behavior of flux tubes. While Chapter 7 provides preliminary, plausible accounts of many phenomena seen in cool stars, it is clear that substantial further work will be required to provide a deeper theoretical understanding of the

role of magnetic fields in the atmospheres of cool stars.

IV. PROSPECTS

Several chapters in this volume were essentially completed long before publication. Many readers will notice that certain contemporary research problems are not discussed extensively. This situation reflects, of course, the health and vigor of the scientific investigation of the atmospheres of cool stars, and the speed at which progress is being made.

The vitality of research on this problem depends on three main factors: (1) the existence of a strong international research program in solar physics, which provides new paradigms for stellar workers; (2) rapid progress in instrumentation, covering vast portions of the electromagnetic spectrum; and (3) a fertile exchange of theoretical concepts, not only with adjacent disciplines in astrophysics but also with workers at the cutting edge of other relevant disciplines, such as fluid mechanics and plasma physics, which lie outside of traditional astrophysics.

It seems that there are sound prospects for continued progress in this field, since each one of the three factors described above will surely be sustained over the next decade.

NONTHERMAL PHENOMENA IN THE PHOTOSPHERES OF COOL STARS

David F. Gray

I. INTRODUCTION

Convective envelopes occur in F, G, and K stars. Stars also rotate. These two, convection and rotation, alone and coupled, drive the non-thermal events in the atmospheres of F-G-K stars. The bottom of the photosphere lies in the top of the convection zone. The gases are churned by the convective motion. One expects pressure waves, gravity waves, and MHD waves. The photosphere is likely permeated with a mozaic of magnetic lines of force. Spatial fluctuations in brightness are generated by the convective motion, and differential rotation is also present. Surface spots and eruptions of various sorts occur. The photosphere of a typical F, G, or K star is a very dynamic place! But at the current epoch, we understand these dynamics only poorly. So, much of our job in the observational arena is to detect and characterize the various physical events. A serious procedural problem arises almost immediately: how can we interpret the observations without model photospheres? And how can we build believable model photospheres if we do not understand the dynamics in the first place? The optimistic approach is to assume that certain characteristics of the observable

radiation are dominated by one or two physical processes. That is to assume that even a poor model is good enough in some cases, because the leverage of the model is so weak that the interpretation is hardly altered by changing the model between wide ranging limits. The result is then a first approximation of the measured quantity, and it can subsequently be incorporated to first order into an upgraded and more comprehensive model.

The photosphere of a star is the link or transition region between the interior and the very tenuous outer atmospheric layers. The wavelength change of the opacity reaches a minimum through the visible wavelengths, and so normal optical observations of stellar spectra tell us about the photosphere. Higher atmospheric layers control the UV and far-IR wavelengths.

This chapter is organized in the following way. First we start with the most fundamental types of observations and premises. We then consider, in turn, the major nonthermal phenomena that have been identified or are strongly suspected in stellar photospheres: turbulence, granulation, rotation,

starspots, magnetic fields, and oscillations. It will become increasingly clear that most, if not all, nonthermal effects are coupled together. Further, it is not really possible to separate the events in the photosphere from the action in the rest of the star, especially in the convection zone and the chromosphere. The star is a unified whole, and ultimately we must understand it as such. An Appendix contains a summary of some basic thermal data for F-G-K stars.

II. SPECTRAL LINES: FUNDAMENTAL OBSERVATIONS

II.A. NONTHERMAL EFFECTS

We do not have to look very hard at a stellar photospheric spectrum before we see clear evidence for nonthermal phenomena. Specifically, we mean the following by "nonthermal": if we take the temperature indicated by the energy distribution or by the excitation or by the ionization levels characterizing the spectrum, the thermal Maxwellian velocity distribution falls far short of describing the widths and shapes of the star's spectral lines.* This is universally true for all stars.

Figure 2-1 shows some examples of nonthermal effects, which, from the point of view of line broadening, include phenomena like convection, even though convection is driven by thermal gradients. The suprathermal broadening does vary with effective temperature and surface gravity, and it is also likely that each individual star has its own peculiarities relative to the broad, average variations across the HR diagram.

Furthermore, we expect thermal broadening to be symmetric, whereas the observed spectral

*This statement of what "nonthermal" means is not intended as a general definition, since it excludes many important phenomena such as the dissipation of waves, nonthermal temperature gradients, mass-loss, flares, and so on. But within the context of the photosphere, such a definition brings into mental focus almost all of the observed nonthermal phenomena which will be discussed.

lines are clearly not. Figure 2-2 shows one way of making the asymmetry clearly visible. Asymmetries, like the extra line widths, are ubiquitous. Differential line shifts can also be seen. (See Chapter 2.IV.C.)

Nonthermal events such as magnetic fields might be expected to produce line polarization through systematic Zeeman splitting, but polarization measurements have been largely negative for F-G-K stars. Even continuum measurements of dMe flare stars show little or no polarization. Lack of polarization is generally taken to mean a lack of strong globally organized magnetic fields. Complex, bipolar, locally organized fields are observed by means of line broadening introduced by the Zeeman displacements.

II.B. THE VELOCITY INTERPRETATION

Our interpretations are guided by what we see on the solar surface, like granulation,

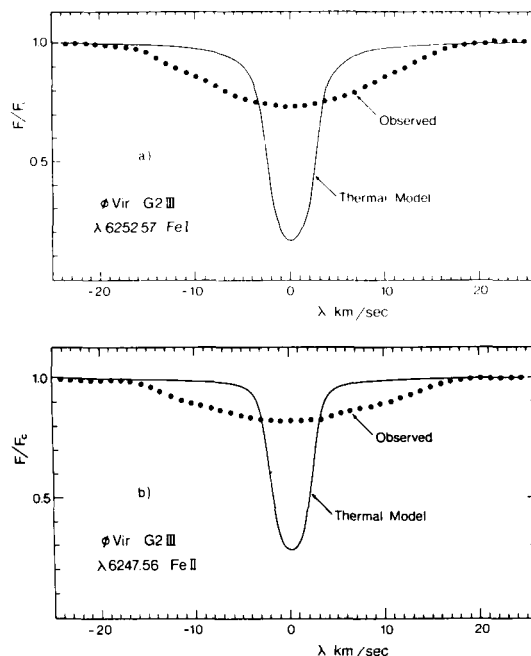


Figure 2-1a and 2-1b. The observed spectral lines of ϕ Vir are shown by the dots. The thermal line computations are indicated by the continuous line.

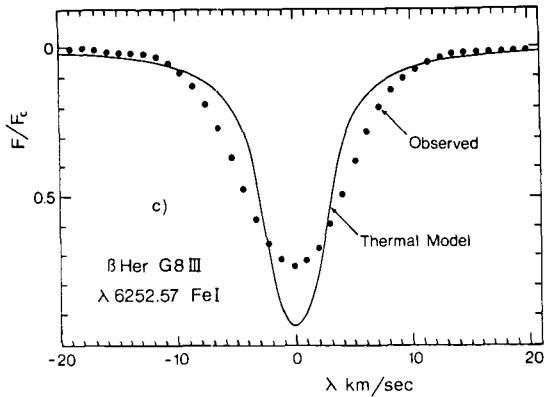


Figure 2-1c. A strong line of β Her is compared to the thermal model.

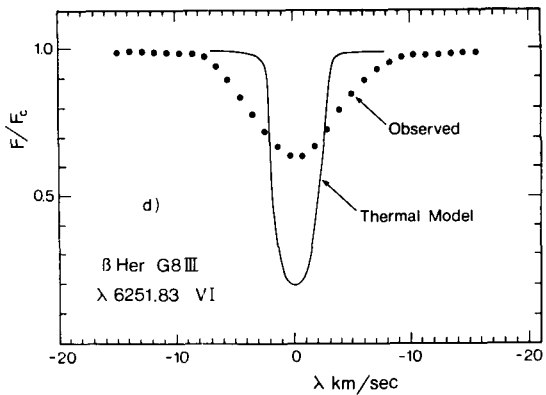


Figure 2-1d. A much weaker line of β Her is compared to a thermal model.

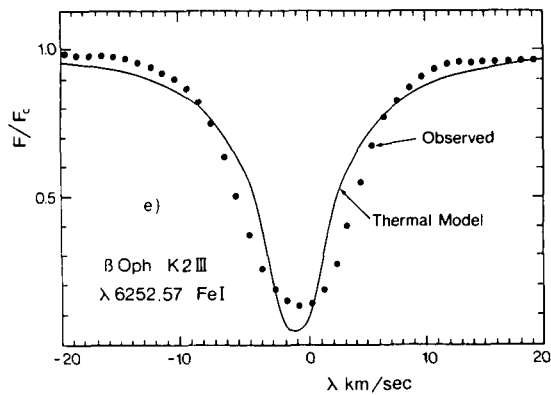


Figure 2-1e. A line of β Oph is compared to a thermal model.

supergranulation, oscillations and waves, magnetic fields, spots, and rotation. The velocities associated with these phenomena

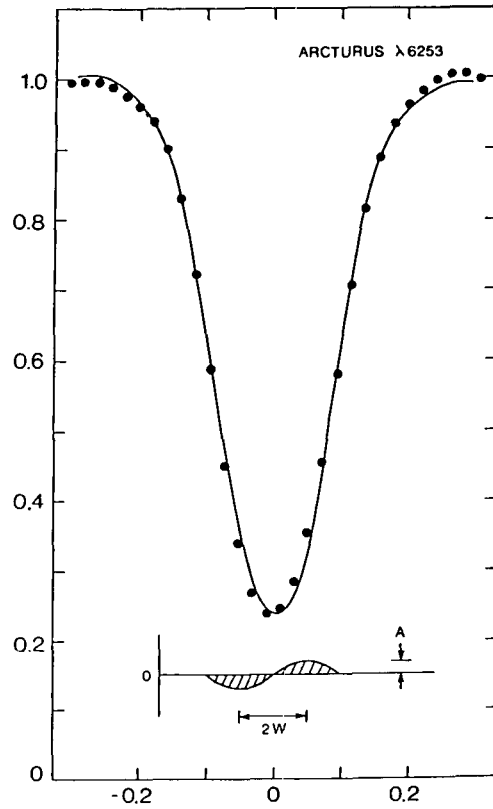


Figure 2-2. The K2III star Arcturus shows typical asymmetries in its spectral lines. The observed profile is shown by the filled circles. The same profile reversed left for right is shown by the continuous curve. The small graph at the bottom shows the difference between the profile and its reversed image. The width, W , and the amplitude, A , are measures of the size of the asymmetry (from Gray, 1980b).

cause Doppler shifts and broadening. Coupled with temperature inhomogeneities, velocities produce asymmetries in lines. We quite naturally look toward Doppler shifts to explain a major portion of the stellar line observations. Suppose velocities *are* the fingerprints of the physical mechanisms in stellar photospheres. One test of the supposition is to see if the broadening is proportional to wavelength in accordance with Doppler's equation. This has been well established by many observers, and a classical example is found in the work of Struve (1930) with his early work on rotation.

We do find deviations from this simple hypothesis in the case of strong lines, where still more broadening is seen. However, curve of growth studies show that pressure broadening, and damping effects generally, become important for such lines; so in fact these are only perturbations on the velocity broadening hypothesis. The observational results described below are predicated on the velocity hypothesis.

We are fortunate that nature produces spectral lines. Being sharp spectral features, they make relatively good detectors of the Doppler effect. Continuum measurements in contrast, tell us almost nothing about nonthermal events in stellar photospheres. This accounts for the fact that virtually all of our studies of nonthermal phenomena in the photospheres of stars amount to a careful scrutiny of spectral lines.

III. PHOTOSPHERIC TURBULENCE

III.A. FORMULATIONS OF TURBULENCE

As we have seen, spectral lines show widths well in excess of the expected thermal Doppler broadening (Figure 2-1). Part of the extra broadening might well be due to rotation, as indeed proves to be the case. Not all of it can be attributed to rotation because we see no stars at all with lines of only thermal width, and certainly some rotation axes would be close enough to pole-on to reduce the rotational broadening to very small values. Furthermore, we can see excess thermal broadening in the solar spectrum where rotation can be explicitly accounted for. In addition, medium strength lines show a desaturation effect that so far can only be attributed to velocity effects on the absorption coefficient (see Equations 1 and 2 below). In stellar astronomy we call these extra velocities by the name of turbulence. In solar astronomy the name nonthermal velocities is more common. Reviews and summaries have been made by Huang and Struve (1960),

Thomas (1961, 1967), Beckers and Canfield (1976), Canfield and Beckers (1976), Cayrel and Steinberg (1976), Gray (1978), and Gray and Linsky (1980).

Since we are just beginning to understand what physical processes are involved in turbulence, it is not surprising that the formulations used so far are somewhat rudimentary and empirical. While it is easy to incorporate microturbulence and macroturbulence into model atmosphere computations, they make relatively little sense physically. In the first instance, intermediate geometrical scales (mesoturbulence) are neglected. Only recently has any effort gone into formulations including mesoturbulence (Hundt 1973; Auvergne et al., 1973; Gail and Sedlmayr, 1974; Traving, 1975; Frisch, 1975; Frisch and Frisch, 1976; among others). In the second instance, it is not very realistic to treat ordered motions such as granulation and oscillations as purely stochastic. Such phenomena show significant deviations from randomness, especially nonisotropy.

III.B. MICROTURBULENCE, MACROTURBULENCE, AND ROTATION

Use of the parameters of microturbulence dispersion (ξ) and macroturbulence dispersion (ζ) to describe unaccounted-for line broadening has become an astronomical tradition. When rotation ($v \sin i$) is added, we have a three parameter "model." If a radial-tangential form (see below) is assumed for the macroturbulence velocity distribution, essentially all photospheric line profiles of F, G, and K stars can be modeled to within the observational errors (Gray, 1982d). We can view the trio ξ , ζ , $v \sin i$ as a sophisticated classification set, a taxonomic tool much like spectral type. We then have three parameters that are connected in some (poorly understood) manner with nonthermal physics, but which can be measured with considerable precision. We understand

with relative clarity the meaning of $v \sin i$; it specifies the projected rotation rate. Less certain is the meaning of macroturbulence, although we certainly expect stars to have large (geometrical) scale motions like those seen in the solar photosphere. Least certain is the nature of microturbulence. We see microturbulence-type broadening in solar lines, but even there we do not know how it arises.

The micro- macroturbulence plus rotation model is purely kinematic. Velocities are inferred from the observed Doppler broadening. The dynamics that go with the motions are ignored. Pilot dynamical calculations have been carried out by Shine (1975), Cram (1976, 1981), Cram et al. (1979), Durrant (1979), Dravins et al. (1981), and others. But the overwhelming majority of the observations have been parameterized by ξ , ζ , and $v \sin i$. We now look briefly at the methods used to obtain them.

III.C. THE CURVE OF GROWTH MICROTURBULENCE

One of the first introductions of nonthermal phenomena into the interpretation of F-G-K spectral lines was when Struve (1946) chose microturbulence as a "patch" to explain the desaturation seen in curves of growth. The parameter was simply chosen to obtain agreement with the observed desaturation. If we write the thermal absorption coefficient as

$$\alpha_\lambda = \frac{\pi e^2}{m c^2} f \lambda^2 \frac{1}{\Delta \lambda_D} \exp(-\Delta \lambda / \Delta \lambda_D), \quad (2-1)$$

where

$$\Delta \lambda_D = \frac{\lambda}{c} \sqrt{\frac{2kT}{m} + \xi^2}, \quad (2-2)$$

we are using a dispersion $\Delta \lambda_D$ appropriate for a convolution of a thermal Gaussian having a dispersion of $\sqrt{2kT/m}$ with a microturbulence

Gaussian having a dispersion of ξ . The curve of growth technique and the concept of microturbulence itself fell into a questionable state owing to numerous uncertainties in physical constants and inadequate modeling of the physics (Gray and Evans, 1973; Worrall and Wilson, 1973). More recent work, for example by Foy (1972, 1978) and Luck (1977), while still using the kinematic physics, shows more believable results, and results that are also consistent with line profile analyses. Figure 2-3 shows an example from Cayrel de Strobel et al. (1981). Statistical errors on ξ are ~ 0.1 to 0.3 km s^{-1} , if the curve of growth is carefully constructed. But one should be aware of the fact that the saturation portion of the curve of growth dwindles drastically with increased photospheric pressure (Cayrel et al., 1977), greatly reducing the leverage.

III.D. THE RADIAL-TANGENTIAL MACROTURBULENCE

In the early studies of macroturbulence, an isotropic Gaussian velocity distribution was

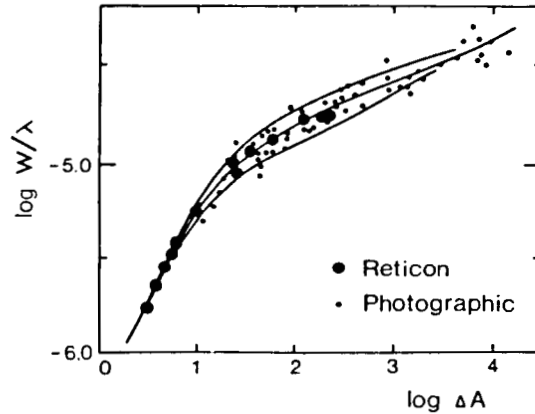


Figure 2-3. The curve of growth for FeI lines in the spectrum of α Ari. The abscissa is the abundance relative to ϵ Vir. Small points represent photographic measurements, large points represent Reticon measurements. The three theoretical curves, shown by the continuous lines, are for $\xi = 0.0, 1.5,$ and 2.0 km s^{-1} (based on data from Cayrel de Strobel et al., 1981).

always assumed. More recent work has shown this to be an incorrect assumption for all late-type stars except perhaps for supergiants for which not enough work has yet been done to say one way or the other. The distribution that is found to be successful in fitting the observations is the anisotropic radial-tangential model in which velocity vectors are postulated to be only in the radial or tangential directions or both (Gray, 1975, 1976, 1978, 1982d). With this condition on the directions, a full Gaussian range of velocities is then used. After integration over the disc, the result is a profile having a sharper peak and more extended wings than a Gaussian (see Figure 2-4). A comparison with other velocity distributions and a discussion of the correctness of the radial-tangential form has been made (Gray, 1978, 1982d). Heuristically, one can argue that the predominant directions for motions of granulation and oscillations are radial and tangential. White and Cha (1973) even find a Gaussian distribution of velocities for the 5-minute oscillation. And Keil and Canfield (1978) show that a velocity distribution for granulation is not far from a Gaussian. But as yet no real physical derivation of the radial-tangential model has ever been given.

In all work to date, the dispersion in the radial and in the tangential directions has been taken to be equal (here denoted by ζ_{RT}). The parameter ζ_{RT} is the most probable velocity (modal value) and is $\sqrt{2}$ times larger than the

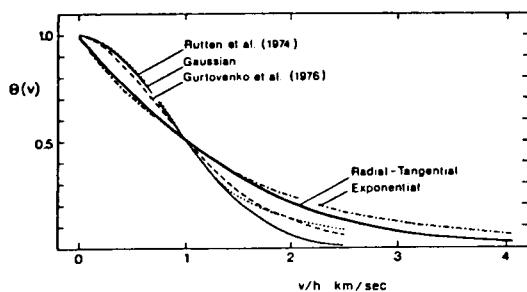


Figure 2-4. The radial-tangential velocity distribution is compared to other velocity functions. Width normalization is to the half-width, h (from Gray, 1978).

root-mean-square velocity that has sometimes been used. (Note in passing that the microturbulence ξ also denotes a most probable velocity.) Furthermore, the radial and tangential components have been equally weighted when computing broadening functions to compare with observations.

III.E. DIRECT FITTING OF LINE PROFILES

One might choose to match an observed profile directly with trial and error combinations of ξ , ζ_{RT} , and $v \sin i$. Or, ξ might be obtained from a curve of growth analysis, followed by the inclusion of ζ_{RT} and/or $v \sin i$ to reproduce the observed profiles. An example of this approach is found in the analysis of β Gem by Ruland et al. (1980). The results for $\lambda\lambda 5576-5577$ are shown in Figure 2-5. This direct approach has also been used in part by Soderblom (1982), and in most of the older investigations (e.g., Abt, 1958; Slettebak, 1956; Ross and Aller, 1968).

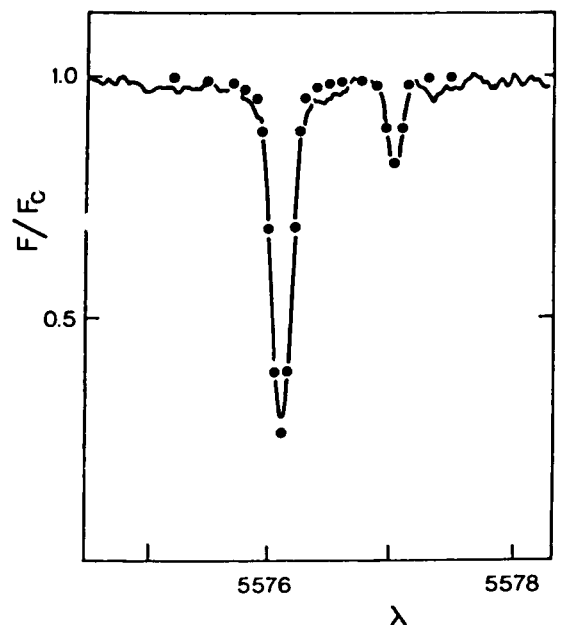


Figure 2-5. This direct fitting of profiles was obtained by Ruland et al. (1980). Here the dots represent the computed points and the continuous line the observations.

III.F. THE FOURIER ANALYSIS

The sidelobe structure in the Fourier transforms of profiles in late G and K star spectra is most often due to desaturation effects, and is therefore parameterized by the microturbulence dispersion, ξ . The typical uncertainty involved can be seen from Figure 2-6 to be $\leq 0.1 \text{ km s}^{-1}$. Elimination of the specific intensity profile, which includes the thermal and microturbulence broadening, leaves a residual transform. The residual transform is shaped by the macroturbulence and rotation. In the most recent work, many such residual transforms are averaged before further analysis. Disc integrations of the combined Doppler shifts of radial-tangential macroturbulence and rotation can then be used to obtain ζ_{RT} and $v \sin i$ (see Gray, 1981a, 1982b). Examples of residual

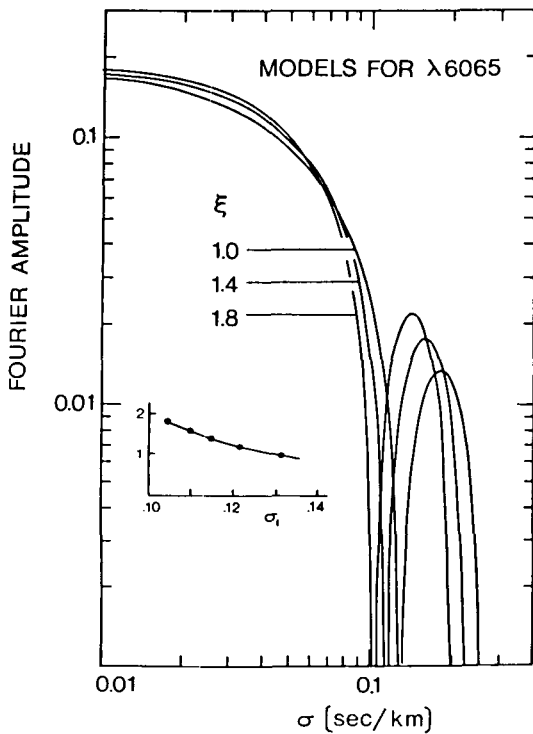


Figure 2-6. Microturbulence dispersion controls the position of the first zero in the Fourier transforms of the lines as shown here for three values of ξ . The inset graph shows the relation between ξ and the Fourier frequency of the first zero denoted by σ_1 (from Gray, 1980a).

transforms and the interpreted mean are shown in Figure 2-7.

Some F and early G stars have profiles dominated by rotation (Figure 2-8). The Fourier transforms in such cases are heavily filtered by the rotation profile transform, as is illustrated in Figure 2-9. We expect any sidelobe structure stemming from microturbulence desaturation to be at Fourier frequencies $\sim 0.1 \text{ s km}^{-1}$, as it is for the slower rotators. Clearly, that portion of the transform has been pushed well below the noise level by the filtering of the rotation profile transform. The sidelobes we see in Figure 2-9 are unambiguously those of the rotation transform itself. Under such circumstances, the profile shapes give only relatively weak information on ζ_{RT} .

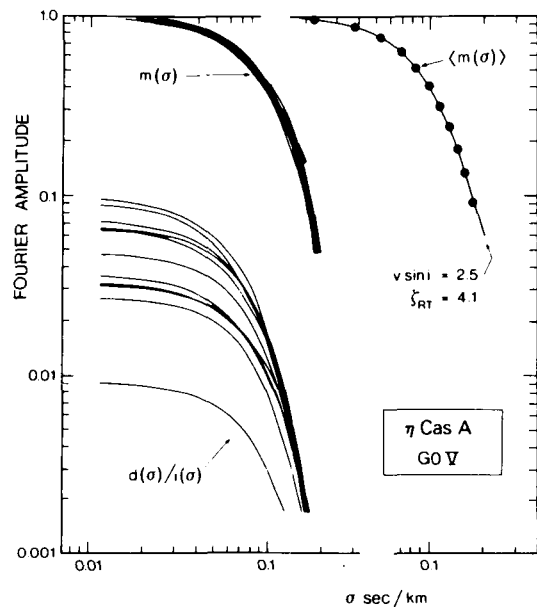


Figure 2-7. The lower set of curves are transforms of the line profiles with the instrumental profile removed. The upper curves, labeled $m(\sigma)$, are the residual transforms with only macroturbulence and rotational broadening left. The mean residual, $\langle m(\sigma) \rangle$ as shown by the dots, is compared with a model (line) to obtain the macroturbulence dispersion, ζ_{RT} and the rotation velocity, $v \sin i$. All the measured lines are from the $\lambda 6250$ region (from Gray, 1984b).

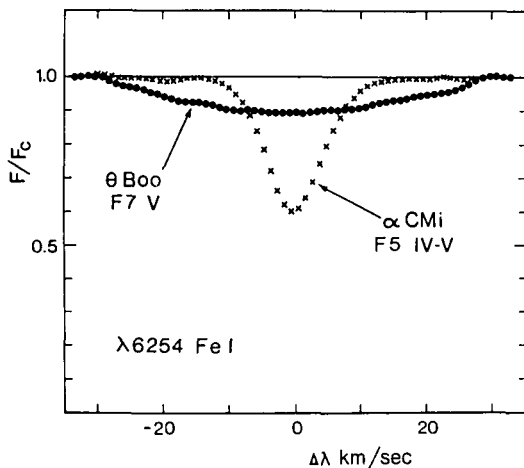


Figure 2-8. The profiles of θ Boo are dominated by rotational broadening ($v \sin i = 28.5 \text{ km s}^{-1}$). This is contrasted to the case for α C Mi, where rotation is less than the macroturbulence ($v \sin i = 2.8 \text{ km s}^{-1}$; $\zeta_{RT} = 7.0 \text{ km s}^{-1}$).

More generally, uncertainties in ζ_{RT} and $v \sin i$ vary markedly depending on the size of these variables and the quality of the data. In instances of large rotation, $v \sin i$ can be measured with a precision exceeding one percent. Such precision is greater than uncertainties introduced by other assumptions such as a cosine limb darkening law or the value of the limb darkening coefficient. For the slower rotators, formal errors are typically 20–30% for both ζ_{RT} and $v \sin i$. Systematic errors depend on the shape of the velocity distribution assumed for the macroturbulence, but a Fourier analysis of the solar flux spectrum yielded $\zeta_{RT} \sim 30\%$, larger than obtained from spatially resolved measurements (Gray, 1977b). It is not clear how much of this discrepancy is due to failure of the analysis of the flux spectrum and how much is due to real solar velocities which are overlooked when only relatively small portions of the solar surface are measured.

Since its introduction in 1973, Fourier analysis has been used in many investigations of spectral line broadening, e.g., Smith (1975, 1976, 1978), Smith and Frisch (1976), Smith and Dominy (1979) Ebbets (1978), Wynne-

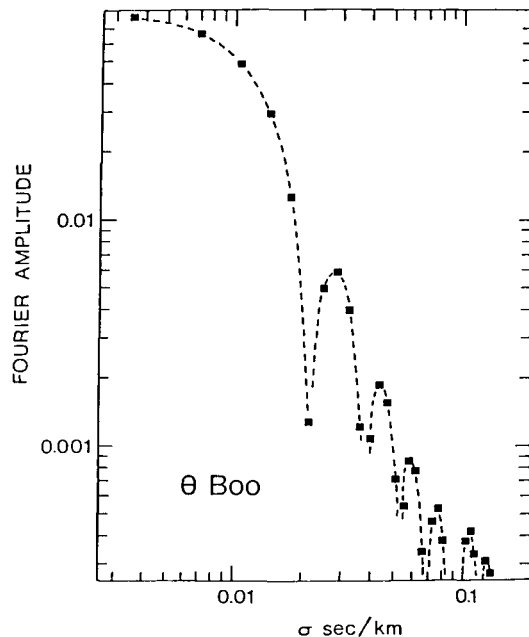


Figure 2-9. The rotation profile transform is clearly visible in this mean residual transform of θ Boo. The dashed line is simply drawn in to guide the eye (from Gray, 1982b).

Jones et al. (1978), Soderblom (1982), Bruning (1981), Bray and Loughhead (1978), Karp and Fillmore (1980), Gray (1982d and references therein), Gray (1984a, b), Gray and Nagar (1985).

III.G. DUAL MACROTURBULENCE DISPERSIONS

For the G and K giants, some recent work (Gray, 1982d) has led to the use of two distinct values of ζ_{RT} . The lines having equivalent widths below about $100 \text{ m}\text{\AA}$ show systematically larger ζ_{RT} than are found for the stronger lines. The size of the difference between the two ζ_{RT} 's varies with spectral type and not all stars of a given spectral type show the effect. Figure 2-10 illustrates one example. It is possible to understand this type of behavior in terms of a depth-dependent macroturbulence, especially if the surface convection velocities are a major contributor to the

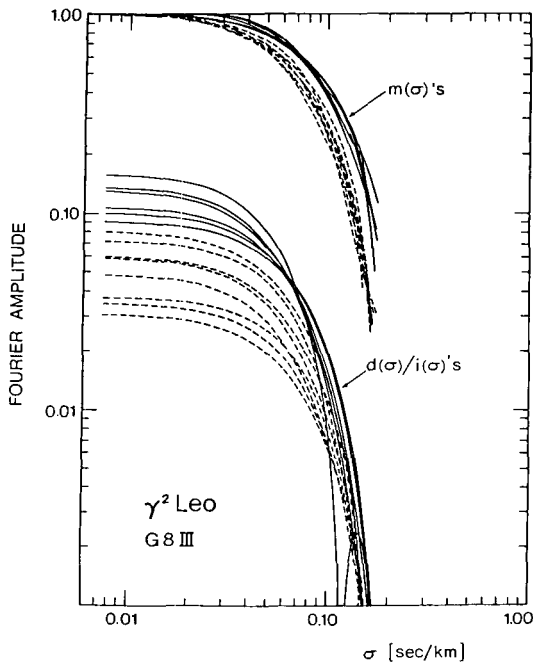


Figure 2-10a. The lower curves are Fourier transforms of the observed line profiles with only the instrumental profile removed. The upper curves are the residual transforms. Lines having equivalent widths less than 100 mÅ are shown with dashed lines. These weaker lines show a macrobroadening that is distinctly larger than for the stronger lines (from Gray, 1982d).

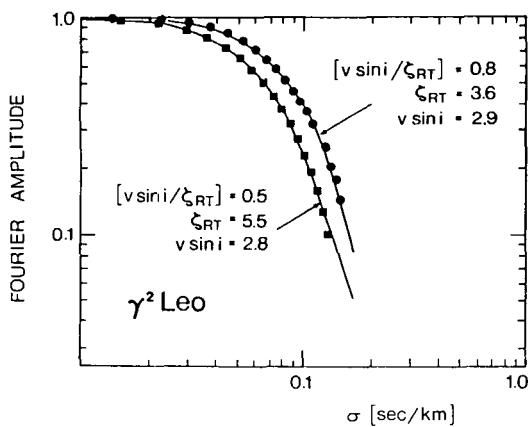


Figure 2-10b. The mean residual transforms for weak (squares) and strong lines (dots) are shown with their modeled macrobroadening functions (lines) (from Gray, 1982d).

macroturbulence. The line asymmetry information points toward an outward decrease in convective velocities (Chapter 2.IV) for stars in this part of the HR diagram. Then too, we have solar measurements which show the same thing in even more detail (Keil and Cram, 1978; Keil, 1980; Canfield, 1976; Durrant et al., 1979; Mattig and Schlebbe, 1974). One simply argues that the stronger lines are formed in higher layers where the convective velocities are somewhat less, and therefore ζ_{RT} is less for lines formed in higher layers. While this makes some sense, it is not proven, for we do not yet know how large a portion of the macroturbulence arises from convective velocities.

III.H. VARIATION OF MACROTURBULENCE ACROSS THE HR DIAGRAM

The general trend of increasing turbulence with increasing luminosity has been known for several decades (Wright, 1955; Slettebak, 1956), and modern observations of macroturbulence corroborate these earlier findings. Figure 2-11 summarizes the observations and their means, $\langle \zeta_{RT} \rangle$. Zeeman broadening occurs in most dwarf spectra later than $\sim G5$, resulting in substantially larger errors on ζ_{RT} for those stars. Only a handful of luminosity class II and I stars have yet been measured; none have been published.

As expected, there is essentially a continuum of points above the main sequence in Figure 2-11, i.e., a smooth continuous transition from one luminosity class to the next. We see that $\langle \zeta_{RT} \rangle$ for each luminosity class drops rapidly with decreasing temperature, and that $\langle \zeta_{RT} \rangle$ increases smoothly toward higher luminosity classes. Some earlier studies (e.g., Smith, 1980a; Smith and Dominy, 1979) seemed to find sharp nonlinearities in plots of macroturbulence dispersion vs. luminosity, but at that time the rather steep temperature dependence of $\langle \zeta_{RT} \rangle$ was not known. There are systematic differences in average spectral types with luminosity class for the stars measured in

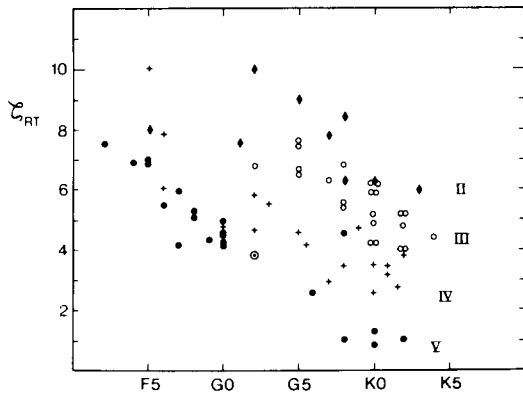


Figure 2-11a. Macroturbulence dispersion is shown as a function of spectral type for luminosity classes II through V, as denoted by different symbols. From Gray (1982d), Gray (1984b), Gray and Nagar (1985), and unpublished data by Gray and Toner.

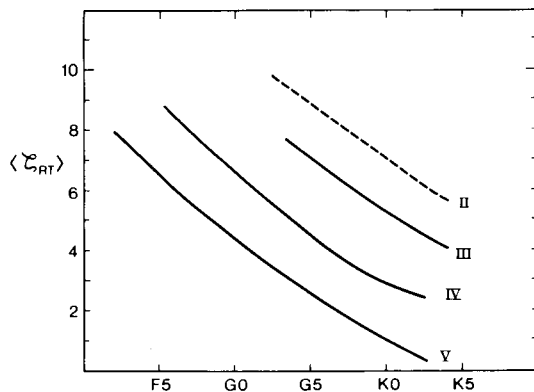


Figure 2-11b. Means of the macroturbulence dispersion from Figure 2-11a are shown.

these investigations. Specifically, most of the dwarfs chosen are G-types; most of the giants and supergiants are K-types. As we can see from Figure 2-11, $\langle \zeta_{RT} \rangle$ for K dwarfs is substantially less than it is for G dwarfs. When this systematic difference is properly allowed for, the nonlinearity of these earlier results disappears.

For supergiants, we have mainly measurements of line half-widths, for no complete analysis spanning a range in spectral type

has been done. The half-widths published by Bonsack and Culver (1966) and Imhoff (1977), and the isotropic values of Luck (1977) indicate a decrease with advancing spectral type from G0 to mid-K. It is not possible to assign a precise velocity to the half-widths, but the velocities are clearly quite large, probably exceeding the velocity of sound by a sizeable margin.

III.I. AGING OF DWARF STAR ATMOSPHERES

Smith (1978) found a systematic decrease in G dwarf macroturbulence dispersions with age, where age estimates were based on CaII H and K line emission and Li abundance. The aging of dwarf star atmospheres in the form of reduced chromospheric activity, chemical composition changes, and rotation are well known (Chapter 2.V.D). It would not be surprising then, to find a weakening of macroturbulence with age. Unfortunately, the correlation found by Smith is greatly weakened when newer measurements are used and when the temperature dependencies noted above are fully accounted for.

On a different front, Foy (1978, 1980, 1981) has maintained that microturbulence values show systematic differences with evolutionary age. He finds the pre-He-flash giants to show $\langle \zeta \rangle \sim 1.5 \text{ km s}^{-1}$ compared to 0.9 km s^{-1} for the post-He-flash giants. Steenbock and Holweger (1981) find some evidence for a larger ζ in stars with active chromospheres.

III.J. MICROTURBULENCE

Microturbulence is the mechanism by which desaturation is introduced into the modeling of a line profile (or equivalent width), as indicated in Chapter 2.III.C, Deubner (1976b, 1976c) favors short period sound waves as the physical explanation. Nordlund (1976, 1978, 1980) finds desaturation in his models of granulation. Shine (1975), Kostyk and Gerbil'skaya (1976), Edmunds (1978), Durrant (1980), and Cram (1981)

have shown how model waves bring in the same effect. The real cause(s) of the desaturation remains unknown. We do not know to what extent density and temperature inhomogeneities enter the picture. Therefore, any physical interpretation of ξ and its variations must be treated with extreme caution. The existence of the desaturation, however, is an observed fact. It is also true that modern curve of growth values of ξ agree with those derived from Fourier analyses of the line profiles, at least for F-G-K stars of luminosity classes III-IV.

Fundamental uncertainties in measuring ξ still remain (in addition to the physical uncertainties). Changes in the temperature distribution, $T(\tau)$, used in the model atmosphere analysis are known to produce changes in the derived ξ of a few tenths of a km s^{-1} (Gray and Martin, 1978). Similar results occur for curves of growth (Strom, 1968). A drop in the source function introduced by non-LTE effects will induce much the same behavior. Our knowledge of $T(\tau)$ is incomplete, and the idea of using only one $T(\tau)$ per star is probably inadequate to begin with.

Then there is the question of the isotropy of microturbulence. Virtually all stellar analyses assume isotropy, while the solar evidence is clearly against it (e.g., Allen, 1949; Canfield and Becks, 1976; Holweger et al., 1978). The depth dependence of ξ is also open to question, and if one is somewhat bold with the depth dependence of the model (e.g., Gray, 1978), wide profile variations can be manufactured. In the case of the dwarfs, pressure broadening infringes on the saturation portion of the curve of growth, further complicating matters. Some of these uncertainties are reviewed by Gray and Evans (1973), Foy (1980), and Cayrel et al. (1977). In many of the investigations prior to ~1970, insufficient comprehension of these details, along with systematic errors in oscillator strengths, caused spuriously large ξ -values to be derived. As each of these physical effects was introduced and their importance more fully appreciated, the residual broaden-

ing attributed to micro-velocity fields became less. However, a linear extrapolation in time would have given negative ξ -values by the 1980's, whereas in reality quite finite and positive desaturation is still required to understand the observations.

The most recent work on giants (Gray 1982d), indicates statistically larger ξ 's for stronger lines. Further, ξ is ~ 0 for the weaker lines (equivalent widths ≤ 75 mÅ) and rises to $\sim 1.7 \text{ km s}^{-1}$ for the stronger lines. This may imply an outward increase in ξ , since stronger lines are formed higher in the photosphere. Depth dependent behavior has frequently been invoked in the past. Dwarf stars have not been carefully investigated with regard to ξ , and most of the published values are byproducts of abundance analyses. Typical values range from 0.5 to 1.5 km s^{-1} . Foy (1978) and Gehren (1980) find statistical increases in ξ with increasing effective temperature and decreasing surface gravity. This agrees, in essence, with an earlier summary (Gray, 1978). The reader is also referred to the reviews by Gehren (1980), Canfield and Beckers (1976), and Huang and Struve (1960) for further details.

IV. STELLAR GRANULATION

IV.A. WHAT TO EXPECT

What can we know about stellar granulation? How can we observe stellar granulation? Naturally, we turn first to the Sun, where spatially resolved photographs show the granules to be substantially brighter than the lanes between granules (Figure 2-12). The rising granules and the falling material in the dark lanes show that the granulation phenomenon is the top of the surface convection zone. The motions alone produce Doppler shifts in spatially resolved (solar) spectra, while in stellar spectra this appears as line broadening. But there is a very important identifier associated with the granulation: the asymmetry it introduces into the line profiles. It is easy to see



Figure 2-12. A photograph of solar granulation shows that most of the surface is covered by granules with relatively narrow intergranular dark lanes. (Photo courtesy of J. B. Zirker, Sacramento Peak Observatory.)

how the asymmetries arise. Consider the rising hot material producing a blue shifted component to the stellar line profile and the falling cooler material producing a red shifted component. To produce an asymmetry the two components must be unequal in strength (Figure 2-13). More specifically, it is the flux contrast combined with the Doppler displacements that causes asymmetrical line profiles. We define the flux contrast, C_F , by

$$C_F = (F_g - F_l)/(F_g + F_l) \quad (2-3)$$

where g and l refer to granule and dark lane and the F's denote the monochromatic fluxes contributed by these two areas, i.e., the "photon weight" resulting from the combined areal and specific intensity differences. [The solar flux contrast is difficult to measure. The area occupied by granules is not well determined, with values ranging from ~44% (Pravdjuk et al., 1974) to ~66% (Müller and

Roudier, 1984). What is called a granule and what is not depends markedly on the spatial resolution and some rather subjective judgment of brightness differences. The same problems make estimates of the relative specific intensities of lanes to granules inexact, but most values are $\sim 79\% \pm 5\%$ (Bray et al., 1984). The contrast also decreases toward longer wavelengths (Albregtsen and Hansen, 1977). Combining numbers, C_F for the Sun would be $\sim 0.3-0.5$.] The centroid as well as the core of the profile of Figure 2-13 shows a slight blueshift. Unfortunately, the unknown radial velocities of stars preclude the explicit use of the shifts, and only differential effects remain.

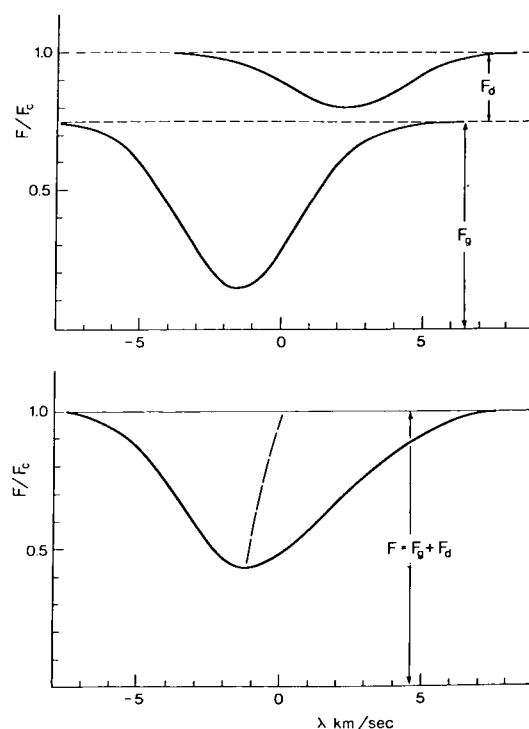


Figure 2-13. The observed spectral lines can be visualized as a simple combination of the light from the granules added to the light from the dark lanes. The upper panel shows these profiles appropriately Doppler shifted (-1.4 and $+2.4 \text{ km s}^{-1}$, respectively). The lower panel shows the sum, with the dashed line indicating the bisector. This figure is purely schematic and does not illustrate real observations.

The complete picture is rather complex because the flux contrast and the Doppler shifts are functions of depth. Different portions of a line profile, formed at different depths, will reflect these functions. To this already complicated picture we must add the statistical distribution of granulation velocities, i.e., the distribution of upward velocities about the mean of the granule velocities and the (different?) distribution of falling velocities about the mean velocity of the dark lanes. The line bisector has proved to be an informative way of expressing observed line asymmetries, although other methods have been used or proposed (Gray, 1980a, 1980b; Bray and Loughhead, 1978). An example of a solar line bisector is seen in Figure 2-14 (see also Adam et al., 1976; Roddier, 1965; Dravins et al., 1981). Bisectors of strong solar lines have a "C" shape showing that the wings and cores have less net blueward displacement than intermediate line depths. Stellar line bisectors show a wider variety of shapes.

What can we expect to learn from such studies? Optimistically, we could learn a great deal, for we begin to get at the photospheric hydrodynamics directly. Our grasp of convection physics is poor and therefore observations of granulation can improve our understanding

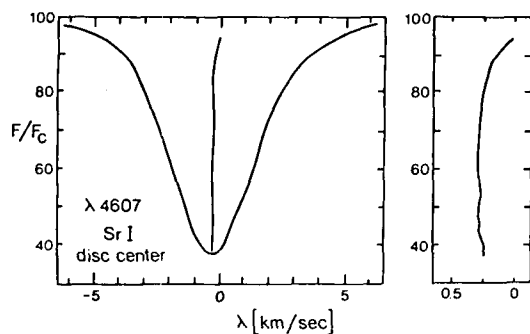


Figure 2-14. The bisector of an unblended solar (disk center) line shows the characteristic C shape. The panel on the right has the wavelength scale expanded by five times compared to the scale for the profile (from Gonczi and Roddier, 1971).

of F-G-K star convection zones and the things which depend on them: convective heat transfer, the generation of oscillations and waves, the support of chromospheres and coronae, mass-loss, and the dynamo generation of magnetic fields.

IV.B. STELLAR ASPECTS OF THE SOLAR GRANULATION

The emphasis here will be on the characteristics obtainable for disc integrated solar radiation, since that is what we have to deal with for all other stars. In particular, we will look at the line bisectors and the asymmetries they represent.

Solar line asymmetries has been an active area of study, although observations have frequently been limited to the center of the solar disc. The initial measurements were those of Voigt (1956, 1959) and Schröter (1957). An extensive list of references to the observations is given by Beckers (1981) and by Dravins (1982). Recent models of granulation have been put forward by Cloutman (1979), Nordlund (1976, 1980), Nelson (1980), and Keil (1980), among others. The most relevant study for stellar purposes is that of Dravins, Lindgren, and Nordlund (1981), which will be abbreviated DLN.

DLN studied 311 FeI lines in the solar spectrum, including measuring their asymmetries and absolute velocity shifts. Further, they showed that the basic properties seen in observations taken at the center of the disc can also be seen in disc-integrated measurements. Although individual line bisectors show many details of interest, means of groups are more informative because the noise and blending are greatly reduced. (In this regard, see also Barambon and Müller, 1979.) Several important characteristics can be seen. First there is the basic "C" shape of the bisectors of the stronger lines, as illustrated in Figure 2-15. All of the absolute shifts (of average bisectors) are toward the blue, with the weaker lines showing the

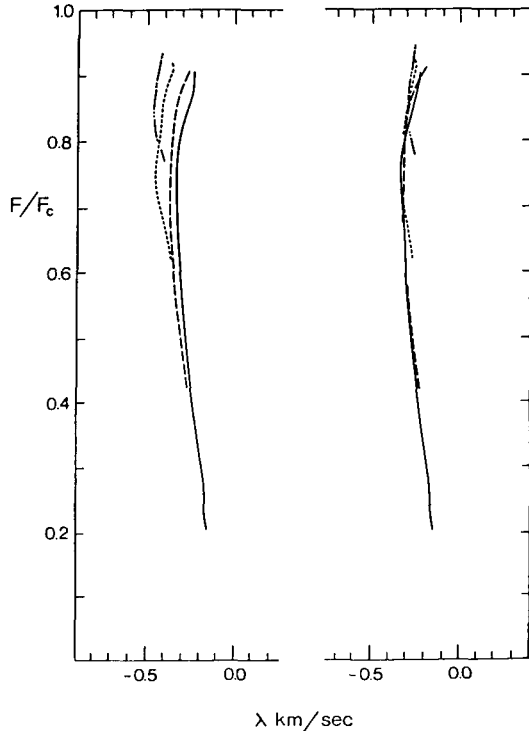


Figure 2-15. Mean line bisectors are shown for the center of the solar disk. Weaker lines (dot-dashed curve) show larger blue-ward displacements (left panel). On the right, the same bisectors are shown shifted in wavelength to illustrate the approximately similar shape of these mean bisectors (adapted from Dravins et al., 1981).

largest displacements. This is readily interpreted in terms of the granulation picture: it is natural to expect the convective velocities to be larger in the deeper layers where the weaker lines are preferentially formed; hence the greater shifts for the weaker lines.

The same phenomenon explains the reduced blue displacements of the cores of the stronger lines, although here the diminishing, with increasing height, of both the convective velocities and flux contrast contributes. The bend toward zero velocity in the upper portion of the bisectors results from downward moving gases having larger velocities than the granules. Bray et al. (1976), for example, find

the average granule rises at 0.7 km s^{-1} , while the material in the dark lanes falls at 1.1 km s^{-1} . DLN favor slightly higher velocities in both directions. Matting (1980) measures the mean vertical granule velocity to be near one km s^{-1} . The full height variation for both the vertical and horizontal components of the granulation velocity has been determined by Keil and Canfield (1978). They find the mean horizontal velocity to range from 3 to $\sim 0.5 \text{ km s}^{-1}$ through the photosphere, while the vertical component is ~ 1.0 to 1.5 km s^{-1} less, but mimics the same decrease with height. Keil and Yackovich (1981) also find that a rapid decrease in granulation velocity with height is needed to explain the solar line asymmetries. Durrant et al. (1979) find a much weaker height dependence.

The DLN solar observations show clear excitation and ionization dependences, a result of the higher energy transitions being formed in the hotter deeper layer where the velocities are also greater.

Finally, there is a mild wavelength dependence arising from the net combination of the competing effects of Doppler shifts (proportional to wavelength) and granulation contrast (nearly proportional to inverse wavelength). Figure 2-16 shows the effect. This is one important example of an effect that is not proportional to wavelength, even though it is rooted in the Doppler displacements of the spectral lines.

We can expect to find all of these same features in stellar spectra, but we must bear in mind that the absolute velocity is not known because of the arbitrary radial velocity of the star.

IV.C. OBSERVATIONS OF STELLAR GRANULATION

Although most of our knowledge of stellar granulation stems from the asymmetries of the lines, the first observational hint of stellar

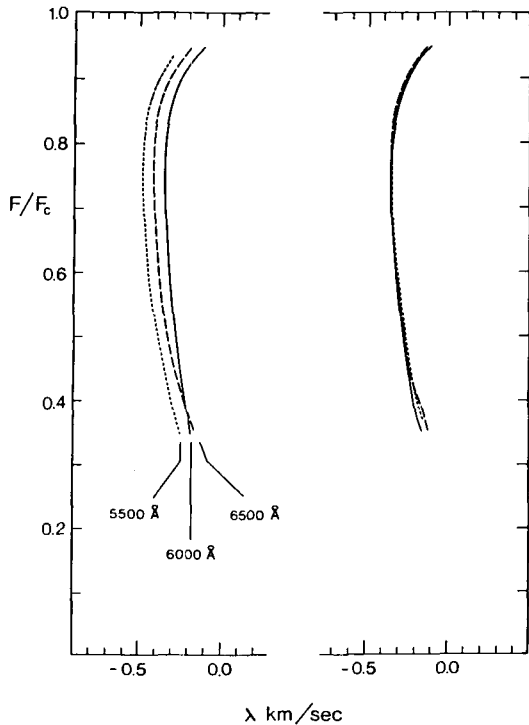


Figure 2-16. Mean bisectors for the center of the solar disk are shown for three wavelength regions (left panel). The right panel shows the same three bisectors shifted in wavelength to show that their shapes are the same (adapted from Dravins et al., 1981).

granulation came from differential radial velocity shifts and their correlation with excitation potential, χ , of the line (Dravins, 1974, 1976). A more extensive work is that of Stawikowski (1976), summarized by Glebocki and Stawikowski (1980). The relations for Procyon and Arcturus are shown in Figure 2-17. The interpretation is that lines of higher excitation potential are formed deeper in the photosphere where the granulation velocities are larger. This is similar to the interpretation for Figure 2-15 above. It is difficult to press this kind of data for further physical interpretation because the actual depth of formation of a line depends on more than χ and frequently spans a substantial portion of the photospheric thickness. Equally difficult is the question of what part of the profile is used by the human eye when a radial velocity is measured.

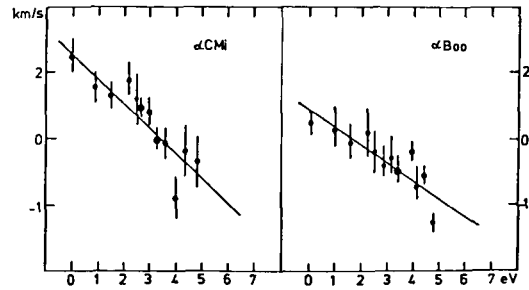


Figure 2-17. Relative line shifts are shown as a function of excitation potential (from Glebocki and Stawikowski, 1980).

Stellar line asymmetries (of the convective type) were first discovered in the spectrum of Arcturus (Gray, 1980a, 1980b), for which Figure 2-18 shows an example, and shortly thereafter for Procyon (Gray, 1981d). An extensive study (Gray, 1982a) of F-G-K giants and dwarfs, using line bisectors, shows not only evidence for the universal existence of stellar granulation, but some interesting trends with spectral type as well. As with the solar case, average line bisectors are found to be useful. Line blending is so serious that frequently only a portion of the bisector can be used. Further, the radial velocity of the star prevents the use of absolute wavelength displacements; so one may as well ignore the absolute shifts and collect all of the measurements for each star into one mean bisector, thereby gaining a higher signal-to-noise ratio. Within the errors of the stellar measurements, all strength lines (in each star) show the same shape bisector (refer to Figures 2-15 and 2-16). In using such a mean, one ignores slight differences in shape with depend on excitation, ionization, line strength, and wavelength.

It is also found that stars of the same spectral type show similar mean bisectors, leading us to construct one grand mean for each position in the HR diagram. Such means are displayed in Figure 2-19. Recent unpublished measurements by S. Ridgway using the Kitt Peak IR Fourier transform spectrometer show that CO-band lines in late-type giants also have qualitatively similar asymmetries (see also

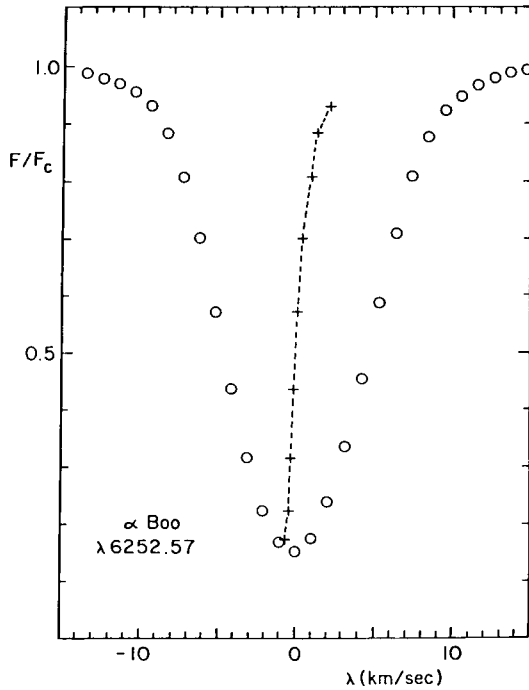


Figure 2-18. The asymmetry in $\lambda 6252.57$ in the spectrum of Arcturus is shown by means of the bisector (crosses and dashed line). The wavelength scale of the bisector is expanded to ten times the scale of the profile itself and the zero position is arbitrary. This method of describing the asymmetry can be contrasted with the portrayal of Figure 2-2. The bisector gives more information but requires finer sample spacing (from Gray, 1982a).

Ridgway and Friel, 1981). One is immediately struck by some similarities to the solar behavior and by some differences as well. All spectral types seem to show the redward displacement in the line wings (relative to the rest of the profile), that is, the top of the "C" is present in all of the stars that were observed. But the lower portion of the bisectors are not generally like those seen for the solar lines. It is true, however, that other early G dwarfs show the full "C" shape.

It has been shown (Gray, 1982a) how the upper halves of the mean bisectors can be scaled (Figure 2-20), and hence all of them have similar shape. This in turn implies that granulation in

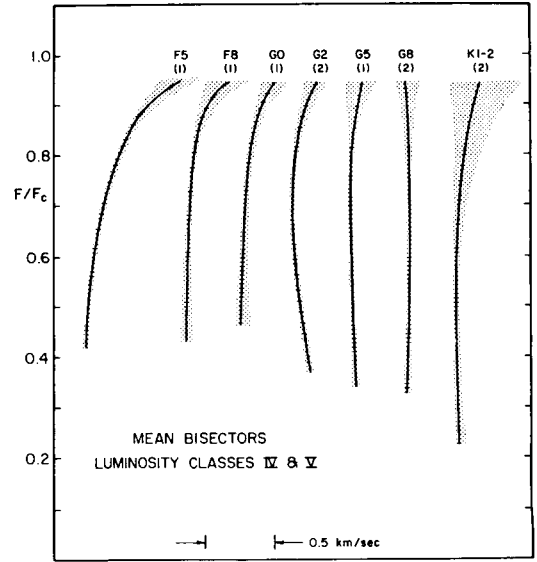


Figure 2-19a. Luminosity classes IV and V stars show mean bisectors with a variety of shapes but with some systematic trends, as a function of spectral type. The C shape is seen only for stars near the sun in the HR diagram. The number of stars entering the means is shown above the bisectors (from Gray, 1982a).

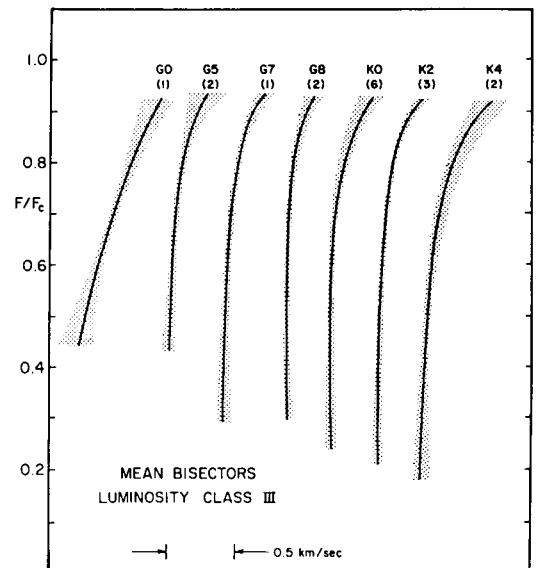


Figure 2-19b. Mean bisectors for luminosity class III are shown as a function of spectral type.

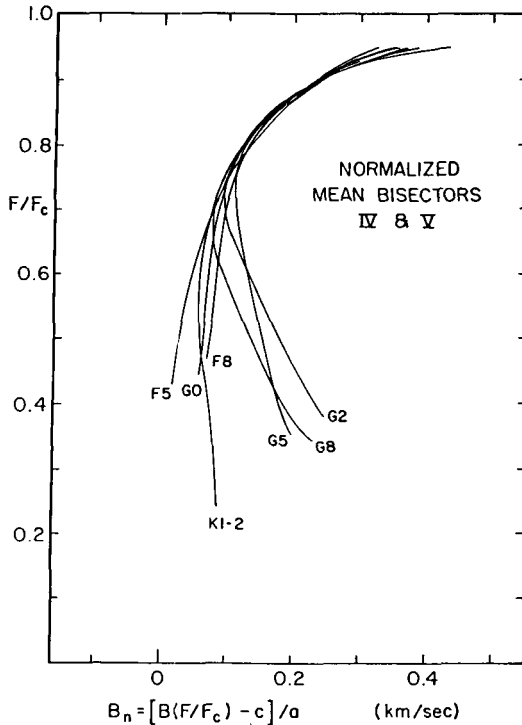


Figure 2-20a. The lower luminosity group bisectors are shown in normalized form. The normalization is brought about by determining the linear scale constants a and c from a parametric plot of bisector displacement (wavelength), with F/F_c as the parametric variable. The upper halves of the bisectors show a unique shape while the lower halves show a systematic change with spectral type (from Gray, 1982a).

all stars has a high flux contrast since the curvature of the top of the bisector depends strongly on the flux contrast (see also Gray and Toner, 1985). The scaling property can then be used to circumvent the lack of absolute zero in the stellar measurements by including the mean solar bisector in the scaling and using its absolute wavelength. Figure 2-21 then shows the mean stellar bisectors on an absolute wavelength scale. For both luminosity class groups, there is a systematic march of the bisectors with spectral type, starting at high blueshifts, dropping toward zero, and then moving blueward again. Using the deduction that the flux contrast is universally high, it

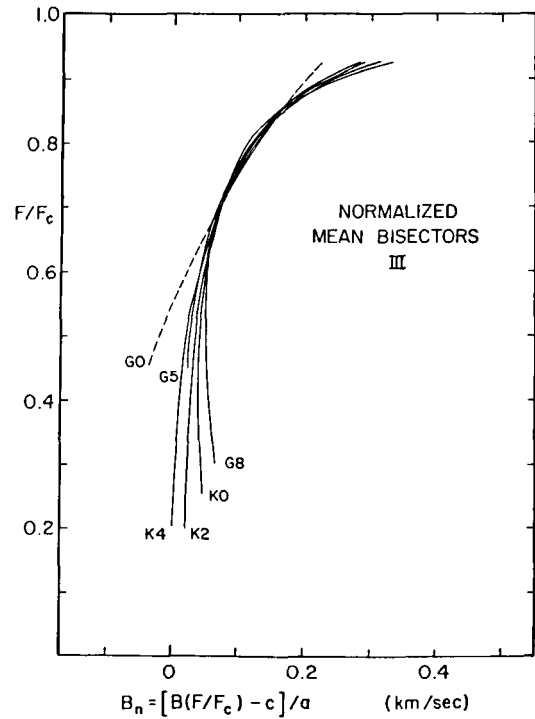


Figure 2-20b. The scaling is shown for the higher luminosity class. The systematic changes in the lower halves of these normalized bisectors show less amplitude but the same qualitative behavior as seen on the a) part of the figure (from Gray, 1982a).

follows that the displacements of these bisectors are proportional to the apparent granulation velocities. In this manner the results of Figure 2-22 were obtained. The apparent granulation velocities for both luminosity groups seem to show a minimum toward late G stars. The relation for the giants is systematically higher by about the solar value. No explanation has yet been offered for either the temperature or the luminosity dependence.

IV.D. COMPLICATIONS WHERE SPATIAL RESOLUTION IS LACKING

We can anticipate certain complications in the interpretation of stellar line bisectors, compared to solar ones, because of the disk-integrated nature of the stellar observations.

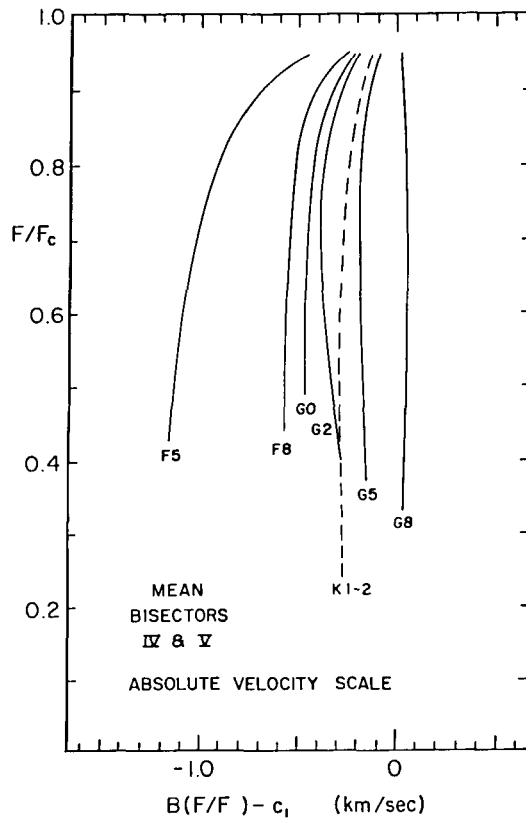


Figure 2-21a. Using the solar mean bisector, the scaled mean bisectors of the previous figure can be plotted on an absolute scale, as shown. The data for luminosity classes IV and V are shown here (from Gray, 1982a).

First, the “Expanding Star Effect” of the granulation (Gray and Toner, 1985) introduces curvature in stellar bisectors opposite the observed curvature, an effect that must be overridden by the contributions from the falling material to produce what we see. The Expanding Star Effect arises because granules dominate the light of the star, and they are all moving outward as if the star were expanding. The distribution of Doppler shifts from the granules will show a tail toward the blue, and the size of the tail depends on the mean absolute velocity of the granules relative to the star. Even though the velocity of the star relative to us blocks our ability to measure absolute velocities, the Expanding Star Effect requires that we include not just the velocity differences

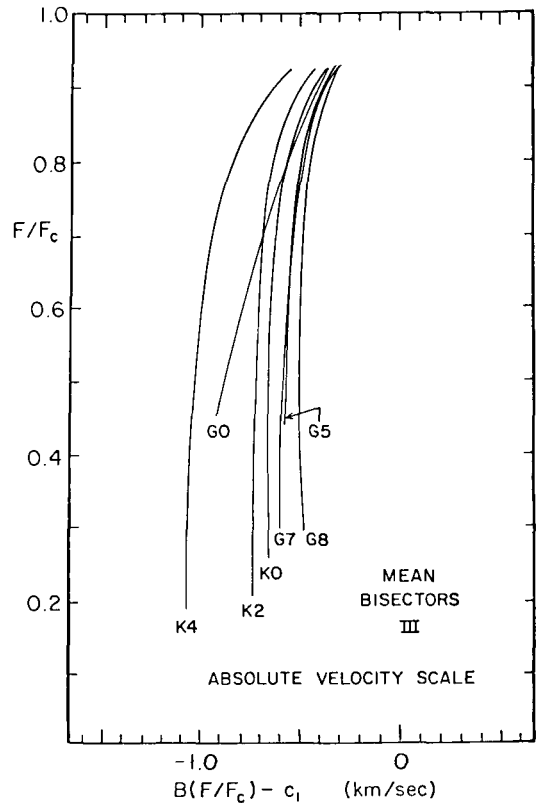


Figure 2-21b. The mean bisectors of the giants are shown on an absolute scale.

between granules and lanes, but absolute velocities, in our modeling.

Second, rotation will produce alterations in the bisector shapes because it redistributes the Doppler shifts. Figure 2-23 shows a simplistic modeling of the effect of rotation. Since many F-G-K stars are slow rotators, the complications will be relatively small, but for $v \sin i$ greater than or similar to the granulation velocities, much larger alterations can be expected. Rotation effects in bisectors have not yet been observed.

IV.E. COMMENTS

Some types of star, supergiant F stars for example, are known to show line bisector radically different from those discussed above (Dravins, 1983, Gray and Toner, unpublished data).

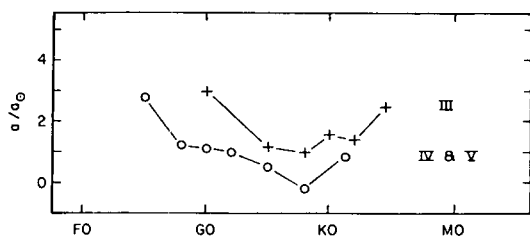


Figure 2-22. The granulation velocities are shown as a function of spectral type for the two luminosity groups, as labeled (from Gray, 1982a).

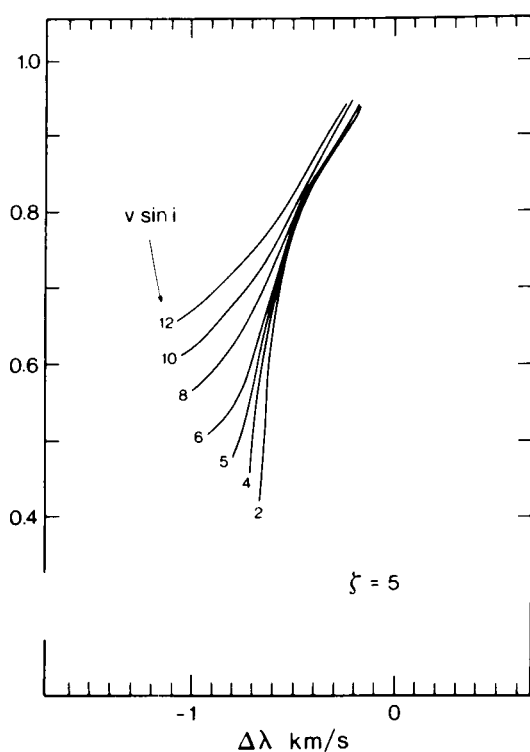


Figure 2-23. The redistribution of Doppler shifts by rotation causes the line bisector to be altered. The strength of the effect depends on the mean velocity of rise of the granules. (Approximate numerical simulation from Gray and Toner, 1985.)

As we shall see below (Chapter 2.VII.C), the granulation may be significantly affected by the strength of the magnetic field permeating the photosphere. The Sun shows a decrease in

granulation velocities and an increase in the number of granules with increasing magnetic activity. Increasingly strong evidence points toward concentration of magnetic field in the dark lanes (see the summary by Beckers, 1981).

Another way to tap inhomogeneities in photospheric structure is through the non-LTE pumping of the FeII $\lambda 3969.4$ line (Cram et al., 1980), but this tool has yet to be applied to stars.

V. ROTATION

V.A. INTRODUCTION

A superficial glance might lead one to expect no connection between the rotation of a star and the dynamics of the stellar atmosphere. But in fact, the rotation can modify the convection patterns in F-G-K star envelopes, it can nurture strong and weak magnetic fields via dynamo action, and it can modify the mass loss and the evolutionary changes of the star. Many secondary features are generated or shaped by these events: cyclic chromospheric activity, generation and strength of starspots, magnetic braking of the rotation, funneling of waves and escaping particles via magnetic forces, the molding of the coronal fields and the X-ray generation, and possibly also the magnetic inhibition of convection. Stellar rotation is a very important driving force in photospheric dynamics.

Two basic methods have been used for measuring stellar rotation rates. The classical approach is to look at the spectral line broadening caused by the differential Doppler shifts across the apparent disk of the rotating star. This method was invented and developed by Rossitter (1924), McLaughlin (1924), Shajn and Struve (1929), and others, and was used extensively by the observers through the middle of the century, e.g., Westgate (1933a, 1933b, 1934), van Dien (1948), Huang and Struve (1953), Huang (1953), Herbig and Spalding (1955), Oke and Greenstein (1954), Slettebak

(1954, 1955, 1956, 1968), Abt (1957, 1958), Abt and Hunter (1962), Abt and Chaffee (1967), Kraft (1965, 1967), Anderson et al. (1966), Slettebak et al. (1975). The method works well for stars where rotation clearly dominates the line broadening, i.e., the early spectral type stars. For G and K stars, rotation must be identified and measured in the presence of the larger macroturbulence broadening. Fourier transform techniques have proved to be a useful tool for the job (refer to Chapter 2.III.F).

All methods using the Doppler effect necessarily yield a projection of the rotation according to the orientation of the axis. There is some evidence for random orientations of rotation axes (Struve, 1945a, 1945b; Slettebak, 1949; Huang and Struve, 1954). The presence of galactic rotation does not seem to influence the orientation of axes, and even cluster stars which share some common origins seem to show random orientations (but see Huang and Struve, 1960 and Rajamohan, 1978). On the other hand, stars in binary systems are likely to show some alignment of rotation and orbital axes (Weis, 1974). Generally speaking though, it is $v \sin i$ that is measured, and the Doppler broadening from rotation drops to zero for a star seen pole-on. The statistical correction from a mean $v \sin i$, $\langle v \sin i \rangle$, to a mean v , $\langle v \rangle$, is given by $\langle v \rangle = 4/\pi \langle v \sin i \rangle$. The Doppler method is applicable to all F-G-K stars, but as $v \sin i$ becomes small compared to other broadening agents, the errors on $v \sin i$ rise.

A second method for measuring rotation is to look for periodicities that can be associated with the appearance and disappearance of features, such as spots or active areas, moved across the visible half of the star by the rotation (Kron, 1950; Eaton and Hall, 1979; Blanco et al., 1979a, 1979b; Stimits and Giles, 1980; Rucinski, 1980). Actually, the concept here has long roots, for, as the Durants (1961) and Bray and Loughhead (1964) point out, Johannes Fabricius and Galileo Galilei independently deduced the rotation period of the Sun from

the periodicity of sunspots in 1611. The most extensive period measurements for other stars have relied on the modulation of the CaII H and K line core emission. The method grew out of the extensive work on stellar cycles by Wilson (1978) and the observed solar modulation (Jebsen and Mitchell, 1978; LaBonte, 1982). It has been carried forth by Vaughan and Preston (1980); Vaughan et al. (1981); and Baliunas et al. (1982). Apparently, active regions on the surface of the majority of stars are far from uniformly distributed and have a lifetime of at least several rotation periods. This in itself is significant information toward a comprehensive understanding of stellar atmospheres, but, for this discussion, we shall concentrate on the rotation periods it yields.

With period studies, projection effects are not important because it is v , not $v \sin i$, that is finally obtained. Of course, if the star is seen too close to pole-on, rotation will not cause the disappearance and re-emergence of surface features, and no rotational periodicities would be seen. For stars off the main sequence, uncertainties in radius may render the conversion of period to v uncertain. The periodicity method is primarily applicable to cooler stars where the H and K line emission, spots, and other surface inhomogeneities are strong. In this respect, the two methods of measuring rotation complement each other, since the cooler K and the M dwarfs are difficult to handle with Doppler broadening. A variant of the periodicity method, using time-moving features in the profiles of more rapidly rotating stars, may also prove useful in rotation studies (refer to Chapter 2.VI.A below).

V.B. THE GIANT STARS

The rotation of giant stars is a good place to start with the observational results because several key issues can be isolated. Post-main sequence evolutionary changes of giants produce nearly horizontal tracks in the HR diagram, and a spectral sequence corresponds to an age

or time sequence. This is very different than the main sequence case where the star remains at essentially constant spectral type for long periods of time, making age discrimination a much more difficult and subtle task. Rotation rates of giant stars have been measured by Alshuler (1975), by the author (Gray, 1975, 1981a, 1981b, 1981c, 1982d; Gray and Martin, 1978), and by Smith and Dominy (1978). Earlier measurements of cooler G and K stars gave only upper limits.

The observations show a rather interesting behavior, as illustrated in Figure 2-24. The run of rotation to the left of G5 III is in excellent agreement with model envelope calculations (Endal and Sofia, 1979; Gray, 1982d). The implication is that the star's internal moment of inertia is in full control of the surface rotation rate up to this point. But at G5 III there is about a five-fold decrease in the observed rotation! Apparently a rather strong brake is suddenly and effectively applied to the star, since the star does not have enough time to evolve more than a few tenths of a spectral class before the whole process is completed.

Model envelope calculations (Gray and Endal, 1982) show that deep convection starts as a star evolves into the G-star region and grows in depth monotonically toward cooler surface temperature. The continuous increase in depth of the convection zone combined with the short convective turnover time (\sim months) show that inward transfer of angular momentum, which would then be a slow continuous process with advancing spectral type, cannot explain the discontinuity at G5 III.

The rotational discontinuity may result from the application of a magnetic brake. Magnetic brakes have often been discussed in the past (e.g., Huang and Struve, 1960; Schatzman, 1962; Kraft, 1970; Mullan, 1976; Weber and Davis, 1967; Belcher and MacGregor, 1976; Barker and Marlborough, 1982; MacGregor and Pizzo, 1983). Ionized material escaping from the star in the form of winds and from

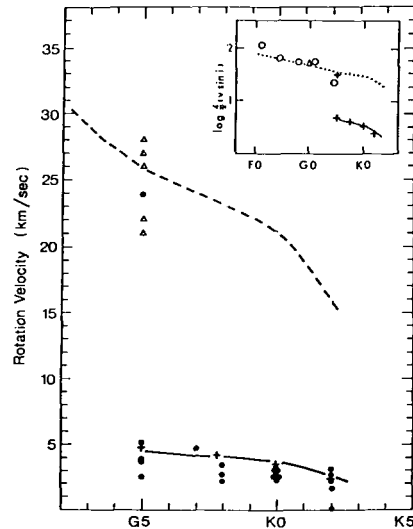


Figure 2-24. Projected rotation velocity is shown as a function of spectral type which for giants is also an evolutionary sequence. The dots represent $v \sin i$ obtained by Fourier analysis while the triangles are taken from the catalogue of Uesugi (1976). Crosses are the means of groups by spectral intervals increased by $4/\pi$ to remove the systematic effect of projection. The dashed line is the computation of expected rotation according to Endal and Sofia (1979). The solid line is the dashed line scaled down by 5.7 times. In the inset graph, the circles are mean values for the spectral classes according to Fukuda (1982), the triangle is the mean for G0 by Alshuler (1975), and the crosses are from the main figure (from Gray, 1982d).

eruptions will become caught up in and channeled by the field lines. The escaping material is disengaged from the magnetic field only at several hundred stellar radii, and so it carries away large amounts of angular momentum, dissipating the star's rotation.

A dynamo generated field is a natural choice, since two ingredients, rotation and convection, are needed to drive it, and it is precisely through the G-giant interval that convection is added to the rotation. We might also expect a stronger

brake to be generated by faster rotators—an effect that would sharpen the discontinuity. As seen in Figure 2-24, the observed discontinuity is rather sharp.

Additional information in Figure 2-24 is important: the giant stars all evolve away from G5 III with the same rotation velocity of about 5 km s^{-1} . Further, the distribution of $v \sin i$ for the post-brake phases (from G5 to K2) indicate one unique rotation rate at each point along this sequence, i.e., a δ -function velocity distribution, as it is sometimes called (Gray, 1982d).

The cessation of the strong brake may result from a major restructuring of the dynamo brought on by the rotation being reduced to the low value of 5 km s^{-1} . It might also be related to a change in the brake mechanism external to the star. Belcher and MacGregor (1976) have shown that, when rotational energy dissipation dominates the thermal component of the stellar wind, the braking is much stronger than for the inverse case. The transition to the thermally dominated situation may occur in giants at a rotation of 5 km s^{-1} .

Magnetic braking can be expected to slow the rotation of the envelope, but probably not of the core of the star. If so, then another important conclusion follows from the slow decrease in rotation from 5 km s^{-1} at G5 III to 2.5 km s^{-1} at K2 III, namely, as the convective envelope deepens, material from the rapidly rotating core will be annexed into the convection zone. This would increase the surface rotation again. Since the observations show a decrease, not an increase, some braking must continue to occur over the G5 III to K2 III interval.

Couple this with the δ -function velocity distribution seen for these stars, and one is led to suspect that an equilibrium exists in which the evolution of the star carries it along a precise rotation boundary above which strong braking occurs.

X-ray observations (Aryes et al., 1981) show a wide range of emission strength for giants earlier than G5 III, but beyond G5 III the giants are X-ray quiet. The X-rays are presumed to originate in the closed magnetic loops of coronae, as they do in the Sun. At the same time, radio observations at 5 GHz (Gibson, 1984) show the inverse behavior: no emission until the giants pass the G5 III discontinuity. Simon (1984) finds a decline in the strength of chromospheric-coronal material ($T \sim 10^5 \text{ }^\circ\text{K}$) in the G0 III to G5 III span. Several other studies have been made of the relation of rotation to chromospheric and coronal emissions, for example, Ayres and Linsky (1980); Walter and Boyer (1981); Pallavicini et al. (1981); Walter, 1981, 1982). Rotation is clearly a driving force in these activities.

V.C. ROTATION OF SUBGIANTS

A recent study of subgiants shows a rotational discontinuity near G0 IV (Gray and Nagar, 1985). See Figure 2-25. Rotation is less than 4 km s^{-1} for stars later than G0 IV. Not all of the stars in the G0 IV to K5 IV interval were rapid rotators on the main sequence

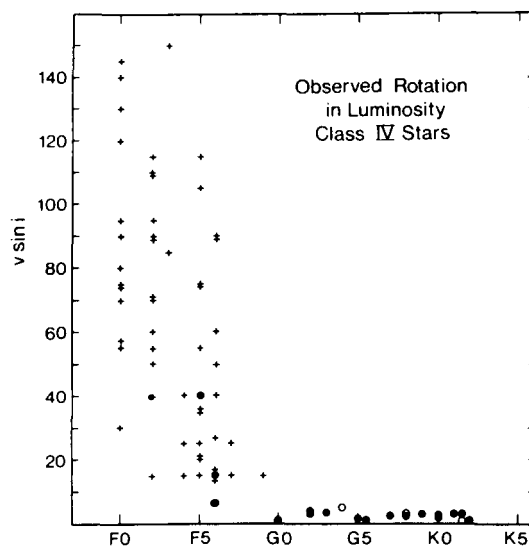


Figure 2-25. The rotational discontinuity in luminosity class IV is seen near F8-G0. (From Gray and Nagar, 1985.)

(unlike the class III giants), but all of the late F-stars on the lefthand side of the diagram are expected to evolve across the G0 to K5 span. Apparently they abruptly lose their angular momentum as they cross over. It would seem that the rotational braking and the dynamo hypothesis, discussed above with regard to the giants, also has application to the subgiants.

V.D. THE MAIN SEQUENCE STARS

The spectral-type dependence of rotation for main-sequence stars is one step more complicated than for the giants because the variables of effective temperature and age are now decoupled. One of the early discoveries was that characteristic rotation rates diminished rather rapidly from late-A through mid-F stars, as is shown in Figure 2-26. Prior to the 1970's, limited spectral resolution and signal-to-noise ratios precluded the detection of $v \sin i$ much below 10 km s^{-1} , so the details of behavior for late F and cooler dwarfs could not be established. Had the rotation been high, however, it would have been spotted easily enough, so it was known that the F-G-K dwarfs

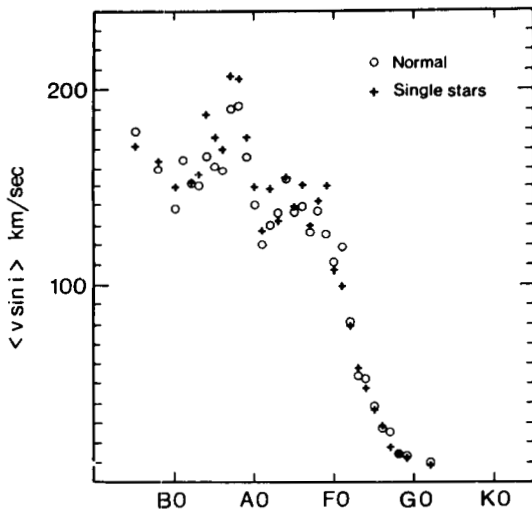


Figure 2-26. Mean rotation is shown as a function of spectral type. The well-known drop in the F stars can be seen (based on Fukuda, 1981).

were slow rotators, but nothing more was known. Recent results obtained by Smith (1980b), Soderblom (1982), and Vaughan et al. (1981) using newer equipment and techniques are plotted in Figure 2-27. It is seen there that the average rotation continues to decrease from G0 V through the K dwarfs—a sort of tail on the major drop from the A stars. There is an upper bound on the rotation seen in Figure 2-27.

The upper bound can be understood by drawing a parallel between the time changes of the rotation for dwarfs and for giants (Gray, 1982c). We suppose that the evolutionary changes in rotation seen in Figure 2-24 (and in Figure 2-25) also occur for dwarfs, with the numerical details being appropriate for dwarfs and dependent on position along the main sequence. First, a strong dynamo brake phase would occur during a star's pre-main-sequence evolution and/or soon after its arrival on the main sequence. This is expected simply because

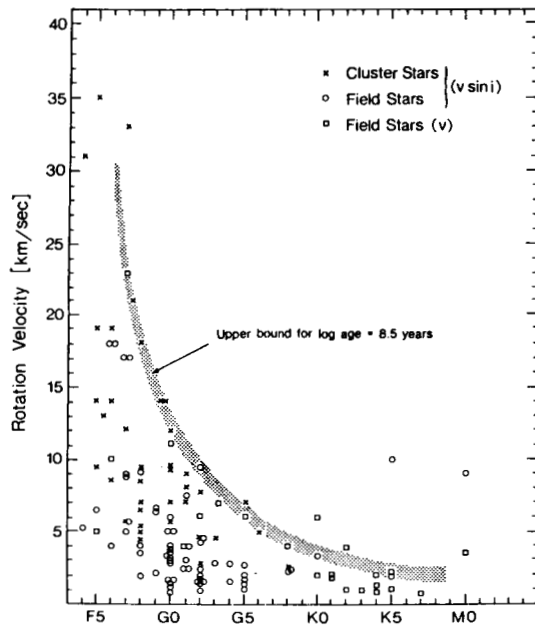


Figure 2-27. Rotation values for main sequence stars are shown as a function of spectral type. The upper bound is indicated by the shaded strip (from Gray, 1982d).

both rotation and extensive convection occur in the “adolescent” life of a star. (We saw what such a combination does for the G giants.) Second, the strong brake turns off abruptly at a rotation rate dependent on the internal structure of the star and hence on its spectral type. Third, there follows a period of weak braking or slow decline in rotation (see below). According to this picture, there should be a sharp upper bound on the rotation, variable with spectral type, and that is what is seen in Figure 2-27. The upper bound itself is, if properly decoded, a map of the strong-brake turn-off velocity versus spectral type.

One expected result of the process described is the destruction of any initial distribution of rotation velocities. The cessation of the strong brake occurs at a rotation velocity unique to each point along the zero-age main sequence (Gray, 1981c, 1982c). Additional observational evidence in support of a δ -function velocity distribution for main sequence stars has been given by van Leeuwen (1983), Duncan (1983), Rengarajan (1984), Duncan et al. (1984), and Stauffer et al. (1984). As with the giants, the physics of these processes is still obscure. Rotation shown in Figure 2-27 can lie below the upper bound because (1) the $\sin i$ factor causes a spread downward from the equatorial rotation rate, and (2) the sample of stars covers a wide range in age with the older stars showing rates below the upper bound.

Let us turn now to this slow time decrease in the rotation that occurs while the star is spending time on the main sequence. Early studies of the main sequence age dependence were done by Wilson (1966b), Kraft (1967), and Skumanich (1972). They showed that age differences could be seen and that the dwarfs spin down in proportion to $\text{age}^{-1/2}$. Figure 2-28 shows the relation based on the rediscussions of Smith (1980b) and Soderblom (1982). (It should also be noted that the chromospheric activity ages in this same manner, although perhaps with a shorter time-scale, as documented by Wilson and Skumanich (1972),

Vaughan (1980), Vaughan and Preston (1980), Mielbrecht and Young (1981), and Middlekoop (1981). The chromospheric aspects are discussed in another chapter of this volume.) The magnetic brake producing the slow spin-down is partially understood, and several variants of the story have been presented, for example, by Huang (1967a), Kraft (1970), Carrasco et al. (1980), and Soderblom (1982). A great deal of work has centered on the solar dynamo. The reader is referred to articles in the solar volume of this series (Zwaan, 1981; Gilman, 1981; Spruit, 1981) and to the chapter in this F-G-K volume by Zwaan.

The evolution of main sequence rotation can also be followed in the angular momentum-mass plane. McNally (1966), Kraft (1968, 1970), and Dicke (1970) considered the angular momentum versus mass relation. The recent lower-main-sequence observations allow us to extend this relation to lower masses, as is illustrated in Figure 2-29. Because we do not know the angular momentum distribution within the star, Figure 2-29 uses a pseudo-angular momentum given by $L = MRv$ where M is the mass, R the radius, and v the rotational velocity. The upper main sequence shows the well known $M^{3/2}$ relation (or specific angular momentum proportional to $M^{3/2}$). This may reflect, at least statistically, uniform angular momentum per unit mass allotted to stars at their birth (Dicke, 1970). A dramatic deviation

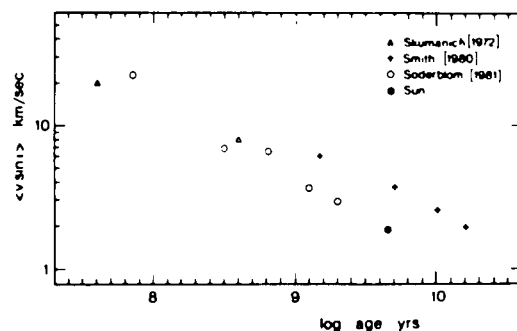


Figure 2-28. Rotational velocities decrease with age approximately as $\text{age}^{-1/2}$.

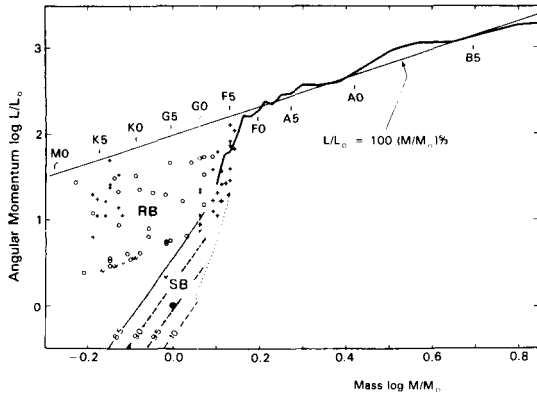


Figure 2-29. The pseudo-angular momentum, $L = MRv$ is shown as a function of mass. The $5/3$ -power dependence is seen to describe the early-type stars and forms an upper envelope to the “rapid braking region” (denoted by RB) for late-type stars. Points in the RB domain are for relatively young clusters: α Per (Stauffer et al., 1985b) and the Pleiades (van Leeuwen and Alphenaar, 1982). Upper limits are shown as v’s. The “slow braking” (SB) region contains most of the F-G-K stars. Lines of \sim constant age are labeled with log age; they show a ~ 7 th power dependence on mass. The line labeled 8.5 corresponds to the upper bound in Figure 2-27. Rotation rates should not fall below the dotted line before evolution takes the stars off the main sequence.

from the $M^{5/3}$ relation occurs for the lower-mass stars, where individual values populate the whole domain. F, G, and K dwarfs probably start with angular momentum near the $M^{5/3}$ line, but then move rapidly downward in this diagram during the rapid braking (RB) phase. The points in the region labeled RB are young Pleiades and α Per cluster stars. Older main-sequence stars in the slow braking phase populate the shaded region labeled SB. The line labeled 8.5 corresponds to the upper bound shown in Figure 2-27 (at an age of $10^{8.5}$ years). The majority of main sequence stars, for obvious reasons, lie within the SB region.

Rotation in pre-main sequence stars has been studied by Vogel and Kuhl (1981) and Kuhl (1983). The change in rotation of stars contract-

ing to the main sequence has been discussed by Stauffer (1985a). The relation between rotation and starspots is considered in Chapter 2.VI.C.

V.E. ROTATION IN HIGHER LUMINOSITY CLASSES

We know relatively little about the rotation in F-G-K stars of luminosity classes I and II. Preliminary studies (Gray and Toner, 1985) show that $\langle v \sin i \rangle \sim 6 \text{ km s}^{-1}$ for II’s and $\sim 8 \text{ km s}^{-1}$ for Ib’s are compatible with the line broadening for several dozen G and K stars. At the time of this writing, we are not certain that the usual radial-tangential formulation for macroturbulence is applicable to these stars, making its separation from rotational broadening suspect. We do know that a substantial portion of the line broadening is not due to rotation because there are no narrow-lined stars in these luminosity classes, i.e., the $\sin i$ projection factor does not dominate in any of them. Consequently, rotation cannot be much larger than the $6\text{--}8 \text{ km s}^{-1}$ quoted above.

Periodic variations in MgII h and k lines have recently been measured by Brosius et al. (1985) for a sample of eight stars, five of which are luminosity class Ib or II. Interpreted as rotational modulation, their results are consistent with line-broadening measurements for the four stars of their eight having $v \sin i < 10 \text{ km s}^{-1}$. For the others, they deduce substantially higher rates, up to 42 km s^{-1} in the case of θ Her (K1 IIa), which is not compatible with the general line-broadening results of I’s and II’s. [But note: rotation in horizontal branch stars is surprisingly high in some cases (Peterson et al., 1983).] Some interesting research remains to be done here.

V.F. DIFFERENTIAL ROTATION

Most theoretical modeling in which the interaction of rotation with convection is considered conclude that some sort of differential

rotation ought to occur (e.g., Durney and Latour, 1978; Gilman, 1980; Belvedere et al., 1980). The rotation varies with depth and with latitude on the star. These effects were observed on the Sun 120 years ago by R.C. Carrington (Meadows, 1966), but more recently in great detail (e.g., Wilcox and Howard, 1970; Howard, 1975; Kearns, 1979; Rhodes et al., 1979; Deubner et al., 1979; Ulrich et al., 1979; Balthasar and Wöhl, 1980; Scherrer et al., 1980; Claverie et al., 1981; Cram et al., 1983; Snodgrass, 1983; Durney et al., 1984). It may also be noted in passing that Doppler measurements of the solar photosphere show a distinctly slower rotation by 1–4% compared to some magnetic tracers such as spots and faculae. Figure 2-30 shows the smooth monotonic decrease of rotation with latitude as delineated by sunspots. A change of $\sim 20\%$ occurs from equator to poles. The angular-velocity latitude dependence is frequently approximated by polynomials such as $\omega = a + b \sin^2 \phi + c \sin^4 \phi$, where ϕ is the latitude (Howard and Harvey, 1970). A summary of such details is given by Schröter and Wöhl (1978). Variations in differential rotation with phase in the 11 year cycle are discussed by Howard and LaBonte (1983). Although non-radial oscillations allow a depth probe in the Sun, the results for $\omega(r)$ are not yet definitive. Deductions from stellar non-radial oscillations of F-G-K stars have not yet begun as of this

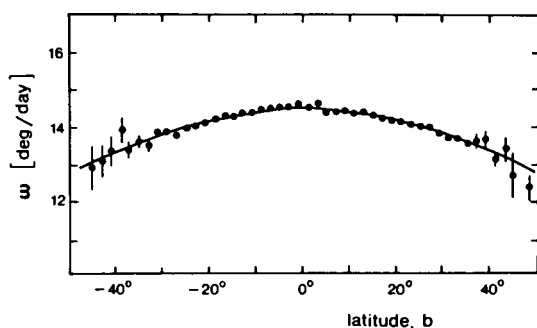


Figure 2-30. The solar differential rotation as delineated by sunspots occurring between 1940 and 1968 is shown. The curve is $\omega = 14.525 - 2.83 \sin^2 b$ (from Balthasar and Wöhl, 1980).

writing (see Chapter 2.VIII), and so we shall confine our attention here to the latitude effect.

Differential rotation will introduce identifiable characteristics into the line profiles and their transforms (Gray, 1977a; Bruning, 1981; Garcia-Alegre et al., 1982; Wöhl, 1983). If we had only rotation and its differential effects to handle, we would be quite capable of measuring details like those seen on the Sun and even smaller. But nature has deemed the stars with convective envelopes (and hence differential rotation) to be relatively slow rotators. For slow rotators, the line broadening is strongly affected, indeed often dominated, by macroturbulence, and the features produced by differential rotation are diluted by a significant factor.

High signal-to-noise ratio observations of main sequence F stars showed upper limits on differential rotation that are significantly lower than the solar amount (Gray, 1982b). Figure 2-31 shows one example. There are several possible explanations for this negative result (e.g., Belvedere and Paterno, 1983; Gray, 1982a; Moss and Vilhu, 1983), but the obvious thing to do next is to try similar measurements in cooler stars. It will not be an easy task. In fact, just measuring rotation itself against the larger macroturbulence can be difficult.

It may be more promising to pursue the method of periodicities. Suppose we do have solar type differential rotation in G and K stars. If we can measure the modulation of starspot-associated activity, and if that activity has a latitude dependence after the manner of the Sun, then, during what corresponds to the solar 11 year cycle, we should see a systematic decrease in the rotation period as the activity moves to lower latitudes. Information of this type is beginning to trickle in. Vogt (1981b), for example, deduced a differential rotation in BY Dra from spot migrations that is very similar to the solar value, $d\omega/d\phi \sim 10^{-8} \text{ rad sec}^{-1} \text{ deg}^{-1}$. Hallam and Wolf (1981) suspect a differential effect in their UV line measurements of six F-G-K stars. Mullan (1975) considers

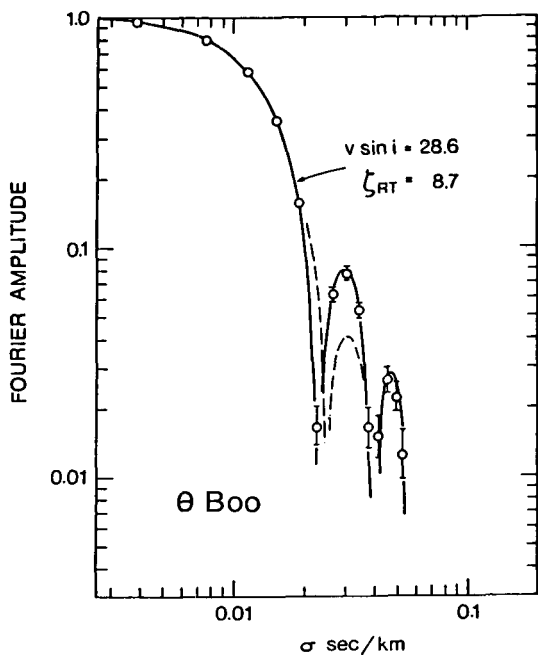


Figure 2-31. The mean residual transform of lines of θ Boo is indicated by circles. Error bars are shown. The continuous curve is for the model having rigid rotation with parameters as labeled. The dashed curve is for differential rotation that is approximately twice as large as the Sun's (based on Gray, 1982b).

related material on W UMa-type binaries. Rotational modulation of stellar H and K line emission may not be useful in this context since the solar measurements do not show the effects of differential rotation (LaBonte, 1982; Drescher et al., 1984), perhaps because the latitude span of plage areas is too large.

VI. STARSPOTS

VI.A. EVIDENCE FOR STARSPOTS

Signs of spots on the surface of stars can be found in both the photometric and the spectroscopic data. Spots were invoked many years ago for various reasons, but the thread of recent research starts with the suggestion by Kron (1950) and, somewhat later, by Krzeminski (1968) that certain low-level photometric

modulations are the result of the passage of a spot carried across the visible disk of the star by its rotation.

We can hardly assume it is coincidence that the stars showing evidence for spots lie on or near the lower main sequence, that part to which the Sun also belongs, and where we have convection zones, rotation, and dynamo activity. It is particularly amongst the active groups such as the BY Dra and RS CVn types*, most of which are close binaries, that spot detections have been made. (This is probably a selection effect, as will become clear in Chapter 2.VI.B. It has been suggested that all dMe stars may show spot modulations (Bopp and Espenak, 1977).

The basic type of photometric behavior is illustrated in Figure 2-32. Photometric amplitudes range from ~ 0.4 magnitudes downward, and depend on wavelength. Periodicities of several days and longer are common, and for the stars we are dealing with, this is too long to be pulsation. At times the variability ceases altogether (Bopp and Espenak, 1977). There are also discontinuous changes in phase (Hartmann and Rosner, 1979; Oskanyan et al., 1977; Rucinski, 1977). Such observations are hard to understand in terms of eclipse or pulsation phenomena, but quite natural if spots or groups of spots wax and wane, the way solar spots are observed to do. Still more convincing are the spectroscopic observations (Vogt, 1979, 1981a; Ramsey and Nations, 1980; Baliunis and Dupree, 1982; Fraquelli, 1982; Fekel, 1983; Vogt and Penrod, 1983) showing enhanced TiO and VO molecular bands along with H α and H & K emission at times of spot transits. A powerful adjunct to

*These are observationally related classes of periodic variables typically of classes III, IV, and V. They are recognized by their small amplitude and changeable light curves and by their active atmospheres which show emission in any or all of: CaII H & K lines, MgII h & k lines, Balmer lines, Lyman lines, X-rays, and radio waves (see Hall, 1976).

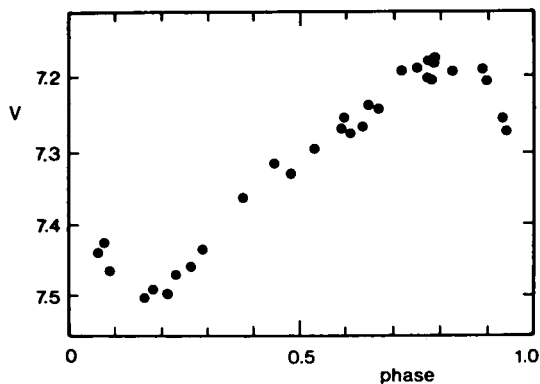


Figure 2-32. The light curve of the spotted star II Peg (HD 224085, K2-3 IV-V) with a photometric period of 6.75 days (based on Bopp and Noah, 1980).

this is the detection of “bumps” in spectral lines that are seen to move across the line profile owing to the changing rotational Doppler shift of the spot as it moves across the disk (Figure 2-33). The emission bumps are not true emission, but result from the spot’s light being unable to contribute as deep a line as the surrounding photosphere.

This curious state comes about because (1) the spot is much cooler (see Chapter 2.VI.B) causing a weaker continuum, and (2) the line is saturated, making \sim zero light a lower limit on its depth. Consequently, the strip on the disk which is parallel to the projected rotation axis and contains the spot cannot contribute its full share of line absorption. The emission bump is simply continuum from disk strips adjacent to the spot.

Given the antics of our Sun, we are not surprised to have spots on other stars, but the evidence in favor of their existence can now be considered hard.

VI.B. CHARACTERISTICS OF SPOTS

In almost all investigations, the spots are found to be cooler than the surrounding photosphere. Temperature differences of 400 K to 1800 K have been deduced (Bopp and

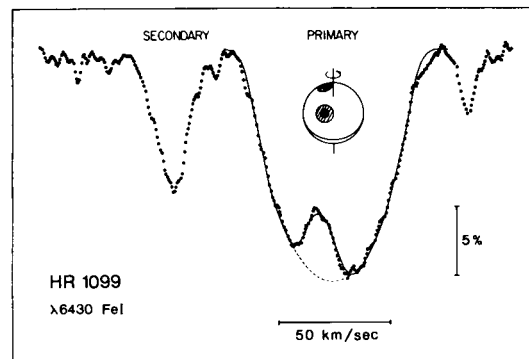


Figure 2-33. The line profile of the primary component of HR 1099 shows a hump that moves across the profile with time. It is interpreted to be caused by spots moved across the visible hemisphere by rotation, as shown by the picture centered within the profile (based on a figure supplied by S. Vogt).

Evans, 1973; Torres and Ferraz Mello, 1973; Davidson and Neff, 1977; Eaton and Hall, 1979; Vogt, 1979, 1981b; Bopp and Noah, 1980; Dorren et al., 1981; Kimble et al., 1981; but see Nha and Kang, 1982). Using the observed enhancement of molecular bands, Vogt (1979, 1981a) has judged a spot on II Peg to have a spectral type near M6 compared to K2 for the star as a whole. Table 2-1 gives some representative numbers assembled by Vogt (1982).

In the cases studied in detail, the darkened area is a sizable fraction of the apparent disk, ranging between 20% and 40%. Mullan (1975) has reasoned that one ought to expect larger spots on stars farther down the main sequence because they have deeper convection zones. Others, for example Rucinski (1979), have suggested that we are seeing groups of spots, and Eaton and Hall (1979) have used a segmented spot model with the darkening tapered at the boundaries. In many cases, the smoothness of the light curve changes dictate a darkened span in longitude of 30° to 40° . Latitude features are more difficult to establish because spots at the same longitude share a common rotational modulation. Nevertheless, Vogt (1981b)

Table 2-1
Characteristics of Starspots

| Star | Spectral type | T _{star} °K | T _{spot} °K | T _{spot} /T _{star} |
|-----------|---------------|-------------------------|-------------------------|--------------------------------------|
| HD 209813 | K0 III | 4790 | <3840 ± 20 | <0.80 |
| SZ Psc | K1 IV | 4700 | 3500 ± 400 | 0.74 |
| II Peg | K2 IV | 4600 | 3400 ± 100 | 0.74 |
| BY Dra | M0 V | 4100 | 3599 ± 450 | 0.85 |

mapped poleward latitude changes on BY Dra and used them to measure a differential rotation rate as discussed in Chapter 2.V.F. Latitude changes have also been seen on HR 1099 by Dorren et al. (1981). Photometric analyses for spots are discussed by Friedman and Gurtler (1975).

Individual spots last for hundreds of rotations (months or years), rather strikingly longer than typical solar behavior. Generally, the spots detected so far point toward a highly organized global structure with one or two large spots or a concentration of spots. This might be an observational bias, since such configurations result in the largest amplitude modulation.

What about magnetic fields in starspots? They are frequently assumed to be there and even to be the cause of the spot (e.g., Bopp and Evans, 1973; Mullan, 1975), but attempts to measure them have given only negative results. Upper limits on average organized magnetic fields of ~150 gauss (10^4 gauss = 1 tesla = 1 weber m⁻²) were found from circular polarization measurements (Vogt, 1980), but strong fields, concentrated in small areas, especially dark ones, cannot be ruled out. It is also possible (probable?) that the field lines are chaotic enough to average out (greatly reduce) the polarization. Detection using detailed Zeeman line broadening measurements may yet be possible (see Chapter 2.VII). Optimism will be needed here because these stars are fairly faint for high resolution work, they are cool enough so that line blending occurs with un-

comfortable frequency, and finally, many of the candidates are rotating sufficiently fast to give line widths considerably larger than the Zeeman broadening. Nevertheless, it is important to try, as we shall see below. (Radio polarization has been measured by Gibson et al., 1978; Mutel and Weisberg, 1978; and Brown and Crane, 1978; but how or if this is related to spots is still an open question.)

Cycles of spot patterns may occur. Secular brightness changes over decades has been reported (Mullan, 1975; Hartmann et al., 1979; Phillips and Hartmann, 1978; Eaton and Hall, 1979; Hartmann et al., 1981). And Vogt (1981b) has traced the same poleward latitude migration of two separate spots on BY Dra. The cyclic nature of H and K line emission in some stars has been well established (Wilson, 1978). In the case of the Sun, sunspot numbers vary in phase with H and K line variations (White and Livingston, 1981). The stellar expectation is therefore obvious, but the proof is still skimpy.

VI.C. THE ROTATION-SPOT COUPLING

Quite aside from the fact that rotational modulation has led to the bulk of our knowledge concerning starspots, there may be a causal relationship here, with rotation being a driving force and spots a driven response. The circumstantial evidence is that most stars showing spots are also fairly rapid rotators for their spectral type (> 5 km s⁻¹). They also show emission in H α and the CaII H and K lines, flares, and other evidence of active chromospheres (Mullan, 1976; Owen et al., 1976; Buscko et al., 1977; Weiler, 1978; Feldman et al., 1978; Aller et al., 1978; Epstein and Briggs, 1978; Bopp and Talcott, 1978; Popper, 1978; Hobbs et al., 1978; Furenlid and Young, 1978; Hearnshaw, 1978; Fraquelli, 1978, 1982; Dorren et al., 1981; Baliunas and Dupree, 1982; Radick et al., 1982). The line of thought is that magnetic fields are likely to be intimately connected to, or the direct cause of,

spots, and that rapid rotation is needed to activate a magnetic dynamo (the other ingredient, convection, is always present in these stars). Unfortunately, as noted above, the magnetic fields have not been seen. But to continue this line of thought, one would expect the rotation to wind down as angular momentum is carried away by escaping mass (Chapter 2.V.B). Therefore, strongly spotted stars, and more generally those showing H α and H and K line emission, must either be young or in binary systems where orbital synchronism has been tidally enforced upon the rotation, preventing its "natural" spin-down. It is well established that most of the strongly spotted stars are binaries and so could simply be in this second category. But some are apparently truly single stars (Bopp and Fekel, 1977; Bopp and Espenak, 1977) and candidates for just being young. Vogt and Fekel (1979) for instance, have pointed to BY Dra A as a young object. It lies above the main sequence, but has too small a mass to have had time enough to complete its sojourn on the main sequence. Its rotation period is shorter than its orbital period (3.84 versus 5.98 days), implying that tidal interaction has not yet had enough time to draw it into synchronism. They view the star as currently terminating its T Tau phase of evolution.

This picture of spot occurrences and rotational changes dovetails with the rotation observations discussed in Chapter 2.V. Carrasco et al. (1980), however, found angular momenta for BY Dra stars to be well above the usual main sequence values (Chapter 2.V.D). This could be a result of orbital coupling maintaining high rotation in the binary components. But the young, rapidly rotating, spotted stars that are single would be completing the rapid braking stage.

VII. MAGNETIC FIELDS

VII.A. TECHNIQUES

Evidence for solar-type magnetic fields in F-G-K stars comes from several kinds of obser-

vations. The most direct is Zeeman splitting of spectral lines. The relatively large velocities of turbulence and rotation dominate the shaping of most photospheric lines, as we have seen in the preceding paragraphs. The Zeeman splitting is therefore going to appear as a small differential effect. Under such circumstances, the usual technique is to use circular polarization measurements (Babcock, 1953, 1958, 1962; Botticher, 1968), but such measurements have proved fruitless (Vogt, 1980; Brown and Landstreet, 1981; Slovak, 1982), although very small linear polarization measurements have been reported by Tinbergen and Zwaan (1981). If the stellar photospheric magnetic fields are organized around granules and supergranules, and if active regions are structured irregularly as they are in the Sun, polarization effects would be small. Viewed globally, the star would present as many positive as negative lines of force to an observer, cancelling the polarization. However, the Zeeman splitting itself remains (e.g., Preston, 1971), even for complex field patterns, and is therefore the more relevant effect to look for in F-G-K stars.

Robinson (1980) and Robinson et al. (1980) have shown how carefully paired sets of lines can be used to detect the Zeeman broadening, and Marcy (1984) has used this technique to survey 29 G and K dwarfs. Analysis in the Fourier domain has also been done (Gray, 1984a). In the triplet case, the s components of the Zeeman pattern are shifted in both directions from the undisplaced position by

$$\Delta\lambda_1 = 1.40 \text{ E-7 } \bar{g} \lambda B \quad (2-4)$$

for the field strength of B gauss (10^4 gauss = 1 testla = 1 weber m^{-2}), the wavelength λ in Å, and the shift $\Delta\lambda_1$ in km s^{-1} . The effective Lande-g factor is \bar{g} . A large table of these has been published by Beckers (1969). Lines having no magnetic broadening are tabulated by Landstreet (1969); by Sistla and Harvey (1970); and by Adelman (1974).

The relative intensity of the shifted component is

$$I_s = 0.25 (1 + \cos^2 \psi), \quad (2-5)$$

and for the unshifted components is

$$I_p = 0.5 \sin^2 \psi, \quad (2-6)$$

where ψ is the angle between the magnetic field lines and the line of sight (Seares, 1913; van den Bösch, 1957; Aller, 1963; Botticher, 1968; Shore and Menzel, 1968). For most stars we know little or nothing about the geometry of the field, except, as mentioned above, that wide ranging orientations are expected; ψ likely is better thought of as a distribution rather than a single value.

A correct approach to Zeeman analysis would convolve the Zeeman pattern into the line absorption coefficient before the radiative transfer equation is evaluated. But since ψ is unknown, only more approximate methods have been used to date. The radiative transfer calculation can be bypassed by using weak unsaturated spectral lines, because then the convolution with the Zeeman pattern can be written

$$I_\nu = I_\nu^0 * Z(\lambda), \quad (2-7)$$

where I_ν is the Zeeman broadened line, I_ν^0 is the same line without Zeeman broadening, and $Z(\lambda)$ is the Zeeman pattern. If we make the further assumption that $Z(\lambda)$ is independent of position on the stellar disk (in a statistical sense), then we can write

$$\begin{aligned} F_\nu &= \oint I_\nu^0 * Z(\lambda) \cos \theta \, dw \\ &= Z(\lambda) * \oint I_\nu^0 \cos \theta \, dw \\ &= Z(\lambda) * F_\nu^0, \end{aligned} \quad (2-8)$$

where F_ν^0 is the flux profile without Zeeman broadening. This approximation has been used in all recent stellar studies.

The observed Zeeman broadened profile, which can be seen readily enough for sunspots (Figure 2-34), will have an undisplaced component consisting of I_p from magnetic regions combined with the undisplaced line arising from nonmagnetic areas of the surface. Neglecting other forms of line broadening for the moment, we can view this central component as a δ -function of strength $1-A_0$. The displaced components will be δ -functions of strength $A_0/2$. The Fourier transform of such a pattern is

$$z(\sigma) = (1 - A_0) + A_0 \cos 2\pi\Delta\lambda_1\sigma. \quad (2-9)$$

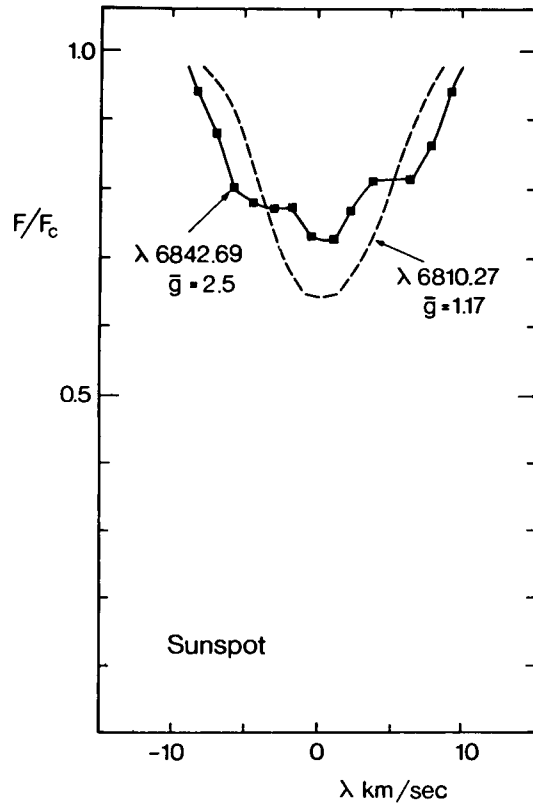


Figure 2-34. The Zeeman effect can be seen in the light from a sunspot (based on Robinson et al., 1980).

In other words, the Zeeman effect will show itself as an oscillatory component in the transform. However, since the Zeeman broadening is relatively small compared to the total line broadening, the cosine term typically encountered shows less than half a cycle, and might look like Figure 2-35. Comparison with stellar observations yields A_0 from the shape of the transform and $\Delta\lambda_1$, and hence B, from the displacement along the abscissa. Examples are shown in Figure 2-38, below.

In principle A_0 can be related to the fraction of the stellar disk covered by magnetic field. Assuming magnetic areas have the same brightness as nonmagnetic areas, and that we can find some suitable average for ψ , say $\langle\psi\rangle$, then Equations (5) and (6) give

$$A_0 = 0.5 \alpha (1 + \cos^2 \langle\psi\rangle), \quad (2-10)$$

where α is the fraction of the disk covered by field. Therefore $2A_0 > \alpha > A_0$.

In cases where the magnetic influence is weak but still detectable, A_0 cannot be separated

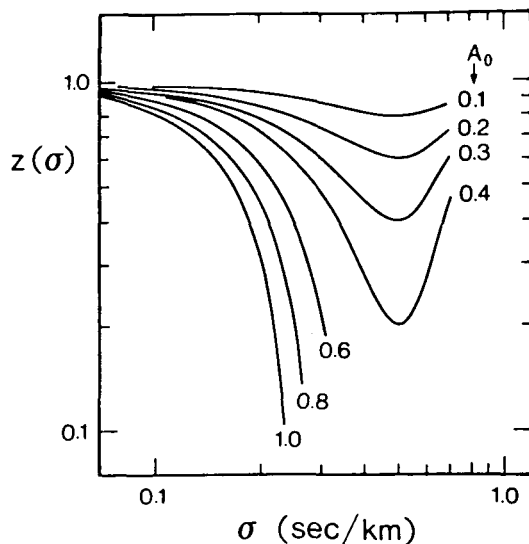


Figure 2-35. A log-log plot of equation (8) is shown for $\Delta\lambda_1 = 1 \text{ km s}^{-1}$ for the values of A_0 shown.

from B and only the product $B\sqrt{A_0}$ can be found (Gray, 1984a). Quite generally, either small fields or small areal coverage can reduce the Zeeman broadening below the level of detection. The current limit of detectability is ~ 0.3 in $B\sqrt{A_0}$ when B is in kilogauss. For example, a one kilogauss field would have to cover more than 9-18% of the disk to be seen, depending on the value of $\langle\psi\rangle$.

A real star is likely to have not one field strength, but a whole distribution of strengths. It is impractical to measure this distribution with the techniques available. But neglect of the distribution will result in systematic overestimates of B and underestimates of A_0 . Overestimates of $B\sqrt{A_0}$ are substantially less (Gray, 1984a).

Further, the actual Zeeman patterns for the lines that have been analyzed are not triplets, but substantially more complex. Examples are given by Babcock (1962) and Meggers (1953). Systematic errors arising from the triplet approximation are expected to be in the same sense as those for the neglected field strength distribution. Since all Zeeman patterns are symmetric, no asymmetry is introduced into the line profiles, and no confusion arises between granulation and Zeeman broadening.

The reduction technique used by Robinson (1980), Robinson et al. (1980), and Marcy (1982, 1984) centers on Equation (2-8). The profile without Zeeman broadening is treated much like an instrumental profile, and its removal from the Zeeman broadened profile can be done using standard Fourier techniques, or by iteration. F_v^o is obtained from a low-g line while F_v corresponds to a high-g line (Figure 2-36). All other characteristics of the two lines should be as similar as possible. Robinson (1980) suggests several pairs of lines suitable for solar-type stars.

Alternatively, reductions can be done in the Fourier domain by comparing the transforms of F_v to $z(\sigma)$ in Equation (2-9), as shown in

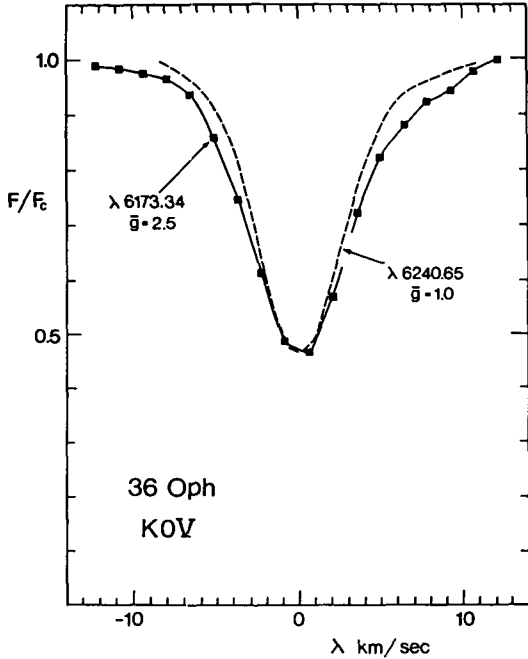


Figure 2-36. Evidence of magnetic broadening can be seen in the lines of 36 Oph (based on data supplied by G. Marcy).

Figure 2-37. This allows any number of lines to be combined into one solution. The wider the range in g , the better the solution.

It is well to remember, however, that for the polarized components of the Zeeman pattern, total saturation occurs not at zero light, but at half the continuum level. With the onset of saturation, the appearance of the profile could change markedly. Typically the triplet pattern of the weak line in a longitudinal field would be replaced by an apparent doublet (Figure 2-38). The doublet profile could be mistakenly taken to indicate a transverse field, i.e., exactly opposite the truth.

Finally we should keep in mind the possible, even likely, occurrence of variations in turbulence broadening between magnetic and non-magnetic regions. If this were the case, the I_V^0 in Equation (2-8) would be nonunique and the linear formulation is once again inappropriate.

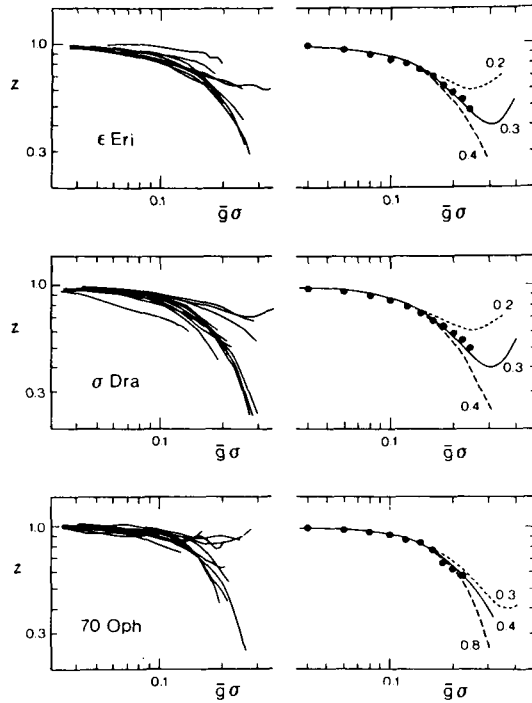


Figure 2-37. Zeeman transforms obtained from stellar data are shown on the left side, where $z(\bar{g}\sigma)$ is shown for ~ 10 individual spectral lines. The dots on the right side are the means of the data shown on the left, and curves from Figure 2-35 are matched to these data. Values of A_0 are shown by the model curves (from Gray, 1984a).

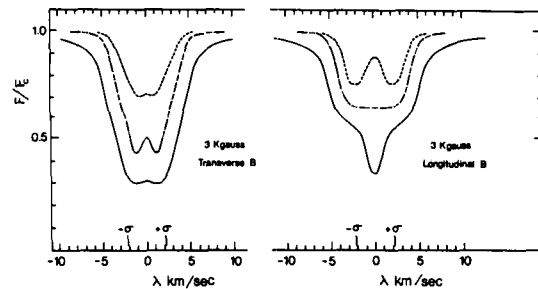


Figure 2-38. Zeeman broadened line profiles, according to model calculations, depend on the amount of saturation. Since the Zeeman components are polarized, they saturate at $F/F_c \sim 0.5$. The overlapping wavelength intervals, however, can absorb both components of polarization and eventually become the deepest parts of the profile (based on calculation done by J. C. Evans).

VII.B. OBSERVATIONS

The first detection of Zeeman broadening in F-G-K-type spectra was reported by Robinson et al. (1980) for ξ Boo A. Variability with time was suspected almost immediately when the magnetic effect was not always seen (Marcy, 1981). All published studies of F, G, and K dwarfs are summarized in Figure 2-39. Here we see a remarkable correlation between the two measurable parameters B and A_0 . Even multiple measurements of the same star, although they may vary widely in B and A_0 , line on this correlation. There are no obvious reasons to expect such a correlation to result from errors of measurement or analysis (Gray, 1985). Assuming a real physical relation here, the correlation slope of -1 implies that BA_0 is a constant, ~ 520 gauss according to Figure 2-39.

BA_0 appears to be independent of spectral type (Figure 2-40). Multiple measurements are shown within the vertical strips for the three stars for which they are available. The scatter about $BA_0 \sim 520$ gauss is no more than expected from the errors of measurement. Nondetections are also shown. Apparently B

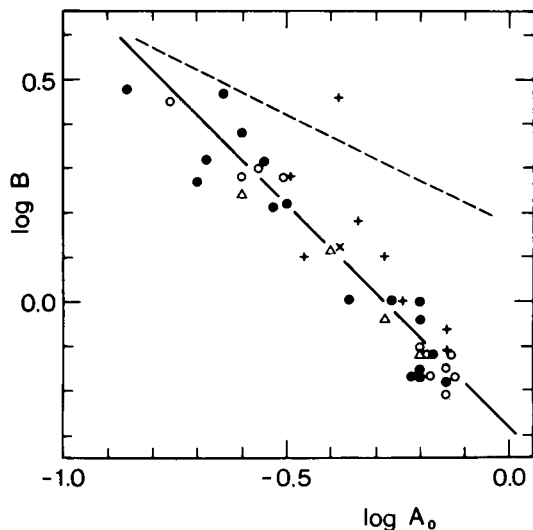


Figure 2-39. The magnetic field strength, B, is inversely related to the areal coverage factor, A_0 . Δ , 70 Ohp A; +, ξ Boo A; o, ϵ Eri; \bullet , stars with < 2 observations (from Gray, 1985).

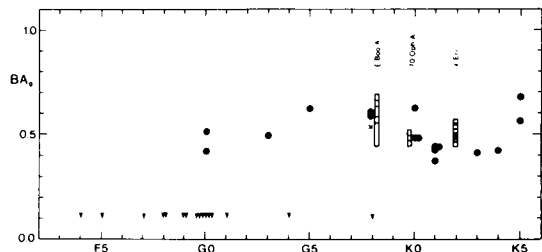


Figure 2-40. BA_0 is independent of spectral type. Multiple measurement for three stars (as labeled) show a span consistent with observational error. Nondetections are shown as arrowheads at the bottom.

or A_0 can be too small to allow detection, but when Zeeman broadening is seen, BA_0 is a constant.

BA_0 is also independent of rotation rate. However, B and A_0 separately do seem to depend on rotation, as shown in Figure 2-41. Although some stars may not fit the correlation, B generally becomes weaker as rotation increases, while A_0 becomes larger by the same fraction.

The total number of magnetic lines of force in the photosphere can be written

$$\eta = 4\pi R^2 \alpha B, \quad (2-11)$$

where R is the radius of the star and α is the fraction of the surface covered by field. η should be carefully distinguished from the magnetic flux which is zero over the whole star. Only the scalar properties of B are used in Equation (11). Replacing α from Equation (10),

$$\frac{\eta}{4\pi R^2} = \frac{BA_0}{0.5(1 + \cos^2 \langle \psi \rangle)}. \quad (2-12)$$

Since $\langle \psi \rangle$ is likely to be essentially constant, and since BA_0 is constant, we see that the number of lines of force per unit area, as

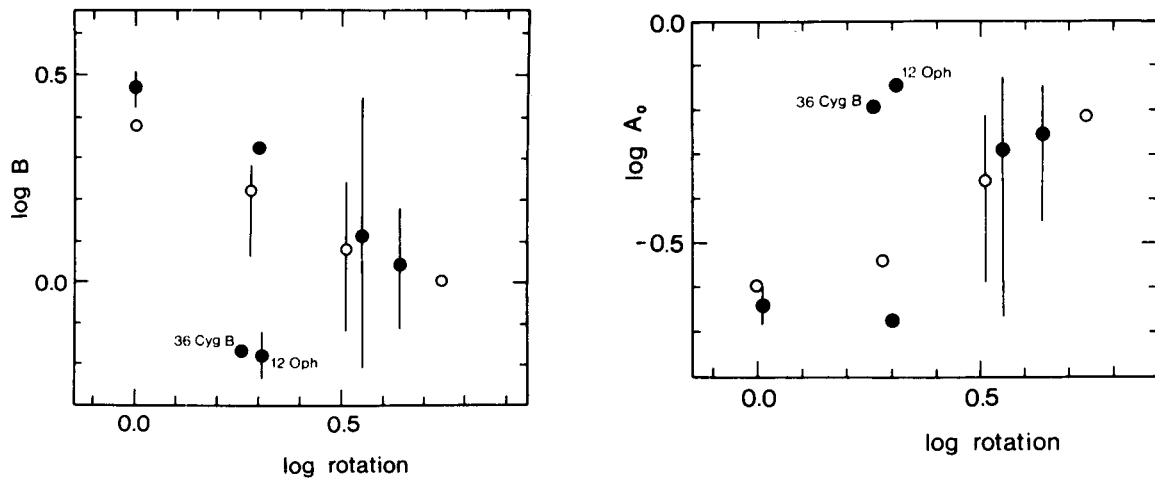


Figure 2-41. Although BA_0 is independent of rotation, B appears to decrease while A_0 increases with more rapid rotation. Some stars, such as 36 Cyg A and 12 Oph, may fall off the correlation.

averaged over the star, is a universal magnetic constant. Apparently the concentration of this fixed number of lines can vary, giving strong fields over small areas at some times, and weak fields over larger areas at other times. The average state of concentration may be affected by the rotation, as we see in Figure 2-41.

Stars above the main sequence do not generally show Zeeman broadening large enough to detect. Marcy and Bruning (1984) looked at eight stars, and Gray and Nagar (1985) looked at 20 stars. On the other hand, the RS CVn star λ And (GB III-IV), which is a rapid rotator and has starspots, was measured by Giampapa et al., (1983) to have a 1.3 kilogauss field over 48% of its surface. These values also fall on the correlation of Figure 2-39.

VII.C. INDIRECT EVIDENCE OF MAGNETIC FIELDS

Magnetic fields in stars are also inferred from a number of indirect lines of evidence. One of these is the rotational braking discussed in Chapter 2.V. Estimates based on the Weber-Davis (1967) formulation for the dissipation of angular momentum indicate that fields of only a few tens of gauss are needed. This refers

only to the "open" field lines, and the total photospheric field could be much larger, as it is for the Sun.

Other indirect evidence of fields is the existence of starspots. The strongest and most extensive magnetic fields on the solar surface occur in spots. A substantial amount of evidence indicates that dark spots on stellar photospheres are not unique to the Sun (Chapter 2.VI). A possible detection of a starspot field is discussed by Vogt (1981a).

Enhanced H and K line emission is associated with magnetic regions on the Sun (see, for example, LaBonte, 1982). It is frequently assumed that the same is true of stars. Middelkoop and Zwaan (1981), Zwaan (1983), and Noyes et al. (1984) have used this assumption to discuss magnetic field variations in cool stars. They find the H and K emission differences among stars to be consistent with theory for dynamo-generated fields, with regard to both rotation and aging. Wilson (1982) has published photoelectric measurements of H and K emission in giant stars.

Finally, X-ray emission is taken as an indication of coronal magnetic fields, and these coronal loop fields are anchored in the

photosphere, or deeper. On the Sun, the open field lines channel the escaping particle flow or wind. These regions are relatively less dense, cool and dark, by virtue of which they have earned the name coronal holes. In contrast, the loops of magnetic field hold onto the plasma, the temperatures are significantly elevated, and thermal X-rays are emitted. (Zirker, 1981). X-rays have been observed from a large variety of stars (Vaiana et al., 1981; Sterne et al., 1981; Mew et al., 1981). A preliminary discussion of possible relations between X-ray emission and Zeeman broadening is presented by Marcy (1984).

A remarkable discovery relating convection and magnetic fields on the Sun has been made by Livingston (1982, 1983). In Chapter 2.IV we saw that the line bisector was a measure of the photospheric convection velocity. Livingston has found a change in the line bisector during the solar magnetic cycle (Figure 2-42). The stronger the average solar field, the smaller the bisector displacement. The presence of the magnetic field appears to inhibit convection. The number of solar granules is also seen to increase with increasing magnetic activity (Müller and Roudier, 1984). The implications here are enormous. Unfortunately, work on stellar bisectors has just begun. The only studies of stellar magnetic cycles are those started by Wilson (1978). Suppose that magnetic activity does parallel the general chromospheric activity. Will all stars show inhibited surface convection with growing activity? What variations are produced in the effective temperature of the star and how does this inhibition arise?

VIII. OSCILLATIONS AND WAVES

VIII.A. THE SOLAR EXAMPLE

The photospheric gases have the forces of gravity, pressure, and magnetic fields acting on them. Each can act as a restoring force on mass displacements, and so potentially gravity waves, sound waves, and MHD waves can exist there.

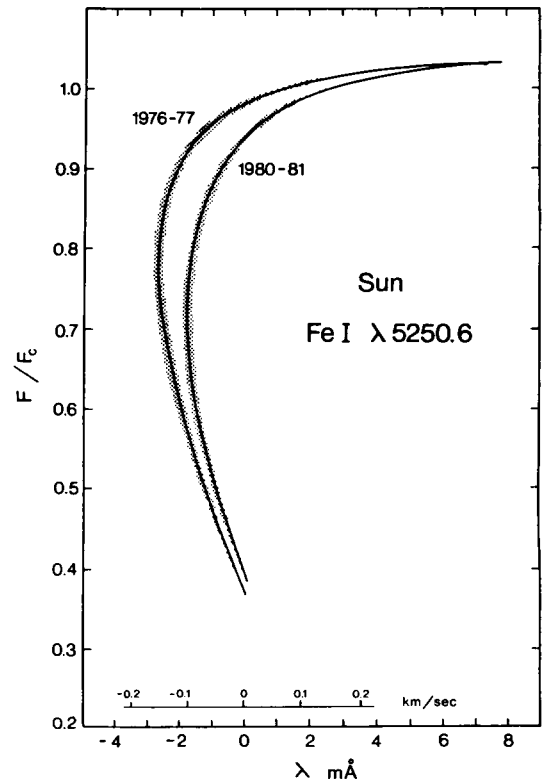


Figure 2-42. Solar line bisectors indicate that the convection changes with time, presumably with phase in the solar cycle. The shaded regions around the bisectors indicate the errors (from Livingston, 1982).

Once more we turn to the solar photosphere for guidance, and indeed a rich ensemble of waves is found. The most striking of these, because of its velocity amplitude and surface coverage, is the 5-minute oscillation. It was discovered relatively recently (Leighton, 1961; Leighton et al., 1962) and has received a great deal of attention. Through the work of Frazier (1968), Ulrich (1970b), Wolff (1972a, 1972b, 1973), Deubner (1974, 1976a, 1981a), Ando and Osaki (1975a), Rhodes et al. (1977), Ulrich and Rhodes (1977), Hill et al. (1982), Duval and Harvey (1983, 1984a), the complex nature of these oscillations has been mapped in time and geometry, and has been interpreted as non-radial pressure-mode oscillations. The complicated temporal and spatial behavior is a result of the interference of many modes of resonance within the convection zone. Careful

interpretation gives essentially the sound speed versus position. Important results follow, namely, a value for the depth of the solar convection zone and the density and temperature at its lower boundary (Rhodes et al., 1977; Christensen-Dalsgaard, 1982). A new method of measuring the solar rotation and its depth dependence results from the rotational splitting of the modes (Rhodes et al., 1979; Deubner et al., 1979; Ulrich et al., 1979; Deubner 1981a; Claverie et al., 1981; Hill et al., 1982; Duval and Harvey, 1984b). A small inward increase in angular velocity is indicated at this writing, but the details are disputed. Any of this type of information for other stars would be of basic importance. Unfortunately, when only integrated light from the stellar disk is available, substantial leverage is stripped away. It appears that only low order modes (< 4) may be detectable in principle (Christensen-Dalsgaard and Gough, 1982; Christensen-Dalsgaard and Frandsen, 1983). Ideally, a mapping of convection zone parameters across the HR diagram should be made. It is not clear that this will be possible. But the first step is to detect the counterpart of the 5-minute oscillations in other F-G-K stars.

VIII.B. STELLAR OSCILLATIONS

Is it possible to see such oscillations on a star where only disk-integrated radiation can be measured? Brightness or radial velocity variations are the tools available. (The term non-radial refers to the wave vectors and not to the photospheric velocities produced.) The lack of phase coherence from one oscillating area to another means that the disk integration will largely average out the effect. Oscillations can be detected in the solar flux (Traub et al., 1978; Claverie et al., 1979, 1980; Grec et al., 1980, 1983; Woodard and Hudson, 1983a, 1983b; Deubner, 1981b), and they exhibit variations of only $\sim 20 \text{ cm s}^{-1}$ in velocity and $\sim 2 \times 10^{-6}$ fractional changes in luminosity. These are remarkably small values! It is no wonder that detection of oscillations in other stars has been a difficult endeavor.

In other stars, particularly the K and M giants and supergiants, the number of oscillating cells may be considerably smaller (e.g., Schwarzschild, 1975), and the number of resonant modes may also be less (Ando and Osaki, 1975; Christensen-Dalsgaard and Frandsen, 1983). This would help by increasing the amplitude of the flux variations by lengthening their period, thereby allowing lower time resolution and higher photon counts per integration. But clearly, the detection of these fluctuations will require careful observing technique, high signal-to-noise ratios, and in the case of velocity measurements good spectral resolution. Some of the limitations are discussed by Fossat (1984).

Traub et al. (1978) used a PEPSIOS spectrometer to measure the position of Fe I $\lambda 6678.0$ in nine F-G-K stars. The $3\text{-}\sigma$ errors ranged from a low of 3 m s^{-1} for α Boo to 46 m s^{-1} for β Gem. No stellar oscillations were seen within the period range of 10 to 5000 seconds.

Smith (1982a, b) searched for stellar oscillations by measuring stellar line positions relative to interlaced telluric lines of the O₂ $\lambda 6300$ band. Oscillations having a 97 ± 28 minute period in α Boo and a 110 ± 16 minute period in α Tau are suspected, but they are still too immersed in the noise ($\pm 7 \text{ m s}^{-1}$ to be certain. Hayes (1981) may have detected non-radial pulsations in the M2Iab star α Ori using linear polarization measurements.

P-mode oscillations in α Cen A, having ~ 5.6 minute period, are reported by Fossat et al. (1984) based on observations using a Na-cell spectrometer. H and K line measurements of ϵ Eri seem to show somewhat longer periods ~ 10 minutes, according to Noyes et al. (1984).

Other types of oscillations may turn out to be significant in F-G-K star photospheres, but until they are detected and some of their characteristics measured, there is little more to be said.

IX. COMMENTS

The last decade of work has led to almost all of our knowledge concerning nonthermal phenomena in stellar photospheres. Observations and ideas go hand in hand. We are largely the product of our times. We frequently stand on technological advances to see ahead. The interpretations and predictions are couched in terms of what our minds can conceive, and this is based on our current understanding coupled with reasoning, but often led by example, e.g., the Sun versus other stars. While it is true that many nonthermal phenomena are first recognized on the Sun, the nature of the physics often remains obscure even there. Studies using other stars may prove to be the fruitful approach in this regard, for in them we obtain the sensitivity of the nonthermal events to temperature, pressure, rotation rate, age, etc., and in some cases even discover stronger versions of the solar-type phenomenon, stellar mass-loss and rotational braking being two examples. Another important illustration is the stellar evidence that acoustic waves are unable to account for the heating of the chromospheres of cool stars (Stein, 1981).

While the foregoing pages have shown how certain nonthermal effects can be detected and measured, there are several others seen on the Sun which may never be detected in stellar photospheres. Consider, for example, the subtle motions of mesogranulation and supergranulation (November et al., 1981; Giovanelli, 1980). Their velocities are small ($<0.5 \text{ km s}^{-1}$) and, more importantly, there is no detectable temperature variation associated with them. These types of motions in other stars may always be confined to an unidentified component of macroturbulence. But spatial intensity variations, such as those associated with granulation and starspots, may be the lever for some dramatic future gains. Speckle interferometry has already whet our imaginations in seeing large surface features (Lynds et al., 1976; Wilkerson and Worden, 1977). Giant interferometers may soon be mapping stellar sur-

faces (Labeyrie, 1982) and thereby adding a powerful new dimension to studies of F-G-K stars. Spectral line measurements are proving to be increasingly valuable as high signal-to-noise ratios and high spectral resolution are attained. The tools for studying nonthermal phenomena in stellar photospheres are maturing and showing results.

X. APPENDIX: THERMAL CHARACTERISTICS

X.A1. INTRODUCTION

Thermal physics adequately describes some of the basic observational characteristics of stellar photospheres. Primary among these are: (1) the energy distribution or continuous spectrum, (2) the spectral type sequence, (3) pressure effects, including ionization equilibria and the growth of damping wings on strong lines, and (4) the chemical composition, especially of weak spectral lines. Within the thermal framework there are the broad subsections of LTE (Local Thermodynamic Equilibrium) and non-LTE.

The building of thermal model atmospheres and the understanding, at least on the first or second levels of iteration, of the appropriate thermal physics occupied astrophysicists extensively from ~1930 to ~1970. The majority of books written on stellar atmospheres deal largely with the thermal aspects of the subject, e.g., Unsöld (1955), Ambartsumyan (1958), Greenstein (1960), Aller (1963), Pecker (1965), Sobolev (1966), Jefferies (1968), Cowley (1970), Athay (1972), Gray (1976), and Mihalas (1978). Since these references already cover the thermal material, we briefly consider here only selected aspects of these topics.

The reason for bringing up the thermal nature of stellar atmospheres in a volume dealing with nonthermal phenomena is that the first step into nonthermal atmospheric studies is from the thermal foundation. Our model

photospheres in particular are likely to be essentially thermal in makeup with our ideas of some nonthermal feature of interest grafted onto them. This is not to say that the thermal models will be sheltered from significant alteration as the nonthermal is introduced. Rather, we are simply seeing the historical progression of studies from what we think we know to what we know we do not yet understand.

To facilitate this process, we need to have ready access to typical thermal characteristics of the stars we study. The following sections summarize information on photometric indices, effective temperatures, surface gravities, and masses of F, G, and K stars. The data are extended slightly to include earlier and later spectral types in order to show the continuity.

X.A2. ENERGY DISTRIBUTIONS

In F-G-K stars, measurements of the energy distribution, typically the Paschen continuum, are used primarily as temperature indicators. Energy distribution measurements bring the observations one step closer to the physics and to photospheric models than do color index measurements (Chapters X.A3 and X.A4, below). More wavelength points are measured, line absorption can be accommodated, atmospheric excitation can be handled without color terms, and transmission-detector sensitivity passbands need not be folded into the computations, so the comparison of model continua to the observations is relatively direct. The important foundation for this type of work is the absolute shape calibration of Vega, the primary standard.

The modern era began with the Vega calibration by Code (1960). There have been several stages of settling in: Kharitonov (1963), Glushneva (1964), Oke (1964, 1965), Willstrop (1965), Oke and Schild (1970), Hayes (1970), Bless and Code (1972), Hayes and Latham (1975), Hayes et al. (1975), and Tug et al. (1977). There is now good agreement ($\sim 1\%$)

among observers. Table 2-A1 gives a reference calibration for Vega.

Secondary spectrophotometric standards have been given by Oke (1964), Hayes (1970), Stone (1977), Taylor (1978), and Tug (1980a, 1980b). A summary and discussion of errors has been published by Breger (1976).

Absolute flux measurements at $\lambda 5556$ in Vega (or alternatively for an A0 V star of zero visual magnitude) are needed for some studies. The value of 3.5×10^{-9} erg s $^{-1}$ cm $^{-2}$ Å $^{-1}$ at $\lambda 5556$ for $V=0.00$ (Gray, 1976) is 2% smaller than the more recent calibration by Tug et al. (1977), and this difference is about the size of the expected errors.

Array detectors make energy distribution measurements more attractive than ever, with

Table 2-A1

An Absolute Shape Calibration of Vega*

| λ | $\log F_{\nu} + \text{const}$ | λ | $\log F_{\nu} + \text{const}$ |
|-----------|-------------------------------|-----------|-------------------------------|
| 3300 | -0.455 | 6056 | -0.044 |
| 3400 | -0.452 | 6436 | -0.067 |
| 3500 | -0.439 | 6800 | -0.088 |
| 3571 | -0.431 | 7100 | -0.109 |
| 3636 | -0.424 | 7550 | -0.144 |
| 4036 | +0.120 | 7780 | -0.159 |
| 4167 | +0.111 | 8090 | -0.172 |
| 4255 | +0.105 | 8400 | -0.190 |
| 4464 | +0.095 | 8708 | -0.180 |
| 4566 | +0.080 | 9700 | -0.194 |
| 4785 | +0.061 | 9950 | -0.209 |
| 5000 | +0.041 | 10250 | -0.228 |
| 5263 | +0.020 | 10400 | -0.234 |
| 5556 | 0.000 | 10800 | -0.260 |
| 5840 | -0.025 | | |

*from Gray (1976). Nearly continuous wavelength coverage is given by Tug et al. (1977).

their ability to measure thousands of spectral intervals simultaneously (e.g., Campbell, 1977; Cochran, 1981; Cochran and Barnes, 1981).

X.A3. TEMPERATURE INDICES

Because the Paschen continuum and the spectral lines are both temperature dependent in F-G-K stars, the spectral type and various photometric color indices are parametrically related. Tables 2-A3, 2-A4, and 2-A5 summarize the empirical mean correspondences, while Table 2-A2 brings together reference material on the photometric systems themselves. Photometric indices measure the continuum as affected by line absorption. Some bandpasses can be placed to measure the

Table 2-A2

Temperature Indices and Their Photometric Systems

| Index* | System | References |
|---------------|---------|--|
| Spectral Type | MK | Morgan et al. (1943), Keenan (1963), Abt et al. (1968), Morgan and Keenan (1973) |
| B-V | UBV | Johnson and Morgan (1953), Johnson and Harris (1954) |
| b-y | uvby | Strömgren (1963, 1966) |
| V-R | 5-color | Iriarte et al. (1965), Moffett and Barnes (1979) |
| G-R | RGU | Becker and Stock (1954), Becker (1967), Steinlin (1968), Buser (1978, 1979) |
| B-V | Geneva | Rufener and Maeder (1971), Rufener (1979), Golay (1979) |
| C(42-45) | DDO | McClure and van den Berg (1968), McClure (1976) |

*Other modern spectral classification atlases are: Houk et al. (1974) and Morgan et al. (1978), but they do not stress the F-G-K stars. There are several less frequently encountered photometric systems which are not included here: VBLUW (Lub and Pel 1979), Vilnius (Straizys 1979), 8-color (Wing 1979), 6-color (Stebbins and Whitford 1943), Washington, among others.

Balmer jump, e.g., u, v on the uvby system, or the strength of the line absorption which is often presumed to be related to the chemical composition, e.g., the C(38-42) index of the DDO system. Only temperature indices, measuring primarily the change in slope of the Paschen continuum are brought together in the Tables. The color-index entries in these Tables were read from graphs of the index (in magnitudes) versus spectral type, using interpolation when necessary to fill out the grid of the tables. Generally the last digit is not significant except, perhaps, in a relative sense.

The spectral type and color indices vary roughly as the logarithm of the temperature. Somewhat better temperature resolution is afforded by the photometric indices, but the spectral type is independent of interstellar reddening and can be assigned more readily for close or unresolved binaries. Many sources are available for the B-V calibration with spectral type (Böhm-Vitense, 1981; Popper, 1980; Bessell, 1979; Osborne, 1979; Hayes, 1978; Gray, 1976), but they are all closely related to, or based directly on, the earlier work of Fitzgerald (1970). The relations adopted for the Tables and shown in Figure 2-A1 differ only slightly from FitzGerald's work.

Other temperature indices are taken from the following sources: Popper (1980) for V-R, Bessell (1979) and Popper (1980) for b-y, Yoss (1977), Osborne (1979), and McClure and Forrester (1981) for C(42-45), Becker (1967) and Buser (1978) for G-R, and Golay (1979) for B_2-V_1 . Differences of ± 0.02 magnitudes in the calibrations at a given spectral type, but from different literature sources, are common. It should be noted that earlier calibrations of G-R in terms of B-V differed markedly from the more recent ones (e.g., Becker and Stock, 1954).

X.A4. EFFECTIVE TEMPERATURES

Relatively few fundamental determinations of effective temperature, T_{eff} , are available for

Table 2-A3

Thermal Parameters for Main Sequence Stars

| Sp | B-V | b-y | V-R | G-R | B ₂ -V ₁ | C(42-45) | Mass | log mass | log g | T _{eff} | M _V |
|----|-------|-------|-------|-------|--------------------------------|----------|------|----------|-------|------------------|----------------|
| A5 | 0.143 | 0.073 | 0.160 | 0.450 | -0.040 | ... | 1.90 | 0.278 | 4.20 | 8250 | 1.8 |
| 6 | .170 | .093 | .173 | .502 | -0.005 | ... | 1.82 | .260 | 4.21 | 8090 | 2.0 |
| 7 | .198 | .118 | .190 | .560 | +0.035 | ... | 1.74 | .240 | 4.22 | 7910 | 2.1 |
| 8 | .228 | .135 | .213 | .630 | .070 | ... | 1.70 | .230 | 4.22 | 7750 | 2.4 |
| 9 | .265 | .150 | .250 | .665 | .106 | ... | 1.63 | .212 | 4.23 | 7530 | 2.6 |
| F0 | 0.300 | 0.165 | 0.300 | 0.720 | 0.130 | ... | 1.57 | 0.195 | 4.23 | 7380 | 2.8 |
| 1 | .329 | .192 | .325 | .750 | .156 | ... | 1.51 | .180 | 4.24 | 7170 | 3.0 |
| 2 | .354 | .220 | .350 | .780 | .175 | ... | 1.45 | .162 | 4.25 | 6980 | 3.1 |
| 3 | .380 | .242 | .366 | .808 | .197 | ... | 1.41 | .150 | 4.25 | 6800 | 3.2 |
| 4 | .404 | .261 | .382 | .835 | .213 | ... | 1.38 | .140 | 4.26 | 6660 | 3.4 |
| 5 | .431 | .285 | .400 | .870 | .233 | ... | 1.34 | .128 | 4.27 | 6500 | 3.5 |
| 6 | .464 | .300 | .423 | .902 | .250 | ... | 1.29 | .112 | 4.28 | 6370 | 3.7 |
| 7 | .496 | .317 | .448 | .932 | .270 | ... | 1.26 | .100 | 4.28 | 6250 | 4.0 |
| 8 | .530 | .331 | .470 | .961 | .285 | .540 | 1.22 | .087 | 4.29 | 6130 | 4.2 |
| 9 | .561 | .348 | .483 | .995 | .302 | .567 | 1.18 | .072 | 4.30 | 6050 | 4.4 |
| G0 | 0.583 | 0.360 | 0.500 | 1.030 | 0.320 | 0.594 | 1.15 | 0.060 | 4.32 | 5980 | 4.4 |
| 1 | .608 | .375 | .515 | 1.054 | .332 | .618 | 1.10 | .042 | 4.34 | 5900 | 4.6 |
| 2 | .625 | .390 | .528 | 1.074 | .346 | .627 | 1.07 | .028 | 4.35 | 5800 | 4.7 |
| 3 | .642 | .404 | .534 | 1.097 | .362 | .644 | 1.04 | .015 | 4.37 | 5710 | 4.7 |
| 4 | .657 | .417 | .538 | 1.120 | .376 | .659 | 1.00 | .002 | 4.38 | 5690 | 4.8 |
| 5 | .672 | .433 | .541 | 1.150 | .390 | .673 | 0.98 | -.010 | 4.40 | 5620 | 4.9 |
| 6 | .690 | .444 | .546 | 1.180 | (.402)* | .692 | .93 | -.030 | 4.42 | 5570 | 5.0 |
| 7 | .713 | .459 | .560 | 1.208 | (.415) | .708 | .90 | -.045 | 4.44 | 5500 | 5.2 |
| 8 | .740 | .473 | .580 | 1.240 | (.428) | .726 | .87 | -.060 | 4.46 | 5450 | 5.4 |
| 9 | .776 | .488 | .606 | 1.270 | (.440) | .768 | .84 | -.075 | 4.48 | 5370 | 5.6 |
| K0 | 0.819 | 0.502 | 0.640 | 1.310 | ... | 0.821 | 0.81 | -0.090 | 4.49 | 5230 | 5.9 |
| 1 | .866 | .518 | .687 | 1.340 | ... | .874 | .79 | -.105 | 4.50 | 5080 | 6.1 |
| 2 | .912 | .534 | .740 | 1.364 | ... | .950 | .76 | -.120 | 4.52 | 4920 | 6.4 |
| 3 | .966 | .565 | .805 | 1.400 | ... | 1.036 | .74 | -.132 | 4.53 | 4810 | 6.7 |
| 4 | 1.030 | .600 | .890 | 1.590 | ... | 1.122 | .70 | -.153 | 4.54 | 4640 | 7.1 |
| 5 | 1.150 | .680 | .990 | 1.780 | ... | 1.213 | .67 | -.175 | 4.55 | 4350 | 7.4 |
| M0 | 1.420 | ... | 1.280 | ... | ... | ... | 0.52 | -0.280 | 4.63 | 3840 | 8.9 |
| 1 | 1.475 | ... | 1.400 | ... | ... | ... | .49 | -.310 | 4.66 | 3710 | 9.6 |
| 2 | 1.512 | ... | 1.500 | ... | ... | ... | .44 | -.358 | 4.70 | 3620 | 10.0 |

*Values in parentheses are extrapolated.

Table 2-A4

Thermal Parameters for Class III Giants

| Spectral Type | B-V | b-y | V-R | B ₂ -V ₁ | C(42-45) | Mass | log mass | log g | T _{eff} | M _V |
|---------------|---------|---------|-------|--------------------------------|----------|-------|----------|-------|------------------|----------------|
| F5 | 0.430 | ... | ... | 0.22 | ... | 2.1 | 0.32 | 3.6 | 6380 | 1.2 |
| 6 | .463 | ... | ... | .26 | ... | — | — | — | 6100 | — |
| 7 | .500 | ... | ... | .29 | ... | — | — | — | 6030 | — |
| 8 | .545 | ... | ... | .34 | .532 | — | — | — | 5860 | — |
| 9 | .595 | ... | ... | .38 | .567 | — | — | — | 5670 | — |
| G0 | 0.650 | ... | 0.530 | 0.41 | 0.608 | 2.1 | 0.32 | 3.3 | 5500 | 1.1 |
| 1 | .710 | ... | .574 | .44 | .655 | — | — | — | 5400 | — |
| 2 | .766 | (.51) * | .608 | .46 | .696 | — | — | — | 5280 | — |
| 3 | .816 | (.52) | .640 | .48 | .733 | — | — | — | 5190 | — |
| 4 | .859 | (.53) | .664 | .51 | .757 | — | — | — | 5060 | — |
| 5 | .893 | .540 | .685 | .54 | .776 | 2.4 | 0.38 | 3.1 | 5010 | 1.0 |
| 6 | .918 | .550 | .696 | .56 | .788 | — | — | — | 4950 | — |
| 7 | .934 | .565 | .706 | .59 | .802 | — | — | — | 4870 | — |
| 8 | .954 | .575 | .720 | .63 | .818 | — | — | — | 4830 | — |
| 9 | .979 | .590 | .740 | .66 | .848 | — | — | — | 4770 | — |
| K0 | 1.015 | 0.610 | 0.770 | 0.70 | 0.880 | 2.3 | 0.36 | 2.6 | 4660 | 0.9 |
| 1 | 1.092 | .650 | .808 | .75 | 0.930 | — | — | — | 4550 | — |
| 2 | 1.159 | .700 | .840 | .80 | 1.002 | — | — | — | 4370 | — |
| 3 | 1.240 | .800 | .960 | .95 | 1.106 | — | — | — | 4140 | — |
| 4 | 1.385 | .865 | 1.060 | 1.07 | 1.218 | — | — | — | 3980 | — |
| 5 | 1.485 | .900 | 1.195 | 1.12 | 1.307 | 2.2 | 0.34 | 1.9 | 3880 | 0.1 |
| M0 | 1.583 | 0.985 | 1.230 | 1.18 | ... | (2.2) | (0.34) | (1.4) | 3750 | -0.4 |
| 1 | 1.600 | 0.994 | 1.280 | 1.19 | ... | — | — | — | 3730 | — |
| 2 | (1.650) | 1.000 | 1.340 | 1.22 | ... | — | — | — | 3650 | — |

*Values in parentheses are extrapolated.

F-G-K stars. So far, most angular diameter measurements have been largely of earlier spectral types or of the large red stars. Consequently, there is considerable reliance on model atmospheres in fixing T_{eff}. Two main classes of

dependence can be seen here: (1) a model of a given T_{eff} is chosen to match a star on the basis of the energy distribution, or (2) a model is chosen on the basis of spectral line strengths through excitation or ionization temperatures.

Table 2-A5

Thermal Parameters for Class I Supergiants

| Spectral Type | B-V | C(42-45) | log g | T _{eff} | M _V (lb) |
|---------------|-------|----------|-------|------------------|---------------------|
| F5 | 0.430 | ... | ... | 6740 | -4.6 |
| 6 | .463 | ... | ... | 6520 | — |
| 7 | .510 | ... | ... | 6280 | — |
| 8 | .566 | .528 | ... | 6000 | — |
| 9 | .642 | .587 | ... | 5790 | — |
| G0 | 0.715 | 0.650 | 1.6 | 5500 | -4.6 |
| 1 | .790 | .682 | — | 5290 | — |
| 2 | .854 | .714 | — | 5120 | — |
| 3 | .910 | .750 | — | 4980 | — |
| 4 | .959 | .781 | — | 4900 | — |
| 5 | 1.000 | .810 | 1.3 | 4780 | -4.5 |
| 6 | 1.033 | .838 | — | 4680 | — |
| 7 | 1.073 | .868 | — | 4630 | — |
| 8 | 1.112 | .900 | — | 4560 | — |
| 9 | 1.145 | .938 | — | 4500 | — |
| K0 | 1.175 | 0.974 | 1.0 | 4440 | -4.5 |
| 1 | 1.227 | 1.022 | — | 4350 | — |
| 2 | 1.315 | 1.120 | — | 4250 | — |
| 3 | 1.415 | 1.222 | — | 4140 | — |
| 4 | 1.515 | 1.276 | — | 4020 | — |
| 5 | 1.595 | 1.300 | 0.7 | 3920 | -4.5 |

*Values in parentheses are extrapolated.

Recent summaries of the results have been given by Böhm-Vitense (1981) and Hayes (1978), and need not be repeated in detail here.

The values for the tables and Figure 2-A2 are compiled from Flower (1977), Hayes (1978), Bessell (1979), Osborne (1979), Ridgway et al. (1980), Böhm-Vitense (1981), and Gehren (1981). Although the different published results often agree within ~ 100°K, absolute errors of ~ 300°K are entirely possible. The recent measurements of G and K giants by Adelman

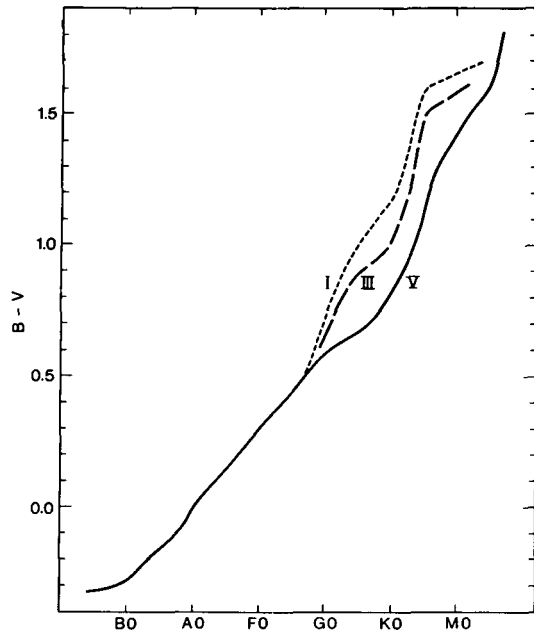


Figure 2-A1. The mean relation between B-V color index and spectral type is shown.

and Shore (1982) are slightly lower than the adopted calibration, but not necessarily significantly so. (There are too few stars to say.) Systematic errors of a conceptual nature may even exist (Nelson 1980). Notice that the T_{eff} values for the giants and supergiants are nearly the same as dwarf values when expressed as a function of B-V, but are distinctly lower at a given spectral type owing to the trifurcation seen in Figure 2-A1.

X.A5. MASSES

The main sequence star masses listed in Table 2-A3 and Figure 2-A3 are based on the tabulation by Popper (1980). These mean values agree well with the earlier tabulations of Harris et al. (1963), but Popper's newer values show much less scatter. For spectral types earlier than G0, the results are based almost exclusively on spectroscopic eclipsing binaries, whereas visual binaries largely define the cooler end. There is no evidence of discontinuity between the two portions.

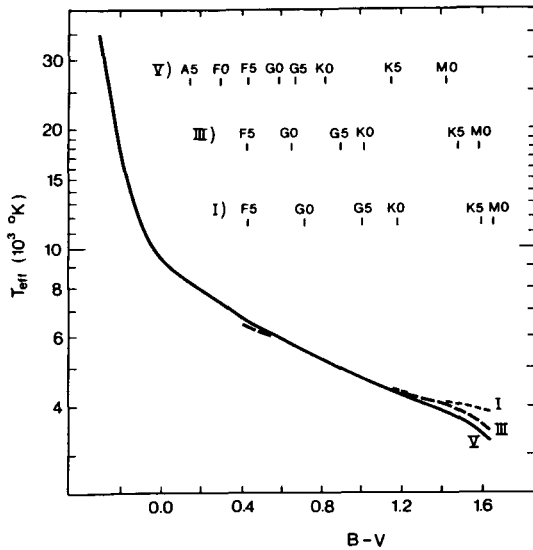


Figure 2-A2. The effective temperature is shown as a function of $B-V$. The F-G-K portion is identical with the entries in Tables 2-A2, 2-A3, and 2-A4, and the remainder is based on the findings of Böhm-Vitense (1981).

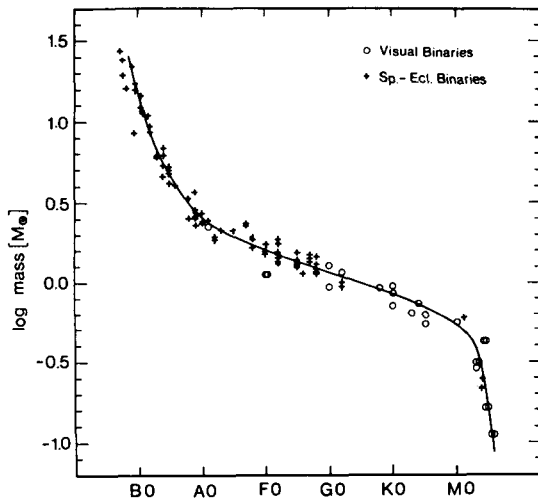


Figure 2-A3. Mass in solar masses is shown as a function of spectral type (based on the data of Popper, 1980).

Near M0 V, there is an abrupt steepening of slope in the mass-spectral type relation. Therefore, a small change in assigned spectral type can lead to substantial differences in deduced mass.

There is some controversy over the values of mass for luminosity class III stars. Scalo et al. (1978) argued in favor of a small mass $\sim 1.0 M_{\odot}$, but the entries in Table 2-A4 are based on the work of Stephenson and Sanwal (1969) and are about twice as large. There is also ample evidence that evolutionary model calculations for two to four solar masses can produce evolutionary tracks appropriate for red giants (e.g., Endal and Sofia 1979). The few binary giants that have been measured have masses on this larger scale, e.g., α Aur (G0 III + G5 III) has 2.55 and 2.65 M_{\odot} . Other systems such as RZ Cnc (K1 III + K4 III), AR Mon (K0 III + K3 III) are probably exchanging mass, but their system masses are 3.7 and 3.5 M_{\odot} , respectively (Popper, 1980).

Unfortunately, masses for late-type supergiants are still less well determined and in general can only be estimated from evolutionary tracks. This is not particularly satisfactory since sizeable mass loss apparently occurs. In consequence, no masses have been listed in Table 2-A5.

X.A.6. SURFACE GRAVITIES

The dependence of surface gravity on spectral type is reasonably well established for the dwarfs (Figure 2-A4). The entries in Table 2-A3 are based mainly on the results of Popper (1980), with lesser contributions from Osborne (1979) and Gray (1976). Log g rises only slightly from about 4.20 to 4.25 (g in cm s^{-2}) from B5 V to F5 V. Toward cooler stars a somewhat steeper increase is seen. The dwarf g -curve has the same two-part nature as the masses upon which they are based, with the spectroscopic binaries yielding the values hotter than G0 and the visual binaries giving those for cooler stars.

The giants' g -values are based on the masses of Stephenson and Sanwal (1969) and the g -values of Osborne (1979). The supergiant gravities have been estimated by van Paradijs (1973), Osborne (1979), and Luck (1982), using model atmosphere results. There is about

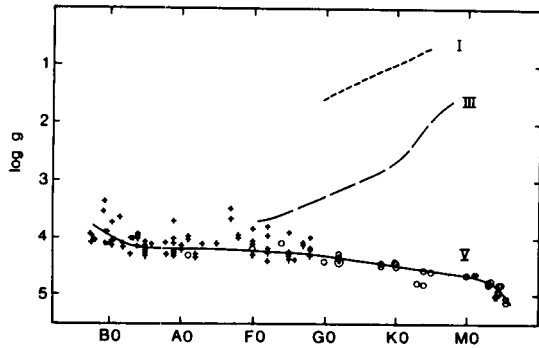


Figure 2-A4. Surface gravity in cm s^{-2} is shown as a function of spectral type. The circle with the dot in it indicates the solar value. Luminosity classes are shown.

a one order of magnitude spread of the individual values about the means. The luminosity class I and III g -values decrease rapidly with decreasing effective temperature owing to the radius increase.

Surface gravities obtained from model atmosphere and interior computations (e.g., van Paradijs and Ruiter, 1972; van Paradijs, 1973; Perrin, 1975a, 1975b; Tomkin et al., 1975; Hearnshaw, 1976a, 1976b; Foy, 1978) are at least approximately consistent with those listed in Tables 2-A3 and 2-A4, although this is not always the case (e.g., Oinas, 1974, 1977; Ayres and Johnson, 1977). In that portion of the HR diagram where the evolutionary tracks curve upward (typically K3 III and later), it becomes increasingly difficult to establish g . The well known discussion for Arcturus illustrates the point (Mackle et al., 1975; van Paradijs and Meurs, 1974; Ayres and Johnson, 1977; Martin, 1977; Spite and Martin, 1981).

X.A7. ABSOLUTE MAGNITUDES

The absolute visual magnitudes are included in the tables for completeness. They are taken from Allen (1973), Blaauw (1963), and Stephenson (1960). The zero-age main-sequence magnitudes are 0.4 magnitude fainter at A5 than the tabulated values, and the difference

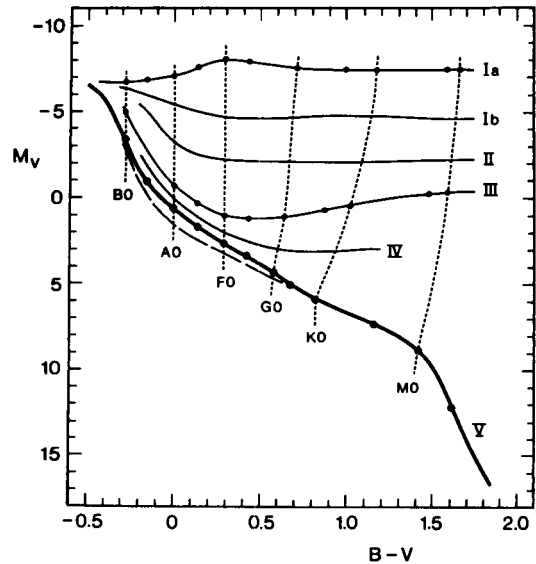


Figure 2-A5. An HR diagram is included here for reference. Constant spectral types are shown by the dashed lines.

tapers to zero by late G stars, as shown in Figure 2-A5.

X.A8. THE SUN

For some purposes the Sun's proximity can be frustrating. Its large angular size and its very brightness make it hard to measure with the equipment and standard techniques applied to other stars. The effective temperature of $5780 \text{ K} \pm 20 \text{ K}$ (Fröhlich, 1977; Willson and Hickey, 1977; Neckel and Labs, 1973) is well determined especially by F-G-K star standards, but its spectral type and color indices are not. Technically speaking, the Sun is a G2 V star by definition, since Johnson and Morgan (1953) adopted it as a G2 V standard in the MK system. But the meaningful questions are: does the Sun have a spectrum that is systematically different from others of G2 V classification? If so, does the solar spectrum indicate a hotter or cooler photosphere than for others of this same class, and by how much?

Garrison (1979) has reviewed the classes of errors commonly committed and gives

references to studies earlier than 1978. Hayes (1979) has summarized the solar B-V measurements and finds values ranging from 0.60 to 0.67. His best estimate is $(B-V)_{\odot} = 0.66 \pm 0.015$. The corresponding spectral type (Table 2-A3) is G4 V. Clements and Neff (1979) also review the published measurements and add some of their own. They conclude that $(B-V)_{\odot} = 0.63 \pm 0.01$. The recent extensive measurements of Tüg and Schmidt-Kaler (1982) give one of the highest values yet: $(B-V)_{\odot} = 0.686 \pm 0.011$. The Sun would fit the tabulated mass relation (Table 2-A3) if it had a spectral type of G4 V and a B-V of 0.66. According to Table 2-A3, the solar surface gravity is not attained until G8 V, at a mass of $0.90 M_{\odot}$. At the same time, we can see from Figures 2-A3 and 2-A4 that the solar values are within the

scatter of the points around the adopted mean relations, and since both mass and g are slowly varying functions of spectral type a small deviation translates into a rather large step in these two variables. Consequently, there may be no significance to the small deviations of the solar values from the means. We should also be aware that the sample of stars may contain a significant fraction of marginally evolved stars, implying that the true main sequence mean in Figure 2-A4 should be drawn somewhat lower.

This manuscript was completed in February of 1985. Additional related material may be found in the recent book "Lecture on Spectral-Line Analysis: F, G, and K Stars," by D.F. Gray (The Publisher: Arva, Ontario), 1988.

3

OBSERVATIONS OF THE CHROMOSPHERES, CORONAE, AND WINDS OF F, G, AND K STARS

Dieter Reimers

I. OVERVIEW: EVIDENCE FOR AND INCIDENCE OF CHROMOSPHERES, CORONAE, AND WINDS IN COOL STARS

In this chapter we consider spectroscopic observations of phenomena that emanate from stellar chromospheres, coronae, or winds, i.e., of those phenomena that involve emission or absorption in atmospheric layers located above the stellar photosphere. To avoid an exercise in semantics concerning what is a chromosphere, etc., we first define the scope of the chapter by listing in this section the kinds of observations that will be discussed in approximately the order of increasing height above the photosphere.

- (i) **Na D:** The cores of the Na D lines in the solar Fraunhofer spectrum give information about the structure and velocity field of the low chromosphere (Gehren, 1975). In some luminous G to K supergiants, the Na D lines have additional blueshifted cores apparently of circumstellar origin (see below). This effect has not yet been well observed, since very high spectral resolution is required and there may be interference with interstellar components.
- (ii) **Infrared CaII triplet:** There is no evidence for distinct emission features in the lines of the CaII IR triplet. However, in late F to early K stars the line cores of active-chromosphere stars are observed to be filled-in relative to those of quiet-chromosphere stars of the same spectral type. Observations of the early M supergiant α Ori with the Fourier Transform Spectrometer at Kitt Peak show that all three infrared CaII lines are strongly asymmetric (Figure 3-1). In α Ori the Doppler shifts of the CaII lines do not follow the radial velocity variations of the photospheric lines; so the infrared CaII lines must be formed in a layer decoupled from the photosphere (Goldberg, 1979).
- (iii) **H α :** In late-type stars the cores of the Balmer lines are usually deep and broad (Figure 3-2). The lines are much too strong, given the low temperatures of the stellar photospheres, an effect that was called "superexcitation" decades ago. In α Ori the point of minimum intensity in the H α profile is displaced to the blue and does not follow the radial velocity variations of

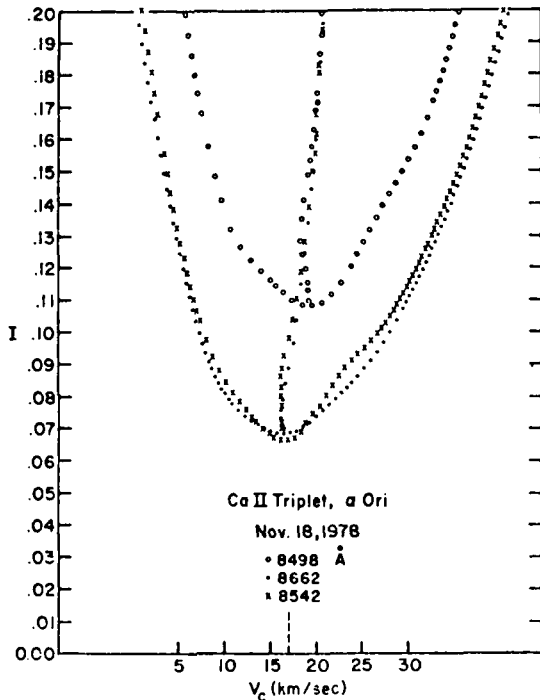


Figure 3-1. Profiles of the cores of the three members of the CaII infrared triplet plotted on a velocity scale. The loci of the bisectors are also plotted. The vertical dashed line on the abscissa scale marks the radial velocity of the photosphere (Goldberg, 1979).

the star (Weymann, 1962). In K supergiants and extremely luminous F and G supergiants blueshifted, variable H α emission has been found in addition to the broad absorption (e.g., Reimers, 1981, cf. Figure 3-9b). In cool Population II giants the H α profile may have substantial asymmetric emission wings (Peterson, 1981; Cacciari and Freeman, 1983).

- (iv) **CaII H and K emission cores:** In late-type stars the CaII H and K lines are strong and have very extended damping wings. An emission feature (Figure 3-3) is often seen at the very center of the line in F to K stars lying to the right of the Cepheid strip in the HR diagram. CaII emission is also seen in

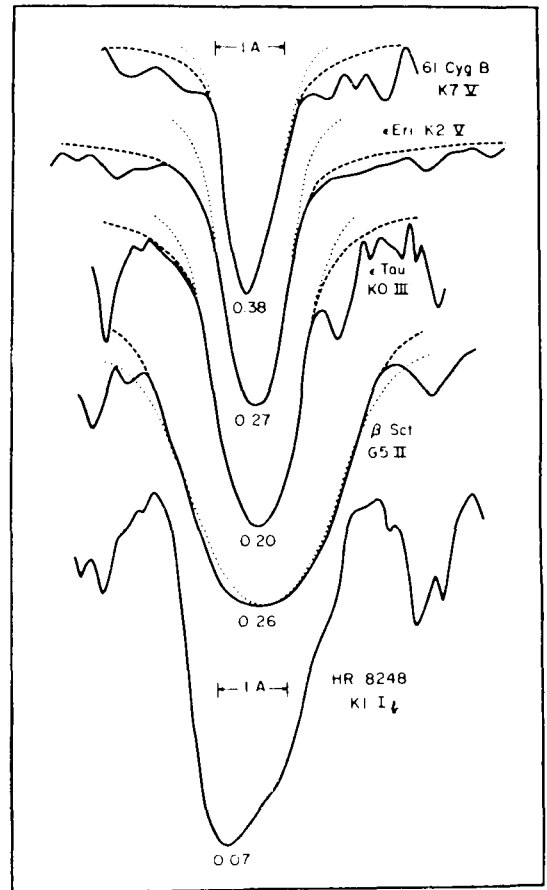


Figure 3-2. Five sample H α profiles. In the top four, the dashed curve is the reconstructed profile, and the dotted curve, a Gaussian profile with the same half-width and central intensity. Note the damping wings in ϵ Eri and the unsymmetric profile of HR 8248 (K1 Ib). The central intensity in units of the hypothetical continuum is given at the bottom of each profile (from Kraft et al., 1964).

Cepheids at certain phases, but such stars are not discussed here. The emission feature is often double peaked. On the main sequence the earliest spectral type at which emission has been seen is F0 (γ Vir N, a magnetically active star, Warner, 1968). There is no evidence for CaII emission from A-type stars (Dravins, 1981b). The widths (cf.

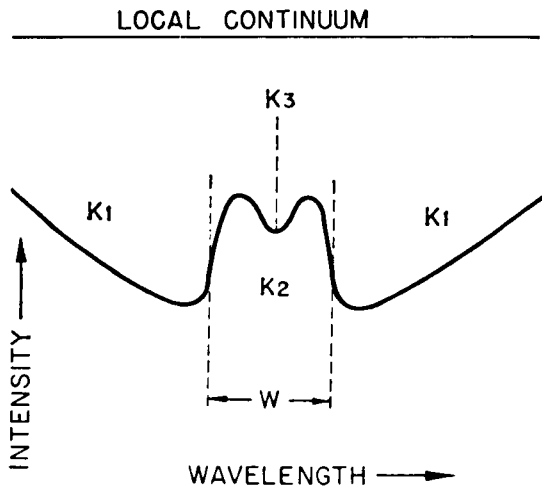


Figure 3-3. Schematic representation of a typical K line as seen in the integrated solar spectrum or in a stellar spectrum. The deep, broad absorption, K_1 , is formed in the photosphere; the emission, K_2 , is produced in the chromosphere (Wilson, 1966a).

Figure 3-4), intensities, time-variability, and dependence on stellar parameters of the CaII H and K lines have been extensively studied, in particular by O.C. Wilson (e.g., 1966a) and subsequently by Vaughan and Preston (1980), Vaughan et al. (1981), and Baliunas et al. (1983).

Relationships between the fine structure on the solar disk seen in CaII H and K, and in $H\alpha$, He $\lambda 10830$, and MgII h and k have been studied by several authors (McMath et al., 1956; Vaughan and Zirin, 1968; Fredga, 1972). It is clear that these relationships are strongly influenced by solar magnetic fields (Skumanich et al., 1975).

- (v) **CaII H and K wing emission lines and He:** Weak emission lines (mainly FeI and FeII) are seen in the absorption wings of CaII H and K in bright giant and supergiant stars of spectral type F to M (Figure 3-4). The properties of He

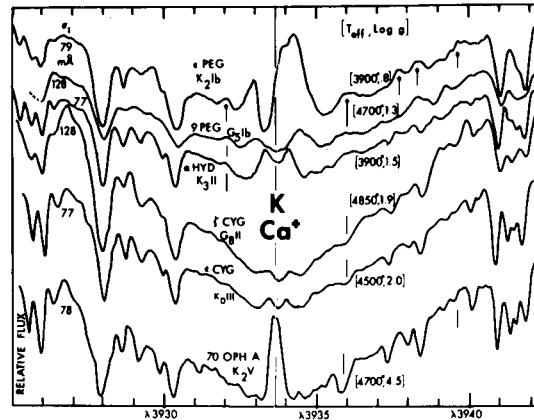


Figure 3-4. The CaII K line in six cool stars of similar effective temperature but differing luminosity as indicated (Stencel 1977).

emission near the center of CaII H were investigated by Wilson (1957).

- (vi) **MgII h and k:** These lines are a UV counterpart to the CaII H and K lines. Due to the high relative abundance of magnesium to calcium (15 times) and the much higher contrast against the photosphere at 2800\AA , MgII doublet emission is often easier to detect than CaII H and K. It has been found to be ubiquitous in late-type stars [see Linsky and Ayres (1978) for earlier references]. Böhm-Vitense and Dettman (1980), in particular, have surveyed the occurrence of MgII emission in late-type stars. On the main sequence they found MgII emission from all spectral types later than F2, and among giants and supergiants from all stars on the red side of the Cepheid instability strip (just as CaII K). The earliest observed star with MgII emission is Altair (A 7 IV-V) (Blanco et al., 1982).

MgII and other UV emission lines have only been detected in main-sequence stars cooler than about $B-V = 0.30$. However, Linsky and Marstad

(1981) have shown that, due to the steep increase of background photospheric surface flux around $B-V = 0.30$ ($\sim F0 V$), emission lines from even the most active chromospheres would be impossible to detect. Because of this contrast problem, other techniques, such as X-rays, must be used to search for evidence of non-radiative heating in A-type stars.

(vii) **Ly α :** Emission line profiles of Ly α were first observed with the Princeton spectrometer on board the Copernicus satellite in nearby main-sequence and giant stars (cf. McClintock et al., 1975). The stellar line appears to be centrally reversed (Dupree, 1976) although the shape of the core is often affected by interstellar Ly α and geocoronal emission.

(viii) **He I 10830 Å:** This highly-excited He I line is the only line in the normal solar Fraunhofer spectrum that originates entirely in the chromosphere, although its intensity may be controlled in part by soft X-ray radiation from the corona. It is weak in quiet regions and increases in absorption strength in plages and filaments. It appears in absorption in some F stars (e.g., α CMi), in many G stars, particularly giants, and at least at some time in all K giants. The line disappears around M1 (Zirin, 1976, O'Brien, 1980). In luminous K giants it appears occasionally in emission, sometimes with a P Cygni-type profile and with far blueshifted absorption components (Figure 3-5).

(ix) **UV emission lines:** Emission lines from OI, CII, CIV and SiIV, indicating temperatures from 10^4 to 2×10^5 K, occur widely in late-type stars. The wealth of spectra obtained with the IUE (International Ultraviolet Explorer) satellite illustrates the range of

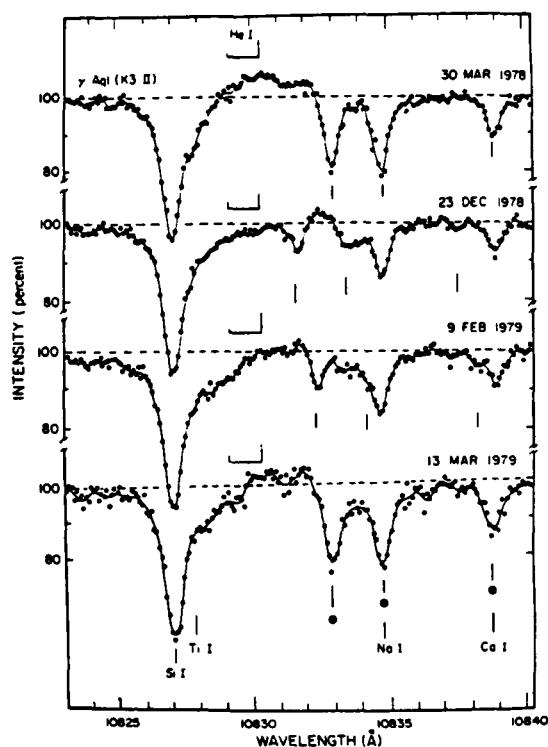


Figure 3-5. He I 10830 Å in the 'hybrid atmosphere' star γ Aql. Notice variable emission as well as far blueshifted absorption (from O'Brien, 1980).

variation. Some of the regularities of this emission can be illustrated by considering CIV, which is indicative of the presence of 10^5 K plasma. Figure 3-6 contains results of IUE measurements of CIV emission from cool stars of various luminosities. Most dwarf stars later than F5 clearly show the presence of CIV in emission, while CIV is not observed at all in the coolest, most luminous stars (i.e., M supergiants). With the exception of these two cases, it is not possible to predict the presence or absence of detectable quantities of high temperature plasma based on position in the H-R diagram alone. Stars at a given position may exhibit CIV and other high temperature ions, or they may have a spectrum showing only lower excitation species, or they

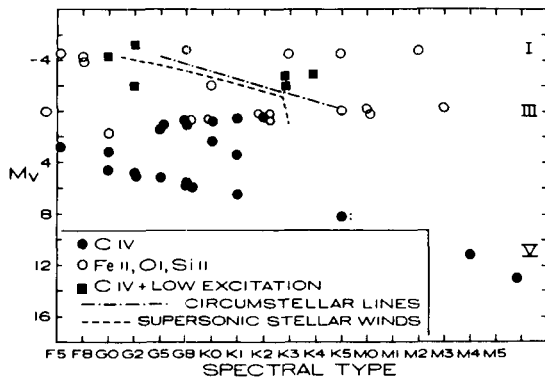


Figure 3-6. Presence of UV emission lines and circumstellar lines in the HR diagram (Reimers, 1981): Hybrid atmosphere stars.

may even have a combination of the two, as in the “hybrid” stars (Hartmann et al., 1981).

Of course, “detection” must be quantified in terms of objective parameters such as surface flux, a matter which is discussed in a later section. It can be difficult to detect an emission line against a strong continuum. There is a particular problem with IUE in the detection of C IV in stars which have a rapid decrease in flux with decreasing wavelength. This effect is especially critical in stars of spectral type F. Aspects of the problem and the difficulty in determining whether or not hot stars have chromospheres are discussed by Böhm-Vitense and Dettman (1980); Linsky and Marstad (1981); and Hartmann et al. (1982). Although C IV may not be “visible” in a spectrum, there is no evidence at present for a sharp cut-off of chromospheres in the early F stars.

- (x) **X-rays:** X-rays have been detected with the HEAO-2 (*Einstein*) satellite from main-sequence stars of every spectral type, from a few white dwarfs, from giant and supergiant stars of early spectral type, and from a handful of G and K giants (Figure 3-7; Vaiana et

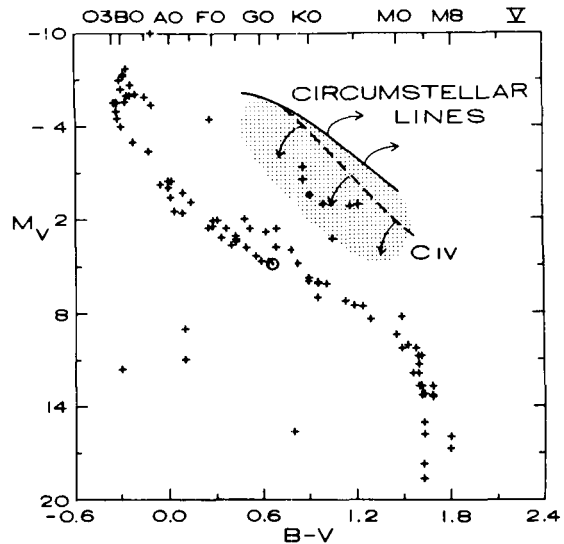


Figure 3-7. Stars that have been detected as X-ray sources with HEAO-2 (“Einstein”). The hatched region indicates where the transition from hot to cool outer atmospheres occur (after Dupree, 1981).

al., 1981). There is a striking failure to detect X-rays from the coolest giant and supergiant stars in the upper right quadrant of the H-R diagram. In the case of these coolest giant and supergiant stars, upper limits to the X-ray surface fluxes in the best-observed cases are substantially lower than the X-ray flux from the quiet Sun and comparable to that from solar coronal holes. In these stars, there may indeed be no X-ray emitting material or it may be present, but only in undetectably small quantities.

A significant decrease in coronal X-ray fluxes has been found in single dwarf stars cooler than about $B-V = 0.30$ (Golub et al., 1983; Schmitt et al., 1983; Walter, 1983). The earliest main-sequence star with a “solar-like” corona and chromosphere appears to be α Aq1 (A7, IV-V, $B-V = 0.22$), while the hottest rapidly rotating W UMa systems with UV emission lines are of later A type (cf. Walter et al., 1983).

- (xi) **Winds and mass loss:** Indicators of mass loss include blueshifted circumstellar absorption in the CaII and MgII resonance lines of giants and G and K supergiants; far shifted HeI 10830Å absorption components in K giants and G and K supergiants; shifted H α emission in K supergiants and particularly in luminous G and F supergiants and bright Pop II stars; a 10 μ infrared excess in luminous K and G supergiants; and circumstellar lines with P Cyg profiles in the spectra of ζ Aur systems, formed by scattering of B star photons in the winds of the K giants.

Further knowledge about the structure of the outer layers of F to K stars comes from direct observations of the geometrical extension of chromospheres and winds in certain eclipsing binary systems. In ζ Aur stars, eclipsing binary systems consisting of a bright K (super) giant and a hot B star, the B star is an astrophysical light source which probes the extended chromosphere and wind of the K giant immediately before and after secondary eclipse. Recently, it has become possible through high-resolution IUE spectra to observe in ζ Aur systems both the extended chromosphere and the expanding wind of the late-type stars at distances of several stellar radii, using observations of B star photons scattered by the wind (Chapman, 1981; Reimers et al., 1981; Che et al., 1983; Schröder, 1985a,b). These results are discussed in Chapter 3.V.B. The existence of large geometrical extension of supergiant chromospheres has also been revealed in early M supergiants (cf. Chapter 3.V.B).

II. CORONAE OF F TO K STARS

Before the launch of IUE (1979) and *Einstein* (1979) we had no real knowledge of coronae in cool stars other than the Sun. With the exception of a few singular detections and upper limits from rocket and satellite experiments (cf. review by Mewe, 1979), there were only theoretical predictions of the existence and proper-

ties of stellar coronae, and nearly all of these have been found to be inadequate.

With the *Einstein* and IUE satellites it has been possible to detect hot plasmas with $T \leq 10^6$ K and $\leq 2 \times 10^5$ K respectively in a large number of stars. The temperature range 2×10^5 to 10^6 is still unexplored. Since at such temperatures abundant ions emit lines only in the EUV range, it depends on the currently unknown degree of interstellar Lyman continuum absorption whether it will be possible to study in depth plasmas at temperatures of several 10^5 K in distant stars.

Unfortunately, the instruments on board *Einstein* were not sensitive enough to do spectroscopy in the X-ray domain, and thus it is very difficult to infer reliable physical properties of the emitting coronae (temperature, density, flow velocities, total energy output, etc.). The only late-type star observed at high resolution with the crystal spectrometer was the bright RS CVn-type giant Capella. On the other hand, the IPC instrument on board *Einstein* showed for the first time which types of stars exhibit X-ray emission, what is the range of soft X-ray luminosity L_x for a given stellar type, and with which stellar parameters L_x is correlated.

The IUE satellite offered the additional advantage — besides merely detecting UV emission — of permitting a determination of electron densities and temperatures from lines of highly ionized atoms (up to NV formed at $1.5 \cdot 10^5$ K). Furthermore, the kinematics of hot regions around cool stars could be studied in a few bright stars from line profiles and/or line displacements.

II.A. SOFT X-RAY EMISSION

The main result of *Einstein* observations of stars was the discovery that X-ray emission is nearly ubiquitous in the HR diagram (Vaiana et al., 1981). Typical detections and upper limits are given in Table 3-1. On the cool side of the main sequence, X-ray emission has been

Table 3-1

Summary of Target Stars, X-Ray Fluxes, and Ultraviolet Emission Properties

| Star (1) | HR No. (2) | Spectral Type (3) | V (mag) (4) | $(V-R)^b$ (mag) (5) | \int_{bol} (10^{-7} ergs cm^{-2} s^{-1}) (6) | $\int_{\text{X}}/\int_{\text{bol}}$ (10^{-7}) (7) | $\int_{\text{Mg II}}/\int_{\text{bol}}^{b,c}$ (10^{-7}) (8) | $\int_{\text{CIV}}/\int_{\text{bol}}^c$ (10^{-7}) (9) | $\int_{\text{He II}}/\int_{\text{bol}}^c$ (10^{-7}) (10) |
|---------------------|---------------|----------------------|---------------------|---------------------------|---|---|---|---|--|
| Dwarfs | | | | | | | | | |
| μ Dra..... | 6369, 70 | dF6+dF6 | +5.06 | (+0.40) | 2.4 | 170 | ... | ... | ... |
| β Vir..... | 4540 | F8 V | +3.60 | +0.48 | 9.7 | 20 | ... | ... | ... |
| π^1 UMa... | 3391 | G0 V | +5.64 | +0.52 | 1.5 | 420 | ... | ... | ... |
| β Com..... | 4983 | G0 V | +4.26 | +0.49 | 5.3 | 40 | ... | ... | ... |
| Sun..... | ... | G2 V | -26.77 | (+0.53) | 1.37×10^{13} | (1.5-4) ^c | 200-280 ^c | 0.9-2.1 ^c | 0.2-0.8 ^c |
| α Cen A.. | 5459 | G2 V | -0.01 | (+0.53) | 270 | 2 ^{d,c} | 180 | 1.0 | 0.3 |
| τ Cet..... | 509 | G8 V | +3.50 | +0.62 | 12 | <4 ^f | ... | ... | ... |
| 70 Oph... | 6752 | K0 V+K5 V | +4.03 | +0.65 | 7.4 | 100 ^f | ... | ... | ... |
| α Cen B.. | 5460 | K1 V | +1.33 | (+0.7) | 95 | 14 ^{d,c} | 250 | 1.2 | 0.2 |
| ϵ Eri..... | 1084 | K2 V | +3.73 | +0.72 | 10 | 150 ^f | 750 | 9.8 | 5.3 |
| 61 Cyg.... | 8085, 86 | K5 + K7 V | +4.80 | +1.08 | 6.1 | 40 ^f | ... | ... | ... |
| Subgiants | | | | | | | | | |
| δ Pav..... | 7665 | G5 IV | +3.56 | +0.61 | 11 | 3 ^d | ... | ... | ... |
| Giants | | | | | | | | | |
| α Aur Ab. | 1708 | F9? III | +0.96 | (+0.46) | 110 | 90 ^{d,c} | 1100 | 32 | 4.5 |
| β Lep..... | 1829 | G5 III | +2.84 | +0.65 | 23 | 1 ^d | ... | ... | ... |
| μ Vel..... | 4216 | G5 III | +2.69 | +0.68 | 27 | 80 | 380 | 3.7 | 2.1 |
| β Crv..... | 4786 | G5 III | +2.64 | +0.61 | 26 | <1 | ... | ... | ... |
| χ Per..... | 662 | gG6 | +6.00 | (+0.78) | 1.4 | 25 ^{d,c} | ... | ... | ... |
| η Dra..... | 6132 | G8 III+dK | +2.74 | +0.61 | 24 | 0.6 ^d | ... | ... | ... |
| β Gem..... | 2990 | K0 III | +1.14 | +0.75 | 120 | 0.4 | 93 | ... | ... |
| ϵ Cyg..... | 7949 | K0 III | +2.46 | +0.73 | 35 | <0.4 | ... | ... | ... |
| β Cet..... | 188 | K1 III | +2.02 | +0.72 | 52 | 40 | 260 | 1.0 | 1.1 |
| α Ari..... | 617 | K2 III | +2.00 | +0.84 | 62 | <0.2 ^d | 81 | ... | ... |
| α Boo..... | 5340 | K2 III | -0.05 | +0.97 | 490 | <0.03 | 95 | <0.2 | <0.3 |
| α Ser..... | 5854 | K2 III | +2.64 | +0.81 | 33 | 0.3 ^d | 67 | 0.6 | <0.3 |
| ϵ Sco..... | 6241 | K2 III-IV | +2.29 | +0.86 | 48 | 0.3 ^d | 71 | 0.6 | <0.3 |
| α Tau..... | 1457 | K5 III | +0.86 | +1.23 | 360 | <0.04 | ... | ... | ... |
| Bright Giants | | | | | | | | | |
| β Dra..... | 6536 | G2 II | +2.78 | +0.68 | 24 | 30 | 660 | 10 | 2.0 |
| ϵ Car..... | 3307 | K0 II+B | +1.85 | (+0.92) | 74 | 0.2 | ... | ... | ... |
| α Cas..... | 168 | K0 II-III | +2.23 | +0.78 | 46 | <0.3 | 82 | ... | ... |
| α UMa.... | 4301 | K0 II-III+? | +1.79 | +0.81 | 68 | <0.2 ^d | 100 | <0.9 | <0.5 |
| β Peg..... | 8775 | M1 II-III | +2.42 | +1.50 | 160 | <0.2 ^d | 36 | ... | ... |

^a Values in parentheses are obtained from $(B-V)$ for the Sun and α Cen A.^b Stencel and Mullan, 1980, and Basri and Linsky, 1979.^c Ayres, Marstad, and Linsky, 1981.^d Vaiana et al., 1981.^e High Resolution Imager.^f Johnson et al., 1981.

Table 3-1 (Continued)

| Star (1) | HR No. (2) | Spectral Type (3) | V (mag) (4) | (V-R) ^b (mag) (5) | \dot{J}_{bol} (10^{-7} ergs cm^{-2} s^{-1}) (6) | f_x/\dot{J}_{bol} (10^{-7}) (7) | $f_{\text{Mg II}}/\dot{J}_{\text{bol}}$ ^{b,c} (10^{-7}) (8) | $f_{\text{CIV}}/\dot{J}_{\text{bol}}$ ^c (10^{-7}) (9) | $f_{\text{He II}}/\dot{J}_{\text{bol}}$ ^c (10^{-7}) (10) |
|---------------------|---------------|----------------------|-------------------|------------------------------------|--|--|--|--|---|
| Supergiants | | | | | | | | | |
| α Car..... | 2326 | F0 Ib-II | -0.75 | +0.24 | 480 | 0.6 | ... | ... | ... |
| η Aql..... | 7570 | F6 Ib + ? | +3.50 | (+0.55) | 11 | <1 | ... | ... | ... |
| δ CMa.... | 2693 | F8 Ia | +1.84 | +0.51 | 50 | <0.3 | 62 | ... | ... |
| β Aqr..... | 8232 | G0 Ib | +2.87 | +0.61 | 20 | <1 | 260 | 1.5 | 0.6 |
| α Aqr..... | 8414 | G2 Ib | +2.93 | +0.66 | 20 | <1 | 590 | 1.6 | 1.0 |
| 9 Peg..... | 8313 | G5 Ib | +4.31 | +0.80 | 6.6 | <2 | 260 | ... | ... |
| ϵ Gem.... | 2473 | G8 Ib | +2.98 | +0.96 | 29 | <0.6 | 280 | <0.3 | ... |
| 12 Peg.... | 8321 | K0 Ib | +5.29 | (+0.99) | 3.6 | <3 | ... | ... | ... |
| ϵ Peg..... | 8308 | K2 Ib | +2.39 | +1.05 | 58 | <0.2 | 210 | ... | ... |
| ξ Cyg..... | 8079 | K5 Ib | +3.70 | +1.20 | 24 | <0.4 | 100 | ... | ... |
| α Sco..... | 6134 | M1 Ib + B | +0.91 | +1.55 | 710 | <0.02 ^d | ... | ... | ... |
| α Ori..... | 2061 | M2 Iab | +0.42 | +1.64 | 1400 | <0.03 ^d | 32 | <0.01 | ... |

^a Values in parentheses are obtained from (B-V) for the Sun and α Cen A.
^b Stencel and Mullan, 1980, and Basri and Linsky, 1979.
^c Ayres, Marstad, and Linsky, 1981.
^d Vaiana et al., 1981.
^e High Resolution Imager.
^f Johnson et al., 1981.

detected in stars of all spectral types later than about F0 and as late as M8.

In late-type supergiants, on the other hand, only a single star (α Car, F0 Ib) has been detected as an X-ray source. All stars in the upper right-hand corner of the HR diagram seem to be free from X-ray emission (Figure 3-8). Among giants, X-ray surface fluxes decrease rapidly as one proceeds from G to early K giants, and no X-rays have been detected by *Einstein* in late K giants (redward of V-R = 0.85). The *Einstein* satellite detected two early K giants (ϵ Sco, K0 III; α Ser, K2 III) with $L_x \approx 10^{28}$ erg s^{-1} and $L_x/L_{\text{bol}} = 3 \times 10^{-8}$, a ratio smaller than that in coronal holes.

It thus seems to be a fundamental fact that soft X-ray emission from single red giants decreases sharply with later spectral type, over the interval from V-R = 0.7 to V-R = 0.85. For example, Arcturus (α Boo, K2 III) and α

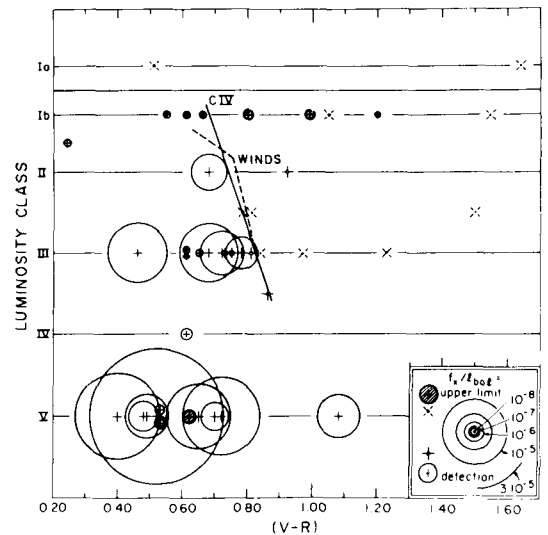


Figure 3-8. An H-R diagram in which soft X-ray detections (open circles) and upper limits (hatched circles) are plotted as bubbles whose areas are proportional to f_x/L_b . CIV and wind boundaries are also plotted (cf. Figure 3-6).

Tau (K5 III) were not detected with upper limits $L_x/L_{\text{bol}} < 3 \times 10^{-9}$, more than an order of magnitude less than in a coronal hole. In the G to M supergiants, no nonbinary star has been detected as a soft X-ray source. The G supergiants α Aqr (G1 Ib) and β Aqr (G0 Ib) have upper limits $L_x/L_{\text{bol}} < 10^{-7}$, while α Ori (M1 Iab) and α Sco (M1 Iab + B) have upper limits $L_x/L_{\text{bol}} < 2 \times 10^{-9}$.

The nondetection of soft X-rays from K giants later than K2 and from supergiants led Ayres et al. (1981) to propose a division of the HR diagram into two regions, one in which there is no evidence for hot coronae in any star (giants later than K2, G to M supergiants), and the other in which X-rays are frequently (but not always) detected. This latter region includes G to K2 giants, subgiants, and early F to M dwarfs. The detection of X-rays from a specified member of this latter class depends on factors such as the current level of activity and instrumental sensitivity.

A similar division had been found previously in the properties of UV emission lines (Linsky and Haisch, 1979), at a location in the HR diagram corresponding closely to that at which detectable circumstellar lines reveal the presence of massive stellar winds (Reimers, 1977a; Stencel and Mullan, 1980). At the time of this writing the physical origin of this apparent remarkable change in atmospheric structure is not known.

X-ray emission was detected in all nearby F to M main-sequence stars, with typical limiting sensitivity of 10^{-13} erg cm⁻² s⁻¹ at the Earth in the 0.25–4 keV band of the *Einstein* IPC for ½ hour exposure time. It has been conclusively shown that it is not the basic stellar parameters — gravity g and effective temperature T_{eff} — that alone determine the X-ray luminosity of a cool dwarf star. Indeed, for a given set of basic stellar parameters there is a spread by a factor of ~ 300 in the X-ray luminosity L_x , with a mean value of $\log L_x \simeq 28.5$ independent of spectral type, despite the

fact that the total bolometric luminosity decreases steeply from F to K or M dwarfs. The X-ray luminosity in late-type dwarfs is apparently controlled by other factors, one of which is probably surface magnetic fields, just as it is in the Sun.

In fact, the observed range of variation in soft X-ray luminosity L_x from different solar-type stars covers the range seen from different parts of the solar corona. For the very quiet Sun L_x would be about $10^{26.8}$ erg s⁻¹, while L_x would be about $10^{29.3}$ erg s⁻¹ if the Sun were completely covered with active regions. The former value lies near the bottom and the latter near the top of the observed distribution of L_x in G dwarfs (Linsky, 1981b).

There is now convincing observational evidence that stellar rotation, acting via dynamo-induced magnetic fields, plays a large role in determining the relative X-ray luminosities for stars with otherwise identical stellar parameters. For example, Pallavicini et al. (1981) have shown that, in the mean, single F7 to M5 stars satisfy $L_x \sim (v \sin i)^{1.9 \pm 0.5}$ (see Figure 3-25), independently of luminosity. This result can be interpreted as $L_x/L_{\text{bol}} \propto \Omega^2$, where Ω is the angular rotation velocity. On the other hand Walter (1981) found $L_x/L_{\text{bol}} \propto \Omega$ for rapidly rotating F8 to G5 stars and RS CVn systems. Walter (1982) has proposed that observations of single solar-type dwarfs can be represented simply by two power laws of the form $L_x/L_{\text{bol}} \propto \Omega^\alpha$, with a break in the value of α near a rotation period of roughly 12 days. This break may be related to the observed change in the form of the time variation of CaII emission that also occurs at rotational periods around 12 days (Vaughan and Preston, 1980; Vaughan, 1980). According to Skumanich's (1972) age-rotation relation $v \sim t^{-1/2}$, this change would occur at an age of about 10^9 years.

The correlation of X-ray activity with age among solar-type stars has been clearly demonstrated in several studies of galactic

clusters and associations of various ages, including the Orion cluster (Micela et al., 1982), Pleiades (Caillault and Helfand, 1981), Ursa Major (Walter et al., 1984), and Hyades (Zolcinski et al., 1982). The observed range of L_x for F to G stars is $30.4 \leq \log L_x \leq 31.5$ for Orion, $29.3 \leq \log L_x \leq 30.4$ for the Pleiades, $28.9 \leq \log L_x \leq 29.6$ for Ursa Major, and $28.3 \leq \log L_x \leq 30.1$ for the Hyades. The most active stars in the 10^8 year old Pleiades have 4×10^3 times the soft X-ray luminosity of the quiet Sun! The brightest source in the Hyades is 71 Tau (F0 V, $v \sin i \sim 200 \text{ km s}^{-1}$), with $L_x \sim 10^{30} \text{ erg s}^{-1}$. This star is about five times brighter in X-rays than the Sun would be if it were covered entirely by active regions, and so the active regions of 71 Tau must be (1) hotter, (2) denser, and/or (3) more extensive than those seen in the Sun.

Some of these very active late-type stars have been found to have measurable magnetic fields. In ξ Boo A (G8 V), a probable member of the young UMa group, and in 70 Oph A (K0 V), Robinson et al. (1980) have detected magnetic fields from the Zeeman splitting observed in unpolarized light. For ξ Boo A they found a field of $2.6 \times 10^3 \pm 400$ Gauss covering 30% of the stellar surface. Other stars with magnetic fields have been detected by Marcy (1980, 1984) [see Chapter 3.II.G].

Independent evidence for magnetic fields comes from microwave emission from X¹ Ori (G0 V), which was detected with the Very Large Array (VLA) at 6 cm and interpreted as gyroresonant emission from electrons in coronal fields of about 300 Gauss (Gary and Linsky, 1981).

II.B. UV EMISSION LINES

As mentioned briefly in the introductory overview, UV emission lines of CIV, SiIV and NV occur in all types of dwarf stars later than early F. However, among giants and supergiants there is a dichotomy similar to that found in X-ray emission. For stars of luminosity class III (Linsky and Haisch, 1979), a substantial

decrease in UV emission has been found at V-R ≈ 0.8 (early K type), while in Class II and Class I objects such UV emission has been found only in early G. In no single K or M supergiant have CIV lines ever been detected. UV emission in lines such as CIV, SiIV, and NV indicates the presence of plasma with temperatures in the range $5 \times 10^4 - 2 \times 10^5 \text{ K}$. In the solar atmosphere, the analysis of differential emission measured in these and similar lines shows that the plasma at such temperatures is compact relative to the volume of either the chromosphere ($T < 2 \times 10^4 \text{ K}$) or the corona ($T > 10^6 \text{ K}$). For this reason, the portion of the solar atmosphere with temperatures lying between "chromospheric" and "coronal" values is often called the transition region (TR). This designation has since been used to describe UV emission from other stars, although the actual geometry is not well understood. It should be noted that a successful prediction of the presence or absence of a hot corona (or TR) in a given star cannot be made on the basis of the basic stellar parameters (*i.e.*, position in the HR diagram) alone. Depending on the level of stellar activity (measured for example in typical low-temperature chromospheric lines such as OI, SI, SiII or MgII), TR emission lines may or may not be observed at a given detection level. This stellar individuality perhaps reflects star-to-star variations in rotation-induced magnetic fields. This individuality leads to a blurring of the dividing line in the HR diagram between stars with hot coronae and stars with cool expanding winds (see below).

The relation between TR emission and chromospheric and X-ray emission for various types of stars has been studied in detail by Hartmann et al. (1982) and Ayres et al. (1981). Their observations can be summarized as follows:

- (i) In most stars, the strength of TR (and X-ray) emission is well correlated with the strength of dominant chromospheric emission lines like MgII h and k [cf. Figure 3-4 in Ayres et al. (1981)].

The correlations between line fluxes in various lines are approximately $f(\text{OI}, \text{SiII}, \dots) \propto f(\text{MgII})$; $f(\text{CII}) \propto f(\text{MgII})^{1.5}$; $f(\text{SiIV} + \text{CIV} + \text{NV}) \propto f(\text{MgII})^{1.5}$; $f(\text{HeII } 1640) \propto f(\text{MgII})^2$; and $f(\text{soft X-rays}) \propto f(\text{MgII})^3$. These correlations suggest that coronae and chromospheres are physically related, but that heating of the hottest, outermost layers has a different functional dependence on the underlying parameters (rotation, magnetic fields, pulsation, ...) than heating of the chromosphere. A possible explanation is that heating mechanisms are different in different atmospheric layers.

- (ii) Although most stars follow the cited correlations, certain groups of stars deviate significantly from the trend. For example, F dwarfs and giants have brighter TRs relative to their chromospheric emission than G and K dwarfs. On the other hand, the OI 1305 Å multiplet is strongly enhanced in giants relative to dwarf stars with comparable MgII h and k fluxes.
- (iii) A significant observation is the simultaneous presence of both CIV, SiIV, and NV TR emission and cool stellar winds in a number of stars near to and on the cool side of the dividing line [e.g., α Aqr (G2 Ib), β Aqr (G0 Ib), Θ Her (K3 II), γ Aql (K3 II), ι Aur (K3 II), α TrA (K3 II), δ TrA (G3 II), HD81817 (K3 II), μ UMa (M0 III), σ Oph (K2 II), 9 Peg (G5 Ib); Hartmann et al., 1981; Reimers, 1982, 1984, 1985]. These stars have been called hybrid atmosphere stars.

Among these hybrid stars only α TrA and possibly Θ Her have been detected as X-ray sources (Brown, 1985). It is remarkable that while the NV surface fluxes in α Aqr and β Aqr are ~ 4 times the mean solar value, the upper

limits to X-ray fluxes are a factor of 2 below that of the quiet Sun. It is important to stress that the X-ray emission from hybrid stars and stars with massive winds, if present at all, must be much weaker than would be predicted by the relation $f_x \propto f(\text{MgII})^3$ (see above). For α Boo and α Aqr, the X-ray flux upper limits lie a factor of 10 or more below a prediction using this relation, which was established using G to K dwarfs and giants that are X-ray sources. On the other hand, TR emission line fluxes of hybrid stars follow the same correlations with chromospheric lines as the giants on the hot side of the dividing line (Reimers, 1982), and the Ayres et al. (1981) relations for TR emission appear valid for hybrid stars. The different behavior of the TR and X-ray emission then suggests that either temperatures in the hot regions of hybrid stars do not exceed $\sim 2 \times 10^5$ K (maximum of the coronal emission measure distribution) or else X-rays have for some other reason remained undetected in stars like α Aqr. One possibility is that X-rays are produced, but are then reabsorbed in the cool stellar winds of these stars.

III. MASS LOSS

The study of mass loss from red giants was initiated by Deutsch (1956, 1960), who observed violet displaced absorption cores in strong metal lines of low excitation in M-type giants and supergiants. By studying suitable binary systems Deutsch proved that these stars eject mass into the interstellar medium. Later, Deutsch's circumstellar line survey was extended to K and G giant and supergiant stars (Reimers, 1977a).

A detailed summary of optical observations of circumstellar (CS) shells made prior to 1975 was given by Reimers (1975b). Here, we concentrate on more recent optical and UV observations of winds in K, G, and early M giants and supergiants. Observations of CS dust, thermal molecular line emission and maser line emission will not be discussed in this volume.

III.A. WIND PROPERTIES

Mass-loss indicators and the incidence of mass-loss in the HR diagram may be summarized as follows:

- (i) **Circumstellar CaII and MgII absorption lines:** All stars cooler and more luminous than those on a line in the HR diagram defined roughly by (K5, $M_V = 0$), (K4, -1.0), (K2, -1.8), (G5, -4), (G0, -4.5) have CaII H and K absorption components (denoted as H_4 , K_4) shifted far beyond the violet edge of the CaII H and K emission core (Reimers, 1977a; see Figures 3-9 and 3-10). In the spectroscopic binaries μ UMa (M0 III) and ξ Cyg (K5 Ib) it was shown that these K_4 absorption lines remain stationary while the photospheric lines move back and forth as a result of the Doppler shifts due to orbital motions, indicating circumstellar matter. In the same group of stars far shifted absorption components have also been detected in the MgII resonance lines (Hartmann et al., 1981; Reimers, 1982; Mullan and Stencel, 1982; Simon et al., 1982). Indeed, owing to the larger optical depths of

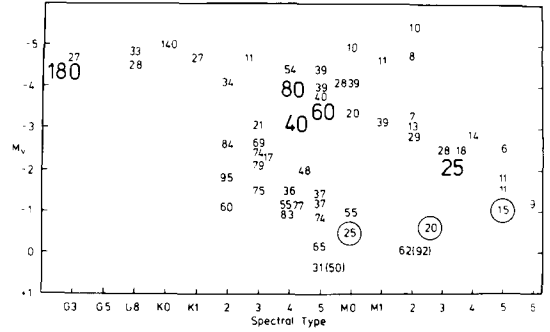


Figure 3-10. Survey of stellar wind velocities [km s^{-1}] observed mainly from shifts of circumstellar CaII absorption (from Reimers, 1977a). Larger size numbers: Wind velocities measured in ζ Aur systems.

the MgII lines, the visibility limit of CS MgII lines compared to CaII lines is shifted to slightly lower luminosities and higher temperatures. A far shifted CS component has also been seen in $\text{Ly}\alpha$ from the K giant α TrA (Hartmann et al., 1981). In K supergiants such as λ Vel, the emission cores of CaII H and K are blueshifted. In such stars, the stellar wind is already readily detected in the chromosphere (Figure 3-11).

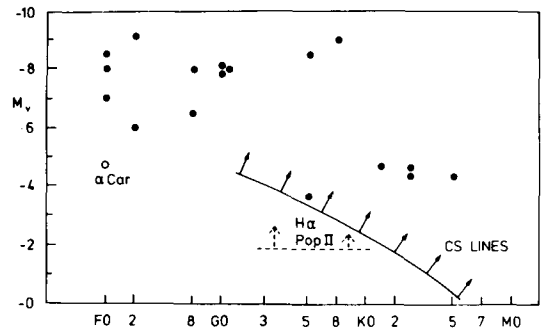
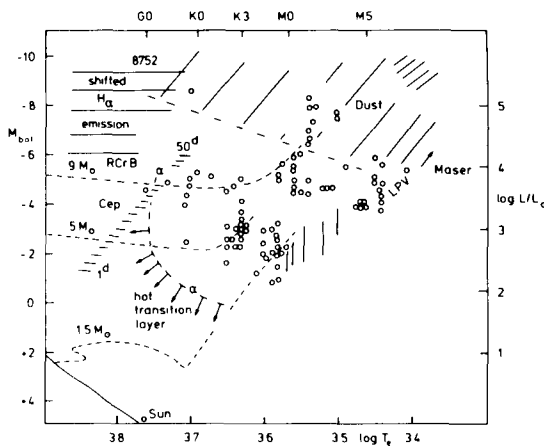


Figure 3-9. Stars with observed circumstellar absorption lines are denoted by open circles (a) and stars with shifted $H\alpha$ emission indicating mass-loss are shown as solid dots (b) (Reimers, 1981).

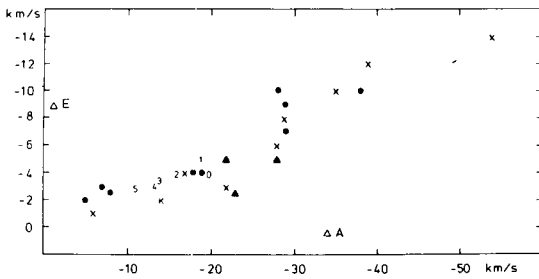


Figure 3-11. Shift ΔA of the circumstellar CaII K_4 absorption feature versus the shift ΔE of the chromospheric CaII K_2 emission feature (from Reimers, 1975a).

(ii) **Ultraviolet P Cygni type lines in ζ Aur systems:** The B star companions serve as astrophysical light sources that probe the extended chromospheres and inner wind regions of the K supergiant primaries. Rich CS spectra formed in the K giant stellar winds have been found with high-resolution IUE observations (see Chapter 3.V.B.1).

(iii) **HeI 10830 Å:** Among K giants there is evidence for a nearly one-to-one correlation between the presence of HeI emission and a CaII K asymmetry ratio $V/R < 1$ (see below). A number of K giants and G supergiants (ζ Aur, α Aqr, Θ Her, γ Aql) have far blueshifted (-150 to -200 km s $^{-1}$) absorption components in HeI (10830 Å).

(iv) **CaII and MgII asymmetry:** The ratio of the intensity of the violet emission peak to that of the red peak (V/R) provides further tentative evidence for outflow of matter from red giants. Stencel (1978) and Stencel and Mullan (1980) have shown that the line in the HR diagram where $V/R > 1$ (no outflow) changes to $V/R < 1$ (outflow) is near to and parallel to the line in the HR diagram beyond which stars have detectable CS lines. It is not clear whether $V/R < 1$ values are caused by

blueshifted absorption by escaping material (far away from the star), or by expanding chromospheres, or by both. Without detailed modeling the origin of the asymmetry of the self-reversed CaII and MgII profile remains unclear, and even the interpretation of $V/R < 1$ as an effect of mass loss perhaps appears insecure.

(v) **H α emission:** Following the work of Kraft et al. (1964) and Gahm and Hultquist (1972) it has been known that in G and K supergiants there is variable H α emission — mostly blueshifted — superimposed upon the broad chromospheric H α absorption line. Similar H α emission components, perhaps due to mass loss, have been found in bright Population II stars (e.g., Cohen, 1976, Cacciari and Freeman, 1983) and in extremely luminous F and G supergiants. Doubts have been cast on simple interpretations of the H α emission in terms of mass loss by Dupree et al. (1984) and much lower mass loss rates may be involved. In α Ori, the H α absorption core — probably formed in the extended chromosphere of the star — is also blueshifted by about half the wind's terminal velocity. In addition, the absorption core does not follow the photospheric pulsation, indicating that the chromosphere of α Ori is decoupled from the photosphere (Goldberg, 1979).

(vi) **Dust:** An infrared excess at 10μ , probably due to silicates in a CS shell, can be observed in the upper right-hand corner of the HR diagram in all stars cooler and more luminous than those on a line defined by M1 Iab, G8 Ia, and G0 Ia $^+$ (for references, see Reimers, 1975b).

(vii) **Radio emission:** In the G0 Ia (super) supergiant HR 8752, radio emission

has been measured between 27 and 90 MHz (Smolinski et al., 1977). This may be due to free-free emission by a spherical expanding envelope which is ionized by a hot companion: the presence of such a companion was discovered with IUE (Stickland and Harmer, 1978). A similar case is HR 5171. Continuum free-free radiation from partially ionized winds has been detected in a few M supergiants and in the K2 III giant α Boo with the VLA at 6 cm (Drake and Linsky, 1983).

- (viii) **Nonstationary shell ejection:** In the F supergiant ρ Cas (Sargent, 1961) and in HR 8752 (Lambert and Luck, 1978) sudden shell ejections with high mass-loss rates accompanied by spectral line changes have been observed.

III.A.1. SPATIAL EXTENSION OF CHROMOSPHERES AND CIRCUMSTELLAR SHELLS

There is growing evidence that mass loss in red giants may be related to the existence of an extensive volume above the photosphere containing gas at chromospheric temperatures. We refer to these regions as extended chromospheres. In ζ Aur stars — eclipsing binary systems consisting of a bright K supergiant and a hot B star — the B star serves as an astrophysical light source that probes the extended chromosphere and wind of the giant. With the flight of the IUE satellite it has become possible to take a long time sequence of B star spectra as the eclipse progresses. These show chromospheric (absorption) lines or wind (P Cyg type) lines which give direct information about the height dependence of density, excitation and ionization, as well as nonthermal velocities in the outer K-giant atmosphere. Chromospheric lines have been observed up to about one stellar radius above the limb in 32 Cyg. In the UV continuum at 1300 Å, the star

is about 20% larger than at optical wavelengths (the total eclipse lasts several days longer).

The chromospheres of early M supergiants are also geometrically extended. During a lunar occultation of 119 Tau, it was observed that $H\alpha$ is emitted from a region having at least twice the diameter of that which produces the continuum (White et al., 1981). In α Ori, Goldberg et al. (1981) observed by means of speckle interferometry that the $H\alpha$ diameter is about 5 times the stellar diameter, and that there are deviations from a spherical shape at the level of a few percent. We should recall that during a solar eclipse an irregular bright red arc ($H\alpha$) is seen around the obscured disk, a phenomenon that led to the name "solar chromosphere."

The density of cool CS envelopes is sufficiently low for resonance line scattering to dominate over true absorption. Re-emission from the envelopes of α Ori and μ Cep has been observed spatially resolved on the sky in the KI 7699 Å and Na D₂ resonance lines (Bernat and Lambert, 1976, Münch et al., 1976). In case of α Ori, the line scattering envelope was detected in the neutral potassium line as far outwards as 50 arc sec (Honeycutt et al., 1980) which corresponds to about 2200 M star radii or 10^4 AU. The travel time from the star for the outermost observed CS material is $\sim 10^4$ years. Contour maps of scattered potassium line radiation show only slight deviations from spherical symmetry (Mauron et al., 1984). Far away from the star, the neutral potassium density decreases, however, more sharply with distance from the star than does the total particle density ($n_{KI} \propto r^{-2.5}$ compared to $\propto r^{-2}$). This is probably due to ionization by the interstellar radiation field.

The inner radius of the scattering shell is not well determined, although it is of the order of 10 stellar radii in M supergiants like α Ori. ζ Aur stars offer the possibility of spatially resolved observations of the transition from a chromosphere to a wind.

III.A.2. WIND VELOCITIES

It was clearly recognized by Deutsch (1960) that the shell expansion velocities in red giants are always much below the escape velocities from the stellar surfaces, contrary to what is known from the solar wind or winds in hot stars (where $v_{\text{wind}} \approx 3 v_{\text{esc}}$).

A survey of stellar wind velocities over the entire red giant region of the HR diagram using mainly K_4 shifts (Figure 3-11) reveals that there is — in the mean and with considerable scatter at any given position in the HR diagram — a continuous trend in the value of the wind velocity from luminous M supergiants ($\sim 10 \text{ km s}^{-1}$) through early M giants ($\sim 25 \text{ km s}^{-1}$) and K and G (super)giants (~ 50 to 150 km s^{-1}) to the solar wind ($\sim 500 \text{ km s}^{-1}$). This trend corresponds roughly to $v_{\text{wind}} \propto v_{\text{esc}}^2$.

Detailed measurements of wind velocities of eclipsing binaries by means of high-resolution IUE spectra taken at various phases yielded values between 40 and 80 km s^{-1} for ζ Aur, 31 Cyg and 32 Cyg (Che et al., 1983). These confirm values found from K_4 shifts. For the G2 Ib supergiant 22 Vul, a wind velocity of about 170 km s^{-1} has been found with the same technique (Reimers and Che-Bohnenstengel, 1986).

In extremely luminous yellow supergiants, the following expansion velocities have been measured: ρ Cas (F8 Ia): 50 km s^{-1} (Sargent, 1961); HR 8752 (G0 Ia0): 30 km s^{-1} (Lambert and Luck, 1978); LMC super-supergiant HD 269723 (G4 0): 10 km s^{-1} (Hagen et al., 1981). Again there is a tendency towards decreasing wind velocity with decreasing gravity (i.e., increasing luminosity). In most of these stars, the observed CS velocities do not exceed the velocity of escape at the stellar surface. This implies that if the material is to escape the star, continued acceleration must occur over several stellar radii.

III.A.3. NONTHERMAL STOCHASTIC VELOCITIES

There are only a few reliable measurements of stochastic, nonthermal velocities (in the language of stellar spectroscopy “microturbulence,” as determined from line profiles and curves-of-growth) in stellar winds. In the outer parts of the α Her (M5 II) envelope (line of sight to α^2 Her) a stochastic, nonthermal velocity or microturbulence, $v_{\text{st}} = 4 \text{ km s}^{-1}$ (compared to 8 km s^{-1} wind velocity) was found (Reimers, 1977b).

In α Ori, the main S_1 component of the circumstellar CO 1-0 vibration-rotation band at 4.6μ (seen also in KI and NaI) yields $v_{\text{st}} = 4 \text{ km s}^{-1}$ (11 km s^{-1} wind velocity), while the weaker S_2 component, probably formed at larger distances from the star, has $v_{\text{st}} = 1 \text{ km s}^{-1}$ with 18 km s^{-1} expansion velocity. The interpretation of CS P Cygni profiles observed with IUE in the spectrum of α Sco B gives $v_{\text{st}} = 8 \text{ km s}^{-1}$, while the wind velocity of α Sco A is 17 km s^{-1} (Hagen, 1984).

The same technique applied to IUE spectra of eclipsing binaries gave a typical value of $v_{\text{st}} \approx 25 \text{ km s}^{-1}$ and 60 km s^{-1} wind velocity for ζ Aur, 32 Cyg, and 31 Cyg (Che et al., 1983). Taken altogether, these results suggest that a typical value for microturbulence seems to be half the wind velocity. If microturbulence is caused mainly by wind velocity variations on a time-scale short compared to typical flow times in the observed shells (10 to 10^3 years), the relative amplitudes of these variations are not unlike those in the solar wind where velocity fluctuations are about 25% of the mean velocity. Alternatively, nonthermal broadening of CS lines could be caused by waves of sizeable amplitudes (e.g., Alfvén waves).

III.A.4. WIND TEMPERATURES

In M supergiants like α Ori, temperatures deduced from radio observations correspond to

values of 8000 to 9000 K within a regime occupying a few stellar radii above the limb (Altenhoff et al., 1979, Wischnewski and Wendker, 1981). In the inner CS shell a temperature below 1000 K was estimated from the observed population of low-lying FeII levels (Weymann, 1962), while CO measurements of the distant shell of α Ori indicate temperatures of ~ 100 K (Bernat et al., 1979). The observed upper limit to the population of excited fine structure levels of TiII in the outer α Her shell (line of sight to α^2 Her, distance several hundred M-star radii) also gave an upper limit of ~ 100 K (Reimers, 1977b). This would be consistent with adiabatic wind expansion ($T_{\infty} r^{-4/3}$) in the outer wind.

A first estimate of wind temperatures in K supergiants was recently given by Che-Bohnenstengel (1984): for the wind of 32 Cyg (K5 Ib) at a distance ≥ 5 stellar radii, an electron temperature of $T_e \geq 4800$ K was found from the population of low-lying FeII levels observed on high-resolution IUE spectra, under the assumption that the degree of hydrogen ionization is $> 1\%$.

Mean temperatures as determined from CII $\lambda 2325/\lambda 1335$ ratios in "noncoronal" giants, i.e., stars on the wind side of the dividing line, are ~ 8500 K at a typical distance of 1 stellar radius above the photosphere (Brown and Carpenter, 1984).

III.A.5. DIVIDING LINES, "HYBRID" STARS, AND VARIABILITY

As mentioned above, CS CaII H and K and MgII h and k lines are found only to the right of a line in the HR diagram running from about M0 III through the K giants to early G supergiants (Figure 3-6). After the first IUE observations it was suggested (Linsky and Haisch, 1979) that among red giants there is a sharp division in the HR diagram between "solar like" stars that emit high excitation UV lines (TR lines such as NV, CIV, SiIV, ...) and "nonsolar-like" stars that emit only low

temperature, chromospheric lines (OI, SI, CI, SiII, ...). Linsky and Haisch suggested that this seemingly sharp line coincides with the lower boundary of stars in the HR diagram with observed cool stellar winds (Reimers, 1977a). X-ray observations of cool giants with the *Einstein* satellite seem to confirm the existence of a similarly located dividing line between stars with and without detectable X-ray emission (e.g., Linsky, 1981a). The most obvious interpretation was that the onset of massive winds inhibits the formation of a transition zone and hot corona through efficient cooling.

However, it has since become clear that the boundary in the HR diagram between stars with solar-type UV and X-ray emission on one hand and those with cool chromospheres and winds on the other is not sharp, and that the instrumental sensitivity of IUE leads to pronounced selection effects. In particular, it has been shown that there are early G supergiants (α Aqr, β Aqr, δ TrA) and K giants of luminosity class II (Θ Her, α TrA, γ Aq1, i Aur), all near to the mentioned boundary lines (Figure 3-6), that have both a cool, massive, high-velocity (~ 70 to 130 km s $^{-1}$) wind and TR line emission (Hartmann et al., 1980, 1981; Reimers, 1981, 1982). These stars have been called "hybrid" stars. In this connection it may be relevant that many, if not all, stars near to the dividing line show highly variable CS lines, variable HeI 10830 Å, and possibly also variable CIV, NV, etc.

In Θ Her, for example, the HeI emission undergoes cyclic variation with emission maxima observed in 1966, 1971 and 1975 (Zirin, 1976). This observation is consistent with the conjecture that hybrid stars are slowly rotating stars with inhomogeneous outer layers containing both magnetically open regions which produce the wind (analogous to coronal holes on the Sun) and magnetically closed regions which are more effectively heated coming alternately into the line of sight. However, this conjecture remains to be proven by future observations.

The characteristic time-scale for larger variations of CS lines in K giants is of the order of one to several months, while minor variations may occur within days. Examples are α Tau, HD 36167, μ UMa, γ Aql, Θ Her, and 63 Cyg (Reimers, 1977a, 1982). The emission lines of NV, CIV, etc., are also variable in stars like Θ Her and α Aqr; and, as mentioned, at least 5 hybrid stars (γ Aql, α Aqr, i Aur, μ UMa, Θ Her) have far blueshifted (> 100 to 200 km s^{-1}), variable HeI 10830 Å components (O'Brien, 1980). If the winds of hybrid stars represent a link between hot solar type winds and cool M-type winds, the question arises whether there is evidence for a "warm wind" of, say, 10^5 K in these stars.

Hartmann et al., (1981) found on high-resolution IUE spectra of α TrA that the SiIII] and CIII] lines have widths of 100 km s^{-1} while CIV 1550 Å is 150 to 200 km s^{-1} broad. These values are much larger than those found in the solar transition layer. Hartmann et al., (1981) therefore took the close correspondence between the half-widths of the CIV lines with the wind terminal velocity of 85 km s^{-1} seen in MgII as evidence for line-broadening of CIV by wind expansion. On the other hand, magnetically active stars like β Dra (G2 II-Ib) with no evidence for a wind also have broad CII etc. lines. There is even strong evidence for downflow of matter (Ayres et al., 1983; Linsky, 1984b).

III.A.6. MASS-LOSS RATES

At the present time there is only one method to measure accurate mass-loss rates: the analysis of CS lines of a predominant stage of ionization (FeII, SiII, SII, TiII, OI, ...) seen against the spectrum of a hotter companion.

There are only a few cases where the components can be separated visually on the sky (α Her, α Sco, o Cet). However, the IUE satellite offered a new possibility; namely, separation through complimentary energy distributions in

those systems where the visual spectrum is dominated by the red giant, while in the UV below $\sim 3000 \text{ Å}$ the spectrum is a pure B-star spectrum. The numbers of binary systems suitable for measuring accurate mass loss rates by this technique is much larger. Table 3-2 summarizes our present knowledge of mass-loss rates in cool stars.

III.B. RED GIANTS WITH HOT COMPANIONS (ζ AUR/VV CEP STARS)

As mentioned above, the spectrum of the outer atmospheres of red giants with hot companions may be studied by using UV and visual observations of the complementary energy distributions of the components. High resolution IUE spectra of the following binary systems have been studied or are under study by a group of astronomers at the University of Hamburg (Reimers et al., 1981; Che et al., 1983; Reimers and Schröder, 1983; Che and Reimers, 1983; Schröder, 1983; Hagen et al., 1987; Hempe, 1982, 1983, Reimers, 1987):

K Supergiants and giants: ζ Aur, 32 Cyg, 31 Cyg, ϵ Car, π Pup, 47 Cyg

M giants and supergiants: α Sco, HD 203338, HR 2902, VV Cep, δ Sge

G supergiants: 22 Vul, HR 6902

Most useful are systems with known orbital elements and known inclination of the orbit. In particular, eclipsing systems yield the most complete results.

The analysis technique involves the use of the B star as an astrophysical light source which orbits in the wind of the red giant. Compared to far separated visual binaries, a number of additional difficulties arise in the interpretation

Table 3-2

Mass-Loss Rates Determined From Circumstellar Lines and Radio Emission

| Star | Sp. | \dot{M} (M_{\odot} /yr) | Technique | References |
|----------------|-----------|------------------------------|-----------|--------------------------------------|
| α^1 Her | M5 II | $1.1 \cdot 10^{-7}$ | Vis. bin. | Reimers (1977b) |
| α Cen | Mira var. | $\sim 1 \cdot 10^{-7}$ | " | Reimers and Cassatella (1985) |
| α Sco | M2 Iab | $7 \cdot 10^{-7}$ | " | Kudritzki and Reimers (1978) |
| | | $5 - 10 \cdot 10^{-7}$ | IUE* | Hagen et al. (1987) |
| ζ Aur | K4 Ib | $0.6 \cdot 10^{-8}$ | IUE* | Che et al. (1983) |
| 32 Cyg | K5 Iab | $2.8 \cdot 20^{-8}$ | " | " |
| 31 Cyg | K4 Ib | $4 \cdot 10^{-8}$ | " | " |
| δ Sge | M3 II | $2 \cdot 10^{-8}$ | " | Reimers and Schröder (1983) |
| 22 Vul | G3 Ib-II | $\sim 4 \cdot 10^{-9}$ | " | Reimers and Che-Bohnenstengel (1986) |
| HR 8752 | G0 Ia | $1 \cdot 10^{-5}$ | Radio | Lambert and Luck (1978) |
| α Boo | K2 IIIp | $\geq 1 \cdot 10^{-10}$ | " | Drake and Linsky (1983) |

*Mass-loss rates for α Sco determined from UV-spectra by van der Hucht et al. (1980) and Bernat (1982) are erroneous since (i) only lines contaminated by interstellar lines have been used and (ii) line transfer was not treated properly (cf. Hagen et al. 1987).

of the spectrum of these usually much closer ζ Aur systems:

- (i) The wind may be disturbed by the nearby companion through both its gravitational field and the formation of a shock front as the B star travels supersonically through the wind.
- (ii) The hot B star ionizes the wind; i.e., it may form an HII region within the red giant wind of considerable size (α Sco, 31 Cyg). Ionization effects have to be taken into account for metals like Fe, Si, etc., which are used for the mass-loss determination. Even time-dependent effects may occur if the time-scales of ionization or recombination are comparable with the orbital period and/or the time-scale for wind expansion.
- (iii) A 3-dimensional, nonspherical, spectral line-transfer problem has to be

solved, since the light source (B star) is eccentric from the wind symmetry center. Computing times for P Cygni profiles in this case are about two orders of magnitude above those for the spherical case.

On the other hand, ζ Aur systems offer a unique opportunity to observe winds and extended chromospheres of red giants with relatively high spatial resolution. This enables us to investigate deviations from spherical symmetry through observations at various binary phases. In particular, the systems offer the possibility to observe the transition from the extended chromosphere to the wind region.

H.B.1. OBSERVED UV LINE SPECTRA

Qualitatively, the UV spectra of ζ Aur systems look like B star spectra (for $\lambda \geq 2800$ Å a contribution from the red giant is visible) upon which numerous P Cygni type profiles,

broad emission/absorption lines, and sometimes double peaked emission lines are superimposed. At total eclipse, all P Cygni profiles turn into pure emission lines. In addition to lines from the photosphere of the B stars and from the interstellar medium, one can distinguish several other types of lines:

- (i) Wind lines: Visible at all phases as lines with P Cygni profiles (in eclipse: emission lines) of ions like FeII, SiII, Al II, MgII, SII, CII, OI. These lines are formed by scattering of B-star photons in the wind of the red giant (Figure 3-12). A few wind lines like FeII Multiplet 9 are seen in pure absorption due to the branching ratios of the upper levels, which favor re-emission as FeII Multiplet 191 photons (Hempe and Reimers, 1982a).
- (ii) Chromospheric lines: Seen near total eclipse (phase 0 ± 0.03), the lines are absorption lines centered at zero velocity, and they are narrower than wind lines. In the lower chromosphere, neutral ions like FeI can also be seen. Compared to optical observations of chromospheric absorption lines in ζ Aur systems, the UV lines have the advantage of having a well defined continuum (pure B star). In addition, the chromosphere can be studied outwards to 1 to 2 stellar radii above the red giant limb.
- (iii) Shock front lines: Depending on phase, the resonance lines of highly ionized metals like CIV, SiIV, Al III, NV and excited lines of FeIII (Multiplet 34) are seen as very broad absorption lines, regular or inverse P Cygni profiles or pure emission lines (Chapman, 1980, 1981; Reimers and Kudritzki, 1980; Reimers et al., 1981). The line-emitting region is moving with the B star and is often partially eclipsed in phase with the B star. Since tempera-

tures of the order of 10^5 K are required for the highest ionization stages, the lines are probably formed in a shock zone formed as the B star moves through the red giant wind with supersonic speed (Chapman, 1981; Che-Bohnenstengel and Reimers, 1986).

- (iv) Lines possibly associated with shock front and/or an accretion disk: Lines of FeII UV multiplets 60, 78, 99 and a few others like CrII (7) do not show P Cygni type profiles, but rather show either broad emission profiles or double-peaked emission lines (e.g., in δ Sge, Reimers and Schröder, 1983, Figure 3-13). At present the origin of these lines is not understood. In ζ Aur and δ Sge, the B stars seem to possess accretion disks formed by accretion from the winds of the cool giants (Che-Bohnenstengel and Reimers, 1986).

III.B.2. THEORY OF LINE FORMATION IN THE WIND

A computer code for solving the non-spherical line transfer problem in ζ Aur systems has been described by Hempe (1982). It has been applied to phase-dependent, high-resolution IUE spectra of the ζ Aur systems 32 Cyg, 31 Cyg, and ζ Aur (Che et al., 1983), to circumstellar P Cygni profiles in the spectrum of α Sco B (Hagen et al., 1987), and to a determination of the wind temperature of 32 Cyg (Che-Bohnenstengel, 1984).

The basic assumption in the theory of resonance line formation in the winds of ζ Aur stars is that the wind is expanding with spherical symmetry from the K supergiant. In the first approximation we thus neglect disturbances of the K-giant wind by the close B star, and we neglect bending of streamlines due to the orbital motion of the giant. Fortunately, in systems like 32 Cyg and ζ Aur, where high-resolution IUE spectra have been obtained at

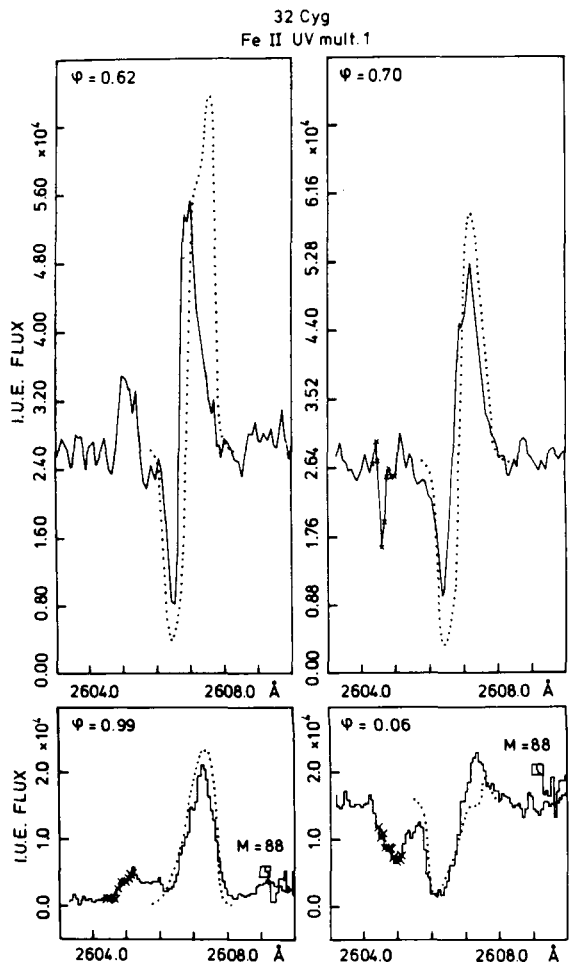
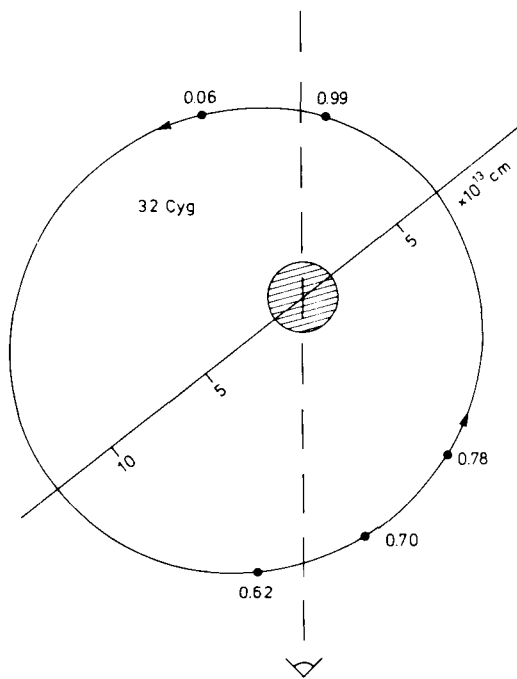


Figure 3-12. Phase-dependence of wind lines of 32 Cyg observed with IUE (a) location of B star relative to K supergiant and to line of sight, (b) observed and computed (dots) profiles of an FeII resonance line (from Che et al., 1983).

all relevant binary phases, the degree of envelope asymmetry of the red giant can be tested and is found to be small. Individual mass-loss rates \dot{M} , determined at various phases, provide a better estimate of the uncertainties compared to previous methods used to determine \dot{M} .

The procedure involved in a determination of wind parameters such as mass-loss rate \dot{M} , wind velocity v_w , and stochastic velocity field v_{st} (or again, "microturbulence," which is here, in a spectroscopic sense, a quantity which includes all velocity contributions due to deviations from a radially expanding wind) from high-resolution IUE spectra at various phases

involves the following steps: (1) Model-atmosphere analysis of the B stars in order to determine the ionizing radiation field; (2) Calculation of structure of HII regions around the B star within the wind of the K giant for various model winds; (3) Calculation of ionization equilibrium of metals; (4) First rough estimate of mass-loss rate, wind velocity and wind "microturbulence" using the FeII UV multiplet 9 absorption lines (pure absorption lines which can be treated easily, cf. tables in Heme, 1983); (5) Refinement of wind parameters using shapes of P Cygni profiles.

It turns out that v_{st} is fixed by observations at phases where the B star is in front of the K

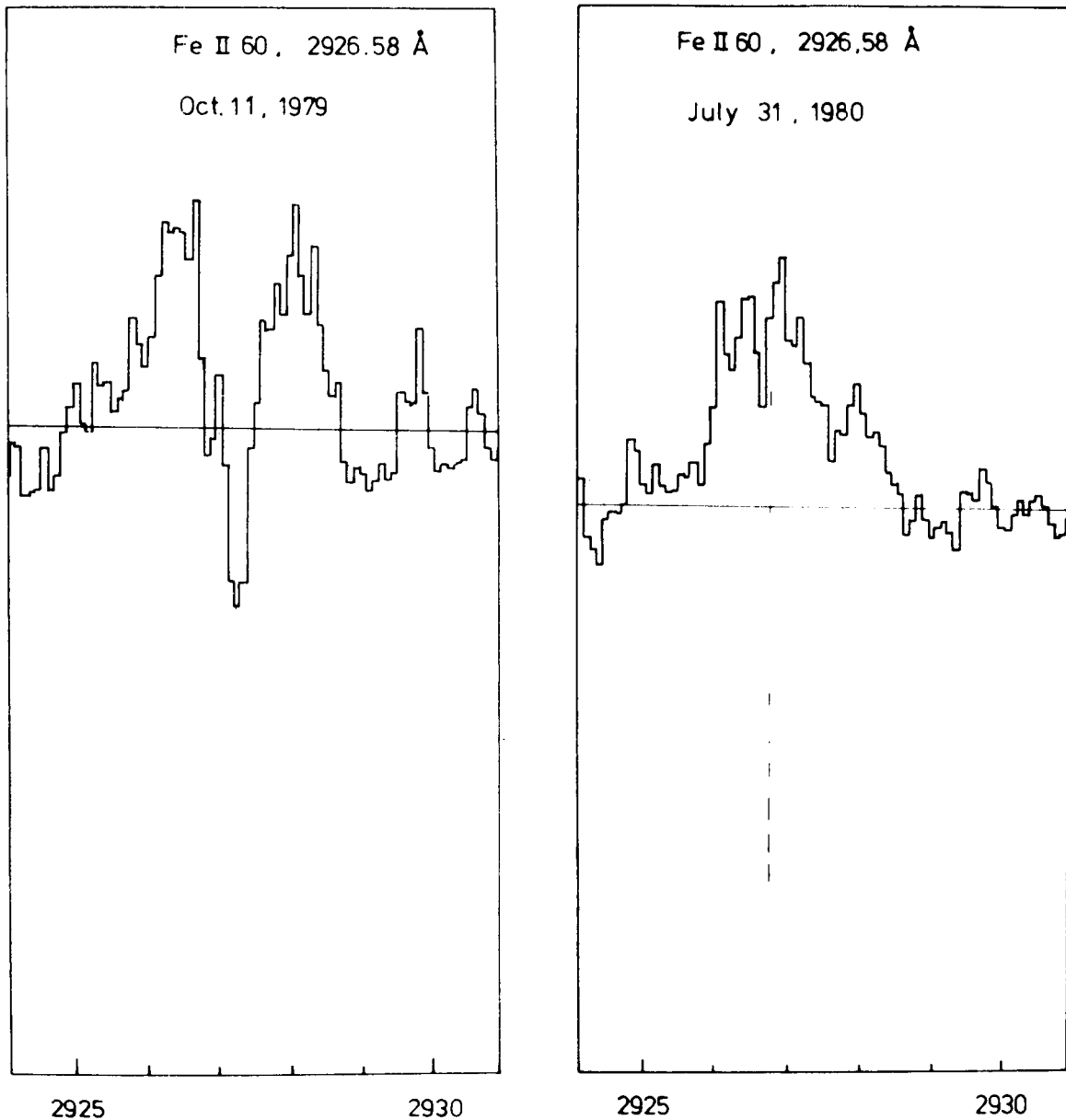


Figure 3-13. Emission and absorption of FeII UV mult. 60 in δ Sge (M2 II + B9 V) typical for a whole group of lines. The broad emission probably comes from a rotating disk that moves with the B star.

giant (absorption part of profile shifted by v_w , broadened by v_{st}), while v_w is best determined at phases with the B star behind the K giant (profile from $-v_w$ to $+v_w$). Further details can be found in the paper by Che et al. (1983).

It was possible in all cases to match the circumstellar line profiles at all phases (including

the pure emission-line phase when the B star is totally eclipsed) with *one* set of wind parameters v_w and v_{st} and — within a factor of 2 — *one* mass-loss rate \dot{M} . This means that at least in the orbital plane the envelope asymmetries (in wind density) are no more than a factor of 2 on the length scale of several K-star radii.

The stochastic velocity v_{st} is rather large, 25 to 30 km s⁻¹ or about half the wind velocity, consistent with what is known from other late-type stellar winds (cf. Chapter 3.II.A.3).

Mass-loss rates determined with the binary star technique using IUE spectra (ζ Aur, 31 Cyg, 32 Cyg, δ Sge, α Sco, and 22 Vul) are given in Table 3-2. Other objects currently under study are VV Cep, ϵ Car, He 203338, and 47 Cyg.

It has not been possible, given the quality of the available data (IUE-spectra), to use this technique to determine empirically the velocity field in the wind-acceleration region from wind lines, although the relevant binary phases have been covered. Improved spectral resolution of the P Cygni profiles, an absolute wavelength scale, and an improved signal to noise ratio are required. The possibility of probing the wind-acceleration zone of red giants makes ζ Aur stars promising objects for detailed investigation with the high-resolution spectrograph on board the Space Telescope.

III.B.3. EVIDENCE FOR NONSTATIONARY WINDS

Clouds moving with velocities up to several hundred km s⁻¹ have been observed for many years near to eclipse as "satellite" lines of CaII H and K in 32 Cyg and other ζ Aur systems (Wilson, 1960b). Multicomponent structure in the stronger CS lines (up to several hundred km s⁻¹) has been observed by Stencel et al., (1979) in 32 Cyg on IUE spectra taken far outside the eclipse phase.

A remarkable example of spectroscopic evidence for "clouds" is found in δ Sge, an M3 II giant with a B9 main sequence companion having a period of about 10 years. The giant has a wind with a velocity slightly less than 30 km s⁻¹ and a mass-loss rate of $2.10^{-8} M_{\odot}/\text{yr}^{-1}$ (Reimers and Schröder, 1983). This is quite normal for an M giant (Figure 3-10).

The strong MgII h and k resonance doublet usually exhibits (on several spectra taken between 1979 and 1982) multicomponent structure with components up to ~ 200 km s⁻¹ expansion velocity. An IUE spectrum taken in September 1983 even shows a strong blueshifted absorption component at a velocity of ~ 380 km s⁻¹ (Figure 3-14). It is not clear whether these high-velocity clouds are due to the binary nature of δ Sge, since they have not been seen in the spectra of single M giants. In K giants, on the other hand, variability of CS lines is normal, and the sudden appearance of sharp, discrete components has been observed, e.g., in α Tau at ~ 50 km s⁻¹ (Reimers, 1977a). Although the high-velocity clouds do not appear to contribute significantly to the total amount of mass loss, they may play a key role in the dynamics of heating of the winds of late-type stars.

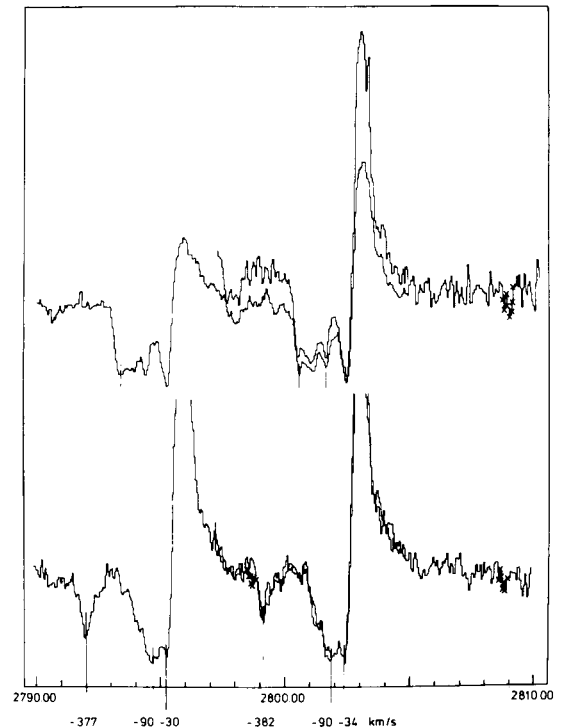


Figure 3-14. Far shifted absorption components in MgII resonance lines observed at different phases of δ Sge.

IV. ENERGY LOSSES BY RADIATION AND WINDS

One of the basic constraints to any theory of nonradiative heating of the outer layers of cool stars is provided by empirical estimates of energy losses by chromospheres and coronae, in electromagnetic radiation and stellar winds.

In this section we discuss three aspects of the observed energy losses: first, direct measurements of radiative losses in the dominant lines and continua in a number of representative stars; second, the variation of such radiative losses with position in the HR diagram; and third, the variation of the mode of energy loss — which finally should give information about the variation of the height distribution of energy losses — with stellar parameters.

An overview of the energy losses (per unit area of stellar surface) from the chromospheres, coronae, and winds of F to K stars is shown in Table 3-3. In the solar chromosphere, MgII

h and k, CaII H and K, and the infrared CaII triplet contribute about 85% of the total integrated net cooling rate (Vernazza et al., 1981a). Note that the values in Columns 7 and 8 of Table 3-3 are not the total energy loss of the corona and transition region, but only refer to the radiative losses. In the case of the Sun, downward thermal conduction from the corona and transition region appears to be a significant component of the total loss rates of about $10^6 \text{ erg cm}^{-2} \text{ s}^{-1}$ from quiet regions, and about $10^7 \text{ erg cm}^{-2} \text{ s}^{-1}$ from active regions. The total amount of heating required to maintain coronae and transition regions of stars other than the Sun cannot be measured directly, although the nonradiative energy loss of the corona (conduction plus wind) may be deduced by detailed modeling, once radiative losses have been measured at all wavelengths.

The variation of chromospheric radiative losses with position in the HR diagram was studied by Blanco et al. (1976), using the CaII H and K lines, and by Basri and Linsky (1979)

Table 3-3

Radiative and Wind Energy Losses ($10^5 \text{ erg s}^{-1} \text{ per cm}^{-2}$ of the Stellar Surface)

| Star | Sp. | CaII H+K | IR CaII | MgII | Ly α | CIV + SiIV + NV | Soft X-rays (0.25 – 4 keV) | \dot{M} (Mo/Yr) | v_w (km/s) | Wind | |
|----------------|----------|----------|---------|------------|-------------|-----------------|-------------------------------|---------------------------------|----------------------------|------------------|------------------|
| | | | | | | | | | | E_{pot} | E_{kin} |
| Quiet Sun | G2 V | 12 | 18 | 9 | 3 | 0.09 | 0.1 | $2 \cdot 10^{-14}$ | 400 | 0.4 | 0.16 |
| ζ Boo A | G8 V | 12 | | 45 | | 1.6 | 31 | | | | |
| α C Min | F5 IV-V | 19 | | 17 | | 0.76 | | | | | |
| ϵ Eri | K2 V | 15 | 35 | 11 | 3.2 | 0.23 | 2.2 | | | | |
| β Dra | G2 II-Ib | 41 | 22 | 28 | | 0.85 | 1.2 | | | | |
| β Gem | K0 III | | 9 | 3.4 | 0.2 | | 0.014 | | | | |
| α Boo | K2 IIIp | 7.5 | 8 | 1.8 | 0.5 | <0.003 | <0.0007 | $\geq 1 \cdot 10^{-10}$ | 40 | ≥ 0.07 | ≥ 0.013 |
| α Aqr | G2 Ib | 29 | 6.5 | 50 | | 0.34 | <0.0001 | | 125 | | |
| 22 Vul | G2 Ib | | | | | | | $4 \cdot 10^{-9}$ | 170 | -2.5 | -1.8 |
| ϵ Gem | G2 Ib | 4.4 | | 7 | | <0.02 | <0.03 | | | | |
| 32 Cyg | K5 Iab | | | | | | | $\sim 3 \cdot 10^{-8}$ | 60 | 0.67 | 0.14 |
| λ Vel | K5 Ib | | | ≤ 0.4 | | <0.02 | | | | | |
| α Ori | M2 Iab | | | 0.26 | | ≤ 0.0001 | ≤ 0.0001 | 10^{-6} | 10 | 1.8 | 0.014 |

References: Basri and Linsky (1979), Linsky et al. (1979a,b), Ayres et al. (1981), Vernazza et al. (1981), Blanco et al. (1976), Drake and Linsky (1983), McClintock et al. (1975), Baliunas et al. (1983), Brown and Jordan (1981), Stencel (1980), Che et al. (1983), Reimers and Che-Bohnenstengel (1986).

and Stencel et al. (1979), using the MgII H and K lines. Their main results are (i) for a given luminosity and temperature there is a considerable range of chromospheric radiative losses (factor ~ 10); (ii) for effective temperatures less than about 5000 K there is a tendency for MgII losses to decrease with increasing temperature; (iii) supergiants appear to lie a factor of ~ 4 above giants in chromospheric radiative losses: (iv) for supergiants, MgII losses decrease steeply with increasing temperature for temperatures greater than 5000 K. This last result may be related to a general tendency for chromospheres to disappear with increasing temperature (e.g., Böhm-Vitense and Dettman, 1980).

For F to K dwarfs and giants, close correlations between chromospheric energy losses (MgII, OI, . . .), energy losses in transition layer lines ($T \sim 10^5$), and broad-band coronal soft X-ray fluxes ($\geq 10^6$ K) are found. The correlations have the specific forms $f(\text{NV} + \text{CIV} + \text{SiIV}) \propto f(\text{MgII})^{1.5}$ and $f(\text{soft-X-ray}) \propto f(\text{MgII})^3$ (Ayres et al., 1981). These correlations cover normal stars of various activity levels, hybrid giants and also RS CVn stars. They demonstrate that the heating mechanisms for chromospheres and coronae in all G and K stars may be closely related.

From inspection of Table 3-3 we see that energy losses through winds do not seem to be closely related to coronal energy losses. This finding is perhaps contrary to expectations regarding the properties of thermally driven winds. From the few data available at present (Table 3-1), it appears that the total energy losses through winds are typically of the order of $10^5 \text{ erg cm}^{-2} \text{ s}^{-1}$ (at the stellar surface for the stars listed), while transition layer and coronal energy losses vary from solar-type main-sequence stars to cool supergiants (α Aqr, α Ori) by factors exceeding 10^3 . This is an indication that the wind acceleration mechanism in giant stars without coronae (see below) may be different from that in the Sun.

There are a few stars that are exceptions to the general trend of coronal energy losses decreasing towards the upper right-hand corner of the HR diagram. For example, the G2 II-Ib supergiant β Dra has no spectroscopically detectable wind — contrary to otherwise similar stars like α Aqr — while its chromosphere and corona are extremely active, with an energy loss $> 2 \times 10^5 \text{ erg cm}^{-2} \text{ s}^{-1}$ in soft X-rays and CIV, SiIV, NV lines (Table 3-3). This energy loss is similar to the amount required in other stars to drive the wind. It may be that β Dra has a closed magnetic field structure that inhibits a wind and so leads to strong nonthermal heating, maintaining an active corona. A further example is the peculiar M giant HD 4174 which has a kilogauss magnetic field and no detectable wind (Stencel and Ionson, 1979).

In addition to the basic stellar parameters, gravity and effective temperature, other factors such as the activity level, magnetic field structure, and variability also determine whether the outer layers of a star are mass-loss dominated or corona dominated. While coronae disappear in G supergiants and middle K giants along the dividing line defined approximately by the appearance of stronger stellar winds, according to IUE and *Einstein* observations (Reimers, 1977a; Linsky and Haisch, 1979), the transition from corona-dominated to wind-dominated outer layers is gradual. The so-called hybrid-atmosphere stars, which are located in the HR diagram near this dividing line, seem to represent a still high level of stellar activity in intermediate mass giants.

The fact that the activity level measured, for example, by the normalized MgII flux is related to the appearance of a K giant at UV and X-ray wavelengths can also be seen among the four Hyades K0 giants of identical age and projected rotational velocity. Two of these stars show CIV and soft X-ray emission, while the others do not (Baliunas et al., 1983). This observation is consistent with the observation that there is

a range of normalized MgII energy losses $F(\text{MgII})/\sigma T_{\text{eff}}^4$ of at least a factor of 10 in field stars at any given location in the HR diagram, independently of T_{eff} (Figure 3-15). While there appears to be some dependence of nonradiative heating on the basic parameters (gravity and effective temperature) which determine the structure of a stellar atmosphere, there is at least one other important parameter. At present we believe that magnetic fields caused by stellar rotation are one such parameter in many stars.

V. ATMOSPHERIC STRUCTURE

The only star for which we have detailed spatially resolved information is of course the Sun. Observations of the Sun give us the following rough picture of the atmospheric structure of a G-type dwarf. The deepest observable layer of the solar atmosphere is the photosphere through which the temperature decreases outwards from ~ 6600 K at $\tau_C = 1$ to the temperature minimum with $T \sim 4600$ K. Above the solar temperature minimum we have the fairly extended, very inhomogeneous chromosphere (up to a few thousand km) in

which the temperature increases only slowly over several pressure scale heights up to $\sim 10^4$ K. Above the chromosphere, in the extremely inhomogeneous and dynamic transition region, the temperature increases rapidly, by a factor of ~ 100 , in less than one pressure scale height. The temperature structure in this narrow region, in particular between 10^5 and 10^6 K, is apparently dominated by heat conduction from the corona. The maximum coronal temperature $T \sim 1.5 \times 10^6$ K is reached at about 2×10^4 km above the limb. The hot corona is very extended, with little temperature variation over one pressure scale height, and mainly thermally drives the solar wind. In magnetically open regions (coronal holes) the energy balance in the solar corona is dominated by energy losses through fast solar wind streams. On the other hand, in coronal active regions, confined by coronal magnetic fields, the wind cannot readily escape and heating causes much higher temperatures. Here the energy balance between the still unknown heating mechanism and downward conduction plus radiative cooling determines the temperature structure. A principal characteristic of the outermost layers of the Sun is extreme inhomogeneity dominated by magnetic fields, and we should keep this in mind when looking at stars. In particular, we will have to take into account that even in a star with a low activity level like the Sun, a few active regions may dominate the UV and X-ray spectrum, while the magnetically open coronal regions that provide most of the wind may be invisible in an integrated UV or X-ray spectrum.

V.A. MAIN-SEQUENCE STARS

For solar-type stars little is known about atmospheric structure. However, there are no observational indications that the Sun is an exceptional G2 V star. Indeed studies of α Cen A (G2 V), a near twin of the Sun, have shown that the very similar chromospheric and coronal emission spectra can be understood with a similar atmospheric structure (Ayres et al., 1982). We have no knowledge of solar-type

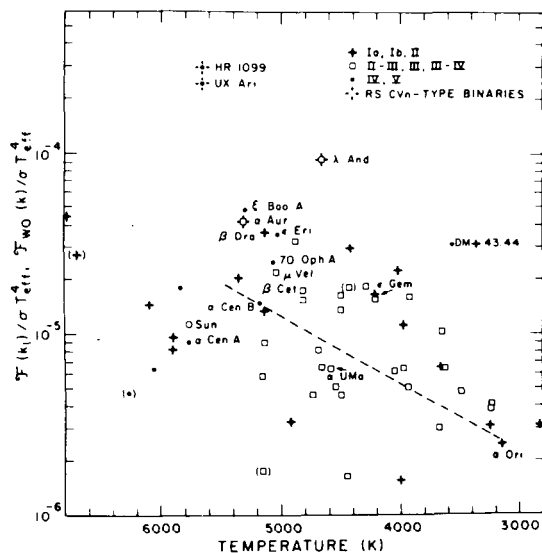


Figure 3-15. Ratio of MgII k surface flux to total surface luminosity σT_{eff} for various cool stars (from Basri and Linsky, 1979).

winds in main-sequence stars since, if they exist, they would be far below the present limits of spectroscopic detectability. Therefore, it is not known how winds in young, magnetically very active, main-sequence G stars are structured.

It is known that TR line fluxes of F dwarfs deviate from the mean (for all late-type stars) correlations between fluxes of lines formed at various temperatures as found by Ayres et al., (1981). This is an indication that the atmospheric structure in these objects may be different from that of the Sun. The only F-type dwarf studied in detail is Procyon (α CMi, F5 IV-V). Brown and Jordan (1981) measured line fluxes and line widths on low- and high-resolution IUE spectra. From the line fluxes, they deduce the emission-measure distribution, the electron pressure and hence a model of the density and temperature as a function of height. A brief summary of the method used by Brown and Jordan (1981) to infer atmospheric structure from disk-averaged line fluxes of stars follows.

In a spherically symmetric atmosphere, the surface flux ($\text{erg cm}^{-2} \text{s}^{-1}$) in an optically thin emission line is given by

$$F = \frac{6.8 \cdot 10^{-22}}{\lambda} \cdot \frac{\Omega_{12}}{W_1} \cdot \frac{N_e}{N_H} \cdot \int_{\Delta h} g(T) \cdot N_e^2 dh, \quad (3-1)$$

where

$$g(T) = T_e^{-1/2} \cdot \frac{N_{\text{ion}}}{N_e} \cdot \exp(-W_{12}/kT_e). \quad (3-2)$$

Here, Ω_{12} is the average collision strength, w_1 is the statistical weight of the lower level, W_{12} is the excitation energy, and Δh is the height range over which the ion in question is formed. The formula holds for lines in which the upper state is collisionally excited.

It has been shown that the function $g(T)$ for most ions has a relatively sharp peak at a temperature T_m , and that a logarithmic

temperature interval of $\Delta \log T = \pm 0.15$ is the typical range over which an emission line is formed. Thus, for this interval a mean value $g(T_m)$ may be found. This lets us extract $g(T)$ from the integral in Equation (3-1), and

the "emission measure" $\int_{T_1}^{T_2} N_e^2 dh$ can then be determined as a function of electron temperature T_e from observed line fluxes of a range of ions.

Combining the results from various ions, the emission-measure distribution $N_e^2 dh$ is obtained as a function of T_e (cf. Figure 3-16 for Procyon). Below temperatures $T_e = 2 \times 10^4$ K, chromospheric models can be obtained by detailed analysis of emission-line profiles of the optically thick lines of MgII, CaII, Ly α and OI, by means of radiative line-transfer studies (cf. Ayres et al., 1974). This yields essentially the distribution of $N_e \cdot N_H dh$ as a function of temperature (Figure 3-16).

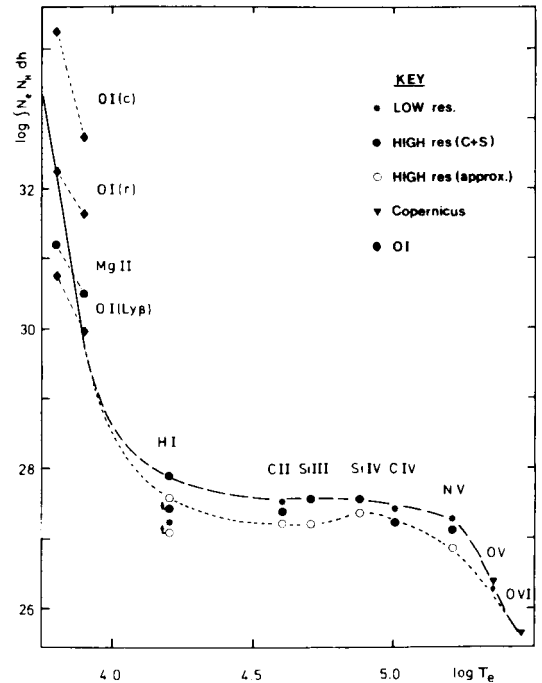


Figure 3-16. Emission measure distribution derived from low and high resolution line fluxes of Procyon (F5 IV-V), from Brown and Jordan (1981).

Once the emission measure distribution has been established the temperature and density structure can be derived using methods developed for the Sun (cf. Brown et al., 1979). The emission measure

$$E_m = \int N_e^2 dh$$

for a given line can be used to obtain the temperature gradient via the relation

$$\frac{dT}{dh} = \frac{P_e^2}{1.4 \cdot E_m \cdot T_e}, \quad (3-3)$$

where it is assumed that P_e and dT/dh are constant over the line formation region. With the additional assumption of hydrostatic equilibrium it may be shown that

$$\frac{dP_e}{dh} = -7.14 \cdot 10^{-9} \cdot P_e \cdot g \cdot T_e, \quad (3-4)$$

where g is the stellar gravity.

If P_e is known, for example from density-sensitive line ratios such as the components of CII λ 2325 Å at one or at several values of T_e and if $E_m(T_e)$ has been measured, the temperature structure of the atmosphere is known from Equations (3-3) and (3-4). If, as in the case of Procyon, no density-sensitive line ratio is available, either a lower limit to P_e may be found by assuming that the hottest observed line is formed in an isothermal corona over one density scale height, or limits to P_e can be imposed from line opacities. In the case of Procyon, Brown and Jordan (1981) determined the following values: $N_e \cdot T_e = P_e = 1.2 \cdot 10^{14} \text{ cm}^{-3} \text{ K}$ at $T_e = 2 \cdot 10^5 \text{ K}$ and $P_e = 3.6 \cdot 10^{14} \text{ cm}^{-3} \text{ K}$ at 10^4 K . The EUV observations suggest a model in which the maximum (coronal?) temperature is only $\sim 3 \cdot 10^5 \text{ K}$ (Brown and Jordan, 1981), much lower than in the solar corona. According to X-ray fluxes measured later with the *Einstein* satellite, it has

been estimated that only about 0.1% of the surface is covered with a $1.5 \cdot 10^6 \text{ K}$ corona (Brown, 1985). The hot gas may be trapped in a few small magnetic loops. The transition layer structure of Procyon is also quite different from that of the Sun in that the conductive energy flux is far less than the radiative losses. If the apparent trend of decreasing (mean) coronal temperature from the Sun to the F5 IV-V dwarf Procyon is typical for F stars — at least for stars of similar age — this would offer an explanation for the observed decrease of coronal emission in early F main-sequence stars.

V.B. GIANTS

The emission measure distribution technique described above has been applied by Brown et al., (1984) to β Dra, a highly active [i.e., high observed surface fluxes of chromospheric and TR emission lines] G2 Ib-II giant (cf. Table 3-3). This star is located to the left and below the wind-corona boundary in the HR diagram. From low- and high-resolution IUE spectra and soft X-ray emission fluxes, Brown et al. have constructed models of the transition region of β Dra using consistent emission-measure distributions between 10^4 K and $2 \cdot 10^5 \text{ K}$ and from density-sensitive line ratios. They find values of $P_e = N_e T_e$ lying in the range $4-9 \cdot 10^{13} \text{ cm}^{-3} \text{ K}$ from CII, CIII, SiIII, OIII, SiIV, CIV and NV line fluxes. This range of transition-region pressures is about an order of magnitude smaller than for the quiet Sun and not inconsistent at the base with the earlier chromospheric models for β Dra (Basri et al., 1981). The geometrical extent of the chromosphere plus TR is ≤ 0.01 stellar radii. The coronal temperature of β Dra as measured with the *Einstein* satellite IPC is $1.5 \cdot 10^7 \text{ K}$. Two possible explanations for this high value are that the hot plasma is confined in magnetic structures or that an efficient heating mechanism is capable of heating the plasma to 20 times the escape temperature.

Thermal conduction is negligible compared to radiative losses in the transition region and

corona of β Dra and there is no detectable wind. There are also significant downflows of hot TR material observed as line redshifts. β Dra represents an extreme example of a "coronal," nonwind giant where inhomogeneities possibly dominate the geometrical structure of the corona and transition region.

V.B.1. EXTENDED ATMOSPHERES OF ζ AUR SYSTEMS

A major breakthrough in the understanding of the extended atmospheres and wind acceleration regions of K supergiants has been achieved by extensive IUE observations of the eclipsing binary systems ζ Aur, 32 Cyg, and 31 Cyg. In such systems, the B-star companion serves as an astrophysical light source that can be used to probe the outer atmospheric structure with spatial resolution. The analysis of a time sequence of the resulting absorption lines visible in the composite spectra gives direct information about the height dependence of density, excitation and ionization, nonthermal velocities, etc., in the chromosphere of the K giant and in the inner-wind region. At present, K supergiants in ζ Aur systems are the only stars besides the Sun for which such information is available.

The extensive optical observations of atmospheric eclipses in ζ Aur systems were summarized by Wilson (1960b) and will not be repeated here. We notice, however, that optical observations are severely hampered by the composite spectrum (B + K) which makes reliable measurements of absorption lines very difficult (the spectra had to be decomposed). On the other hand, the B star is the only light source in the satellite-UV, and the numerous chromospheric lines visible during atmospheric eclipse are seen in absorption against a fairly smooth B-star continuum.

In addition, chromospheric absorption lines can be seen in the satellite-UV at projected distances of up to 2 K-giant radii. Furthermore, the duration of eclipse increases with decreas-

ing wavelength (15.5 days at 1350 Å compared to ~9 days at 2000 Å in 32 Cyg). The reason is a steep increase of opacity towards shorter wavelengths in the extended chromosphere. This behavior can be used to obtain an independent determination of the density structure in the inner chromosphere (up to ~0.2 stellar radii above the limb).

The optical observations summarized by Wilson (1960b) already unambiguously revealed extended chromospheres around K supergiants (Figure 3-17). In ζ Aur itself, for example, the density scale height at a distance of half a stellar radius above the photosphere

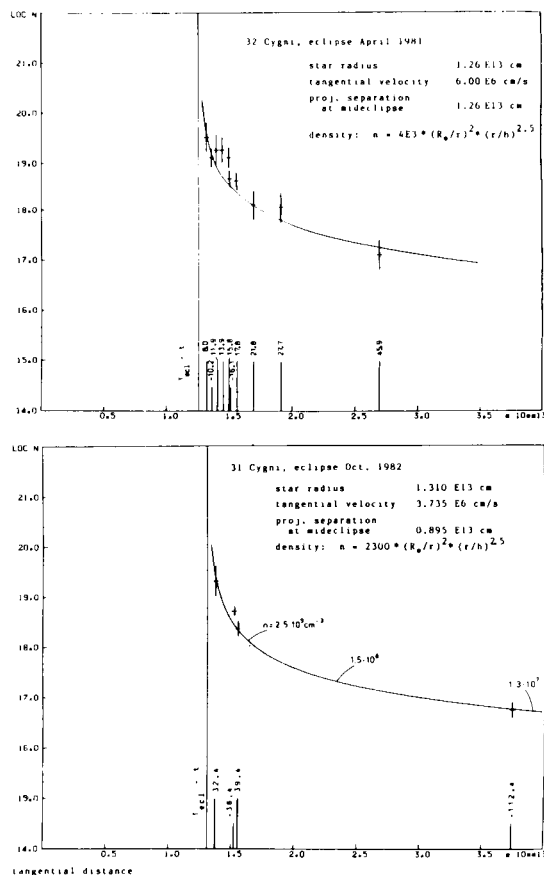


Figure 3-17. Observed column densities of Fe II (from ingress and egress of chromospheric eclipses) versus tangential distance. Solid lines represent column densities calculated from the density functions as given in the plot.

is of the order of one tenth of a K-star radius (Wilson and Abt, 1954; Groth, 1957). The presence of significant excitation of the 2nd quantum level of neutral hydrogen, which seems to increase (Figure 3-18) with height, at least up to $0.5 R_*$ ($R_* =$ stellar radius), indicates the existence of nonradiative heating of the outer layers. The occasional multicomponent structure of CaII H and K absorption reveals the “cloudy” structure of the extended atmosphere of ζ Aur, somewhat reminiscent of prominences on the Sun.

Modern observations made in the UV by IUE provide a more complete picture. Since it is well known that wind acceleration is already detectable in the chromospheres of late-type supergiants (Reimers, 1975a), the first step in understanding wind acceleration is to construct an empirical model of the high chromosphere. Using a close time sequence of IUE spectra taken during the atmospheric eclipses of 32 Cyg, 31 Cyg, and ζ Aur, Schröder (1985a) found that the chromospheric density distributions of 32 Cyg and 31 Cyg can be represented in the range $h \leq 2 R$ by the relation

$$n = n_0 \cdot \left(\frac{R}{r}\right)^2 \cdot \left(\frac{r}{h}\right)^a \quad (3-5)$$

with $a = 2.5$ and $n_0 = 4 \cdot 10^3 \text{ cm}^{-3}$ (32 Cyg) and $2.3 \cdot 10^3 \text{ cm}^{-3}$ (31 Cyg) respectively. R is the stellar radius, r the radial distance from the center of the K star, and h is the height above the stellar photosphere. In case of ζ Aur, the chromospheric density was found to be much smaller ($n_0 = 1.5 \cdot 10^2 \text{ cm}^{-3}$) and be decreasing much faster with height ($a = 3.5$). Derived distributions are shown in Figure 3-17 and Table 3-4 (Schröder, 1985b). As can be seen from Table 3-4, both the electron temperature and the fraction of ionized hydrogen increase with height up to at least half a stellar radius above the limb. This is consistent with Groth’s (1957) finding that the number density of excited hydrogen atoms stays nearly constant with height (Figure 3-19). The maximum

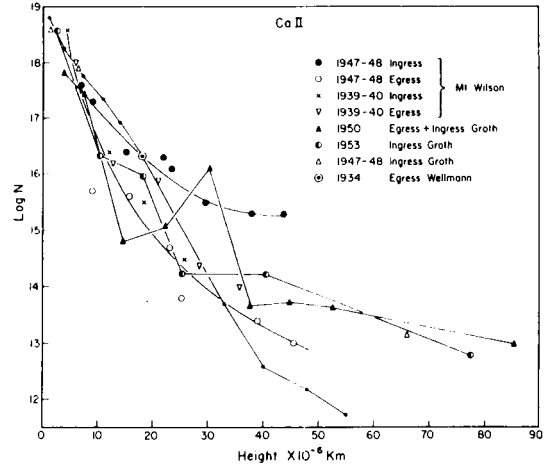


Figure 3-18. Column densities $\log N$ versus height above the photosphere of ζ Aur observed during various eclipses (from Wilson, 1960b).

temperature and its height above the limb are not known yet. We know only that at a height of $\geq 5R$ the wind has cooled again to $\sim 5000 \text{ K}$ (Che-Bohnstengel, 1984).

We may now estimate the radial distribution of the outflow velocity by combining the results of the mass-loss study for these systems (Che et al., 1983; Chapter 3.III), namely values of mass-loss rate \dot{M} and terminal velocity v_{wind} determined at radial distances $r \geq 5R$ (essentially outside the B-star orbit), with the empirical density model. We find with $\dot{M} = 4\pi r^2 v(r) \rho(r)$ ($\rho =$ mass density) the value

$$v(r) = \frac{\dot{M}}{4\pi \rho_0 \cdot R^2} \left(1 - \frac{R}{r}\right)^a, \quad (3-6)$$

and

$$v_\infty = \frac{\dot{M}}{4\pi \rho_0 \cdot R^2} \text{ for } r \gg R. \quad (3-7)$$

The assumption of continuous outflow would be supported by this argument if v_∞ as calculated from Equation (3-7), using the empirically determined \dot{M} (far away from the star)

Table 3-4a

Empirical Chromospheric Model Derived from the 1981 Eclipse of 32 Cyg Observed With IUE
(Schröder, 1985a,b) h = Height Above the K Giant Limb, R_k = Radius of K Giant,
 α = Scale Height.

| $h[\text{cm}]$ | h/R_k | $n_H[\text{cm}^{-3}]$ | $\alpha[\text{cm}]$ | n_e/n_H | T_e | |
|---------------------|---------|-----------------------|---------------------|----------------|--------------|------------|
| $1.0 \cdot 10^{11}$ | 0.008 | $1.7 \cdot 10^{12}$ | $5.6 \cdot 10^{10}$ | | | |
| $2.0 \cdot 10^{10}$ | 0.016 | $4.8 \cdot 10^{11}$ | $1.1 \cdot 10^{11}$ | | | UV |
| $5.0 \cdot 10^{11}$ | 0.04 | $9.3 \cdot 10^{10}$ | $2.8 \cdot 10^{11}$ | | | continuum |
| $1.0 \cdot 10^{12}$ | 0.08 | $2.6 \cdot 10^{10}$ | $5.5 \cdot 10^{11}$ | | | data |
| $2.0 \cdot 10^{12}$ | 0.16 | $7.5 \cdot 10^9$ | $1.1 \cdot 10^{12}$ | $\sim 10^{-3}$ | ≤ 8500 | |
| $3.0 \cdot 10^{12}$ | 0.24 | $3.2 \cdot 10^9$ | $1.5 \cdot 10^{12}$ | | ~ 10000 | absorption |
| $5.0 \cdot 10^{12}$ | 0.40 | $1.0 \cdot 10^9$ | $2.3 \cdot 10^{12}$ | | | line |
| $7.0 \cdot 10^{12}$ | 0.56 | $4.9 \cdot 10^8$ | $3.2 \cdot 10^{12}$ | $\sim 10^{-2}$ | ~ 11000 | data |
| $1.0 \cdot 10^{13}$ | 0.79 | $2.2 \cdot 10^8$ | $4.5 \cdot 10^{12}$ | | | |
| $1.5 \cdot 10^{13}$ | 1.19 | $9.2 \cdot 10^7$ | $6.9 \cdot 10^{12}$ | | | |

Table 3-4b

Total Chromospheric Particle Densities and Scale Heights as a Function
of Height Above the Limb (Schröder, 1985b)

| h/cm | ζ Aur | | 32 Cyg | | 31 Cyg | |
|---------------------|---------------------|---------------------|---------------------|---------------------|---------------------|---------------------|
| | n/cm^{-3} | α/cm | n/cm^{-3} | α/cm | n/cm^{-3} | α/cm |
| $3.0 \cdot 10^{11}$ | $7.7 \cdot 10^{11}$ | $8.7 \cdot 10^{10}$ | $1.2 \cdot 10^{12}$ | $1.2 \cdot 10^{11}$ | $7.3 \cdot 10^{11}$ | $1.2 \cdot 10^{11}$ |
| $5.0 \cdot 10^{11}$ | $1.3 \cdot 10^{11}$ | $1.7 \cdot 10^{11}$ | $3.3 \cdot 10^{11}$ | $2.0 \cdot 10^{11}$ | $2.1 \cdot 10^{11}$ | $2.0 \cdot 10^{11}$ |
| $1.0 \cdot 10^{12}$ | $1.3 \cdot 10^{10}$ | $3.0 \cdot 10^{11}$ | $5.9 \cdot 10^{10}$ | $4.1 \cdot 10^{11}$ | $3.7 \cdot 10^{10}$ | $4.1 \cdot 10^{11}$ |
| $3.0 \cdot 10^{12}$ | $3.5 \cdot 10^8$ | $9.5 \cdot 10^{11}$ | $4.0 \cdot 10^9$ | $1.3 \cdot 10^{12}$ | $2.5 \cdot 10^9$ | $1.3 \cdot 10^{12}$ |
| $1.0 \cdot 10^{13}$ | $9.4 \cdot 10^6$ | $3.7 \cdot 10^{12}$ | $2.3 \cdot 10^8$ | $4.4 \cdot 10^{12}$ | $1.5 \cdot 10^8$ | $4.4 \cdot 10^{12}$ |
| $3.0 \cdot 10^{13}$ | $6.0 \cdot 10^5$ | $1.3 \cdot 10^{13}$ | $2.1 \cdot 10^7$ | $1.4 \cdot 10^{13}$ | $1.3 \cdot 10^7$ | $1.4 \cdot 10^{13}$ |

and e_0 (in the chromosphere), agreed with the independently measured wind velocity $v_\infty = v_{\text{wind}}$. In that case Equation (3-6) represents an empirical velocity law in the wind acceleration region, which is valid for $r \leq 2 R$, where chromospheric densities have been measured. Table 3-5 contains the derived numbers.

For both 32 Cyg and 31 Cyg the observed and calculated values of v_∞ agree, and Equations (3-5) and (3-6) can be considered as the first empirically determined density and velocity distributions in the chromospheres and wind acceleration regions of K supergiants. However, for the height range $2 R \leq h \leq 5 R$, Equation

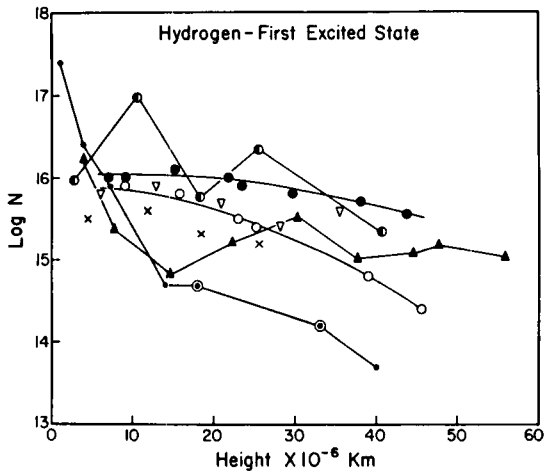


Figure 3-19. Column densities $\log N$ versus height for the first excited state of hydrogen in the chromosphere of ζ Aur (from Wilson, 1960b).

(3-6) is only an interpolation formula between the high chromosphere and the outer wind region. This region cannot be observed with IUE, since the genuine chromospheric absorption lines are too faint for the low S/N of IUE, and the wind P Cygni profiles are optically thick.

As could be expected from the very low density in the chromosphere of ζ Aur and its steep decrease in comparison with observed wind densities, the assumption of steady outflow breaks down. Since mass loss from ζ Aur has

been determined from IUE spectra at 5 different phases (B star in front of and behind K giant), and since the wind lines are formed over larger volumes, the anomalously low chromospheric density of ζ Aur probably means that at that particular phase we were looking through a large-scale low-density structure that may be analogous to a solar coronal hole. Earlier optical observations implying that the extension of the chromospheres may vary from one eclipse to another in ζ Aur stars is consistent with this picture. A further structural analogy to the Sun is the huge prominence detected during egress of the 1981 eclipse of 32 Cyg.

V.B.2. OBSERVATIONS OF A "PROMINENCE" IN 32 CYG

Optical observations showed prominence-like features only through satellite lines of CaII H and K near total eclipse; i.e., close to the limb. In comparison, high resolution ultraviolet observations with IUE offer advantages for the study of inhomogeneities in the outer atmospheres of K supergiants in ζ Aur stars, including (i) the B-star light source that probes the outer atmosphere of the K giant is uncontaminated in the UV light from the cool star, and (ii) observations are possible at all phases, i.e., at various projected separations of the components.

Table 3-5

Wind Parameters for Eclipsing Binary Systems

| | 32 Cyg | 31 Cyg | ζ Aur |
|-------------------------------------|---------------------|------------------------|------------------|
| \dot{M} (M_{\odot}/yr) | $2.8 \cdot 10^{-8}$ | $\leq 4 \cdot 10^{-8}$ | $0.6 \cdot 10^8$ |
| v_{wind} (km/s) | 60 | 80 | 80 |
| v_{∞} (eq 3.7) | 55 | ≤ 88 | 380 |

Che et al. (1983)

In addition to high-velocity clouds seen in the wind at distances of ~ 5 K star radii (see 3.IV.B.3), we have detected in 32 Cyg an absorbing cloud reminiscent of a solar quiescent prominence (Schröder, 1983). Using a sequence of high-resolution IUE spectra taken around the 1981 eclipse of 32 Cyg, light curves have been constructed at seven ultraviolet wavelengths. As was already known from OAO2, observations of the 1971 eclipse of 32 Cyg (Saijo and Saito, 1977), the duration of totality increases with decreasing wavelengths (~ 15.5 days at 1350 \AA compared to ~ 9 days at 1980 \AA). This is due to a steep increase of opacity of the extended chromosphere of the supergiant with higher frequencies.

In addition, a dip in the light curve can be seen after egress from eclipse for $\lambda < 2000 \text{ \AA}$ (Figure 3-20). The additional absorption can be seen for at least 6 days. Since the observed "prominence" was optically thin in the continuum, the wavelength dependence of optical depth, $\tau_\nu \propto \nu^{5.5}$, could be used to identify the opacity source as Rayleigh scattering by HI ground states.

One prominence has a typical column density of neutral hydrogen of $N_H = 2.8 \cdot 10^{24} \text{ cm}^{-2}$. A linear extension perpendicular to the line of sight of about $1/6$ stellar radii ($\sim 30 R_\odot$) and an apparent height of $\sim 15 R_\odot$ above the limb (at 1350 \AA) could be estimated from the light curves (Schröder, 1983). The typical density in the observed prominence was $n_H \sim 10^{12} \text{ cm}^{-3}$, a factor of 10 higher than in the surrounding chromosphere. If the excess pressure is balanced by magnetic fields, a field of ~ 4 Gauss would be required.

The low observed velocity ($\leq +20 \text{ km s}^{-1}$) of a few absorption lines, such as (?) VII 3110.7 \AA seen in addition to the normal chromospheric lines indicates a quiescent or slowly moving prominence. Also, even a moderate proper motion perpendicular to the line of sight, e.g., a moving prominence rising upwards with the wind velocity of 60 km s^{-1} , can be excluded,

since, within the 6 days the absorbing cloud was seen, it would have moved by about $45 R_\odot$ (3 times the observed height above the limb!).

V.B.3. OTHER EVIDENCE FOR EXTENDED CHROMOSPHERES IN COOL GIANTS

Since only few stars can be studied by the binary technique, the question arises as to the general application of the results concerning extended cool chromospheres to other stars.

This question has been addressed by Brown and Carpenter (1984), and Carpenter et al. (1985), who determined the electron density and electron temperature as well as the geometrical extent of chromospheres of 15 late-type stars using line ratios within the CII (UV 0.01) $\lambda 2325 \text{ \AA}$ multiplet, the CII $\lambda 2325/\lambda 1335$ ratio and the total CII $\lambda 2325 \text{ \AA}$ flux. This method was first described by Stencel et al. (1981), and details can be found in the original papers.

Brown and Carpenter (1984) found a distinct dichotomy in the CII $\lambda 2325/\lambda 1335$ ratios between coronal and noncoronal stars, i.e., between stars on the hot and the cool side of the dividing line that separates giant stars with hot coronae and no detectable wind from stars with cool massive winds and no detectable corona (Reimers, 1977a, Linsky and Haisch, 1979). Brown and Carpenter found that CII emission from noncoronal giants and supergiants comes from plasmas with electron temperatures in the range 7000–9000 K, with the mean temperature being ~ 8500 K, whereas the CII emission from coronal stars probably comes from much hotter regions. Even more significant is the clear distinction between coronal and noncoronal giants with respect to the electron density and geometrical extent R/R_* (R_* = stellar radius) of the CII emitting region: coronal stars have $R/R_* < 1.001$ and $\log N_e \approx 10-11$, while noncoronal giants have typically $R/R_* \sim 2$ (range 1.4 to ~ 5) and $\log N_e \approx 8$. The latter results apply to K and M giants as well as to late G to M supergiants (cf. Table 3-6).

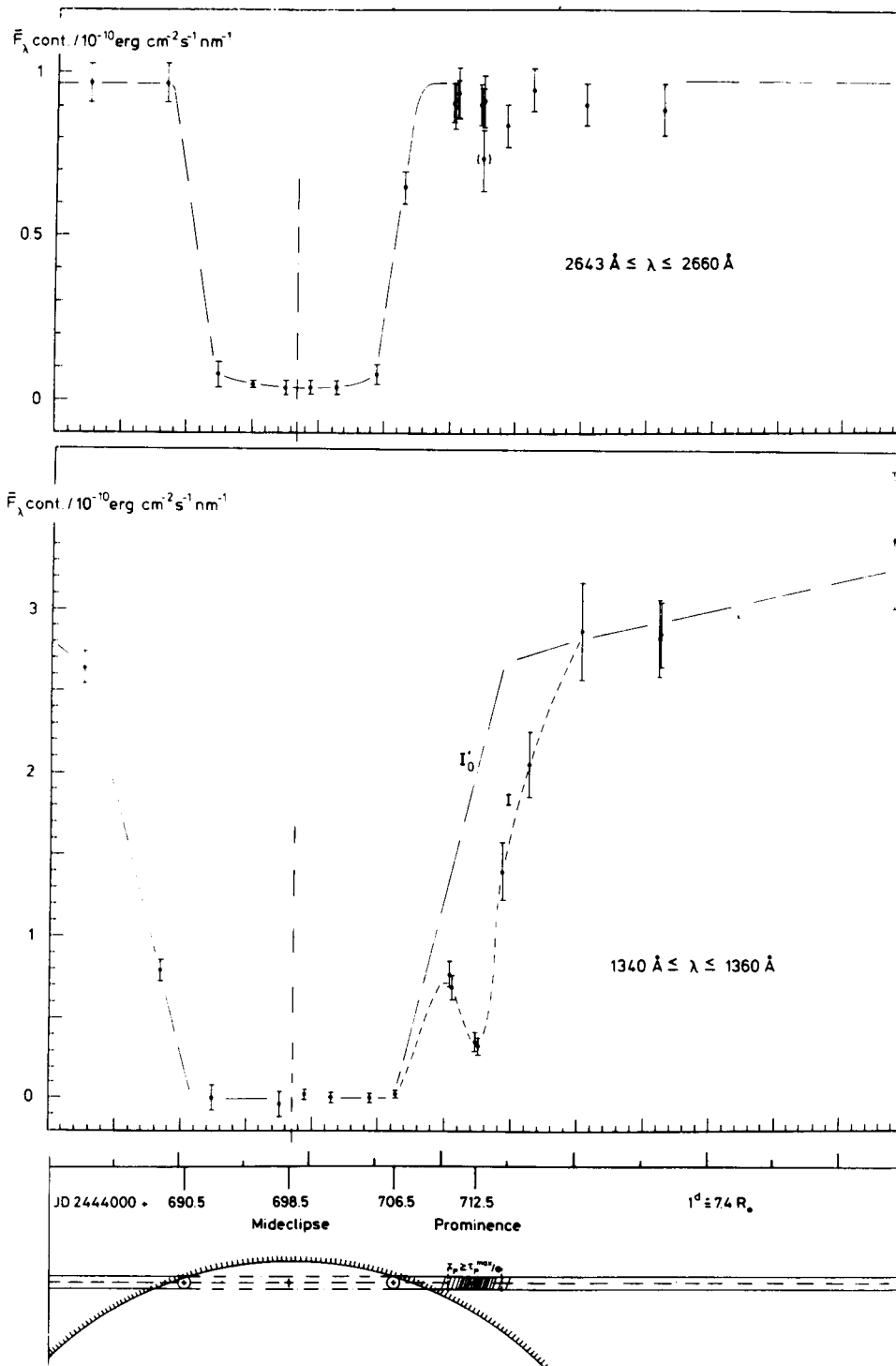


Figure 3-20. Light curves for 32 Cyg during 1981 eclipse at λ 2650 Å (unaffected by prominence) and at λ 1350 Å clearly showing the additional absorption dip due to a "prominence" (Schröder, 1983).

Table 3-6

Density (N_e), Temperature (T_e) and Geometrical Extent (R/R^*) of CII Emitting Regions (Brown and Carpenter, 1984; Carpenter et al., 1985)

| Star | Spectral type | Log N_e (cm^{-3}) | T_e (K) | R/R^* |
|----------------|---------------|--------------------------------|-----------|---------|
| α Cen B | K1 V | 10.9: | > 11,800 | <1.001 |
| β Cet | G9.5 III | 10.9: | > 7,300 | <1.001 |
| β Gem | K0 III | 10.3 | > 9,000 | <1.001 |
| α Boo | K2 III | 8.5 | 8,100 | 2.0 |
| α Tau | K5 III | 8.3 | 10,000 | 1.4 |
| β And | M0 III | 8.2 | < 8,300 | 2.4 |
| λ Cru | M3.4 III | 8.2 | 8,200 | 1.4 |
| α TrA | K2 IIb-IIIa | 8.1 | 11,800 | 2.0 |
| β Peg | M2.5 II-III | 7.9 | 8,700 | 3.2 |
| β Gru | M3 II | 8.1 | 7,500 | 1.7 |
| ϵ Gem | G8 Ib | 7.8 | 8,100 | 5.9 |
| ϵ Peg | K2 Ib | 8.0 | 11,300 | 1.9 |
| λ Vel | K5 Ib | 8.3 | 7,800 | 2.1 |
| σ CMa | M0 Iab | [8.0] | < 6,900 | 4.8 |
| α Ori | M2 Ib | 7.5-8.1 | 8,900 | 2.1 |

The values of geometrical extent and temperature found for the noncoronal giants with the CII method are in agreement with what has been seen in the more direct, spatially resolved studies of chromospheres in ζ Aur type giants. Electron temperatures found from radio observations of the upper chromosphere of α Ori also support this picture with respect to the temperature (Altenhoff et al., 1979).

Let us now summarize the overall picture of the expanding chromospheres and winds of noncoronal giants located on the cool side of the dividing line in the HR diagram. This picture will impose stringent conditions which any stellar wind theory for these stars will have to meet.

The density and velocity structure can be described roughly by

$$\rho = \rho_0 \left(\frac{R}{r}\right)^2 \left(\frac{r}{1-R}\right)^{2.5}, \quad (3-8)$$

and

$$v(r) = \frac{\dot{M}}{4\pi R^2} \left(1 - \frac{R}{r}\right)^{2.5}. \quad (3-9)$$

At $r = 2R$, the wind has roughly $N_e \approx 10^8 \text{ cm}^{-3}$, $T_e = 8500 \text{ K}$ and has reached about $1/4$ of the terminal velocity. As can be seen from Figure 3-21, the heating rate P/ρ , i.e., the rate of energy input into the wind per unit mass, reaches its maximum value at about this height in K supergiants. The existence of distributed nonradiative heating is also indicated by the steeply increasing hydrogen excitation. Indeed, as shown in Figure 3-19 (Wilson, 1960b), the column density of H atoms in the 2nd quantum level stays nearly constant outwards to at least $0.5 R_*$. At a distance of 5 stellar radii, $N_e \approx 10^6 \text{ cm}^{-3}$, the flow speed has almost attained the terminal velocity, and the wind has cooled down to $T_e \leq 5000 \text{ K}$ (Che-Bohnenstengel, 1984).

Whether the density and velocity structure determined for K supergiants applies also in detail to M supergiants like α Ori remains to be shown. In the case of α Ori itself, the mass-loss rate is higher than that of 32 Cyg by a factor of ~ 40 , and we find a consistent picture only if the fraction of ionized hydrogen is assumed to be $\sim 1\%$ in α Ori. In K supergiants hydrogen is $\sim 10\%$ ionized. Radio observations of α Ori, α Sco, and α Her with the VLA at 6 cm also show that about 1% of H is ionized (Drake and Linsky, 1983) in the inner wind of these M supergiants.

A further significant observation that models of stellar winds have to meet is the sudden change in atmospheric structure from coronal

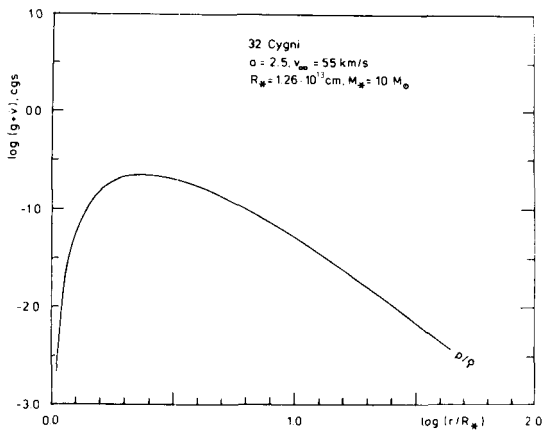


Figure 3-21. Observed energy input per unit mass into the wind (P/ρ) versus height for 32 Cyg (Schröder, 1984).

to noncoronal giants. There is some evidence that this transition in atmospheric structure is related to an abrupt decrease of the rate of rotation (Gray, 1982d; Simon, 1984).

According to one picture, the so-called hybrid stars are intermediate mass stars ($\sim 5 M_{\odot}$) that are just crossing the Hertzsprung gap from left to right. They still maintain a high degree of chromospheric activity, but the CII 2325/1335 diagnostic has shown for one hybrid object, α TrA, that the star has mainly a noncoronal, extended cool atmosphere. The G3 Ib-II supergiant 22 Vul, a young star of $\sim 4 M_{\odot}$ located near to the dividing line, also has been seen during its May 1985 eclipse to have an extended chromosphere ($\sim 1 R_{\odot}$) but a fast stellar wind (170 km s^{-1} ; Schröder and Che-Bohnenstengel, 1985). The transition region plasma emission in hybrid stars, i.e., the hottest observed gas in these stars, is probably confined to closed magnetic loops which cover only a small fraction of the stellar surface. These stars can be expected to have highly inhomogeneous outer layers, and a one-dimensional model may be a misleading oversimplification (cf. Chapter 3.VII.C on RS CVn stars). The observed presence of huge “prominences” and “coronal holes” in K supergiants (see above) is a further indication that inhomogeneity may be an important aspect of at-

mospheric structure in cool giants, as it is in the Sun. It is probable that this inhomogeneity is intimately related to magnetic fields.

VI. LINEWIDTH-LUMINOSITY RELATIONS AND NONTHERMAL MOTIONS

Observed emission fluxes of chromospheric lines provide information on the temperature and density structure and the rate of nonthermal heating. On the other hand, line profiles contain information on velocity fields in chromospheres, coronae, and winds.

One basic phenomenon that has been well known for decades is that in late-type stars the line widths of chromospheric (and photospheric) lines increase with increasing luminosity (see Figure 3-4). Examples of the effect are widespread:

- (i) Wilson and Bappu (1957) discovered that in a great number of G, K, and M type stars the width W_0 of the CaII H and K emission cores increases markedly with the luminosity (or absolute magnitude M_v) of the stars over a range of more than 15 magnitudes. The specific relation is $M_v = -14.94 \log W_0 + 27.59$, where W_0 is measured in km s^{-1} . The relation has been calibrated by means of the Sun, the Hyades giants, trigonometric parallax stars, and other cluster stars (Wilson, 1967, 1970). Instead of the CaII K half-intensity emission width W_0 , the K1 minimum features (cf. Figure 3-3) and other parts of the emission line core can be correlated with M_v , with similar results (Ayres et al., 1975, Cram et al., 1978).
- (ii) The $H\alpha$ absorption core widths H_0 are also correlated with M_v (Kraft et al., 1964). The width-luminosity relation for $H\alpha$ breaks down in supergiants later than K2, because blueshifted,

variable $H\alpha$ emission is also present (Gahm and Hultquist, 1972). After correction for the effects of emission, a well defined width-luminosity relation in $H\alpha$ is also observed in supergiants (Imhoff, 1977).

- (iii) The MgII h and k resonance emission doublet also displays a width-luminosity effect (Kondo et al., 1975, and earlier references therein). From a large collection of spectra, Weiler and Oegerle found $M_v = 15.15 \log W + 34.93$.
- (iv) Observations made with the Copernicus satellite showed that $L\alpha$ exhibits a width-luminosity effect (McClintock et al., 1975).
- (v) High-resolution IUE spectra have shown that there is also a width-luminosity effect in transition layer lines like SiIII] λ 1982 and CIII] λ 1909. These lines are broader in β Dra (G2 Ib-II) and α Aur than in active dwarfs, implying that the amplitudes of nonthermal motions increase with luminosity (Linsky, 1984a).

The Wilson-Bappu relations of CaII, MgII, and $L\alpha$ are parallel with approximate width ratios 1:3:7.5. The increasing line widths possibly reflect a variation of the broadening mechanism (nonthermal velocities?) with height in stellar chromospheres. In this connection it is remarkable that the widths W of weak photospheric lines and the photospheric microturbulence ξ both appear to display a width-luminosity effect with a constant ratio $\xi:W:W_0$ 1:2:15 (Reimers, 1976 and references therein; Imhoff, 1977; Nissen and Gustafsson, 1978).

Theoretical interpretations of width-luminosity relations must explain (1) why line widths increase by a factor of ~ 50 in a single star in lines formed from the photosphere up to the high chromosphere and transition region,

and (2) why the widths of all lines increase with luminosity. An important indication to a possible resolution of these questions might lie in the emission lines in the wings of CaII H and K, which are formed over a range of heights (Stencel, 1977). These lines exhibit the following tendencies: (i) a number exhibit a line-width-to-luminosity correlation analogous to the Wilson-Bappu effect; (ii) the emission lines exhibit a width variation with wavelength shift from the CaII H or K line center. This variation contains direct information about the depth-dependence of the broadening mechanism. Finally, (iii) the slope of the line-width-to-luminosity correlation of H and K emission lines varies monotonically with $(\Delta\lambda)^{-2}$ (H or K line damping-wing opacity is $\sim (\Delta\lambda)^{-2}$), which suggests that we are observing a depth-dependent phenomenon.

The observed variations of line width with increasing height of formations are readily explained in terms of a total nonthermal broadening velocity that increases with height (Stencel, 1977). This is consistent with a line-broadening agent (velocity field) that increases from the photosphere up to the height of formation of $L\alpha$.

It may also be useful to mention the attempts to reformulate the Wilson-Bappu effect in terms of basic stellar parameters $\log g$ and T_{eff} , since theoretical models usually start with these parameters. It can be shown empirically that $M_v = -15 \log W_0 + \text{const}$ is equivalent to $\log W_0 = \alpha \log g + \beta \log T_c$ with $\alpha \sim -0.2$ and $\beta \approx 1.2$ (Reimers, 1973). Lutz and Pagel (1982) and Ayres (1979) found slightly different exponents and added terms to account for metal abundance.

In addition to linewidth-luminosity relations which show the presence of nonthermal motions in all layers of late-type stars, it has been discovered with IUE that the transition-layer lines are redshifted relative to low-temperature lines in a number of stars with active chromospheres and transition layers (e.g.,

β Dra, α Aur, λ And, and active G and K dwarfs). The redshifts, confirmed on an absolute scale, increase with the temperature of the line formation region and reach values of $\sim 20 \text{ km s}^{-1}$ in lines of OIV] and NV. This is reminiscent of a similar effect in solar active regions. Since the redshifts have been found also in intercombination lines, they cannot be produced by differential motions, and imply that some 10^5 K plasma is actually moving downward in these stars (Ayres et al., 1983; Linsky, 1984b).

VII. STELLAR ACTIVITY IN COOL STARS

VII.A. MAIN-SEQUENCE STARS

The Sun is the only star whose outer layers and activity can be studied in detail. Therefore, in order to understand stellar activity, chromospheres, coronae, and winds in late-type stars, we must start with understanding these phenomena in the Sun. On the other hand, it may be helpful toward understanding the underlying physics to place the Sun in the general context of stellar activity, by studies of the dependence of the various activity phenomena on parameters like effective temperature, gravity, age, chemical composition, rotation, and binary membership. In particular, the variation of certain indicators of chromospheric activity with some of these stellar parameters has been studied extensively during the last two decades.

VII.A.1. STELLAR CYCLES

It is well known from CaII K spectroheliograms that CaII emission in the solar chromosphere varies with the sunspot cycle. The net CaII emission of the Sun is also modulated by rotation due to the nonuniform distribution over the solar surface of CaII emitting plages. Stimulated by these facts, O.C. Wilson started in 1966 a series of observations over more than a decade to answer the general question: Does chromospheric activity of main-sequence stars

vary with time, and if so, how (Wilson, 1978)? To answer this question, he monitored the relative fluxes in 1\AA bands at the centers of the H and K lines in 91 main-sequence stars from F5 to M2, and came to the following conclusions:

- (i) It is likely that no chromospheres are constant in time, and, in particular, short-term fluctuations are universal. The short-term fluctuations increase in amplitude with the increase of the average flux.
- (ii) Cyclic variations with periods ranging upwards from seven years to at least twice as long were found in about two dozen stars, the earliest-type star with definitely cyclical behavior being G2. These long-period cycles seem to be analogous to that of the Sun (Figure 3-22). The incidence of cycles appears to increase with later spectral types (cf. Table 5 in Wilson, 1978), although this finding could be biased by the easier detectability of such variations in stars with later spectral types, as Wilson points out.

There is not yet a satisfactory answer to the question of what fraction of solar-type stars exhibits cycles at a given time and what fraction of their lives is spent in this state. The answer to this question is important in the light of the detection of the so-called solar Maunder minimum. For a period of 70 years beginning with A.D. 1645 the Sun did not show signs of its usual level of sunspot activity. In addition to the Maunder minimum, further epochs of minimum solar activity have been identified (A.D. 1420–1530, A.D. 1280–1340, A.D. 1010–1020). The existence of these minima is established through auroral histories, radiocarbon records in tree rings, and modern historical sunspot observations (Baliunas and Vaughan, 1985). An apparently similar phenomenon is known in a number of late-type dwarf stars. For example, HD 224085 is a late-type

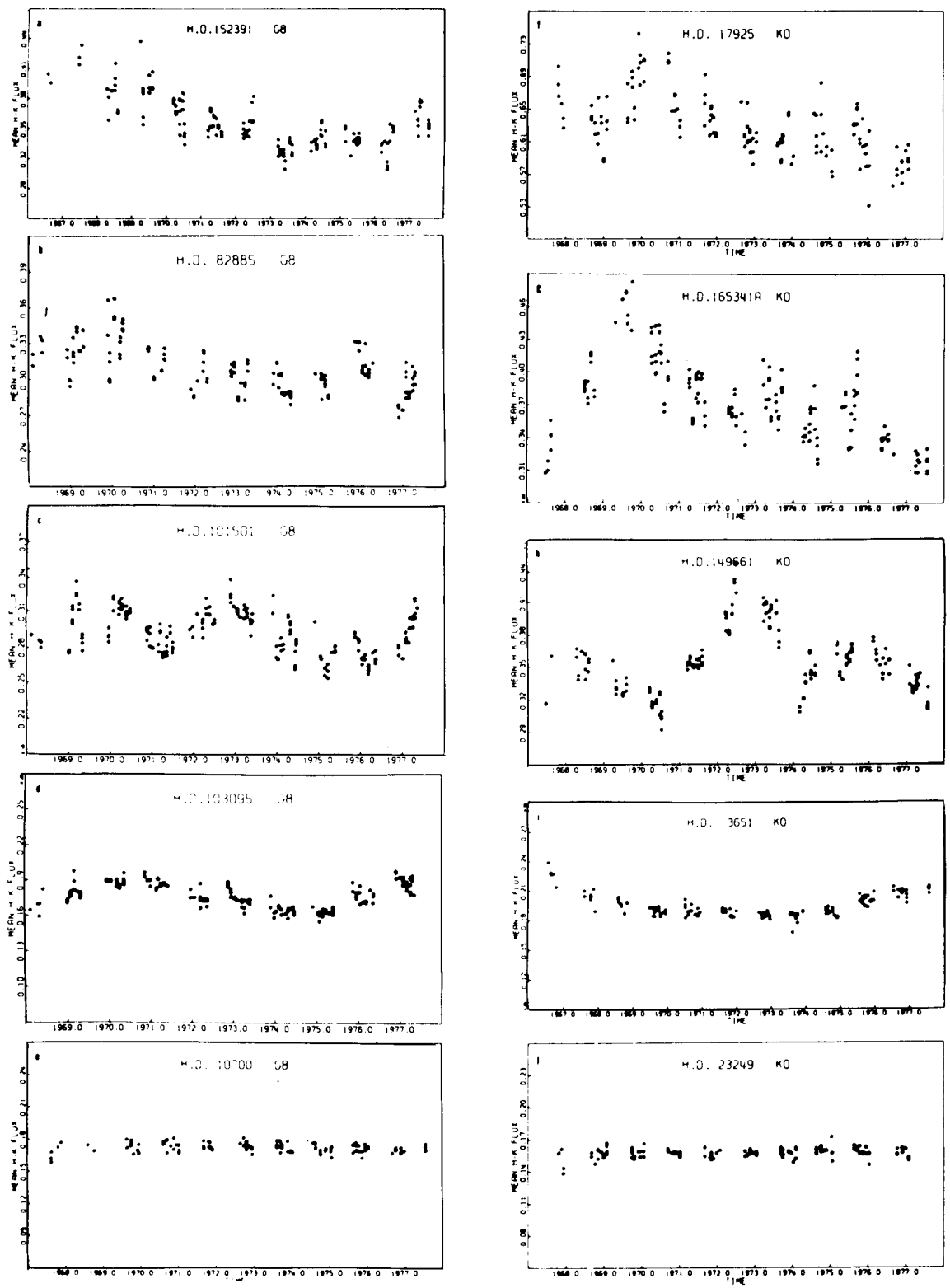


Figure 3-22. Stellar cycles of various late-type main sequence stars observed in CaII K fluxes (Wilson, 1978).

emission-line star (K2) with light variations that have been interpreted as being due to starspots. Hartmann et al., (1979) found that the star was essentially constant in mean light for ~ 40 years before beginning to exhibit changes ≥ 0.3 mag, both in short period variability and in mean light. The data suggest that stars with spots may have long periods of relative inactivity.

In a recent study of the short-term variability of CaII K emission apparent in Wilson's data, 46 main-sequence stars were observed nearly continuously at nightly intervals in a 14-week observing run with the technique used by Wilson (Vaughan et al., 1981). Clear evidence of rotational modulation of the CaII intensity was found in many stars. In 19 stars, rotational periods could be assigned by visual inspection (Figure 3-23), and in a further 9 stars by autocorrelation analysis. The rotation velocities obtained from the measured periods are in accordance with spectroscopically determined $v \sin i$ values when available. Much of the short-term scatter in H and K fluxes observed by Wilson is apparently due to rotational modulation, although variations on other time-scales are also present.

Vaughan et al., (1981) found that periodic cycles resembling the Sun's are almost exclusively found in stars with rotation periods in excess of about 20 days, and that the cycle periods are uncorrelated with rotation rate. On the other hand, fast rotators ($P_{\text{rot}} < 20$ days) show incoherent variations on long time-scales. Among the younger, faster rotating stars, rotational modulation of CaII emission fluxes was seen in $\sim 80\%$ of the stars, implying that for much of the time these kinds of stars have asymmetric distributions of active regions on their surfaces. In some stars, amplitude variations and phase shifts were observed in the rotational modulation as expected when individual active regions grow and decay. On the other hand, for some younger active stars, Noyes found that active longitudes may persist over times ranging up to a decade (e.g., HD 82885). He stated that "in some stars the rotational

modulation curves are less suggestive of the growth and decay of individual active regions than of the 'beating' of at least two active regions at different longitudes whose longitude difference changes with time."

VII.A.2. THE AGE/ROTATION/ ACTIVITY CONNECTION

Through the extensive studies of O.C. Wilson (1963, 1966a, 1966b); Wilson and Skumanich (1964); and Wilson and Woolley (1970), it is well known that the CaII emission intensities of main-sequence stars depend on rotation rate and age. Since the rotation velocities of these stars decrease with age (Kraft, 1967; Soderblom, 1983) it is possible that the basic underlying motor for chromospheric activity is simply rotation. However, it is also possible that evolutionary changes in the internal structure of the stars exert an influence on chromospheric activity which is independent of rotation.

However, the connections between chromospheric activity and rotation, activity and age, and rotation and age may be quite subtle, and it seems wise to discuss these correlations at first separately:

- (i) Activity-rotation: It was first noticed by Wilson (1966a,b) that, on the main sequence, there is a close correspondence between the onset of fast rotation in stars with spectral types earlier than about F4 and the termination of chromospheres at the same spectral type. This was taken as evidence for a braking mechanism related to convection and activity in late-type stars.

On the other hand, in a study of F2 to G3 IV and V stars, Kraft (1967) showed that the average rotational velocity is higher among stars with CaII emission than among those without. Soderblom (1983) found that for solar-type main-sequence stars, the

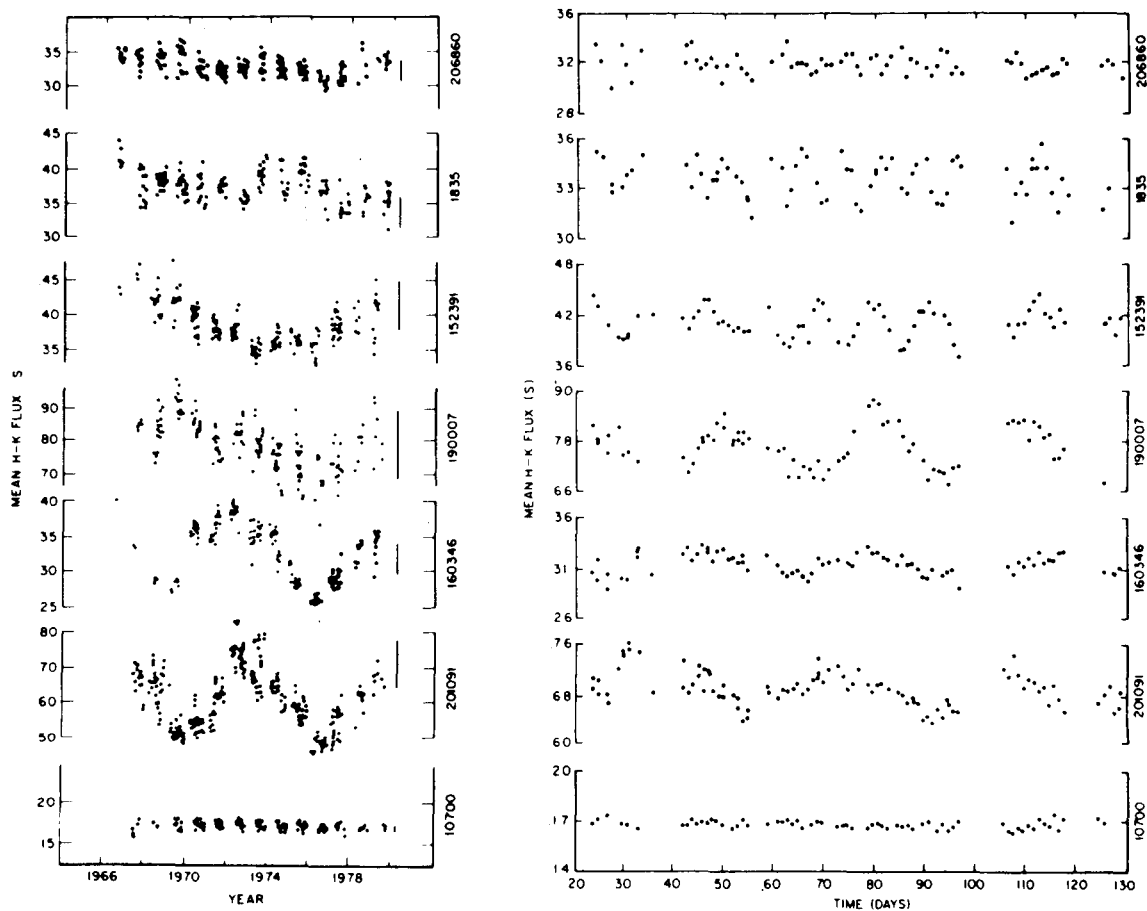


Figure 3-23. Mean H-K fluxes for selected MS stars (right) as observed at daily intervals, from Vaughan et al. (1981).

relative fraction of the star's energy appearing in the central emission reversal of CaII K is proportional to the rotation speed and that stars cooler than 6000 K exhibit much stronger K emission than somewhat hotter stars with the same rotational velocity. This is confirmed by the data shown in Figure 3-24, a $\log S - P_{\text{rot}}$ diagram (S is a measure of the CaII flux) for different temperature groups. Figure 3-25 shows a similar relation between X-ray luminosity and rotation, established by Pallavicini et al., (1981).

Finally, it has become clear from rates of rotation measured by observations of modulation of CaII K fluxes

(Vaughan et al., 1981) that the strength of H and K emission varies as a function of rate of rotation at a given color $B-V < 1.0$. This suggests that rotation rather than individual conditions of age *per se* is the chief parameter influencing chromospheric emission.

The relationship between CaII K emission and rotation (or age) is probably nonlinear (Vaughan and Preston, 1980; Vaughan, 1980). A survey of CaII flux S in several hundred main-sequence stars shows that in the $\log S - (B-V)$ diagram there is a clear division into two branches (two distinct groups) in stars of spectral type G0-K1. Stars in the upper branch

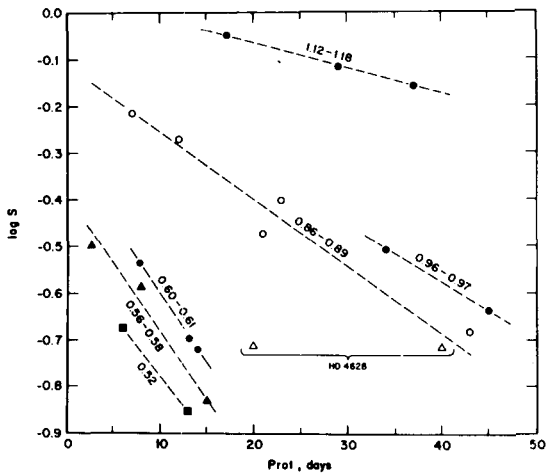


Figure 3-24. Strength of H-K emission ($\log S$) versus rotation period (P_{rot}) for stars in selected narrow intervals of B-V. For a given color, the points appear to lie on well-defined sequences (Vaughan et al., 1981).

(young stars) reveal erratic behavior over a considerable range of time-scales (typically 1 to 2 years), plus additional stochastic variations; while stars in the lower branch have solar-like cycles with smooth, undulating variations where the rapidly varying

component is always larger in the maximum of the cycle, as it is in the Sun.

- (ii) Activity-Age: It was first pointed out by Wilson (1963) that the average intensity of H and K emission is much higher for main-sequence stars of spectral type G0 to K2 in the Hyades, Praesepe, Coma, and Pleiades clusters than for similar field stars, and that it is appreciably higher for the Pleiades than for the other clusters. In a subsequent study, Wilson and Skumanich (1964) concluded from the distribution of H and K intensities of field stars in a $C_1 - (b-y)$ diagram that chromospheric activity of main-sequence stars decreases with age.

Furthermore, a clear correlation was found between the calcium emission intensities and the eccentricities and inclinations of the galactic orbits of stars. This supports the view that main-sequence stars with strong H and K emission lines are young stars which have nearly circular orbits with low inclination to the galactic plane, while

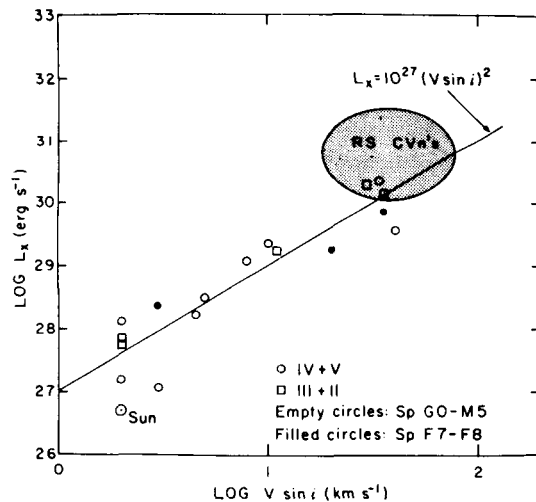
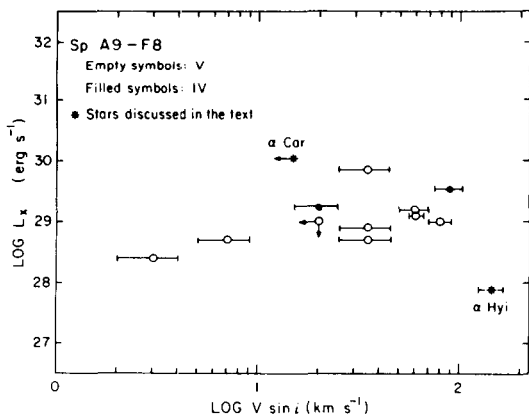


Figure 3-25. Correlation of X-ray luminosities with projected rotational velocities of late-type stars. Figure (3-25a) shows main-sequence and subgiant stars of spectral type A9-F8, while Figure (3-25b) shows stars of spectral type later than F7 (Pallavicini et al., 1981).

stars with weak emission are old stars which have, statistically, high eccentricities and high inclinations to the galactic plane (Wilson and Woolley, 1970).

As already mentioned, the data of Vaughan and Preston (1980) show a gap in the distribution of K emission intensities versus color, from which they suggested that chromospheric activity might decline abruptly at an age of $\sim 10^9$ years (nonlinear behavior). This conclusion was also reached by Soderblom (1983). The alternative possibility, that there is a lack of stars in the solar neighborhood with ages to fill the gap, seems to be ruled out by Soderblom's (1983) observation that there are a sufficient number of nearby sample stars whose age, according to their Li abundance, is intermediate between the Hyades and the Sun.

The reality of the gap and a possible nonlinear variation of H and K emission flux with age are supported by the observation of Vaughan et al. (1981), showing that stars with rotation periods longer than about 20 days have solar-type activity cycles, while in faster rotators noncyclic activity was found. This dichotomy may be explained in terms of the existence of two different modes of magnetic field generation. On the other hand, Noyes et al. (1984) have found from a study of 41 stars with well determined rotation periods that the dependence of mean chromospheric emission on rotation and spectral type is essentially the same for stars above and below the Vaughan-Preston gap. An explanation of the gap in terms of a discontinuity in dynamo characteristics therefore appears doubtful.

As shown in Figure 3-26, Noyes et al. (1984) found that the mean level of CaII H and K emission (averaged over 15 years) of these 41 main-sequence stars, when expressed as ratio of chromospheric flux to total bolometric flux, is well correlated with the parameter P_{obs}/τ_c , where P_{obs} is the observed rotation period and $\tau_c = f(B-V)$ is a theoretically determined convective overturn time calculated with a mixing length to scale height ratio $\alpha = 2$. The quantity P_{obs}/τ_c is the Rossby number, R, measuring the ratio of Coriolis force to inertial force acting on a convective eddy. It therefore measures the efficiency of an α - ω dynamo process in generating magnetic fields.

The finding of Noyes et al. (1984) is in accordance with the predictions of magnetic field behavior based on dynamo theory, provided that the relation between chromospheric emission and dynamo-generated fields is essentially independent of rotation rate and spectral type of the stars. Of course,

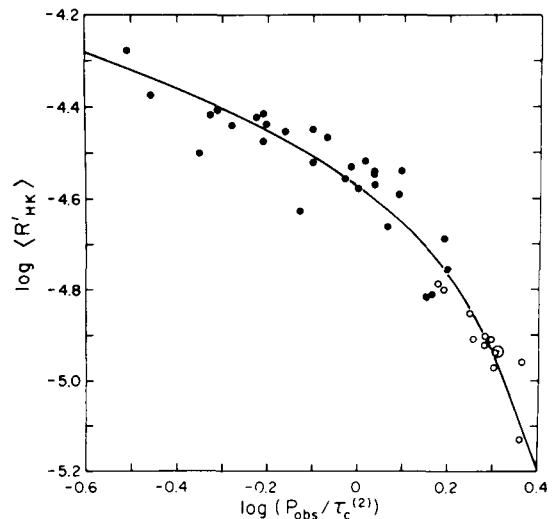


Figure 3-26. CaII H-K emission flux versus Rossby number P_{obs}/τ_c (see text), from Noyes et al. (1984).

theory is currently unable to predict observed quantities such as CaII K emission strengths. A further preliminary result is that the activity cycle period of solar-type stars with regular cycles apparently varies with Rossby number as $P_{\text{cyc}} \sim R^{1.25 \pm 0.5}$ (Noyes, 1984).

The surface flux of CaII emission also appears to decline as the square root of age $F_{\text{CaII}} \sim t^{-1/2}$ (Skumanich, 1972). Emission from higher temperature layers (TR and corona) declines more rapidly than does CaII emission. It is found that $F_{\text{CIV}} \propto t^{-0.9}$, while the soft X-ray flux $F_x \propto t^{-1.3}$ (Boesgaard and Simon, 1981; Stern et al., 1981). The $t^{-1/2}$ relation is not valid for CaII emission from stars younger than the Pleiades (Linsky, 1984b).

- (iii) **Rotation-age:** Kraft (1967) found in a study of high-dispersion spectra of F5 to G3 stars in the Pleiades and Hyades that the rotational velocity decreases with age. Skumanich (1972) deduced from Kraft's data and the rotational velocity of the Sun a decrease of the mean projected rotational velocity $\langle v \sin i \rangle$ with age t of the form $\langle v \sin i \rangle \propto t^{-1/2}$.

In a more detailed study, Soderblom (1983) determined rotational velocities using lithium abundances (an age indicator) obtained from high-resolution line profiles for a large number of stars with ages between $\sim 10^8$ and $5 \cdot 10^9$ years. The relation $\langle v \sin i \rangle \propto t^{-1/2}$ was clearly confirmed to within the uncertainties of measurements.

VII.B. SINGLE GIANT STARS

Early evidence for the existence of variability in CaII K emission in normal, nonvariable stars was found in α Boo by Griffin (1963) and in

α Tau by Deutsch (1956). The same two stars were later shown to exhibit CaII H and K emission flux variations over periods ranging from hours to months (Liller, 1968).

A number of K and G (super) giants show a variable HeI 10830 line. Variations on a time-scale of months are common, although in α Boo they have been seen on a time-scale of less than a week. (Vaughan and Zirin, 1968; Zirin 1976; O'Brien, 1980). There seems to be a well-defined boundary in the HR diagram separating those stars showing such variable 10830 Å from the solar-type stars (O'Brien, 1980). This boundary coincides with the dividing line between stars with hot solar-type (nonwind) chromospheres and coronae and those with cool extended chromospheres (wind) (Reimers, 1977a,b; Linsky and Haisch, 1979; Carpenter et al., 1985).

A number of bright K and G giants (e.g., Θ Her, γ Aql, α Aqr, i Aur) show highly variable HeI 10830 with both absorption and emission components. These stars have absorption features in 10830 Å which are shifted far to the blue, indicating a high velocity mass flow. These stars were identified subsequently as "hybrid" atmosphere stars (cf. Chapter 3.II.B). The time-scale for larger variations of HeI emission in Θ Her is several years.

Hybrid stars are located on the HR diagram near to the previously mentioned dividing lines. It was recognized, from extensive observations of circumstellar CaII H and K absorption lines in K and G giants and supergiants, that CS CaII H and K lines are usually variable in stars near to this dividing line (Reimers, 1977a). The CS lines may in fact be sharp, diffuse, or invisibly weak at different times, and they are often accompanied by considerable velocity shifts (Reimers, 1977a). The time-scale of noticeable variations is of the order of months in μ UMa. In α Tau, a sharp circumstellar line appeared over a period of less than two months, and remained visible for more than a year. The line in α Tau was observed to change its position

within two days (Reimers, 1977a). Kelch et al. (1978) also found variations of CS CaII K on a time-scale of days in α Tau. A similarly short time-scale was observed in α Aqr: the V/R ratio (intensity ratio of violet to red emission peak) of CaII K changes even within a day (Hollars and Beebe, 1976). So far, the shortest time-scales for chromospheric variations in giant stars have been detected in α Tau. Baliunas et al. (1981), monitored the CaII flux variability and found a maximum in the power spectrum near 30 minutes. The change in energy in an event on November 5, 1978, lasting ~ 2.5 hours, encompassing an 8% change over 12 minutes, was observed to be $\sim 2.10^{32}$ erg in H and K.

In addition to variations on these short time-scales (which may be related to flare- or prominence-like phenomena in certain regions of the stellar surface) the same stars undergo variations on a time-scale of years. For example, α Aqr underwent a substantial decrease in the blue peak of its MgII emission over a period of ~ 1 year, apparently as a result of increasing MgII absorption in the wind (Dupree and Baliunas, 1979). During the same time the asymmetry of the CaII K line varied on a time-scale of days (Dupree, 1982). The increased opacity in the high-velocity part of the wind appears to result from a long-lived structural change, since the MgII profile has exhibited its new form for about two years. Cyclic variations on a time-scale of about 5 years have also been detected in the HeI 10830 Å emission of the hybrid star Θ Her.

Such long periods might be due to rotational modulation of activity in giant stars, but definite periods have not yet been established. A spot-activity picture is supported by observed variations of UV emission-line fluxes (OI, CII, ...) by factors of ~ 2 in hybrid stars like α Aqr (Dupree and Baliunas, 1979, Böhm-Vitense and Dettmann, 1980). An alternative explanation would involve irregular pulsation, since most of the discussed stars are indeed semi-regular variables.

VII.C. RS CVn-STARS

RS CVn systems are close, detached, late-type G and K giant and subgiant binaries. Although binary interactions cannot be neglected in discussing their active chromospheres and coronae, the main (giant) components appear to define the extreme end of a rotation-activity relation similar to that observed in late-type dwarf stars. This extreme behavior may thus help us to gain insight into structural phenomena not easily seen in single stars.

The defining characteristics of RS CVn systems are (cf. Linsky, 1984a): (i) They are binaries with periods of 1-14 days, with rotation and orbital periods synchronized by tidal interactions; (ii) they show strong CaII emission (outside eclipse); (iii) the hotter star is usually of spectral type F or G, and on or near to the main sequence, while the secondaries are not always detected; (iv) a further important characteristic is the presence of dark starspots that migrate in phase, as observed from wave-like distortions of the optical light-curves.

Large spots or spot concentrations have been observed to drift very slowly relative to the stellar rotation, for as long as ~ 10 years in one case. The spots are presumably magnetic. However, magnetic fields are difficult to measure in rapidly rotating stars, and the only star with detected fields is λ And with 1290 ± 320 G covering half the visible surface (Giampapa et al., 1983). Further evidence for coronal magnetic fields in RS CVn stars comes from nonthermal radio emission (Linsky, 1984b).

The following phenomena observed in RS CVn stars may be particularly relevant to understanding single stars. [The chosen topics are highly selective: detailed reviews of optical and in particular UV and X-ray observations have been given by Hall (1976, 1981), Dupree (1981), Rodono (1983), Catalano (1983), and Linsky (1984a)].

A close connection between the minimum photometric light and the maximum UV line flux was first revealed by IUE observations of λ And (Baliunas and Dupree, 1982) and AR Lac (Walter et al., 1983). The effect is also seen in II Peg, for which Figure 3-27 (Marstad et al., 1982) shows the remarkable sharp rise of emission-line flux at phase 0.45, and the corresponding steep decline at phase 0.95. Marstad (1983) used observations of II Peg to develop a geometrical model of the active region. He found that the UV active region was located

near the leading edge of the larger of two distinct spot groups. The UV region covered only $\sim 6\%$ of the stellar surface, compared with a total spot area of 25–30% of the visible hemisphere. This pattern is the reverse of the situation on the Sun, where active regions are much larger than the sunspots themselves.

A further consequence of the fractional coverage of only $\sim 6\%$ is the extremely high estimated value of the CIV surface flux (4×10^3 times that of the quiet Sun). These data imply that one-component models of chromospheres and transition regions of active stars using integrated fluxes are not very realistic, and that active region filling factors must be determined before adequate models can be constructed.

A powerful new technique, “Doppler Imaging,” has been applied to wavelength-calibrated IUE spectra of AR Lac for an identification (localization) of active regions on the stellar surface (Linsky, 1984a). The technique exploits the fact that in the spectrum of a rotating star there is a one-to-one correspondence between the wavelength of a spectral line (or part of a spectral line) emitted by a given bright (or dark) structure and the spatial position across the stellar disk. The technique, which allows a one-dimensional mapping of the stellar disk, was first applied to optical spectra of BY Dra and RS CVn stars (cf. Vogt and Penrod, 1983).

RS CVn stars are well known to be bright X-ray sources. In fact, they were the only cool giant stars that could be observed with the *Einstein* solid state spectrometer (Swank et al., 1981) and α Aur was even observed at high resolution with the crystal spectrometer. The main results of X-ray observations were (Linsky, 1984a): (i) all observed RS CVn systems have two components in their corona, one at “low” temperatures of $T_e \sim 4-8 \cdot 10^6$ K with $\log L_x = 30-31$ and one at $T_e > 5.0 \cdot 10^7$ with $\log L_x \sim 29-31$; (ii) the high-temperature components are more variable than the low temperature components; and (iii) the longest period system

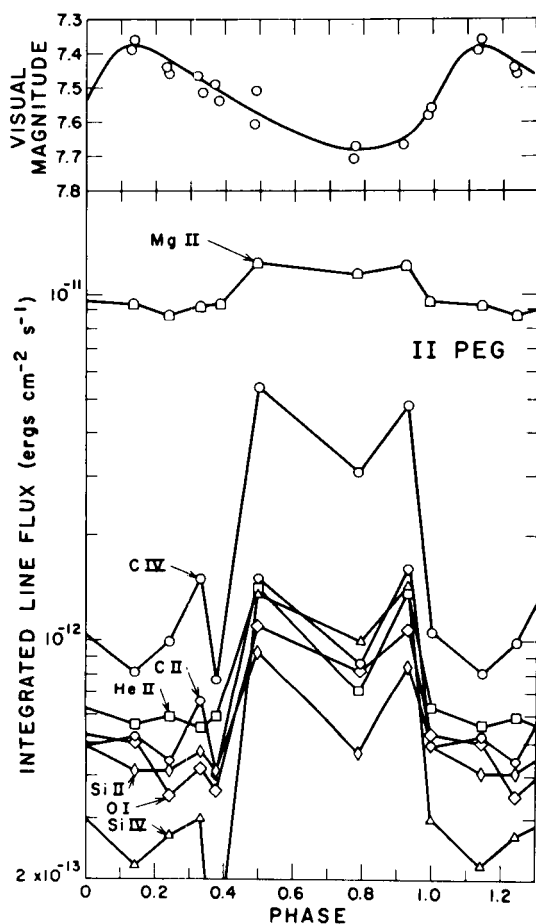


Figure 3-27. Phase dependence of visual brightness and of integrated fluxes of various chromospheric and transition region emission lines of the RS CVn variable II Peg. Notice the rapid rise and fall of line fluxes indicating the rotational modulation of a compact active region across the disk (Marstad et al., 1982).

4

T TAURI STARS

L.V. Kuhi and L.E. Cram

I. TAXONOMY OF T TAURI STARS AND RELATED OBJECTS

The irregular variability of T Tauri itself has been known for more than a century. However, the first systematic study of the T Tauri stars as a separate class appears to be that of Joy (1942, 1945, 1949), who chose as defining criteria: (a) rapid irregular light-variations of as much as 3 mag, (b) spectral type F5-G5, with overlying emission lines resembling those of the solar chromosphere, particularly manifest in the great strength of H and K of ionized calcium, (c) low intrinsic luminosity, and (d) association with bright or dark nebulosity.

Herbig (1958, 1962) refined the definition in terms of primary spectroscopic criteria: (a) the hydrogen lines and the H and K lines of CaII are in emission, (b) the fluorescent FeI emission lines at 4036 Å and 4132 Å are present, and (c) the [SII] emission lines at 4068 Å and 4076 Å are very often, but not always, present. The emission lines are usually superimposed upon a continuous spectrum ranging from a pure continuum to a normal absorption spectrum. Herbig noted that stars with these primary characteristics possess, in addition, the following properties: (d) when an absorption spectrum is visible, the spectral type lies in the

range from late F to M, and strong Li 6707 absorption is present; (e) the stars are invariably superimposed upon, or lie very near the edges of, obscured regions; (f) the general level of excitation of the emission spectrum is never high, although HeI is frequently present, and weak HeII has been reported; and (g) all stars of this type that have been adequately investigated are variable in light, and exhibit a wide variety in the nature of the variability.

Classification according to variability has not been very successful. In early editions of the General Catalogue of Variable Stars, T Tauri stars are identified as a subclass of the RW Aurigae variables, the latter being primarily defined in terms of irregular variability and proximity to the main sequence. Connection with bright or dark diffuse nebulosity is also a property of the overwhelming majority of RW Aur stars. The T Tauri subclass is further defined by having spectral class G-M and characteristic emission spectra in which bright fluorescent lines of FeI and forbidden lines of [SII] and [FeII] are present.

The diversity of spectroscopic and photometric features exhibited by T Tauri stars and related objects has led to considerable discussion and confusion regarding the precise

definition of the T Tauri type. One of the main sources of ambiguity lies in the fact that broadband photometric light curves have been used often to provide primary criteria for classification [this is the origin of the RW Aur class, the T Ori class, and the designations of light-curve types I, II, III and IV introduced by Parenago (1933)]. However, in general the features of the light curves that define the subclasses are neither prominent, nor stable, nor unique (cf. Glasby, 1968, pp 11–12), and in many cases they do not correspond to any characteristics distinguishable in spectrally resolved observations. As Joy (1945) noted, “The variations in light of the T Tauri stars are so irregular and unpredictable that classification by means of their light-curves is practically impossible. Thus far, observations have been insufficient to determine definite sequences of light changes which are uniquely characteristic of the group.”

Perhaps recognizing these problems, IAU Commission 27 (1964) adopted the following classification scheme which relies on both photometric and spectroscopic criteria:

“I. Eruptive Variable Stars

1. Nebular and rapid irregular variables

Int – T Tauri-type variables connected with diffuse nebulae. Brightness variations are irregular. They are characterized by F to M-type spectra with emission lines of FeI 4064, 4132, of [SII] 6717, 6731, of [OI] 6300, 6363, and emission lines of H, HeI, CaII, FeII, TiII together with the absorption lines Li 6707 are characteristic of the spectrum. A typical representative is T Tau.

IT – T Tauri-type variables not connected evidently with nebulosity. The same spectral characteristics. A typical representative is RW Aur.”

It appears that many workers currently in the field would be prepared to adopt Herbig’s definition with assignment to the T Tauri class be-

ing made only on the basis of his specific spectroscopic criteria. These criteria separate the T Tauri stars from all other kinds of emission-line stars, but such a rigid definition may exclude objects from the class for reasons that are “not very fundamental” (Herbig, 1958).

In particular, there is a large, rather inhomogeneous group of stars, containing the T Tauri stars as a subgroup, whose members are characterized by the presence of some of the following properties: (a) association with nebulosity, (b) irregular variability, (c) emission lines with level of excitation approximately that of the solar chromosphere, and (d) UV and/or IR excesses. The entire group has been loosely termed “nebular variables” (e.g., Glasby, 1968) or the “Orion population” (Herbig and Rao, 1972). In addition, weak emission-line T Tauri stars look very much like normal dwarfs, and late-type T Tauri stars are often indistinguishable from dMe stars. Bastian et al. (1983) have attempted to update the definition of T Tauri stars to distinguish them as a subset of these objects. Their phenomenological definition is “stellar objects associated with a region of obscuration; in their spectrum they exhibit Balmer lines of hydrogen and the CaII H and K lines in emission, the equivalent width of H α being at least 5 Å. There is no supergiant or early-type (earlier than late-F) photospheric absorption spectrum.” In this chapter we will be somewhat more flexible in our discussion than strict adherence to the defining criteria would require, since the boundaries of the T Tauri “class” are presumably not related to clear cut physical differences.

Haro (1976) has offered a tentative definition of the minimum requirements for a bona fide T Tauri star: (a) spectral type F8 or later, (b) irregular variability and usually associated with detectable interstellar material, and (c) the CaII H and K lines and some of the hydrogen lines must be in emission and detectable on low-dispersion (430 Å/mm) slit spectrograms. This definition is adequate for our purposes, although it probably should also address the

question of how persistent the line emission should be in order for the star to qualify for the T Tauri description.

The characteristics which serve to distinguish T Tauri stars from normal stars occur with a range of prominence from one star to another, and often vary with time in any one star. In fact it is often possible to arrange a given set of observations of a group of T Tauri stars, or a time sequence of observations of a given star, into an ordered sequence reflecting the degree of prominence of a particular T Tauri characteristic. Such ordering might be done, for example, in terms of the amplitude or rate of photometric variability, the strength or color of excess continuum emission, or the intensity and shape of certain emission lines. Figure 4-1 shows such a sequence arranged in order of increasing strength of emission-line prominence, and illustrates the important characteristics of T Tauri spectra as observed at a resolution of 7\AA (Cohen and Kuhi, 1979). Sequences arranged in this way presumably reflect in some way trends in the structure of the underlying atmospheres. It is not true that sequences defined by two different characteristics of this kind will always coincide, presumably because the contributions of different parts of the atmosphere occur with different relative weights in different stars at different times. Indeed, we might expect to learn much about the structure of the atmospheres of T Tauri stars by identifying both the presence and absence of correlations among various spectral features.

Given that a set of T Tauri observations is often amenable to systematic arrangement, it is reasonable to adopt terminology similar to that introduced by Herbig (1958), i.e., those stars with the strongest, densest emission-line spectrum and the strongest excess blue continuum are considered to be the most "advanced" T Tauri stars. Several authors have suggested that the advanced objects are perhaps also the youngest T Tauri stars, but it is very hard to confirm the validity of this suggestion, inasmuch as there is a general correlation of

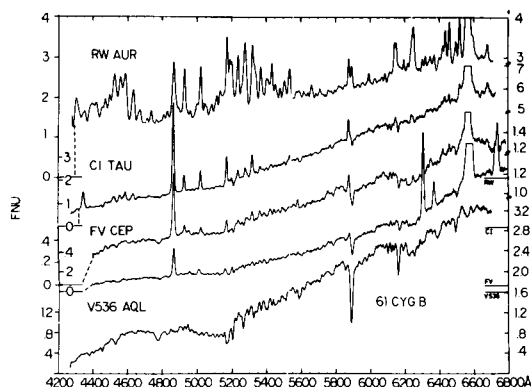


Figure 4-1. A sequence of K7 spectra beginning with the normal star, 61 Cyg B, showing the effect of increasing emission characteristics in the T Tauri stars. The extreme T Tauri star, RW Aur, shows no photospheric components in this observation (Cohen and Kuhi, 1979).

emission-line strength with bolometric luminosity, hence age (Cohen and Kuhi, 1976). In view of this possibility we will use the term "extreme." The extreme T Tauri stars are of special interest because the atmospheric phenomena producing the T Tauri spectral characteristics are obviously developed to a very high degree.

The extreme T Tauri stars constitute only some 10% of the T Tauri population, but they are often thought of as the typical T Tauri stars. In fact Cohen and Kuhi (1979) have shown that the most common T Tauri star is probably of spectral type K7 with modest $H\alpha$ and CaII emission. A more amenable approach to understanding these less bizarre stars might be to consider normal stars with suitable changes in physical parameters designed to produce minimal T Tauri characteristics.

Ambartsumyan (1958) was the first to suggest that T Tauri stars are in fact new stars only recently formed from nebular material. This view is widely accepted today, and T Tauri stars are considered to be "pre-main-sequence" (PMS) objects. The spectral peculiarities are

therefore ascribed to certain atmospheric properties associated principally with "youth." The arguments that have been advanced to support this view include: (a) the high space density of T Tauri stars in the so-called T-associations located in regions of nebulosity; (b) common radial velocities between T Tauri stars and their associated molecular clouds (Herbig, 1977a), indicating that there is little differential motion between the stars and the cloud, and implying that the stars have not had enough time to diffuse away from the cloud and must therefore be very young; (c) the location of T Tauri stars on color-magnitude diagrams (Walker, 1956) and Hertzsprung-Russell diagrams of young clusters in the region predicted for low-mass pre-main-sequence stars from theoretical evolutionary tracks (Cohen and Kuhn, 1976, 1979); and (d) the very high abundance of lithium. Skumanich (1972) showed that lithium decreased as the inverse square root of the age for main-sequence stars, and T Tauri lithium abundances seem to be consistent with interstellar abundances (Zappala, 1972) which presumably are primeval.

Fainter T Tauri stars have most frequently been discovered by slitless $H\alpha$ surveys (e.g., Joy, 1949; Haro et al., 1953; Herbig, 1954; Herbig and Kuhn, 1963). A very comprehensive catalog of 300 T Tauri stars and related objects was compiled by Herbig and Rao (1972). It provides coordinates, magnitudes, colors, variability data, spectral data, and emission-line class [a measure of the general strength of the emission-line spectrum (Herbig, 1962) ranging from class 1 with weak $H\alpha$ to class 5 with very strong $H\alpha$]. Cohen and Kuhn (1979) studied some 500 northern $H\alpha$ emission objects and provide the most comprehensive collection of basic data about T Tauri stars to date, based on their spectrum scanner and infrared observations. Their work was extended to southern-hemisphere stars by Appenzeller et al. (1983). A useful catalogue of spectral energy distributions of many T Tauri stars has been published by Rydgren et al. (1984a). These basic compendia contain references to much of

the original literature on T Tauri stars. Reviews by Bertout (1984), Cohen (1984), and Herbig (1985) also provide compact accounts of observations and the theory of T Tauri stars.

II. BROAD-BAND PHOTOMETRIC OBSERVATIONS

In her book on "Stars and Clusters," Payne-Gaposchkin (1979) vividly illustrates the manner in which studies of associations and groups underpin many of our current ideas regarding the internal structure and development of stars. In studies of the early phases of stellar development, for example, the classic, broad-band photometric studies which provided color-magnitude diagrams of young clusters such as NGC 2264 (Walker, 1956; Figure 4-2) were seen as strong support for the idea that stars approach the main sequence as cool, luminous objects contracting under the influence of gravity (e.g., Schwarzschild, 1958). In particular, the fact that the fainter stars in NGC 2264 tend to lie above the main sequence (Walker, 1956; Adams et al., 1983) is usually interpreted in

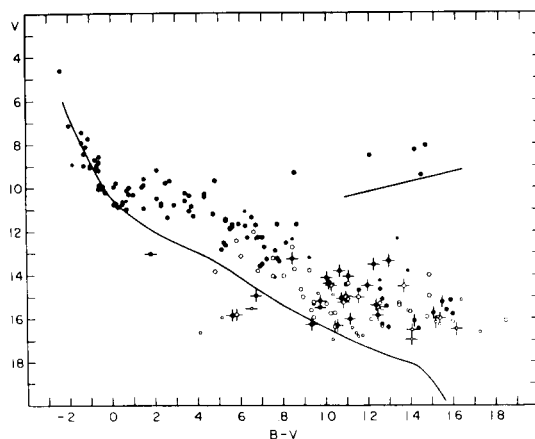


Figure 4-2. Color-magnitude diagram of the young cluster NGC 2264 (Walker, 1956). Vertical bars signify known variables, while horizontal bars denote stars with $H\alpha$ emission. The curves denote the standard main-sequence and giant branches.

terms of the relatively slow pre-main-sequence development of low-mass stars (e.g., Stahler, 1983).

There are however several factors that complicate the interpretation of color-magnitude and two-color diagrams of groups of T Tauri stars. For example, some T Tauri stars possess such extremely blue colors relative to their luminosity that they actually lie below the main sequence (cf. Figure 4-2, and Mendoza et al., 1985). Many T Tauri stars also emit strong infrared radiation which must be taken into account in any attempt to estimate the bolometric luminosity and hence total power output of the stars. Further, corrections for reddening are difficult to determine with any precision because the intrinsic colors are essentially unknown. Finally, T Tauri stars are irregular variables and, consequently, they move about in the color-magnitude (or HR) diagram. In this section, these and other aspects of broad-band photometric observations of T Tauri stars are discussed.

II.A. PHOTOMETRIC VARIABILITY

The "peculiar" nature of the T Tauri stars and related objects was first recognized through their irregular variability. There have subsequently been many attempts to provide a useful classification of these objects in terms of the forms of their light curves (e.g., Parenago, 1933; Hoffmeister, 1957; Wenzel, 1968; Glasby, 1968). However, these attempts have not been successful. For example, the prototype of one of Glasby's classifications (T Tauri itself) exhibited in September, 1932, an episode of variability characteristic of another of his classes (Hoffmeister, 1957). Thus, while the form of the light curve of T Tauri stars can be used to describe their behavior at a given epoch, it does not seem to be a basis for fundamental classification (Herbig, 1962). The failure of the light curves to categorize uniquely the T Tauri stars was one of the main reasons why Herbig (1958, 1962) introduced his above mentioned spectroscopic criteria.

The light curves of T Tauri stars exhibit variability over a very wide range of amplitudes and durations (Herbst, 1986). The most spectacular variations are certainly the outbursts of the FU Orionis stars, which involve brightening by several magnitudes over a time scale of ~200 days followed by decay over many years. The possible connection between FU Ori itself, which brightened in 1936-37 from an unclassified star, and the T Tauri stars was discussed by Herbig (1962) and subsequently confirmed by a similar brightening of the T Tauri star V1057 Cyg (Welin, 1971). Other stars have also been observed to undergo similar transformations. Although the phenomenon is "rare" in terms of the lifetime of astronomers, Herbig (1977b) postulates that virtually all T Tauri stars undergo one or more such episodes in their development. This possibility opens up profoundly important questions regarding the validity of the current picture of the structure and evolution of such stars. Further discussions of the "Fuor" syndrome may be found in Ambartsumyan (1958), Herbig (1962, 1977b), Welin (1978), Magnan (1979), Hartmann and Kenyon (1985) and Reipurth (1985).

Variability on a scale less spectacular than that of the FU Ori phenomenon, but still involving very large amplitudes and a wide range of time scales, is very common among the T Tauri stars. The light-curve samples (Glasby, 1968) exhibited in Figure 4-3 illustrate some of the kinds of variability encountered. On time scales of weeks or longer, amplitude changes of several magnitudes are observed in many stars, but attempts to arrange or classify these changes have resulted in the identification of only two weak tendencies that may be significant: (1) the time scale of variations in a given star tends to lengthen as the amplitude of the variations increases (Ishchenko, 1937), and (2) in some cases the light curve apparently undergoes relatively short (few days or weeks) episodes of abnormally irregular variability.

Several attempts have been made to identify periodicities in the light curves of T Tauri stars.

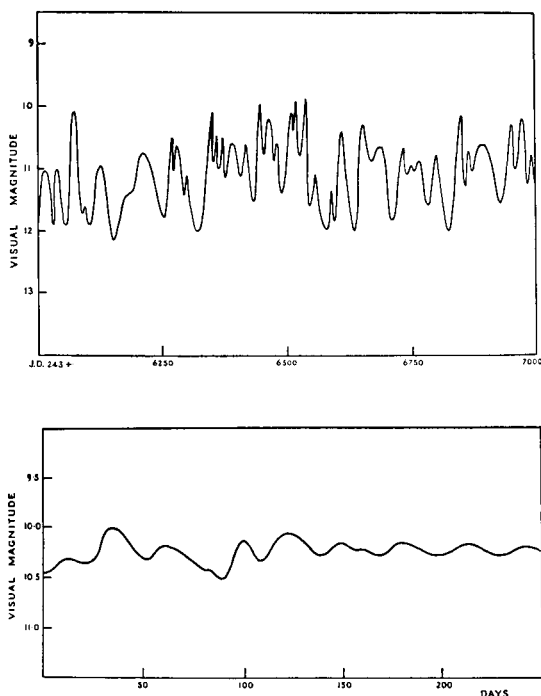


Figure 4-3. Light curves for RW Aur (a) and T Tau (b) from Glasby (1968). Attempts to provide a systematic classification of “nebular variables” on the basis of their light curves have not been very successful.

The earliest was that of Hoffmeister (1958), who claimed the detection of pseudo-periodicities in the range 4 to 6 days in RW Aur, S CrA and RU Lup. Neither Plagemann (1960) nor Klyees and Lobaser (1975), using the techniques of Fourier power spectrum analysis, found any significant evidence for regular variations, although the latter authors claimed to have established that the variations did not have the character of white noise. On the other hand, Grinin et al. (1983) detected a period of about 5.40 days in time-series observations of the $H\beta$ line emitted by RW Aur, a result which confirms Hoffmeister’s conclusion that RW Aur has a period of “about 5 days.” Schaefer (1983) reports a period of 6.1 days for a 1.6 mag variation in $H\beta$ for SY Cha. Rydgren and Vrba (1983b) have reported observations of four T Tauri-like stars that display quasi-sinusoidal light variations on time scales of 2–4 days, and

further work has confirmed that such variability is fairly common (Vrba et al., 1986; Bouvier et al., 1986a; Herbst et al., 1986). These quasi-periodic variations have been interpreted in terms of the rotation of a star with an inhomogeneous surface structure, somewhat analogous to the photometric variations of the BY Draconis stars (Phillips and Hartmann, 1978) and the K-line variations observed in some late-type dwarf field stars (Vaughan et al., 1981). Indeed, Bouvier et al. (1986b) have claimed to have detected clear evidence for starspots on DN Tau, using multi-wavelength photometry and spectroscopy to derive quantitative estimates of the spot properties. The implications of these results in relation to the rotation and the surface structure of T Tauri stars will be addressed in later chapters. No eclipsing systems have yet been discovered.

Some T Tauri stars exhibit photometric variability on time scales shorter than one day (Gahm, 1986). Figure 4-4 shows the light curves of a “flare” of T Tauri observed by Klyachkov and Schevaschenko (1976), and Figure 4-5 shows observations of rapid “flickering” in several T Tauri stars observed by Kuan (1976). Similar flickering has been observed by Zajtseva and Lyuty (1976) in DF Tau and by Worden et al. (1981) in several T Tauri stars with a power spectrum frequency dependence of $\sim f^{-2}$. The latter authors suggested an interpretation in terms of a multitude of irregular “flares” on timescales of 10^2 to 10^4 sec in the stellar atmosphere. A penetrating discussion of the implications of the existence of flares on T Tauri stars and related objects has been given by Haro (1976), who has advanced empirical evidence indicating that dwarf flare stars in the field and flash stars in Orion and other stellar associations may develop from T Tauri stars or T Tauri-like stars. In view of the growing interest in the development of phenomena akin to solar “activity” in other stars, this suggestion clearly warrants further exploration.

Multi-color broad-band (UBVRI) photometric observations have been made by

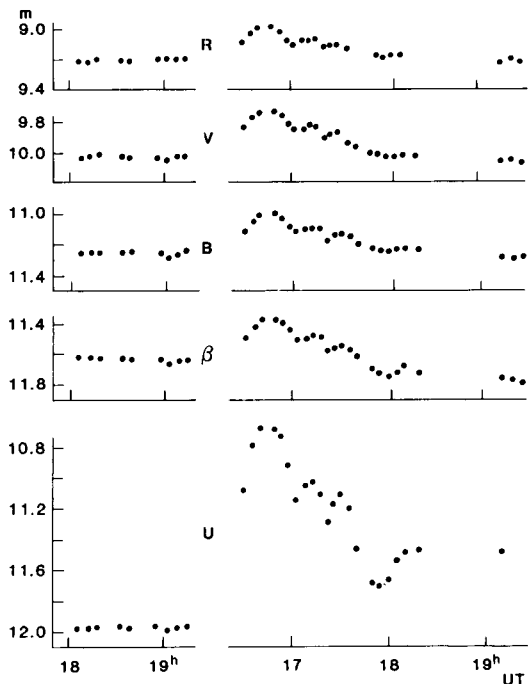


Figure 4-4. Multi-color photometric observations of a “flare” on T Tauri (Klyachkov and Shevaschenko, 1976).

numerous investigators (e.g., Mendoza, 1966, 1968; Varsavsky, 1959; Smak, 1964; Rydgren et al., 1976; Schaefer, 1983; Kolotilov, 1986). In general, for a given T Tauri star, the amplitude of variation is largest in the ultraviolet; it decreases with increasing wavelength and is smallest in the near-infrared. Furthermore, most T Tauri stars get redder as they become fainter: DF Tau and BP Tau are good examples, with the former once undergoing an increase in (B-V) of ~ 0.6 mag while decreasing in brightness at V by 1.5 mag. However, extreme T Tauri stars often show no marked color change over as much as 2 mag variation in V. In an attempt to find general correlations, Cohen and Schwarz (1976) made simultaneous optical and infrared observations over a six-day period: they found that almost all possible trends actually occurred. Nearly simultaneous visible and infrared photometry (UBVRI and KHKL) has been carried out for some 50 T Tauri stars by Rydgren and coworkers (Rydgren and Vrba, 1981, 1983a;

Rydgren et al., 1984b; Vrba et al., 1985), who find for five actively variable T Tauri stars that changes in (B-V) and (V-I) with V differ widely from star to star; (J-H), (H-K) and (K-L) colors become larger when V is fainter, and the amplitude of variations in L is much smaller than that in V. They also confirm the earlier conclusion that (B-V) and (R-I) correlate well with V, i.e., the stars become redder as they become fainter. The behavior of (U-B), however, is much more erratic and indicates the presence of some other mechanism. Herbst and coworkers (Herbst and Stine, 1984; Holtzman et al., 1986) have carried out UBVRI and $H\alpha$ photometry over many years on several T Tauri stars, and have observed a number of trends (albeit with some counter examples) including “bluer when brighter” and an increase in the $H\alpha$ equivalent width with fainter V magnitude.

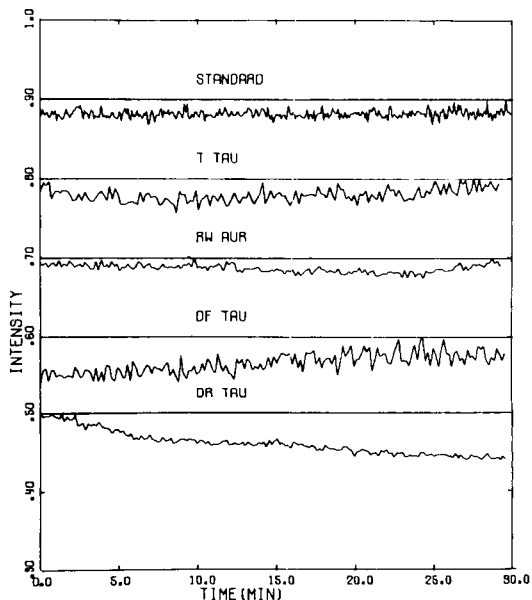


Figure 4-5. Time-series U-band observations of several T Tauri stars obtained by Kuan (1976). The stars DF Tau and T Tau seem to undergo rapid fluctuations on a time scale of a few minutes, which may be a result of the superposition of many explosive flare events on the star.

Explanations for the wide range of behavior are equally wide ranging: obscuring clouds or variable circumstellar extinction, [Gahm et al., 1974 for RU Lup; Walker, 1978, 1980 for the YY Orionis stars], flare activity (Worden et al., 1981), variation of temperature over the stellar surface as produced by hot plage regions (e.g., Herbig and Soderblom, 1980) or other magnetic effects (Schaefer, 1983; Appenzeller and Dearborn, 1984), and changes in chromospheric properties or in circumstellar envelope properties perhaps produced by changes in mass flow or excitation conditions (Rydgren et al., 1976). Finally the rotational modulation of the light curve expected from spotted stars has been detected in several stars and will be discussed further below. It is most likely that several different mechanisms are acting to produce the variability observed in any particular T Tauri star, and the study of the correlations between these may be very important in elucidating their physical character (Schmelz, 1984).

II.B. BLUE AND ULTRAVIOLET CONTINUUM

In the U-filter, T Tauri stars may be as much as 1.5 Mag brighter than normal G or K stars of the same spectral type (Haro and Herbig, 1954, Walker, 1956), a peculiarity which has become known as the ultraviolet excess. Observations made with moderate spectral resolution suggest that the UV excess occurs at wavelengths shorter than about 3750 Å (Haro and Herbig, 1954; Herbig, 1962; Kuhl, 1970) and sets in rather abruptly. It seems likely that this excess is due predominantly to continuum radiation and to the confluence of the higher Balmer lines (e.g., Anderson and Kuhl, 1968). Herbig and Goodrich (1986) have carefully merged far-UV spectra obtained with the IUE satellite with nearby simultaneous visible spectroscopy to show that the UV excess persists at a remarkably high level to wavelengths at least as short as 1500 Å. Indeed, the far-UV colors are those of A stars, even for relatively weak K-type T Tauri stars. Herbig and Goodrich show that the measured colors are consistent

with a model of enhanced chromospheric activity, and they point out the relevance of their results for the UV photochemistry of the primitive atmosphere of the Earth.

Some T Tauri stars also display a “curious filling-in” (Haro and Herbig, 1954) or “veiling” (Joy, 1949) of their absorption line spectra at wavelengths longer than 3800 Å. Joy (1949) ascribed this veiling to an overlying continuous emission, although other workers (Herbig, 1962; Cram, 1979; Calvet et al., 1984) have suggested that it could reflect principally a true weakening of the absorption lines themselves because of the presence of a very strong chromosphere. Figure 4-6 illustrates how this kind of veiling effect occurs in the star T Tau.

Figure 4-7 exhibits the visible continuum excess of the T Tauri star DG Tau, evaluated by subtracting from the observed spectrum of DG

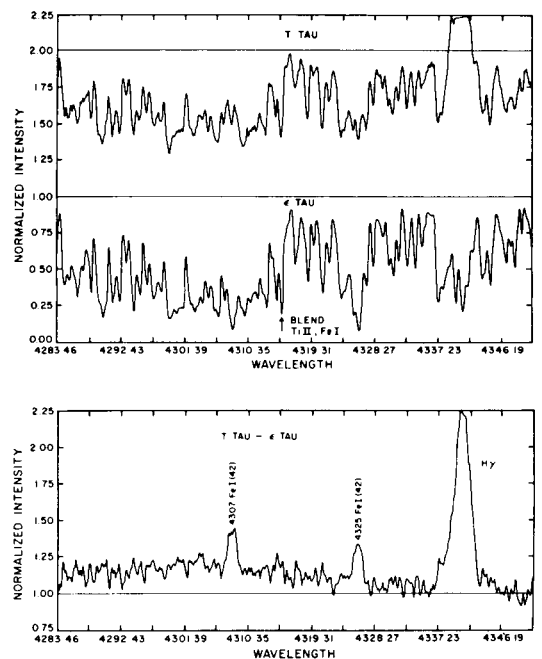


Figure 4-6. The top frame (a) compares the spectrum of T Tauri (K0-K1 IV) with that of ϵ Tau (K0 III), following the introduction of slight smoothing. The lower frame shows the difference spectrum, revealing that the lines of Fe I (multiplet 42) are filled in.

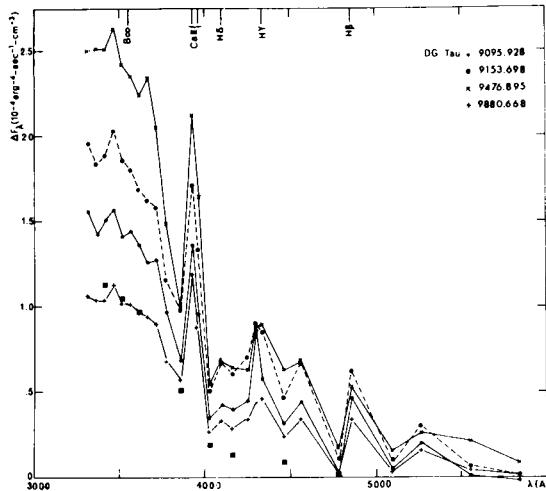


Figure 4-7. The difference ΔF between the energy distribution of DG Tau on different dates and that of a reference G5 V star. The square symbols represent the fluxes on J.D. 2439880.668 corrected for the effects of overlapping emission and absorption lines. Continuum emission appears to extend to about 4800 Å (Kuhi, 1974).

Tau the spectrum of a normal G5 V star. The figure illustrates the general rise in the excess emission towards the UV, and the strong variation of the excess emission over an interval of a few months. It also illustrates the difficulty of distinguishing between true excess continuum radiation and an unresolved blend of spectral lines whose profiles may be significantly altered by the T Tauri character of the stellar atmosphere. In Figure 4-7 the squares show the result of applying a correction for the presence of unresolved emission lines made on the basis of measurements by Gahm (1980). After the correction is made, the excess still extends beyond 4500 Å and the designation "blue" rather than "UV" would be appropriate to characterize the continuum in this star. However, in a study of another T Tauri star, RU Lupi, Gahm et al. (1974) determined that a much larger correction for line emission was required in the spectral range >3700 Å. These authors find that the apparent continuum excess in the blue spectral region for RU Lupi is

essentially completely removed after these corrections.

It appears that the UV excess and the blue veiling may not be manifestations of the same emission process. For example, in the stars Lick H α 22 (Haro and Herbig, 1954) and GG Tau, DE Tau (Rydgren et al., 1976) the veiling is rather weak, although the UV excess is very strong. In RW Aur both the veiling and the UV excess are strong (Haro and Herbig, 1954). Candidates for stars with relatively strong veiling but weak UV excess can be found as objects with relatively small (B-V) and large (U-V) in two-color diagrams or in the catalogue of Herbig and Rao (1972): possibilities include HL Tau and GW Ori. Moreover, two-color observations of the photometric variations of T Tauri stars sometimes reveal poorly correlated changes in (B-V) and U-B as already mentioned (see also Zajtcva and Lyuty, 1976). The same results are evident in the ~ 50 Å resolution scanner data obtained by Kuhi (1974). It is clearly of considerable interest to obtain well-calibrated observations with high spectral resolution of the visible and UV excess emission from a selection of T Tauri stars, in order to delineate carefully the true shape of the continuum excess, and to reveal how it changes with time. Rydgren et al. (1976) discuss the continuum excess in the blue and UV spectral regions of T Tauri stars in some detail, and conclude that there is evidence for both Balmer continuum emission and a separate blue continuum responsible for veiling at wavelengths longer than the Balmer edge. The extent to which the blue veiling reflects a true continuum emission process rather than a general weakening of the photospheric absorption lines is unclear at present.

In this context, it should be noted that so-called "white-light" solar flares produce excess radiation which has characteristics not unlike that of the blue excess of T Tauri stars. Neidig (1983) has provided a recent and comprehensive account of the observed properties of such white-light flares, and discusses possible

theoretical interpretations of them. Neidig's work (see Figure 4-8) shows how difficult it is to separate true continuum emission from changes in line emission even with high-quality solar data. Conclusions drawn from the quantitative analysis of low-resolution stellar spectra should therefore be viewed with considerable caution.

II.C. INFRARED OBSERVATIONS

The fact that T Tauri stars are bright sources at wavelengths longer than $1 \mu\text{m}$ was discovered by Mendoza (1966, 1968) and Low and Smith (1966). More recently Strom et al. (1972); Cohen (1973a,b,c.; 1974; 1975); Rydgren et al. (1976); Cohen and Schwartz (1976); Cohen and Kuhi (1979); Rydgren and Vrba (1981, 1983b); Rydgren et al. (1982); and others have under-

taken studies of T Tauri stars and related objects at IR wavelengths out to $20 \mu\text{m}$. Some T Tauri stars have also been observed out to $160 \mu\text{m}$ (Harvey et al., 1979), and Rucinski (1985) has published IRAS flux measurements for several dozen T Tauri stars. The spectral distribution in the far-IR can be attributed to radiation from dust grains, perhaps in the form of a disk. The temperatures appear to be somewhat lower ($\sim 100 \text{ K}$) than the values (600 to 1000 K) found by earlier observers attempting to fit the infrared data with blackbody radiation (e.g., Mendoza, 1966; Low and Smith, 1966). T Tauri itself has been found to be extremely bright in the far IR, and it is thought that this is related to the binary nature of the object (Dyck et al., 1982; Schwartz et al., 1986).

IR observations have also been made with relatively high spectral resolution to search for IR emission or absorption features. An early attempt was unsuccessful (Cohen, 1974) but Rydgren et al. (1976) did find that some T Tauri stars exhibit evidence of "silicate" at $10 \mu\text{m}$. In particular, T Tau and HL Tau displayed $10 \mu\text{m}$ absorption while RY Tau showed emission. The extreme T Tauri star, HL Tau, also displayed a strong absorption feature at $3 \mu\text{m}$ which has been attributed to water ice (Cohen, 1974, 1975, 1980; Strazzulla et al., 1983). More recently Cohen and Witteborn (1984) completed a spectrophotometric survey of 40 T Tauri stars at $10 \mu\text{m}$ and found that emission features attributable to silicates are relatively common, but that silicate absorption is quite rare. Figure 4-9 shows typical observations of the $10 \mu\text{m}$ emission feature which are most readily matched by silicate materials. These observations imply that most of the IR emission from these stars is produced by small solid material (i.e., dust grains), and that such thermal re-emission must play at least a part in explaining the IR observations of other, less extreme T Tauri stars. It should be noted that there is a strong tendency for those objects associated with visible nebulosity to exhibit strong IR emission at $10 \mu\text{m}$.

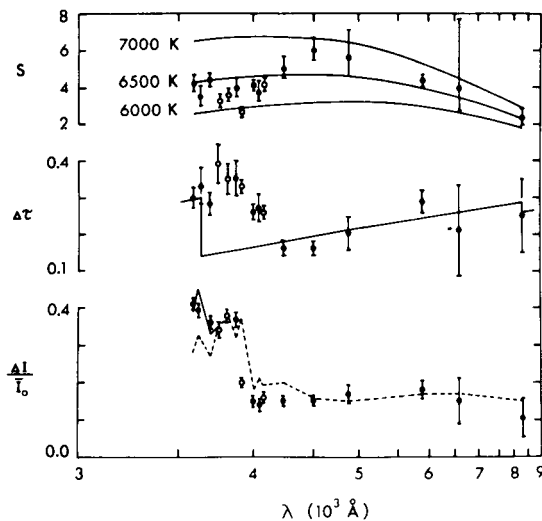


Figure 4-8. Observations and analysis of a solar white-light flare whose continuum spectrum bears some resemblance to the "UV excess" of T Tauri stars. Top: inferred flare source function compared with black-body curves. Center: inferred optical thickness compared with the absorption produced by H and H. Bottom: observed intensity enhancements compared with predictions based on free-free emission from a thin LTE layer (after Neidig, 1983).

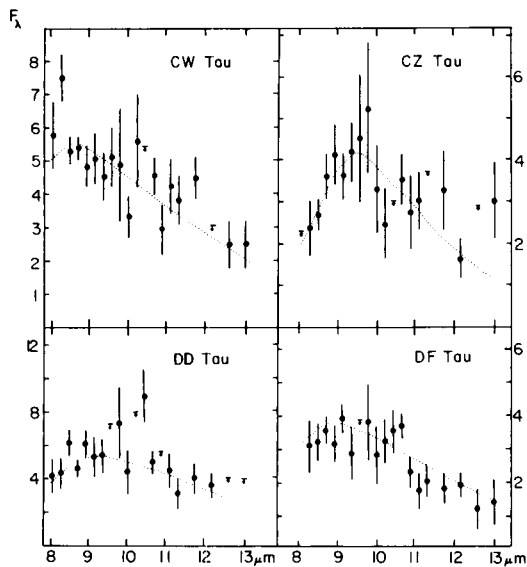


Figure 4-9. Observations of $10\ \mu\text{m}$ spectra of several T Tauri stars, showing the match (dotted lines) to thermal emission from silicate grains with a temperature of 250–550 K (Cohen and Witteborn, 1984).

A fascinating aspect of the correlation concerns the IR emission from T Tauri stars associated with the small, structured nebulosities historically known as “cometary nebulæ” (e.g., Dibai, 1971). Cohen (1974) found that IR emission from these stars is invariably very strong, while the emission from T Tauri stars associated with other kinds of amorphous nebulosity is generally weaker. Since the cometary nebulæ are almost always associated with T Tauri stars (or similar star-like condensations) which lie in positions of obvious geometrical significance, it appears that there is an intimate connection between the nature of the IR emission and the interaction between the star and its surrounding environment. An interesting interpretation of this connection has been offered by Cohen (1974) in terms of the phases involved in clearing away material shrouding young stars. The CCD imaging work of Mundt and Fried (1983) shows that the emission nebulosities surrounding several T Tauri stars (e.g., DG Tau, HL Tau) are jet-like in character rather than spherically symmetric. This argues

strongly for highly collimated flow from the central star. Optical studies of associated Herbig-Haro objects (Herbig and Jones, 1981) indicate a very high degree of collimation, with velocity vectors pointing back to a central object. The investigation of connections between extreme T Tauri stars (and their associated nebulosities) and the Herbig-Haro objects has become a fascinating field of endeavor (cf. Canto and Mendoza, 1983).

Observations have not yet established conclusively the relationships between the character of the IR emission and other spectrophotometric properties of Tauri stars. Cohen (1974) discovered a loose correlation between the stellar magnitude at $18\ \mu\text{m}$ and the maximum observed photographic magnitude measured at any epoch. This correlation does not hold between the IR magnitude at $18\ \mu\text{m}$ and the photographic magnitude at minimum light.

Cohen (1974) has also defined an index which measures the relative partition of the stellar emission between the UV (i.e., $0.36\text{--}0.55\ \mu\text{m}$) and IR (i.e., $>0.55\ \mu\text{m}$) spectral ranges. This index is very large for stars that are associated with visible nebulosity and small for those with no visible nebulosity. It is not strongly associated with the strength of the visible emission-line spectrum of the stars. This relation indicates that the IR emission from T Tauri stars is connected more with the extended nebulosity around some stars than with the processes responsible for exciting the emission line spectrum.

The nature of the variability of the IR emission of T Tauri stars has also been the subject of investigation. For example, Cohen (1974) found a tendency for the color index $V\text{--}[3.5\ \mu\text{m}]$ to decrease with increasing $3.5\ \mu\text{m}$ magnitude in T Tau, indicating that as this star becomes visually fainter, the proportion of its IR flux increases. This result is reminiscent of Herbig’s (1962) discovery that the color temperature of RW Aur apparently decreases markedly as the star becomes fainter, a result

that could be interpreted in terms of cold "spots" on the star. However, it must be emphasized that this trend is not found universally, and it appears that virtually any combination of visible and IR variability can exist. This may again indicate that at least part of the IR variability is associated with phenomena that take place at locations rather remote from the region emitting visible radiation.

The interpretation of the continuum IR emission of T Tauri stars has been controversial, perhaps because of a tendency to try to explain all of the observed characteristics with a single mechanism. The form of the excess actually varies markedly from star to star, in some cases being only a slight excess for all wavelengths beyond $1 \mu\text{m}$ (relative to a "normal" late-type star), and in other cases representing an excess of several magnitudes at longer wavelengths. Several early authors (e.g., Poveda, 1967; Huang, 1967b; Cohen, 1973a) interpreted the IR emission as thermal radiation from circumstellar "dust." A range of temperatures and/or particle sizes was called upon to explain most observations. However, Rydgren et al. (1976) proposed that free-free and free-bound emission from ionized hydrogen at 10,000 K could be responsible. They were able to account for the IR energy distribution in a number of T Tauri stars, and in fact claimed that "the primary emission features characteristic of T Tauri stars arise from bound-bound, free-bound, and free-free emission in a hot ($T = 20,000 \text{ K}$) ionized gaseous envelope surrounding the stars; this model of envelope emission can account for the ultraviolet, blue, and IR continua of these objects and can also explain the observed irregular variations at visible wavelengths."

However, in order to effect the matches between observation and theory that support these claims, Rydgren et al. (1976) had to use anomalous reddening laws with the ratio of total to selective extinction of order 6 to 8, instead of the more usual value of 3.2. While there is some evidence that the high value does

occur for early-type stars deeply embedded in dense clouds such as the ρ Oph region, there is little convincing evidence for anomalous extinction of T Tauri stars, which are usually found at the edges of dark clouds. For this and other reasons, Cohen and Kuhi (1979) rejected the hypothesis that free-free radiation from ionized hydrogen provides the explanation of the IR emission in all cases and emphasized again the importance of dust. They constructed a two-color diagram [(1.6–2.3 μm) versus (2.3–3.5 μm)] shown in Figure 4-10 to illustrate the observational data and the predicted results of the two conflicting interpretations. The diagram clearly shows that many T Tauri stars lie in areas that can only be occupied by objects radiating as black bodies. Many others lie in a region of ambiguity that could be due to free-free emission from an ionized gas or to thermal re-radiation from dust superimposed on a K-type stellar spectrum. Reddening plays little role in this diagram, and we may conclude that thermal radiation from dust (at temperatures of 1000 to 1500 K) is important in a significant fraction of stars. Free-free emission may be important for those stars lying close to the free-free line in Figure 4-10, especially for those stars that also exhibit strong Balmer lines and continuum emission at visible wavelengths.

Since then, Rydgren et al. (1982) and Rydgren and Vrba (1983b) have independently come to the same conclusion from their JHKL and UB-VRI photometry of T Tauri stars in Taurus and NGC 2264. They found evidence for a correlation between the color excess in (V–I) and the IR color index (H–K) which suggests a circumstellar contribution to the reddening. In addition, after correction for reddening, the loci of T Tauri stars in (J–H) versus (H–K) and (H–K) versus (K–L) diagrams are very narrow and are consistent with circumstellar models having dust temperatures of $\sim 1300 \text{ K}$. Thus, the typical IR excess of a T Tauri star can most readily be explained by dust. However, the same authors found that some of the weak-line emission stars showed no evidence for circumstellar dust while others clearly did. Most

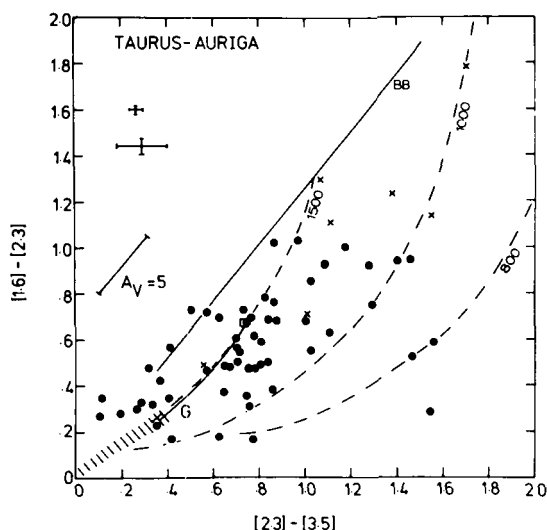


Figure 4-10. IR two-color diagram for stars in the Taurus-Auriga cloud. Filled symbols represent observations corrected for extinction, while crosses represent stars for which no correction has been made. The hatched area is the locus of main-sequence photospheres, and the solid extension (b) represents the effect of superimposing on a K7 V photosphere an increasing amount of optically thin continuum emission at 10,000 K. The black-body curve is denoted by BB, while the dashed curves represent a K7 V photosphere with superimposed emission from dust at the indicated temperatures (Cohen and Kuhi, 1979).

likely there is no unique explanation. A further point is that in many cases (e.g., HL Tau), the dust may be distributed in a circumstellar disk (cf. Cohen, 1983; Rucinski, 1985; Beall, 1986; Shu et al., 1987).

II.D. RADIO OBSERVATIONS

The first detections of radio emission from T Tauri stars were reported by Spencer and Schwartz (1974), Altenhoff et al. (1976), and Schwartz and Spencer (1977), all of whom detected T Tauri itself. These authors reported detections of several other stellar objects exhibiting evidence of youth and atmospheric activity (e.g., Lk H α 101 and MWC 349), but these are not bona fide T Tauri stars. Sensitive

radio surveys for emission from young stellar objects, including T Tauri stars, have been reported by Cohen et al. (1982), Felli et al. (1982), Bertout and Thum (1982), Beiging et al. (1984), and André et al. (1987). These surveys have found radio emission from only a very small number of bona fide T Tauri stars, although emission has been found in a larger population of apparently young stellar objects.

The radio emission observed from T Tauri and other T Tauri stars was initially ascribed to thermal emission by an ionized circumstellar region (Schwartz and Spencer, 1977; Cohen et al., 1982; Felli et al., 1982; Bertout and Thum, 1982). However, observations of relatively rapid, large-amplitude variability and “non-thermal” spectral indices imply that other radio-emission mechanisms may also be operating (Beiging et al., 1984; Feigelson and Montmerle, 1985; André et al., 1987). In this regard, the observation that radio-bright T Tauri stars tend to be preferentially associated with Herbig-Haro objects may imply some connection with the remarkable IR and radio properties of the young stellar objects associated with collimated flows (Shu et al., 1987). On the other hand, the strong radio flaring of the object DoAr 21, which exhibits only weak T Tauri characteristics, may imply a connection with nonthermal processes more akin to solar flares (Feigelson and Montmerle, 1985). Yet other factors may be pertinent for the emission from T Tauri itself, since the presence of a peculiar companion may account for much of the emission (Hanson et al., 1983; Schwartz et al., 1986).

II.E. X-RAY OBSERVATIONS

X-rays were first detected from pre-main sequence objects in the Trapezium region of Orion by Ku and Chanan (1979), who found many sources at flux levels of $\sim 10^{30}$ erg s $^{-1}$ whose positions coincided with some 25 known nebular variables. About one half of these were T Tauri stars and the other half were flare stars. Gahm (1981) observed several T Tauri stars and

detected only one of them at $L_x = 6 \times 10^{30}$ erg s^{-1} . Surprisingly, two extreme T Tauri stars, RW Aur and RU Lup, were not detected. Feigelson and DeCampi (1981) then observed a further 20 T Tauri stars and detected 8 of them with $L_x \sim 10^{30}$ to 10^{31} erg s^{-1} . The ratio of X-ray to bolometric luminosity in the detected stars was typically 10^{-3} . No convincing correlations with optical characteristics were found, although Gahm (1981) postulated that those stars of light-curve classes I and II (i.e., stars which are most often bright) were most likely to be detected as X-ray sources when the star flared. This suggestion was based on the detection by Feigelson and DeCampi (1981) of an X-ray flare from DG Tau, a strong emission-line star whose flux was observed to increase by a factor of 10 in an interval of ~ 200 s. The observations were not long enough to show an appreciable decay. Walter and Kuhi (1981) observed a further 23 T Tauri stars in Taurus and detected 8 sources with $L_x \sim 10^{30}$ to 10^{31} erg s^{-1} . DG Tau was not detected. No flaring activity was detected in any of the stars.

Walter and Kuhi (1981) also found an apparent limiting visual magnitude in Taurus-Auriga below which no stars were detected; this implies a roughly constant ratio of X-ray to visual luminosity in the brightest X-ray stars. Within this limit, only one suggestion of a correlation with optical features was found, namely, the stronger the $H\alpha$ emission flux the less likely the X-ray detection. For example, no stars with $H\alpha$ equivalent widths greater than 100 \AA were detected as X-ray sources, whereas for equivalent widths less than 50 \AA all stars were detected. Walter and Kuhi (1981) suggested that these results could be explained by a low-lying corona "smothered" by overlying cooler gas whose presence was indicated by the extremely strong $H\alpha$ emission. An alternative hypothesis is that stars with very strong $H\alpha$ simply have no coronae.

In a subsequent study, Walter and Kuhi (1984) observed a few selected regions with long

X-ray exposures to obtain spectral data as well as to test the apparent $H\alpha$ inverse correlation. They observed a large flare on the T Tauri star AS205, which had previously shown no quiescent X-ray flux. However, they did not detect AA Tau, which previously had been a strong source: for this object, the $H\alpha$ intensity had, however, increased by a factor of five over its previous value. These observations also showed that the most probable value of the temperature for the X-ray emitting region is approximately 10^7 K.

An important result of X-ray studies of young stars was the discovery of "serendipitous X-ray sources" with fluxes in the range 10^{30} – 10^{31} erg s^{-1} , in Taurus-Auriga fields containing known T Tauri stars (Walter and Kuhi, 1981; Feigelson and Kriss, 1981). When examined optically (Mundt et al., 1983), the X-ray sources were found to resemble weak-line T Tauri stars. They may be post-T Tauri stars. Long-term observations of the ρ Ophiuchi region by Montmerle et al. (1983, 1984) showed very clearly the complex behavior of T Tauri X-ray sources: they called the region an X-ray Christmas tree! These authors discovered about 50 X-ray sources, half of which are known to be pre-main-sequence objects. Most sources were highly variable with amplitudes as large as an order of magnitude in a day. The distribution of the observed normalized amplitude variations obeys a power law with index 1.4. The observations have been interpreted in terms of widespread flare activity, since most stars would be detected at these flux levels only when a strong X-ray flare is taking place (the strongest flare had a luminosity of 10^{32} erg s^{-1}). On any individual exposure only 10% to 50% of the known T Tauri stars are detected.

Walter (1986) has reported an extensive study of the X-ray stars found in regions of star formation. His sources are not characterized by an "advanced" T Tauri spectrum. Rather, they display weak $H\alpha$ emission, reminiscent of dKe, dMe stars, and in many cases the $H\alpha$ is virtually absent. Walter suggests that these X-ray stars

may fall into two classes; (1) genuine post-T Tauri stars whose high level of activity is consistent with the youthful end of the activity-age relationship observed in main-sequence stars (see Chapter 1), and (2) naked T Tauri stars, which are of the same age as the normal T Tauri stars, but which lack the circumstellar environment which produces the characteristic $H\alpha$ and forbidden-line emission and the IR excess of T Tauri stars.

II.F. POLARIZATION OBSERVATIONS

The earliest attempts to measure linear polarization of T Tauri stars were reported by Hunger and Kron (1957), Hiltner and Iriarte (1958), Vardanian (1964), and Serkowski (1969). More recently, large scale surveys have been carried out by Bastien and Landstreet (1979) and by Bastien (1981, 1982, 1985). Bastien (1982) also presents a table of all published polarization observations of young stars. Linear polarization has been detected at the 0.2% to 1% level for many T Tauri stars and at even higher values for RY Tau (2.7%), DG Tau (6.0%), DO Tau (3.1%) and HL Tau (11.2%). The wavelength dependence of linear polarization was discussed by Bastien (1981), who found that the polarization amplitude may either increase or decrease with increasing wavelength and also that this dependence may vary strongly.

The linear polarization is usually interpreted in terms of an extended circumstellar dust envelope which is slightly flattened or in which the grains are partially aligned. Since only a modest degree of flattening is needed to produce the observed polarization for single scattering, this is the most likely explanation. Any such dust also must lie outside the visible line-emitting region, since there is no change in polarization across the $H\alpha$ profile. The observed variation with wavelength can be explained by large variations in grain size in the dust scattering regions. The extreme degree of polarization observed for HL Tau has been

taken as further evidence for the presence of a circumstellar disk by Cohen (1983), who estimated that the star itself is seen through an edge-on disk and an extinction of 7 magnitudes at V.

In his survey of polarization properties of T Tauri stars, Bastien (1982) found variability of polarization in at least 35% of his sample of 50 stars. However, the variability was not correlated with changes in luminosity, nor was there any correlation between the linear polarization and emission-line intensity, color indices or rotational velocity. There was some correlation of polarization with the infrared color indices, especially (V-I), i.e., stars with large infrared excesses usually had higher linear polarization. In fact, those stars with very strong emission line spectra and no underlying photospheric spectrum (HL Tau, DG Tau and V536 Aql) had the highest polarizations. Also the stars with IR colors lying closest to the free-free emission curve had smaller polarizations than those lying above it (in flux). This supports the idea that most of the infrared excess is likely to be produced by the absorption of stellar radiation and its subsequent thermal re-emission by dust grains rather than free-free emission from a hot gas. This same dust is also responsible for the linear polarization. Bastien's (1985) study of polarization in southern T Tauri stars supports many of these points, and specifically confirms the close relationship between the IR properties and the polarization.

Schulte-Ladbeck (1983) has presented time-series observations of linear polarization in several T Tauri stars, confirming many of Bastien's results, and showing how the systematic trends with time can be interpreted in terms of variable mass-flow rates and orbiting scattering regions. Detection of circular polarization from T Tauri stars (Nadeau and Bastien, 1986) presents a challenge to scattering theories, although multiple scattering from aspheric grains in an anisotropic region might account for the observations.

An alternative explanation of the polarization observed in T Tauri spectra has been offered by Gredin and Red'Kina (1984). These authors suggest that scattering by free electrons in an optically thin circumstellar envelope with a dipole magnetic field could account for the observed polarization amplitudes and wavelength dependence, if the field strengths are a few hundred gauss. A weakness of this proposal is the postulated high degree of ionization in the circumstellar material: while this is not inconsistent with models which ascribe the IR excess to free-free radiation from an ionized gas, we have seen (Chapter 4.II.A) that recent results support strongly the idea that the IR-emitting material is too cool to be substantially ionized.

III. LINE SPECTRUM

T Tauri stars are distinguished by the presence of an emission-line spectrum superimposed on an underlying absorption-line spectrum typical of a late-type dwarf star. The defining characteristics were described earlier, but some more specific remarks are now in order. At dispersions useful for classification ($\sim 10 \text{ \AA/mm}$; see for example, Yi li Sun et al., 1985), the most striking lines are $H\alpha$ and CaII H and K, which in many stars are the only emission lines visible. For stars with a relatively sparse emission spectrum, the underlying absorption features can be classified by using the standard criteria of the MKK system. The major absorption anomaly is the strong feature of LiI 6707. As the T Tauri character becomes stronger, more Balmer lines appear in emission, as do lines of many neutral and singly ionized metals, e.g., FeI, FeII, TiII, MgI, NaI, CaI and CaII. The fluorescent lines FeI 4063 and 4132, excited by CaII H + $H\epsilon$, also become more evident. The absorption spectrum begins to appear peculiar, especially in the blue region: absorption lines seem to be filled in or overlain by continuum emission and spectroscopic classification becomes more difficult or impossible. The effect is called "veiling," a term which refers to the washed-out appearance of the photo-

spheric lines. Appenzeller et al. (1985) and Korotin and Krasnobabtsev (1986) have published spectra of T Tauri stars made with intermediate dispersions, which reveal the complexity of the detailed spectrum.

The photospheric lines ultimately disappear among the extreme T Tauri stars, leaving a rich emission-line spectrum akin to that of the solar chromosphere (Joy, 1945). HeI 5875 is seen in emission, along with many multiplets of neutral and singly ionized metals. Figure 4-1 displays these changes in comparison to the spectrum of a normal K7 star. A strong-line star such as RW Aur typically has in emission all the lines normally found in absorption in the photospheric spectrum of a late K star. In addition many stars have forbidden lines of OI, OII, and SII in emission, indicating the presence of low-density gas. These stars are often associated with visible nebulosity. Cohen and Kuhl (1979) found that, for stars showing at least hydrogen emission, 33% showed emission in FeII, 56% in HeI, 33% in [OI], and 8% in NaI D.

The emission and absorption-line spectra can vary on a variety of time scales. Figure 4-11 shows spectra with 7 \AA resolution obtained at Lick Observatory of XZ Tau, a T Tauri star of late spectral type, RW Aur, an extreme emission-line star, and several other stars. Over a period of 1 month, XZ Tau shows an increase of FeII emission line strength, but even more striking is the apparent change in absorption to the TiO molecular bands which have weakened considerably. This may be due to a change in the continuum intensity or may instead reflect an increase in temperature of the TiO absorbing region. Figure 4-11 also shows the marked changes observed in the emission-line strength of the star RW Aur over a period of two hours, with NaI D decreasing by a factor of two. Over the course of one night, the general emission-line strength has been seen to decrease quite substantially (easily a factor 2 to 3 in most lines) and NaI D has gone from emission to absorption. The spectrum of RW Aur has also been reported on occasions to be in a

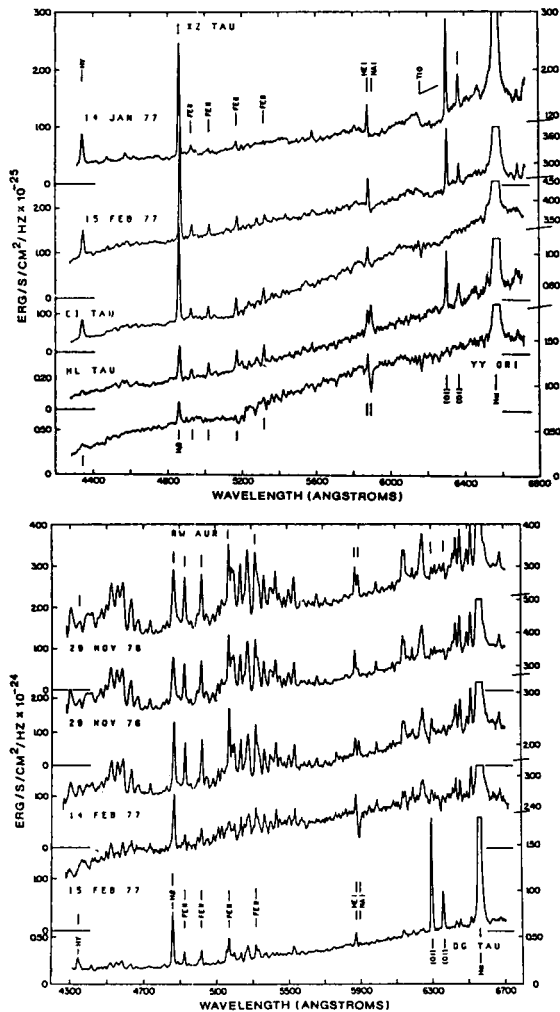


Figure 4-11. Scanner spectra (7 \AA resolution) of T Tauri stars, showing the wide variety of spectra which are observed. Note particularly the marked changes in the spectra of XZ Tau and RW Aur.

weak emission-line phase in which some features of a K-type photospheric spectrum were visible (Mundt and Giampapa, 1982; Aiad et al., 1983). Similar changes occur in most T Tauri stars that have been monitored, but on different time scales. Some stars have shown no changes of any kind; others seem to be different each time they are observed. No patterns of regularity have yet been found.

Strong emission lines (hydrogen and CaII H and K) often show an absorption component

displaced to shorter wavelengths, even at classification dispersions. This was initially interpreted in terms of mass loss from the star (Herbig, 1962; Kuhi, 1964a), striking examples are V 1331 Cyg, AS 205, and AS 353A. Another subset of T Tauri stars described by Walker (1972) showed longward displaced absorption components, especially in the higher members of the Balmer series (but not at $H\alpha$), usually had strong ultraviolet excesses, and were interpreted in terms of mass infall. These are known as the YY Orionis stars, and have been claimed to represent stars at the very end of their accretion phase (e.g., Appenzeller and Wolf, 1977). Changes in emission line strengths are very common for this group (Walker, 1972).

The advent of the IUE made the far-ultraviolet spectral regions accessible and revealed a host of emission lines covering a large range in excitation and ionization: FeII, MgII, CII to CIV, SiII to SiIV and NII to NV (Appenzeller et al., 1980) have been observed to be present. These observations lend considerable credence to chromospheric models for the production of the emission line spectrum.

III.A. THE ABSORPTION SPECTRUM

Spectral classification based on the absorption spectrum was originally attempted by Joy (1945) who assigned only rough spectral types. A complete compilation of data available at the time was published by Herbig and Rao (1972); spectral types were determined from the traditional photographic regimes using the MKK classification system. Further classifications were provided by Rydgren et al. (1976) and by Herbig (1977a). Herbig used the spectral region between 5860 \AA and 6700 \AA for classification, and he also measured radial velocities for some 50 T Tauri stars. He found no systematic differences between the absorption-line velocities of the stars in Taurus-Auriga and the velocities of the molecular clouds upon which they are projected. The velocity dispersion was less than 3 km s^{-1} . Spectral types ranged from early G to about M4 with a peak in the distribution of

types at M0. Herbig also found that most stars resemble luminosity class V.

Further spectral classification of over 400 stars was done by Cohen and Kuhi (1979), who used scanner data of 7 Å resolution in conjunction with scans of stars of known spectral types. These authors used features of CaI, FeI, CrI, MgI, as well as band strengths of TiO. They found that T Tauri stars of very late spectral type (later than M3) could be considered to be of luminosity class IV, but for other late-type stars there is little distinction between classes III and V as indicated by the TiO bands. Most other T Tauri stars are probably of class IV according to Mould and Wallis (1977), who used the CaH 6940 band for luminosity classification.

Cohen and Kuhi (1979) found the latest types to be M5 or M5.5, with most stars being of spectral type late K. Comparison of their types with those of Herbig and other workers indicate that appreciable variations must have occurred in the strengths of various indicators of spectral type in many stars. An example is DF Tau, which Herbig classified as M3, whereas Cohen and Kuhi classify it M0.5. In this range of spectral type, such differences are much too large to be attributed to differences in classification schemes.

Figure 4-11 shows the large changes in relative TiO band strengths observed in XZ Tau. The presence of "veiling" must also be noted, since it can change relative line strengths and hence influence classification. The selective character of veiling was pointed out by Vogel and Kuhi (1981), who found that the filling-in was largest for the strongest absorption lines (Figure 4-12), which are those most likely to have a chromospheric contribution. These lines appear in emission first as the T Tauri character becomes more prominent. The veiling effect in general is largest in the blue and ultraviolet and decreases greatly to the red and near infrared; it is also variable with time. This behavior rules out explanations involving large

numbers of unresolved emission lines (Gahm et al., 1974).

In view of the possible importance of magnetic fields in explaining aspects of the behavior of T Tauri stars, it is of interest to note the results of attempts to detect circular polarization and hence to measure Zeeman splitting in T Tauri stars. Brown and Landstreet (1981) set a limit of $B = 600 \pm 270\text{G}$ for T Tauri itself, while Johnstone and Penston (1986) studied several stars, finding net circular polarization consistent with a field of about 550G on RU Lupi. Observations of this kind are conducted at the limits of current instrumental capacity, and a successful application of the polarization-independent Zeeman splitting method of Robinson (1980) would be valuable.

III.B. SPECTROSCOPIC STUDIES OF ROTATION

Since the T Tauri stars are very young, one might expect that they would have considerable angular momentum and hence should rotate

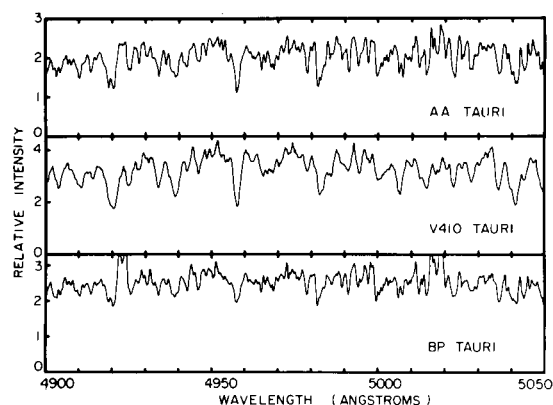


Figure 4-12. Comparison of spectra of three K7 T Tauri stars. AA Tau and BP Tau have projected rotational velocities below 25 km s^{-1} , while V 410 Tau has $v \sin i = 76 \text{ km s}^{-1}$. The spectrum of BP Tau is heavily influenced by "veiling" and at low dispersion this could be mistaken for broadening due to rapid rotation (Vogel and Kuhi, 1981).

rapidly. Differential galactic rotation alone would result in a specific angular momentum approximately 10^6 times larger than that of the Sun. The work of Kraft (1967) indicated that rotational velocity decreased with increasing age for G and K stars. Skumanich (1972) summarized the work of many investigators and showed that rotational velocity, CaII K emission and LiI strength all decay inversely as the square root of the age. Extrapolating these results back in time would suggest that T Tauri stars, being very young, should be rapid rotators. Indeed the measurements of 4 stars by Herbig (1957) gave values of $v \sin i$ in the range 25 to 75 km s^{-1} , and hence suggested that this was the case. The CaII K line is certainly very strong in T Tauri stars, but it is not yet clear whether it follows the Skumanich relation.

To study these questions further, Vogel and Kuhi (1981) attempted to measure $v \sin i$ for a large number of pre-main-sequence stars in Taurus-Auriga and NGC 2264. They used a Fourier transform technique which essentially compares the power spectrum of several 100 Å bands of the visible spectrum close to the MgI b band of program stars with that of a standard star of known $v \sin i$ and similar spectral type. Lines known to appear in emission in T Tauri stars (e.g., H β , MgI, FeII) were removed from the analysis. In addition Vogel and Kuhi noted that some stars of the same spectral type display absorption features that look broadened but which are most likely influenced by a chromospheric contribution (Figure 4-12). The effect is most pronounced for stronger lines which are likely to be affected by a chromospheric contribution in their cores. Rotational broadening, on the other hand, affects all lines equally. This difference is illustrated in Figure 4-13, which shows the power spectra of the three stars of Figure 4-12: it is clear that only one of them, V410 Tau, is rotating rapidly. Vogel and Kuhi (1981) claimed that this observation provides evidence for a chromospheric contribution, implying that the so-called “veiling” (Chapter 4.I.B) is not really the result of a smooth overlying continuum (although some

such contribution may still be present), but rather is due to a selective filling-in of the cores of absorption lines of large optical depth.

The rotation results obtained by Vogel and Kuhi (1981) were unexpected. Although they confirmed Herbig’s measurements, they found only upper limits for all other low-mass stars. Figure 4-14 shows the HR diagram and measured velocities for NGC 2264, and demonstrates that most low-mass star ($M < 1.5 M_{\odot}$) have $v \sin i \leq 25 \text{ km s}^{-1}$, as do most H α emission stars. Only stars with $M > 1.5 M_{\odot}$ have large values of $v \sin i$. In addition, most stars on the convective track show no measurable rotation velocity. This result led Vogel and Kuhi to conclude that the angular-momentum “problem” (within factors of 2 to 5) has been basically solved *before* the stars become visible and show a photospheric absorption spectrum. In addition, the dichotomy between low- and high-mass stars is already present when the stars first become visible.

Vogel and Kuhi’s (1981) results have been confirmed by more recent measurements of $v \sin i$ by Giampapa et al. (1981) of some 30 T Tauri stars. The authors found that about 30% of the stars had $v \sin i \leq 10 \text{ km s}^{-1}$ and most of the rest had $10 \leq v \sin i \leq 25 \text{ km s}^{-1}$. They also detected sharp photospheric absorption features indicating $v \sin i \leq 20 \text{ km s}^{-1}$ in several extreme T Tauri stars (e.g., S CrA, UZ Tau E, DI Tau, CI Tau, and RW Aur). These results imply that the conclusions of Vogel and Kuhi extend to the strong emission-line stars. Similar results with data having somewhat higher sensitivity have been found by Hartmann et al. (1987) and Bouvier et al. (1986a), and these two studies draw comparable conclusions about the distribution of rotation velocities. Recent studies of rotation rates of low-mass stars which are older than T Tauri stars have revealed a complex picture of mass-dependent spin-up and spin-down near the main sequence: the interested reader may consult Hartmann and Noyes (1987) for an overview of these results.

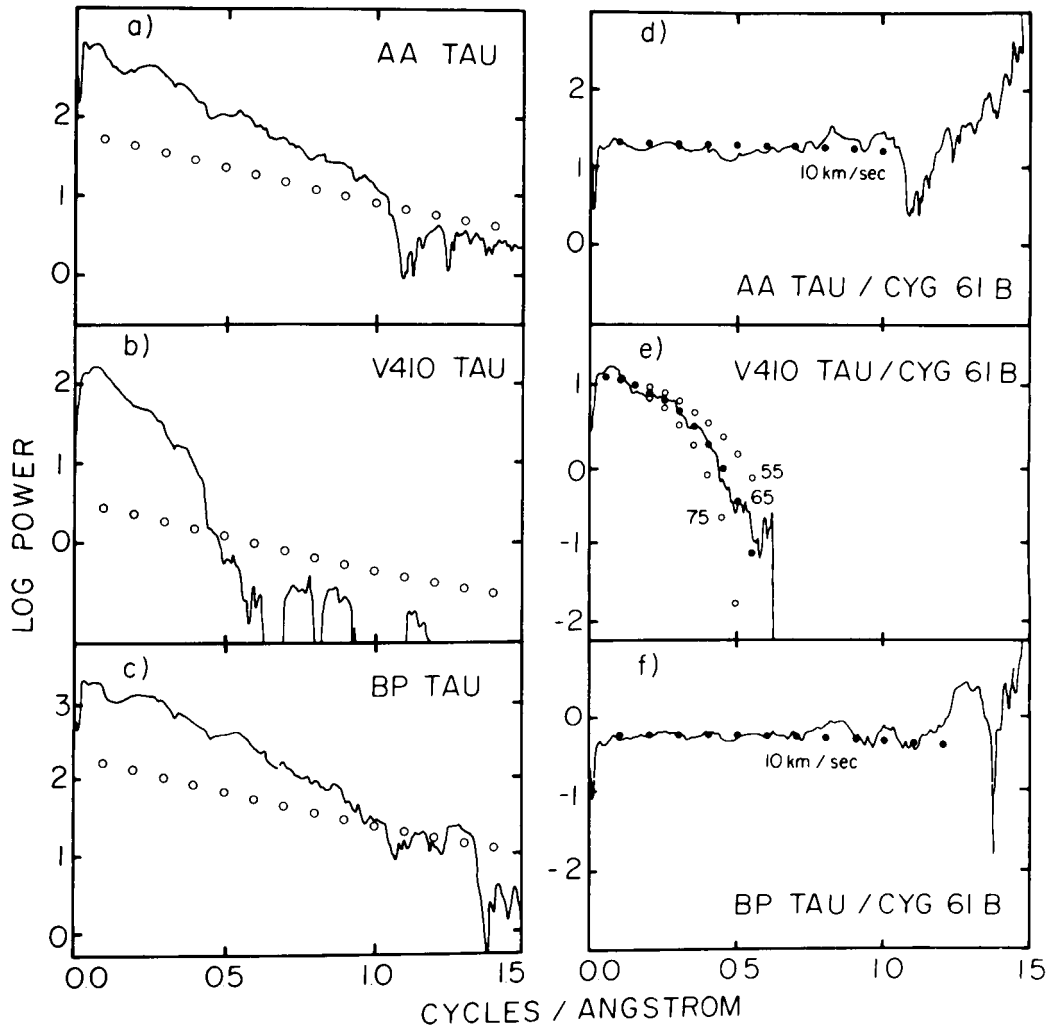


Figure 4-13. Power spectral density of the absorption spectrum of the three stars shown in Figure 4-12. Only V 410 Tau exhibits the high-frequency cut-off characteristic of rapid rotation.

Rotational modulation of light curves has already been discussed in connection with the variability of T Tauri stars (Chapter 4.II.A). Rydgren and Vrba (1983b) discovered such modulation in four pre-main-sequence stars (including V 410 Tau) with amplitudes of 0.06 to 0.23 mag in V and periods of 1.9 to 4.1 days. By calculating a radius from the effective temperature and luminosity they obtain rotational velocities in the range 19 to 75 km s⁻¹. All four stars are weak-lined stars showing on-

ly weak H α emission. Schaefer (1983) observed a similar variation for SY Cha which showed an amplitude of 1.6 mag in B and a period of 6.129 days. Rydgren et al. (1984b) found rotational periods of 2.8 to 7.0 days for more weak-emission pre-main-sequence stars but were unsuccessful in detecting any periodic variation in DF or DK Tau. The modulation technique would probably be more sensitive if the CaII K line were monitored, and such observations would be extremely valuable.

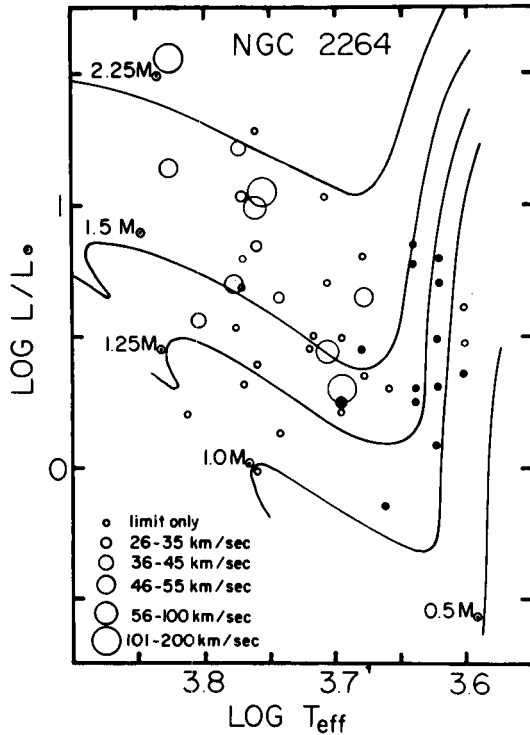


Figure 4-14. HR diagram of NGC 2264, with symbols indicating stellar rotation velocities. Most low-mass stars and most $H\alpha$ emission stars have slow rotation rates.

III.C. OPTICAL EMISSION LINES

The emission-line profiles observed in T Tauri stars have provided no end of speculation concerning possible explanations for their origin. We will first describe the general characteristics of the emission lines and then return to the models later in this chapter.

The behavior of the Balmer series of hydrogen encompasses all types of line profiles observed in T Tauri spectra. For example, $H\alpha$ profiles are often of Beals (1950) P Cygni Type III, i.e., two emission peaks with the shortward displaced peak (“blue”) being weaker than the longward peak (“red”), the peaks being separated by a shortward displaced “absorption” feature at velocities from 30 to 250 km s^{-1} (e.g., Ry Tau, S CrA, and RW Aur). However, they may often exhibit a single, quite

symmetrical peak with little if any central displacement, frequently Gaussian in shape (e.g., BP Tau). In the case of BM And (P Cygni Type III profile) the absorption feature clearly goes below the continuum, confirming that it really is produced by absorption and not simply by the absence of emission as had been suggested by Ulrich (1976) for other double-peaked profiles. There are a few stars that show very strong P Cygni Type I profiles at $H\alpha$, i.e., strong shortward displaced absorption going almost to zero intensity at velocities of 100 to 300 km s^{-1} , (e.g., AS 205, V 1331 Cyg, and AS 353A). Such profiles give very strong evidence for mass outflow. It should be noted that there exists a population of $H\alpha$ emission-line stars with emission equivalent widths lying below the value of 5 \AA conventionally used as a lower limit for the T Tauri designation (cf. Bastian et al., 1983). Feigelson and Kriss (1981) have detected several “pre-main-sequence” stars with $0.4 \text{\AA} \leq EW(H\alpha) \leq 4.2 \text{\AA}$ at 15 \AA resolution, while Walter (1986) has published spectra of several “post” or “naked” T Tauri stars showing weak, rather symmetric $H\alpha$ emission. Herbig et al. (1986) have detected what appear to be a similar class of stars in the Taurus-Auriga dark clouds, using CaII objective prism exposures for the primary search. This work confirmed that the positions of the weak $H\alpha$ objects in the Hertzsprung-Russell diagram are similar to the more extreme T Tauri stars. This result implies that the weak $H\alpha$ stars may be coeval with the strong $H\alpha$ stars, suggesting that differences in stellar environment rather than age may lead to the observed spectroscopic differences (cf. Walter, 1986).

Well-resolved profiles of emission lines have been published by numerous authors; e.g., Kuhi (1964a); Ulrich and Knapp (1979), (1982); Mundt and Giampapa (1982); Aiad et al. (1984); Mundt (1984); Boesgaard (1984); Grinin et al. (1985); Sá et al. (1986); and Edwards et al. (1987). Figure 4-15 shows several examples of $H\alpha$ profiles, and illustrates the wide variety of observed contours. Hydrogen line profiles

in some stars can be variable on time scales ranging upwards from hours. For example, variability of Balmer line profiles in S CrA is shown in Figure 4-16 (from Bertout et al., 1982) over a 4 day sequence; the relative intensities of the blue and red peaks change by as much as a factor of two on time scales of a day. The red peak occasionally disappears completely, as if it were destroyed by overlying strong absorption. The CaII H and K emission lines show a redward displaced absorption component at most times, but the most striking feature is a strong, sharp, shortward-shifted component at -105 km s^{-1} in both H and K which maintains a constant velocity over the 11 days. The velocity of this feature is too high for it to be interstellar. One is thus forced to contemplate the presence of high velocity outflow (presumably at a great distance from the star) from an object which also shows evidence of infalling material in the hydrogen lines at various times. Even more drastic behavior has been shown by DR Tau (Krautter and Bastien, 1980), in which Balmer line profiles changed from P Cygni to inverse P Cygni in a day or so. In addition H_γ showed a normal P Cygni profile, whereas the upper Balmer lines showed inverse P Cygni profiles on the same spectrogram! This kind of behavior seems to imply that some components of the hydrogen lines are produced locally (e.g., by large-scale prominence activity or other chaotic behavior), while there also exists a stellar wind which takes over at large distances. The behavior of solar coronal loops and holes may provide insight into the behavior of S CrA.

The NaI D lines are very sensitive to local conditions, being so easily ionized, and they should thus be very useful in setting constraints on atmospheric models. They are also resonance lines. However, they show a bewildering complexity of behavior. Surveys of the D lines have been carried out by Ulrich and Knapp (1979) and Mundt (1982, 1984). The former authors found that most stars with blue-shifted absorption (below the continuum) at H_α also showed such absorption in the NaI D lines.

However, other stars having a doubly peaked profile at H_α often show red-shifted absorption components in NaD. In two cases, both blue and red components were observed, and AS 205 had both red and blue absorption features present on the same night. Ulrich and Knapp (1979) concluded that mass infall and

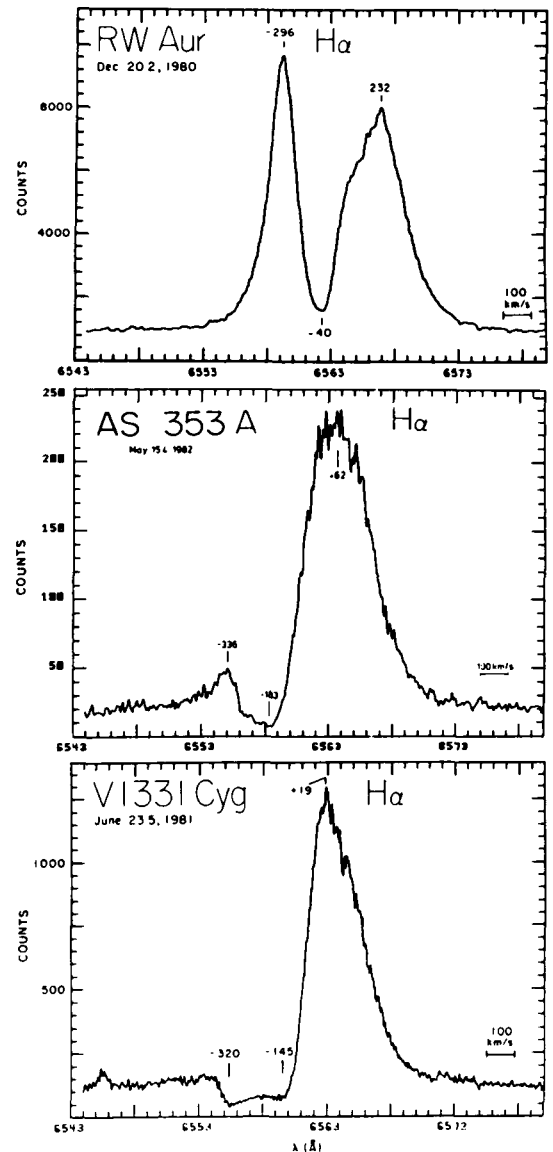


Figure 4-15. A selection of H_α profiles from various T Tauri stars (after Mundt and Giampapa, 1982). Displacements of various features in the profiles from line center are given in km s^{-1} (Mundt and Giampapa, 1982).

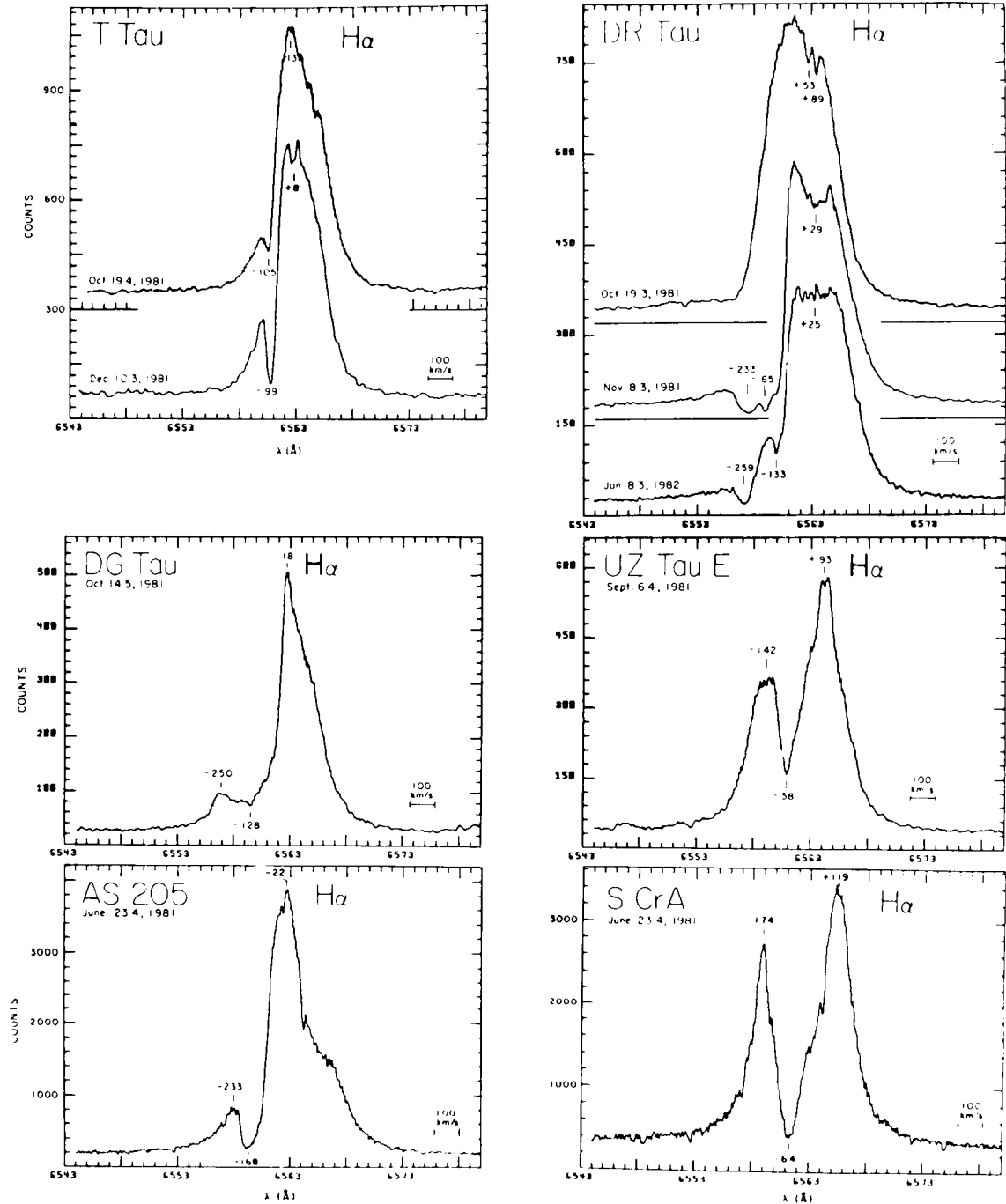


Figure 4-15. (Continued).

outflow were both present, and they suggested that the outflow was due to flaring activity in a primarily accreting flow. They further suggested that the large brightness increases observed for FU Ori, V1057 Cyg and other T

Tauri stars (e.g., Herbig, 1977b) were probably due to a reversal in the direction of mass flow from accretion to outflow. V1057 Cyg, for example, appears to be ejecting matter since its flare-up.

Mundt (1984) published line profiles of NaI D as well as H α and CaII K with high spectral resolution and high signal-to-noise ratio. Figure 4-17, taken from this paper, shows representative examples of NaI D profiles which can be described as follows:

- a. a very broad, blue-shifted absorption component with a strong emission peak (the classical P Cygni profile) e.g., DG Tau, and AS 353A.
- b. strong blue-shifted absorption components with a strong emission peak, e.g., AS 205, S CrA, and DR Tau.
- c. multiple blue-shifted absorption components with an emission peak, e.g., T Tau and UZ Tau E.
- d. multiple blue-shifted components with little if any emission, e.g., V1057 Cyg and V1331 Cyg.
- e. a blue-shifted emission peak with redward absorption components (which are still negative in velocity with respect to the stellar velocity) e.g., RW Aur.
- f. normal absorption profile (probably photospheric) with no shifted absorption components.

The multiple components seen in T Tau are currently at -71 and -99 km s $^{-1}$. Over the past 40 years these components have shown a decrease in velocity with time amounting to ~ 2 km s $^{-1}$ yr $^{-1}$, indicating a decelerating flow. The components are relatively sharp and they must, therefore, be formed at some distance from the star. S CrA also shows this deceleration in a narrow blue-shifted component; the CaII H and K components first observed at -120 km s $^{-1}$ are now observed at -102 km s $^{-1}$.

Other stars observed by Mundt (1984), i.e., DR Tau, AS 205, and LKH α 321, show no such

deceleration: the narrow blue-shifted component remains at a constant velocity over many years. Typical velocities are in the range, -70 to -145 km s $^{-1}$. The most spectacular case of multiple blue-shifted components is V1057 Cyg, which changed from an extreme T Tauri star in some 200 days first to a B-type spectrum (Welin, 1971) and then gradually to an F-type after an increase of ~ 5 mag in brightness. The NaI D lines show at least four components with velocities from -90 to -180 km s $^{-1}$. The largest velocity component seems to be broader than the lowest, indicating a decelerating flow but also showing that ejection occurs in the form of shells, with the -180 km s $^{-1}$ component being the most recent. While it is not entirely clear what happened in this object, it is now considered to be another example of the FU Orionis phenomenon (Herbig, 1977b). Mundt (1984) also reports that stars with blue-shifted NaI D absorption components have on the average a stronger ultraviolet excess and ~ 3 times stronger emission lines than those stars without such components.

The NaI D lines can be very variable in emission intensity (e.g., DR Tau), in strength of the blue-shifted component (e.g., T Tau) and in the appearance and disappearance of a redward-displaced absorption component (e.g., BP Tau). For DR Tau (Mundt, 1984) the emission strength changes by more than 50%, but the blue-shifted absorption component remains constant in strength and velocity. Mundt concludes that the NaI D lines are formed very close to the stellar surface (given the ratio of VB to VR), and hence that there must be a strong wind acceleration in that region. The sharp absorption components must be formed at much larger distances and suggest some deceleration of the wind further from the surface. Mundt further interprets the occasional appearance of inverse P Cygni profiles in the higher Balmer lines of the YY Orionis stars in terms of an inefficient mechanism for the initial acceleration of the wind close to the star. As a result, some material does not reach sufficiently high velocities to escape and simply

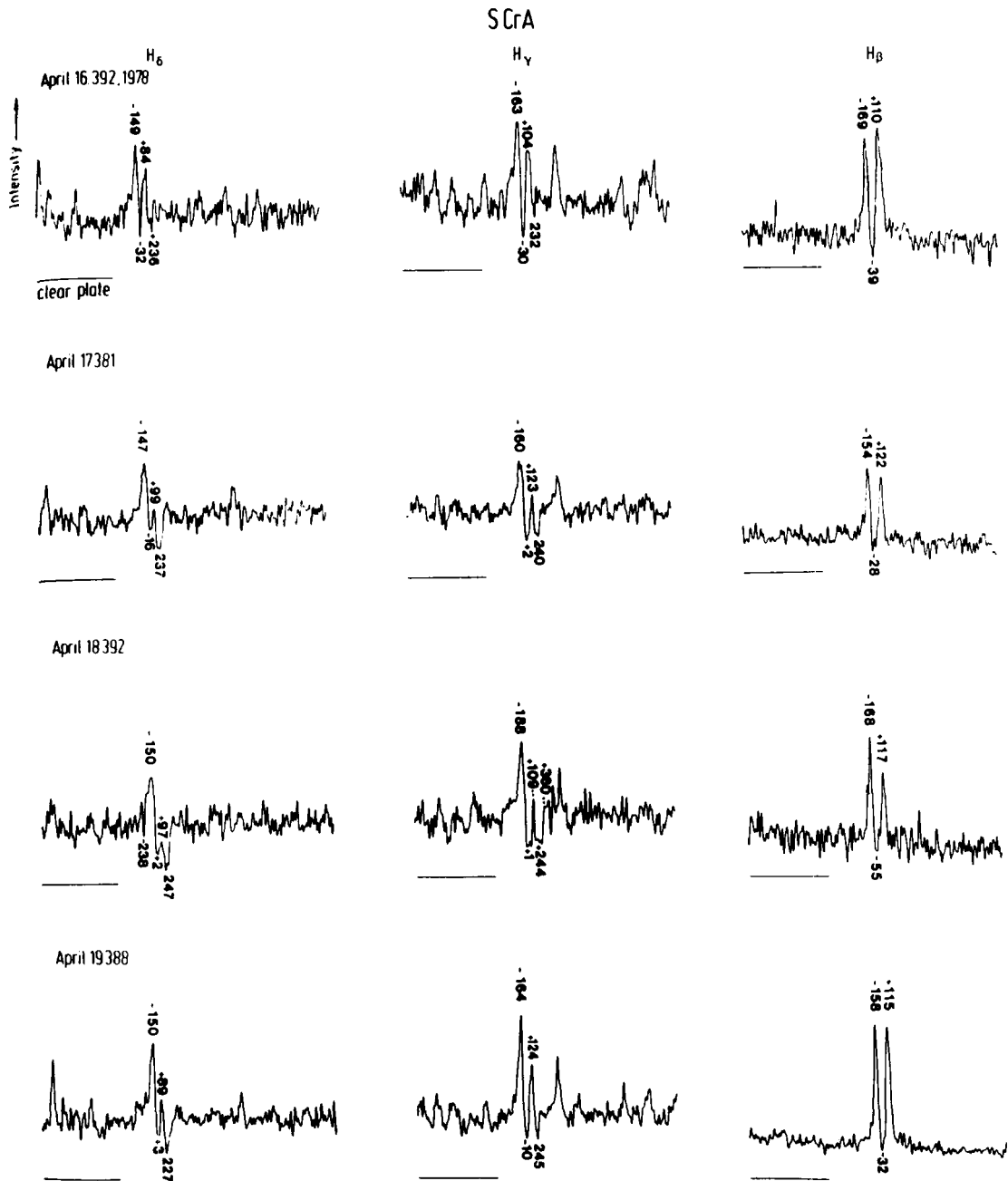


Figure 4-16. Time series of spectra of the bright T Tauri star S CrA (from Bertout et al., 1982).

falls back to the stellar surface. This would account for the complexity of behavior observed in these stars, and also explain why a prime example of YY Orionis type behavior, S CrA, shows such strong signs of outflow in the NaI D and CaII H and K lines. The requirement of very unusual conditions to explain the blue

asymmetries of the NaI D lines in terms of infall led Mundt to reject infall models entirely.

A striking confirmation of the presence of a wind outside the region of formation of the CaII line is found in the interaction between photons of CaII H and hydrogen atoms at H ϵ

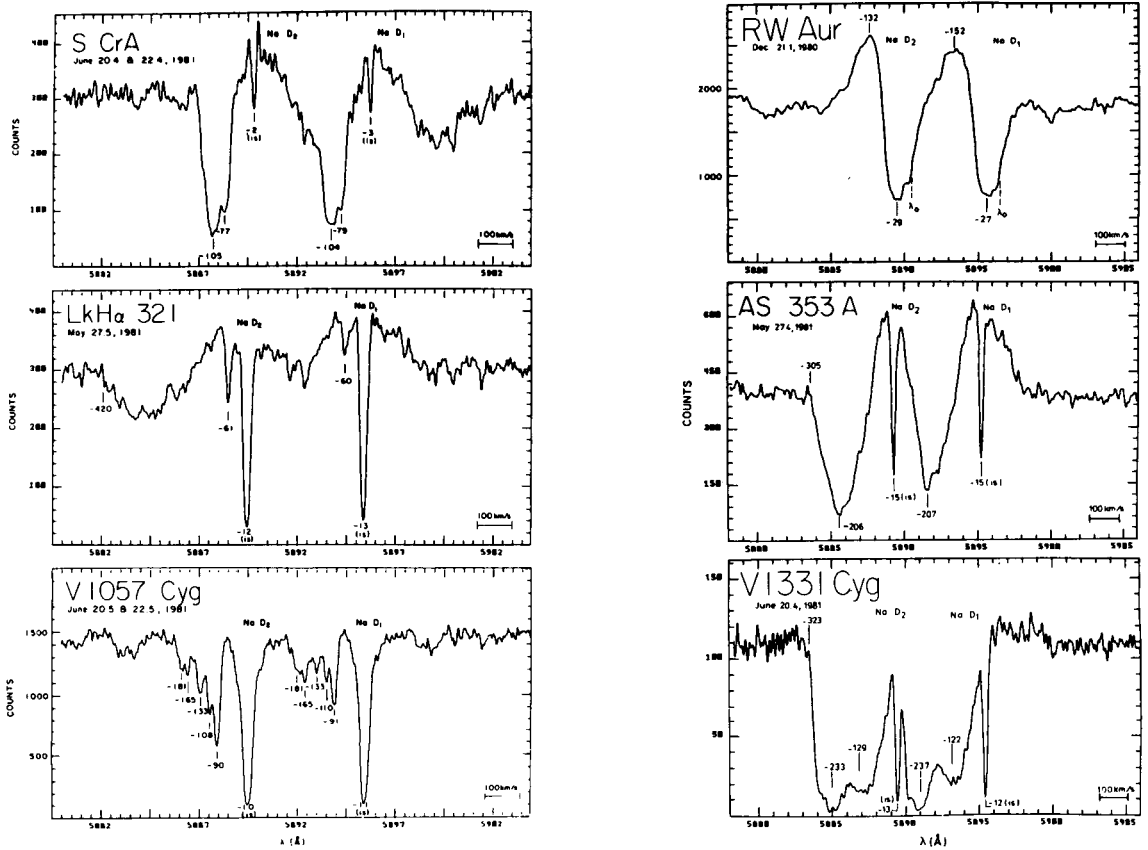


Figure 4-17. A sample of high-resolution spectra of the Na D lines of T Tauri stars, showing the tremendous diversity of emission and absorption components which are observed (Mundt, 1984).

in stars like V1331 Cyg. The Balmer lines (including H ϵ) have very strong blue-shifted absorption (the classical P Cygni profile) and the CaII K line is very strong in emission. However, CaII H is barely present, having been absorbed almost completely by the outwardly flowing hydrogen atoms which produce the blue-shifted absorption component of H ϵ .

HeI profiles at 5876 Å and 10830 Å have been observed by Ulrich and Wood (1981) for eight T Tauri stars. They found a blue-shifted absorption feature at 10830 Å only for T Tau, and they concluded that this feature must come from a stellar wind. Other stars showed more or less symmetrical profiles in both He lines.

Ulrich and Wood interpreted these results as arising from chromospheric emission, except for DF Tau in which the emission was most likely nebular in origin. Calvet (1984) confirmed that collisional ionization, rather than X-ray photoexcitation, is likely to excite the HeI spectrum in most T Tauri stars.

The other permitted emission lines seen in T Tauri spectra (e.g., FeII) as in Herbig, 1977b; Boesgaard, 1984) are most often symmetric in profile (but not always of equal width) with no absorption components. In the most extreme T Tauri stars, the strongest FeII lines will occasionally show absorption components. There has been little work done on the quantitative analysis of these spectral features.

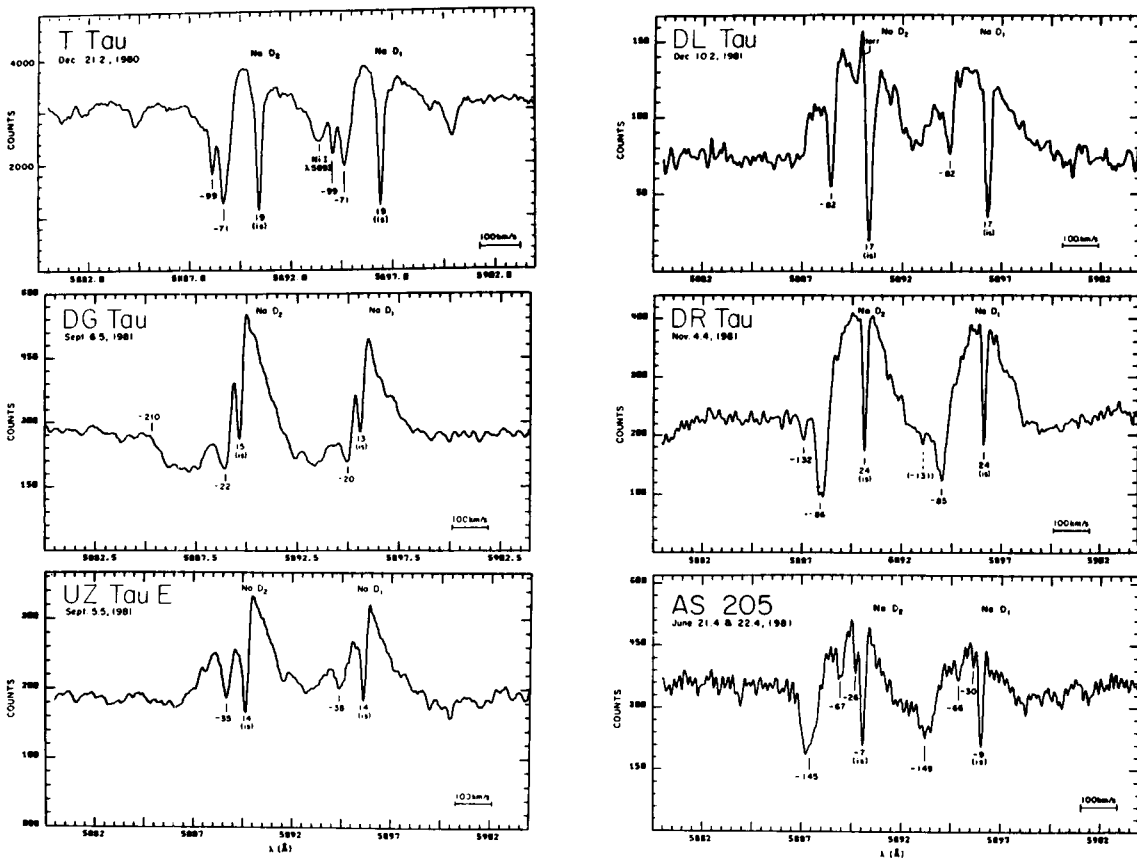


Figure 4-17. (Continued).

The forbidden lines, when present, are almost always sharp, indicating a small velocity dispersion and low density. These lines are likely to be formed at very great distances from the star. The forbidden lines of [OI], [SII] and [NII] have been studied by Appenzeller et al. (1984), who found that they often showed radial velocities from -40 to -160 km s^{-1} , i.e., blue-shifted with respect to the star. Appenzeller et al. (1984) obtained line profiles for the forbidden lines in 12 T Tauri stars. Most show symmetrical profiles but some show two blue-shifted peaks (V536 Aql) with the same profiles for all forbidden lines, while others (e.g., DG Tau) show similar structure but with different relative strengths of the two peaks in [OI] and [SII]. Appenzeller et al. suggested that the apparent blue shifts were caused by the extinction of part of an axially symmetric, focused flow by a circumstellar disk. Edwards et al. (1987) obtained further high quality spec-

tra of forbidden lines, confirming the results of Appenzeller et al. (1984), and essentially supporting the main thrust of their postulated formation mechanisms. Edwards et al. inferred a density of $\sim 10^4 \text{ cm}^{-3}$ and a radius of $\sim 20\text{--}100 \text{ AU}$ for the emitting volume, with a mass-loss rate of $\sim 10^{-8} M_{\odot} \text{ yr}^{-1}$.

Another interesting feature in the visible region is the presence of several emission lines which are excited by a fluorescence mechanism. The best example is the FeI pair of lines at 4063 \AA and 4132 \AA , which is excited by the blend of CaII H and H-epsilon (Willson, 1974, 1975). The behavior of these lines can be used to provide insight into the radial distribution of velocity fields in the atmosphere.

Following the discovery that some T Tauri (or T Tauri-like) stars are powerful X-ray sources, several workers sought evidence for

forbidden coronal lines in their visible spectra. Gahm et al. (1979) and Gahm and Krautter (1982) established significant upper limits, while the low upper limit obtained by Lago et al. (1985) for the known X-ray T Tauri star GW Ori has shown that the coronal conditions in this star are likely to be significantly different from those in the Sun. Lamzin (1985) has investigated the formation of visible coronal lines taking account of EUV and X-ray data, and has concluded that their detection will prove to be very difficult.

III.D. IUE OBSERVATIONS

The *International Ultraviolet Explorer* satellite has provided many observations of T Tauri stars in the previously inaccessible far-ultraviolet spectral region. Low dispersion spectra cover the range 1150 Å to 3200 Å in two steps with some overlap around 1900–1950 Å at a resolution of 6 Å. A high resolution mode (0.2 Å) can also be used to obtain emission-line profiles. Early efforts were primarily spectral surveys of the brighter T Tauri stars in the low-resolution mode in which line identifications were made, e.g., Gahm et al. (1979), Appenzeller and Wolf (1979), Gondhalekar et al. (1979), Appenzeller et al. (1980), Imhoff and Giampapa (1980a,b), and Mundt et al. (1981). The emission lines observed cover a range of ionization potential: CI to CIV, SiII to SiIV, NII to NV, FeII, MgII, HeII, and other metallic ions with a temperature range from below 10^4 K to above 10^5 K.

The appearance of the visible spectrum of T Tauri stars is no guide as to what one sees in the far-ultraviolet. Figure 4-18 shows the IUE spectrum of the star L H α 332-21, which represents one extreme in the richness of emission lines seen in the ultraviolet. More typical spectra show strong MgII lines, a moderate CIV line and a few other weaker lines. The correlation between the visible and EUV spectra of T Tauri stars is not very tight. For example, the visible spectrum of T Tauri is a complete con-

trast to its rich ultraviolet spectrum: only CaII H, K, and the hydrogen lines are strong in emission. On the other hand, RW Aur is extremely rich in the visible, but it shows only a few emission lines in the ultraviolet. The MgII h, k emission lines are striking in their overall strength in all T Tauri stars, and typically have a surface flux exceeding that of the Sun by a factor of 50 or more. The far-ultraviolet lines typically have a total flux about 3000 times that of the same lines in the Sun and contribute 0.1% to 0.2% of the total luminosity. In addition, many T Tauri stars show a strong ultraviolet continuum in the 1500 Å to 3100 Å range (i.e., up to the wavelength cutoff of the detector), which appears to be a continuation of the excess ultraviolet observed at longer wavelengths (Herbig and Goodrich, 1986).

The range of temperatures represented by the detected ions implies that the ultraviolet emission lines can be used to study the physical characteristics of many parts of the T Tauri atmosphere, in particular the chromosphere and the transition region. The gross similarity of the far ultraviolet spectra to those of normal G, K and M main-sequence stars provides strong qualitative support for the idea that similar activity (albeit at a much enhanced level) is responsible for the spectra of both groups of stars. However, a few significant differences have emerged. For example, the most extreme T Tauri stars do not show the strong high-temperature lines seen in normal G and K stars and the more typical T Tauri stars. In the extreme stars, NV and HeII emission lines are not present and CIV is weakened with respect to SiIV (CIV is always stronger than SiIV in normal late-type stars). This suggests that high temperature gas might not be present in the extreme stars. For such stars, there is no evidence of a transition region to a hot corona and, indeed, no corona may be present. Recall that these same stars (e.g., RW Aur) have not been detected in X-rays. For the less extreme stars, it is found that all emission lines become stronger as the ultraviolet spectrum gets more intense, although the higher temperature lines

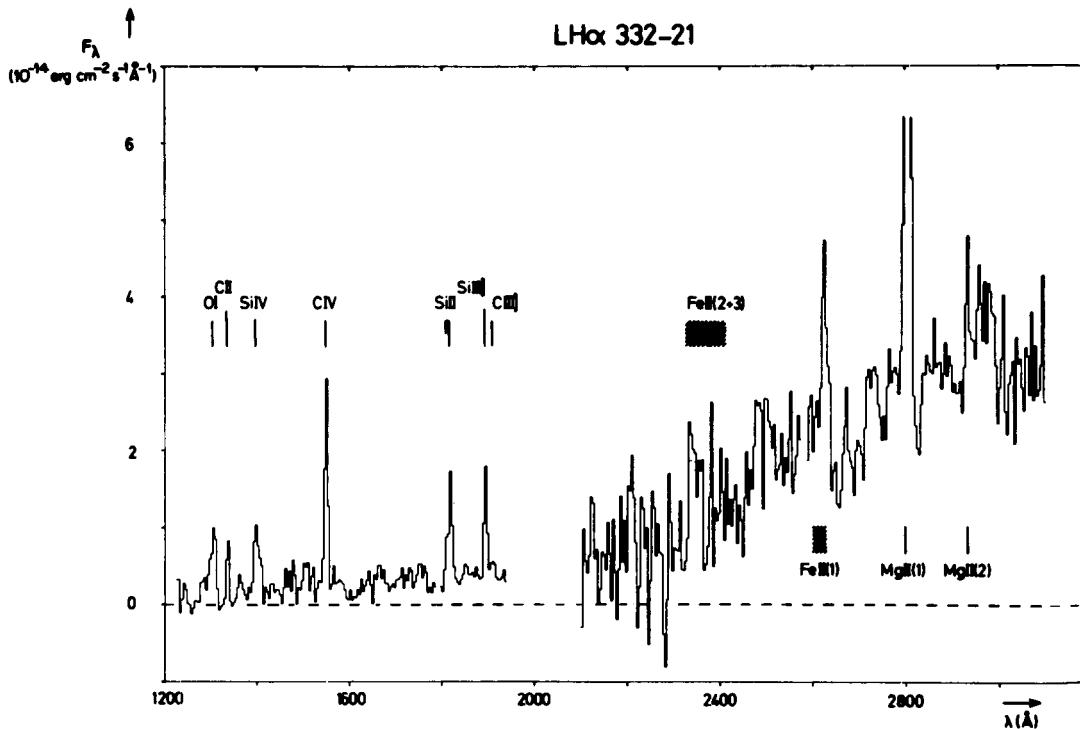


Figure 4-18. IUE spectrum of the T Tauri star L H α 332-21, showing a fairly complex EUV spectrum (from Penston and Lago, 1983).

increase in strength more rapidly. This behavior is similar to that of normal cool stars.

The variability of the ultraviolet spectrum has been investigated for only a few stars. Imhoff (private communication) has followed RW Aur for several years, finding that the emission spectrum is strongest when the star is brightest. She found that the emission lines of CII and SiII increase by a factor of 2.5 and CIV and SiIV by as much as a factor of 5. At the same time, the ultraviolet continuum increased by an order of magnitude at 3000 Å. Such increases in activity seem to last for a few days, but the available observations are inadequate for proper variability studies. It is tempting to interpret these changes as flaring activity similar to that seen on other stars, although the time scales for normal stellar flares are shorter.

Giampapa et al. (1981) determined surface fluxes for the MgII h, k, and CaII H, K lines for several T Tauri stars and used a chromo-

spheric model to interpret their measurements. They found CaII fluxes to be 10 to 75 times stronger than typical solar values, and MgII fluxes from 10 to 130 times stronger. The MgII to CaII flux ratios in the resonance lines ranged from 0.5 to 9.4 with a mean of 3.7; however, when the CaII infrared triplet lines are included they conclude that the CaII lines may be more important than the MgII lines as a radiative cooling path. A crude estimate of the filling factor for active regions based upon the MgII and CaII resonance line fluxes ranges from 0.10 to 1.0 (the solar value is 0.001), suggesting that the surfaces of T Tauri stars may be covered by extensive regions of high chromospheric activity similar to solar plages. The conclusion that T Tauri stars exhibit spotted surface activity was also reached by Herbig and Soderblom (1980). In a study of the CaII infrared triplet, these authors found essentially the same line-strength ratios in most stars, but vastly different line-to-continuum ratios from star to star. Giampapa et al. (1981)

estimated the chromospheric mass-column-density and mean electron density, finding that the former is about 20 times larger than that of the quiet Sun, and the latter is $\sim 10^{11} \text{ cm}^{-3}$. However, these studies were hampered by the lack of simultaneous observations in the relevant lines.

A later study by Calvet et al. (1985) provided the first simultaneous, calibrated flux measurements of the CaII K and MgII resonance lines for 12 T Tauri stars. They found that the ratio of MgII k to CaII K surface fluxes in low-mass T Tauri stars follows a natural extension of the ratio found in normal late-type stars, although the fluxes are a factor of ~ 100 times larger. For the more massive T Tauri stars ($> 1.5M_{\odot}$), the correlation breaks down in the sense that MgII k is relatively much stronger. This result may imply that the MgII line is formed in a more extended region, perhaps contiguously with $H\alpha$. Calvet et al. (1985) also noted that the MgII k line does not change significantly on time scales of hours or days (except for DR Tau) although changes as large as a factor of two on a much longer time scale do take place (Giampapa et al., 1981). On the other hand very large changes (60% in GW Ori) in the CaII K line flux do take place on shorter time scales. While such flux measurements are difficult to make, the available data seem to suggest that the CaII K line is formed in localized patches on the surface of the stars.

The ultraviolet emission line intensities of T Tau have been used by Jordan et al. (1982) and Brown et al. (1984) to deduce the run of emission measure with temperature. Results from Jordan et al. (1982) are presented in Figure 4-19, which shows the emission measure as a function of electron temperature for each ion from hydrogen to NV. Brown et al. (1984) combined IUE data with other observations to construct a number of quite detailed models of the hot regions in the atmosphere of T Tauri. This analysis provided evidence of a multicomponent transition region and corona, and revealed weaknesses in several models for T Tauri stars.

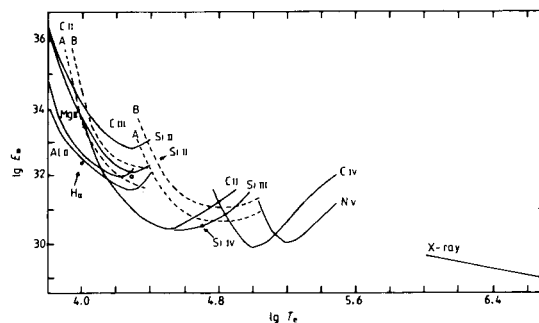


Figure 4-19. Distribution of emission measure with temperature in the star T Tauri, deduced by Jordan et al. (1982) from IUE observations.

A most unexpected result of IUE observations was the detection of the Lyman bands of H_2 in emission in the far ultraviolet spectrum of T Tau (Brown et al., 1981). These bands have also been detected in the spectrum of a sunspot, where they are thought to be excited by fluorescence via Lyman- α of hydrogen. However, Brown et al. conclude that the H_2 emission in T Tauri stars is excited by collisions at an excitation temperature of at least 2000 K, in a region some 10^{16} cm in extent around the star. This region probably corresponds to the optical nebulosity.

High-resolution IUE observations of UV emission-line profiles have been obtained for several stars, e.g., L H α 332-21 (Penston and Lago, 1983), RW Aur (Imhoff and Giampapa, 1980b), S CrA (Appenzeller et al., 1981), and T Tau (Brown et al., 1981). The only lines with high signal-to-noise ratios are the MgII h and k lines, which show components and structures that often seem to bear little resemblance to their optical counterparts, CaII H and K. Figure 4-20 compares the MgII h, k with CaII H, K, $H\alpha$ and $H\beta$ for L H α 332-21. A very broad, strong absorption feature shifted to shorter wavelengths is present at MgII h and k, but only a hint of its presence is seen at CaII H and K. The Balmer lines in this star are almost symmetrical, with a little distortion on the shortward side. Among other T Tauri stars, S CrA displays a double-peaked structure in

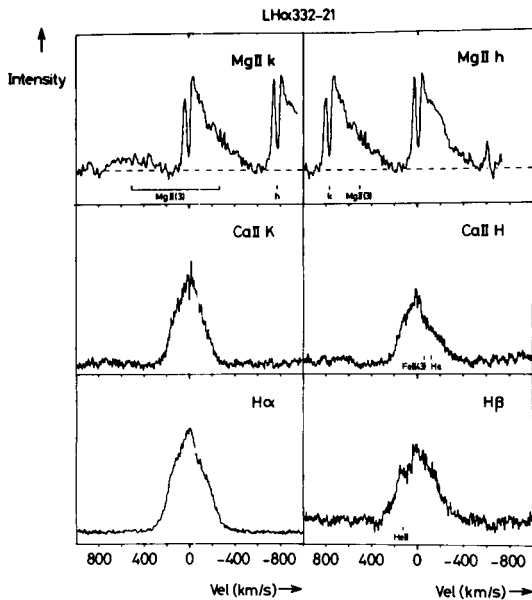


Figure 4-20. Emission line profiles in various lines for the T Tauri star L H α 332-21 (Penston and Lago, 1983).

MgII with a broad absorption feature displaced 175 km s^{-1} shortward from the peak of the stronger emission component. T Tauri shows very strong emission peaks in MgII which are not symmetrical, but appear to have strong shortward displaced absorption. The profiles can also be variable, not only in total strength but also in the absorption structure on the shortward side of the lines over a year and a half. Over this interval the emission extends further from line center, and the absorption appears to become deeper.

IV. THE INTERPRETATION OF T TAURI SPECTRA

IV.A. LOCATION IN THE HR DIAGRAM

Early UVB measurements of young clusters such as NGC 2264 by Walker (1956) indicated that the T Tauri stars lie above and to the right of the zero-age-main-sequence on the color-magnitude diagram, where pre-main-sequence objects were expected to occur. However, positioning T Tauri stars on the HR diagram is a

difficult task because of uncertainties in the reddening corrections, which reflect a lack of knowledge of the intrinsic color and effective temperature of these stars. Traditional bolometric corrections do not apply, because of the peculiar nature of both the spectrum and the continuous energy distribution. Instead of using such corrections, one thus tries to make reddening corrections to flux measurements made over as wide a wavelength range as possible, and then to integrate the resulting distribution to determine the bolometric luminosity. A basic assumption in this procedure is that of spherical symmetry, which may not hold for the extreme T Tauri stars such as HL Tau (Cohen, 1983). Further, it is particularly difficult to divide the reddening into interstellar and circumstellar components, even though such a division must be made to distinguish between emission from the star itself and re-radiation from circumstellar material. Finally, spectrophotometric observations over an extended wavelength range have rarely been made simultaneously, and thus may not be very reliable because of the intrinsic variability of T Tauri stars. Bolometric luminosities are thus subject to considerable uncertainty, perhaps as large as 50%.

In spite of these other difficulties, Cohen and Kuhi (1979) undertook a major survey of some 500 T Tauri stars which had as one of its goals the more precise location of these stars on the HR diagram. Spectral types were determined from low-resolution (7 \AA) scanner data by comparison with a sequence of standard star spectra. The spectral types were translated to effective temperatures by assuming that a unique relation exists between T_{eff} and spectral type for these peculiar stars. Since most T Tauri stars are not very different from late K stars, in the spectral range (5000 \AA to 7000 \AA) used for classification, this assumption is likely to be valid except for the extreme objects. For the latter, no classification could be made because of the lack of photospheric features. In addition, Cohen and Kuhi assumed that the effective temperature and the intrinsic color over the

observed spectral region are uniquely defined by the spectral type. A reddening correction could then be determined using a standard reddening law. Integration over the corrected fluxes (usually from -0.4μ to 3.5μ) then gave the luminosity of the object. For the extreme T Tauri stars ($\sim 5\text{--}10\%$ of the population) no corrections were possible, and only a lower limit could be determined.

In studies such as this, the errors in spectroscopic classification are likely to be quite small, so one expects little change along the T_{eff} -axis. An error in the reddening correction would usually tend to increase the luminosity. Figure 4-21 shows the HR diagram for the Taurus-Auriga dark cloud. It can be seen that most of the stars are of spectral type late K, with luminosities between 0.5 and $5 L_{\odot}$. The evolutionary tracks displayed in Figure 4-21 were modified from Iben's (1965) convective-radiative tracks. These tracks suggest that a representative mass for a T Tauri star would be $0.7 M_{\odot}$ with an age of $\sim 10^6$ years.

Cohen and Kuhi (1979) draw the following general conclusions from their work on the convective-radiative tracks: most stars with $H\alpha$ emission are still fully convective, and range in age from $\sim 10^4$ to 6×10^6 years, with masses from 0.2 to $3 M_{\odot}$ and radii from 1 to $5 R_{\odot}$. In a statistical sense the youngest stars (1) show the richest emission line spectra, (2) are still associated with nebulosity (as indicated by the forbidden lines), (3) show the largest ratio of infrared to optical luminosity and (4) give the impression that emission activity decreases with increasing age. However, from the data for any individual star, one cannot draw any conclusion about its evolutionary state or behavior; the spread in characteristics and the intrinsic variability are simply too large. Similar results were found for other clusters and associations and leave little doubt that the T Tauri population is very young.

Using newly calculated stellar collapse models, Stahler (1983) confirmed that the stars

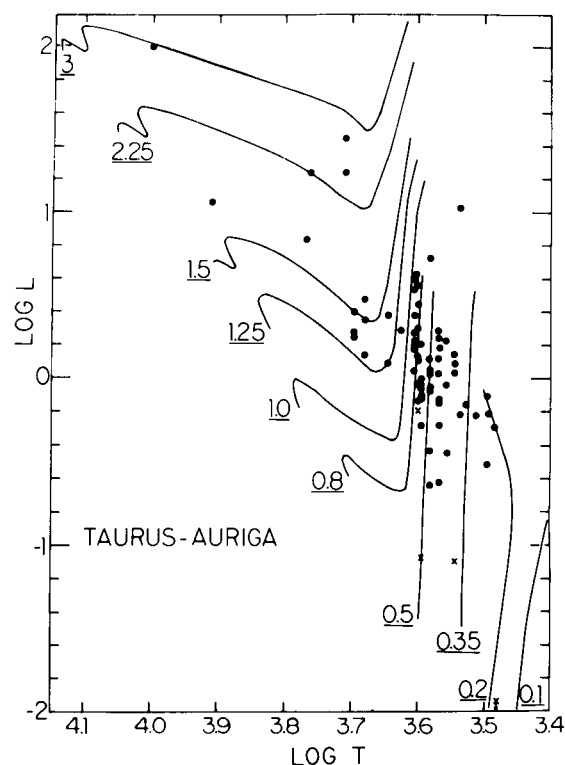


Figure 4-21. Hertzsprung-Russell diagram for the T Tauri stars in the Taurus-Auriga region, superimposed on evolutionary tracks modified from the calculations of Iben. The diagram has been constructed and discussed in detail by Cohen and Kuhi (1979).

observed by Cohen and Kuhi (1979) indeed tend to lie on the convective parts of the theoretical tracks in the HR diagram. Furthermore, Stahler showed that many of the stars are clustered near the theoretical birthline at which contracting stars become visible, and he used statistics of the estimated times since "birth" to explore the changing rate of star formation in several star-forming regions. Weaver (1984) also determined ages of T Tauri stars from their locations in the HR diagram, and from these ages determined a quantity he terms the "youth," i.e., the time remaining before the star will arrive at the zero-age-main-sequence. Weaver noted a marked gap in the number of stars with a "youth" corresponding to 5% of the time to the main sequence, and pointed out that this gap coincides with the convective-radiative

transition in theoretical models of star formation.

IV.B. ATMOSPHERIC STRUCTURE

No current model satisfactorily explains the observational data for even a single T Tauri star, let alone for the entire group. The development of models of the atmospheres of T Tauri stars has always been hampered by the tendency to include many free parameters in models which show little concern for overall physical self-consistency. We present here an overview of the early modeling efforts with some discussion of their shortcomings. We will also review some more recent models, some of which attempt to introduce more physical consistency. These models, based upon the hypothesis that some of the emission lines originate in a chromosphere, rely on self-consistent radiative transfer calculations to treat the formation of such spectral lines, be they in absorption or emission. Further discussion of models of T Tauri atmospheres can be found in Chapter 6.

The presence of classical P Cygni profiles and closely related types with shortward displaced absorption components led early investigators (Herbig, 1962; Kuhl, 1964a) to an interpretation based on mass outflow. Kuhl predicted emission line profiles by combining a simplified treatment of line transfer with the assumption that material was physically ejected from the star and then subjected only to gravitational forces, i.e., ballistic ejection. He inferred mass-loss rates in the range 0.3 to $6 \times 10^{-7} M_{\odot} \text{ yr}^{-1}$ with a mean of $3 \times 10^{-8} M_{\odot} \text{ yr}^{-1}$ for the nine stars studied. Velocities of ejection were found to be a few hundred km s^{-1} , often below the escape velocity. No attempt was made to account for the returning material, atomic level populations for hydrogen were calculated assuming nebular departure coefficients, no ionization or excitation mechanism was advanced, radiative transfer effects were ignored, spherical symmetry was assumed, no initial acceleration mechanism was provided, and con-

tinuum radiation was not considered. The model did reproduce the hydrogen and calcium line profiles reasonably well, but the ad hoc nature of aspects of the model implied the need for a more physically consistent treatment.

IV.B.1. INFALL MODELS

The apparent paradox that young stars (still presumably in their gravitational contraction phase) should be losing mass instead of gaining it led Ulrich (1976) to develop a model based on mass infall instead of outflow. The model postulates nonspherically symmetric infall of gas, initially guided by a magnetic field but then by the conservation of angular momentum under free-fall conditions to within some critical distance from the star. An accretion shock produced at the surface of the hydrostatic core by the infalling gas produces X-rays which in turn ionize the infalling material outside the shock. The secondary cooling layer then produces essentially a recombination spectrum of hydrogen, although the high densities imply a significant role for collisional excitation. Ulrich did not solve the radiative transfer problem for either the initial shock region or the secondary cooling layer, but instead he made a number of assumptions (e.g., a constant ratio of line to continuum source function) to allow the calculation of the line profiles expected from such a flow. Ulrich predicted line profiles for a wide range of parameters, and succeeded in reproducing the commonly observed double-peaked Type II P Cygni profile. A more precise fitting to the observed profiles for RY Tauri led to an inferred infall rate of $10^{-7} M_{\odot} \text{ yr}^{-1}$ with a gas temperature between 10,000 and 15,000 K for the hydrogen line-forming region. According to this model, the apparent "absorption" feature is produced not by true absorption, but by the absence of emitting atoms in a certain range of bulk velocities. Initially, the success of the model cast doubt on Kuhl's (1964a) mass-loss interpretation for most T Tauri stars (except, of course, those showing Type I P Cygni profiles with absorption features extending below the continuum).

In fact, the interpretation of symmetric profiles has always been ambiguous, but Ulrich's work suggested that other profiles present the same problem.

However, a closer examination of Ulrich's (1976) work has revealed a number of problems. Specifically, there are three regions in the model where the $H\alpha$ line is produced: the secondary cooling layer at the stellar surface, the infalling material in the envelope outside the shock, and the accretion disk formed by the infalling material. Ulrich considered emission from the first region only, even though he recognized that the emission from the disk in the form of a double-peaked, symmetric line could dominate the line profile. Such a disk profile would bear little resemblance to the observed profiles and hence Ulrich arbitrarily suppressed the disk component. We conclude that the specific infall model produced by Ulrich cannot account for the observed line profiles. The work of Ulrich and Knapp (1979) supports this conclusion.

A different class of infall models was developed by Appenzeller and Wolf (1977) and Wolf et al. (1977), to explain the higher Balmer lines in YY Orionis stars which often exhibit inverse P Cygni profiles. This work concentrated on S CrA, a bright southern YY Orionis star, which shows inverse P Cygni profiles for most metallic lines, narrow symmetric profiles for HeI and HeII, symmetric profiles of CaII H and K with a narrow blue-shifted absorption component, and a very complex and variable structure for the Balmer lines which were typically double-peaked at $H\beta$, $H\gamma$ and $H\delta$. The higher Balmer lines show only vestiges of double-peaked structure, and on one night they were seen to display significant changes in the shape of the redward absorption features. Appenzeller and his coworkers showed that the observed Balmer line profiles could be reproduced by a combination of emission from an extended infalling envelope and radiation produced by hot gas in the immediate vicinity of the core. Variability was ascribed to fluctua-

tions in the mass-infall rate. A number of untested approximations were made to simplify the treatment of non-LTE radiative transfer in the infalling envelope, and of the dynamics of the shock cooling region. An inverse P Cygni profile was relatively easy to produce with this semi-quantitative approach.

Bertout (1977, 1978, 1979), Bastien (1982), and Wagenblast et al. (1983) developed a more quantitative theory of the infall model of T Tauri stars. Bertout investigated the line formation problem for a two-level atom in the cases of spherically symmetric infall, combining spherical infall and outflow with axially symmetric flows. Local Sobolev theory was used initially, and subsequently a generalized Sobolev theory was developed to include non-local radiative coupling between certain velocity fields. Bastien (1982) treated the problem of incorporating a many-level atom into the generalized Sobolev theory in the case of spherically symmetric infall. In this model there remain a large number of free parameters, and many approximations have to be made. These include the following: (1) the core (i.e., the photosphere and shocked region) radiates a pure continuum; (2) the envelope temperature is $\sim 10^4$ K, decreasing with increasing radius; (3) the hydrogen continua are optically thin; and (4) the use of the "on-the-spot" approximation, which does not apply to Lyman- α , since this line is so optically thick. The profiles produced by Bastien's models have stronger emission and absorption components than those from Bertout's (1979) two-level atom treatment, and they qualitatively reproduced the inverse P Cygni profiles observed in the higher Balmer lines in S CrA. However, the $H\alpha$ profile predicted by the model always has a redward-displaced absorption feature which cannot be suppressed except by an envelope with a radially increasing temperature (12,000 K to 20,000 K). The often observed double-peaked profile at $H\alpha$ cannot be explained by this model.

This difficulty led Wagenblast et al. (1983) to consider yet another special geometry for the

infalling material, namely a shell that is thin in radial extent and located some distance from the star. Such a shell might be produced at the interface between a growing stellar corona and the remnants of the infalling material. With a suitable set of parameters the model can be forced to produce double-peaked emission profiles, ranging from equal intensity peaks with an additional redward-absorption component, to a profile with a very strong blue peak and a weak red peak located in the center of a strong redward-absorption feature, to a profile resembling the observed $H\alpha$ profile. According to the model, a blue displacement of the minimum between the emission peaks is produced by asymmetric excitation and absorption across the shell, even though the flow is directed inwards. Of course, the same profile can be produced by changing the sign of the velocity field and the run of opacity and source function across the shell. Thus, for profiles of this type the position of the minimum does not really permit any conclusion to be drawn about the sign or the magnitude of the gas flow. Although infall models enjoy some qualitative success, the need to make increasingly narrow assumptions to explain the observations in detail can be seen as a significant liability.

IV.B.2. OUTFLOW MODELS

Several efforts have been made to develop models based on outflow. For example, Kuan (1975) considered a hot (10,000 K to 20,000 K) expanding envelope, which he found could explain the average Balmer line profiles, the Balmer decrement, and even the blue veiling longward of the Balmer discontinuity which was ascribed to Paschen continuum emission. Rydgren et al. (1976) showed that Kuan's model could account for the observed energy distribution, including spectral veiling and most of the infrared excess. However, they had to assume abnormally large values of total-to-selective extinction, an assumption which has been invalidated by the infrared data of Cohen and Kuhi (1979).

Our understanding of the structure of winds from T Tauri stars was analyzed at some length by DeCampli (1981), who showed that the mass-loss rates derived from models such as those discussed above are uncertain by at least three orders of magnitude. The largest uncertainties arise from estimates based on symmetrical emission-line profiles, which are ambiguous regarding flow rate (which could be zero!) and the direction of flow. DeCampli argues that the uncertainties decrease as the profiles become more asymmetric and complex in structure, so that reasonably reliable estimates of flow rates could be obtained by combining data from many lines covering the entire observable spectral range. DeCampli also investigated the variability of various acceleration mechanisms which have been proposed to drive the T Tauri winds. For mass-loss rates of less than $10^{-9} M_{\odot} \text{ yr}^{-1}$, thermal coronal expansion or radiation pressure in the lines could work; for rates up to a few $\times 10^{-8} M_{\odot} \text{ yr}^{-1}$, a possible mechanism could be the deposition of momentum by Alfvén waves generated in the convection zone. Magnetic fields of a few hundred gauss would be required. He found no acceptable mechanism to maintain winds with mass-loss rates larger than a few $\times 10^{-8} M_{\odot} \text{ yr}^{-1}$. Of course, the removal of spherical symmetry in the models used to fit line profiles could reduce the estimates of mass-loss rates by at least an order of magnitude. To explore non-spherically symmetric models, DeCampli also presented computations for a wave-driven wind from a rotating star. The resulting envelope has an emission region around the equator where the magnetic pressure holds the gas in hydrostatic equilibrium and there is no flow. Nearer the poles, the flowing wind would be bipolar in appearance. Appropriate P Cygni profiles could be produced using the Sobolev approximation for an optically thick envelope constrained to flow along the magnetic field lines.

The Alfvén wave-driven wind model was developed further by Edwards et al. (1981) and Hartmann et al. (1982). These workers assumed

that wave dissipation heats the wind, and by specifying the heating function they could calculate the temperature of the wind and its emission measure. Since no theory of the wave generation process is available, it was necessary to adopt an ad hoc energy flux by assuming values of initial density, wave amplitude, and magnetic field strength. Further, they assumed purely radial steady flow, radial magnetic fields and that linear Alfvén waves are the only MHD mode present. This work showed that mass-loss rates of 10^{-9} to $10^{-8} M_{\odot} \text{ yr}^{-1}$ require surface field strengths of a few hundred gauss and wave energy fluxes from 10% to 100% of the luminosity of the underlying T Tauri star. The highest mass-loss rates led to wind temperatures which were in fair agreement with observed emission measures for ultraviolet lines, but the predicted density-sensitive line-strength ratios did not agree with measurements.

Wave-driven models predict large wave amplitudes in the envelope. In fact, in much of the wind the turbulent velocity is comparable to the terminal velocity. These turbulent flows would appear as large broadening velocities in spectral line profiles. Close to the star, the turbulent velocity can exceed the local expansion velocity so that the line broadening is not controlled by the expansion velocity law but rather by the turbulent velocity. This aspect of the model has a strong effect on the line profiles, and it invalidates the application of the Sobolev approximation to profile calculations. To address this problem, Hartmann et al. (1982) assume that the contribution to the emission-line profile at a given radius arises from an optically thin shell at that radius, and they use a static plane-parallel formulation to determine the source function of the optically thick hydrogen lines. They find that the large equivalent widths of $H\alpha$ (over 100 \AA in some cases) and the large Balmer decrement can be produced with mass-loss rates about one tenth as large as those estimated originally by Kuhl (1964a). However, the resulting line profiles do not correspond closely to the observed profiles. The authors emphasize the rudimentary nature

of their approach, and the uncertainties likely to be introduced by their neglect of, or oversimplified treatment of, important physical phenomena such as conduction, wave damping, and radiative transfer. Nevertheless, the study does show that Alfvén waves could drive a stellar wind and could produce enough turbulence to explain the line widths of the hydrogen emission lines.

An intensive study of the emission lines in RU Lup (Lago, 1984; Penston and Lago, 1983) was also based on an Alfvén-wave-driven model, albeit with somewhat different assumptions and parameters. Again, this study showed that the run of velocity, density, and temperature predicted by such a model leads to line profiles which are in acceptable agreement with observation. However, the model still contains a number of unjustified simplifying assumptions, particularly in relation to the structure of the underlying magnetic field.

Another model relying on strong turbulence has been proposed by Ulrich et al. (1983) to explain observations of the spectral energy distribution of DR Tau from 0.32μ to 1.1μ , including a Balmer discontinuity in emission. The model requires the existence of an optically hot gas akin to a chromosphere, with a temperature of 65,000 K maintained by the dissipation of strong turbulence through many weak shocks. The model suggests that turbulence is driven by inhomogeneities in an accretion flow. The description of this “turbosphere” is still almost entirely qualitative.

IV.B.3. DISKS

The appearance of the solar system, supplemented by one of many cosmogonies, suggests that a young star may be accompanied by an equatorial disk. Direct imaging of the extreme T Tauri star HL Tau (Grasdalen et al., 1984) reveals structure with a disk-like appearance, while fits to the observed amplitude and spectrum of the IR excess of several T

Tauri stars are also consistent with the presence of a disk (e.g., Strom et al., 1987).

The hydrodynamic theory of equatorial disks is very rudimentary and difficult to develop, because the flows generally involve a state intermediate between noninteracting Keplerian orbits and a fully collisional gas. Furthermore, the energy budget may involve not only "reprocessed" photospheric radiation (e.g., Adams and Shu, 1986) but also mechanical energy may be converted to radiation in the disk itself by friction or electrodynamic processes.

At least three consequences of disks have been considered in theories designed to account for T Tauri spectra: (1) IR and visible continuum radiation from warm dust (e.g., Adams and Shu, 1986); (2) emission from ionized gas at the disk-photosphere interface (e.g., Bertout et al., 1987); and (3) occultation of the receding part of a stellar wind, leading to blue-shifted spectral lines (Edwards et al., 1987). While disk models are evidently capable of providing an explanation of many spectral features, our present understanding of the relevant hydrodynamics and energy balance is highly speculative.

Models involving anisotropic mass outflow offer scope for explaining a wide variety of emission-line shapes. One might, of course, be inclined to apply Occam's razor to models containing a large number of free particles, but there is clear evidence of anisotropic bipolar outflows in some young stellar objects (e.g., Lada, 1985). Although such flows are rare among T Tauri stars, they have been detected (e.g., Mundt et al., 1987) and hence it is not unreasonable to explore the possible effects of anisotropic flows which, if present, could not be directly observed at present. Edwards et al. (1987) have published many theoretical profiles which demonstrate how most of the shapes seen in T Tauri spectra can be explained by adjustments in aspect, collimation degree, and velocity law.

IV.B.4. CHROMOSPHERIC MODELS

The striking resemblance between the emission line spectra of extreme T Tauri stars and the solar chromosphere, first noted by Joy (1945), led Herbig (1970) to suggest that the T Tauri spectrum might be produced by a chromosphere with a temperature minimum lying deep in the atmosphere, i.e., at $\tau_{5000} \sim 10^{-1}$ or 10^{-2} instead of 10^{-3} as in the Sun. Dumont et al. (1973) developed Herbig's suggestion, and showed that it is possible to predict $H\alpha$ emission fluxes in agreement with those observed in T Tauri stars under the basic assumption of a photoionization-dominated source function. The model did not require the presence of an extended envelope. Such models always produce a strong central reversal which is not usually present in the observed line profiles. Dumont et al. suggested that better agreement could be obtained by the introduction of a systematic velocity field, which would broaden the line, reduce the central absorption and produce an asymmetric profile. The treatment was semi-empirical in character, since the $H\alpha$ emission was predicted using the observed Paschen and Balmer continua; the self-consistent multi-level hydrogen problem was not solved.

The chromospheric model was explored further by Heidmann and Thomas (1980). In particular, the effects of a velocity field and changed density distributions were considered, and several different models for emission line formation were considered. These included: (1) wholly geometric emission with broadening due either to turbulence or to expansion, contraction and/or rotation and (2) chromospheric and coronal emission (both low-lying and extended). Heidmann and Thomas concluded that it is relatively easy to adjust such models to get weak emission in $H\alpha$. However, to produce a line strongly in emission requires a large temperature rise in the chromosphere, e.g., $H\alpha$ emission with a peak-to-continuum ratio of even a factor of 2 requires $T_e > 7500$ K above 350 km, with unit optical depth in the

C-3

Balmer continuum at that height. To produce typical T Tauri Balmer profiles with this model, the chromosphere must begin very deep, and there must be a very steep temperature rise. Even with such a model, comparison with the observed profiles indicates two points of disagreement: (1) the predicted peak intensities are too low, and (2) the predicted profiles are symmetric and double-peaked with strong central absorption. Heidmann and Thomas suggested that larger line strengths could be obtained from an extended chromosphere or a post-coronal emitting region, i.e., from a geometrically extended envelope.

Cram (1979) developed a model by grafting an ad hoc chromospheric temperature rise onto a photospheric temperature structure corresponding to a line-blanketed LTE model in hydrostatic equilibrium with $T_{\text{eff}} = 4500$ K and $\log g = 4$. Non-LTE effects were considered for the ionization equilibrium of hydrogen, and the radiative transfer equations were solved explicitly for $H\alpha$, $H\beta$, and $H\gamma$ and for the Lyman, Balmer, Paschen, and Brackett continua. The temperature minimum of 3670 K occurred at a mass column density of 0.65 ($\tau_{5000} = 0.03$). A temperature of 10^4 K is reached at a mass density of 10^{-3} gm cm $^{-2}$. The model produces a continuum energy distribution with a large ultraviolet excess and a strong Balmer discontinuity in emission whose value depends sensitively on the position of the temperature minimum and the temperature gradient above the minimum. Small changes in either of these parameters produce large changes in the ultraviolet emission. Further, Cram synthesized a portion of the iron line spectrum (4475 Å to 4500 Å), and showed that the apparent "veiling" could be reproduced by the fact that these lines are mostly in emission in the deep-chromosphere model. Profiles for $H\alpha$, CaII K, and NaI D all show the central reversals already discussed. The reversal at CaII K is narrow and would not be detectable at resolutions poorer than 0.1 Å. Although the model predicts several of the spectral characteristics of extreme T Tauri stars, it pro-

duced only modest $H\alpha$ emission line strengths and could not produce the observed $H\alpha/H\beta$ flux ratios. Consequently, Cram concluded that extended atmospheres with systematic velocity fields would be needed to explain the strong and asymmetric profiles of $H\alpha$ and the large ratio of $H\alpha$ to $H\beta$. Nevertheless, this work implied that the existence of a low-lying chromosphere might explain many of the other emission characteristics of T Tauri stars. For example, the predicted CaII IR triplet ratios were found to agree quite well with the later measurements of Herbig and Soderblom (1980).

The characteristics of chromospheric models were explored further by Calvet et al. (1984), who determined the most important factors affecting the resultant spectrum. They used the semi-empirical approach employed by Linsky (1980) and collaborators to construct model atmospheres consisting of a late-type photosphere ($T = 4000$ K) plus a hydrostatic chromosphere with a deep-lying temperature minimum, a chromospheric temperature rise, and a transition region. The crucial parameters are the depth of the temperature minimum and its temperature, the gradient of the temperature rise, and the density of the transition region. The models reproduce reasonably well such features as the total fluxes in the CaII K and MgII k emission lines, the continuum energy distribution, the absorption lines and the ultraviolet emission lines. The chromospheric contribution is dominant in the ultraviolet and produces a Balmer discontinuity in emission, whereas the spectrum in the visible and infrared is mostly photospheric in origin. Veiling is selective and most noticeable in strong lines which exhibit a chromospheric component. Increasing the chromospheric contribution eventually causes such lines to pass completely into emission. Thus, many characteristics of a typical T Tauri star can be readily produced by a chromospheric model. However, Calvet et al. also concluded that an extended emitting region was necessary to produce the large $H\alpha$ fluxes, and that velocity fields must be included in order to reproduce the observed asymmetric

line profiles. They suggested that further modeling should include non-LTE calculations for the metallic lines, better treatment of line-blanketing effects, velocity fields, and an extended emitting region as well as the transition region and corona. It should be noted that existing chromospheric models are based on ad hoc temperature distributions and that self-consistent energy-balance models have not as yet been constructed.

IV.C.3. SUMMARY

As a result of the studies described in this section we may conclude that the atmosphere of a typical T Tauri star is likely to encompass most or all of the following:

1. A photosphere responsible for the almost normal absorption spectrum of most T Tauri stars, and the almost normal visible-infrared spectral region of the more extreme T Tauri stars;
2. A chromosphere with a deep-lying temperature minimum and steep temperature rise to a transition region producing much of the metallic emission lines, some of the CaII H, K, and MgII h, k emission, the so-called veiling, and some of the Balmer line and continuum emission;
3. Regions of variable surface activity producing some of the CaII H, K, and MgII h, k emission as well as the NaI D emission;
4. A transition region and corona which are responsible for the multiply ionized metallic lines in the ultraviolet and the X-ray emission (some stars may not have a normal corona but may produce X-rays via powerful flares);
5. An extended envelope responsible for most of the hydrogen line emission, especially H α , with a velocity field characteristic of a stellar wind with mass outflow;
6. Regions produced by ejection of material followed by return to the stellar surface, to account for the rapid changes observed in the NaI D lines and in the higher Balmer lines (there must be episodes of shell ejection activity);
7. Greatly extended, aspheric regions containing dust particles responsible for the infrared emission;
8. Even more extended regions from which the various molecules detected at radio frequencies must be located; and finally,
9. Herbig-Haro objects and other effects of ejection of matter such as bipolar nebulae, associated with the most extreme T Tauri stars.

5

CLASSICAL THEORY OF STELLAR ATMOSPHERES

Lawrence E. Cram

I. INTRODUCTION

Astronomy is an empirical science rather than an experimental science: we can observe stellar atmospheres, but we cannot influence them. Although we would like to verify (or refute) our theories by predicting and observing how the atmospheric structure changes in response to controlled changes in selected parameters, we cannot make the stars carry out these changes. To help overcome this problem we may study relevant problems in the laboratory, where experimental conditions are controllable, and we may also study groups of similar stars whose atmospheres nevertheless differ as a result of different patterns and stages of stellar evolution.

The inherent problems of astrophysical research have been recognized by many astrophysicists. For example, Eddington (1926, p.1) discussed the "chain of deduction" which starts with observations of the radiant energy which escapes from the star, and proceeds to learn about the stars by the application of the "most universal rules of nature — the conservation of energy and momentum, the laws of chance and

averages, the second law of thermodynamics, the fundamental properties of the atom, and so on." Although Eddington recognized the need to employ observations to check conclusions based on theoretical deductions, it appears that he may have been over-confident in the power of theory alone to lead to an appropriate description of the stars.

The "deductive" work of Eddington and others has produced a model for stellar atmospheric structure which has been of considerable value in the past, and which is still widely used in contemporary studies. This "classical" model is based on the assumption that the stellar atmosphere is a quiescent, homogeneous gaseous envelope around the star, in which the distributions of temperature and pressure are completely determined by the conditions of radiative and hydrostatic equilibrium. The structure of a classical model atmosphere of given chemical composition is completely determined by two basic parameters, the effective temperature, T_{eff} , and the surface gravity, g , once the microscopic physics of the equation of state and the emission and absorption of radiation have been specified. Applications of

classical models generally involve the inference of T_{eff} , g , and chemical composition from observations of the stellar spectrum.

The classical model does not provide a satisfactory and complete description of the structure of stellar atmospheres. Eddington's chain of deduction based on the "rules of nature" is weak because theory, by itself, does not automatically reveal the complexity of natural phenomena which obey these rules. *It is observed that the structure of stellar atmospheres is not accurately described by simple solutions of simple governing equations*, and the principle challenge of contemporary theoretical stellar astrophysics is to identify relevant models and then to explore the richness of solutions of complex governing equations. Nevertheless, the classical model has been used to draw important conclusions about stellar atmospheres, and these appear to provide a reasonably robust foundation for more complete and realistic investigations. This chapter of the monograph therefore deals with the classical theory of stellar atmospheres.

We begin (Section II) with a brief survey of the historical background to the classical theory of stellar atmospheres. The survey shows how the contemporary classical theory has gelled from a number of diverse lines of investigation, and emphasizes that the deficiencies of the classical theory have long been recognized. We then discuss (Section III) the theory of radiative transfer, since this is basic to all studies of stellar atmospheric structure. We review briefly not only LTE radiation transfer theory, which has been used in most studies of classical model atmospheres, but also non-LTE theory and the related spectroscopic diagnostic techniques that are applicable in the radio, far UV, and X-ray portions of the electromagnetic spectrum. It is only by the use of an extensive set of diagnostics that the full radial structure of stellar atmospheres is revealed. We then (Section IV) describe methods for the construction of classical model atmospheres, and present (Section V) a critical survey of the successes and

failures of these models when confronted with observations. This survey uncovers a number of problems with the classical model. The chapter concludes (Section VI) with a description of various "semi-empirical constructs" that have been incorporated into the classical model to improve agreement between theory and observation. These semi-empirical constructs, such as nonthermal velocities, atmospheric extension, and nonradiative heating, represent a first attempt to provide a more realistic description of stellar atmospheres.

II. HISTORICAL BACKGROUND

In this section we briefly summarize the development of understanding regarding stellar atmospheres. We show how the classical model links several physical themes — radiation thermodynamics, atomic theory, radiative and hydrostatic equilibrium — into a theory whose main achievements have been the derivation of stellar surface temperatures, gravities, and abundances. These quantities have been used in turn as data for verification of theories of the structure and evolution of stars and galaxies. The classical model has thus played a key role in the development of modern astrophysics.

We also review the historical background to the proposition that the classical model does not account for all observations of stars. It is shown that throughout the period of development and application of the classical model, a large body of observational material was accumulated concerning decidedly nonclassical phenomena, such as variability, emission lines, and a host of poorly understood processes in the solar atmosphere. Unfortunately, we are unable to examine here the reasons why key theoreticians in stellar atmospheric research chose to overlook this material, and hence were motivated to follow patterns of thought that led to the entrenchment of the classical models. However, we do briefly review the history of observational studies of nonclassical phenomena to demonstrate that the limitations of the

classical model should always have been apparent.

In her monograph on Stellar Atmospheres, Cecilia Payne (1925, p. 199) stated that

“the future of a subject is the product of its past . . . the direction in which progress lies will depend on the (observational) material available, on the development of theory, and on the trend of thought.”

Although astrophysicists have always recognized the widespread existence of phenomena which could not be explained by the classical model, their “trend of thought” has been directed, in general, towards the use of the classical model to infer effective temperature, surface gravity, and chemical composition from optical observations: these are the parameters on which classical models depend. This tendency has led to the thorough understanding of the classical model that we possess today. However, it has also led to an unfortunate tendency to overlook the many phenomena that lie outside classical theory and equilibrium thermodynamics. New observations, especially those made from outside the Earth’s atmosphere, have now revealed a host of previously unknown properties of stellar atmospheres. Theories must be developed to accommodate these new observations, and, consequently, we are now witnessing remarkable changes in the trends of thought regarding the structure of stellar atmospheres and the thermodynamic principles needed to describe them.

II.A. RADIATION THEORY AND STELLAR ATMOSPHERIC STRUCTURE

An essential prerequisite for a clear understanding of the physics of stellar atmospheres was the development of the theory of the thermodynamics of radiation that occurred in the second half of the 19th century. An impor-

tant early result was Kirchhoff’s demonstration (ca. 1860) that the emission and absorption coefficients (η_ν and κ_ν respectively) of any substance in thermodynamic equilibrium must be related by a universal function of temperature (T) and frequency (ν) which also characterizes black-body radiation:

$$\kappa_\nu/\eta_\nu = B_\nu(T) \quad (5-1)$$

The period 1860–1900 saw the development of Kirchhoff’s law into results such as the Stefan-Boltzmann relation

$$\int B_\nu d\nu = \frac{\sigma}{\pi} T^4 \quad , \quad (5-2)$$

Wien’s law,

$$T/\nu = \text{constant}, \quad (5-3)$$

and the Rayleigh-Jeans relation:

$$B_\nu(T) = \frac{2\nu^2}{c^2} \cdot kT \quad (5-4)$$

In 1900, Planck applied quantum statistics to the radiation field to derive finally the comprehensive law

$$B_\nu(T) = \frac{2h\nu^3}{c^2} (e^{h\nu/kT} - 1)^{-1} \quad (5-5)$$

These developments led to a physical interpretation of stellar colors, and thence to an understanding of the connection between spectral type and temperature (recall that even the LTE theory of the relation between spectral line strength and temperature was not understood at the time). Combined with measurements of parallaxes, this connection led to the recognition of the existence of dwarf and giant stars (ca. 1905) and to the Hertzsprung-Russell (H-R) diagram (ca. 1913). The H-R diagram is a cornerstone in the development of theories of stellar structure and evolution. Following

these discoveries, a large part of stellar atmospheric research in the early 20th century was devoted to developing methods for measuring and calibrating stellar colors, absolute magnitudes, and radii, mainly to improve and extend the H-R diagram. The work of Adams and Kohlschütter (1914) on the spectroscopic determination of absolute magnitudes was an important milestone in this research.

The fundamental ingredients of the classical theory of stellar atmospheres were assembled by Schwarzschild (1906). Introducing the concept of radiative equilibrium and applying Kirchhoff's relation and the Stefan-Boltzmann law, Schwarzschild derived an approximate equation for the temperature distribution in a stellar atmosphere,

$$T^4(\tau) = \frac{1}{2} T_{\text{eff}}^4 (\tau + 1) \quad , \quad (5-6)$$

where τ is the "average" optical depth, and T_{eff} the effective temperature. Schwarzschild showed that a radiative equilibrium model of this kind predicted a solar limb-darkening curve which fits the observations much better than an adiabatic model. He demonstrated that such a radiative equilibrium model would be stable if its ratio of specific heats, γ , were greater than 4/3. Schwarzschild also showed how the scale height of a stellar atmosphere could be computed, but his actual estimate was wrong, because accurate values of the opacities and molecular weights were not available to him.

Since 1906 an enormous effort has been devoted to improving Schwarzschild's model. Much of this effort was initially directed towards a solution of the Schwarzschild-Milne equation,

$$B(\tau) = \frac{1}{2} \int_0^{\infty} B(t) E_1(|\tau - t|) dt \quad , \quad (5-7)$$

which combines the condition of radiative equilibrium with the equation of radiation

transfer in a gray atmosphere. Approximate solutions of this fundamental equation were derived by Eddington, Chandrasekhar, and others, and by 1950 the exact solution had been found by several different methods.

Many attempts were made to verify the theory, particularly by using observations of the wavelength dependence of solar limb darkening. As the accuracy of measurement improved, and as better techniques were developed to correct the observations for extinction and line blanketing, the theory had to be modified and refined. An early debate (ca. 1915) on the relative importance of scattering and absorption was resolved in favor of absorption in the continuum but, as we shall see, the debate lingered on in line-formation studies for many years. Unsöld's work on the existence of a hydrogen convection zone (ca. 1930) led to several attempts to observe departures from radiative equilibrium in the deep photosphere, and to theoretical attempts to include convection in the energy transport equation (Vitense, 1953). The problem of line blanketing received attention, and most of the important physical effects of lines were revealed by applications of Chandrasekhar's picket-fence model (ca. 1936).

One of the most important obstacles to the orderly development of Schwarzschild's classical model concerned the nature of the "general" or continuum absorption coefficient of stellar photospheres. The gray model predicted continuous spectra that agreed well with both solar observations and a black-body distribution, and prior to about 1925, the agreement rather than the disagreement was the point which was emphasized (Greaves, 1956). However, the studies of solar limb darkening undertaken by Lundblad, Minnaert, Mulders and others eventually demonstrated not only that the solar continuum absorption coefficient is frequency-dependent, but also that it is quite different from that predicted by Kramers' theory (ca. 1923). The problem was finally solved by Wildt (1939) who identified the H^-

ion as the primary source of opacity in the photospheres of cool stars. With the accurate theoretical calculation of the H^- absorption coefficient, the classical theory of the structure of the solar photosphere (and therefore the photospheres of other cool stars) reached the high degree of refinement described in Minnaert's (1953) review. Developments over the past three decades have involved improved H^- absorption coefficients, more comprehensive treatment of line blanketing, and some cosmetic improvements to the convective transport model.

II.B. ABSORPTION LINES

In parallel with this development of the classical theory of stellar atmospheric structure, there was intensive research on spectral line formation in stellar atmospheres, particularly after Bohr's theory (ca. 1916) of electronic transitions and Saha's theory (ca. 1920) of ionization and excitation equilibria were formulated. Although controversy and confusion concerning the specific mechanisms of line formation were rife throughout the period 1920–1970, the processes were understood well enough to allow the development of coarse diagnostic methods.

In the 1920s, Fowler, Milne, Payne, Russell and others developed techniques for interpreting measurements of relative line strengths in terms of atmospheric properties such as temperature and pressure. This research provided an indication of the low pressure of stellar atmospheres in general, and the very low pressure of giant atmospheres in particular. Once the role of temperature and pressure in spectral line formation had been clarified, it became possible to make fairly accurate estimates of the relative abundances of the elements, a task in which Russell (1933) played a key role. This work, although based on an "egregiously simplified model", suggested that hydrogen was the main constituent of stars, and demonstrated the approximate constancy of element abundances from star to star for most stars.

Further theoretical investigations of line broadening mechanisms and of the relative importance of scattering and absorption led to advanced diagnostic techniques such as the curve-of-growth and the method of weighting functions (Unsöld, 1955, Chapter XVII). In the period 1940–1970, these techniques were applied in a large number of studies of the spectra of the Sun and other stars, with an emphasis on detecting abundance differences between stars. Although there are important problems remaining even today (e.g., abundance gradients in galaxies and the abundances in globular clusters), these studies led to a general picture of the chemical evolution of the galaxies which matches fairly well with the theoretical ideas built up from studies of nuclear processes thought to occur deep within the stars (Burbidge et al., 1957).

Since 1960, theories of spectral line formation based on nonlocal thermodynamic equilibrium (non-LTE) have been widely applied in studies of stellar atmospheres (Thomas, 1965). These theories have led to a few major revisions of LTE results (Mihalas, 1974), but in the context of classical atmospheres non-LTE theory has not had a revolutionary impact. Nevertheless, the development of self-consistent non-LTE diagnostic methods was the key step in revealing the full character of chromospheres as evidence of major departures from the classical model (e.g., Thomas and Athay, 1961).

One of the major applications of the theory of spectral line formation has been the provision of a sounder framework for the use of spectral lines in stellar classification. In questioning the basis of stellar classification, Struve (1933, p. 75) asked "if two stars of equal atmospheric temperature and pressure are given, are their spectra necessarily identical?" Struve's intention was to demonstrate that the answer is clearly no. Russell, Payne-Gaposchkin, and Menzel (1935) also knew that the answer was negative, but nevertheless they argued that the theory of line formation implied that the

parameters necessary to define a stellar spectrum could be listed in order of decreasing importance: (1) effective temperature and surface gravity, (2) abundances, and (3) "modifying" factors such as rotation, turbulence, size, interstellar absorption, and color excess. This ordering of importance by the Harvard workers set the scene for an interpretation of stellar classifications in terms of the classical theory, and this has persisted as a major theme of stellar atmospheric research until recent times.

II.C. EMISSION LINES

Bright or emission lines in stellar spectra form a class of phenomena which lie in almost all cases outside the classical theory. Throughout the first half of this century a considerable effort was devoted to observational studies of emission line stars, particularly those of early type (Oe, Of, Be, Wolf-Rayet, P Cygni, etc.). Much of this observational material has been summarized by Struve (1942) and in Volumes II, III, and IV of this monograph series. Theoretical discussions of the origins of the emission lines usually concentrated solely on the line formation mechanisms and not on the origin of the associated atmospheric structure. By ca. 1950 it was widely accepted that the predominant cause of line emission in early-type stars was a low-density extended atmosphere or shell, which in many cases appeared to be ejected from the star. The work of Sobolev (1960) and others provided a comprehensive account of techniques of spectroscopic diagnostics of such extended atmospheres. However, few attempts were made to explain the existence of extended atmospheres and outflows in terms of physical processes occurring in and beneath the stellar atmosphere. Interest in these early-type objects has been heightened in the past decade by EUV observations showing that atmospheric extension and rapid variable mass loss are very common phenomena.

Emission lines are also observed in the spectra of many late-type stars. Calcium and

hydrogen emission occurs in the cool supergiants (e.g., Imhoff, 1977), but the phenomenon has received very little attention. T Tauri stars and dMe (flare) stars have prominent emission line spectra, but because these stars are invariably faint, it has been possible to make detailed spectroscopic studies only in the past few years. As yet there is no crystallization of ideas regarding either the atmospheric structure or the underlying dynamical processes that might be responsible for these various emission features. However, the similarity of the line spectra of these objects to that of the solar chromosphere has led several workers to suggest that there may be deeper relationships, possibly connected to the widespread existence of magnetic fields and associated activity. A chromospheric "explanation" also seems plausible for the CaII and MgII resonance line emission cores that are present in many cool stars, but again there is no well-developed theory of chromospheric structure, or of the phenomena which produce chromospheres, in these stars.

II.D. VARIABLE STARS

Variable stars have always been a popular subject for astronomical observations, and each breakthrough in instrumentation has led rapidly to new data on the time dependence of variable-star properties. This wealth of observations, combined with tentative ideas regarding the physical origin of various kinds of variability, has allowed astronomers to develop a classification of variable stars. The taxonomy used nowadays has been relatively stable for about 30 years (Payne-Gaposchkin and Gaposchkin, 1938; Ledoux and Walraven, 1958; Cox, 1974), although there are still forms of variability that defy a straightforward classification. In general terms, variable stars are classified as follows:

I. Pseudo-variables (geometric variables)

eclipsing systems
magnetic rotators

II. The Great Sequence (pulsational variables)

- Cepheids and related types
- long-period variables
- semi-regular variables
- β Cephei and related types

III. Explosive and/or erratic variables

- supernovae
- novae
- symbiotic stars
- R Coronae Borealis types
- cataclysmic variables
- T Tauri types
- flare stars
- active binary systems (Algol, W UMa, RS CVn. . .).

It is, however, not always clear how variability should be classified. For example, one may ask whether the variability of T Tauri stars has an origin similar to that of the flare stars (Johnson, 1953), or whether it is due to eclipses by proto-planetary material (Gahm et al., 1974), or to a combination of these and other factors. Questions such as these highlight the close connection between the taxonomy and the theoretical interpretation of stellar variability.

In the past, the Cepheids and related types have been the main subjects for theoretical studies of stellar variability. Following a long debate on the cause of regular variability in the Cepheids, Eddington (1917) provided one of the first useful models of stellar pulsation. [It is interesting to note that Eddington (1926, Appendix II) identifies this question as the origin of his work on radiative equilibrium and stellar structure.] However, the pulsational theory was accepted only slowly, since it did not provide a convincing explanation of some aspects of the observations (Rosseland, 1949). Because of the importance of (1) the period-luminosity law in the determination of cosmic distances, and (2) pulsation morphology as a probe of interior structure, a great deal of work

has since been done on the theory of Cepheid pulsations (e.g., Ledoux and Walraven, 1958; Cox, 1974). Most of this work has concentrated on the dynamics of the stellar interior, and little work has been done on the response of realistic models of Cepheid atmospheres to the internal motions. Over the past decade, evidence has been accumulating for the presence of low-amplitude, nonradial pulsations in stars of many types and classes, and there is growing interest in theoretical models for this form of variability (Unno et al., 1979).

In contrast to the fairly advanced state of theory regarding radial and nonradial pulsations of stars, the origins of explosive and/or erratic variability are poorly understood. Although many conjectures have been made regarding the nature of variability of this kind, it is only in the past decade that quantitative modeling has begun. This new research has been prompted in part by the birth of X-ray astronomy as a subdiscipline, and has become associated with growing interest in phenomena such as mass transfer, accretion, and pulsed nuclear energy release. Although the theories that treat these problems have been rarely developed to the stage where they actually predict the atmospheric response, detailed comparisons with quantitative observations are now becoming possible in a few cases.

In concluding this section we must emphasize: all stellar variability (except strictly geometrical effects) vitiates the use of the classical model. Moreover, the changes required are not merely cosmetic, but they represent fundamental changes in the adopted thermodynamic framework.

II.E. THE SOLAR PARADIGM

These examples show how analogies between solar atmospheric structures or spectroscopic characteristics and similar features in other stars have often been exploited to help formulate and refine theories of stellar atmospheric structure. The central role played by

studies of the solar photosphere in the development of the classical model has been discussed already. Solar studies have played, and will continue to play, an equally important role in the development of models for nonclassical phenomena such as chromospheres, coronae, winds, and activity. It is therefore useful to review briefly the historical background of studies of the solar atmosphere.

Observational studies of the solar chromosphere, first with spectroscopes at eclipses (ca. 1868), and later with spectroheliographs (ca. 1891), coronagraphs, and filters (ca. 1930–1940), had led by 1940 to a reasonably complete qualitative account of chromospheric meteorology [Eddington (1927) seems to have introduced this possibly pejorative analogy between terrestrial and solar atmospheric changeability]. Perhaps because of a concentration on eclipse observations of the jagged solar limb, it was widely accepted in the period 1900–1940 that the key problem of chromospheric physics was to explain nonhydrostatic atmospheric extension. Milne's (1924) theory of radiation support of the calcium chromosphere, and McCreia's (1929) theory of turbulent support were designed to explain large chromospheric scale heights. With the recognition of the existence of unexpectedly high (on the basis of radiative equilibrium) temperatures in the chromosphere (ca. 1940–1950) and density scale heights not inconsistent with hydrostatic equilibrium, attention was directed away from the problem of chromospheric support and towards the problem of chromospheric heating. Since ca. 1950, most theoretical work on the chromosphere has involved either diagnostic studies (e.g., Thomas and Athay, 1961; Vernazza et al., 1981) or studies of heating processes (Jordan, 1981b); models of phenomena such as spicules are relatively undeveloped.

Until ca. 1940, studies of the solar corona were severely hampered by the failure to appreciate its extremely high electron temperature. After it was recognized that coronal temperatures were of the order of 10^6 K,

theoretical coronal physics concentrated on the coronal heating problem. There has been a close relationship between theories of coronal and of chromospheric heating with models based on shock dissipation of acoustic noise being heavily promoted until recently. The gradual acceptance of the existence of the solar wind (ca. 1930–1957) has now developed into an extremely important branch of astronomical and terrestrial research, which has seen in recent years increasing interest in coronal dynamics and structure (Zirker, 1981).

As can be seen from the subject matter in our companion volume "The Sun as a Star" (Jordan, 1981), the main thrust of contemporary research on the solar atmosphere is directed towards theoretical and observational studies of magnetic fields and their consequences. This research extends back to Hale's (ca. 1908) work on sunspot magnetic fields, and Bartels' (ca. 1932) work on terrestrial magnetic storms. As reviewed by Cowling (1953), many of the fundamental concepts of cosmic electrodynamics had been developed by ca. 1950, and the ensuring three decades have been devoted, in the main, to applications of these concepts. An interesting and critical review of the development of this branch of astrophysics has been given by Alfvén (1967). Many fundamental problems concerning the structure and evolution of solar magnetic fields, and the atmospheric response to magnetic fields and current systems, are still unsolved at this time. There has been a rapid growth of interest in these problems in the past few years, however, and there is growing evidence for widespread magnetic-related activity in many other stars (see Chapters 3 and 7).

From this brief history of the development of some aspects of solar physics, it is clear that studies of the Sun have often been used to formulate initial ideas about the atmospheres of other stars, and to test and verify these ideas with greater precision and speed than is possible in other stars. It is stimulating to conjecture that the changing emphasis in solar studies,

from “classical” (ca. 1920–1940), via “dynamic” (ca. 1940–1970), to “magnetic” (ca. 1970–present) will be reflected in a parallel, but delayed, change in the emphasis of stellar atmospheric studies.

III. RADIATION TRANSFER

The theory of radiation transfer is important in studies of stellar atmospheres for three distinct reasons:

- (1) Radiation emitted by the stellar atmosphere and detected at Earth provides almost all of the data we have on stars. The goal of spectroscopic diagnostics is to develop techniques to permit us to infer from such data various properties of the radiating atmosphere. Unfortunately, such inferences are not straightforward, and there are fundamental limitations on the amount of information that can be extracted, as well as fundamental ambiguities that can be resolved only by external hypotheses regarding the structure of the source.
- (2) Radiation is an important mode of energy transfer in most parts of most stellar atmospheres. A measure of the importance of radiation in energy transfer is the Boltzmann number,

$$Bo = \rho u C_p T_e / \sigma T_R^4, \quad (5-8)$$

where ρ is the density, u the bulk velocity, C_p the specific heat at constant pressure, σ the Stefan-Boltzmann constant, and T_e and T_R the electron and radiation temperatures, respectively. If we take u to be of the order of the sound speed, we may estimate that $Bo < 1$ throughout the entire atmosphere of most cool stars, from photosphere to corona. Radiation thus dominates the energy transfer, and small changes in the radiation flux can have profound effects

on the thermal and macroscopic kinetic energy content of the gas.

- (3) Radiation plays a key role in controlling the occupation numbers of the microscopic atomic states of the stellar atmospheric plasma. Gas densities are so low and radiation intensities are so high that radiative processes dominate many of the microscopic rate equations. The absence of thermal equilibrium in the radiation field that is a necessary consequence of the presence of an optical boundary in the atmosphere then leads immediately to non-equilibrium populations. This is the basic reason why non-LTE methods, with all their difficulties, should be used to describe stellar atmospheres, in both “classical” and “nonclassical” investigations.

The goal of spectroscopic studies of stellar radiation is to determine the physical properties of the radiating atmosphere. As discussed by Jefferies (1968, p. 200), there are two broad paths to this goal. Firstly, suppose that we know how to predict the emergent radiation field from an atmosphere of given physical structure (temperature, pressure, velocity, and so on). We could then proceed to postulate a model, predict the spectrum, and compare the predictions with observations. Any disagreement could be used to refine the physical model. This is called a synthetic approach. Alternatively, we could attempt to infer directly from the observations the properties of the gas. This is the analytic approach. In practice, most stellar spectroscopy is synthetic in character, primarily because the analytic problem is not well posed, and is in any case dependent in part on a prior understanding of the synthetic problem.

Synthetic and analytic approaches both involve essential ambiguities and uncertainties, since many different atmospheric configurations produce indistinguishable spectra.

Because of this, it is particularly desirable to ensure that the structure of any proposed atmospheric configuration is consistent with the “laws of nature,” but even when this is done, there are still an infinite variety of structures that can produce the same spectrum.

We are consequently led to ask the question: “Can we develop an approach to stellar spectroscopic diagnostics that can accommodate the essential uncertainties and ambiguities?” It seems that three sequential steps are involved in the affirmative answer to this question:

- (a) Spectroscopic detection of the existence of certain material in the stellar atmosphere and elucidation of the thermodynamic framework needed to describe its state,
- (b) spectroscopic determination of the quantity of material with certain thermodynamic attributes, and
- (c) investigations which reveal the space- and time-dependent *organization* of the different physical components of the atmosphere.

The sequence — existence, quantity, and organization — presents increasing diagnostic difficulty and increasing risk of ambiguity. The remainder of this section provides an account of the spectroscopic diagnostic techniques that are used to extract these characteristics from observations of stellar atmospheres.

We note firstly that astrophysicists distinguish between “thermal” and “nonthermal” radiation mechanisms from cosmic plasmas. Nonthermal radiation is generally produced by sources containing particles with strongly non-Maxwellian microscopic velocity distributions, while thermal sources contain distributions which deviate only slightly from a Maxwellian. The detection of nonthermal radiation from cool stars immediately provides important clues

to atmospheric structure, and we will discuss some relevant nonthermal mechanisms in Section III.B. However, thermal radiation is much more widely used as a diagnostic in cool stars, and most of the present section therefore concentrates on an account of the theory of thermal radiation, emphasizing those physical processes that are of greatest importance in controlling and/or diagnosing the atmospheric structure.

III.A. THERMAL RADIATION

An account of the theory of thermal radiation emitted by a stellar atmosphere is conveniently divided into two parts, one dealing with radiation transfer and the other with the microscopic physics of the interaction between radiation and matter. Insofar as the microscopic physics involves the nonlocal radiation field, these two parts are not independent. However, the use of the theory by an astrophysicist seeking to study the existence, quantity, and organization of matter in the atmosphere is best explained by emphasizing either one or the other of these parts.

III.A.1. TRANSFER EQUATION

The radiation transfer equation along a specified line-of-sight can be written in the form

$$\begin{aligned} \Omega \cdot \nabla I(\nu, \Omega, r, t) &= \kappa(\nu, \Omega, r, t)I(\nu, \Omega, r, t) + \eta(\nu, \Omega, r, t) \\ &= \kappa(\nu, \Omega, r, t)[I(\nu, \Omega, r, t) - S(\nu, \Omega, r, t)] \quad , \quad (5-9) \end{aligned}$$

where I is the specific intensity of the radiation field at a point r and time t , with frequency, ν , propagating in a direction specified by the vector Ω . The terms κ and η are, respectively, the absorption and emission coefficients, and the ratio $S = \eta/\kappa$ is the source function. These latter terms reflect the microphysics of the interaction between matter and radiation. This form of the transfer equation neglects time derivatives, which are not important in the present context (see Mihalas, 1978, pp. 490–510),

and refers only to unpolarized light. Polarization, which can be used as a diagnostic for magnetic and electric fields, and asymmetrical geometries, will not be discussed here.

According to Equation 5-9, the intensity emerging from a particular point r_o on the "surface" of the star in the direction Ω_o can be obtained from an integral

$$I^o(r_o, \Omega_o) = \int_{\ell_o}^{\infty} \eta(\ell) e^{-\tau(\ell)} d\ell$$

$$= \int_{\ell_o}^{\infty} S(\ell) e^{-\tau(\ell)} d\tau(\ell) \quad , \quad (5-10)$$

where ℓ measures distance along the line of sight. The optical depth is defined by:

$$d\tau(\ell) = \kappa(\nu, \Omega', r, t) d\ell \quad . \quad (5-11)$$

The intensity emerging from a particular line of sight depends on the distribution of the absorption coefficient and source function along the line of sight, from the surface to a point where the optical depth becomes large ($\tau \gg 1$) in the optically-thick case, or to a point where the emission coefficient becomes negligibly small in the optically thin case.

Because of the very small angular size subtended by stellar disks at the Earth, it is generally impossible to observe the intensity along individual lines of sight into the stellar atmosphere. Rather, an integral over a small area on the celestial sphere containing the entire stellar disk is measured, giving the flux:

$$F(\nu, t) = \int_{\text{disk}} I^o(\nu, \Omega, r_o, t) \Omega \, d\Omega \quad (5-12)$$

In attempting to discover the quantity and organization of matter in a stellar atmosphere, it is often assumed that the atmosphere is plane-parallel and laterally homogenous. In this case,

the emergent intensity depends only on the angle between the line of sight and the normal to the atmosphere, so that

$$F(\nu, t) = 2\pi \int_{-1}^1 I^o(\nu, \mu, t) \mu d\mu \quad , \quad (5-13)$$

where $\mu = \cos \theta$, and θ is the angle between the outward normal and the line of sight.

While a plane-parallel, laterally homogenous model atmosphere is conceptually and computationally convenient, Figure 5-1 shows that the atmosphere of at least one cool star, namely the Sun, is highly structured. Other direct evidence for structures in the atmospheres of cool stars includes images of supergiant disks (Lynds, Worden, and Harvey, 1976), observations of irregular circumstellar material near T Tauri stars (Joy, 1945) and around α Orionis (Honeycutt et al., 1980), time-varying discrete spectroscopic features seen during egress and ingress in binary systems such as ξ Aurigae (Wilson, 1957, Section 3), and regular modulation of the light curves of rotating stars due to asymmetric patterns of dark or bright material on their surfaces (Bopp and Evans, 1973; Vaughan et al., 1981).

A hotly debated issue in contemporary studies of stellar atmospheres is the general question whether such structures are dominant components of the atmosphere, or whether they represent only minor fluctuations about an underlying one-dimensional, radially stratified state. We would argue that it is unnecessary to decide between these alternatives at present. On the one hand, there is overwhelming evidence for the existence of lateral inhomogeneities, and strong evidence that these inhomogeneities themselves reflect fundamental physical processes. But on the other hand, there is also strong evidence for the almost ubiquitous existence of a universal pattern of gross, radial structure. It seems prudent to undertake research that seeks to understand *both* the origins of the gross radial patterns and the

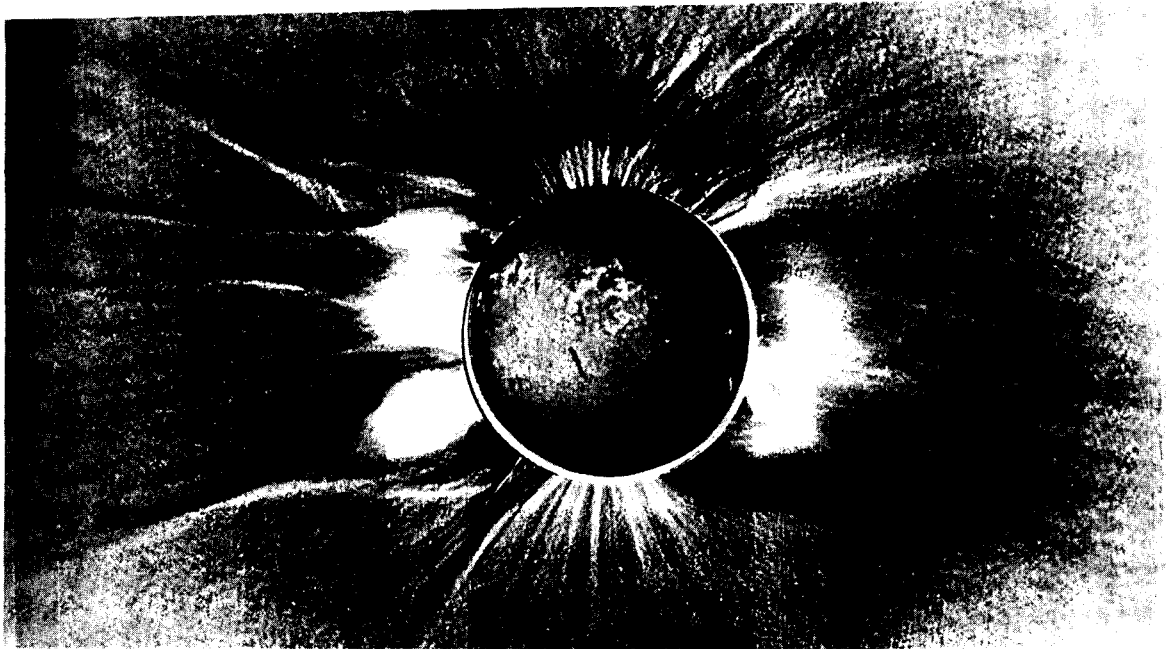
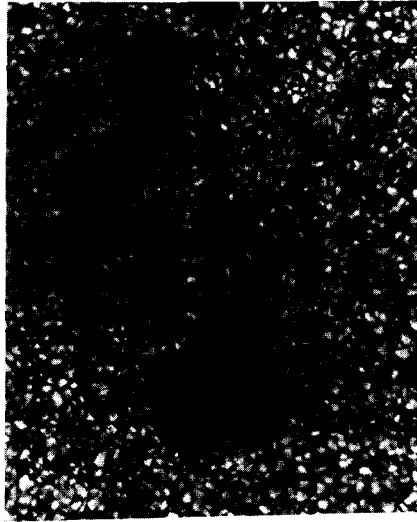


Figure 5-1. Photographs showing the inhomogeneous structure of the solar atmosphere. (Top left) Photograph of a new sunspot group emerging through the solar photosphere, taken in broad-band visible light. Granulation, thought to be a manifestation of convection, is apparent around the border of the picture: individual granules are about 2000 km in diameter. (Top right) Photograph of the solar chromosphere made through a narrow filter tuned to the $H\alpha$ line. The elongated objects are spicules, and the irregular structure at lower center is an active region. The solar limb is visible at the top. The spicules are about 10,000 km long. (Bottom) Photograph of the solar corona obtained in white light at an eclipse. The picture has been “dodged” to accentuate the streamers in the corona, and superimposed on a full-disk $H\alpha$ spectroheliogram.

Top figures are (c) AURA Inc., courtesy of Sacramento Peak Observatory. The bottom figure is courtesy of Dr. S. Koutchmy.

physical processes that produce the inhomogeneities. Ultimately, it is likely the two kinds of structure will be seen to have common origins.

Attempts to diagnose the form of the gross radial atmospheric structure and to detect atmospheric inhomogeneities are severely compromised by ambiguities caused by the integration of the radiation transfer equation along specified lines of sight, and by the flux integration over the stellar disk. Although the synthesis of emergent intensities and fluxes from atmospheres with specified organizations of opacity and emissivity (or more fundamental attributes) is now straightforward, the analytic problem of inferring the organization from the observations is in fact insoluble. Since fruitful astrophysical research must begin with observations (Eddington's "cloudbound" physicist notwithstanding) the very first step involves inherent ambiguities. It is, therefore, all too easy to begin on the wrong track.

III.A.2. EMISSION, ABSORPTION, AND SCATTERING PROCESSES

The physical conditions of the atmospheric plasma are impressed on the emergent radiation field by way of their influence on emission, absorption and scattering processes. Although a detailed account of the theory of these processes cannot be given here (see Mihalas, 1978), it will be useful to summarize the equations describing the scattering, emission, and absorption coefficients and to briefly indicate where the various processes are currently known to be relevant in the atmospheres of cool stars.

The extinction coefficient due to Thompson (or electron) scattering is

$$\kappa_\nu = n_e \sigma_e g_e(\Omega, \Omega'); \quad \sigma_e = \frac{8\pi e^4}{3m^2 c^4} \quad (5-14)$$

Here, n_e is the electron density, σ_e the electron-scattering cross-section, and g_e is the phase function. This formula ignores frequency

redistribution which occurs as a result of the thermal motion of the electrons. The extinction coefficient due to Rayleigh scattering by atoms or molecules of species s is

$$\kappa_\nu = n_s \cdot \sigma_e f_s \cdot \frac{\nu^4}{(\nu_s^2 - \nu^2)^2} g_s(\Omega, \Omega'), \quad (5-15)$$

where ν_s , f_s are respectively the frequency and oscillator strength of the scattering resonance of species s . The emission coefficient for these scattering processes is

$$\eta_\nu = \int \kappa_\nu I_\nu \frac{d\Omega}{4\pi} \quad (5-16)$$

In the photospheres of cool stars, Rayleigh scattering by the ground state of neutral hydrogen and by H_2 molecules is a significant, but not dominant, component of the extinction coefficient. In the ionized chromospheres and coronae of cool stars, electron scattering is again a significant, but usually not dominant, contributor to the extinction coefficient. Although the total electron-scattering optical thickness of the solar chromosphere and corona is only about 10^{-6} , diagnostics based on observations of the intensity and polarization of the electron-scattered K corona of the Sun have been an extremely important tool in solar coronal studies (Shklovskii, 1965). In the very massive ionized atmospheric regions in objects such as T Tauri stars, electron scattering may be an important opacity source if the column electron density $\int n_e d\ell > 10^{24} \text{ cm}^{-2}$.

The theory of free-free radiation (Bremsstrahlung) has been summarized by Brussard and van de Hulst (1962). If the process takes place as a result of free electrons with a Maxwellian velocity distribution (thermal Bremsstrahlung), the emission coefficient is

$$\eta_\nu = 4\pi \cdot \frac{8Z^3 e^6}{3m^2 c^3} \cdot \left(\frac{2\pi m}{3kT_e} \right)^{1/2} \cdot n_i n_e g(T_e, \nu) e^{-h\nu/kT_e} \quad (5-17)$$

where Z is the ionic charge and g is a gaunt factor. For such radiation the source function is given by the Planck function:

$$S_\nu = \frac{\eta_\nu}{\chi_\nu} = B_\nu(T_e) = \frac{2h\nu^3}{c^2}(e^{h\nu/kT_e} - 1)^{-1} \quad (5-18)$$

The corresponding absorption coefficient can be deduced from these two relations.

In the photospheres of cool stars, free-free processes associated with the H^- ion are a dominant component of the absorption coefficient redward of $1.5 \mu\text{m}$. Refined theoretical calculations of the free-free H^- absorption coefficient have been undertaken by Stille and Callaway (1970). Free-free emission from hydrogen (electrons-protons) is apparently responsible for the "thermal" radio emission (Wright and Barlow, 1975) which can be detected from extended ionized regions in stellar atmospheres. Free-free radiation from electrons moving in the electric fields of highly ionized species is also an important component of the X-ray radiation produced by the coronae of cool stars. Culhane and Acton (1970) give useful approximations to the X-ray emission coefficient from coronal plasmas, and Craig and Brown (1976) show how the spectral distribution of coronal emission can be used to infer some (but not all) of the properties of the emitting plasma.

The absorption coefficient for free-bound radiation (in one specified transition) can be written

$$\chi_\nu = n_1^* \alpha_\nu (b_1 - e^{-h\nu/kT_e}), \quad b_1 = n_1/n_1^* \quad (5-19)$$

where n_1 and n_1^* are respectively the actual and LTE populations of the bound level, and α_ν is the frequency-dependent cross-section. The term $e^{-h\nu/kT_e}$ represents stimulated emissions, and it is only important in the long wavelength radiation from relatively hot regions. The emission coefficient for bound-free radiation is

$$\eta_\nu = n_1^* \alpha_\nu (1 - e^{-h\nu/kT_e}) B_\nu(T_e) \quad , \quad (5-20)$$

where $B_\nu(T_e)$ is Planck's function. This result holds because the recombining electrons are supposed to possess a Maxwellian thermal velocity distribution. From Equations 5-11 and 5-12, it is clear that the bound-free source function is

$$S_\nu = \frac{n_1^* \alpha_\nu (1 - e^{-h\nu/kT_e}) B_\nu(T_e)}{n_1^* \alpha_\nu (b_1 - e^{-h\nu/kT_e})} \approx \frac{B_\nu(T_e)}{b_1} \quad , \quad (5-21)$$

where the approximation holds if stimulated emissions are neglected. This result has been used in studies of the solar Lyman continuum, (Thomas and Athay, 1961; Noyes and Kalkofen, 1970), where there are very large departures of free-bound radiation intensities from LTE values because b_1 is very large.

In the photospheres of cool stars, bound-free absorption by the H^- ion dominates the opacity in the visible and near-IR parts of the spectrum. Empirical studies of the frequency dependence of the photospheric continuum opacity (mostly using solar limb-darkening data) and the subsequent identification of the absorber as H^- (Wildt, 1939) were key stages in the refinement of the classical theory of stellar atmospheres. Bound-free absorption in neutral hydrogen is a significant continuous opacity source in stellar chromospheres, and it has proved to be a powerful and reliable diagnostic of physical conditions in the low solar chromosphere (Thomas and Athay, 1961). It is unfortunate that this diagnostic is not accessible in most other stars, since eclipses are required to exploit the technique. The continuous EUV spectrum of cool stars is dominated by free-bound chromospheric radiation from species such as SiI, CI, FeI, MgI, and AlI. The atomic parameters of most of the relevant transitions are summarized by Vernazza et al. (1973, 1976, 1981b); the ionization and excitation state of these species generally departs significantly from LTE. Free-bound

transitions of highly ionized species are also important in coronal X-ray emission.

The absorption coefficient for bound-bound (line) radiation is

$$\kappa_\nu = (n_\ell B_{\ell u} - n_u B_{u\ell}) \frac{h\nu}{4\pi} \phi_\nu(\Omega), \quad (5-22)$$

where n_ℓ and n_u are respectively the lower and upper level populations, $B_{\ell u}$ and $B_{u\ell}$ are Einstein coefficients, and $\phi_\nu(\Omega)$ is the absorption profile. The term $B_{u\ell}$ represents stimulated emissions: its inclusion in this way is only approximate, but it is almost always small (see Oxenius, 1965, for a more detailed account).

The emission coefficient for line radiation is

$$\eta_\nu = n_u A_{u\ell} \Psi_\nu(\Omega), \quad (5-23)$$

where $A_{u\ell}$ is another Einstein coefficient and Ψ_ν is the emission profile. The source function is therefore:

$$S_\nu = \frac{n_u A_{u\ell}}{n_\ell B_{\ell u} - n_u B_{u\ell}} \cdot \frac{\Psi_\nu}{\phi_\nu} \quad \text{or} \quad (5-24)$$

$$S_\nu = \frac{2h\nu^3}{c^2} \left(\frac{n_\ell g_u - 1}{n_u g_\ell - 1} \right) \cdot \frac{\Psi_\nu}{\phi_\nu} \quad (5-25)$$

The importance of bound-bound transitions to astrophysical spectroscopy lies in the fact that the strengths and shapes of spectral lines sensitively reflect the physical conditions in the emitting atmosphere. In many cases, the line strengths are influenced principally by atomic parameters and by level populations that are in turn often controlled by the electron temperature, the density, and the abundance of the elements. The shapes are principally influenced by the distribution of the absorption profile along the line of sight, which in turn reflects atomic properties (natural damping), atmospheric densities (resonance, van der Waals, and Stark damping), and Doppler broadening and shifting produced by thermal motions, gas-

dynamic motions, and stellar proper motion. Examples of the application of these diagnostics will be discussed below. We cannot develop the theory more fully here, and the reader is referred to Unsöld (1955), Aller (1963), or Mihalas (1978) for extensive discussions of its physical basis.

III.A.3. INTERACTION BETWEEN RADIATION AND MATTER

The emission and absorption coefficients discussed above contain two kinds of factors: physical or atomic constants, and occupation numbers. The constants do not depend on physical conditions in the atmosphere, but the occupation numbers do. The evaluation of occupation numbers in the particular conditions of a stellar atmosphere is often a challenging task, but one that must be undertaken if we are to study the quantity and organization — rather than just the existence — of material with certain attributes.

One technique that has been used extensively to evaluate occupation numbers relies on the assumption of local thermodynamic equilibrium (LTE). The occupation numbers are then determined by the constraints of Maxwell-Boltzmann-Saha equilibrium, evaluated using the local electron temperature. The radiation field $I_\nu(\Omega)$ is allowed to depart from equilibrium as a result of transfer, but apart from a possible contribution from “pure scattering,” the source function has its equilibrium (Planckian) value.

Throughout the period 1920–1960, many attempts were made to justify the use of LTE in studies of stellar photospheres (see, e.g., Woolley and Stibbs, 1953). These attempts were linked to the struggle to provide a satisfactory theory for the formation of strong spectral lines whose measured central intensities were known to be much too low to have been formed by an LTE “pure absorption” process. A clearer picture of the interaction of matter and radiation in stellar atmospheres and of the degree of

departure from LTE has emerged over the past 30 years with the introduction of non-LTE techniques.

As emphasized by Thomas (1965), the accurate evaluation of occupation numbers requires a solution of the coupled rate equations describing the various paths by which atomic levels are populated and depopulated. Because the rates of certain processes depend on the intensity of the radiation field which is out of equilibrium as a result of transfer effects, the occupation numbers depart from their LTE values. There are close connections between the radiation field, the transfer equation, the rate equations, and the emission and absorption coefficients.

To illustrate this connection between matter and radiation in the general (non-LTE) case, we consider a simple example involving a model atom with two bound levels and a continuum. Thomas (1957) showed that the general form of the line source function S_L corresponding to a bound-bound transition in such an atom is

$$S_L = \frac{\int J_\nu \phi_\nu d\nu + \epsilon B_\nu + \eta B^*}{1 + \epsilon + \eta} \cdot \frac{\Psi_\nu}{\phi_\nu}, \quad (5-26)$$

where Ψ_ν , ϕ_ν are respectively the normalized emission and absorption profiles, and J_ν is the angle-averaged monochromatic intensity. The term ϵ ($\approx C_{u\ell}/A_{u\ell}$) is the ratio of the rate of collisional to radiative decay from the upper level, and B_ν is the Planck function. The terms η and ηB^* contain the rate coefficients connecting the upper and lower levels to the continuum, and represent the creation or destruction of photons in the line by radiative or collisional processes involving other bound levels or the continuum. Thomas (1957) showed that scattering is almost completely non-coherent in the Doppler core of a spectral line, so that in this case one has $\Psi_\nu/\phi_\nu \approx 1$ and S_L independent of frequency.

Numerically the term $\int J_\nu \phi_\nu d\nu$ is generally dominant in the expression for the source function. However, the mean intensity J_ν appearing in this term can only be obtained by solving the radiation transfer equation

$$\mu \frac{dI_\nu}{d\tau} = I_\nu - S_L, \quad (5-27)$$

using expression 5-26 to specify the source function.

The resulting integro-differential equation implies that the value of the source function at any position in the atmosphere ultimately depends on the distribution of the source and sink terms ϵB , ηB^* , ϵ , and η throughout the atmosphere. These depend in turn on the distribution of electron density, temperature, and continuum intensities. There is, therefore, only a rather tenuous connection between the organization of the material in the atmosphere and the information ultimately available to the terrestrial observer. The reader is referred to Thomas (1965), Jefferies (1968), Athay (1972), and Mihalas (1978) for a detailed account of this "tenuous connection" in various astrophysical situations, and with more realistic atomic models.

Powerful numerical techniques have been developed to treat the complicated systems of nonlinear equations which arise when non-LTE problems are considered in practical applications. Because the application of these techniques generally requires access to large computers, they have not been employed universally. Nevertheless, sufficient work has been done to provide insight into how and where non-LTE effects influence the radiation fields of stellar atmospheres. Studies of particular importance to cool stars include Thomas and Athay (1961 - solar H); Lites (1973 - solar FeI) — see also Lites and Cowley (1974); Vernazza et al. (1973, 1976, 1981b); and the work on stellar chromospheres summarized by Linsky (1980, Table 1) and in Chapter 3.

It may be useful at this point to give some perspective on the impact of non-LTE methods in work on stellar atmospheres. Note firstly that it would have been possible for non-LTE diagnostics to develop from studies of RE/HSE photospheres, but this did not happen. Rather, non-LTE methods were developed to study the decidedly non-HSE planetary nebulae, and the decidedly non-RE solar chromosphere. In the latter case, the character of the elusive layer lying between the solar photosphere and corona could only be satisfactorily understood by combining non-LTE diagnostics with an investigation of departures from RE and HSE (e.g., Thomas and Athay, 1961).

With the passage of time, non-LTE methodology has been increasingly accepted and applied with significant impact in many other areas, including RE models of the photospheres of hot stars (Auer and Mihalas, 1969), strong lines in stellar chromospheres (Linsky, 1980), and the violent ejection products found in supernovae (Hoffleich, private communication). Often, the non-LTE methods have led to crucial revisions of theoretical models, and hence to major reinterpretations of observations. At present, we are beginning to see the development of models linking non-LTE radiative theory with rarefied gas dynamics, and it is likely that the insights gained by these studies will provide new interpretations of observations of stellar atmospheric dynamics (see also Mihalas, 1974).

The discussion in this section has concentrated on the interaction between matter and radiation in optically thick and relatively dense stellar photospheres and chromospheres. The importance of non-LTE effects has also been recognized for a long time in low density, optically thin, cosmic plasmas such as planetary nebulae and the solar corona. The increasing importance of X-ray and EUV space observations has recently promoted more interest in non-LTE diagnostics for such optically thin plasmas, where the radiation transfer problem becomes much simpler. Reliable diagnostics

based on these observations require improvements in the theoretical and empirical determination of atomic constants, and in the theory of statistical equilibrium in moving, structured atmospheres.

III.B. NONTHERMAL RADIATION

Flares and other manifestations of solar activity produce nonthermal radiation in γ -rays, X-rays, microwaves, long radio waves, and possibly in the optical continuum (white-light flares). The monographs by Svestka (1976) and Melrose (1980) provide descriptions of the observational data and the basic physical mechanisms of nonthermal solar radiation.

Nonthermal γ -rays and hard X-rays from cool stars other than the Sun have not yet been detected. This failure presumably reflects low instrumental sensitivity and limited time coverage on promising objects. However, strong transient nonthermal microwave (~ 6 cm) emission has been detected from many binary systems containing a cool component (Spangler et al., 1977), in particular from RS CVn systems (Feldman, 1983). The star χ^1 Ori has been detected as a steady nonthermal microwave source with the very large array (VLA) telescope (Gary and Linsky, 1982), and we might expect further detections of this kind with this extremely sensitive instrument.

On the basis of its polarization, spectrum, and rapid time variability, the microwave radiation from RS CVn systems has been interpreted as gyrosynchrotron radiation, analogous to solar moving Type IV bursts (Feldman et al., 1978). This nonthermal mechanism involves mildly relativistic electrons ($E \sim \gamma mc^2 \sim 500$ keV) gyrating about a magnetic field and radiating in harmonics of the gyrofrequency $f_G(\text{MHz}) = 2.8 B$ gauss (10^4 gauss = 1 tesla), where B is the field strength. This identification of the radiation mechanism from flares in RS CVn systems leads to estimates of source size and magnetic field strength. For a flare on the system RS CVn itself, Feldman et al. (1978)

deduce a size of $\sim 5 \times 10^{11}$ cm, and a field strength of 50 gauss. The source size is approximately the separation of the binary system. The observation of such nonthermal radiation provides compelling evidence for the existence of structured and unstable magnetic fields in these active systems, similar to those in the solar corona but leading to much more intense nonthermal radiation.

It should be emphasized that if the Sun were placed at stellar distances, none of its variety of nonthermal radio emissions could be detected with present-day instruments because of their limited sensitivity. The RS CVn systems are detected only because their radiation intensity is many orders of magnitude larger than that of solar bursts. There is evidence that some T Tauri stars are microwave sources (Chapter 4), but this radiation is usually identified as thermal bremsstrahlung from an extended atmosphere (Wright and Barlow, 1975).

IV. CLASSICAL ATMOSPHERIC MODELS

The structure of a classical model of the atmosphere of a cool star is determined by the simultaneous solution of the equations of radiative-convective equilibrium (RCE)

$$\nabla \cdot (\mathbf{F}_R + \mathbf{F}_C) = 0 \quad , \quad (5-28)$$

and hydrostatic equilibrium (HSE):

$$\nabla (P_g + P_c) = -\rho g \quad (5-29)$$

In these equations, \mathbf{F}_R is the radiative flux, \mathbf{F}_C the convective flux, P_g and ρ the gas pressure and density, and P_c the "turbulent pressure" due to Reynolds stresses in the convection. To solve these equations, one needs to specify the chemical composition of the model atmosphere, and to define procedures for evaluating the plasma properties ($\chi_\nu, \eta_\nu, P_g, \rho, \dots$) in terms of this specified composition and the physical processes that are assumed to occur in the model (e.g., the description of convec-

tion, and the choice between LTE or non-LTE radiation transfer theory).

The present section discusses some of the physical processes involved in RCE and HSE models for cool stars. The objective is to provide sufficient background to allow a critical comparison between (a) predictions based on classical models of various degrees of sophistication and (b) observed properties of stars. In particular, we want to be able to classify any failings of classical models that are uncovered into one of two classes: those in which the deficiency could apparently be rectified by improved modeling techniques and greater attention to detail within the limits of RCE and HSE, and those which are apparently due to fundamental problems in the assumptions underlying the classical model.

In discussing the physics of RCE/HSE models we follow the approach of Gebbie and Thomas (1970, 1971), using the concept of a temperature control bracket. In this way we can systematically describe a hierarchy of models of increasing levels of sophistication, and thereby compare and contrast the errors and uncertainties in the different models. Attention will be focussed mainly on the condition of radiative equilibrium (RE), since this is the process that has received the greatest diversity of treatment by modelers, and the one involving a large number of subtle effects. The condition of hydrostatic equilibrium has rather straightforward consequences in classical models, while the condition of convective equilibrium (CE) involves extremely complex and very poorly understood physical processes and consequences which will be more fully discussed in Chapter 6.

Gebbie and Thomas (1971) write the equation describing radiative energy balance in the form:

$$4\pi n_c \int_0^\infty \alpha_{ff}^* (J_\nu - B_\nu) d\nu \quad +$$

$$4\pi \sum_j (n_j \int_{\nu_j}^{\infty} \alpha_{jc} J_{\nu} d\nu - n_j^* \int_{\nu_j}^{\infty} \alpha_{jc}^* B_{\nu} d\nu) -$$

$$\sum_i n_i A_{ul} h\nu_i [\text{NRB}]_i + e_m = 0 \quad (5-30)$$

In this equation the first three terms are, respectively, the flux divergences in the free-free continuum, the free-bound continua, and the lines, while the fourth represents any non-radiative energy flux divergence which is present. The quantities denoted by α represent cross-sections, while those denoted by n are population densities. The asterisk * denotes LTE quantities, while [NRB] is the net radiative bracket, $1-J/S_L$. Equation 5-30 can be written in the form

$$\sum_j \frac{E_{Bj}}{N_{Bj}} P_j + E_B P_{ff} =$$

$$\sum_j \left(\frac{E_{Jj}}{N_{Jj}} + \Delta \right) (b_j \frac{N_{Jj}}{N_{Bj}}) P_j + E_j P_{ff} \quad , \quad (5-31)$$

where

$$E_J = \int_0^{\infty} \alpha_{ff}^* J_{\nu} d\nu, \quad E_{Jj} = \int_{\nu_j}^{\infty} \alpha_{jc} J_{\nu} d\nu ,$$

$$N_{Jj} = \int_{\nu_j}^{\infty} \alpha_{jc} J_{\nu} d\nu / h\nu ,$$

$$E_B = \int_0^{\infty} \alpha_{ff}^* B_{\nu} d\nu, \quad E_{Bj} = \int_{\nu_j}^{\infty} \alpha_{jc}^* B_{\nu} d\nu ,$$

$$N_{Bj} = \int_{\nu_j}^{\infty} \alpha_{jc}^* B_{\nu} d\nu / h\nu \quad ,$$

$$\Delta = \frac{e_m - e_L}{4\pi \sum_j n_j N_{Jj}} \quad ,$$

$$e_L = \sum_j n_j A_{ul} h\nu_i [\text{NRB}]_i \quad ,$$

$$P_j = \frac{n_j^* N_{Bj}}{\sum_j n_j^* N_{Bj}} \quad ,$$

$$P_{ff} = \frac{n_c}{\sum_j n_j N_{Bj}} \frac{n_c}{n_j^* N_{Bj}}$$

The E-integrals measure the total energy absorbed, and the N-integrals the total number of photons absorbed.

A simple and illuminating form of Equation 5-31 is obtained by neglecting free-free processes, and including only one bound-free continuum. One finds

$$E_B / N_B = (E_J / N_J + \Delta) (b N_J / N_B) \quad , \quad (5-32)$$

where $b = n/n^*$ is a non-LTE departure coefficient. In this equation the LHS is an explicit function of the electron temperature. The first factor on the RHS, $E_J / N_J + \Delta$, represents the effect of radiation transfer. It is the rate at which energy is directly supplied to the system (by radiation in the continuum and lines, and by nonradiative heating), normalized to the rate of photoionization. The second factor,

$$b N_J / N_B = [\text{TCB}] \quad (5-33)$$

is the temperature control bracket. It reflects the way in which the microscopic physics of the interaction between radiation and matter controls the level populations, and hence influences the temperature. Of course the factorization of the RHS into ‘‘transfer’’ and ‘‘population’’ effects is only a first-order division, because the size of the population effect is ultimately determined by transfer. With these equations at

hand, we can now consider a series of stellar atmospheric models which illustrate the physics of RCE models.

IV.A. GRAY, LTE MODELS

In a gray atmosphere there are no lines, and the absorption coefficient is independent of frequency. In LTE, $b = 1$. The energy equation for such an atmosphere may thus be written

$$E_B = E_J \quad ,$$

or

$$\frac{\sigma T_e^4}{\pi} = \int B_\nu d\nu = \int J_\nu d\nu \quad (5-34)$$

The temperature distribution $T_e(\tau)$ is determined by the local mean intensity, which in turn is determined by a solution of the radiation transfer equation. The solution of this problem is

$$T_e^4(\tau) = \frac{3}{4} T_{\text{eff}}^4 [\tau + q(\tau)] \quad , \quad (5-35)$$

where $q(\tau)$ is a monotonically increasing function of τ satisfying $q(0) = 0.58$ and $q(\infty) = 0.71$. The temperature decreases monotonically with decreasing optical depth, to a boundary value of $0.81 T_{\text{eff}}$. This decrease reflects the decrease in the *quantity* of radiation due to the presence of an optical boundary. Given this equation for $T_e(\tau)$, the equation of hydrostatic equilibrium can be readily integrated if the pressure and temperature dependence of the opacity is known (e.g., Schwarzschild, 1906; Eddington, 1926, Section 233). For all classical models of cool stars this integration shows that the atmosphere is compact, with the density scale height $H_\rho \ll R^*$. This conclusion is not changed by any refinements of the atmospheric model within the constraints of RCE and HSE.

Although the LTE gray model has been superseded, it formed the basis of many of the

early fundamental studies on classical atmospheres. For example, Schwarzschild's (1906) work on convective-radiative equilibrium was based on a simple solution of the gray problem, and the identification of the importance of H^- opacity in the Sun was based on the use of the gray model as a reference structure (see Chandrasekhar, 1960, Section 80.3).

IV.B. GRAY, NON-LTE MODELS

Consider again a gray absorption coefficient, in an atmosphere where the population n_1 of the single bound level is determined by the rate equation

$$n_1 \left[\int J_\nu d\nu / h\nu + n_e q_{c1} \right]$$

$$= n_1^* \left[\int \alpha B_\nu d\nu / h\nu + n_e q_{c1} \right] \quad ,$$

$$b_1 = \frac{N_B + n_e q_{c1}}{N_J + n_e q_{c1}} \quad (5-36)$$

Here, $n_e q_{c1}$ is the collisional ionization rate. When collisions dominate ($n_e q_{c1} \gg N_B, N_J$), then $b_1 = 1$, and we have the LTE case discussed above. When collisions are unimportant, we have

$$b_1 = N_B / N_J \quad , \quad (5-37)$$

so that

$$E_B = E_J [b_1] \quad (5-38)$$

An approximation for E_J and N_J in the outer layers of the atmosphere ($\tau < 0.1$) is obtained by setting $J_\nu = 0.5 B_\nu(T_{\text{eff}})$, so that the temperature and departure coefficient become

$$T_e(0) = T_{\text{eff}}; \quad b_1(0) = 2 \quad (5-39)$$

In the limit of low collision rates we therefore find a non-LTE boundary temperature which is about 25% higher than in the LTE case. The

detailed structure of a non-LTE gray model depends on the run of collision rate with depth, and therefore on the pressure balance and the details of the ionization equilibrium. The possibility of a non-LTE temperature rise in the outer parts of the solar atmosphere was first noted by Cayrel (1963 — see also Cram, 1978), and there has been vigorous debate over the question whether such a rise contributes to the temperature rise in the solar chromosphere. Many workers now agree that the non-LTE temperature rise is suppressed by line blanketing (Athay, 1981), but nevertheless the effect is more than a curiosity, since it represents a direct manifestation of the change in control of the atmospheric state parameters from the quantity or density of radiation in the deep layers to the quality or color in the outer layers. This effect could introduce significant nonlocal, non-equilibrium behavior in dynamical processes in stellar atmospheres, through nonlocal control of the equation of state and the radiative flux divergence.

IV.C. NONGRAY LTE MODELS

There are two kinds of nongray effects that are important in the photospheres of cool stars: those arising from frequency-dependence of the continuum absorption coefficient, and those due to the lines. Let us first consider a simple model which illustrates the effect of a nongray continuum.

Following Rosseland (1936, p.116), suppose that the absorption coefficient is confined to the ultraviolet, and has the form:

$$k_\nu \sim \nu^{-3}, \quad \nu > \nu_m \quad (5-40)$$

The equation of radiative equilibrium, $E_J = E_B$, then gives an implicit equation for the boundary temperature T_o :

$$\frac{T_{\text{eff}} - T_o}{T_o} = \frac{kT_{\text{eff}}}{h\nu_m} \ell n \left(\frac{2T_o}{T_{\text{eff}}} \right) \quad (5-41)$$

For increasingly high cut-off frequencies ν_m , this relation implies that T_o becomes arbitrarily close to T_{eff} . This form of opacity thus leads to an elevated boundary temperature relative to the gray case. In practice, a nongray absorption coefficient may change the temperature distribution in either direction, depending on the relative frequency distribution of the absorption and emission coefficients. Gebbie and Thomas (1970) have estimated the effects of departures from grayness in the solar continuum. They conclude that the nongrayness in the absorption coefficient in the outer parts of the photosphere (due to H^- ions and H bound-free processes) lowers the boundary temperature by only a few percent relative to a gray model.

In an LTE atmosphere, spectral lines influence the temperature distribution of a radiative equilibrium atmosphere in two ways: backwarming and surface cooling. Backwarming results from the blocking effect of the lines, which simply increases the mean absorption coefficient and thereby drives up the temperature gradient so that the same radiative flux can be transported. In terms of our unified model, backwarming can be explained by noting that the equation of radiative equilibrium basically determines the temperature distribution as a function of Rosseland optical depth, $T_e(\tau_R)$. When lines are added, the Rosseland optical depth at any specified physical depth increases, and so the temperature at that physical depth is elevated. An additional modification to the atmospheric temperature structure $T_e(\tau_R)$ is also produced, because the lines change the frequency dependence of the internal radiation field.

Surface cooling is represented by the E_L term in Equation 5-31. The physical behavior of the term may be described by considering the equation of radiative flux divergence in a spectral line

$$\frac{1}{4\pi} \frac{dF}{dh} = \frac{h\nu}{4\pi} [(n_l B_{lu} - n_u B_{ul}) - n_u A_{ul}]$$

$$\begin{aligned}
&= \frac{h\nu}{4\pi} n_u A_{u\ell} [1 - \bar{J}/S_L] \quad (5-42) \\
&= \frac{h\nu}{4\pi} n_u A_{u\ell} [\text{NRB}] \quad ,
\end{aligned}$$

where $S_L = n_u A_{u\ell} / (n_\ell B_{\ell n} - n_u B_{u\ell}) (= B_\nu(T_e)$ in LTE). The net radiative bracket therefore measures the imbalance between emission and absorption in the line, or the net flow of energy between the radiation field in the line and the thermal electrons. The particular value of NRB depends on J , the frequency-integrated mean intensity in the spectral line. This quantity depends in turn on the temperature stratification of the atmosphere and on the parameters affecting the line formation. Any one line may therefore heat or cool the atmosphere at any specified depth, but the main overall effect of spectral lines is a marked tendency to cool the surface layers.

Nongray, line-blanketed, LTE, classical atmospheric models are widely used, and have been produced by methods which apply increasingly refined numerical methods and improved spectral line data. The enormous number of spectral lines that appear in the spectra of cool stars can be treated by a variety of LTE sampling techniques (e.g., Gustaffson et al., 1975; Kurucz, 1979) and a compilation of theoretical spectral line data is available (Kurucz and Peyremann, 1975). Line-blanketed LTE models for cool star photospheres are now quite sophisticated, although uncertainties remain in the UV opacity (160–400 nm), probably related to a haze of weak lines (Sacotte and Bonnet, 1972), and in the effects of certain IR molecular features (CO and H₂O in particular).

IV.D. NONGRAY, NON-LTE MODELS

The line blanketing processes described above also occur when non-LTE theory is used, although the difference between the sizes of LTE and non-LTE blanketing effects is often

hard to predict. For example, two non-LTE effects compete to determine the net change in backwarming: the equivalent width of the blocked continuum generally increases as a result of noncoherent scattering, while the nonlocal control of the mean intensity \bar{J} inside the line allows the influence of the optical boundary to be felt deeper in the atmosphere. The net result of the two competing processes is small in most cases (Athay and Skumanich, 1968), and can be determined only by calculation.

Non-LTE effects on surface cooling are more easily predicted, at least for a collision-dominated line. For such a line, the [NRB] is given by (Thomas, 1965, p.51):

$$\begin{aligned}
[\text{NRB}] &= 1 - \bar{J}/S_L \\
&= \epsilon(B - \bar{J}) / [(1 - \epsilon)\bar{J} + \epsilon B] \quad (5-43)
\end{aligned}$$

Since $\epsilon \ll 1$, the [NRB] is reduced by a factor of order ϵ relative to the LTE case, so that the tendency for surface cooling is markedly reduced by this non-LTE effect. The reduction in the cooling effect occurs because most photons that escape in a non-LTE line have been multiply scattered; only a few result from collisional decay and hence directly cool the electron thermal distribution. Athay (1970a) has argued that a non-LTE increase in the line opacity often compensates for the reduction in the [NRB]: this is equivalent to increasing the population factor n_u in Equation 5-42. Calculations for specific species in specific model atmospheres are ultimately the only reliable way to obtain quantitative estimates of the effects of non-LTE blanketing (Athay and Skumanich, 1968).

In addition to the backwarming and surface cooling effects which are transfer phenomena common to both LTE and non-LTE models, non-LTE blanketing introduces further atmospheric heating or cooling through the population effects implied by the temperature control bracket. In particular, the theoretical value of

the [TCB] for the lower bound levels of hydrogen depends on the specific atomic model used in a non-LTE study. Thus, the introduction of non-LTE transfer in, say, $H\alpha$ changes the [TCB] in the layers where the 2-3 transition passes out of detailed balance, and this population effect leads to atmospheric heating or cooling. Note that population effects due to spectral lines (as opposed to continua, which were discussed above) are felt only when line transfer influences the [TCB] in the continua that actually carry the bulk of the radiative flux. In the photospheres of cool stars, where H^- is the dominant opacity, there cannot be a large population effect due to lines, since bound-bound transitions in H^- are irrelevant. However, indirect population effects due to the non-LTE ionization equilibrium in important electron-donor minority species (e.g., Si, Fe, K, Mg...) can occur, and require further study.

Most studies of nongray non-LTE classical models have referred to hot stars (e.g., Auer and Mihalas, 1969; Gebbie and Thomas, 1971). Athay's (1970a) work on the structure of the solar photosphere is a unique and fundamentally important study of non-LTE line blanketing in a cool star. However, the numerical results of Athay's work depend on a number of currently untested assumptions (e.g., neglect of population effect, simplified atomic models, neglect of molecules), and no final conclusions may be drawn from the similarity between the temperature distribution in Athay's model and that in LTE line-blanketed models. In particular, LTE models necessarily involve extremely low boundary temperatures (< 3500 K), while Athay's model predicts an isothermal boundary at ≈ 4300 K, a fact which has often been overlooked when comparisons have been made between LTE and non-LTE models.

IV.E. CONVECTION

The development of ideas concerning the relative importance of convective and radiative energy transport in the photospheres of cool

stars has been a slow and difficult task, and even today the problem is by no means solved. Early work on stellar models was based on polytropes, whose "adiabatic" temperature distributions implied convective transport. However, Schwarzschild (1906) derived a criterion for the convective stability of a radiative-equilibrium atmosphere which led him to conclude that the solar atmosphere would be convectively stable. But Unsöld (1931) pointed out that in certain circumstances the ratio of specific heats $\gamma = C_p/C_v$ in an ionizing gas could fall below the critical value of 4/3 found by Schwarzschild, and therefore Unsöld concluded that there would be a "hydrogen convection zone" in the outermost layers of the solar envelope.

The question of the relative importance of convective and radiative energy transfer in the solar photosphere was subsequently addressed on several occasions. For example, by inverting limb-darkening observations, Plaskett (1936) inferred that convection produced marked changes in the temperature distribution in layers $\tau < 1.3$, in contradiction to an earlier study by Milne (1922) which had apparently confirmed the theory of radiative equilibrium. Woolley (1941) used a crude model of convection to show that Plaskett's result was certainly in error, and this theoretical approach was refined by Vitense (1953) to provide a phenomenological model of convective energy transport based on the mixing-length theory. This approach, which is used in most contemporary theoretical studies, can be described as follows.

In a convecting medium, the mean convective flux can be written as (Gough and Spiegel, 1977)

$$F_c = \frac{1}{4} \rho C_p \left(\frac{g\delta}{T} \right)^{1/2} \ell^2 \beta^{3/2} \quad , \quad (5-44)$$

where β is the superadiabatic lapse rate

$$\beta = - \left[\frac{\partial T}{\partial z} - \frac{1}{\rho C_p} \frac{\partial P}{\partial z} \right] \quad (5-45)$$

The parameter δ is the gradient $-(\partial \ln \rho / \partial \ell \text{ in } T)_p$, while ℓ is the mixing-length, which is usually introduced in the form

$$\ell = \alpha H_p, \quad (5-46)$$

where H_p is the pressure scale height, and α is a constant. In an RCE model, the energy equation is

$$\nabla \cdot (\mathbf{F}_R + \mathbf{F}_C) = 0, \quad (5-47)$$

where \mathbf{F}_C is computed from (Equation 5-44) wherever the atmosphere is found to be convectively unstable by Schwarzschild's test ($\beta > 0$).

Gough and Spiegel (1977) have discussed the validity of Equations 5-44 through 5-46, pointing out that these mixing-length formulae (or their possible refinements) are based on rough, order-of-magnitude estimates, and that the physical arguments supporting them are based on imprecisely defined models. But Gough also points out that there are bleak prospects for significant improvements in the near future, and, moreover, that in some problems the uncertainties in the theory may not be critical (see also Gough and Weiss, 1976). Unfortunately the deficiencies of mixing-length theory are most apparent in the outer envelopes of cool stars, particularly at the interface between the convective envelope and the radiative atmosphere, and these are precisely the layers where we are seeking a reliable boundary condition for atmospheric studies. We shall discuss the gas dynamics of convection further in Chapter 6, emphasizing the dynamical behavior of the convection-radiation interface and the role of convection as a source of atmospheric motions.

IV.F. COMPUTING CLASSICAL MODELS

The art of computing classical models of the atmospheres of cool stars has been highly refined, although the challenge of non-LTE line

blanketing has not yet been solved. To give the reader perspective on the techniques used and, more importantly, the problems encountered in these computations, we critically summarize some recent work on classical models for cool-star photospheres by Kurucz (1979) and Gustaffson et al. (1975). The latter work provides a particularly lucid account of the methods and problems, and the quotations in the ensuing discussion are taken from it.

The basic assumptions in these models are "plane-parallel stratification in homogeneous stationary layers, hydrostatic equilibrium, and LTE." The plane-parallel assumption can be checked and it is found to introduce errors < 50 K at $\tau = 10^{-2}$ in a very low gravity model with a $\log g = 0.75$. The error is even smaller in models with higher gravities. The other assumptions are harder to check and their implications are more uncertain. For example, the models are almost always calculated with microturbulence included in the line broadening, in a crude attempt to model "dynamical effects." Fortunately, the changes in model structure introduced by the microturbulence are usually small.

The model calculations require that the abundances of some 10 elements be specified, since in cool stellar photospheres many of the electrons come from "metals." These elements participate in the formation of neutral atoms, ions, and molecules, whose equilibrium concentrations depend on partition functions and dissociation constants which are somewhat uncertain. Many thousands of spectral lines are included in the line-blanketing calculations, either explicitly or by means of statistical functions which reflect the distribution of line opacity in wavelength and depth. The distribution functions rely on oscillator strengths and damping coefficients which are often very uncertain. In models for cool stars, molecules such as CN, CO, and H₂O are important blanketing agents in the outer photospheres, but the multitude of molecular lines must usually be treated by approximate methods.

A number of comments can be made about contemporary computations of classical models. Firstly, the numerical techniques now appear to produce reliable and accurate solutions. A considerable amount of analytical and numerical mathematical work has been applied to the solution of the classical atmospheres problem, and now digital computers permit accurate investigations of quite complicated models. The remaining errors and uncertainties in the models stem from the use of opacity distribution functions and the absence of accurate atomic data, especially for UV lines. Secondly, we can note that model photospheres of cool stars may be strongly influenced by convection (Gustaffson et al, 1975). The effects are particularly evident in stars with low gravity, low effective temperature, and low metal abundances. Gustaffson et al. note that even if the primary effect of convection (energy transport) on the model is small the secondary effects such as photospheric velocity fields and inhomogeneities are not well understood. Finally, we note that a comparison of recent classical models with semi-empirical solar models (see Figure 5-2) shows significant unexplained dif-

ferences in the outermost ($\tau < 10^{-2}$) and innermost ($\tau > 1$) regions. These differences have important implications. For example, Athay (1981, p.93) has noted that uncertainties at small optical depths are so large that "no one knows whether the mechanical energy input at the temperature minimum region is of major or minor importance."

Although contemporary models for the photospheres of cool stars are highly refined in some aspects, they are quite poorly developed in others. As Gustaffson et al. (1975) point out, because of the assumptions of homogeneity and LTE, and the neglect of "possibly heavy turbulence and chromospheric activity," it is "still at present unclear for which depths models of this type may be used with confidence in quantitative work on stellar spectra and colors."

V. APPLICATIONS AND LIMITATIONS OF CLASSICAL MODELS

Classical models for stellar atmospheres are used to provide not only an understanding of the physical structure of the outer layers of a star, but also to determine stellar luminosities and other stellar parameters in those common circumstances where more fundamental methods are inapplicable (Hack and Struve, 1969). This latter application implies that the theory of stellar atmospheres underpins work on the problems of the structure and evolution of the stars, and the structure and evolution of the galaxies.

The successes and failures of classical models in these dual roles can be judged by comparisons between (1) predictions based on the models and (2) actual observations of stars. Classical models are still widely applied, and one might conclude that the results of such comparisons have satisfied many uncritical astrophysicists that the models are adequate in specific circumstances. However, a growing body of evidence conclusively demonstrates the inability of the classical model to account for all observations of stellar atmospheres. This

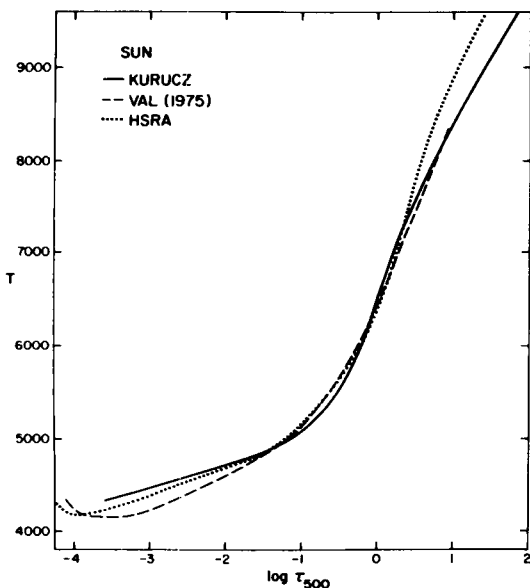


Figure 5-2. Comparison between a theoretical solar model due to Kurucz (1979) and "semi-empirical" models derived from observed spectra. From Kurucz (1979).

section examines these apparently contradictory assessments of the classical model.

V.A. THE SOLAR ATMOSPHERE

We begin with a comparison between the spectrum predicted for a solar atmospheric model, and the corresponding observations. Figure 5-3 shows how the (line-blanketed) theoretical continuum is in fair agreement with observations in the spectral range 300–700 nm. Some of the major disagreements in this range are probably due to an inadequate treatment of line blanketing. For example, the systematic error in the red may reflect the absence of molecular line blanketing in the model (or it may be related to an inadequate model of convection). The poor fit in the G band at 430 nm is almost certainly due to neglect of the CH molecule. The predicted UV spectrum in this model is generally too bright, a problem which is usually cured by application of an ad hoc “opacity enhancement factor” which increases the theoretical opacity by as much as a factor of 3 (Vernazza et al., 1976). Whether this factor reflects a deficiency in the UV line opacity

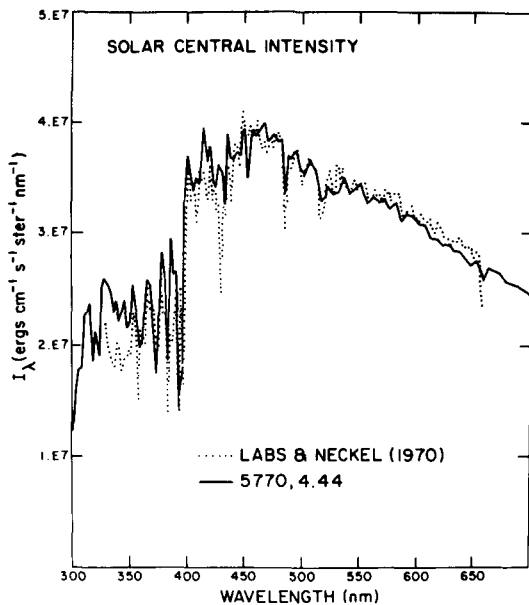


Figure 5-3. Comparison between the solar central intensity predicted by Kurucz (1979) and the measured spectrum. From Kurucz (1979).

calculations, or whether it is due to the effects of atmospheric temperature inhomogeneities (e.g., Ayres and Testerman, 1981), or to some other effect, is presently unclear.

When used to predict properties of spectral lines formed in the solar atmosphere, this highly refined classical model encounters major problems. Figure 5-4, from Kurucz and Avrett (1981), compares a part of the theoretical UV spectrum with observations, and shows prominent errors which may be ascribed to several factors: there are uncertainties in atomic parameters such as line identifications, oscillator strengths, and damping constants; there are poorly understood effects due to gas dynamic processes in the solar atmosphere (turbulence and temperature inhomogeneities); and for many lines there are effects due to the existence of a chromosphere, and to departures from LTE.

Of course the classical model completely fails to account for the far IR ($\lambda > 100 \mu\text{m}$) and far UV ($\lambda < 200 \text{ nm}$) radiation of the Sun, which originates primarily in the chromosphere and corona, just as it fails to predict the line profiles of the cores of strong lines in the visible spectrum. The classical model cannot explain the wealth of structure seen in spatially resolved solar observations, nor can it explain activity centers and the time-dependent response of the atmosphere to magnetic fields. In fact, the classical model is unable to explain any of the multitude of phenomena which are the primary subject of modern solar physics. Clearly, the classical model is totally inapplicable in the solar atmosphere, except perhaps in the deeper layers.

Many astrophysicists might respond to these criticisms of the classical solar model by arguing that it was never intended that classical models should explain phenomena such as chromospheres, coronae, and dynamical processes (which is certainly true), and, furthermore, that in many applications these phenomena can indeed be ignored. It appears that this

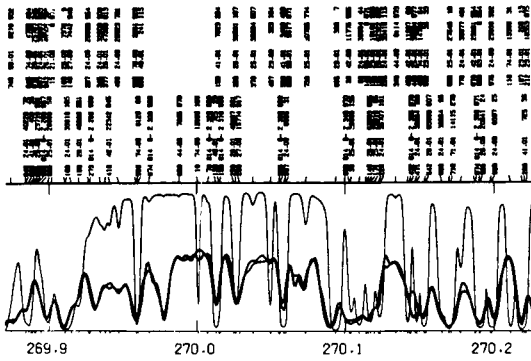


Figure 5-4. Comparison between the predicted shape of a portion of the solar UV spectrum (thin line) and the observed spectrum (solid line). From Kurucz and Avrett (1981).

argument has some merit, since it is true that classical models have been used with apparent success in several kinds of studies. To discover why this is so, let us consider how classical models are used to study the atmospheres of the stars.

V.B. APPLICATIONS OF CLASSICAL MODELS

Most applications of classical models rely on the fact that they provide theoretical calibrations of spectroscopic properties that can be used to infer stellar surface temperatures, surface gravities, and surface chemical compositions from observations of continuum and line spectra, generally in the optical spectral range. For example, surface temperatures may be roughly inferred from estimates of line strengths in low dispersion spectra (i.e., from spectral type), and from the colors of the continuum. Temperature estimates may be refined and calibrated, using quantitative observations and detailed modeling of the strengths of continuum features (such as the Balmer jump) and selected spectral line ratios which happen to be exceptionally sensitive to temperature at the temperature in question. Once the temperature has been estimated, the surface gravity can be derived from pressure-sensitive line strengths or line broadening, either by direct observations

of sensitive lines, or by the blanketing effects on photometric indices. When both the temperature and gravity have been estimated, the abundances of the elements in the atmosphere can be obtained by using a curve of growth, narrow-band spectrophotometry, or more refined "fine analysis." The temperatures, surface gravities, and abundances so derived can then be used to infer other stellar parameters such as absolute bolometric luminosity, effective temperature, mass, and age. Knowledge of these properties of a large number of stars provides the empirical foundation of the theory of the structure and evolution of stars, star clusters, and galaxies.

To provide a specific illustration of the use of classical models in investigations of stellar atmospheres, we consider here in some detail the study of lithium in cool stars. It has been known for some time that the abundance of lithium in cool dwarf stars appears to diminish with age. Recently, several workers (e.g., Duncan, 1981; Soderblom, 1983) have attempted to calibrate the lithium-age relation in order to provide improved quantitative data on the evolution of chromospheric activity and rotation in these stars. The results of these studies offer potentially valuable insight into the nature of secular changes in stellar "activity" (see Chapter 7), and it is consequently of considerable importance to assess the validity of inferences based on the use of classical model atmospheres in this context.

Duncan's (1981) study of lithium abundances in solar-type stars relies on the classical model in two separate ways: (1) to effect an "empirical" estimation of fundamental parameters such as surface gravity, effective temperature, and metallicity; and (2) to provide theoretical curves of growth of $\text{Li } \lambda 670.7 \text{ nm}$ in stars with different fundamental parameters. His use of classical model atmospheres to estimate fundamental parameters relies on calibrations of the relation between a given fundamental parameter and an observed color index. For example, gravities are obtained from the Strömberg index

δc_1 , which corresponds to the difference between the measured color index $c_1 = (u-v) - (v-b)$ (a measure of the Balmer discontinuity) and the value of c_1 for a zero-age star with the same $b-y$ color. Similarly, metallicities for many stars are deduced from the Strömgren index δm_1 . Relyea and Kurucz (1978) have undertaken a refined analysis of the connection between the theoretical color indices δm_1 and δc_1 and fundamental parameters. Their analysis revealed the presence of significant errors in the theoretical estimates of color indices, which they ascribed largely to uncertainties in the representation of line blanketing, convection, and turbulence in the classical model.

Duncan (1981) determined the effective temperatures of his sample of stars using in most cases measured R-I color indices, calibrated by the "fine analysis" of Perrin et al. (1977). The technique of "fine analysis" underlying the work of Perrin et al. is described by Cayrel and Cayrel (1963) in their classic investigation of the spectrum of the normal red giant ϵ Vir. The technique uses a semi-empirical solar model to provide the run of temperature with depth, rather than a strictly theoretical model based on RCE. In other respects, however, the classical assumptions of a plane-parallel, homogeneous atmosphere with microturbulence and LTE are adopted. For ϵ Vir, estimates of effective temperature (4940 ± 150 K), surface gravity ($\log g = 2.7 \pm 0.2$), metallicity ($\log A/A_{\odot} = 0 \pm 0.2$, macroturbulence (3.6 ± 1 km s⁻¹) or rotation ($v \sin i = 4.8 \pm 1.3$ km s⁻¹) and microturbulence ($2-3$ km s⁻¹) are derived by fitting (1) the energy distribution in the continuum, (2) the excitation temperature of FeI, (3) the strength of the wings of H α , (4) the absolute visual magnitude of the star, and (5) the intensity ratio of ionized to neutral species. Subsequently abundances of specific elements are determined from individual curves of growth.

Cayrel and Cayrel (1963) conclude their widely applied fine analysis of ϵ Vir with the

sobering statement that "there are, unfortunately, many sources of errors, either observational or arising from oversimplification in the theory, which conceal the rather small effects [i.e., abundance differences — ed. note] predicted by current theories of nucleogenesis". There is no reason to think that the sources of error encountered in this careful pioneering study of ϵ Vir have been removed by more recent techniques. Consequently, there may be significant systematic errors underlying the tabulations of Perrin et al. (1977) and corresponding uncertainties in effective temperatures derived by Duncan (1981) from photometric data.

By applying the calibrations described above, Duncan (1981) was able to determine the effective temperature, surface gravity, and metallicity of his sample of solar-type stars. With this information available, he could then estimate lithium abundances by using curves of growth for the line Li λ 670.7 nm, computed with the aid of a sequence of classical atmospheric models. Figure 5-5 displays the theoretical curve of growth. Since Duncan's (1981) work addressed the problem of the depletion of lithium with age, yet another application of classical models is implicitly involved in his determination of cluster ages from color-magnitude diagrams.

Duncan (1981) [see also Soderblom, 1983] used these techniques to derive a regression relationship between lithium abundance and age for solar-mass stars. Using this regression, Duncan and Soderblom discussed the age dependence of chromospheric CaII emission and rotation rate, respectively, thereby contributing basic "empirical" data of relevance in the study of stellar activity.

This rather detailed account of the methodology used in these recent investigations has revealed the crucial role played by classical models in the investigation of important astrophysical questions. Insight accumulated from such investigations has been absorbed

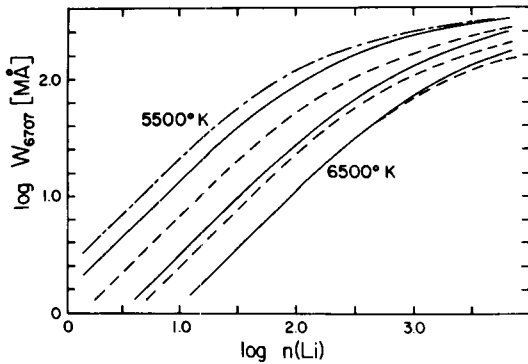


Figure 5-5. Curves of growth for $\text{Li } \lambda \text{ 6707}$. (Solid) $\log g = 4.5$, $T_{\text{eff}} = 5500, 6000, 6500$ K; (dashed) metallicity reduced by a factor of 10; (dash-dot) $T_{\text{eff}} = 5500$ K, $\log g = 4.0$. From Duncan (1981).

(often after considerable debate) into the general body of astrophysical “knowledge” to become part of the overall theory of the structure and evolution of stars. The foundations of this theory rest therefore on the *quantitative* validity of classical models. As the validity of conclusions based on classical models is now often tacitly accepted in many studies of stellar atmospheres and interiors, it has become increasingly hard to identify and assess the *empirical* basis of certain critical concepts.

For example, it is almost always assumed that line-strength differences between cool stars of identical spectral type and class reflect differences in the abundances of elements. The quantitative determination of abundances by the use of a curve of growth is a well-established technique. However, an empirical study by Giampapa et al. (1979) suggests that differences in the level of magnetic activity between stars can produce effects which might be misinterpreted as differences in abundances. The extent to which this effect influences the determination of lithium abundances is unclear. It should be clear from the discussion in this section that the application of the classical model is fraught with uncertainties.

V.C. A CRITIQUE OF THE CLASSICAL MODEL

As discussed above, a comparison between the predictions of a classical solar model and observations of the Sun reveals a number of disparities. The observations described in Chapter 2 reveal similar disparities, to a greater or lesser degree, in most cool stars. Some of these discrepancies are undoubtedly due to *rectifiable problems* within the basic framework of the classical model, and a number of potentially rewarding lines of investigation within this framework can be identified (Auer and Newell, 1978). These include the quest for improved values of atomic parameters such as oscillator strengths and damping constants, improved methods for treating line blanketing (especially the part due to molecules), an improved theory of convection, and the study of non-LTE effects on classical models.

But there is another class of *fundamental problems* that will never be rectified by investigations within the constraints of the assumptions underlying the classical model. These include the observed existence of stellar chromospheres and coronae, widespread stellar variability, and evidence that stellar atmospheres are in a state of vigorous motion. These fundamental problems point to the need for a new atmospheric model that can account for these phenomena.

It is becoming increasingly important to develop a theory that can account for the actually observed deviations from the classical model of a stellar photosphere. For example, if we can show that part of the phenomena known as stellar photospheric micro- and macro-turbulence is associated with convective overshoot, we may conclude that processes analogous to solar granulation occur in other stars. This knowledge could improve the theory of convection in stars. A clearer understanding of the relationship between photospheric turbulence and lateral temperature fluctuations associated with convection could let us examine

more deeply the assumption of plane-parallel stratification in the photosphere (cf. Böhm-Vitense, 1977). We might also note the growing evidence for the existence of significant nonradiative heating in the upper photospheres of the Sun and other cool stars (Linsky, 1980). Such heating will compromise the use of classical models in any spectroscopic diagnostics that are based on observations of strong Fraunhofer lines.

Some of the fundamental astrophysical concepts that have emerged from the application of classical models may survive when a new model is introduced. For example, the use of spectral type or color index to indicate the temperature scale in the Hertzsprung-Russell diagram requires only the assumption that stars radiate roughly as black bodies with a temperature given by the effective temperature of the star. From this simple beginning, fundamental studies such as Eggen's (1960) work on the ages of star systems may be undertaken. Popper's (1974) investigation of lowered element abundances in Population II stars did not require a "fine analysis" of their spectra. Basic insights such as these will probably survive, as classical atmospheric models are revised to represent more closely real stellar atmospheres. On the other hand, equally "simple" concepts such as the "veiling" effect in T Tauri photospheres (Chapter 4) are likely to be radically reinterpreted in the light of new, nonclassical treatments.

VI. SEMI-EMPIRICAL CONSTRUCTS

Differences between theoretical predictions based on classical models and observations of stars have prompted astrophysicists to modify the classical model by introducing *semi-empirical* constructs such as "turbulence" to account for observed spectral line widths, and "chromospheric temperature rises" to account for emission lines. *The semi-empirical constructs* are generally introduced by well-defined empirical procedures which are primarily concerned with improving the agreement between

theory and observation, and only secondarily with the physical basis of the construct and its further ramifications.

Insofar as semi-empirical constructs lead to improved agreement between theory and observation, and suggest at the same time a physical mechanism underlying the improvement, they are a valuable step in revising the classical model. However, developments in the theory of stellar atmospheres have sometimes stagnated with the introduction of such constructs, since they have been used occasionally as diagnostic crutches rather than as clues to improved physical models. When used in this way, semi-empirical constructs are akin to Ptolemaic epicycles, and equally meaningless. It is thus important to make a sustained effort to understand the physical basis of these constructs. In this section we consider some of the semi-empirical constructs frequently used today, emphasizing both their application in patching up the classical model, and the hints which they provide to a more satisfactory model of stellar atmospheres. The constructs to be discussed are nonthermal velocity fields, chromospheres and coronae, and extended atmospheres.

VI.A. NONTHERMAL VELOCITY FIELDS

The observed widths of most lines in the spectra of most stars are greater than predictions based on classical model atmospheres and line formation theory. This disparity could conceivably be due entirely to rectifiable difficulties in the models (such as erroneous RE temperature gradients, or neglect of non-LTE effects), but errors of this magnitude seem to be improbable in the light of current views of the reliability of classical models.

The observed extra widening therefore suggests that the classical model must be modified, and this modification is usually effected by means of a hypothetical nonthermal velocity field which broadens the lines by Doppler

shifts. Almost invariably, the structure of this velocity field is assumed to be known a priori, rather than deduced from the data or from sound physics, and moreover, any consequences of the velocity field, other than line broadening through Doppler shifts, are ignored.

The first clear evidence for the existence of nonthermal line broadening was reported by Struve and Elvey (1934), who found that the curves-of-growth of the F supergiants ϵ Aur and α Per implied total Doppler widths that were as much as an order of magnitude larger than the expected thermal Doppler widths. They attributed this extra broadening to isotropic Gaussian “turbulence” of the kind which had been proposed by McCrea (1929) to account for the geometrical extension of the solar chromosphere, and estimated its amplitude from the observed Doppler width $\Delta\lambda_D$ by the formula

$$\Delta\lambda_D = \frac{\lambda_o}{c} \left(\frac{2RT_e}{m} + \xi^2 \right)^{1/2} , \quad (5-48)$$

where $2RT_e/m$ is the mean-square thermal velocity, and ξ is the turbulent velocity. Milne (see Chandrasekhar, 1949) recognized that a “turbulent” velocity which broadens spectral lines in this way has to have a spatial scale which is small compared with unit optical path length, and the phenomenon thus became known as *microturbulence*.

Struve (1946) also found that the measured line widths in the F supergiant δ C Ma are not only greater than that expected if thermal broadening were acting alone, but also greater than that expected from the combined effect of thermal broadening and microturbulence, as inferred from the curve of growth. Schwarzschild, Schwarzschild, and Adams (1948) found a similar effect in the spectrum of η Aql (cG4), and suggested that it might result from large-scale turbulent eddies which produced net line shifts along each line-of-sight into the atmosphere. Broadening of this kind is now known as *macroturbulence*.

A number of researchers have attempted to improve or modify the basic models underlying micro- and macroturbulence. The subject has been put on a fairly rigorous mathematical footing by studies of stochastic models of spectral line formation in the presence of *mesoturbulence* (Gail et al., 1974; Auvergne et al., 1973). But the turbulence models used in these studies are chosen for their mathematical convenience and not on the basis of theories of hydrodynamical turbulence. There is consequently no valid reason for employing the results in actual stellar diagnostics.

Another nonthermal broadening process which affects the shape of stellar spectral lines is *rotation*. Rotational line broadening is usually regarded as a relatively well understood process. However, it is often difficult to separate the effects of rotation from macroturbulence (Abt, 1957; Gray, 1973). Moreover, as we discuss in Chapter 7, rotation may lead indirectly to major changes in atmospheric structure through the agency of magnetic fields, and it is a challenging diagnostic problem to investigate the relationships between rotational broadening and spectroscopic evidence of these other changes.

Other manifestations of nonthermal velocity fields include *shifts* and *asymmetries* of spectral lines (Dravins, 1981a). Many different processes have been proposed to account for these effects, and it is extremely difficult to derive a unique model of a nonthermal velocity field from observations of line shifts and asymmetries alone. Despite this difficulty, the combination of line shift and asymmetry measurements with evidence of atmospheric heating and extension provides insight into the kinds of phenomena that might be considered in a revision of the classical model.

It might be expected that observations of the Sun would be able to clarify the nature of nonthermal line broadening in cool stars, but this is not the case. As discussed by Beckers (1981), spatially resolved solar observations do reveal

a pattern of large-scale (spatially resolved) flows associated principally with oscillations, granulation, supergranulation, and differential rotation. All of these phenomena contribute to macroturbulent and rotational broadening of spectral lines in the solar flux spectrum. However, spatially resolved spectral lines are invariable asymmetric and weakened or strengthened in the fine structures, showing clearly that classical macroturbulence is unable to adequately represent line formation in the presence of waves and convective overshoot. Moreover, there is also ample evidence (see Beckers, 1981) for the existence of microturbulent broadening of solar spectral lines, and because the relevant scales cannot be resolved, there are no observations which could help identify the physical origin of this form of line broadening. The range of the values of solar macroturbulence and microturbulence obtained by different authors is extremely large (a factor of 10), and it depends markedly on the diagnostic procedure adopted.

In Chapter 2 of this volume, Gray has provided a comprehensive account of the results of studies designed to refine our knowledge of the characteristic variations among the cool stars of semi-empirical constructs associated with nonthermal velocity fields. Here, we focus somewhat more sharply on the question of the physical origins of the observed phenomena.

VI.A.1. MICROTURBULENCE

Microturbulence is thought to be produced by velocity fluctuations on scales that are small compared with a photon mean free path ($< 50\text{km}$ in the photospheres of cool dwarfs). Gaussian microturbulence enters the radiation transfer equation exactly parallel to thermal Doppler broadening (Equation 5-48). The signature of classical microturbulence is an inferred total Doppler width that is significantly larger than the inferred thermal Doppler width.

Various methods can be used to determine total and thermal Doppler widths, and hence

to estimate the amplitude of microturbulence. The curve of growth has been used widely, and its application has reached a high degree of refinement (e.g., Foy, 1980). However, the statistical nature of this method means that a lot of information contained in the line profiles may be lost (Struve, 1943). Other methods which yield Doppler widths include detailed profile fitting (Gray, 1973, and Chapter 2.III.E), the Goldberg-Unno method (Stenholm, 1977a,b), and the use of narrow-band filters in blanketed spectral windows (Gustafsson et al., 1974). In all of these methods the diagnostic procedures are based on a number of questionable (and unclear) assumptions, and there may be significant systematic errors in the derived microturbulence values. Sources of uncertainty include (1) the assumption of an isotropic gaussian velocity distribution, (2) the neglect of dynamical effects (Cram, 1981), (3) the use of inappropriate Schuster-Schwarzschild or LTE Milne-Eddington models of line formation, (4) uncertain atomic parameters (especially oscillator strengths and damping rates), (5) confusion between microturbulence and other forms of nonthermal line broadening, and (6) neglect of any alterations in the atmospheric structure that might arise as a consequence of the dynamical processes actually responsible for microturbulence.

It is clear that microturbulence is not a particularly well defined semi-empirical construct. Therefore it is perhaps not surprising that studies of the trends in microturbulence in cool stars yield results that are often confusing and contradictory.

Results of several studies of microturbulence in main-sequence cool stars are summarized in Figure 5-6. At any spectral type there is wide scatter, principally due to observational uncertainty and diagnostic error. It is impossible to determine whether there are real star-to-star differences at any given spectral type, related, e.g., to different levels of chromospheric activity. A number of studies have revealed a tendency for microturbulence to increase as one considers

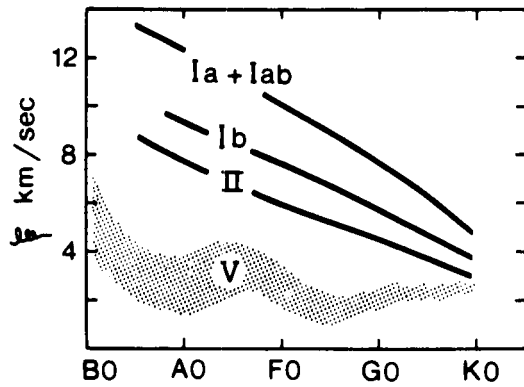


Figure 5-6. Variation of microturbulence (from curve-of-growth analyses) with spectral type and luminosity. From Gray (1978).

stars that are progressively hotter, or cooler, than the Sun. These trends may only reflect systematic errors in differential analysis methods.

Several studies have suggested that microturbulence increases with increasing luminosity at any spectral type among the cool stars. The situation is summarized in Figure 5-6, which shows both the increase of microturbulence with increasing luminosity at a given spectral type, and the increase of microturbulence with earlier spectral type at given luminosity class. However, studies of smaller, more homogeneous, regions of the HR diagram reveal radically different dependencies on gravity (Stenholm, 1977b) and temperature (Gustaffson et al., 1974).

The question of a dependence of microturbulence on metal abundance has been debated often since Conti and Deutsch (1966) claimed that "differences in microturbulence are chiefly responsible for the ultraviolet excesses and Strömgren residuals Δm that abound in solar-type stars of the disk population." This suggestion questions the conventional view that the UV excesses and Δm residuals reflect abundance differences, and thus it throws doubt on fundamental ideas regarding galactic structure and evolution. Consequently much work has

been done in an attempt to rebut it (e.g., Chaffee, 1970), although the problem does not seem to have been satisfactorily resolved. For stars that are extremely metal deficient the situation is also unclear. Foy (1980) finds no evidence for decreased microturbulence in metal-poor giants, but Aller and Greenstein (1960) find evidence for very small microturbulence in cool subdwarfs. In fact these later authors find that the microturbulence is negative in certain subdwarfs, a result which surely says as much about the reliability of differential curve-of-growth analyses as it says about nonthermal velocities in the atmospheres of subdwarfs!

Foy (1980) has suggested that microturbulence could be correlated with the evolution of stars in the sense that more evolved giants show higher microturbulence values. Foy offers an explanation of this result in terms of evolutionary changes in the structure of convection inside the star, but the empirical result is only marginally significant, and the theoretical explanation fails to connect small-scale atmospheric microturbulence with large-scale internal convection. There do not appear to be any studies that attempt to relate a decay of microturbulence with stellar aging on the main sequence, despite the possibility that the known decay of chromospheric activity with age in main-sequence stars would require significant changes in microturbulence, if microturbulence were indeed related to nonradiative heating (e.g., Edmonds, 1978).

A number of authors have attempted to study the anisotropy and variation with height of microturbulence in the visible parts of stellar atmospheres. As summarized by Beckers (1981), solar microturbulence appears to be anisotropic, with the horizontal velocity component about 50% larger than the vertical. The amplitude appears to decrease with increasing height in the photosphere, and then to increase in the chromosphere. Studies of the dependence of stellar microturbulence on excitation potential led Rosendahl (1970) to conclude that microturbulence exhibits an outward decrease

in the photospheres of cool giants, a result supported by Stenholm's (1977a) study of the total nonthermal velocity field. But Osmer (1972) adopted a microturbulence variation which rises monotonically with decreasing density, in an effort to match FeI and FeII observations in F supergiants. Chaffee (1970) attempted to interpret the dependence of microturbulence on spectral type in main-sequence cool stars in terms of changes in the depth dependence of microturbulence, but unfortunately he found that "the solar microturbulence does not fit into this scheme."

From this discussion of microturbulence, two safe conclusions may be drawn:

1. Microturbulence does exist in cool stars, in the sense that the Doppler widths of spectral lines are generally larger than would be produced by wholly thermal broadening.
2. There is an enormous range in the microturbulence values inferred for a group of stars of approximately the same spectral type and class. This range might reflect the fact that a component of the star-to-star variation of microturbulence is independent of the classical atmospheric parameters, or it might be due entirely to diagnostic ambiguities, errors, and uncertainties.

In view of these conclusions it is evidently premature to attempt to relate the systematics of microturbulence among the cool stars to any physical mechanism that might be thought to underlie microturbulence. For example, we would place little weight on arguments given by Gehren (1980) and Böhm-Vitense (1980), to the effect that the systematics of microturbulence among cool stars can be fairly well understood in terms of the expected variations in convection among these stars. The observations are themselves uncertain, and there is no sound physical basis for connecting values of atmospheric microturbulence with the structure

and amplitude of envelope convection. We have no satisfactory understanding of the relation between microturbulence and the manifestations of convective overshooting (granulation), even in the solar atmosphere where spatially resolved observations can be made. It might also be noted that it is generally unwise to use a selected set of microturbulence "trends" to support a particular physical model, since one can always find other observations which run counter to any such trend.

VI.A.2. MACROTURBULENCE

Macroturbulence corresponds to velocity fluctuations that are large compared with the depth of the line-forming layer. Macroturbulence is introduced into line formation theory by first computing "intrinsic" intensity profiles, and then applying statistical Doppler shifts before performing the flux average. The classical symptom of macroturbulence is therefore a line width that is significantly greater than that which would be expected on the basis of the Doppler and damping widths.

Diagnostic methods for measuring macroturbulence are perhaps even less certain than those used to measure microturbulence. Line widths are more difficult to define and to measure than are equivalent widths, and they are more directly influenced by the instrument and by rotation. It is often difficult to separate macroturbulence from rotation (Abt, 1957; Gray, 1973; and Chapter 2.III.F), although the two broadening mechanisms presumably have unrelated physical origins. Derived values of macroturbulence are probably no more and no less reliable and meaningful than those of microturbulence, although some systematic variations of macroturbulence among cool stars do seem to be detected reliably.

The most spectacular systematic trend in macroturbulence is the observation that supergiant stars exhibit large values, sometimes $> 10 \text{ km s}^{-1}$. Figure 2-11 suggests that macroturbulence decreases with later spectral

type in a given luminosity class, and decreases with decreasing luminosity in a given spectral type. Although Bonsack and Culver (1966) found a fairly uniform increase in macroturbulence with increasing luminosity, Smith and Dominy (1979) argued that there is a rather sudden jump in macroturbulence from values of $< 3 \text{ km s}^{-1}$ for $M_B < -2$ to values $> 5 \text{ km s}^{-1}$ in the higher luminosity range. Gray (Chapter 2.III.H) suggests that recent observations do not sustain this argument. We might note that Bonsack and Culver's result implies a tight connection between photospheric macroturbulence and the Wilson-Bappu width of the chromospheric K line (Chapter 3.VI). Such a connection is required by models which identify the K-line width with "turbulent broadening." The result of Smith and Dominy suggests a weaker correlation.

There is evidence that stars of the same spectral type and class may have different values of atmospheric macroturbulence. For example, Gray (1975) finds significant differences between the K3 II stars γ Aq1 and γ^1 and, while Smith and Dominy (1979) find that β Cet (K1 III) has significantly higher macroturbulence than other apparently similar cool giants. It seems that the random errors in these two studies are so small that the star-to-star differences are significant.

There is strong evidence for a dependence of macroturbulence on atmospheric metal abundances. Smith (1980c) has claimed that macroturbulence might be related to age on the main sequence. Comparisons between photospheric and chromospheric line widths have led to suggestions that macroturbulence may increase with height (Bonsack and Culver, 1966). While such a result is compatible with solar observations, there is considerable doubt that the widths of stellar chromospheric lines are a reliable measure of nonthermal velocity fields and this result may not be significant. Gray (1977b) has suggested that microturbulence ζ and macroturbulence ξ may be related by the formula $\zeta = 0.5 \xi^{3/4}$. This result, suggestive as

it is, is not supported by the homogeneous set of data published by Bonsack and Culver (1966), nor is it apparently satisfied by the Sun.

Although the systematic trends of macroturbulence in the cool stars are not always clear, two safe conclusions can be drawn:

1. Macroturbulence is larger in cool supergiants and bright giants than it is in main sequence cool stars.
2. There are some reliable cases where two stars of the same spectral type and class have significantly different values of atmospheric macroturbulence. This result should be considered against the difficulty of separating rotation and macroturbulence.

VI.A.3. ROTATION

The effect of rapid rotation on stellar spectral lines was recognized long ago (e.g., Rosseland, 1936, Chapter XIV). Under the assumption that the intrinsic stellar intensity profiles are known, the theory of rotational line broadening is straightforward, and relatively simple procedures may be applied to derive the projected rotation velocity $v \sin i$ from an observed spectrum (e.g., Sletteback, 1970; Gray, Chapter 2.III.F). Of course, estimates of $v \sin i$ can be in error if the rotation itself alters the intrinsic line profile, or if the lines are changed by other factors such as weak central emission (Doazan, 1970). Nevertheless fairly reliable and comprehensive observations of rotation rates are available for the early-type stars, which generally rotate rapidly.

However, with only a few exceptions, single cool stars do not rotate rapidly [Kraft, 1967 — there are a few stars, such as 37 Com (Smith and Dominy, 1979) and some Pleiades G dwarfs (Marcy et al., 1985), which violate this rule], so that it is often extremely difficult to untangle the rotational broadening from other

broadening mechanisms such as macroturbulence (Abt, 1957; Gray, 1973). The Fourier dissection technique (Gray, 1976, and Chapter 2.III.F) is the most sensitive line profile diagnostic method currently available, and when applied to low-noise data it can reveal rotational broadening as small as $\sim 2 \text{ km s}^{-1}$. Recently Vaughan et al. (1981) have shown that periodic modulations of the CaII K-line emission strength in some late-type stars can be used to derive rotation periods (independent of inclination), and this method agrees well with the results of Fourier analysis where comparisons are possible.

Slow rotation by itself, produces insignificant changes in the structure of a classical stellar atmosphere (since the figure of the star remains spherical). However, there is growing evidence to support the idea that rotation, interacting with envelope convection, is the prime agent responsible for magnetic fields in cool stars. Such fields apparently play a very important role in controlling the nonclassical atmospheric structure (Chapter 7). This consequence of rotation is an example of the fact that apparently minor changes in certain *critical* properties of a natural system can lead to extremely significant changes in the behavior of the system (Glansdorff and Prigogine, 1971).

The systematics of rotation rates among the cool stars have been reviewed in Chapter 2. Among the single stars there is a wide range of $v \sin i$ values at any spectral type and class (Smith, 1980c), but the sample size is too small to reliably unravel intrinsic systematic changes from inclination effects. Among dwarf stars later than about F5, there does seem to be a tendency for rotation rates to decrease with increasing age on the main sequence (e.g., Skumanich, 1972). Some relatively young cool giants apparently rotate quite rapidly, presumably because they have evolved from rapidly rotating stars on the upper main sequence [e.g., 37 Com (G9 II-III) as reported in Smith and Dominy, 1979; Gray, Chapter 2.V.B]. Stars in close binary systems rotate

faster than single stars, because orbital angular momentum is ultimately transferred to both stars. A very important clue to the connection between rotation, magnetism, and stellar activity is provided by the observed correlation between increased activity and shorter period in binary systems (Ayres and Linsky, 1980, Figure 7). This result is discussed in Chapters 3 and 7.

VI.A.4. SYSTEMATIC VELOCITIES

Evidence for large-scale systematic radial velocities is provided by observations of asymmetric line profiles. Although such profiles may be produced by many processes, stellar line asymmetries are frequently ascribed to patterns of radial flow in stellar atmospheres. It is convenient to divide the postulated flow patterns into two kinds: those involving steady one-dimensional flow, and those involving lateral inhomogeneity and/or time dependence. Observations of P Cygni profiles or displaced circumstellar lines are usually interpreted in terms of the first kind of flow pattern, while observations of asymmetries in disk-integrated solar and stellar photospheric absorption lines are usually interpreted in terms of the second.

It is generally impossible to deduce a unique atmospheric flow pattern from observations of line asymmetries alone. A prime example of the ambiguity is found in the interpretation of the V/R asymmetry of the self-reversed emission core of the CaII resonance lines in cool stars, which is evidently due to some form of chromospheric velocity field. At least two explanations may be considered.

Firstly, solar observations made with high spatial resolution (Figure 5-7) show that some parts of the solar disk have a dominant violet peak in the emission reversal ($V/R > 1$), while others have a dominant red peak ($V/R < 1$). At any fixed position on the Sun the V/R ratio changes within a minute or so. As discussed by Athay (1970b), the V/R ratio measures the velocity gradient along the line of sight, but offers no measure of the absolute velocity. The

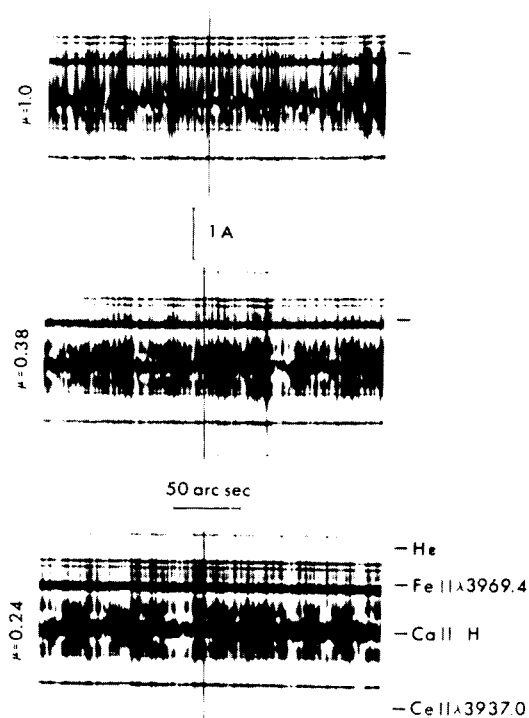


Figure 5-7. High-resolution spectra of the Ca II H line at several heliocentric positions. Note the extreme variation of the self-reversal at the line core. From Cram, Rutten, and Lites (1980).

point-to-point correlation between emission intensity and the sign of the V/R ratio that occurs in the solar chromosphere is ultimately translated into a solar flux profile with $V/R > 1$. The explanation for this net effect in terms of atmospheric dynamics presumably lies in the phase relationships between velocity and temperature in chromospheric oscillations (Cram et al., 1977).

In contrast to the asymmetry of the Sun and other cool dwarfs, cool giant and supergiant stars often have $V/R > 1$. This asymmetry is usually explained in terms of a steady, spherically symmetric outflow (e.g., Chiu et al., 1977) and not in terms of velocity-temperature correlations. The systematics of V/R ratios in the cool part of the HR diagram have recently aroused considerable attention, since they ap-

pear to be related to the systematic changes in coronal structure and mass-loss rates observed among late-type giants. However, it is clearly difficult to decide between outflow or inhomogeneity as the cause of asymmetry in a particular star, particularly when V/R is close to unity, or when V/R depends on line strength in a particular star (Stencel, 1982).

Asymmetries of photospheric absorption lines in cool stars are generally interpreted in terms of a laterally inhomogeneous atmosphere. As reviewed by Dravins (1981a), such asymmetries are potentially very powerful probes of velocity-temperature correlations in stellar photospheres, and hence they can be used to study waves and convective flows which are otherwise unobservable. Unfortunately it is hard to observe line asymmetries with precision (see Gray, 1982a, and Chapter 2.IV), and the interpretation of observed asymmetries is extremely ambiguous. Nevertheless, these kinds of studies could provide future checks for models of photospheric dynamics, and help considerably in clarifying the physical origins of micro- and macro-turbulence (Cram et al., 1979; Dravins et al., 1981).

A form of line asymmetry which has been particularly important in developing models of the atmospheres of cool stars is circumstellar absorption. This phenomenon is manifested as weak absorption lines appearing in the blue wings of the stronger photospheric absorption lines. These may be ascribed to an outward-moving shell or envelope between the star and the observer. The strengths, shifts, and shapes of such circumstellar lines may be used to infer temperatures, densities, velocities, and sizes of the intervening envelope, although the diagnostic procedures are not particularly trustworthy (Goldberg, 1979). The systematics of circumstellar absorption, and its relation to atmospheric properties such as coronal structure, chromospheric depths, and mass-loss rates, have been reviewed by Reimers (1975a and Chapter 3.III).

A related form of line asymmetry involves displaced absorption cores in the blue wing of emission lines. Such a feature could be interpreted as the result of an emitting envelope whose volume is large enough to produce an emission line (see Section VI.C), which also possesses an internal velocity pattern and radial source-function structure that leads to a displaced absorption component. However, it is difficult to reliably identify the atmospheric structure that leads to such line asymmetries. For example, a certain form of asymmetric emission line seen in T Tauri stars may be interpreted in terms of either spherically symmetric outflow, or spherically symmetric inflow, or a rotation-accretion shock. While it is evident that such line asymmetries indicate departures from the classical model, their use as a probe of nonclassical atmospheric structure presents some extremely challenging problems.

VI.B. NONRADIATIVE HEATING

One of the clearest failings of classical models is their inability to explain the existence of spectral lines of high excitation potential and other manifestations of unexpectedly high states of ionization and excitation in stellar spectra. Although some of these features may be explained by radiative effects in classical models (Section IV), there can be no doubt that the vast majority of such features are a symptom of unexpectedly hot (in terms of the classical model) regions in the atmosphere.

From observations of stellar spectra alone it is difficult to determine the geometrical configuration of the hot regions of stellar atmospheres. However, if the structure of the solar atmosphere may be used as a guide in the interpretation of these spectra, we should first consider the possibility that the hot material is located in structures analogous to the heated solar chromosphere and corona, enveloping the relatively cool stellar photosphere. Estimates of gas pressures in the hot parts of stellar atmospheres (Section II) support this idea, since the

pressures are generally found to be much lower than those in the photosphere.

To facilitate diagnosis of the structure of the hot regions of stellar atmospheres it is often assumed that the atmosphere is laterally homogeneous and spherically symmetric. Such an assumption greatly reduces the number of degrees of freedom in a model, and in many cases leads to a model of the radial stratification of the atmosphere that appears to be consistent with the available data. Of course, we know from observation that the chromosphere and corona of the Sun are laterally inhomogeneous, and it is probable that similar inhomogeneities occur in other stars (cf., Chapter 2.V.B.2). In general, however, the available stellar data are unable to constrain the increased number of degrees of freedom that arise when lateral inhomogeneities are introduced into a model.

Over the past decade, a number of semi-empirical models for the chromospheric parts of the atmospheres of cool stars have been constructed (Linsky, 1980, Table 2). Observations of optically thick spectral lines were the basis for the derived temperature structure in most of these models. More recently, observations of UV emission lines and X-rays have widened the range of applicable diagnostics, allowing the construction of more reliable models of chromospheres and the extension of models to higher temperatures. In the remainder of this section we discuss the methods used to construct semi-empirical models of nonradiatively heated stellar atmospheres, and review the trends that emerge from the application of such methods to a range of stars.

The resonance lines of CaII and MgII have been the most widely applied diagnostic of the temperature distribution in stellar chromospheres. The source functions of these lines are collision dominated (Thomas, 1957), and so the emission core that is often observed in the emergent flux profile contains information on the distribution of electron temperature (T_e)

and density (N_e) in the deeper parts of the chromosphere. This information is extracted by the following “semi-empirical” procedure:

- (a) A classical photospheric model for the subject star is selected;
- (b) The temperature distribution in the outer parts of this model is arbitrarily altered and extrapolated so that there is a region of outwardly increasing temperature which roughly mimics the solar chromosphere;
- (c) With the added assumption of hydrostatic equilibrium, equations describing the ionization and excitation equilibrium are solved to obtain the electron density;
- (d) The model atmosphere defined in this way is used in a detailed line-formation calculation to predict the shapes of the chosen spectral lines, and the predicted line profiles are compared with observation. An attempt is made to minimize the differences between observed and theoretical profiles by adjusting the temperature distribution and including extra factors such as microturbulence, macroturbulence, and in some cases systematic velocities.

This technique has been greatly refined by Vernazza et al. (1973, 1976, 1981b) in their progressive refinement of semi-empirical solar models. These authors have solved the non-LTE ionization equilibria for many of the important electron donor elements, and in their recent work have derived one-dimensional models of a variety of solar structures. The semi-empirical models are based on fits to a large number of nonredundant observations including the hydrogen Lyman continuum, the UV, visible, and IR continua, and the resonance lines of H I, Ca II, and Mg II. However, despite the thoroughness of this work a number

of critical problems remain. These include the uncertainty in the actual value of the temperature minimum, a critical quantity for estimating nonradiative heating rates; the inability to account for the UV continuum intensities (near 250 nm) without an opacity enhancement factor; errors of at least a factor of 10 in the fit to spatially unresolved observations of resonance line profiles of Ca II and Mg II; and the failure of any one of their six one-dimensional components to even crudely represent the observed ubiquitous presence of cool material several thousand kilometers above the limb (spicules, prominences, etc.).

Work on models of stellar chromospheres has not yet reached the refined level of semi-empirical solar modeling, the main impediment being the lack of stellar observations of good quality. Stellar models have hitherto been based primarily on observations of the Ca II and Mg II resonance lines, which are not well understood even on the Sun, and which in any case cannot provide reliable models for temperatures in excess of ~ 7000 K. Despite these problems, studies of semi-empirical stellar chromospheric models have revealed a number of significant trends in the chromospheres of cool stars (Linsky, 1980; Chapter 3), which may be summarized as follows.

- (a) There exists a wide range of chromospheric structure in stars of similar spectral type and class. The clearest evidence for this is the existence of a wide range of Ca II and Mg II line strengths in stars of almost identical spectral type and class (e.g., Wilson and Bappu, 1957). The range of chromospheric structure may reflect the range of chromospheric temperature gradients in spherically-symmetric models (Kelch et al., 1979) or the relative areas covered by “active” and “quiet” regions (Leighton, 1959; Zwaan, 1981). For giant stars the origin of the variation is less clear. We will discuss these questions further in Chapter 7.

- (b) There is evidence for nonradiative heating in the upper photospheres of many stars (Kelch et al., 1979, Figure 3). The basis for this inference is an apparent need to raise the photospheric temperature relative to radiative equilibrium models in order to account for the shapes of the inner damping wings of strong lines. The magnitude of the effect is uncertain because of large uncertainties in classical models in these outermost layers, and because of uncertainties in line-formation theory. But this property of semi-empirical models suggests that the assumption of radiative equilibrium that underlies classical models may break down in the outer layers of the photosphere, where the cores of strong and medium-strong absorption lines are formed.
- (c) There are certain trends in the properties of stellar chromospheres that are closely tied to the parameters describing the underlying "classical" photosphere. The most striking of these is the width-luminosity relationship discovered by Wilson and Bappu (1957), involving a very tight correlation between the width of the CaII resonance-line reversal and the absolute visual luminosity of the star. Many proposed explanations of this correlation have been based on a tentative connection between chromospheric turbulence and the fundamental atmospheric parameters (e.g., Hoyle and Wilson, 1958), but the work of Ayres (1979) and others suggests that the origin of the correlation may lie more in the variation of chromospheric pressure and temperature with effective temperature and surface gravity.
- (d) Variability of chromospheric structure, with time scales ranging from seconds to decades, is a very widespread phenomenon. The manifestations of variability include short-duration "flares" such as

those which occur on RS CVn systems (Hall, 1978); periodic modulation with a time scale of days, presumably related to the combined effects of asymmetric chromospheric structure and stellar rotation (Vaughan et al., 1981); cyclic variations with time scales of years, presumably reflecting stellar analogues of the solar activity cycle (Wilson, 1978); short period oscillatory changes possibly associated with atmospheric waves (Baliunas et al., 1981); and irregular variations of the kind seen in T Tauri stars (Gahm et al., 1974), supergiants (O'Brien and Lambert, 1979) and Arcturus (Chiu et al., 1977).

The properties described above have been deduced principally from studies of the resonance lines of CaII and MgII. Observations of the far-UV emission-line spectra of cool stars (principally by *IUE*) and of the broad-band X-ray flux (by *Einstein*) have reinforced these conclusions, and uncovered new systematic properties which were not obvious from spectral features formed only in the cool parts of the chromosphere.

For example, among dwarf K stars the X-ray flux varies from star to star by more than two orders of magnitude (Vaiana et al., 1981; Chapter 3.II.A). There is a loose correlation between the coronal X-ray flux and fluxes in spectral lines formed in the chromosphere and transition region (Ayres and Linsky, 1981), suggesting a connection between the heating of chromospheric and of coronal atmospheric regions. However, there are deviations from the correlation that suggest that the ratio of coronal to chromospheric heating rates may depend on the actual level of heating (Chapter 3.II.B). There is little evidence for correlation between observed changes in coronal and in chromospheric emission. This partially reflects the absence of sufficient data, although there are examples of events on flare stars where simultaneous observations seem to imply that

concomitant variations do not occur in the corona and in deeper layers (Haisch et al., 1981). A notable exception is the anti-correlation between X-ray luminosity and $H\alpha$ emission strength in T Tauri stars (Chapter 4).

There are some systematic variations in UV and X-ray spectral features across the HR diagram. Perhaps the most striking of these is the tendency for evidence of hot atmospheric plasma ($T_e > 20,000$ K) to disappear with increasing luminosity among the late-type giants. This systematic variation, which is found in a number of different spectral features, is described in detail in Chapter 3. The variation apparently reflects a fundamental change in coronal structure with decreasing gravity, and there is evidence that this change is connected with related changes in the radial extent of the chromosphere and in the rate of mass loss.

VI.C. ATMOSPHERIC EXTENSION

The scale height in a classical model of a stellar atmosphere is approximately $k T_{\text{eff}}/g\mu$ where μ is the mean molecular weight. The ratio of atmospheric scale height H to stellar radius R therefore is $H/R \sim 3 \times 10^{-4} T_{\text{eff}}R/M$, where T_{eff} , R and M are the effective temperature, radius, and mass scaled to solar values. With the possible exception of a few extremely large supergiants, this relation shows that classical stellar photospheres are compact, and represent only a thin layer surrounding the star. In this section we discuss a semi-empirical construct which entails atmospheric structures which are significantly extended relative to the classical model, and which generally involve model atmospheres which are one or more stellar radii in depth.

Among the hot stars the widespread existence of optical (e.g., $H\alpha$) and UV emission lines has been taken as evidence for the presence of extended atmospheres. A great deal of work has been done on observations, diagnostics, and theories pertaining to this phenomenon (see Volumes II, III, and IV of this series). Among

the cool stars optical emission lines are not common, being confined (in the main) to supergiants, close binary systems, cool dwarf stars (dMe types), and T Tauri stars. Emission lines from dMe stars, and generally those from close binary systems, are not usually ascribed to atmospheric extension, but rather to the existence of a hot, dense, compact chromosphere. The emission from supergiants and T Tauri stars does seem to indicate atmosphere extension, although a compact chromospheric component may contribute to the emission strength in these stars too. Direct evidence for the existence of atmospheric extension in cool stars comes from observations of eclipsing systems such as ζ Aur (Wilson, 1957; Chapter 3.V.B), and from the solar corona and wind. Recently, a novel EUV diagnostic has been exploited to show that the chromospheric regions of several cool giants have depths of the order of several stellar radii (Stencel et al., 1981; Chapter 3, Sections III.A.1 and V.B.3).

A certain degree of hydrostatic atmospheric extension is necessarily associated with a stellar chromosphere as a result of the increased temperature and decreased mean molecular weight relative to a classical photosphere (e.g., Thomas and Athay, 1961, Chapter 6). For a stellar corona, this hydrostatic extension may be quite large, since the temperature is high. However, most models for extended atmospheres in cool stars ascribe the atmospheric extension to a departure from hydrostatic equilibrium. In some models it is assumed that Reynolds stresses associated with turbulence or waves are responsible for atmospheric support, in others it is assumed that magnetic stresses are acting, while in still others it is supposed that the extended atmosphere is related to a high-density, spherically symmetric flow pattern.

The shifts and asymmetries observed in some spectral lines possibly represent evidence for the systematic flows required for nonhydrostatic support, and in some stars crude diagnostic methods have been applied to estimate the size,

density, temperature, and flow rate in the extended atmosphere (Chapter 3.III). However, as discussed in our survey of nonthermal velocities, there are essential ambiguities involved in these diagnostics. At present these are usually resolved without paying much regard to the hydrodynamic consistency of the model of the extended atmosphere.

There have been frequent proposals that some cool stars possess extremely inhomogeneous extended atmospheres in which structures akin to solar prominences are common (e.g., Spitzer, 1939). Observations of spectroscopic fine structure in eclipsing binary systems and time-dependent discrete absorption components in spectra of RS CVn systems support this idea. It is perhaps worth mentioning that solar prominences, spectacular as they are, produce absolutely no detectable symptoms of atmospheric extension in the integrated solar spectrum.

The existence of the solar corona implies that low-density extended atmospheres may be common among cool dwarf stars. However, at present there is no observational technique which is sufficiently sensitive to detect low density coronae and winds, and we are therefore unable to determine how atmospheric extension varies among cool main-sequence stars. The evidence for atmospheric extension (circumstellar and emission lines) becomes more promi-

nent with decreasing gravity, presumably as a result of increasing density (or mass) in the extended atmosphere. As discussed above, there is a tendency for stars in the cool, low-gravity part of the HR diagram to have weak transition-zone emission, and strong indications of high mass-loss rates. Such stars must have massive extended atmospheres.

The extended atmospheres of T Tauri stars have been studied by a number of semi-empirical methods, but the diagnostics are unreliable and the structural organization of the gas in T Tauri atmospheres remains unclear. In an early study Kuhi (1964b) assumed that the density ρ and velocity distribution v in a model extended atmosphere were given by $r^2\rho v = R_o^2\rho_o v_o$, with $v(r)^2 = v_o^2 + R_o/r - 1$. Kuhi compared the strengths and shapes of predicted and observed emission lines, and adjusted the atmospheric structure until there was a reasonable match. From this work he deduced the high mass-loss rates which are thought to occur in T Tauri stars. Kuhi's model was refined by later workers, who adopted different structures and used different methods to compute the line profiles. There is another class of model for T Tauri atmospheres which involves inflowing material, and it is evident that further work is required to clarify the structure of the extended atmospheres of T Tauri stars. This problem will be discussed further in Chapter 6.

6

DYNAMICAL PROCESSES AND THE ORIGIN OF ATMOSPHERIC STRUCTURE IN COOL STARS

Lawrence E. Cram

I. INTRODUCTION

The critique of the classical model of stellar atmospheres presented in Chapter 5 emphasized that many observed properties of cool stars (and, indeed, hot stars) are not explained by that model. Prominent symptoms of the limitations of the classical model include:

- (1) anomalous degrees of ionization and excitation, in many cases indicating the existence of nonradiative heating of parts of the stellar atmosphere, but in some cases indicating the existence of a remarkable quantity of cool material;
- (2) anomalous spectral line widths and shapes, indicating the existence of chaotic and/or ordered flow patterns in the radiating region;
- (3) emission lines and other spectroscopic features, indicating the presence of an extension of the atmosphere beyond the altitudes where material can be supported hydrostatically; and
- (4) evidence of widespread variability, both regular and irregular, showing that the atmospheres are not static.

The goal of the present chapter is to provide a synopsis of contemporary thought regarding the origin of these and other related "anomalous" phenomena.

It should be noted at the outset that we are treating here a relatively young branch of astrophysics. The available data are severely limited in several respects, particularly in (1) signal-to-noise, (2) spectral range and resolution, (3) coverage of faint objects, and (4) time span and resolution. Moreover, some of the relevant observational material has been obtained only within the past decade, and there has been barely sufficient time to digest it and, more importantly, to integrate it with older data.

However, despite their defects, the available data have stimulated a large number of theoretical investigations aimed at developing explanations or "models" which illustrate how particular structures or mechanisms might act to produce a particular set of observations. As a result, there exists a bewildering variety of models for various parts of the atmospheres of cool stars which have as yet been subjected only to preliminary scientific assessment. While it

will not be possible in this chapter to undertake a significant integration, refinement, or simplification of these models, we do need to erect a framework which permits a systematic treatment of current knowledge. To this end we have adopted the following guidelines:

- (1) Based on the evidence of systematic trends in the spectroscopic characteristics of stars, we conclude that there exists a common pattern in the gross atmospheric structure of most cool stars. The pattern is characterized primarily by a radial sequence of zones analogous in many respects (but not all) to the solar photosphere, chromosphere, corona, and wind.
- (2) It is assumed that the structure of the atmosphere is the net result of the action of a (relatively small) number of physical mechanisms which in broad terms may be characterized as gasdynamic and/or electrodynamic processes.
- (3) In most cases, these processes are ultimately controlled by physical mechanisms which occur in the interior of the star — i.e., in the “subatmosphere.”

In Section II of this chapter, we expand on the first point in particular, discussing evidence for the existence not only of a common structural pattern, but also of systematic deviations from the solar atmospheric paradigm. Section III provides a brief summary of relevant aspects of gasdynamics, with an emphasis on the assumptions which underlie most theoretical studies of stellar atmospheric dynamics. Current ideas regarding the nature of several sub-atmospheric dynamical processes are presented in Section IV, while Section V discusses gas-dynamical processes in the stellar atmospheres themselves.

II. SPECTROSCOPIC TAXONOMY AND ATMOSPHERIC STRUCTURE

The goal of this section is to attempt to provide a global, qualitative description of the

structure of the atmospheres of cool stars. In essence, we return to the questions raised in Chapter 5.III, and ask how the available observational data help to reveal:

- (1) intrinsic atmospheric properties such as temperature, density, and ionization state;
- (2) extrinsic atmospheric properties such as the total amount of material having a certain temperature and bulk velocity; and
- (3) organization of the material of the atmosphere in space and time.

Several of the ideas presented here have been developed from concepts originally discussed by Gebbie and Thomas (1968, 1971), Praderie (1973), Pecker, Praderie, and Thomas (1973) and Thomas (1973). A companion monograph by Thomas (1983) treats the issue from a somewhat different point of view.

This series of papers develops the concept that a star is essentially a concentration of matter and energy located in the dilute, highly nonequilibrium interstellar medium. The star presumably forms from the interstellar medium as a result of a fluctuation (random or externally excited) whose amplitude grows because the interstellar medium at that time and place is unstable to nonadiabatic, nonreversible collapse and condensation. Under the influence of gravitational, magnetic, and pressure forces, a large volume of material accumulates into a region which ultimately develops into a grossly stable and slowly evolving “star.”

The empirical and theoretical study of *star formation* is one of the major themes of contemporary astrophysics (e.g., Gehrels, 1978). Two aspects of the subject are of special interest in the present volume. *First*, it is important to consider the degree to which a star and its neighboring interstellar medium “remember” the specific conditions pertaining during the star’s birth. Insofar as these conditions are not

“forgotten,” they represent a potentially important way to account for differences between mature stars. Examples of initial conditions which may persist for a long time and influence atmospheric structure in mature stars include the initial chemical composition, the distribution of angular momentum, primordial magnetic fields, and the existence of companion stars. *Second*, we are naturally concerned with changes which occur in the stellar atmosphere during the early evolution of the star. In particular, it seems likely that some aspects of the behavior of T Tauri stars can be best understood as the result of the interplay between (1) accretion from the interstellar medium and (2) mass outflow related to a kind of stellar wind (Chevallier, 1983). This process will be discussed below in more detail.

At some instant during the process of stellar collapse, the center of the collapsing object will become opaque to all electromagnetic radiation. This instant can be conveniently identified as the birth date of the star and its atmosphere. We may then define *the stellar interior* as being all regions which are invisible to an external observer (at any electromagnetic wavelength), and *the stellar atmosphere* as being all regions lying outside the interior, extending out to the point where the state of the adjacent interstellar medium is no longer dominated by the single star (or stellar system) in question. Note that this definition of the atmosphere encompasses all of the subregions which have been previously termed photospheres, chromospheres, coronae, winds, shells, ejecta, circumstellar dust, planetary nebulae, or extended envelopes. The identification of the base of the atmosphere with the deepest observable layers of the star is a reasonable approach from the observational point of view. It has the added merit of placing the base of the atmosphere at a point where diffusive radiative transfer in the interior yields to radiative escape (at least at some frequencies) in the atmosphere. This transition is of special relevance because radiation plays such an important role in the energy balance of the star and its atmosphere.

The definition given above implies that the stellar atmosphere is a region of transition between the relatively dense and therefore quasi-equilibrium interstellar medium. Matter and energy flow through the transition region, or atmosphere, coupling the interior and exterior, and certain characteristic structural patterns are imposed on the atmosphere as the process occurs. Some of these patterns are subsequently impressed on the emergent spectrum of the star, and information about the structure may then be extracted by the procedures of spectroscopic diagnostics.

A general but rudimentary theory of the formation of patterns in “transition regions” between extensive thermodynamic systems has been discussed by Glansdorff and Prigogine (1971). This theory distinguishes between (a) equilibrium structures formed and maintained through reversible transformations (e.g., crystallization from a eutectic), and (b) dissipative structures, formed and maintained through the effect of exchange of energy and matter in nonequilibrium conditions (e.g., convective cells in a fluid which is subject to a temperature gradient). Stellar atmospheres are evidently complex dissipative structures. Studies of such systems usually focus on two kinds of problems: (1) identification and characterization of the structures which do appear, and (2) explanations of these structures in terms of the flows of matter and energy. In the remainder of this section we discuss the construction of *empirical models* of the structure of stellar atmospheres, thereby addressing the first of these problems. The second problem will be taken up in subsequent parts of the chapter.

II.A. GROSS RADIAL STRUCTURE OF STELLAR ATMOSPHERES

Our experience of large dissipative structures (such as living organisms, and the atmospheres of the Earth, planets, and the Sun) reveals a tendency for such structures to be organized into fairly distinct subregions or zones. Scientific

investigations are often facilitated when such zones are identified, since the individual zones and the interactions between zones may be dominated by only a small number of physical processes. Of course, too narrow a focus on the properties of single zones can obscure understanding of the global structure of the system. It seems that a productive line of enquiry must involve both the fine analysis of single zones and pairwise interactions, and the construction of coarser models of the overall system.

The reader will recognize that many of the observations reported in Chapters 2, 3, and 4 invite an interpretation in terms of zonal structure in stellar atmospheres. Recognizing this, Thomas (1983), in particular, has undertaken the herculean task of attempting to represent the full range of observations of stellar spectra in terms of a "limited variety of distinctive atmospheric regions." This variety is to encompass all stars, although "some regions are more prominent than others, in different kinds of stars, and in different stars of the same kind, and in some phases of a given star relative to other phases." Thomas has made substantial progress in this task, although the fragmentary nature of most of the observational data — long time sequences of multispectral observations extending over many years — has frustrated the completion of the project. Thomas' results are summarized here because they provide a bridge between the bewildering variety of observations described in Chapters 2, 3, and 4, and the equally bewildering variety of theoretical speculations which have been advanced to account for these observations.

Thomas (1983, p. 330) concludes that the available observations require at least four types of structural sequences to account for all stars. Two of these sequences (type-3 and type-4) involve large amplitude variability of the mass-flux at the photospheric level, either through "episodic" (type-3) or "pulsational" (type-4) behavior. The other two sequences are constructed above "quasi-thermal photospheres" and are distinguished by the fact that

type-2 sequences have a prominent $H\alpha$ emission envelope and a well developed "local stellar environment" (intimately related to variable mass flux), while type-1 sequences do not. While Thomas has not successfully identified a common pattern covering all of these sequences, he has constructed (Thomas, 1983, pp. 283-322) a general structural pattern which covers many (and perhaps all) of the stars discussed in this volume. This structural pattern consists of the following zones (the words used here to describe the zones are not always equivalent to those used by Thomas, and in some cases the essence of Thomas' definitions has been slightly altered in some respects):

A. Quasi-thermal Photosphere

A radiation-dominated region lying immediately above the base of the atmosphere (defined above), characterized by differential velocity fields with amplitudes so small (less than about $\frac{1}{3}$ of the local sound speed) that they do not lead to substantial dissipation or to substantial deviation from hydrostatic equilibrium. Any variability present involves time scales longer than all radiative relaxation rates.

B. Chromospheres

Lying just above the photosphere, the chromosphere is characterized by the dissipation of a nonradiative energy flux which raises the kinetic temperature significantly above the non-LTE photospheric limit ($\sim T_{eff}$). The chromosphere ends where the differential flow velocities are sufficiently high to lead to marked distension relative to hydrostatic equilibrium.

C. Lower Corona

Lying just above the chromosphere, the lower corona is characterized by trans-thermal flows, i.e., by velocity amplitudes lying close to the sound speed, and by dissipation which leads to an outward

increase in kinetic temperature. Thomas presents a novel theory of trans-sonic flow (see also Cannon and Thomas, 1976) to support the definition of this region, which he points out is not part of the "conventional theoretical" model.

D. Upper Corona

The upper corona lies just above the lower corona, and begins where the mean velocity of outflow exceeds the escape velocity. The upper corona ends where strong nonradiative energy dissipation ends. Somewhat arbitrarily, Thomas defines this point observationally, as the point where the kinetic temperature begins to fall.

E. Postcoronal Domain

The postcoronal domain is an "ambiguously characterized set of distinctive atmospheric regions of which . . . there appear to be at least two varieties." Those two varieties are defined in subsections F. and G. which follow.

F. Nondecelerated Postcorona

This variety of postcorona exhibits a slowly decreasing outward kinetic temperature and a density distribution fixed by the mass-flux expansion. Thomas argues that this form of postcorona appears to exist only in stars showing minor variability in mass-flux, and that in such stars it is the last region of the atmosphere proper. Its outer extreme may exhibit detectable interactions with the interstellar medium.

G. Decelerated Postcorona

This variety of postcorona exhibits a complex, nonmonotonic temperature distribution reflecting (Thomas argues) collisions between present flows and "slower moving mass flow from a previous epoch." The region is poorly understood because its radiation field is

best observed shortward of the Lyman edge. A decelerated postcorona is characteristic of stars with grossly variable mass flux. In such stars there are several zones in the "local stellar environment," including, in particular, an $H\alpha$ emission envelope.

H. $H\alpha$ Emission Envelope

This region lies immediately above the decelerated postcorona, and is characterized by densities and (more importantly) temperatures which lead to significant $H\alpha$ emission. The region is characterized by a relatively slow flow velocity relative to the coronal and postcoronal regions. In some stars it merges outward into more extended regions.

I-J-K. . .

The remaining regions of the local stellar environment. These regions may reflect different levels of cooling from the $H\alpha$ envelope. They include regions producing narrow absorption components in visible spectral lines, forbidden lines, and IR dust emission and absorption features.

The great value of Thomas' (1983) work lies in two achievements: (1) the attempt to sketch a spatially continuous sequence of atmospheric zones, with no "gaps" or "holes" in the radial direction, and (2) the provisions for each zone of a description characterizing it in terms of (a) observations, (b) "thermodynamics," and (c) diagnostics. In the next section we explore the correspondence between observations of cool stars and the structural paradigm erected by Thomas.

II.B. DIFFERENCES BETWEEN STARS

Chapters 2, 3, and 4 describe a bewildering variety of observational characteristics of the population we have called "cool stars." The common property of this population is the fact

that the "effective temperatures" span a relatively narrow range (4000–7000 K). As a result, the atmospheres of almost all of these stars are illuminated from below by a radiation field with an intensity and spectral quality not very different from that of the Sun. The discussion of classical atmospheres in Chapter 5 has indicated that this radiation field, acting alone, would lead to a set of rather similar atmospheres for the entire range of cool stars. This is of course not what is observed!

In this section, we explore the variation of "nonclassical" atmospheric properties from star to star. In an effort to concentrate on what seems to be the most significant differences, we use the structural paradigm of Thomas (Section II.A) as a point of reference, and focus on three broad classes of cool stars:

- (A) "Solar-like" main-sequence stars,
- (B) "T Tauri-like" stars, and
- (C) Giant stars lying above the "dividing line" defined by Reimers (Chapter 3.III.A.5).

Of course, other classifications and subdivisions of the cool-star population are possible, but this one serves well to illustrate some of the most obvious similarities and differences between cool stars.

In Table 6-1 we have indicated the evidence for correspondences between Thomas' paradigm and the observationally inferred atmospheric structure of the three stellar types. While there are encouraging indications that several correspondences can be established, it is clear that there are also several doubtful areas. Whether these are due to defects in the paradigm or to gaps in the observational material (or both) is unclear at present. Our attempt to complete this table has emphasized *the crucial importance of developing instruments capable of measuring the time-dependent shapes of spectral lines in the EUV and X-ray spectral regions*. Such information would be of tremendous value in studies of flow patterns in

high-temperature regions, and hence would help greatly in the construction of a plausible description of the radial structure of temperature, chaotic velocity, and net mass flux.

II.C. VARIABILITY

It is probable that all classes of cool stars possess forms of spectrum variability which could be detectable with current equipment if appropriate observing campaigns were undertaken. However, the demanding requirements for instrumental sensitivity and availability have inhibited extensive studies of variability in all but a few cool stars. Consequently, our empirical knowledge regarding such variability is quite fragmentary and incomplete.

A convenient way to approach the problem of providing a coherent summary of observations of variability in cool stars is to consider evidence for variability in each of the zones in the general atmospheric structure summarized above. This is so because only in a few cases among cool stars (FU Ori stars, X-ray emission from some pre-main-sequence stars) do we have evidence of major disruptions in the gross atmospheric structure (this is not the case for the hot B/Be stars, for example). Rather, most observations of variability seem to reflect variations taking place within one or more "zones" or "regions" of an atmosphere, which during these variations preserve most of their gross radial organization. Because of this, observations of variability promise to elucidate important aspects of the spatial organization of stellar atmospheres (e.g., by tracing sequential disruptions or variations through sequential layers), as well as the physical processes at work.

In a large proportion of cool stars, the observed forms of variability strongly suggest that the atmospheric zones are laterally inhomogeneous. Examples include: (1) the rotational and long-term cyclic modulation of photometric and K-line observations of cool dwarfs, suggestive of laterally extended "active regions" (Chapter 3.VII); (2) evidence of rapid

Table 6-1
Atmospheric Zones in Cool Stars

| Region | Solar-type | T Tauri-type | Giant-type |
|--|------------------------|---|------------------------|
| quasi-thermal photosphere | present | either structurally distorted or veiled in "advanced" types | present |
| chromosphere | present | present | present ^(a) |
| lower corona | present | present ^(b) | present ^(b) |
| upper corona | present ^(c) | presence indicated by X-rays only in some stars | unclear ^(c) |
| postcorona-non-decelerated | present ^(d) | n.a. ^(e) | n.a. ^(e) |
| postcorona-decelerated | n.a. ^(e) | unclear ^(f) | unclear ^(g) |
| H α -emission envelope | n.a. ^(e) | present ^(h) | present ⁽ⁱ⁾ |
| outer parts of local stellar environment | n.a. ^(e) | present ^(h) | present ⁽ⁱ⁾ |

(a) Studies of emission-line profile shapes in some giant types indicate that the atmosphere may be distended in all layers above the photosphere: this phenomenon has been called an "extended chromosphere" (Chapter 3.III.A.1), but the usage is not really consistent with Thomas' (possibly in-applicable) scheme.

(b) Confirmation of the existence of a "lower corona" properly requires evidence of transonic, sub-escape velocities. The sparse evidence available indicates that the widths of "transition zone" EUV lines are consistent with transonic Doppler broadening effects (see Chapters 3.II.A.3 and 4.III.B.2).

(c) We have no information on coronal flow velocities or mass-fluxes for solar-type stars, other than the Sun itself.

(d) Thomas insists that the nondecelerated postcoronal structure be characterized observationally and thermodynamically by radiative equilibrium under the combined photospheric, chromospheric, and coronal radiation field. Direct observations of the solar wind at Earth show that thermal conductivity and other poorly understood electrodynamic processes play a dominant role in the energy balance of the solar wind. I believe Thomas' definitions are inadequate in this region.

(e) n.a.: not applicable. Nondecelerated and decelerated postcoronas are mutually exclusive.

(f) It is possible that some of the EUV emission spectrum of T Tauri stars emerges from a postcoronal region. Further work on density diagnostics and line shapes may shed some light on this question (Chapter 4.III.B.2).

(g) The relationships between temperature, density, and mean radial flow velocity as a function of radius in the "local stellar environment" of giant types is not clear (Chapter 3.V.B).

(h) There is abundant evidence of collisions and episodic mass-flux excitation in the outer parts of T Tauri-type atmospheres. However, it is unclear at present whether the effects are primarily related to material ejected from the star, or whether "pre-stellar cloud" material is also involved (Chapter 4.IV.B).

(i) As emphasized by Thomas in the original definitions, there is a tremendously diverse set of spectroscopic indicators of conditions in these outer regions. Not all cool giant stars have clear evidence of an outer local stellar environment.

variability in T Tauri stars, on time scales inconsistent with globally coherent phenomena (Chapter 4.II and 4.III); and (3) evidence of large-scale cohesive structures in eclipsing giant stars, reminiscent of solar prominences (Chapter 3.V.B.2). It is evident that further observational studies are required of the relationship between variability and lateral inhomogeneity in the atmospheres of cool stars.

Thomas' (1983) study of the outer parts of stellar atmospheres — the so-called "local stellar environment" — has revealed evidence of a significant correlation between (1) the presence of a well-developed decelerated postcorona with $H\alpha$ emission, dust radiation, and circumstellar absorption, and (2) prominent, episodic variability in atmospheric structure and, most importantly, in mass flux. Thomas paid great attention to the Be and T Tauri stars, where the effect is manifested through several well-studied phenomena. The situation of the cool giant stars located "above" the hybrid-star dividing line is less clear, although there is some evidence supporting Thomas' conjecture for these objects, too. In particular, the eclipsing systems reveal the presence of gross atmospheric inhomogeneities, while many cool supergiants are semiregular variables with large amplitudes on time scales of months. It is probable that nonradial pulsations, perhaps associated with electrodynamic processes, play an important role in promoting variability and mass loss in these stars. It is a challenging and important task to devise observing programs to investigate the character of variability in several different stars, over different spectral regions and over an extended time scale. The examples of startling new results provided by patient monitoring of B/Be stars (e.g., Underhill and Doazan, 1982) show what can be achieved.

III. BASIC THEORY OF ATMOSPHERIC GASDYNAMICS

In the previous section, we explored what Thomas (1983) has termed "empirical-

theoretical" descriptions of stellar atmospheres. It was shown that substantial progress has been made towards a general empirical model of the radial organization of zones in the atmospheres of cool stars, although large gaps remain to be filled. In the remainder of this chapter, we discuss current theoretical ideas regarding the mechanisms which might be responsible for forming the various zones seen in stellar atmospheres. The present section is included to provide a discussion of some of the more fundamental assumptions made in theoretical studies of these problems.

The stellar atmosphere consists of a low-density, ionized mixture of gases, bathed in a strong radiation field, and subjected to gravitational and electrodynamic body forces. Particle densities, kinetic temperatures, magnetic field strengths, and many other key parameters span several orders of magnitude, and there is enormous diversity in the phenomena to be described. Because the density is so low, the natural starting point to describe such a system is the Boltzmann or Fokker-Planck equation. However, the detail implied by this equation is unnecessary in practical applications, and many techniques have been developed to provide a set of low-order moment equations which give an adequate description of the macroscopic behavior of the fluid system. Even the simplest moment systems exhibit a remarkable range of potential physical interactions that are often ignored in studies of stellar atmospheric dynamics. Although it is not possible to present here a detailed account of the theory of the Boltzmann or Fokker-Planck equation and the moment systems that may be derived from them, it is important to provide some background to the critical problems and results which are relevant in the development of a dynamical theory of stellar atmospheres.

It is widely believed that an adequate description of the dynamics of a large gaseous system such as a stellar atmosphere can be based on a knowledge of the one-point velocity distribution function $f_1(\mathbf{v}, \mathbf{r}, t)$, where $f_1 d\mathbf{v} d\mathbf{r}$ is the

number of particles of species i with velocities in the range $(\mathbf{v}, \mathbf{v} + d\mathbf{v})$ lying in the volume element $(\mathbf{r}, \mathbf{r} + d\mathbf{r})$ at time t . The species index i is multi-dimensional and provides a complete characterization of the isotopic and quantum state of the designated species. The evolution of the distribution function is described by the equation (see Grad, 1958; Chapman and Cowling, 1970):

$$\begin{aligned} D_i f_i &= \frac{\partial f_i}{\partial t} + \mathbf{v} \cdot \frac{\partial f_i}{\partial \mathbf{r}} + \mathbf{F}_i \cdot \frac{\partial f_i}{\partial \mathbf{v}} \\ &= \sum_j C_{ij}(f_i, f_j) \quad , \quad (6-1) \end{aligned}$$

where \mathbf{F}_i is the external or body force:

$$\mathbf{F}_i = m_i \mathbf{g} + q_i (\mathbf{E} + \mathbf{v} \times \mathbf{B}) \quad (6-2)$$

Here, m_i and q_i are respectively the mass and electric charge on species i , and \mathbf{g} , \mathbf{E} and \mathbf{B} are respectively the macroscopic gravitation, electric, and magnetic fields.

The LHS of Equation 6-1, represented by the operator D_i , describes the evolution of f_i as each particle moves under the influence of the external force, without taking account of interactions between the particles. The RHS of Equation 6-1, represented by the operator C_{ij} , describes the changes of f_i due to interactions between particles of type i and j .

It should be mentioned here that the Boltzmann equation may not provide an adequate model for certain aspects of stellar atmospheric dynamics. For example, in a highly ionized gas the dominant interactions may be long-range Coulomb collisions for which two-body collision theory is not always an adequate description. In such cases, the collision term may be modeled by a screened Coulomb potential or, more properly, by the Fokker-Planck equation or its generalizations (Balescu, 1963). This

added complexity gives rise to a number of important questions, including (i) what is the appropriate way to separate the force on a particle into its external and microfield components, (ii) how does f_i change during long-range, long-duration collisions, and (iii) are two-point and higher velocity correlation functions needed to describe some important collective effects. In the context of stellar atmospheres these questions arise immediately in the theory of collisional damping of spectral lines, since this process arises from the interactions that take place between two or more particles in the presence of a photon. The question must also be considered in attempts to model high-frequency phenomena in structured magnetic fields, such as those that might occur in stellar coronae and winds. We shall not consider this aspect of plasma dynamics further in this monograph: the interested reader may refer to discussions of collective plasma processes in texts such as Montgomery and Tidman (1964) and Golant et al. (1977).

The collision operator in the Boltzmann equation may be conveniently divided into three components, each one representing a summation over all two-body interactions:

$$C = \sum C_{ij}^E + \sum C_{ij}^I + \int C_{i\nu} d\nu \quad (6-3)$$

The component C_{ij}^E represents elastic collisions, C_{ij}^I represents inelastic collisions, and $C_{i\nu}$ represents processes involving interactions between species i and electromagnetic radiation of frequency ν . Electromagnetic radiation obeys a Boltzmann-like equation for the specific intensity $I_\nu(\Omega)$ at frequency ν traveling in direction Ω (Simon, 1963; Sampson, 1965):

$$\begin{aligned} \frac{1}{c} \frac{\partial I_\nu}{\partial t} + \Omega \cdot \frac{\partial I_\nu}{\partial \mathbf{r}} &= \\ \sum_i \eta_{i\nu} - \sum_i \kappa_{i\nu} I_\nu & \quad (6-4) \end{aligned}$$

Here, $\kappa_{i\nu}$ and $\eta_{i\nu}$ are, respectively, the absorption and emission coefficients of species i at frequency ν (cf., Equations 5-26, 5-27). Each component of the collision operator C_{ij} in Expression 6-3 contains two parts, the one representing interactions which extract particles of species i from the distribution function in the volume element $drd\nu$, and the other representing interactions which deliver particles into the distribution function as species i at $drd\nu$. Some of these interactions involve three-body processes which may require a slight modification of the Boltzmann equation.

The system of Equations 6-1 through 6-4 is extremely complex, and in practical applications it provides much more information than is actually required to understand the gasdynamics of stellar atmospheres. Thus, although there are some relevant unsolved problems related to the solution of Boltzmann's equation itself in the presence of a non-LTE radiation field (cf. Hubený, 1981a; Beckman and Crivellari, 1985), the practical study of stellar atmospheric dynamics is almost always based on a reduced system of macroscopic (or fluid) equations describing the evolution of low-order moments of the velocity distribution function. Some of the moments, and quantities which may be derived from them, include:

$$\text{number density } n_i = \int f_i d\nu$$

$$\text{mass density } \rho_i = m_i n_i$$

$$\text{mean density } \rho = \sum_i \rho_i$$

$$\text{directed velocity } \mathbf{v}_i = \frac{1}{n_i} \int \mathbf{v} f_i d\nu$$

$$\text{mean velocity } \mathbf{v} = \frac{1}{\rho} \sum_i \rho_i \mathbf{v}_i$$

$$\text{peculiar velocity } \mathbf{c}_i = \mathbf{v}_i - \mathbf{v}$$

$$\text{partial pressure tensor } \mathbf{P}_i \approx m_i \int \mathbf{c}_i \mathbf{c}_i f_i d\nu$$

$$\text{total pressure tensor } \mathbf{P} \approx \sum_i \mathbf{P}_i$$

$$\text{kinetic temperature } T_i^k = \frac{1}{3kn_i} \int mc_i^2 f_i d\nu$$

$$\text{heat flux vector } \mathbf{q}_i = \int \frac{1}{2} m_i c_i^2 \mathbf{c}_i f_i d\nu$$

$$\text{energy density } U_i = \int (\frac{1}{2} m_i c_i^2 + \chi_i) f_i d\nu$$

$$\text{radiation pressure tensor } \mathbf{P}_\nu^R \approx \frac{1}{c} \int \Omega \mathbf{I}(\Omega) d\Omega$$

$$\text{radiation flux vector } \mathbf{F}_\nu^R = \int \Omega \mathbf{I}_\nu(\Omega) d\Omega$$

The formal application of corresponding moment operators to the Boltzmann equation is straightforward, and leads to the following equations:

$$\frac{\partial n_i}{\partial t} + \frac{\partial}{\partial \mathbf{r}} \cdot (n_i \mathbf{v}) + \frac{\partial}{\partial \mathbf{r}} \cdot (n_i \mathbf{v}_i) = S_i \quad (6-5)$$

$$\begin{aligned} & \frac{\partial}{\partial t} (\rho_i \mathbf{v}_i) + \frac{\partial}{\partial \mathbf{r}} \cdot (\rho_i \mathbf{v}_i \mathbf{v}) + \frac{\partial}{\partial \mathbf{r}} \cdot \mathbf{P} \\ & + \rho_i \left[\frac{D\mathbf{v}}{Dt} + \mathbf{v}_i \cdot \frac{\partial \mathbf{v}}{\partial \mathbf{r}} \right] - \rho_i \mathbf{F}_i = \mathbf{M}_i \quad (6-6) \end{aligned}$$

$$\begin{aligned} & \frac{\partial}{\partial t} (\rho_i E_i) + \frac{\partial}{\partial \mathbf{r}} \cdot \mathbf{q}_i \\ & + \rho_i \left[\mathbf{P} \cdot \frac{\partial \mathbf{v}}{\partial \mathbf{r}} + \mathbf{v}_i \cdot \frac{D\mathbf{v}}{Dt} \right] - \rho_i \mathbf{F}_i \cdot \mathbf{v}_i \\ & = W_i \quad (6-7) \end{aligned}$$

These equations are, respectively, expressions for the conservation of number density, drift momentum, and microscopic (internal and translational) energy of species i .

The terms S_i , \mathbf{M}_i , and W_i are net production terms resulting from moments of the collision integrals.

This system of equations is particularly complex because it allows for the flow of individual

species relative to the mean velocity. Such drift and diffusion may be relevant in element diffusion (Vauclair et al., 1978), spectral line formation (Hubený, 1981b), element segregation in coronae (Nakada, 1970), gas entry into magnetic structures (Giovanelli, 1977), and the computation of electrical conductivity in the presence of a magnetic field.

Low-order moments of the radiative transfer equation are also useful:

$$\frac{\partial J_\nu}{\partial t} + \frac{\partial}{\partial \mathbf{r}} \cdot \mathbf{F}_\nu = \overline{\kappa_\nu J_\nu} - \overline{\eta_\nu} \quad (6-8)$$

$$\frac{\partial \mathbf{F}_\nu}{\partial t} + \frac{\partial}{\partial \mathbf{r}} \cdot \mathbf{P}_\nu^R = \overline{\kappa_\nu \mathbf{F}_\nu} - \overline{\eta_\nu} \quad (6-9)$$

In these equations, the overbar denotes a weighted angular average. The terms $\overline{\kappa_\nu J_\nu}$ and $\overline{\kappa_\nu \mathbf{F}_\nu}$ cannot in general be separated, because the Doppler effect produces angular correlations between the absorption coefficient and the radiation field.

A set of equations describing the macroscopic behavior of the plasma as a whole may be derived by summing Equations 6-5 through 6-9 over all species. The production terms cancel as a result of the laws of conservation, and the resulting system is:

$$\frac{\partial \rho}{\partial t} + \frac{\partial}{\partial \mathbf{r}} \cdot (\rho \mathbf{v}) = 0 \quad (6-10)$$

$$\begin{aligned} \frac{\partial(\rho \mathbf{v})}{\partial t} + \frac{\partial}{\partial \mathbf{r}} \cdot (\rho \mathbf{v} \mathbf{v}) \\ + \frac{\partial}{\partial \mathbf{r}} \cdot (\mathbf{P} + \mathbf{P}^R) = \mathbf{F} \end{aligned} \quad (6-11)$$

$$\frac{\partial}{\partial t} (\rho E + \frac{1}{2} \rho v^2) +$$

$$\begin{aligned} \frac{\partial}{\partial \mathbf{r}} \cdot [(\rho E + \frac{1}{2} \rho v^2) \mathbf{v} + (\mathbf{P} + \mathbf{P}^R) \cdot \mathbf{v} \\ + \mathbf{q}_T + \mathbf{F}^R] = \mathbf{v} \cdot \mathbf{F} \end{aligned} \quad (6-12)$$

The total pressure tensor is the sum of the particle pressure tensor and the frequency-integrated radiation pressure tensor.

The system (Equations 6-10 through 6-12) is deceptively simple, since the velocity distribution functions no longer appear. However, in principle, quantities such as ρ , \mathbf{v} , \mathbf{P} and \mathbf{q} can be evaluated only when the distribution functions are known. Since the benefit of the reduced moment system is lost if we have to obtain these distribution functions, approximations are made to describe the distribution functions and their moments. These lead to various models of transport processes in the stellar atmospheric plasma.

One simple hypothesis is that the distribution function for each species is everywhere Maxwellian, with a unique kinetic temperature that varies with position and time, $T_e(\mathbf{r}, t)$. We then have:

$$f_i = n_i \left(\frac{m_i}{2\pi k T_e} \right)^{3/2} \exp[-m_i c^2 / k T_e] \quad (6-13)$$

With this model, all drift velocities are zero, and the pressure tensor is diagonal and isotropic:

$$\mathbf{P} = P_g \mathbf{I} \quad (6-14)$$

The equivalent hypothesis on the radiation field is that the intensity is given by the black-body Planck function:

$$I_\nu = B_\nu(T_e) \quad (6-15)$$

The hypotheses (Equations 6-13 through 6-15) are sufficient to ensure that the production terms are zero, in view of the principle of

detailed balance. Consequently, the excitation and ionization equilibria are given by Saha-Boltzmann relations. The equations that result from this hypothesis are known as the "Euler equations," describing the motion of a compressible, inviscid gas without heat conduction or radiative energy transport:

$$\frac{\partial \rho}{\partial t} + \frac{\partial}{\partial \mathbf{r}} \cdot (\rho \mathbf{v}) = 0 \quad (6-16)$$

$$\frac{\partial(\rho \mathbf{v})}{\partial t} + \frac{\partial}{\partial \mathbf{r}} (\rho \mathbf{v}^2) + \frac{\partial \mathbf{P}}{\partial \mathbf{r}} \cong \mathbf{F} \quad (6-17)$$

$$\begin{aligned} & \frac{\partial}{\partial t} (\rho E + \frac{1}{2} \rho v^2) \\ & + \frac{\partial}{\partial \mathbf{r}} \cdot [(\rho E + \frac{1}{2} \rho v^2) \mathbf{v} \\ & + \mathbf{P} \cdot \mathbf{v}] = \mathbf{v} \cdot \mathbf{F} \end{aligned} \quad (6-18)$$

The motion described by this system is adiabatic along particle paths, except where the paths cross shock fronts. The system of equations is not self-consistent except in the case of strict thermodynamic equilibrium (i.e., T_e constant in time and space), since the existence of flows and/or gradients would necessarily involve a nonisotropic distribution function. Nevertheless, there are many circumstances in which Euler's equations provide an adequate description of the gasdynamics of stellar atmospheres. They are widely used to model aerodynamic flow in terrestrial studies, although they must be supplemented by boundary-layer (viscous) theory in all practical cases where the flow is confined by boundaries. Combined with Maxwell's equations, Euler's system of Equations (6-16 through 6-18) provides the starting point for many studies of magnetohydrodynamics, although some subtle manipulations are required to preserve the first-order effects due to electric currents in this strictly equilibrium model (Chapman and Cowling, 1970; Ferraro and Plumpton, 1966).

In a stellar atmosphere the strict LTE requirement of Expression 6-15 is eventually violated, since the opacity at some wavelengths is small enough to allow a uni-directional flow of radiative energy. A simple approximation which can account for this effect is to maintain the assumption of Maxwell-Saha-Boltzmann distributions for the particles, but to allow the radiation intensity I_ν to be determined by a solution of the radiative transfer equation. Maxwell-Saha-Boltzmann equilibrium implies that the source function $S_\nu = \eta_\nu/\kappa_\nu = B_\nu(T_e)$, but the radiative variables J_ν , \mathbf{F}^R , \mathbf{P}^R , etc., may depart from their equilibrium values. This model of radiation transfer is known as astrophysical LTE, or LTE-R (Thomas, 1965). The modified Euler equations become:

$$\frac{\partial \rho}{\partial t} + \frac{\partial}{\partial \mathbf{r}} \cdot (\rho \mathbf{v}) = 0 \quad (6-19)$$

$$\begin{aligned} & \frac{\partial \rho \mathbf{v}}{\partial t} + \frac{\partial}{\partial \mathbf{r}} (\rho \mathbf{v}^2) \\ & + \frac{\partial}{\partial \mathbf{r}} \cdot (\mathbf{P} + \mathbf{P}^R) = \mathbf{F} \end{aligned} \quad (6-20)$$

$$\begin{aligned} & \frac{\partial}{\partial t} (\rho E + \frac{1}{2} \rho v^2) + \\ & \frac{\partial}{\partial \mathbf{r}} \cdot [(\rho E + \frac{1}{2} \rho v^2) \mathbf{v} + (\mathbf{P} + \mathbf{P}^R) \cdot \mathbf{v} + \mathbf{F}^R] \\ & = \mathbf{v} \cdot \mathbf{F} \end{aligned} \quad (6-21)$$

with the radiative transport equation:

$$\Omega \cdot \frac{\partial}{\partial \mathbf{r}} I_\nu = -\kappa_\nu I_\nu + B_\nu(T_e) \quad (6-22)$$

To introduce processes such as diffusion, thermal conductivity, viscosity, and electrical

resistivity into the gasdynamic equations, the assumption 6-13 of a strictly Maxwellian velocity distribution must be relaxed. Several different approaches are available to effect this relaxation. In the Chapman-Enskog method (Chapman and Cowling, 1970), the distribution functions are expanded in a series of the form:

$$f_i = f_i^{(0)} + f_i^{(1)} + f_i^{(2)} + \dots \quad (6-23)$$

If this expansion is substituted into the Boltzmann equation, a sequence of integral equations is obtained, connecting $f_i^{(n)}$ with $f_i^{(0)}, \dots, f_i^{(n-1)}$.

The solutions of these integral equations, when used in the moment equations (Equations 6-5 through 6-7), provide estimates of the transport coefficients describing diffusion, resistivity, viscosity, and thermal conduction in terms of the spatial gradients of velocity, electric field, velocity shear, and temperature. The coefficients are obtained as integrals of the collision cross-sections.

The Chapman-Enskog procedure provides a restricted class of solutions of the Boltzmann equation known as normal solutions (Grad, 1958). Other solution methods, such as expansion in pre-specified polynomials, expansions in spherical harmonics, or half-range expansions find useful application in appropriate circumstances. Yet other methods are used to solve the Fokker-Planck equation (Spitzer, 1962).

In general, there are very close similarities between low-order systems of moment equations derived by any of these methods. This is due to the fact that the first symptoms of departure from equilibrium are fluxes which are expressible as linear combinations of the first derivatives of the thermodynamic quantities. For example, we have the diffusion current expressible in terms of a diffusion coefficient D_i ,

$$\mathbf{j}_i = \mathbf{D}_i \cdot \frac{\partial n_i}{\partial \mathbf{r}}, \quad (6-24)$$

the thermal conduction flux expressible in terms of the conduction coefficient k_T ,

$$\mathbf{q} = k_T \frac{\partial T_e}{\partial \mathbf{r}}, \quad (6-25)$$

and the electric current expressible as a linear combination of several fluxes in the form of a generalized Ohm's law

$$\mathbf{j}_e = \sigma_e (\mathbf{E} + \mathbf{v} \times \mathbf{B}) +$$

$$\sigma_T \frac{\partial T_e}{\partial \mathbf{r}} + \sigma_D \frac{\partial n_e}{\partial \mathbf{r}} + \dots \quad (6-26)$$

There may be some small quantitative differences in the actual derived values of the various coefficients, depending on the expansion methods employed; but the basic structure of the transport terms stays fixed, provided the departures from a Maxwellian distribution are so small that the fluxes are linear functions of the gradients of the state variables.

There are of course some situations where the first-order equations will break down. An important case involves modifications to thermal conductivity in the presence of a steep temperature gradient such as that which might be encountered in the chromosphere-corona transition zone (Spicer, 1978). Other regions where we might anticipate major deviations from the first-order gasdynamic equations are the low-density parts of stellar winds. The solar wind, because it is magnetized and highly ionized, retains most of its typical fluid behavior despite being "collisionless," although it does exhibit important temperature anisotropies and multi-fluid effects (e.g., Axford, 1985). Cool stellar winds with low degrees of ionization may evolve towards the Knudsen regime, where the free path between collisions is of the order of dynamical length scales, and important modifications may then be needed to the usual fluid equations.

The interaction between matter and radiation plays a central role in stellar atmospheric dynamics, and may also lead to significant deviations from near-equilibrium fluid equations. The most obvious example of this is the existence of highly nonequilibrium occupation numbers of excited bound levels whose population is controlled largely by effectively optically thin radiation fields. Non-LTE effects of this kind in static atmospheres were discussed in Chapter 5.III.B.3. Another potentially important non-LTE effect involves the strong departures from Maxwellian velocity distributions that occur when anisotropic, nongray radiation fields selectively populate certain velocity substates. Such departures are related to the problem of frequency redistribution in bound-bound radiative processes, and some simple examples have been discussed by Hubený (1981a). If velocity substate selection by radiative processes is important, diagnostic methods for gasdynamic phenomena will require improvement. There are some important problems that should be explored in this general area.

IV. SUBATMOSPHERIC DYNAMICS

The nonclassical behavior of a stellar atmosphere represents the ultimate response of the atmosphere to dynamical phenomena occurring beneath the stellar photosphere. These phenomena include convection, differential rotation, oscillations, electrodynamic effects, and episodic processes. In this section we deal with theories of these subphotospheric processes.

IV.A. CONVECTION

In the outer parts of the envelopes of cool stars, the fact that hydrogen is only partially ionized leads to a marked reduction in the ratio of specific heats, $\gamma = C_p/C_v$, and hence to the violation of Schwarzschild's criterion for convective stability (Chapter 5.II.A). Unsöld (1930) first identified this instability and termed the dynamical structure that results from it the

hydrogen convection zone. Theoretical studies (see Biermann, 1977, for an illuminating historical account) suggest that the convection zone in most cool stars extends inwards from the photosphere for a significant fraction of the stellar radius.

The influence of the convection zone on the atmosphere can be considered from two rather different points of view (Schwarzschild, 1961). On the one hand, it has long been recognized that envelope convection in cool stars has a direct influence on energy transport in the lower photosphere and hence on the classical radiative equilibrium model. It was for this reason that we referred to radiative-convective equilibrium (RCE) in Chapter 5.IV. In this context the key problem centers on the variation with altitude of the ratio of convective to radiative energy flux, as the former yields to the latter at the base of the photosphere. On the other hand, it has also been long recognized that envelope convection may produce a relatively small flux of mechanical energy, which travels through the photosphere to produce significant nonradiative heating in low-density regions lying at very small optical depths. This flux may also produce important effects on spectroscopic diagnostics. These two points of view foster two different thrusts in attempts to address the underlying problem of how the mechanical (convective) energy flux changes with height in the atmosphere. We shall first discuss the effect of convection on energy transport in the deep photosphere.

The change from convection to radiation as the dominant transport process at the base of the photosphere has two important effects in cool stars. First, the presence of convective transport in layers with continuum optical depths $\tau_c > 1$ leads to deviations from the radiative-equilibrium distribution of $T_e(\tau_c)$ in these deep layers. These deviations lead in turn to changes in the radiation field and hence the temperature distribution in the atmosphere where $\tau_c < 1$. Theories describing the self-consistent coupling between convection and

radiation at the base of the photosphere have been discussed by Sack (1966) and others.

A second important effect of the change from convection to radiation in cool stars arises in stars where a significant fraction of the stellar interior is occupied by inefficient convection. This situation occurs in the envelopes of cool giant and supergiant stars, where the low density and consequent low heat capacity of the outer 75% or so of the stellar volume implies that a significant departure from adiabatic stratification is required to transport, by radiation, that part of the luminosity that cannot be carried by convection (see Schwarzschild, 1975, Figure 3). In models of such stars, important fundamental parameters such as the radius, surface gravity, and effective temperature depend sensitively on departures from adiabaticity at the base of the photosphere. These departures depend in turn on the radiative properties of the deep photosphere and on uncertain parameters involved in the theory of envelope convection.

Quantitative theories of energy transport by convection in stellar envelopes are generally based on mixing-length theory (Spiegel, 1971; Gough and Weiss, 1976). Of course, there have been many astrophysicists who have expressed strong reservations about the validity of this theory when applied to stellar convection (cf., Spiegel and Zahn, 1977). However, without expressing wholesale acceptance of the mixing-length approach, Gough and Spiegel (1977) have argued that it is possible to place mixing-length theory in a fairly satisfactory framework. It appears that a pragmatic astrophysicist whose interests were directed towards the study of stellar structure and evolution might view mixing-length theory as a crude but useful tool.

However, in relation to the central theme of this volume — the atmospheres of stars — the mixing-length theories used in envelope calculations are quite unsatisfactory. In particular, in their usual form, these theories cannot explain the phenomenon of “overshoot” or “penetra-

tion” of convective structures into the stably stratified region of the photosphere (Moore, 1981; Bray et al., 1984). Some authors (e.g., Ulrich, 1970a) have extended and modified the mixing-length theory to describe the transfer of convective energy into the photosphere, but the modifications are of a semi-empirical nature and not firmly based on gasdynamic theory.

A number of attempts have been made to develop theories of convection in the solar envelope that are based more firmly on the principles of gasdynamics, particularly to provide an account of solar granulation (Bray et al. 1984). Among these are the semi-empirical model of Nelson and Musman (1977) and the full gasdynamic model of Nordlund (1982). Figure 6-1 displays the results of a time-dependent, three-dimensional, numerical simulation of the development of a single granule (turbulent convective eddy) computed by Dravins et al. (1981), using Nordlund’s method. It is evident from this figure that considerable progress has been made in our ability to predict the effects of convection on photospheric structure, although, as Bray et al. (1984) emphasized, there is still no definitive model of a solar granule.

There have been only a few studies of the theory of convective overshoot in stars other than the Sun. Toomre et al. (1976) used a single-mode nonlinear theory to study simple models of convection within the envelope of an A-star. Nelson (1980) extended the solar model of Nelson and Musman (1977) to provide a theoretical prediction of the nature of convective overshoot in main-sequence F stars. Böhm-Vitense (1977) has described some possible photometric observational tests of Nelson’s work. Observations of the asymmetries and shifts of stellar absorption lines promise to provide other kinds of tests of theories of convective overshoot in stars (Bray and Loughhead, 1978; Chapter 2.IV).

Understanding of convection and convective overshoot in the Sun and other cool stars is still

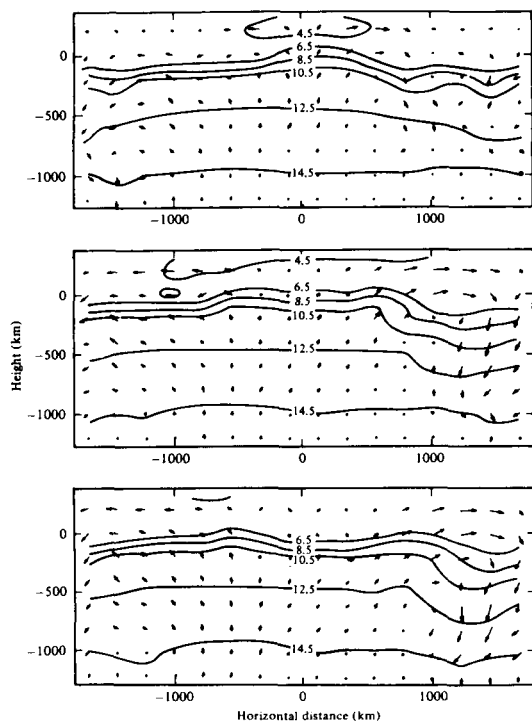


Figure 6-1. Granule development according to the numerical model developed by Nordlund (see Dravins et al., 1981). The arrows show the velocity vectors and the solid curves are isotherms (in units of 1000 K). From top to bottom the frames correspond to times of 0, 4, and 6 minutes.

in a rudimentary state. However, useful progress is now being made on the difficult theoretical and observational questions. In particular, observations of solar granulation provide some insight into the nature of penetrative convection in a stellar atmosphere. The results of such observations may be summarized in terms of the quantities listed in Table 6-2 (Bray et al., 1984). It should be noted that the observations underlying the compilation were obtained using instruments that are able to resolve granulation only on scales larger than about 500 km. At present we have no direct knowledge of solar atmospheric conditions on scales smaller than this. This is a severe limitation, since the phenomenon of spectroscopic turbulence (especially microturbulence) suggests that there could be a large amount of kinetic energy

on these small scales. The ability to resolve scales substantially smaller than 500 km could provide considerable insight into the mechanism of the turbulent cascade from the driven (granular) scale to the viscous dissipation scale (Bray et al., 1984).

Table 6-2
Properties of Solar Granulation

| | |
|-----------------------|------------------------|
| Average diameter | 1 Mm |
| Average lifetime | 15 min |
| rms vertical velocity | 1.5 km s ⁻¹ |
| Temperature contrast | 300 K |

Table 6-2 provides quantitative information regarding some of the boundary conditions imposed at the solar photosphere by conditions in the solar envelope. Comparable information is not available for other stars and, consequently, our ideas regarding conditions imposed by analogous processes in other stars are speculative. The following arguments have been advanced in the past in attempts to estimate convective effects deep in the photospheres of cool stars.

The velocity amplitude may be first estimated by assuming that all of the stellar luminosity is to be carried by convection. For example, Wilson and Hoyle (1958) suggest that the convective flux is:

$$F_c = (\frac{1}{2}\rho v_c^2) v_p \quad , \quad (6-27)$$

where $\frac{1}{2}\rho v_c^2$ is the kinetic energy density of the convection, and v_p is the effective transport velocity of convection. If it is assumed that $v_p = v_c$, the velocity estimates shown in Table 6-3 are obtained. For main-sequence stars the values are subsonic, but they are highly supersonic in low-gravity stars. This implies that the flow will be strongly dissipated and modified: for example, Hoyle and Schwarzschild (1955) suggest that v_p and v_c should both be limited

by the sound speed, implying that convection near the surface cannot be efficient in highly luminous stars. Christy (1962) and Cox and Guili (1968) discuss this problem further.

Table 6-3
Convective Velocities from Equation (6-27)

| Spectral Type | T_{eff} | $\log g$ | $v_c(\text{km s}^{-1})$ |
|---------------|------------------|----------|-------------------------|
| G0 V | 6030 | 4.4 | 8 |
| G0 III | 5600 | 3.3 | 10 |
| G0 I | 5700 | 1.5 | 18 |
| K5 V | 4130 | 4.5 | 3 |
| K5 III | 3800 | 1.9 | 9 |
| K5 I | 3500 | 0.6 | 13 |

The crude approximation (6-27) may be refined by employing the mixing-length theory. In particular, we recognize that in addition to the convection of kinetic energy, the convection of enthalpy is an important component of F_c . If this component is included, a given convective flux may be carried with a lower velocity amplitude. Detailed calculations including this effect have been carried out by Renzini et al. (1977), who used a modification of the mixing-length theory presented by Cox and Guili (1968). Their results are reproduced in Figure 6-2, where it may be deduced that the estimated convective velocities are somewhat less than the sound speed, except for the stars with very low gravity. Renzini et al. (1977) give a velocity scaling law in the form:

$$\bar{v} = \min [v_s, 0.3 v_s (\frac{g_{\odot}}{g})^{0.2} (\frac{T}{T_{\odot}})^{2.2}] \text{ km s}^{-1}, \quad (6-28)$$

where v_s is the sound speed, and a value $\bar{v} = 2 \text{ km s}^{-1}$ has been adopted for the Sun.

According to mixing-length theory the temperature fluctuation ΔT scales as v_s , so,

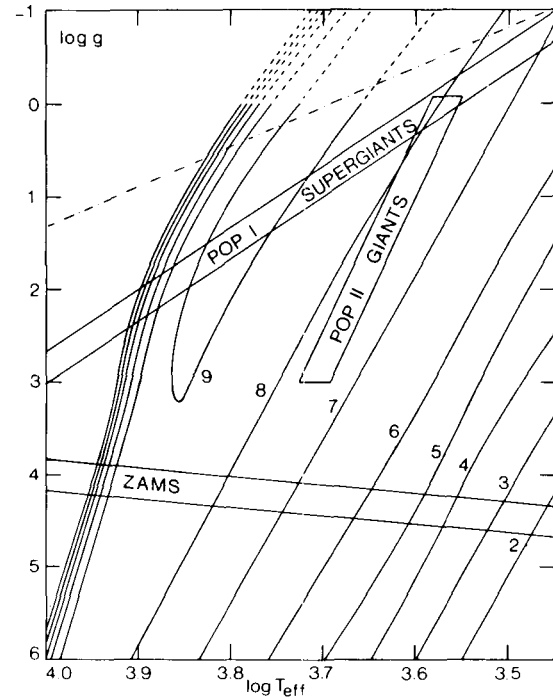


Figure 6-2. Curves of equal acoustic flux in the (g, T_{eff}) plane, computed using the theory of Renzini et al. (1977). Curves are labelled with the logarithm of the flux in $\text{erg cm}^{-2} \text{ s}^{-1}$.

assuming a value of $\Delta T = 300 \text{ K}$ for the Sun, we find a temperature fluctuation scaling law of the form:

$$\Delta T = 300 (\frac{g_{\odot}}{g})^{0.4} (\frac{T}{T_{\odot}})^{4.4} \text{ K}, \quad (6-29)$$

with an upper limit of about 1000 K related to the condition $\bar{v} < v_s$. This relation predicts the existence of large temperature fluctuations ($\sim 50\%$) in the deep photospheres of cool, low-gravity stars. Radiative cooling effects, not included in the theory, could drastically modify this prediction and also radically alter the velocity amplitudes.

To derive a scaling law for the lateral scale of convection, λ_c , we might argue that λ_c is proportional to the mixing length, which in turn might vary in proportion to the pressure scale

height. Then, assuming that $\lambda = 1000$ km for the Sun, we have:

$$\lambda_c = 1000 \left(\frac{T}{T_\odot} \right) \left(\frac{g_\odot}{g} \right) \text{ km} \quad (6-30)$$

This formula predicts length scales approaching 10% of a stellar radius in giant stars. This and other arguments led Schwarzschild (1975) to speculate that there may be only a few very large convective cells on the surfaces of giant stars. Nelson and Musman (1978) suggest, however, that the lateral scale of solar granulation may be determined by radiation transfer rather than the mixing length.

In addition to the production of penetrating eddies as discussed above, vigorous turbulent convection at the base of the photosphere can lead to the production of sound waves that propagate into the photosphere. Several authors (see Jordan, 1981 for a critical review) have identified the shock dissipation of such waves as the primary cause of nonradiative heating in stellar chromospheres and even coronae. It is therefore of interest to briefly review the theory of sound generation in turbulent convection zones. This theory is due to Lighthill (1952), who showed that the acoustic wave field in a quiet region surrounding a small turbulent volume can be derived from the inhomogeneous wave equation:

$$\frac{\partial^2 \rho'}{\partial t^2} - a_0^2 \nabla^2 \rho' = \nabla \cdot \underline{\underline{\mathbf{T}}} \quad , \quad (6-31)$$

where $\underline{\underline{\mathbf{T}}} = \rho \mathbf{v}\mathbf{v} + \underline{\underline{\mathbf{P}}} - c^2 \rho \mathbf{I}$ is a measure of the stresses existing in the turbulent volume.

Lighthill's method has been refined by Stein (1967) to treat noise generation in turbulent convection zones. Stein made a number of assumptions regarding the form of the stress tensor $\underline{\underline{\mathbf{T}}}$, including results predicted on the basis of homogeneous, isotropic, and incompressible turbulence and the assumption of low

Mach-number flow. The quantitative results depend on details of the adopted turbulence spectrum, but a useful approximation is that the acoustic power output per unit volume is approximately

$$\dot{E} = 10^3 \frac{\rho_0 v_0^3}{\ell_0} M^5 \text{ erg cm}^{-3} \text{ s}^{-1} \quad , \quad (6-32)$$

where ρ_0 is the mean density, and v_0 and ℓ_0 are, respectively, the velocity scale and length scale of the turbulence. Note that the emissivity depends on the 8th power of the velocity. The predicted spectrum of the acoustic flux exhibits a broad peak centered on a period $P = 2\pi \ell_0 / v_0$.

Estimates of the total acoustic emission derived from integration of the volume emission coefficient over the upper convection zone of models for cool stars have been reported by Renzini et al. (1977, see Figure 6-2). The convection models underlying these calculations are based on mixing-length theory, so the velocity amplitudes are not reliably estimated. This fact, combined with limitations in Stein's formalism, implies that the predicted fluxes are extremely uncertain. It does not seem to be possible to verify the theoretical estimates by direct observations of the Sun or other stars, so that one of the main ingredients of the acoustic shock-heating theory is poorly constrained at the present time (see also Cram, 1977).

IV.B. PULSATION AND OSCILLATIONS

Until quite recently the study of stellar pulsations concentrated on radial oscillations, principally in connection with Cepheids and related types of variable stars (Ledoux and Walraven, 1958; Cox, 1980). Such stars are not a topic of this volume. However, the discovery that the solar 5-minute oscillations are high-order, nonradial modes (Ulrich, 1970b; Wolff, 1972; Deubner, 1975), combined with the detection of low-order, low-amplitude modes (Brooks et

al., 1978; Grec et al., 1980) has led to a surge of interest in pulsations in cool stars. This work may prove to be of great importance in understanding the dynamics of the atmospheres of cool stars, and we therefore present a brief account of the theory. A more detailed account may be found in the volume by Unno et al. (1979) and in the review by Christiansen-Dalsgaard (1984).

The analysis of oscillatory modes in stellar envelopes begins with the linearized Euler equations, supplemented in some cases by models of radiative and/or convective energy transport. In the notation of Ando and Osaki (1975a,b) the equations are:

$$\frac{\partial \rho}{\partial t} + \nabla \cdot (\rho_0 \mathbf{v}) = 0 \quad (6-33)$$

$$\frac{\partial \mathbf{v}}{\partial t} + \frac{1}{\rho_0} \nabla P = -\mathbf{g} \quad (6-34)$$

$$\rho_0 C_p \left(\frac{dT}{dt} - \nabla A \frac{\rho_0}{P_0} \frac{dP}{dt} \right) = -\pi \nabla \cdot \mathbf{F}^R \quad (6-35)$$

$$\mathbf{F}^R = \frac{4}{3\kappa \rho_0} \nabla J \quad (6-36)$$

$$J = \frac{\sigma}{\pi} T^4 + \frac{1}{4\kappa \rho_0} \nabla \cdot \mathbf{F}^R \quad (6-37)$$

The Eddington approximation for radiation transfer underlies Expressions 6-36 and 6-37. Perturbations in convective transport are ignored.

The system of Equations (6-33 through 6-37) admits solutions of the form

$$f(r, \Theta, \phi, t) = f_n(r) Y_\ell^m(\Theta, \phi) \cdot \exp [i(\sigma_R + i\sigma_I)t] \quad (6-38)$$

where $f_r(r)$ is the radial eigenfunction, $Y_\ell^m = P_\ell^m(\cos \Theta) \cos m\phi$ is a surface harmonic of the first kind, and $\sigma = \sigma_R + i\sigma_I$ is the complex frequency. The period is $P = 2\pi/\sigma_R$, and the growth rate is $\eta = -\sigma_I/\sigma_R$. An eigenvalue problem may be formulated for the linear model by imposing conditions of regularity at the center and boundedness at the surface. Rosenwald and Hill (1980) have argued that the usual surface boundary conditions are incorrect, and it is also probable that nonlinear processes become important within the atmospheres of oscillating stars; but we will not pursue these points.

A solution of the eigenvalue problem yields a spectrum of eigenfrequencies whose eigenfunction structure can be used to classify the modes. The modal classification is based on the spherical harmonic indices (ℓ , m) and an index n which counts the number of nodes in the radial eigenfunction. Modes with $\ell = 0$ are radial modes, the one with $n = 0$ being the fundamental. The mode with n nodes ($n > 0$) and $\ell = 0$ is known as the n th overtone. If $\ell \neq 0$, each set (ℓ , m , n) has two corresponding eigenfrequencies and eigenfunctions. One of these, the g -mode, is dominated by gravitational restoring forces and has a period longer than that of the radial mode with the same (ℓ , n). The other is the p -mode, which is dominated by pressure forces and has a period shorter than the corresponding radial (ℓ , n) mode. Eigenfunctions of the g -modes tend to peak deep inside the star, while those of the p -modes tend to peak near the surface. The radial structure of the eigenfunctions depends on the detailed internal structure of the star, and can be best understood in terms of reflection and trapping phenomena, which are illustrated graphically by propagation diagrams (Unno et al., 1979; Leibacher and Stein, 1981).

Observations of the Sun have shown that many of the p -modes with periods near 5 min are excited. According to the theoretical dispersion equation, $\omega = \omega(\ell, m, n)$, this restricts the combinations of ℓ and n which are excited.

Modes with large ℓ (>200) and correspondingly small n (<15) have been studied by Deubner et al. (1979) and others. These modes are responsible for almost all of the oscillatory power in the photospheric velocity field. Modes with small ℓ (<2) and corresponding large n (>25) have been detected in integrated sunlight. Such modes make no significant contribution to the atmospheric velocity field, but they are extremely important for studies of the solar interior. It is not clear whether g-modes or p-modes with periods longer than about 15 min have yet been detected in the solar oscillation spectrum (Hill and Dziembowski, 1980).

At present it is unclear how the solar oscillations are excited, or what processes determine their amplitudes. Ando and Osaki (1975a,b — see also Ulrich, 1970b and Leibacher and Stein, 1971) suggested that the instability of large- ℓ modes could arise through the temperature dependence of the opacity by a process similar to that which is thought to account for Cepheid instability. Other work (Goldreich and Keeley, 1977) suggests that the modes might be excited by random buffeting due to convection. Without an understanding of the excitation mechanism and of the countervailing damping mechanism, it is impossible to make reliable, quantitative predictions of the amplitudes of those modes which are excited.

It is a relatively straightforward problem to calculate eigenfrequencies and eigenfunctions for linear modes of oscillations in cool stars other than the Sun. Christy (1962) and Ando (1976) have suggested that the periods of the dominant modes should scale as the acoustic cut-off period of the atmosphere

$$P \sim c/g \sim T^{1/2}/g, \quad (6-39)$$

so that a period of 5 min in the Sun corresponds to a period of 7 h in giant stars, and 24 d in supergiants. Ando's (1976) calculations suggest that the value of ℓ for the most unstable mode decreases with decreasing gravity, from $\ell \sim 1000$ in the Sun, to $\ell \sim 30$ in supergiants.

The growth rate of the oscillations was predicted to be much larger in low-gravity models.

An estimate of the amplitude of the oscillatory velocity at the base of the photosphere may be based on Christy's (1962) work, which suggested that nonradial pulsations are the principal means of energy transport in the hydrogen ionization zones in cool giants and bright giants. This suggestion was prompted by the fact that in such stars, convective velocities were predicted to be supersonic so that convection would presumably be inefficient. Christy proposed that the oscillatory velocity amplitude would be given by the approximation:

$$v^2 = \frac{2\pi H_c c}{P_0}, \quad (6-40)$$

where H_c is the heat flux and P_0 the pressure at the base of the photosphere. Table 6-4 provides quantitative estimates of v based on Expression 6-40.

Table 6-4
Pulsation Amplitudes from Equation (6-40)

| Spectral Type | Pulsation Amplitude (km s ⁻¹) |
|---------------|---|
| G5 V | 18 |
| G5 III | 32 |
| G5 I | 74 |

There is only limited direct observational evidence for the existence of nonradial oscillations in cool stars other than the Sun. This is not surprising, since cancellation of nonradial modes in the flux spectrum leads to an enormous reduction in the residual Doppler shift, even when the modal amplitudes are large. Fossat et al. (1984) have reported that 5 minute oscillations are detectable in the Na D lines of α Cen, and several other stars are now being investigated using the resonance cell used to ob-

tain this result. Some indirect evidence for nonradial oscillations might lie in the semi-regular variability of cool supergiants and bright giants (Abt, 1957, Figure 6), and in the remarkably high "macroturbulence" in such stars. Smith (1980a) has noted a relation between macroturbulence amplitudes and absolute luminosity which parallels theoretical estimates of the relationship between oscillation amplitude and luminosity. However, this is only circumstantial evidence, and it is important to mount observational programs to search for nonradial oscillations in cool stars other than the Sun.

IV.C. ROTATION

Rotation is a fundamental and extremely important aspect of the dynamical behavior of stars. However, as Tassoul (1978) has remarked, "the field of stellar rotation has become one of the most differentiated of all astrophysical disciplines in terms of research specialties." In this section we provide a brief sketch of some of the consequences of stellar rotation, emphasizing those which bear most directly on atmospheric dynamical processes. A comprehensive account of the subject is given in the monograph by Tassoul (1978) and in several recent reviews (e.g., Glatzmaier and Gilmore, 1981).

Being gaseous objects, stars are not forced to rotate as rigid bodies. Even in the absence of flows driven by convective and pulsational instabilities, a rotating star will tend to generate currents as a result of centrifugal and Coriolis forces, and these currents will redistribute energy and angular momentum within the star. However, as discussed in Section IV.A, the outer layers of the interior of a cool star are unstable to convection, and convective flows will also be influenced by centrifugal and Coriolis forces, as well as the rotationally induced currents. Consequently, there is an exceedingly complicated dynamical interaction between convection and rotation, leading ultimately to differential rotation (with latitude and depth),

non-axisymmetric currents, and modifications to the structure of large convective cells. Although there have been a number of theoretical studies of important aspects of the problem (e.g., Glatzmaier and Gilmore, 1981), we are far from having a satisfactory understanding of the interaction between convection and rotation.

At first sight, it might appear that our understanding of the interaction between pulsation and rotation is more satisfactory. In particular, it is a relatively straightforward task to use linearized hydrodynamic equations (cf., Equations 6-33 through 6-37), supplemented by a specified distribution of angular velocity, to predict the influence of slow rotation on the eigenfrequencies and eigenfunctions of radial and nonradial oscillations. Analyses of this kind predict that p-modes propagating with prograde and retrograde phase velocities will have slightly different frequencies. Observations of the Sun (e.g., Deubner et al., 1979) and certain B-stars have supported some aspects of this theory. However, there are already hints that unexpected differences in amplitudes between different spherical harmonics are present. It is probable that, as observational techniques are improved, new requirements will emerge for refined, nonlinear models of the interaction between convection, pulsation, and rotation.

Perhaps the most important effects of rotation in cool stars are related to the generation and structuring of magnetic fields. It is believed that these fields are intimately related to the nonradiative heating of stellar chromospheres and coronae. Moreover, atmospheric magnetic fields combined with a stellar wind play a key role in the evolutionary decay of stellar angular momentum (e.g., Roxburgh, 1983). Some aspects of these important problems are discussed in Chapter 7.

IV.D. EPISODIC PROCESSES

An important but often overlooked property of cool stars is the evidence for irregular

variability on time scales ranging from seconds (flare stars) to decades (activity cycles, RV Tauri stars, etc.). An interpretation of irregular variability requires a mechanism involving irregular dynamical phenomena inside the star, or an irregular response of the atmosphere to forces imposed from within the star or by the interstellar medium.

Perhaps the most obvious source of irregular variability in cool stars is the irregularity associated with magnetic activity. It is observed on the Sun that the sizes and emergence sites of active regions are virtually unpredictable at present, and that the envelope of the activity cycle is quite irregular. It is unclear whether this irregularity is due to the essential randomness of turbulent convection, or rather to an intrinsic property of nonlinear dynamo action (Chapter 7.II.C; Weiss, 1983).

Another source of possible irregular and episodic variability in stars like the Sun is the possible dynamical instability of the radiative core, due to molecular-weight gradients or other factors. Investigations of these instabilities have been stimulated by the low values of the solar neutrino flux (e.g., Bahcall et al., 1982). It is conceivable that internal mixing and consequent changes to nuclear reaction rates and stellar structure could also occur during relatively rapid evolutionary phases, such as pre-main-sequence evolution (T Tauri stars) and the crossing of the Hertzsprung gap (G-giants).

The most spectacular forms of episodic variability yet detected among the cool stars are the outbursts displayed by FU Orionis stars (e.g., Herbig, 1977b). Among the mechanisms which have been proposed to account for this phenomenon are (1) the rapid clearing of circumstellar material, possibly associated with the dynamics of H II regions (Magnan, 1979), and (2) irregular accretion onto a hot, optically thick disk (Hartmann and Kenyon, 1985). It is possible that the variability of FU Orionis

stars is an extreme case of a mechanism which acts with a smaller amplitude among T Tauri stars and perhaps other cool stars.

Spectroscopic studies of T Tauri stars and cool giants (both eclipsing and single stars) have revealed evidence of large-scale inhomogeneous structure in their outer atmospheres. The evidence includes multiple absorption systems at different radial velocities, and time-dependent structures within spectral lines. Theoretical understanding of the mass-loss mechanisms in these stars would be greatly improved if observations could be undertaken to establish whether there is a connection between these structures and irregular (or regular) changes in the inner parts of the atmosphere. The length scales and, hence, time scales involved in such observations are very long (months to years), and the astrophysical community may need to consider new approaches to the acquisition of astronomical data to obtain material relevant to this kind of problem.

V. ATMOSPHERIC DYNAMICS AND STRUCTURE

The subphotospheric dynamical phenomena discussed above impose highly structured, time-dependent boundary conditions on the base of the stellar atmosphere. These conditions are responsible for the transfer of mass, momentum, and energy throughout the atmosphere (possibly modified by conditions imposed from outside the atmosphere) and, ultimately, for the gross radial patterns discussed in Section II. Clearly, one of the central problems we must address concerns the link between small-scale, time-dependent, dynamical processes and the emergence of gross atmospheric structural patterns clearly detectable in the integrated emission from a star. This question is examined in this section, although we will see that a satisfactory solution is not available at present. Our treatment of the problem follows the sequence of regions described in Section II.

V.A. PHOTOSPHERES

As discussed above, the layers immediately beneath the photospheres of cool stars are convectively unstable, and the resulting motions excite a number of important atmospheric phenomena. In the solar photosphere, the granulation and supergranulation are presumably manifestations of convective cells or eddies which penetrate into the stable atmosphere. In other stars where the analogues of granulation cannot be observed directly, observations of broadening, shifts, and asymmetries in photospheric absorption lines provide only weak clues to the existence and nature of convective overshoot.

An illuminating account of penetrative convection by Moore (1981) describes many of the atmospheric phenomena which result from convective overshoot. These may be divided roughly into two classes, those associated with the evolution and morphology of the eddies themselves, and those related to the generation of atmospheric oscillations. We discuss each in turn.

An important question regarding the eddies themselves concerns the altitude to which convective overshooting produces temperature and velocity fluctuations. A simple view of this phenomenon might suggest that a relatively hot, buoyant eddy will overshoot and experience an upward buoyancy force until it rises to a point where radiative relaxation leads to thermal equilibrium with the ambient medium. Subsequently the eddy will decelerate, but still continue to rise, until all of its initial momentum is lost. Arguments along these "mixing-length" lines predict penetration altitudes that are much higher than those observed in the terrestrial atmosphere or the solar photosphere.

It appears that processes such as shear turbulence or entrainment remove momentum from the rising eddy, but the mechanism is

poorly understood. Numerical studies of solar granulation have sometimes included a small-scale turbulent component which, when appropriately adjusted, can be used to confine the penetration to agree with observation (e.g., Nelson and Musman, 1977; Cloutman, 1979).

It might be conjectured that small-scale turbulence of the kind involved in these numerical models actually exists in stellar atmospheres and, moreover, is responsible for part of the phenomenon known as spectroscopic microturbulence. However, more work must be done before this correspondence can be established. It is important to emphasize that phenomena on the scale of solar granulation are certainly not small enough to appear as microturbulence in spectroscopic diagnostics, since the horizontal and vertical length scales of granulation are not small compared with the photon mean free path. However, it is probable that a part of the nonthermal broadening of weak solar lines is dominated by convective overshoot, since velocity gradients associated with the penetrative flow may appear as microturbulence in conventional diagnostic procedures. The review by Dravins (1982) addresses aspects of this question, and shows that there are subtle and important processes which must be considered in any attempt to relate measured nonthermal line widths to actual atmospheric velocity fields. On the basis of this work it is clear that arguments seeking to connect properties of envelope (interior) convection to values of "turbulence" parameters derived from spectroscopic methods should entail a sound understanding of the nature of spectral line formation in the presence of penetrative convection.

Laboratory experiments and studies of the terrestrial atmosphere show that convective overshoot is associated with the generation of gravity waves in the overlying stable region (Adrian, 1975). These observations have prompted a number of solar physicists to seek evidence of gravity waves in the photosphere,

and to study the associated theoretical problems. It is perhaps surprising that these studies have not been rewarded by the identification of a high density of gravity waves. Presumably, the strong radiative damping experienced by gravity waves in the deep photosphere partially counteracts their strong excitation by convective overshoot (Souffrin, 1966). However, it may be that a substantial density of gravity waves does exist, but has escaped identification because the resulting spectroscopic signature appears as microturbulence to normal diagnostic techniques (Mihalas, 1981). Whitaker (1963) conjectured that gravity waves could be implicated in the heating of the chromosphere and corona, but for a number of reasons the idea is currently unfashionable (e.g., Ulmschneider, 1976). Despite this, gravity waves in stellar atmospheres should not be ignored as sources of spectroscopic turbulence, nor as agents that can be responsible for the transfer of significant fluxes of mass, momentum, and energy.

We noted in Section IV that there have been many studies of the generation of acoustic waves by turbulent convection, principally directed towards the development of theories of chromospheric heating (see below). However, a few authors have studied some of the effects which might occur if wave fluxes of the predicted strength were actually present in stellar photospheres. Perhaps the most refined calculations have been undertaken by Ulmschneider and his co-workers (e.g., Ulmschneider, 1979), who considered the propagation of nonlinear, radiatively damped waves in a gravitationally stratified photosphere. An important result of these calculations was the demonstration that, throughout much of the model photosphere, radiative dissipation retards the expected growth in wave amplitude. Even with quite substantial fluxes of mechanical energy, RMS wave amplitudes remained well below 1 km s^{-1} in the photosphere. This result suggests that short-period acoustic waves may not play a major role in photospheric turbulence, a conjecture supported by calculations showing that acoustic waves lead to line pro-

file shapes which are not commonly observed (Cram et al., 1979).

Our understanding of convective penetration and wave generation in the solar photosphere is rudimentary, and our insight into the corresponding processes in other stars is even poorer. Our current picture of these phenomena in the solar photosphere implies that the following three points are important: (1) convective penetration and gravity-wave generation are significant (possibly major) contributors to the nonthermal broadening of photospheric lines and may dominate the processes which lead to shifts and asymmetries of such lines, (2) convective penetration does not play an important direct role in the physics of regions lying above the photosphere-chromosphere interface, and (3) there is little evidence that short-period acoustic waves play an important role in photospheres.

As we saw in Section IV, convection is only one of many phenomena which may excite dynamical process in stellar photospheres. Envelope oscillations or pulsations may also generate atmospheric motions which are of considerable importance. Some theoretical studies of the linearized equations of motion have involved a fairly detailed treatment of the oscillation in the atmosphere (Ando and Osaki, 1975a,b; Rosenwald and Hill, 1980; Christiansen-Dalgaard and Gough, 1982). The results of these studies suggest that the oscillations are essentially "adiabatic" throughout most of the atmosphere, so that they are not implicated in significant atmospheric heating despite the relatively large amplitudes of the observed velocities (Ulmschneider, 1976). Nonlinear calculations could lead to a revision of this view, particularly if the chromospheric radiation relaxation time is as short as suggested by Giovanelli (1978). Even if they are not responsible for atmospheric heating, nonradial oscillations could lead to significant atmospheric "turbulence" (Smith, 1980a). They could also provide a significant flux of momen-

tum into the base of the stellar wind of low-gravity cool stars.

The mean temperature and density stratification of a stellar atmosphere containing a photosphere, chromosphere, and corona corresponds to a number of "cavities" which could support trapped atmospheric oscillations in the same way that the 5-minute oscillations are trapped in the outer envelope of the Sun (see Leibacher and Stein, 1981, Figure 10-3). The most interesting example of a mode trapped in this way is the chromospheric oscillation, which in the Sun appears to be intimately connected with 3-minute oscillations and nonradiative heating (Cram and Damé, 1982). Leibacher et al. (1982) have provided nonlinear, one-dimensional models for these oscillations, and have had some success in explaining aspects of spectral line formation in the presence of this phenomenon.

The structure of atmospheric cavities in stars other than the Sun will depend on both the classical parameters, T_{eff} and g , and on the processes responsible for the run of mean temperature and density in the chromosphere. At present it is impossible to assess the importance of trapped atmospheric oscillations in transferring energy and momentum in stars other than the Sun.

Regarding the general influence of oscillations on atmospheric structure we may conclude the following: (1) analogues of solar 5-minute oscillations are likely to be an important line-broadening agency, and they may be important in the energy balance of the atmosphere; (2) there are some indications that nonradial oscillations may attain very large amplitudes in cool, low-gravity stars [if this is so, the oscillation will dominate the nonthermal line broadening, but their role in atmospheric heating or extension is unknown]; and (3) oscillations trapped in stellar chromospheres may have an important influence on line-profile shapes, and they may be responsible for heating the quiet chromosphere.

V.B. CHROMOSPHERES

For almost four decades, a central theme in the theoretical study of the chromospheres of the Sun and other cool stars has been the idea that the nonradiative atmospheric heating is produced by shock dissipation of short-period acoustic waves (Jordan, 1981). Early theoretical models (e.g., Schatzman, 1949) used weak shock theory and other techniques to average over many of the details of the dynamics, and hence to provide directly a coarse description of the global structure of the photosphere and chromosphere.

The temperature distribution $T_c(h)$ in a plane-parallel, stationary, global, chromospheric model of this kind is given implicitly by an energy equation which balances the radiative flux divergence against the power supplied by mechanical heating:

$$\frac{d\pi\bar{F}^R}{dh} = 4\pi\bar{\kappa}(\bar{J} - \bar{S}) \approx \pi\bar{q}(h) \quad (6-41)$$

Here, $\bar{q}(h)$ is the mean rate of heating, and the overbar is used to denote averaged quantities. Several studies based on Equation 6-41 have used models for $\bar{q}(h)$ derived from weak shock theory. This theory provides an estimate of the power dissipated in a volume of gas by a monofrequency train of shock waves whose characteristics are determined by crude approximations to transonic, radiative gasdynamics (e.g., Stein and Schwartz, 1972). According to this theory the function \bar{q} has the form

$$\pi\bar{q}(h) = - \frac{1}{12} \frac{\gamma(\gamma+1)}{T} P\eta^3, \quad (6-42)$$

where $\gamma = C_p/C_v$, P is the pressure, T the temperature, and $\eta = (\rho_2 - \rho_1)/\rho_1$ is the shock strength measured in terms of the relative density discontinuity. The shock strength is given by a nonlinear transport equation in the form

$$\frac{d}{dh} [A(h)\eta^2] = B(h)\eta^3, \quad (6-43)$$

where $A(h)$, $B(h)$ are known functionals of the atmospheric conditions. A self-consistent model atmosphere may be obtained by solving simultaneously Equations 6-41 through 6-43 (e.g., Ulmschneider, 1976).

Stein and Schwartz (1972) and Ulmschneider and his co-workers (Ulmschneider, 1979) have presented numerical solutions of one-dimensional, nonlinear wave equations which shed further light on the propagation and dissipation of acoustic waves in chromospheres. Their results (e.g., see Figure 6-3) provide estimates of the time-dependent fluctuations of pressure, temperature, velocity, and other parameters in a one-dimensional, monofrequency wave train. Ulmschneider et al. (1978), treat the radiative damping of the wave in the photosphere, showing that about 90% of the wave-energy flux is lost through this process. The remaining energy is transformed from wave energy to thermal energy through shock dissipation in the "chromosphere."

The results of such calculations may be averaged over time to produce global models which are comparable with semi-empirical models of stellar chromospheres (Ulmschneider, 1979). The detailed models may also be used to explore the effects of acoustic waves on spectral line formation (Cram et al., 1979). These kinds of studies may be readily applied to cool stars other than the Sun.

Although numerical models for the formation of chromospheres by the dissipation of acoustic waves are highly refined, they suffer from a number of drawbacks. As discussed above, one key uncertainty concerns the properties of acoustic noise generated by the convection zone. The calculations might also be misleading insofar as they treat one-dimensional dynamics and a monofrequency

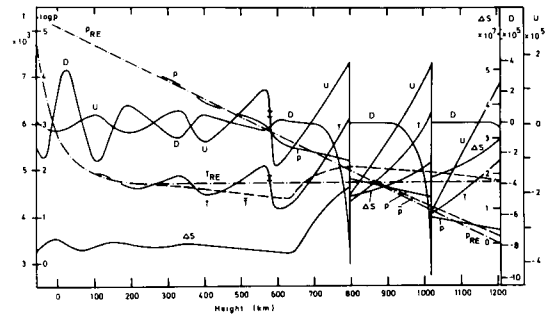


Figure 6-3. Predicted structure of an acoustic wave propagating into a model of the solar atmosphere (Ulmschneider et al., 1978).

wave train. Finally, the physical nature of radiative damping in those parts of the atmosphere which are optically thin in the continuum is a vexing problem, and the usual postulate that the cooling times are long is probably wrong (Giovanelli, 1978).

A prescription for the heating function \bar{q} is only part of the solution of the problem of nonradiatively heated stellar chromospheres. The other part of the solution concerns the evaluation of the radiative flux divergence, and the subsequent inference of the temperature and other atmospheric parameters. This task is made difficult by the fact that the heated atmospheric regions of particular interest correspond to regions where non-LTE spectral lines dominate the radiative energy transport. Fully self-consistent models would require the inclusion of many atomic and ionic states, each treated as a multi-level system (see Vernazza et al., 1981a). This approach has not been used to date. Some work has been based on approximations to the radiative flux divergence, expressed in terms of the net radiative brackets or escape probabilities (e.g., Jordan, 1969), but most models which derive a temperature distribution from energy balance considerations are based on the assumption that LTE continuum radiation dominates the energy loss. The predictions of such models may be quite wrong (Cram, 1977; Giovanelli, 1978).

The hypothesis that stellar chromospheres are produced by shock dissipation of short-period acoustic waves has fallen into some disfavor, and the hypothesis of electrodynamic heating (see Chapter 7) has tended to replace it. The main reason for this switch appears to have been growing interest in "activity" in late-type stars, which is clearly related to electrodynamic processes. However, acoustic heating should not be discounted as an important process, particularly in "quiet" stars. Moreover, as Ulmschneider and Stein (1982) have emphasized, the study of shock dissipation of many kinds of electrodynamic waves may not require major revisions of results already derived from acoustic wave studies.

Studies based on weak shock theory or on solutions of the nonlinear wave equation, with or without magnetic fields, suggest that a significant fraction of any mechanical flux carried into the chromosphere will be dissipated in regions where the RMS velocity amplitudes are less than about half the speed of sound. This result is consistent with Thomas' (1983) empirical-theoretical discussion of transonic flows in stellar chromospheres. Of course, it is obvious that a given rate of heating per unit volume will produce a larger temperature rise when applied to regions of smaller volume emissivity. For this reason, departures from the classical model due to nonradiative heating are hard to detect if they occur deep in the photosphere, even when the mechanical heating is vigorous (e.g., 10^7 erg cm⁻² s⁻¹). On the other hand, only a tiny fraction of the stellar luminosity need be dissipated in the outermost layers to produce an extremely hot corona (e.g., 10^{4-5} erg cm⁻² s⁻¹).

For this simple reason, a wide variety of heating processes will lead to an atmospheric structure whose outwardly decreasing emissivity is paralleled by an outwardly increasing temperature. Plateaus will occur in the temperature distribution near temperatures that correspond to relatively high emissivity or relatively low heating rates, while steep

temperature rises will occur where the emissivity is low or the heating rate high. The emissivity may be strongly influenced by non-LTE effects, through both transport and population mechanisms (see Chapter 5.IV). Athay (1981) has summarized these considerations, and shown how they may be applied to give insight into the global structure of stellar chromospheres.

V.C. CORONAE

According to Thomas (1983 — see also Cannon and Thomas, 1976), the "lower corona" is characterized by the simultaneous presence of (1) nonradiative heating of sufficient magnitude to lead to an outwardly increasing kinetic temperature, and (2) fluctuating or chaotic velocity fields with amplitudes of the order of the sound speed. Our understanding of this region is very limited, and Thomas' picture is not at present widely accepted. However, the data acquired by the IUE satellite have aroused considerable interest in the atmospheric region responsible for the EUV emission spectrum in cool stars. It is likely that much of this emission comes from a region corresponding in several respects to the "lower corona," as defined by Thomas.

In the atmosphere of the Sun, the region with properties corresponding to the "lower corona" is usually called the "transition zone." Observationally, the solar transition zone is characterized by extremely large fluctuations in velocity and temperature associated with spicules and other phenomena (see Brueckner and Bartoe, 1983). Although there are diagnostic procedures and ab initio theories which seek to explain, in simple terms, the mean structure of the transition zone or lower corona (e.g., Jordan and Brown, 1981), there is a tremendous difference between the complex picture revealed by observations and the crude simplifications of contemporary theory. It is likely that major revisions will be made to our current picture of the solar transition zone, especially when methods are developed to

observe and construct theories of the violent small-scale dynamical processes which are the direct manifestation of "transonic" gas-dynamics.

Diagnostic techniques initially developed to study low-resolution solar observations may be applied to interpret some aspects of IUE observations of EUV emission from other cool dwarf stars (e.g., Jordan and Brown, 1981; Chapter III.B.2). Specifically, it is observed that (1) surface fluxes in EUV emission lines vary markedly from star to star, a result which is generally interpreted as the consequence of different surface coverages by "active" regions (see Chapter 7), and (2) the distribution of emission measure with temperature suggests that there is only a relatively small amount of material with temperatures in the neighborhood of 500,000 K. This result is sometimes taken to indicate the importance of thermal conductivity, with an associated steep temperature gradient, in the energy balance of the emitting region. However, the existence of radiative instabilities and other dynamical effects may be equally important (e.g., Thomas and Athay, 1961; Athay, 1981; Linsky, 1983).

T Tauri stars frequently exhibit very intense EUV emission, with mean surface fluxes sometimes more than 3 orders of magnitude larger than solar values. Since the spectroscopically determined densities in the emission region are not very much greater than solar values (Cram et al., 1980; Jordan et al., 1982), it follows that the geometrical extent of the emitting region must be substantially larger than the admittedly compact solar transition zone. At present it is not certain that all of the EUV line emission of T Tauri stars comes from a "low corona" or "transition region" immediately above the chromosphere; observations comparing variability in (visible) chromospheric lines and EUV lines would be very helpful in resolving this question. It should be noted that we have very limited information on the nature of the non-thermal velocity fields in the EUV emitting region of T Tauri stars. Attempts to match the

profiles of "chromospheric" lines such as H α and CaII K by Hartmann et al. (1982) show that quite large (transonic and supersonic) chaotic flows may be present, but the limited availability of relevant data and the rudimentary nature of the theory imply that this result is not very firm at present.

The question of the structure, even the very existence, of a "lower corona" in cool giant stars raises some important issues regarding the general applicability of Thomas' atmospheric structural pattern. As discussed in Chapter 3, there is growing evidence for the existence of geometrically extended regions which are non-radiatively heated and probably involve chaotic transonic flows. Several workers have dubbed this region the "extended chromosphere" (cf., Brown and Carpenter, 1984), since the degree of excitation is similar to that of the solar chromosphere. It appears that well developed regions of this kind do not occur in stars displaying highly excited EUV lines (CIV, NV) and X-rays; this is one manifestation of the dichotomy discussed in Chapter 3.III.A.5. While the use of Thomas' word "coronal" to describe such atmospheric regions will not be readily accepted, it is nevertheless useful to have a vocabulary which can distinguish between regions which are (1) nonradiatively heated and essentially hydrostatic (like the solar chromosphere), and those which are (2) nonradiatively heated and nonhydrostatic (like "extended chromospheres" in cool giants or the base of the "wind" in the solar corona).

Perhaps the key to understanding the relation between these concepts lies in the resurrection of the "fountain" metaphor for chromospheric/coronal structure. The term has been used recently by Hartmann and Avrett (1984) to summarize some aspects of the possible structure of the "extended chromosphere" of α Ori, in a context reminiscent of the descriptions of solar chromospheric structure advanced many years ago by Chandrasekhar (1933) and Menzel (1939). While there has been substantial progress in our understanding of these

parts of the solar chromosphere, we are still far from a satisfactory account of the disorganized, high-velocity flow patterns which are present there (e.g., Pneuman and Kopp, 1977).

Another observation which may have an important bearing on the structure of the region dubbed "lower corona" concerns the EUV spectrum of hybrid stars (Chapter 3.III.A.5). Preliminary efforts to interpret the spectra of these objects (e.g., Hartman et al., 1985) suggest that their "lower corona" is characterized by temperatures of order 200,000 K, physical extension over a scale of the order of the stellar radius, and small-scale, irregular velocities which are transonic or even supersonic. Since these stars seem to exhibit an intermediate state between the compact "lower corona" of the Sun and the so-called "extended chromosphere" of cool giants, they obviously warrant close and comprehensive study.

According to Thomas (1983), the upper corona emerges from the lower corona through a transition in the nature of the velocity field. The velocity field is transonically unstable in the lower corona, but stable, superthermic, and monotonically accelerated in the upper corona. Nonradiative dissipation in the upper corona continues to be adequate to ensure that the temperature increases outwards. Thomas defines the upper limit of the upper corona as the point of maximum temperature, arguing that this is the level "where a strong effect of nonradiative energy dissipation ends." Of course, it is possible that nonradiative heating and transport are still crucially important beyond the temperature maximum.

The upper corona is perhaps the most poorly studied region of stellar atmospheres. Even for the Sun, observations of this region are mainly restricted to spectrophotometric studies in X-rays or radio wavelengths. The data provide intriguing information on the morphology and evolution of coronal structures, but they have only a limited value in estimating thermodynamic properties such as temperature and

pressure. Information on velocity fields is very sparse, being obtained from forbidden coronal lines and a few experiments which provide adequate spectral resolution in X-rays. In the absence of more complete data, only rudimentary theories are available: these treat such topics as the origin of the solar wind (see below) and the role of coronal holes and coronal loops in the solar atmosphere (Chapter 7.III.B).

The *Einstein* satellite revealed the existence of X-ray emission from a wide range of cool stars (Chapter 3.II.A). There is an urgent need for improved instrumentation to permit a fuller study of stellar coronal temperatures and pressures. At present, only a few theoretical studies of stellar coronae are available. Those based on the acoustic heating theory (e.g., Nairai, 1969) have been strongly challenged by the fact that coronal emission is not a simple function of stellar spectral type, while those based on an electrodynamic theory (Chapter 7.III.B) are virtually unconstrained by the available observations. Without instrumentation capable of resolving spectral lines at X-ray wavelengths, it is difficult to see how the nature of upper coronal velocity fields can be investigated.

An important aspect of X-ray emission from stellar coronae is the possibility that significant X-ray absorption may occur in material lying outside the corona itself. In particular, observations showing a tendency for strong X-ray emission to be correlated with weak H α emission among T Tauri stars led Walter and Kuhi (1981) to propose the concept of a "smothered corona" in such stars. A similar effect may be present in other stars.

V.D. POSTCORONAE AND STELLAR WINDS

Thomas' (1983) classification of stellar atmospheric structure bifurcates in the post-coronal region into either (1) a smoothly decelerated postcorona, or (2) a complex postcoronal

region characterized by time-dependent structure and H α emission “envelopes.” Among the cool stars, this bifurcation is perhaps best illustrated by the distinction between solar postcoronal structure (Jordan, 1981), and the behavior of T Tauri stars (Chapter 4) and luminous cool stars (Chapter 3.IV). With the possible exception of T Tauri stars (where accretion phenomena have been frequently considered), the interpretation of these observations is usually sought through the application of the theory of stellar winds.

Many of the foundations of this theory were laid by Parker (1958, 1963a), whose initial studies were directed to the problem of the stability of a hydrostatic model of the solar corona. Parker showed that the pressure at the outer boundary of a hydrostatic corona is too high to smoothly match that of the interstellar medium, and he concluded that the solar corona would therefore be in a state of hydrodynamic expansion. He proposed that this expansion could be described by the steady Euler equations describing conservation of mass and momentum in a spherical co-ordinate system:

$$\frac{1}{r^2} \frac{d(\rho v r^2)}{dr} = 0 \quad (6-44)$$

$$\frac{1}{r^2} \frac{d(\rho v^2 r^2)}{dr} + \frac{dP}{dr} = -\rho \frac{GM}{r^2} \quad (6-45)$$

Combined with the ideal gas law these equations give

$$\left(\frac{q^2}{v^2} - 1\right) \frac{dv^2}{dr} =$$

$$\frac{1}{r} \left[\frac{w^2}{2} - q^2 \left(1 - \frac{d \ln T}{d \ln r^2}\right) \right], \quad (6-46)$$

where $q^2 = kT/\mu$ is the one-dimensional thermal velocity (or sound speed), and $w^2 = GM/r$ is the escape velocity.

The RHS of Equation 6-46 is positive in the photosphere, since $q < w$. Thus, an initial small photospheric flow $u < q$ will increase outwards. There is a singularity in Equation 6-46 at the point $u = q$, where the flow velocity is equal to the one-dimensional thermal velocity. A smooth transition to supersonic velocities $u > q$ is possible, provided the RHS of Equation 6-46 becomes zero at this singularity. The point where $u = q = w$ is known as the critical point. In stars with hot coronae (such as the Sun), the critical point occurs a few stellar radii above the photosphere. An important part of Parker's theory is the argument that high thermal conductivity will maintain a high temperature far out from the base of the corona. While this fundamental point does not seem to be adequately recognized by Thomas (1983) in his discussion of the thermodynamics of postcoronal regions, it is equally true that a high rate of mass loss in the cool giants is apparently not related to thermal conduction of heat into the outer atmosphere.

Parker's original treatment of the solar wind has undergone major revisions and extensions as space observations have provided an increasingly clear picture of the structure of the wind. Some of the important features of contemporary solar-wind models include a multi-fluid description of the wind plasma, allowing for distributed sources of momentum and energy in the initial parts of the wind, and attempts to allow for the importance of magnetic fields in determining the flow geometry and other properties. The developments are summarized in the volume by Jordan (1981). Despite a great deal of work there remain important discrepancies between theoretical predictions and the observed properties of the wind near the Earth.

The extension of Parker's wind model to stars other than the Sun is relatively straightforward. As Parker (1963) has argued, stars near the Sun in the HR diagram probably have coronae and winds similar to those of the Sun. Unfortunately, there is currently no way to

observe winds in such stars, and it is impossible to verify this conjecture. It is particularly unfortunate that it is impossible to study the relationship between wind properties and coronal parameters determined from X-ray observations in solar-type stars, since this kind of data could help considerably in clarifying the role of magnetic fields in coronal heating and winds (Chapter 7.III.C).

In a discussion of the application of the hydrodynamic expansion model to other stars, Parker (1963a) speculated on the origins of mass loss from cool giant stars. He recognized that coronal temperatures in such stars would probably be low (because high expansion rates lead to efficient coronal cooling), and concluded that the solar hydrodynamic model could not account for the high rates of mass loss from these stars. Parker suggested that extended heating could account for the high mass-loss rate, but Weyman (1963) showed that this was unlikely.

The central problem in developing theories of stellar winds in late-type stars appears to be the need to explain why the Sun (and presumably stars like the Sun) should have a high velocity wind with a low rate of mass loss, while giant stars should have low velocity winds with a high rate of mass loss. Presumably this dichotomy is connected with the fact that solar-type stars have extensive hot coronae while cool giants probably do not, although some stars (e.g., some T Tauri stars) seem to have both high mass-loss rates *and* hot coronae. Most explanations of these observations fall into one of two categories, those which propose that increased mass loss occurs because the density at the critical point of a thermally driven wind is high, and those which identify momentum addition as the agency responsible for enhanced mass-loss rates.

Models which place the critical point in regions of high density were first advanced by Roberts and Soward (1972—see also Durney,

1973). These authors argued that conditions at the outer boundary of a stellar wind impose certain relationships between the number density, flow velocity, and temperature at the base of the wind. In particular, for any given value of energy at a point infinitely far from the star, there is a density even at the base of the corona above which the flow velocity must be supersonic. If such high densities occur, the mass-transfer rate is very large.

Mullan (1978) combined this idea with a theory connecting coronal density and temperature [based on Hearn's (1975) minimum flux corona, which is not now widely accepted to be valid] to predict the presence of a supersonic transition locus (STL) in the HR diagram. On the solar side of this locus the flow is subsonic at the base of the corona, and the mass-loss rate is low, while on the giant side the flow is supersonic at the base of the corona, and the mass-loss rate is high. Mullan's model has been modified and extended by Wallenhorst (1980), who considered a more detailed model of the transition zone.

Other models for mass loss in cool giant stars are based on momentum addition to the flow. Radiative forces due to scattering of Ly α radiation have been studied by Haisch et al. (1980), who found that the outward force due to Ly α exceeded the inward force due to gravity in a part of a semi-empirical model for the atmosphere of Arcturus, a star with a high mass-loss rate. The consequences of this discovery have not been worked out. Some authors have suggested that radiation forces on dust grains could be important, although it is not clear how dust can form in the deeper parts of stellar atmospheres. The possible importance of momentum addition from a field of waves in the atmosphere was emphasized by Hartmann and McGregor (1980). These authors showed that the force exerted by a wave flux sufficient to heat the outer atmosphere of a cool giant star would lead to significant atmospheric extension. They focussed attention on Alfvén waves, modeling the dissipation in terms of an ad hoc

damping length L and using a model for wave-influenced winds developed by Jacques (1977). Hartmann et al. (1982) suggested that wave momentum could also be an important factor in the mass loss from T Tauri stars.

None of these theories of stellar winds in cool stars provides a satisfactory description of the observed phenomena. The theory of thermally driven winds cannot account for high mass-loss rates in stars with no coronae, and in its highly refined solar application it cannot account for properties of the solar wind observed near Earth. The theory of the supersonic transition locus rests on an application of the minimum-flux-corona theory where it is not valid, and does not describe the initial acceleration of the wind to supersonic velocities. Models based on radiation forces are incomplete. The theory of winds driven by wave-momentum transfer rests on ad hoc models of the wave-dissipation process: in the words of Castor (1981) "its sins are unobservable." In addition to these problems, models for stellar winds have been criticized for bypassing key questions regarding the primary processes responsible for the winds, a point to which we now turn.

One basic property of thermally driven wind models is that, once the temperature structure of the atmosphere is specified, the mass-loss rate is determined by the temperature (sound speed) and density at the critical points. Momentum-driven wind models may involve a more complicated connection between temperature, density, and velocity; but for them also there is a unique relationship between the input wave energy and the resulting mass-loss rate. An early and particularly clear account of the basic method for developing models of mass loss along these lines has been provided by Weyman (1963):

"...one should decide first what quantities can safely be considered 'given' — that is, which quantities are essentially independent of any characteristics of the flow itself. It seems reasonable to assume

that below a certain level — say the photosphere — the character of the flow has little effect on the structure of the star below the photosphere... Since most of the mechanical energy is thought to be generated in the subphotosphere layers, the total rate of mechanical energy generation L_m can be regarded as 'given,' along with the density, temperature, radiation field, and magnetic field at optical depth unity in the visible continuum. The problem is then how to determine the quantities — dM/dt (mass-loss rate), ϵ_∞ (total mechanical energy expended per gram), E_{rad} (total net radiation losses in the chromosphere and corona) and dU/dt (U is the total energy content of the corona), such that they satisfy:

$$L_m = dU/dt + E_{\text{rad}} + \epsilon_\infty \left| \frac{dM}{dt} \right| \quad (6-47)$$

$$\epsilon_\infty = \frac{V_\infty^2}{2} + \frac{V_{\text{esc}}^2}{2} + \Lambda \frac{\Gamma_\infty P_\infty}{\rho_\infty}, \quad (6-48)$$

where Λ is a measure of the anisotropy of the flow..."

In contradiction to this approach, Thomas and his co-workers (e.g., Thomas, 1973, 1976; Cannon and Thomas, 1976; Heidmann and Thomas, 1981) have argued that it is neither sufficient nor necessary to specify the mechanical flux L_m in the subphotosphere. Rather, these workers stress the necessity of studying atmospheric structure parametrically,

"...by choosing either matter flux, or outward velocity associated with it at some level, or the beginning height of the chromosphere as parameters; probably we also need to take as parameter the mechanical energy flux which is not associated with the matter-flux; possibly we also need as parameter a horizontal scale, for nonspherically symmetric flow."

The key issue in this debate is whether it is necessary to focus on the mass flux as a quantity imposed from below, or as a quantity determined by atmospheric factors. It is likely that self-consistent models of either kind may be constructed (although this has not yet been done). Thus, the decision between the alternatives must rest on observations. Unfortunately it is not possible to reach a firm conclusion at present, although the following relevant points may be made:

1. Observations show that it is impossible to explain stellar atmospheres in the framework of a model which introduces L_m as the only extra parameter, unless L_m depends on parameters other than T_{eff} and g alone (acoustic shock dissipation models are thus ruled out). The inadequacy of such models is shown by observations which reveal marked differences in the chromospheric and coronal spectra of stars of identical spectral type and class.
2. The connection between the temperature structure of an atmosphere and the amount of mass loss remains unclear. It is known that there is a tendency for cool stars of high luminosity to exhibit relatively cool atmospheres and high mass-loss rates, but T Tauri stars and (possibly) Pop II objects violate this trend. However, it must be noted that the weakness of the observational evidence for a connection between temperature and mass-loss rate does not necessarily imply that the physical connection is weak: the relevant observations are sparse and hard to interpret.
3. There is no known example of a pair of stars with closely similar global heating rates but widely different mass-loss rates,

although such would occur if L_m and \dot{M} were completely unrelated. Again, the absence of such evidence may reflect inaccuracies in diagnostic methods, and it cannot be taken as strong evidence against the partial independence of \dot{M} and L_m .

From these points it may be concluded that currently available observations of cool stars do not demand models in which L_m and \dot{M} are specified as independent parameters. Models which specify L_m and subsequently derive \dot{M} from the resulting atmospheric structure could be consistent with observation, provided that L_m is not solely a function of T_{eff} and g . However, it is by no means clear that models based on specification of L_m alone are adequate, and it would appear to be a prudent course to consider further those classes of models for which L_m and \dot{M} are specified separately. It might be noted that a class of models based on the specification of \dot{M} alone, as suggested by Cannon and Thomas (1976), is unlikely to provide viable models of stellar atmospheres (Parker, 1981).

The question of the appropriate boundary conditions for wind models is further complicated by the fact that many observations demand models involving space and time dependent structure. To model such structures it is necessary to impose space and time dependent boundary conditions in the photosphere. Over a long time scale, variations in L_m alone could be sufficient to explain the observed variability of the atmosphere. On short time scales (months or less), however, it seems that changes in L_m alone would be unable to provide adequate models. For such stars, the possibility of linking theories of time-dependent wave propagation through the post-coronal regions (or extended chromospheres) of luminous cool stars (e.g., Willson and Bowen, 1985) to theories of nonradial pulsations in such stars (cf., Section IV.B) is particularly interesting.

THEORY OF MAGNETIC FIELDS IN COOL STARS

Cornelis Zwaan and Lawrence E. Cram

I. INTRODUCTION

Observations of the Sun reveal the profound effect of magnetic fields upon its atmospheric structure. Without magnetic fields the dynamical behavior of the solar atmosphere would be controlled by "normal" convective phenomena, such as granulation and supergranulation, and by wave phenomena, such as the 5-minute and 3-minute oscillations; the chromosphere and corona, if they existed at all, would be quite different. However, magnetic fields are present, and a wealth of atmospheric structure, from sunspots and faculae in the photosphere, through the intricate fabric of the chromosphere, into the complex corona, is controlled by them.

Present theoretical understanding of the Sun relates the magnetic structure in the solar atmosphere to magnetohydrodynamic properties of the underlying convective "envelope." It is suggested that similar relations exist in other stars. Indeed, phenomena that may be attributed to the presence of magnetic fields have been observed in many F-, G-, and K-type stars. These include (1) photometric variations that are attributed to the passage across the visible hemisphere of dark "starspots," (2) chromospheric, transition-region and coronal emissions

that appear to be closely interrelated, and (3) long-term variations in chromospheric emission that resemble the solar activity cycle (see Chapters 2 and 3, and Stenflo (1983) for descriptions of observational material). The magnetic origin of these stellar phenomena is supported by recent direct measurements of strong magnetic fields covering a significant fraction of the surfaces of several late-type dwarfs (Marcy, 1984; Saar and Linsky, 1985).

Studies of phenomena that are considered to be magnetically controlled demonstrate that stars of the same spectral type and luminosity class may show very different levels of activity.* So it appears that the level of magnetic activity in stars is not completely determined

* The expression, "level of activity," refers to any quantitative measure of any spectroscopic feature that is considered to be controlled by magnetic fields in a stellar atmosphere. Such measures include, for example, the integrated flux in one or more chromospheric emission lines, such as the CaII H and K line cores. At present we have only rudimentary empirical calibrations of the relationships between magnetic flux and chromospheric emission, and our theoretical understanding is also very limited. Presumably the level of activity in a given star is closely related to the mean magnetic flux density, irrespective of polarity, passing into the atmosphere. However, the existence of A-type stars with large magnetic fluxes and low "levels of activity" (Section III.A.5) shows that other factors are also relevant.

by the parameters that describe the structure of a classical model atmosphere, i.e., the effective temperature, surface gravity, and abundances (cf., Chapter 5). Indeed, observations indicate that the level of magnetic activity depends on both the classical parameters and additional factors such as the stellar rotation rate, evolutionary status, and existence of companion stars.

The presence of magnetic fields in cool stars leads to several conspicuous effects that are not explained by the classical theory of model atmospheres: (1) marked nonuniformities in the atmosphere, (2) variability of the atmosphere on time scales ranging from seconds to at least decades, and (3) energetic processes that lead to nonthermal emission especially prominent in the radio and hard X-ray spectral regions (cf., Chapter 5.III.B).

This chapter reviews current ideas regarding the role played by magnetic fields in cool stars. Continuing to follow the concepts developed in Chapter 6.II, we first discuss the theory of the magnetic field in the convection zone that lies beneath the visible atmospheric layers. We are particularly interested in the interaction between convection and the magnetic field, and in the processes that lead to the formation of active regions and to activity cycles, since these effects exert a marked influence on the atmosphere. We then discuss the theory of magnetic fields in the atmosphere, concentrating on the topology of atmospheric fields—flux tubes and loops in particular—and on the mechanisms whereby magnetic fields affect the flow of matter and energy. Finally we turn to the change of magnetic activity during the evolution of the stars.

II. MAGNETIC FIELDS IN STELLAR INTERIORS

The magnetic fields that influence so strongly the atmospheres of cool stars are generated and organized by processes that occur in the sub-atmospheric convection zones of these stars.

This section discusses basic theoretical ideas regarding these processes. More extensive accounts of the theory have been presented by Parker (1979a), Priest (1984), and several earlier authors and editors (Cowling, 1953, 1957, 1976; de Jager, 1959; Chandrasekhar, 1961; Lüst, 1965; Roberts, 1967; Cameron, 1967; Howard, 1971; Bumba and Kleczek, 1976).

II.A. BASIC EQUATIONS

Chapter 6.III has provided a brief account of the theory leading to a set of hydrodynamic equations that may be used to investigate dynamical phenomena in stellar atmospheres. Here, we focus on the terms in those equations that reflect the influence of electrodynamic processes, in particular magnetic fields and electric currents. Many important magnetohydrodynamic (MHD) processes in stars can be explained in terms of the force-balance equation

$$\rho \frac{d\mathbf{v}}{dt} = -\nabla P + \rho \mathbf{g} + \mathbf{J} \times \mathbf{B} \quad (7-1)$$

where ρ is the gas density, P the gas pressure, \mathbf{g} the gravitational acceleration, \mathbf{J} the electric current density, and \mathbf{B} the magnetic field. The last term in Equation 7-1, $\mathbf{J} \times \mathbf{B}$, is known as the Lorentz force. The effects of viscosity and radiation pressure forces have been neglected.

The electrodynamic quantities \mathbf{J} and \mathbf{B} appearing in Equation 7-1 may be determined by solving Maxwell's equations, which for application to stellar interiors may be approximated by:

$$\nabla \times \mathbf{B} = \mu \mathbf{J} \quad (7-2)$$

$$\nabla \cdot \mathbf{B} = 0 \quad (7-3)$$

$$\nabla \times \mathbf{E} = -\frac{\partial \mathbf{B}}{\partial t} \quad (7-4)$$

$$\nabla \cdot \mathbf{E} = 0 \quad (7-5)$$

The quantity \mathbf{E} is the electric field, and $\mu = 4\pi \times 10^{-7}$ henry m^{-1} is the magnetic

permeability. A frequently used form of Ohm's law is

$$\mathbf{J} = \sigma (\mathbf{E} + \mathbf{v} \times \mathbf{B}) \quad , \quad (7-6)$$

where σ is the scalar electrical conductivity. By combining Equations 7-2 through 7-6, we may recast Equation 7-4 into the form

$$\frac{\partial \mathbf{B}}{\partial t} = \nabla \times (\mathbf{v} \times \mathbf{B}) + \eta \nabla^2 \mathbf{B} \quad , \quad (7-7)$$

where the magnetic diffusivity η (assumed constant in the derivation of Equation 7-7) is given by:

$$\eta = \frac{1}{\mu \sigma} \quad (7-8)$$

The order of magnitude of the first and second terms on the right-hand side of the induction Equation 7-7 are vB/L and $\eta B/L^2$, respectively where L , v , and B are characteristic values of length, velocity, and magnetic field strength, respectively. The ratio of these terms is known as the *magnetic Reynolds number* (see Parker, 1979a, Chapter 4.5):

$$R_m = \frac{vL}{\eta} \quad (7-9)$$

If R_m is small compared with unity, the right-hand side of Equation 7-7 is dominated by the diffusion term, and plasma motion is not important. The corresponding characteristic decay time is then:

$$\tau_d \approx \frac{L^2}{\eta} \quad (7-10)$$

In the laboratory τ_d is quite small, being less than 10 s for a copper sphere of radius 1 m. However, in most astrophysical conditions the length L is so large that τ_d is very long, even though the magnetic diffusivity η is several times that of copper. For example, Cowling (1953) showed that the MHD diffusion time of a sunspot is about 300 years, and for a global solar magnetic field it is about 10^{10} years. In astrophysics, magnetic diffusion is important only when L is very small as a result of com-

plex magnetic topology, or when η is very large as a result of anomalous transport properties.

When R_m is large compared with unity the first term on the right-hand side of Equation 7-7 is dominant. In this case, the magnetic flux is constant through a closed contour moving with the fluid, and the field is said to be "frozen-in to the plasma" (see Parker, 1979a, Chapter 4). There is virtually no relative motion between the magnetic field and the fluid in the direction perpendicular to the field, but flow parallel to the field is not inhibited.

In astrophysical conditions that have been observed to date, the magnetic Reynolds number R_m is usually large. Even for a thin "tube" of magnetic flux ($L = 100$ km) located at the top of the solar convection zone ($\eta = 200 \text{ m}^2 \text{ s}^{-1}$) in a slow flow ($v = 1 \text{ m s}^{-1}$), we find $R_m = 500$. Hence, almost all observable changes in the magnetic fields in stellar atmospheres are principally due to plasma motions.

The long decay times in astrophysical plasmas make the relation between magnetic field and electric current different from everyday experience with electromagnetism. In domestic and most laboratory conditions, the effects of electric resistivity are predominant: electromotive forces are needed to maintain electric currents and magnetic fields. In these conditions, changes of the magnetic field are caused by changes of the electromotive force or of the resistance of the current circuit.

In many astrophysical conditions the effects of resistivity are minor because of the large scales: once magnetic fields and electric currents are set up, no electromotive force is needed to maintain them. Electric current and magnetic field then represent two complementary vector quantities connected by Ampère's law: $\nabla \times \mathbf{B} = \mu \mathbf{J}$. At the typically large magnetic Reynolds numbers, the local changes in the magnetic field are then determined by plasma motions via $\partial \mathbf{B} / \partial t = \nabla \times (\mathbf{v} \times \mathbf{B})$.

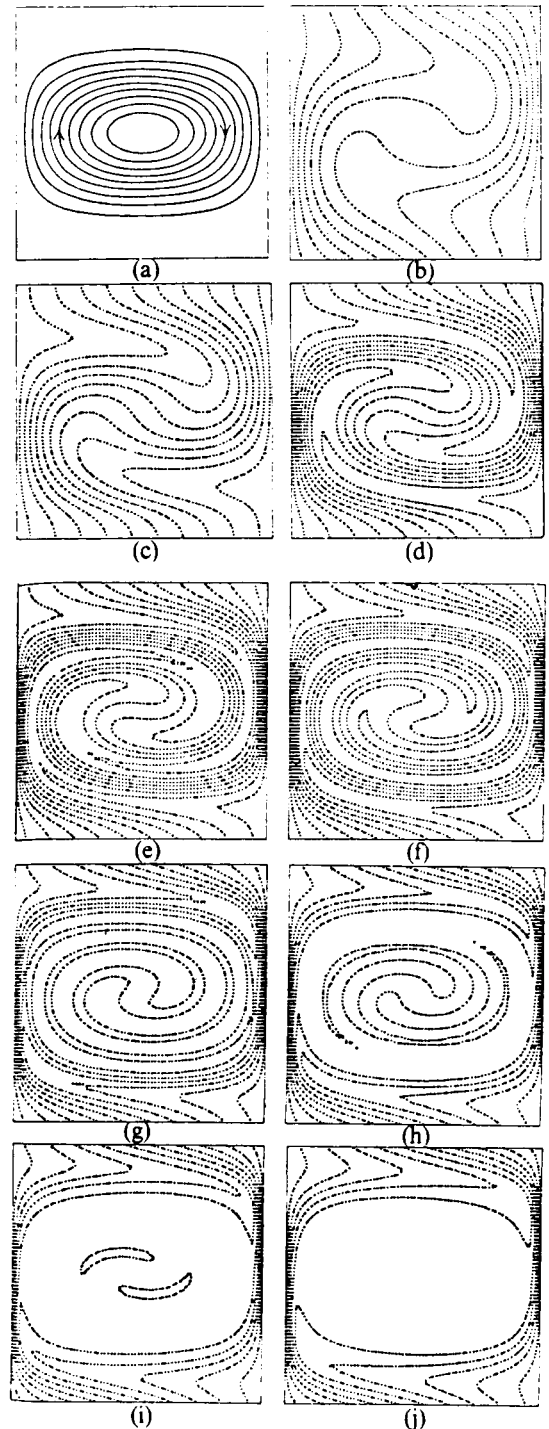
Then the electromagnetic state of the medium may be described by the magnetic field \mathbf{B} alone. In these conditions with $R_m \gg 1$, the magnetic field lines and flux tubes may be pictured as "strings" and "rubber tubes" that are transported, and maybe deformed, by plasma flows. This picture of strings or tubes of permanent identity being carried by the fluid fails in conditions of small R_m (small spatial scale); then the magnetic field diffuses. In simple cases of diffusion the picture of strings or tubes may be maintained in the sense that the "field lines slip across the fluid." [An interesting example, discussed below, is shown in Figure 7-1; panel (b) shows a steady pattern of field lines, with the fluid flow crossing; see the streamlines in panel (a).] In conditions with local $R_m \leq 1$, field reconnection may occur if adjacent field lines are in different directions, and in some cases fields of opposite direction may cancel [these processes are illustrated in Figure 7-1, panels (e) through (j)].

II.B. INTERACTION BETWEEN CONVECTION AND MAGNETIC FIELD

The structure and evolution of the magnetic field in a stellar atmosphere are primarily determined by the interaction between turbulent convection, rotation, and the magnetic field in the interior of the star. At present, theoretical understanding of this interaction is quite limited and only a few aspects have been studied.

Figure 7-1. The effect of a persistent velocity cell on an originally weak, vertical and homogeneous magnetic field. The streamlines of the fluid flow are plotted in (a). Panel (b) shows the final state of the lines of force for the modest magnetic Reynolds number $R_m = 40$. For $R_m = 10^3$ the development of the lines of force is shown in panels (c) through (j) at intervals $\Delta t = 0.5$ times the turnover time of the velocity cell, beginning with $t = 0.5$ in (c) and ending with $t = 4.0$ when the asymptotic state is nearly reached (from Weiss, 1966). The R_m value here is averaged over the system.

Parker (1963b) and Weiss (1966) investigated the influence of systems of persistent velocity cells on initially weak and homogeneous magnetic fields (cf., Figure 7-1). These studies have shown that, for a range of flow patterns at large



values of R_m , the magnetic field is swept into regions between the cells. Within even one turnover time of the cells, this “expulsion” or “concentration” effect is quite conspicuous. On a longer time scale (several turnover times), the field in the cell interiors is strongly sheared; hence $\nabla^2 \mathbf{B}$ becomes very large; so reconnection and eventually field annihilation occur (see Figure 7-1; panels (e) through (j)). The field disappears from the cell interiors, and becomes concentrated at the cell boundaries. Ultimately a stationary state is reached, when diffusion of the field from between the cells balances advection.

These theoretical studies of the interaction between cellular flows and magnetic fields suggest that these flows concentrate magnetic fields into regions between cells, until the Lorentz force $\mathbf{J} \times \mathbf{B} = \mu^{-1}(\nabla \times \mathbf{B}) \times \mathbf{B}$ is sufficiently intensified to halt the flow locally. A crude estimate of the field strength produced by this process may be obtained by equating the magnetic energy density $B^2/2\mu$ and the kinetic energy density $\rho v^2/2$ to yield the “equipartition field strength”:

$$B_{\text{eq}} = (\mu \rho v^2)^{1/2} \quad (7-11)$$

The actual state of convection in stars is much more complex than the systems of well-ordered, long-lasting cells that have been investigated theoretically. Our present understanding of the behavior of magnetic fields in the presence of turbulent convection is consequently quite rudimentary (cf., Parker, 1979a, Chapter 17). Qualitatively, it appears that the magnetic field in a zone of turbulent convection will be very inhomogeneous if the magnetic Reynolds number is high (often called “intermittent”). A high value of R_m implies that magnetic field concentrations outlive the individual turbulent eddies, and so the concentration process described above tends to form and maintain a field configuration consisting of tortuous strands of magnetic flux. Within any strand, the field strength would be of the order of the equipartition value, and the gross

topology of the system of strands would evolve on a time scale considerably longer than the characteristic lifetime of the convective flow. In other words, magnetic field and convection coexist beside one another: most of the field is concentrated in strands without appreciable internal turbulence, while the medium between the magnetic strands is vigorously convective, and without appreciable magnetic flux. This qualitative description is consistent with the observed inhomogeneity of the magnetic field in the solar photosphere.

The partition between convection and magnetic field suggests, as a useful approximation for magnetic fields in convection zones, a two-component model consisting of distinct flux tubes separated by field-free plasma. So we consider the theory of flux tubes (Figure 7-2) in a convective envelope (see also Parker, 1979a, especially Chapter 8). If there are no appreciable flows within and outside the flux tubes, the mechanical equilibrium of a flux tube in a field-free medium is described by the magnetostatic equation:

$$\begin{aligned} -\nabla P + \rho \mathbf{g} + \frac{1}{\mu} (\nabla \times \mathbf{B}) \times \mathbf{B} = \\ -\nabla P + \rho \mathbf{g} - \nabla \left(\frac{B^2}{2\mu} \right) + \frac{1}{\mu} (\mathbf{B} \cdot \nabla) \mathbf{B} = 0 \end{aligned} \quad (7-12)$$

On the right-hand side of Equation 7-12 the Lorentz force has been separated into two terms, the first $(-\nabla B^2/2\mu)$ being the gradient of an *isotropic magnetic pressure* $B^2/2\mu$, and the second being a force arising from a *magnetic tension* B^2/μ along the lines of force. The tension term is zero for rectilinear lines of force.

Some basic properties of the magnetic field may be described by considering a slender flux tube, whose diameter D is smaller than the characteristic scale of variation along the tube (i.e., D is small compared with both the radius of curvature of the field and the pressure scale height). Since the magnetic field exerts no force on the plasma in the direction of the field (\mathbf{l}),

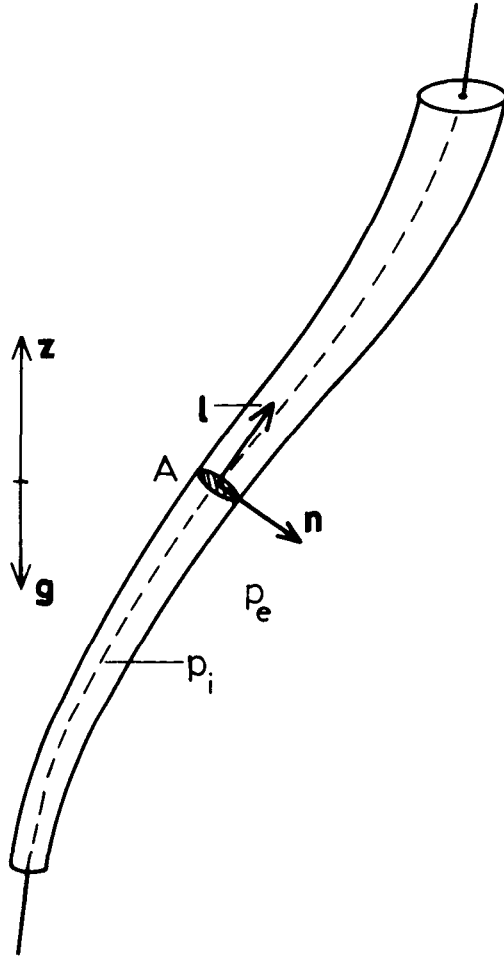


Figure 7-2. The geometry of a magnetic flux tube with an internal field \mathbf{B} (l), cross-section A , internal pressure P_i , and external pressure P_e .

the component of Equation 7-12 in that direction becomes

$$-\frac{\partial P}{\partial l} + \rho (\mathbf{g} \cdot \mathbf{l}) = 0 \quad (7-13)$$

while in the direction \mathbf{n} perpendicular to the tube we have:

$$\frac{\partial}{\partial n} \left(P + \frac{B^2}{2\mu} \right) = 0 \quad (7-14)$$

If we suppose that the magnetic field strength is independent of position across the tube, it follows from Equation 7-14 that the internal

pressure P_i and the external pressure P_e are related by:

$$P_i + \frac{B^2}{2\mu} = P_e \quad (7-15)$$

In this model, there is a pressure jump, $P_e - P_i$, at the edge of the flux tube, supported by the Lorentz force of the thin current sheet bounding the flux tube. Equations 7-13 through 7-15 imply that the variation of field strength and cross-section along a flux tube can be evaluated if the temperature distributions both inside and outside the tube are known, together with the field strength, cross section, and either the internal or external gas pressure at one position. Specifically, the field strength at any height z is given by

$$B(z) = \{2\mu[P_e(z) - P_i(z)]\}^{1/2} \quad (7-16)$$

while the cross-sectional area $A(z)$ is given by the flux-conservation equation:

$$B(z)A(z) = \phi = \text{constant} \quad (7-17)$$

The distributions $B(z)$ and $P_i(z)$ depend on the height z , but not on the path (i.e., the shape of the axis) of the flux tube through the medium.

The path of the flux tube in the convection zone is determined by the velocity shear, the buoyancy of the flux tube, and the magnetic tension along the tube. Note that if a flux tube is stretched by a sheared flow the field is enhanced. Consider a section of a flux tube of strength B , cross Section A and length l . Conservation of flux implies that BA remains constant; ρlA is constant because of conservation of mass. Hence $B \sim \rho l$, or, if the mass density ρ remains constant, $B \sim l$.

In the special case that the flux tube is in thermal equilibrium with its surroundings [$T_e(z) = T_i(z)$], the pressure scale height is the same inside and outside the tube. Equations 7-13 through 7-17 then imply that the field strength

decreases with height according to (Parker, 1979a, Chapter 8.2):

$$B(z) = B(z_0) \exp \{ -(z-z_0)/2H_p \} \quad (7-18)$$

The decrease of the field strength with height according to Equation 7-18 is much more drastic than the variation of the equipartition field strength $B_{eq}(z)$ according to equation 7-11. For instance, a flux tube of equipartition strength in the top of the solar convection zone ($B = B_{eq} \approx 5 \times 10^{-2} \text{ Wb m}^{-2}$), if it extends down to the bottom of the convection zone while in thermal equilibrium with its surroundings, would reach a field strength ($B \approx 10^3 \text{ Wb m}^{-2}$) which is three orders of magnitude larger than the local equipartition strength. Such very high field strengths in the deep convection zone are not likely: the flux tubes would rise very rapidly because of the strong buoyancy (see below).

Observations of solar active regions suggest that magnetic flux tubes do extend over many scale heights in the convection zone, at field strengths of about the equipartition field strength or somewhat larger (cf., Chapter 7.II.C.4), such that the field strength varies with height by a modest factor. In order to explain such a departure from the steep dependence on height predicted by Equation 7-18, two mechanisms have been proposed. The first one, the convective collapse, which is discussed in Chapter 7.III.A.2, cools the flux tube in the top of the convection zone below the temperature of the surrounding medium, which decreases the internal gas pressure and so increases the magnetic pressure. This mechanism causes the magnetic field strength to decrease much more slowly with height than Equation 7-18 indicates.

The second mechanism is associated with the convective turbulence in the medium surrounding the flux tube, which can contain the flux tube at a field strength of nearly the equipartition strength $B_{eq}(z)$ over a range of many scale heights. Van Ballegoijen (1984) investigated

this idea, accounting for the deviation from hydrostatic equilibrium in the external medium by including the vertical component of the Reynolds stress $\langle \rho_e v_z^2 \rangle$ in the equilibrium equation

$$\frac{d}{dz} (P_e + \langle \rho_e v_z^2 \rangle) = -\rho_e g \quad (7-19)$$

where v_z is the vertical velocity, and the diamond brackets indicate an average over a horizontal surface. He assumed that the interior of the tube is strictly static (no turbulence) and in thermal equilibrium with the surrounding medium ($T_i = T_e$). He adopted the temperature distribution $T_e(z)$ and the velocity distribution from Spruit's (1976) mixing-length model for the solar convection zone. The flux tubes were assumed to be vertical and anchored in the bottom of the convection zone with a field strength of about one, four, or ten times the local equipartition field strength B_{eq} . Van Ballegoijen found that the field strength decreases smoothly with height z , first down to $B(z) \approx 0.6 B_{eq}(z)$, and then following $0.6 B_{eq}(z)$ up to about 1000 km below the photosphere. This relatively slow decrease of the field strength with height may be understood as follows: the increase of $\langle \rho v_z^2 \rangle$ with depth slightly uplifts the higher layers, causing the gas pressure $P_e(z)$ to be somewhat larger than in the strictly hydrostatic case. Since this effect does not occur within the flux tubes, the magnetic field can be confined by the increase of the external pressure (see Equation 7-15).

A buoyancy force acts on a flux tube which is (nearly) in thermal equilibrium with its surroundings, since the reduced interior pressure implies a reduced density. The buoyancy force per unit length, F_b , is given by

$$F_b = A g (\rho_e - \rho_i) \quad (7-20)$$

where $\rho_e - \rho_i$ is the difference between the external and internal densities. Parker (1979a, Chapter 8.7) estimates that the rate of rise of a horizontal isothermal flux tube would be approximately the Alfvén speed, whence it follows

for plausible field strengths that buoyancy would expel flux tubes within a few weeks or months. Some mechanism is needed to keep flux tubes anchored in the convection zone; we return to this problem in Section II.C.4.

In this section it is argued that the magnetic field in convection zones must be concentrated in strands at field strengths of the order of the equipartition strength B_{eq} (see Equation 7-11). Solar observations suggest that in the solar convection zone the magnetic field is contained in bundles of flux tubes which are of at least equipartition strength (Zwaan, 1978). Flux tubes at strength $B \gtrsim B_{\text{eq}}$ efficiently exclude turbulence; hence the convective heat exchange between the plasma in the tube and the ambient plasma is severely hampered. Radiative diffusion is very inefficient as well: for all depths larger than 3000 km in Spruit's (1976) model for the solar convection zone the mean photon free path is less than 1 cm, and so the radiative diffusivity η_{rad} is less than $10^3 \text{ m}^2 \text{ s}^{-1}$. At the depth of 8000 km, η_{rad} is smallest: $\eta_{\text{rad}} \approx 0.5 \text{ m}^2 \text{ s}^{-1}$. Hence the radiative diffusion time scale for a tube with radius r , viz., $\tau_{\text{rad}} = r^2/\eta_{\text{rad}}$, is very large: for a tube with $r = 100 \text{ km}$ we find $\tau_{\text{rad}} > 3$ months for all depths below 3000 km; around 8000 km depth, $\tau_{\text{rad}} \approx 600$ years.

We conclude that the flux tubes in the convection zone are thermally insulated. One interesting consequence is that flux tubes tend to move adiabatically, so that plasma flows within the tubes also will be close to adiabatic. Hence the flux tube will be out of thermal equilibrium with its new environment after a vertical displacement ($T_i(z) \neq T_e(z)$), and their thermal imbalance may last for months, because of the long radiative diffusion time. These effects are important in case of displacements through the strongly superadiabatic top part of the convection zone. For the bulk of the convection zone the mean temperature stratification $T_e(z)$ is very close to adiabatic, and there the thermal effect of displacements is slight.

In summary, the main feature of the interaction between magnetic field and convection is the partition: magnetic strands without appreciable internal turbulence coexist beside vigorously convective cells without appreciable magnetic flux. The magnetic field strength in the magnetic strands is estimated to be of the order of the equipartition field strength. Models may be constructed for flux tubes extending over the full height of the convection zone at field strengths $B(z)$ of about the local equipartition strength $B_{\text{eq}}(z)$, provided that the departure of hydrostatic equilibrium caused by the turbulence in the ambient convection zone is taken into account.

Several features of the magnetic field, which are inferred from observational data, cannot be explained from the interaction between magnetic field and convection alone, however: how may relatively strong flux bundles be kept for periods of years within the convective envelope, against the buoyancy? During the activity cycle the solar magnetic field displays several large-scale patterns. How are these produced? Why does magnetic activity in late-type stars depend on the stellar rotation rate? These types of questions are addressed in the next section.

II.C. DYNAMO THEORY

There are two types of theories on the origin of magnetic fields in stars like the Sun: (a) dynamo theories in which the magnetic field is amplified and modified by fluid flow, and (b) theories based on the existence of a primordial field trapped deep inside the stars. Both kinds of theories have been proposed in a variety of forms, but most theoretical effort is put into dynamo models. For a critique of oscillator models based on a primordial field (Piddington, 1976; Layzer et al., 1979), we refer to Cowling (1981) and Schüssler (1983). Here we discuss dynamo models only. For more comprehensive treatments we refer to Parker (1979a, Chapters 17, 18, 19 and 21.2), Priest

(1984, Chapter 9), and monographs devoted to dynamo theory by Moffatt (1978), Krause and Rädler (1980), and Vainshtein, Zel'dovich, and Ruzmaikin (1980). Recent developments have been reviewed by Cowling (1981), Gilman (1981), Schüssler (1983, 1984), Stix (1981), Weiss (1983) and Yoshimura (1982).

II.C.1. PRINCIPLES OF DYNAMO ACTION

In dynamo processes the magnetic field is maintained by currents induced by fluid motions across the field lines. The magnetic field is thought to develop from a "seed" field. The interaction between the velocity field \mathbf{v} and the magnetic field \mathbf{B} , given by the induction Equation 7-7, leads to a steady or oscillating magnetic field. The magnetic energy lost by diffusion and by escape at the boundary is replenished by the convective turbulence acting on the field. Certain simple magnetic configurations are ruled out by Cowling's (1934) theorem: *a steady axisymmetric magnetic field cannot be maintained by a dynamo effect.*

For the discussion of fields in rotating spherical bodies, it is convenient to split \mathbf{B} into a toroidal (or azimuthal) component \mathbf{B}_ϕ and a poloidal component \mathbf{B}_p (which is contained in a meridional plane). *In the dynamo action in stellar convection zones, three processes may be distinguished:*

- (1) The *differential rotation* pulls out the magnetic field lines in the direction of rotation, and so a strong toroidal component \mathbf{B}_ϕ is created (Figure 7-3). Differential rotation is observed on the Sun: the equatorial region rotates faster than the polar regions. This nonuniform rotation is understood as the result of a coupling between rotation and convection (see Gilman, 1981). Stretching in the toroidal direction is in agreement with the nearly east-west orientation of the solar active regions, with their opposite polarity ar-

angement on the northern and southern hemispheres. The amplification of the magnetic field would continue until it is balanced by Ohmic diffusion and the field emerges at the boundary. Such an equilibrium would only apply to the toroidal component, since the poloidal component is not affected by differential rotation. In fact, the poloidal component would slowly decay because of dissipation, and the dynamo would stop. Hence, another process is needed to maintain the poloidal component or, as in the solar case, to reverse the poloidal component periodically.

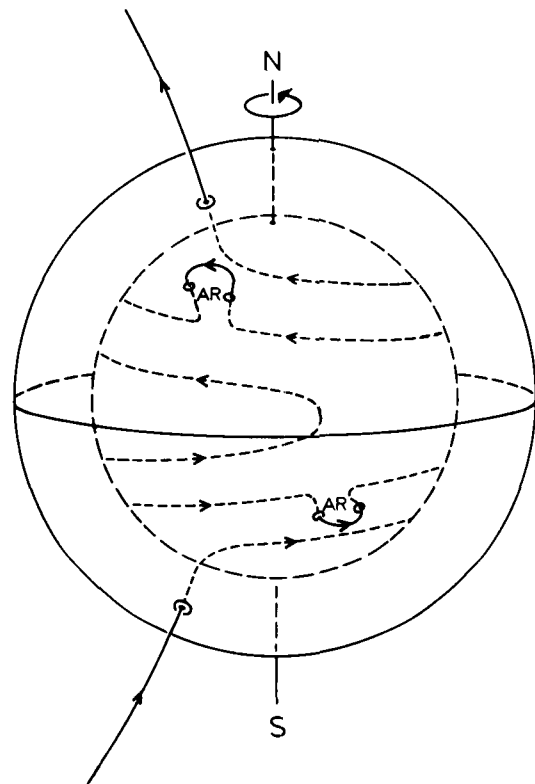


Figure 7-3. The formation of a strong toroidal component in the magnetic field by differential rotation. The differential rotation stretches the field in the east-west direction. When a loop of flux tubes breaks through the photosphere, a bipolar active region (AR) is formed (from van Ballegoijen, 1982).

(2) Parker (1955) suggested that poloidal field may be regenerated by *the effect of cyclonic convective cells*. Because the pressure decreases with height, rising blobs expand and hence tend to rotate because of the Coriolis force. Rising Ω -shaped flux loops tend to rotate clockwise on the northern hemisphere and counterclockwise on the southern hemisphere (Figure 7-4). These twists convert toroidal field \mathbf{B}_ϕ into poloidal field \mathbf{B}_P with the direction opposite to the direction of the previous poloidal field. The

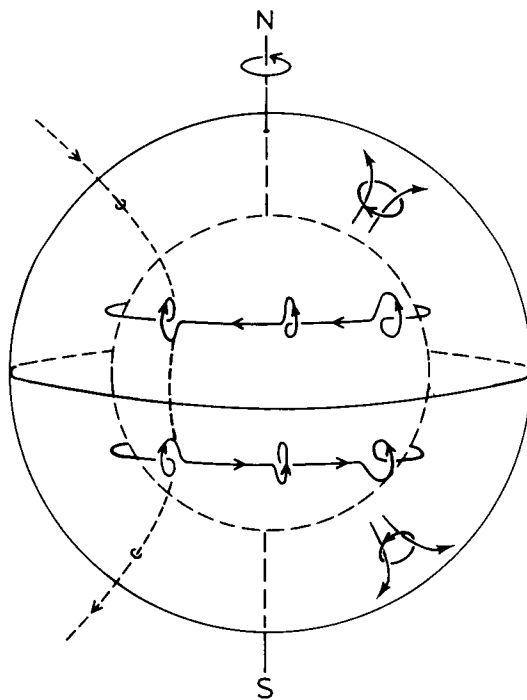


Figure 7-4. The regeneration of poloidal magnetic field from the toroidal field as envisaged in dynamo theory. The Coriolis force causes rising convective bubbles, and hence rising flux loops, to rotate about the vertical. In this way, spiral loops are formed in the toroidal field strands; in each of these loops the field has a component in the meridional plane. Thus a new mean poloidal field is produced. The dotted line symbolizes this poloidal field, which is opposite to the original poloidal field during the generation of the toroidal field; see also Figure 7-3 (from van Ballegooijen, 1982).

rate of generation of \mathbf{B}_P is proportional to the toroidal field \mathbf{B}_ϕ ; hence Parker described the net effect of many convection cells by an extra term in the large-scale electric field:

$$\mathbf{E}_\phi = \alpha \mathbf{B}_\phi \quad (7-21)$$

The coefficient α , which has the dimension of velocity, is a measure of the mean rotational speed of the eddies. It has given the regeneration process of the poloidal field the name “ α -effect” (although Parker introduced a different notation). The new large-scale poloidal field is built up from small loops of the correct circulation.

(3) Parker (1955) assumed the process of *turbulent diffusion* of the magnetic field, which is much more efficient than the Ohmic diffusion. Turbulent diffusion is important in dynamo action, since it redistributes the magnetic field over large parts of the convection zone on a relatively short time scale. In fact, this makes possible a periodic dynamo with a period as short as 22 years.

II.C.2. LEIGHTON'S PHENOMENOLOGICAL MODEL

Leighton (1969) incorporated the dynamo principles into a numerical model that relies on observational data. The toroidal field is amplified by differential rotation. Once the toroidal field strength exceeds some critical value, magnetic flux loops are supposed to rise to the surface and form bipolar active regions. The regeneration of the poloidal field is attributed to the Coriolis force acting on the rising flux loops; in Leighton's model the observed tilt of the active regions with respect to the E-W direction is used as the measure for this effect. The turbulent diffusion is attributed to the supergranulation; the diffusion is modeled as a random-walk process. Because of the tilt of active regions with respect to the direction of

rotation, the “following” polarity (trailing in the solar rotation) is closest to the pole, hence it is predominantly flux of following polarity which is diffused toward the pole. This leads to the reversal of the polar fields at about the time of sunspot maximum, which is interpreted as an indication for a poloidal field pervading the convection zone with the correct direction for the next sunspot cycle.

Adapting the adjustable parameters in his model, Leighton could reproduce the main features of the solar cycle very well.

II.C.3. KINEMATIC DYNAMOS: MEAN-FIELD THEORY

The simultaneous solution of the equations of induction and motion presents the formidable, hydromagnetic dynamo problem which has not yet been solved. To date most attention has been paid to the kinematic dynamo problem: here the velocity field, which may contain adjustable parameters, is postulated and the response of the magnetic field is studied, but the feedback of the Lorentz force on the velocity field is either ignored, or it is treated in a very schematic fashion.

Parker’s (1955) principles of a large-scale electric field $\alpha \mathbf{B}_o$ (Equation 7-21), produced by the net effect of many small-scale convective eddies, and of the effect of turbulent diffusion became incorporated in the so-called mean-field theory (see Krause and Rädler, 1980). In this theory, the magnetic field \mathbf{B} and the velocity \mathbf{v} are split into mean fields \mathbf{B}_o and \mathbf{v}_o , which vary over the large scale L of the convection zone, and fluctuations \mathbf{B}_1 and \mathbf{v}_1 , which vary over scales $l \ll L$. Substitution into the Induction Equation 7-7 and specific assumptions regarding the turbulence led to the so-called *dynamo equation* for the large-scale magnetic field \mathbf{B}_o :

$$\frac{\partial \mathbf{B}_o}{\partial t} = \nabla \times (\mathbf{v}_o \times \mathbf{B}_o + \alpha \mathbf{B}_o) + (\eta + \beta) \nabla^2 \mathbf{B}_o \quad (7-22)$$

The extra terms in this modified induction equation represent the effects of the turbulence mentioned in Section II.C.1: $\alpha \mathbf{B}_o$ is the electric field generated along the mean field \mathbf{B}_o by cyclonic turbulence, and $\beta \nabla^2 \mathbf{B}_o$ represents turbulent diffusion. The values for α and β depend on properties of convective turbulence; crude scalar approximations are:

$$\alpha \approx -\frac{1}{3} \tau \langle \mathbf{v}_1 \cdot \nabla \times \mathbf{v}_1 \rangle \approx -\frac{v_1^2 \tau^2 \omega \cos \Theta}{H_\rho} \quad (7-23)$$

and

$$\beta \approx \frac{1}{3} \tau \langle v_1^2 \rangle, \quad (7-24)$$

where τ is the correlation time for the eddies, the diamond brackets indicate averages over length scales much larger than the scale l of the turbulence, ω is the stellar angular rotation rate, Θ is the latitude, and H_ρ is the density scale height.

Since the dynamo Equation 7-22 is linear in \mathbf{B}_o , the solutions are growing or decaying oscillations. The migrating dynamo waves travel along surfaces of constant angular rotation rate. The solution depends on the dynamo number N_D , which is a dimensionless measure for the effects determining the field generation: the α -effect, differential rotation, and diffusion:

$$N_D = \frac{\alpha \Delta \omega L^3}{\beta^2}, \quad (7-25)$$

where $\Delta \omega$ is the difference in angular velocity across the depth of the dynamo region.

Dynamos are possible only if N_D is sufficiently large. The direction in which the dynamo wave is traveling depends on the sign of $d\omega/dr$. In order to explain the butterfly diagram, i.e., the propagation of the emergence site of solar active regions toward the equator during the activity cycle, the rotation rate should increase with depth ($d\omega/dr < 0$). The main features of the cyclic magnetic activity of

the Sun may be reproduced by mean-field models, provided that the adjustable parameters in the model are suitably chosen.

Dynamo models based on the mean-field approach suffer from several serious problems including (1) the value α required in the model to reproduce the solar cycle is between 1 and 10 cm s^{-1} , which is several orders of magnitude smaller than values of α computed from mixing-length arguments ($\alpha \approx 100 \text{ m s}^{-1}$); (2) the mean-field approach is based on the idea of two widely different scales: a small-scale l for the convective turbulence, and a large-scale L for differential rotation and the mean \mathbf{B}_0 field. This two-scale approximation breaks down if large-scale convection in the form of "giant cells" exists; and (3) mean-field dynamos require that the rotation rate $\omega(r)$ increase with depth, but such a depth dependence seems to be inconsistent with $\omega(r)$ derived from measurements of solar oscillations (Duvall et al., 1986).

II.C.4. FLUX-TUBE DYNAMOS AND BOUNDARY-LAYER DYNAMOS

The observational and theoretical indications for the mutual exclusion of magnetic field and convective turbulence have raised the question whether the mean-field approach is relevant to describe the interaction between convection and magnetic field. Consequently, several recent studies have explored the feasibility of *flux-tube dynamos* — see Schüssler (1983) for a review and references.

Whereas a continuous magnetic field is tied to the plasma because of the high electric conductivity, flux tubes are bound to the surrounding nonmagnetic medium by the drag force. Flux tubes slip through the medium with a velocity \mathbf{u} that is determined by the equilibrium between the curvature force \mathbf{F}_C , the buoyancy force \mathbf{F}_B , and the drag force $\mathbf{F}_D(\mathbf{u})$:

$$\mathbf{F}_C + \mathbf{F}_B + \mathbf{F}_D(\mathbf{u}) = 0 \quad (7-26)$$

Because of the efficient separation between the field and the convective flows in a flux-tube dynamo, the α -effect is expected to be much smaller than in mean-field dynamos, and one of the problems mentioned in Section II.C.3 may be removed. It is not clear, however, that other problems, such as the wrong sign of $d\omega/dr$, may be avoided in flux-tube dynamos.

In order to secure the nearly E-W orientation of the active regions and Hale's polarity laws, the flux ropes should be able to resist deformation by convective turbulence. Hence the field strengths should be about the equipartition value (Equation 7-11), or larger. But strong flux tubes are buoyant, and therefore are difficult to store within the convection zone for times comparable to the period of the sunspot cycle (Parker, 1975). In an effort to solve this buoyancy problem, several authors have argued that strong magnetic field may reside near the bottom of the convection zone, possibly within the relatively thin layer of convective overshoot below the convection zone. Schüssler (1983) lists several arguments why magnetic flux accumulates in the inner boundary layer and why the field may be stored there for several years. This flux accumulation may be attributed to the expulsion of magnetic field from regions of convective turbulence, here applied to the convection zone as a whole. However, in order to make a *boundary-layer dynamo* work, it is necessary that there be differential rotation in this boundary layer. Referring to the well-known analogy between the induction Equation 7-7 and the vorticity equation, Schüssler (1984) argues that the convection zone expels both magnetic field and vorticity. Hence, a boundary layer is expected to be formed where magnetic field and velocity shear are concentrated, but where the overshooting convection is weak. In such a layer, a dynamo might operate without the problems posed by mean-field dynamos operating throughout the convection zone. Schüssler (1984) discusses some aspects of boundary-layer dynamos. As yet, however, no detailed model for such a dynamo has been published.

The present theory of stellar dynamos cannot explain the observed large-scale regularities in the appearance of active regions, in particular the existence of activity complexes, or nests. Such nests are sequences of active regions that appear within a small area on the solar surface over periods ranging from about 6 to 15 months. The solar example suggests that activity nests are responsible for the phase coherence in stellar radiative fluxes that are modulated by stellar rotation.

III. MAGNETIC FIELDS IN STELLAR ATMOSPHERES

Most, if not all, of the magnetic flux that is present in the Sun's atmosphere passes through the base of the photosphere in patches with high field strength. The largest elements appear as *sunspots*, with dark umbrae surrounded by penumbrae. Somewhat smaller elements are seen as sunspot *pores* (umbrae without penumbrae). The smallest magnetic elements are associated with bright patches, called *faculae* and *network elements*. These magnetic elements form a hierarchy, the properties of which depend on the total magnetic flux in the element as the parameter (see Zwaan, 1978, 1981b for descriptions).

The existence of this hierarchy and the main properties of its elements have been interpreted as consequences of the interaction between convection and magnetic field inside the Sun. Consequently, it may be expected that similarly inhomogeneous fields occur in other late-type stars. Evidence supporting this expectation is provided by direct measurements of photospheric magnetic field strengths and fluxes in a few stars (Chapter II.G), and by indirect observations of chromospheric and coronal emissions that vary in time (Chapter III.G).

This section discusses the theory of inhomogeneous magnetic fields in the atmospheres of late-type stars.

III.A. PHOTOSPHERIC MAGNETIC STRUCTURE

Observations of the Sun show that the highly structured photospheric magnetic field exerts a strong influence on the distribution of matter and the flow of energy in the photosphere. Important aspects of these influences can be discussed in terms of the theory of magnetostatic flux tubes, to which we now turn.

III.A.1. MAGNETOSTATIC FLUX TUBES

Consider an axially symmetric, untwisted ($B_\phi = 0$) flux tube, with its axis vertical, surrounded by a nonmagnetic medium (Figure 7-5). Let us assume that any mass flow that occurs inside or outside the tube is so small that the force-balance equation (Equation 7-1) reduces to *the magnetostatic equation*, which determines the pressure balance between the interior of the flux tube and the ambient medium:

$$\begin{aligned} -\nabla P + \rho \mathbf{g} + \mathbf{J} \times \mathbf{B} &= \\ -\nabla \left(P + \frac{B^2}{2\mu} \right) + \rho \mathbf{g} + \frac{1}{\mu} (\mathbf{B} \cdot \nabla) \mathbf{B} &= 0 \end{aligned} \quad (7-27)$$

(Note identity to version given by Equation 7-12, except for \mathbf{J} term.)

Furthermore, we assume that at the top of the convection zone, that is, just below the photosphere, the field strength in the tube is sufficiently large to inhibit energy transfer by convection. This assumption implies that (1) the heat flux F_i inside the tube is much smaller than the flux F_e in the external medium, and (2) the only lateral heat flow is due to radiative energy transfer, which is important only in the transparent top part of the tube. The deeper part of the tube is essentially insulated from the convection zone.

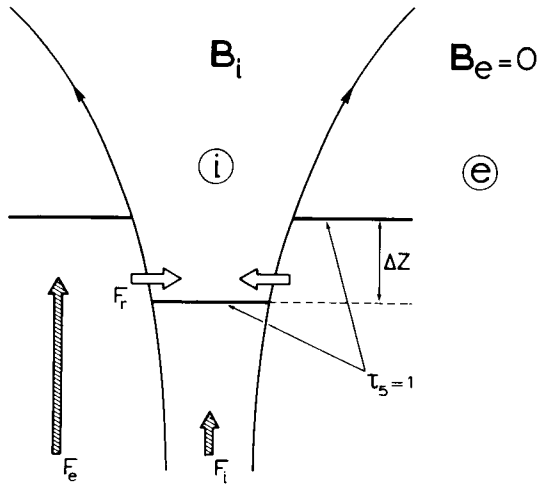


Figure 7-5. Concept of the magnetostatic flux-tube model. One level of constant optical depth τ_5 is shown, with the Wilson depression Δz . The filled arrows F_i and F_e stand for the (nonradiative) energy fluxes. The open arrows F_r indicate the influx of radiation into the transparent top part of the tube.

Because $F_i < F_e$, the plasma inside the tube is cooler than the plasma outside, at the same height: $T_i(z) < T_e(z)$. This temperature difference is largest in the deepest atmospheric layers within the flux tube, where the radiative cooling is most effective. Magnetostatic equilibrium implies that nowhere in the flux tube is the gas pressure larger than the external pressure — see Equation 7-16. In the height range where $T_i(z) < T_e(z)$ the pressure scale height $H_{p,i}$ within the tube is smaller than the external scale height $H_{p,e}$. Consequently the isobars inside the tube are depressed relative to those outside, creating a positive pressure difference

$$\Delta P(z) = P_e(z) - P_i(z) \quad , \quad (7-28)$$

which is balanced by the Lorentz force (in the slender-tube approximation the pressure excess $\Delta P(z)$ is precisely balanced by the magnetic pressure $B^2(z)/(2\mu)$). The depressed isobars are associated with depressed density isopleths, which in turn lead to lower opacities and the

so-called Wilson depression (see Bray and Loughhead, 1964, p. 94; see also Figure 7-5). The Wilson depression of large sunspots is observed to be about 600 km, corresponding to several pressure scale heights in the external medium.

Spruit (1976, 1977) constructed numerical models of thin flux tubes, assuming the existence of a potential field ($\nabla \times \mathbf{B} = 0$) within the tube. Such models possess infinitely thin current sheets at the interface between the field and the external plasma. Spruit calculated the temperature distribution in the flux tube, using an energy equation based on diffusion with an anisotropic and depth-dependent diffusion coefficient. Of course a diffusion equation provides only a crude model of energy transport by radiation and convection, particularly in the part of the tube which is not optically thick.

Spruit showed that flux-tube models may be constructed if three parameters are specified: (1) q , the ratio of nonradiative energy flux inside the tube to that outside, (2) Δz , the Wilson depression, and (3) R , the radius of the tube at a specified height. With these quantities adopted, the magnetic field and temperature distribution may be obtained by a simultaneous solution of the magnetostatic and diffusion equations. Spruit's calculations reproduce the main photospheric characteristics of magnetic elements in the range of sizes from tiny bright elements to dark sunspot pores.

Deinzer et al. (1984) describe a flux-tube model obtained by solving equations describing a time-dependent, axisymmetric field configuration. The properties of the model are similar to those of Spruit's model. The dynamical calculations support the existence of a very sharp boundary between the field and the external medium.

Models for thick magnetostatic flux tubes, designed to represent sunspots, have been constructed by several authors, usually on the basis of a similarity assumption suggested by Schlüter

and Temesvary (1958); see also Deinzer (1965) and Yun (1970). Given an appropriate value of the ad hoc factor describing the reduced efficiency of nonradiative energy transport in the magnetic region, such models can be adjusted to predict field strengths and umbral temperatures in reasonable agreement with observation. However, the similarity assumption underlying these models leads to unrealistic distributions of gas pressure and density, and there is a need for an internally consistent approach to the problem. The "return-flux" model proposed by Osherovich (1982) may yield a more realistic model.

Sunspot models based on a single, thick, and continuous flux tube do not readily explain the observed process of sunspot formation by coalescence of smaller elements (Vrabec, 1973), nor do they explain the occurrence of umbral dots (Danielson, 1964) or the mechanism of energy transport which transmits as much as 20% of the photospheric flux through the umbra. Many authors have suggested that a resolution to these problems may lie in the conjecture that a sunspot actually consists of a "bundle" of smaller flux tubes (Figure 7-6). It is suggested that these smaller flux tubes become quite distinct from one another beneath the photosphere, with essentially field-free, convecting plasma between them. There is as yet no quantitative account of such a composite model, although Parker (1979a) has investigated some important aspects of the energy balance in such a system.

The exponential decrease of gas pressure with increasing height in the external plasma implies that the internal magnetic pressure will also decrease with increasing height. Since the flux must be constant, the field lines diverge rapidly with increasing height above the photosphere. Within a few pressure scale heights the field becomes nearly force free, or, if electric currents are completely absent, it becomes a potential field. In the latter case the field resembles that outside the end of a solenoid.

The degree of divergence of the field lines depends on the total magnetic flux in the structure: for increasing flux, the divergence starts at a progressively lower level in the atmosphere. For structures with large magnetic fluxes (sunspots), a strong horizontal component in the magnetic field is expected on their periphery at levels as deep as the photosphere. This horizontal component is held responsible for penumbrae in large spots.

As a consequence of the reduced internal temperature in the top part of the flux tubes, the internal mass density ρ_i is much smaller than the density ρ_e in the ambient convection zone. Hence the tops of the flux tubes are buoyant, and the assumption that the magnetostatic tubes stand vertical is consistent.

III.A.2. EMERGENCE AND FORMATION OF INTENSE FLUX TUBES

The interpretation of the photospheric magnetic field in terms of the static flux-tube models described in Section III.A.1 does not explain how the intense flux tubes are formed. There is no evidence that magnetic field emerges from the solar convection zone with a high field strength (between 0.1 and 0.2 Wb m⁻²) already present. Indeed, the field strength just before emergence is probably not more than the equipartition field strength in the top of the convection zone, $B_{eq} \approx 0.05$ Wb m⁻² (Section II). This section therefore discusses the processes that may lead to the formation of intense flux tubes.

New magnetic flux appears in the atmosphere as a bundle of rising flux loops (see, e.g., Zwaan, 1978, 1985). Once a flux loop has emerged, the radiative loss from its photospheric parts is not balanced by convective exchange of heat, because convection is impeded in the magnetic field. Hence the photospheric parts of a newly emerged flux loop tend to cool,

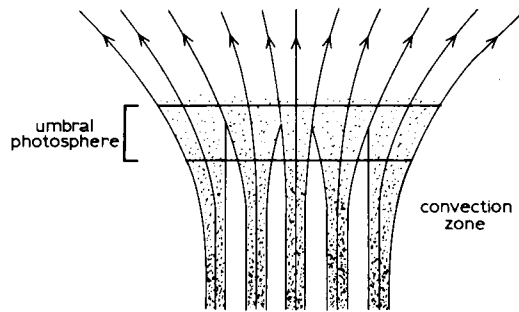


Figure 7-6. Composite model for a sunspot umbra. In the convection zone, the constituting flux tubes (gray) are separated by field-free plasma.

resulting in the slumping of the internal gas. The slump starts a convective downflow, which in turn promotes cooling at greater depths. As the temperature decreases the gas pressure also decreases, and the flux tube is compressed until the increased magnetic pressure $B^2/(2\mu)$ balances the gas-pressure difference between the interior of the tube and the exterior. This process of “convective collapse” ends in an equilibrium state with an intense magnetic field.

The rising-loop model for emergent flux may describe the growth of sunspots by coalescence of smaller elements if the tubes, surfacing separately, join into thicker strands further down. The coalescence is attributed to the buoyancy of the flux tubes in the top of the convection zone (Section III.A.1), and to some process deep in the convection zone that keeps the flux tubes constituting the sunspot together during the lifetime of the sunspot.

In the formation of intense flux tubes the convective collapse appears to be a basic process and, consequently, several authors have investigated the convective instability of slender flux tubes (see Spruit, 1981 for review and references). The mechanism is quite similar to that which occurs in ordinary convection without a magnetic field. In a flux tube, however, the magnetic field impedes the flow of gas around a moving element of gas, so that

the convective instability of a flux tube requires that the superadiabatic coefficient

$$\delta = \frac{d \ln T}{d \ln P} - \left(1 - \frac{1}{\gamma}\right) \quad (7-29)$$

be larger than some positive critical value that depends on the field strength and gas pressure (γ is the ratio of specific heats C_p/C_v). In the field-free case, Schwarzschild’s criterion $\delta > 0$ is sufficient. Note that the convective instability may work both ways: an initial downflow leads to contraction of the flux tube, as described above, while an initial upflow makes the magnetic field weaker, eventually dispersing the field.

Because the superadiabaticity δ varies rapidly in the top layers of a model of the convection zone, the instability condition for an entire flux-tube model has to be obtained numerically. For the Sun it is found that flux tubes with $B > B_c \approx 0.13 \text{ Wb m}^{-2}$ are convectively stable, and, hence, field strengths should usually be greater than this value. This is reassuring, because the measured field strengths of magnetic structures in the solar photosphere are around this critical value, or higher. Weaker flux tubes are expected to collapse, if there is an initial downflow. Spruit (1979) calculated the structure of flux tubes in the equilibrium state after collapse. His calculations reveal that the effect of collapse is limited to the strongly superadiabatic top layers of the convection zone, i.e., to the first 1000 to 2000 km beneath the photosphere (see also van Ballegoijen, 1984). It was also found that, after the collapse, the magnetic field strength in the photosphere is virtually independent of the initial state of the flux tube, with a value of $B \approx 0.18 \text{ Wb m}^{-2}$.

A numerical simulation by Nordlund (1983) has demonstrated how an initially weak, homogeneous, and vertical magnetic field becomes concentrated in the intergranular lanes to high field strength, in a model with granular convection. In Nordlund’s model of the evolution of three-dimensional magneto-convection,

the physics of gas dynamics, MHD, and radiative transport are treated in a consistent manner, and the “convective collapse” of the magnetic structure is a natural consequence. A particularly important aspect of the numerical simulation is that it extends over ten pressure scale heights in the photosphere and the top of the convection zone.

The evolution of the magnetic field and of the granulation is found to proceed as follows in this model: within a fraction of the granular lifetime the magnetic flux is carried into the intergranular lanes. With increasing concentration of the field, the Lorentz force becomes more important, and it tends to retard the concentration. At the same time, however, the heat supply to the magnetic structure by convection is hampered, and the photospheric gas cools and descends. The magnetic structure thus contracts to even higher field strength. After a short time a quasi-stationary state is reached. The magnetic field is concentrated in the intergranular lanes at a field strength $B \approx 0.15 \text{ Wb m}^{-2}$. In the granular updrafts, the plasma is almost field-free.

It is found that the development of the granulation in the presence of a magnetic field is similar to that in the absence of such a field. Because the flow is turbulent, the pattern of both velocity field and magnetic field is perpetually changing. No magnetic flux is destroyed, however; the flux is merely shuffled in response to the evolution of the granules in the field-free areas.

Nordlund’s numerical simulation leads to an intricate magnetic fine structure, but not to individual flux tubes. This may be due to Nordlund’s initial condition of a weak, homogeneous, and vertical magnetic field. Observations indicate, however, that the magnetic field enters the photosphere from below as systems of discrete magnetic loops, whose feet may consist of isolated flux tubes rooted deep in the convection zone.

The extreme concentration of the magnetic field results from the radiative cooling in the photosphere, and the high superadiabaticity of the top layers of the convection zone. Two conclusions follow. First, similar results are expected for other stars with vigorously convective envelopes, even though Nordlund’s investigation has been carried out for the solar case. Second, Nordlund’s results cannot be generalized to describe the behavior of magnetic flux tubes in deep parts of convection zones (see Section II.B), since there the superadiabaticity is extremely small and there are no large radiative losses.

III.A.3. MAGNETIC STRUCTURE AND HEAT FLOW

As heat flows outwards through the convection zone and photosphere, dark spots impede the flow, while faculae enhance it. First we consider the effects caused by dark spots. Two groups of questions come to mind:

- (1) What happens to the “missing radiative flux” over sunspot areas? Why is no conspicuous bright ring visible around a sunspot, and why do starspots show up so well as a rotational modulation in the radiative fluxes from BY Dra stars (Chapters 2.VII and 3.VII)? Is the missing heat flux redistributed simultaneously over a very large area, or is it stored in the stellar envelope?
- (2) What is the effect of a large spot on the global stellar parameters: the total luminosity L , the radius R , and the effective temperature T_{eff} of the unspotted surface?

Two properties of convective envelopes determine the transfer of obstructed heat (Spruit, 1976, 1977). First, the turbulent heat conductivity increases strongly with increasing depth. Hence a temperature disturbance at some depth propagates over large depths and

large horizontal distances. Second, the capacity of the heat reservoir of a thick convective envelope is enormous, which favors temporary storage of the heat that is prevented from leaving the star in the direct way.

The thermal response of a star to a blocking of radiative flux is a time-dependent problem (Spruit, 1982; Foukal et al., 1983). There are two time scales. That part of the blocked flux which reappears in the atmosphere without temporary storage reaches the stellar surface on the *diffusive time scale*

$$\tau_d = d^2/\eta_t \quad , \quad (7-30)$$

where d is the depth of the convective layer involved in the diffusion of blocked heat and η_t is the turbulent diffusivity, $\eta_t \approx 1/3 lv$, where l is the mixing length and v is the convective velocity. If heat flow is stopped by an object in the shallow, strongly superadiabatic layers, which are within a few scale heights below the photosphere, only these layers are involved in the redirection of the flux. In such a case, the diffusive time scale amounts to several days for the Sun. However, it is likely that real starspots block the heat flow many scale heights below the photosphere, and then all depths of the convection zone participate in the redirection of the flux. Inserting the total depth $d = D$ of the convection zone into Equation 7-30, a diffusive time scale of about one year is found for the Sun, which is longer than the lifetime of individual sunspots.

The second time scale involved in the process is the *thermal time scale of the convective envelope*: this is the time span that the convective envelope needs to reach a new thermal equilibrium

$$\tau_{CE} = U_{CE}/L \quad , \quad (7-31)$$

where U_{CE} is the thermal energy content of the convective envelope and L is the stellar luminosity. This thermal time scale is much longer than the diffusive time scale: $\tau_{CE} \approx 1 \times 10^5$ years for the solar convection zone.

A simple description of the time-dependent response to an obstruction to the heat flow may be obtained by treating the spots as cylinders that reach down to a depth d into the convection zone and block a fraction f of the surface. Suppose that the cylinders are suddenly inserted at $t = t_0$, and that the blocking fraction is constant over more than the thermal time scale τ_{CE} . For a time span $(t-t_0) \ll \tau_D$, the luminosity is thus reduced to $L = (1-f)L_0$ (see Figure 7-7). After a time interval $t \approx \tau_d = d^2/\eta$, a fraction of the blocked flux reappears and L increases again, until after a time $\tau_D \approx D^2/\eta$ (where D is again the depth of the convection zone) the luminosity stabilizes for the long time span to $t-t_0$ in the range $\tau_D < t-t_0 \ll \tau_{CE}$ at a value:

$$L = [1 - (1-\alpha)f] L_0 \quad (7-32)$$

The fraction α of the blocked flux appearing in the atmosphere after a time $t-t_0 \geq \tau_D$ depends on the ratio of the blocking depth d to the pressure scale height H_0 at the top of the convection zone. Spruit (1982) estimates, as an order of magnitude:

$$\alpha = [1 + d/(3H_0)]^{-2} \quad (7-33)$$

If spots extend further downwards than the thin, superadiabatic top layer (i.e., deeper than about 2000 km in the Sun), α is smaller than 0.01. Most models of sunspots reach much deeper.

During the quasi-stable equilibrium period $t-t_0 \ll \tau_{CE}$, virtually all of the blocked flux is stored in the deep parts of the convection zone. Since the radiative core and, hence, the rate of energy generation are not affected by thermal disturbances in the convective envelope, the deep part of the convection zone is slowly heated. During this period, nothing changes in the unspotted part of the superadiabatic top layer or the atmosphere. The radiative flux density remains constant, except for the small flux fraction αf , and the flux spectrum remains the same. In the spectral regions where the spots

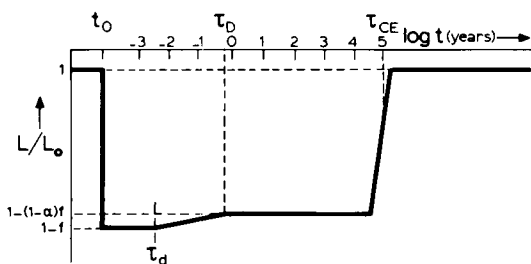


Figure 7-7. Variation of the stellar luminosity (schematic) after spots covering a fraction f of the surface have been switched on at $t = t_0$. The return to the original luminosity occurs on two time scales τ_D and τ_{CE} which are explained in the text (after Spruit, 1982).

may be considered as black, the color indices of the star as a whole do not change. The gradual heating expands the convective envelope, but for $t - t_0 \ll \tau_{CE}$ the change in stellar radius is too small to have observable effects.

After an interval of about the thermal time scale τ_{CE} , the backwarming process has made the convective envelope ready to settle into a final equilibrium. For $t - t_0 \gg \tau_{CE}$ the total luminosity is returned to the original level $L = L_0$ (see Figure 7-7), corresponding to the steady energy production in the stellar core. The superadiabatic layer and the photosphere in the unspotted parts now transmit the total heat flow L_0 through the area fraction $(1-f)$, because the surface temperature is higher and the radius is slightly larger than in the case without spots. Hence, the star has moved to the left in the Hertzsprung-Russell diagram: a star of the mass and luminosity of a main-sequence star now appears as a subluminescent dwarf. As an example, Spruit (1982) considered a star of mass and luminosity corresponding to a main-sequence star of spectral type G5, covered for 50% with spots. Such an object appears photometrically as a G0 star, with its radius increased by 6%.

Since the assumption of a constant spot coverage over more than the thermal time scale

is not realistic, it is desirable to consider time-dependent effects. If all spots were removed at any instant, the heat stored would be released as a flux excess to the steady luminosity L_0 . The luminosity of the star would return slowly to L_0 on time scales ranging from the diffusive time scale to the thermal time scale τ_{CE} . The structure of a star with a spot coverage that varies with time according to the function $f(t)$ is determined mainly by the mean coverage $\langle f(t) \rangle_{\tau_{CE}}$, averaged over one thermal time scale τ_{CE} . This quantity does not affect the total luminosity; but it does influence the surface temperature and the radius.

Any fluctuations in the coverage, $\delta f(t)$, that occur on time scales much shorter than τ_{CE} cause instantaneous fluctuations in the luminosity given by $\delta L(t)/L_0 \approx -\delta f(t)$. If the spots were black, there would be no variations in color associated with the luminosity variations $\delta L(t)$. However, the radiative flux from real spots, particularly from the penumbrae, does contribute to the average flux spectrum of the spotted star in a sense which makes the star redder. This effect thus reduces the tendency for the star to become bluer as its convective envelope adjusts to the average covering $\langle f(t) \rangle_{\tau_{CE}}$. To our knowledge, no quantitative study incorporating both effects has yet been published.

Any bright faculae or network elements in a stellar photosphere cause effects opposite to those produced by spots. There is another difference, however: whereas the spots block the heat flux well below the superadiabatic top layer of the convective envelope, the extra heat loss in faculae occurs mainly in the thin superadiabatic top layer. Hence the fraction α for faculae is much larger than for spots (see Equation 7-33). This implies that a large fraction of the extra flux radiated by a small bright element is provided by the reduced radiative flux through the element's immediate environment, which causes a darker ring around the element (Spruit, 1977). No detailed study of the time-

dependent effect of faculae on stellar luminosity has yet been published. Precise solar irradiance measurements from satellites have indicated that many of the observed variations in the "solar constant" are due to sunspots. However, prominent residuals that cannot be explained by spots correlate well with the bright faculae in active regions, as is indicated by correlations with the solar radio flux at 10.7 cm (Hudson and Willson, 1981).

In summary, a study of diffusive heat flow around dark objects in a model stellar convective envelope explains (1) the absence of bright rings around sunspots and (2) the conspicuous brightness variation of spotted stars, which takes place with little color variation. The theory of the thermal adjustment of the convective envelope to the backwarming caused by dark spots predicts a somewhat higher effective temperature of the unspotted parts of the atmosphere.

III.A.4. STARSPOTS AND STELLAR FACULAE

Insight gained from the theoretical interpretation of the observed solar magnetic structure suggests that stellar magnetic structure will be inhomogeneous in a manner analogous to the solar magnetic field, provided that the star possesses a convective envelope that is several pressure scale heights thick. Because of the high magnetic Reynolds number R_m (Equation 7-9) in convection zones, the magnetic field is expected to be concentrated in strands whose field strengths are estimated to be of the order of the equipartition field strength B_{eq} (Equation 7-11) in the deep part of the convection zone. In the top layers the field concentration is more extreme: the convective collapse, which is the consequence of the strongly superadiabatic temperature gradient and the radiative losses through the photosphere (Section III.A.2) nearly evacuates the tops of the flux tubes, and so increases the field strength far above the equipartition strength.

We thus infer that the photospheres of stars with thick convective envelopes are characterized by two components:

- (1) magnetic flux tubes of various sizes, or bundles of flux tubes, in which the field strengths are relatively large, larger than the local equipartition strength B_{eq} (Equation 7-11), and
- (2) virtually field-free medium between the flux tubes.

As a first step towards two-component modeling of photospheres of late-type stars, we now derive scaling properties of the magnetic field strength B and of the sizes, shapes, and thermodynamic properties of (bundles of) flux tubes of different magnetic flux. The photospheric field strength B^* in small-scale magnetic structures that may be described by the slender flux-tube approximation, with a Wilson depression Δz of about one pressure scale height H_p , is approximately:

$$B^* = B_p (\tau_5 = 1) \equiv [2\mu P(\tau_5 = 1)]^{1/2} \quad (7-34)$$

Here τ_5 is the monochromatic optical depth at $\lambda = 500$ nm, and P is the gas pressure in the field-free atmosphere. The level $\tau_5 = 1.0$ corresponds closely to the level $\tau_{Ross} = 1.0$ (τ_{Ross} is based on the Rosseland mean opacity), lying just above the top of the convection zone. For the Sun, $B^* = 0.180 \text{ Wb m}^{-2}$ (1800 gauss) is a representative mean value for field strengths actually measured in facular elements (between 0.13 and 0.20 Wb m^{-2}) and in small dark pores (between 0.20 and 0.23 Wb m^{-2}).

Field strengths calculated from Equation 7-34, using pressures P listed in model atmospheres published by Carbon and Gingerich (1969), are shown in Figure 7-8. From this grid of models, values of B^* for main-sequence and giant stars may be found by interpolation and some extrapolation. These values are displayed in Figure 7-8 as well. Along the main sequence,

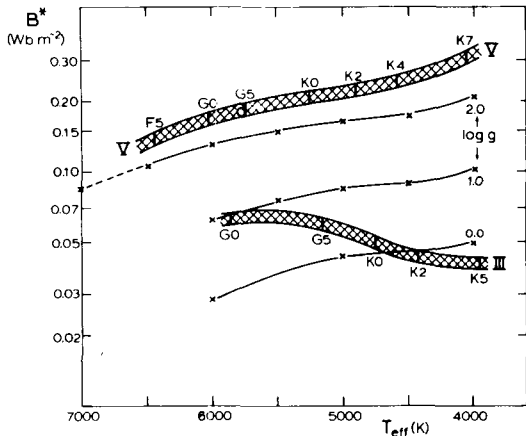


Figure 7-8. The typical photospheric field strength B^* (in Wb m^{-2} , or 10^4 g) for small-scale flux tubes in stellar photospheres (see Equation 7-34), as a function of effective temperature T_{eff} and surface gravity g (m s^{-2}), as computed from the grid of models published by Carbon and Gingerich (1969). The bands indicate the relations for dwarfs (V) and giants (III).

the predicted field strengths range from $B^* = 0.14 \text{ Wb m}^{-2}$ in the mid F-type stars to $B^* = 0.32 \text{ Wb m}^{-2}$ in late K-type dwarfs. For early G-type giants, B^* is between 0.06 and 0.07 Wb m^{-2} , decreasing to $B^* = 0.04 \text{ Wb m}^{-2}$ at K5 III.

As discussed in Section III.A.1, the field lines of photospheric flux tubes fan outward with increasing height, in a way analogous to the field lines near the end of a vertical solenoid. The fanning sets are progressively deeper in the atmosphere with increasing flux tube-radius R , so that large magnetic elements appear as umbrae, surrounded by penumbrae with a strongly inclined magnetic field. The measure of the fanning in the photosphere depends on the ratio R/H_p of the photospheric radius R of the flux bundle to the pressure scale height H_p . For the Sun, the division between dark pores without penumbrae and spots with penumbrae occurs around $R(\tau_5 = 1)/H_p(\tau_5 = 1) = 13$. A similar value of $R/H_p = 13$ may apply to the pore-spot transition in all stars with convective

envelopes, since the effect is one of the results of magnetostatic equilibrium.

The transition from small flux tubes which appear bright in the photosphere to large flux tubes that appear dark depends on two ratios: (1) photospheric tube radius $R(\tau_5 = 1)$ to Wilson depression $\Delta z(\tau_5 = 1)$, and (2) photospheric tube radius $R(\tau_5 = 1)$ to photon mean free path $l_{\text{Ross}}(\tau_5 = 1)$ (Spruit, 1976, 1977).

From the above considerations, it follows that the geometrical and thermodynamic structure of the flux tubes or flux-tube bundles depends on three length scales: (1) the photospheric flux-tube radius $R(\tau_5 = 1)$, (2) the Wilson depression $\Delta z(\tau_5 = 1)$, and (3) the mean free path of photons $l_{\text{Ross}}(\tau_5 = 1)$. Below, we argue that the structural parameters $\Delta z(\tau_5 = 1)$ and $l_{\text{Ross}}(\tau_5 = 1)$, if normalized to the pressure scale height $H_p(\tau_5 = 1)$, depend only slightly on stellar effective temperature T_{eff} and surface gravity g .

Spruit (1977) found that values of the relative Wilson depression $\Delta z/H_p$ lying between 0.6 and 1.3 yield fits to observed properties of solar facular elements and small pores (see Section III.A.1). From these results, and from a consideration of the efficiency of the convective collapse (Section III.A.2), we estimate that the ratio $\Delta z/H_p$ for thin flux tubes in cool main-sequence and giant stars may lie between 0.5 (for the smallest tubes) and 2.0.

The relative photon mean free path $l_{\text{Ross}}(\tau_5 = 1)/H_p(\tau_5 = 1)$ may be estimated from the Carbon-Gingerich (1969) models and Kurucz's (1979) Rosseland opacity tables. For main-sequence stars ranging from F5 to M0, and for giants from G0 III to K5 III, the ratio l_{Ross}/H_p differs by less than a factor 2 from the solar value of 0.22. So the dependence of $l_{\text{Ross}}(\tau_5 = 1)$ on g and T_{eff} is almost removed by the normalization to H_p . Moreover, the dependence of $l_{\text{Ross}}(\tau_5 = 1)$ on metal abundance is not very strong: for a G-type dwarf

with $T_{\text{eff}} = 5500$ K, l_{Ross} drops from 117 km (solar metal abundance) to 53 km (metal abundance reduced by factor 100).

Thus it appears that the main structural parameter is R/H_p , which is determined by the magnetic flux Φ within the flux tube or flux-tube bundle. Because of this, we argue that the atmospheres of stars with convective envelopes are occupied by a hierarchy of magnetic elements similar to the hierarchy observed in the Sun (Zwaan, 1978, 1981a), the star-to-star differences being the differences in the total magnetic flux present in the atmosphere. Among stars with different effective temperature and surface gravity, the photospheric radii of the elements of this hierarchy with given properties are expected to scale roughly in proportion to the pressure scale height H_p . The relative Wilson depression $\Delta z/H_p$ depends on R/H_p ; the normalization of the structural parameters by H_p effectively eliminates the dependence on the photon mean free path l_{Ross} . By analogy with the Sun we then conjecture that the flux tubes in any cool star form a hierarchy consisting of four classes (the properties are summarized in Table 7-1):

- (i) *Network elements and stellar faculae:* The thinnest flux tubes will appear bright in the photospheric continuum over their entire cross sections. Although such elements are surrounded by a darker ring (Section III.A.3), the radiative flux integrated over such an element and the surrounding dark ring is expected to be larger than the radiative flux from an equal area of field-free photosphere. Because the lateral influx of radiation decreases with increasing flux-tube radius, the Wilson depression Δz and the magnetic field strength both increase with increasing radius. From a comparison between Spruit's (1976, 1977) models and solar observational data, we estimate that (Equation 7-34; Figure 7-8) for large stellar faculae $B \approx$

B^* . The field strength is smaller in the thinner flux tubes.

- (ii) *Transition from bright to dark features — micropores or magnetic knots:* At a sufficiently large flux-tube radius, around $R(\tau_5 = 1) \approx 2.0 H_p$, the interior of a flux tube is expected to consist of a cool core that is darker than the field-free photosphere, surrounded by a hot cylindrical shell that is brighter than the field-free photosphere. Observed at sufficient angular resolution, such flux tubes would appear as "micropores," perhaps similar to those observed by Dunn and Zirker (1973) at the center of the solar disk. The total radiative flux integrated over such a magnetic element plus the surrounding darker ring would be approximately equal to the radiative flux of an equal area of the field-free photosphere. In other words, unless they are spatially resolved these elements would be inconspicuous in white light. They would just appear as magnetic field concentrations, hence the term "magnetic knot." For the magnetic field strength we estimate $B \approx B^*$. On the Sun, knots appear prominent as bright chromospheric faculae in CaII H and K.
- (iii) *Dark pores:* Any flux tube with a radius satisfying $3.5 \leq R(\tau_5 = 1)/H_p \leq 13$ would probably show up as a dark pore, with a nearly vertical magnetic field. Because the lateral influx of radiation is smaller, the internal temperatures are lower and hence the Wilson depression is larger than in faculae and magnetic knots. Solar observations suggest for pores $\Delta z \approx 2 H_p$, with magnetic field strengths in the range $1.1 B^* \leq B \leq 1.3 B^*$.
- (iv) *Starspots—umbrae surrounded by penumbrae:* Large magnetic elements in stellar photospheres would appear as

Table 7-1
Properties of Magnetic Elements in Photospheres of Stars With Convective Envelopes

| | Faculae and Network Elements | Magnetic Knots or Micropores | Pores | Starspots |
|---------------------------------------|-----------------------------------|---|---------------------------------------|---|
| Appearance at high angular resolution | bright, surrounded by dark ring | dark core with bright ring, surrounded by dark ring | dark, B vertical | dark umbra (B vertical), surrounded by penumbra (B strongly inclined) |
| Overall appearance in white light | bright | inconspicuous | dark | dark |
| Size | $R \lesssim 1.5 H_p$ | $R \approx 2 H_p$ | $3.5 H_p \lesssim R \lesssim 13 H_p$ | $R \gtrsim 13 H_p$ |
| Magnetic field strength | $0.5 B^* \lesssim B \lesssim B^*$ | $B \approx B^*$ | $1.1 B^* \lesssim B \lesssim 1.3 B^*$ | $1.4 B^* \lesssim B_u \lesssim 1.7 B^*$ |

Notation: R : photospheric radius at $\tau_5 = 1$
 H_p : pressure scale height
 B : magnetic field strength
 B* : characteristic field strength, Figure 7-8
 B_u : umbral field strength

dark umbrae with a nearly vertical magnetic field, surrounded by penumbrae with a strongly inclined field. Observations of the Sun suggest as a critical photospheric radius for the formation of a penumbra $R \approx 13 H_p$. In sunspots, Wilson depressions are observed to $\Delta z \approx 4 H_p$. If a similar value obtains in other stars, the field strengths, B_u , in starspot umbrae will lie in the range $1.4 B^* \lesssim B_u \lesssim 1.7 B^*$.

Table 7-1 summarizes the predicted properties of magnetic elements in stellar photospheres.

The properties of the individual magnetic elements depend on the classical parameters T_{eff} , g, and metal abundance. In this section we have argued that these dependencies are partly, perhaps largely, removed by scaling the

radius R and the Wilson depression Δz by the pressure scale height H_p . The “filling factor” of magnetic structure in the photosphere, and hence the “level of activity,” depend on the “dynamo efficiency,” in which parameters other than the classical parameters are important (Section IV).

Note that the scaling of solar magnetic structure to stars, as summarized in Table 7-1, probably fails in the very active stars with large magnetic filling factors. In such photospheres, the magnetic structure can no longer be considered as a collection of distinct elements of known characteristics. For instance, sunspots have no room to unfurl their penumbrae in closely packed magnetic structure. More fundamentally, the interaction between magnetic field and convection may be different in cases in which the outer convection zone is largely blocked by the field.

Since starspots contribute little to the stellar flux spectrum in the visible, we expect that the magnetic signature of the visible spectrum is largely determined by the bright magnetic elements: the faculae and the knots. The observable magnetic field would be characterized by the filling factor of the bright magnetic structure and a mean field strength $\langle B \rangle \approx B^*$. This point should be remembered when observations of stellar field strengths and filling factors are considered (Chapter 2.VII).

III.A.5. STARS WITHOUT CONVECTIVE ENVELOPES

The intricate and time-dependent magnetic structure that is directly observed in the solar atmosphere, and that is inferred to be present in other late-type stellar atmospheres, is attributed to the interaction of magnetic field, convection, and rotation in the stellar envelope at high magnetic Reynolds number (Sections II.B and II.C). This interpretation hinges on the presence of vigorous convection in the envelope immediately below the atmosphere. Magnetic field is concentrated in strands in convection zones, and within magnetic structure the temperature gradient may differ from that in the ambient medium. The gas pressure may vary in horizontal planes. The theory of dynamo action requires convection.

In stars of spectral type A and earlier, there are no observational or theoretical indications for vigorous convection in the envelope. Hence there are no convective velocities to concentrate and reorganize magnetic fields, and there is no known mechanism to set up temperature gradients that depart strongly from the radiative-equilibrium gradient. There is no reason to expect temperature gradients or pressure gradients with an appreciable horizontal component. If magnetic field is present in an envelope in radiative equilibrium, the field strength is expected to vary rather smoothly over the stellar surface. If the field were weak, it would adjust to any large-scale flow that might be present. If the field were strong (e.g., $B > 0.05$ Wb

m^{-2} for an A4 V star), it must be virtually force-free throughout the atmosphere, and static over periods comparable to the evolutionary time scale of the star. These considerations apparently apply to the magnetic Ap stars, which have strong and long-lived magnetic fields of a simple structure, which is usually described as an eccentric magnetic dipole or as the sum of a strong dipole field and a modest quadrupole field (see Wolff, 1983).

Figure 7-9 shows that the separation between the magnetic Ap stars, with their simple and vir-

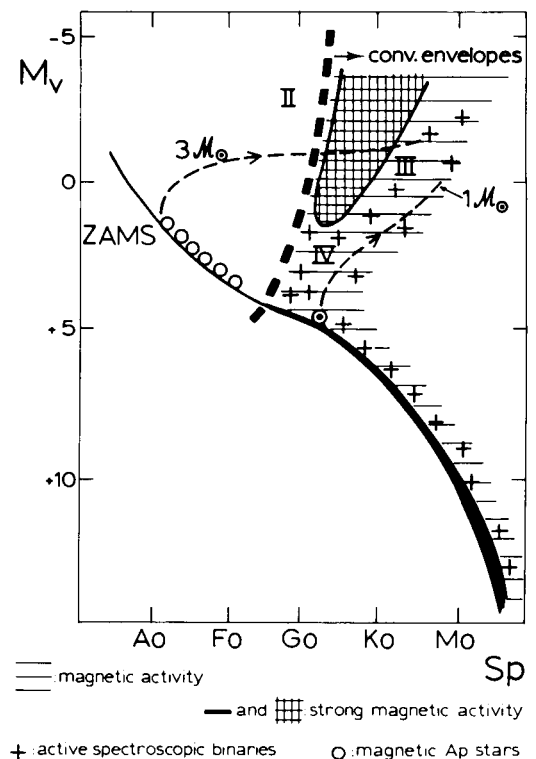


Figure 7-9. Distribution of magnetically active stars over the Hertzsprung-Russell Diagram (schematic). Magnetic activity is found in the region of stars with convective envelopes, which is bounded to the left by the fat broken line. Note that the magnetic Ap stars are found in stars without appreciable convection in their envelopes. The thin broken lines approximate evolutionary tracks for stars of 1 and 3 solar masses.

tually time-independent structure, and the magnetically active F-, G-, and K-type stars, with their complex and time-dependent structure, coincides in the Hertzsprung-Russell diagram with the line which separates stars without appreciable convection in their envelopes from those with vigorous convection. This illustrates the powerful effect of convection on stellar magnetic structure (Zwaan, 1977, 1981a).

III.B. CHROMOSPHERIC AND CORONAL EFFECTS

The topology and evolution of chromospheric and coronal magnetic fields are controlled by the structure of the field in the photosphere. The marked decrease in gas pressure in the chromosphere implies that the magnetic field spreads out to occupy a much larger fraction of the surface than it does in the photosphere. The entire corona is pervaded by magnetic field. Moreover, the decreasing gas pressure promotes the occurrence of various plasma processes associated with the magnetic field, and a large number of intriguing astrophysical phenomena appear. Consequently, the manifestations of stellar magnetic fields are particularly obvious in stellar chromospheres and coronae: this section discusses the theory of these phenomena (see also Spruit 1982, 1983).

III.B.1. MAGNETIC STRUCTURE IN CHROMOSPHERES AND CORONAE

One of the most important factors controlling the structure of magnetic fields in chromospheres and coronae is the exponential decrease of gas pressure with height. To accommodate to the outwardly decreasing pressure, the field in the magnetic elements which are confined to small areas of the deep photosphere fans outwards with increasing height. The fractional area occupied by the magnetic fields (or "filling factor") increases with increasing height, until the individual flux tubes merge. Spruit (1983) estimates the merging height

above the photosphere by

$$h_m \approx 2 H_p \ln (f_p^{-1}) \quad , \quad (7-35)$$

where H_p is the pressure scale height and f_p is the photospheric filling factor, $f_p = \langle B_p \rangle / B_p$, in which $\langle B_p \rangle$ represents the mean magnetic flux density in the photosphere and B_p is the magnetic flux density within a flux tube. The merging height separates the "photospheric regime" of discrete flux tubes from the "coronal regime" where the plasma is everywhere magnetized. Expression 7-35 shows that the merging height h_m depends only weakly on the filling factor: in the quiet solar atmosphere, $h_m \approx 1500$ km [i.e., within the chromosphere], while in solar active regions, $h_m \approx 750$ km.

Another important consequence of the exponentially decreasing gas pressure is that the ratio of the gas pressure to the magnetic pressure,

$$\beta = \frac{2\mu P}{B^2} \quad , \quad (7-36)$$

decreases rapidly with height. In the top of the convection zone, β is of the order unity within flux tubes, and much larger than unity outside the tubes. In the corona, β is much smaller than unity everywhere.

Wherever $\beta \ll 1$ the gas pressure plays an insignificant role in controlling the form of a magnetostatic structure, and hence the magnetic fields tend to become "force free": $(\nabla \times \mathbf{B}) \times \mathbf{B} = 0$. In a force-free state, any electric currents that are present must satisfy $\mathbf{J} = \nu \times \mathbf{B} / \mu$, so that \mathbf{J} will be parallel to \mathbf{B} . If $\mathbf{J} = 0$, the magnetic field is called a "potential field." The observed structure of the low solar corona is often similar to the form of the potential magnetic field computed self-consistently from the observed distribution of magnetic flux in the photosphere (e.g., Levine and Altschuler, 1974). In nearly force-free conditions, small relative variations in magnetic field strength can balance large relative variations in gas pressure or dynamic pressure.

The intricate structure of the solar corona, which is apparent in X-ray or EUV pictures, is made possible by the properties of heat transport in dilute, strongly magnetized plasmas. The thermal conductivity perpendicular to the magnetic field lines is strongly reduced in comparison with the conductivity parallel to the field (see Priest, 1984, p. 85), and plasma flows generally occur parallel to the field lines. Moreover, the corona is optically thin to almost all radiation, and thus there is little radiative heat exchange between different parts of the corona. Therefore, since plasma flow, conduction, and radiative transfer dominate the energy flow in most parts of the corona, flux loops in the corona tend to be thermally isolated from each other. The temperatures in neighboring flux loops may thus differ considerably.

The intricate structure of the solar corona implies that the nonthermal heating rate varies markedly from one magnetic loop to another. Once a part of a magnetic loop is heated, thermal conduction by electrons efficiently smoothes the temperature distribution along the loop. As a consequence, heat flows to the footpoints of the loop, where the temperature rises. The scale heights of pressure and density increase with the increasing temperature, and matter at the footpoints "evaporates" into the loop. The density in the loop increases, and consequently so does the heat loss from the loop by radiation. Eventually, if the heating rate is steady, a balance between heating and loss rate is reached and maintained (see Section III.B.2).

In the chromosphere the ratio β , though smaller than unity, is larger than it is in the corona. Moreover, the opacity is higher, and hence the thermal insulation between neighboring bundles of field lines is less effective than in the corona. Nevertheless, large lateral variations in chromospheric pressure and density still result from uneven heating and from violent magnetohydrodynamical processes. Spruit (1981) pointed out that even without motion, any small tem-

perature variation that extends over several pressure scale heights can lead to large pressure variations in the chromosphere. For example, consider two chromospheric columns (labeled 1 and 2) which differ in temperature by a height-independent factor $1 + \epsilon$ ($0 < \epsilon \ll 1$), i.e.,

$$T_2(h) = (1 + \epsilon) T_1(h) \quad (7-37)$$

If hydrostatic equilibrium obtains, the gas pressures in the two columns are related by

$$\ln \frac{P_2(h)}{P_1(h)} = \epsilon n(h) \quad , \quad (7-38)$$

where $n(h)$ is the number of scale heights above $h = 0$. Even when ϵ is quite small, the pressure ratio becomes large because the chromosphere spans about 10 pressure scale heights.

Figure 7-10 illustrates some of the concepts of magnetic structure in the atmosphere of a star with a convective envelope. In the "flux-tube regime," i.e., in the convective envelope and the photosphere, only a fraction of the

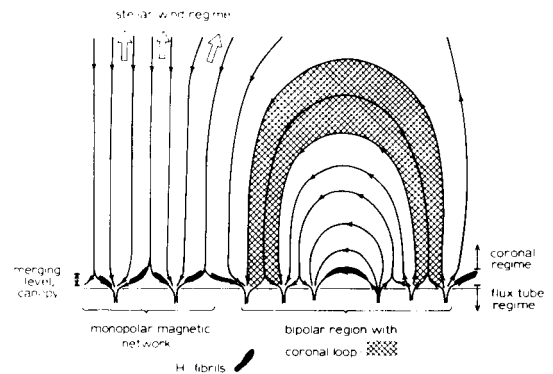


Figure 7-10. Illustrating concepts of the magnetic structure in atmospheres of stars with convective envelopes, showing the field rooted in strong flux tubes in the convection zone. The "flux-tube regime" of discrete flux tubes, separated by nearly field-free plasma, extends upward through the photosphere and into the low chromosphere. In the upper chromosphere the flux tubes merge, creating the magnetic canopy. The corona is pervaded by magnetic field. The stellar wind flows along the magnetic field wherever it is open to interstellar space.

plasma is filled with intense flux tubes. Here, the pressure gradient ∇P is always important in the force-balance equation (Equation 7-1) and in the magnetostatic equation (Equation 7-12 or 7-27). On the other hand, the magnetic fields of individual flux tubes have merged in the “coronal regime,” and the whole corona is pervaded by magnetic field. There the ratio β is much smaller than unity, the magnetic field is nearly force-free, and the gas pressure gradient is of secondary importance.

The topology of the magnetic field in stellar chromospheres and coronae may be extremely complex. Studies of the solar coronal field structure suggest that an approximate representation may be obtained by adopting a potential or a force-free configuration, whose structure at any time is determined uniquely by the instantaneous distribution on a spherical surface at the base of the corona (e.g., Bogdan, 1986). Since this distribution is itself inhomogeneous, the coronal field is complex. Moreover, convective motions tend to “shuffle” and “buffet” the boundary fields, inducing nonpotential structures and metastable configurations in the corona (e.g., Parker 1983; see also van Ballegooijen, 1985). These may give rise to flares, coronal mass ejections, and other episodic, violent, coronal processes.

The interaction between the coronal field and any stellar wind which may be present also tends to produce nonpotential fields. While studies of the Sun show us what may happen in late-type main-sequence stars having hot coronae and low mass-loss rates, it is likely that significantly different processes occur in the coronae and chromospheres of late-type giants and supergiants with extended chromospheres and massive, cool, stellar winds.

Because reconnection occurs, the footpoints of any coronal loop need not correspond to single flux tubes in the photosphere. Most coronal loops are likely to consist of field lines passing through several different photospheric flux tubes. Not all coronal field lines are rooted

to the photosphere at both ends: part of the magnetic structure may be “open,” extending into interstellar space. Large areas with open structure correspond to solar coronal holes (Zirker, 1977, 1981). Indeed, beyond some altitude (about 2.5 solar radii for the Sun) there can be no steady closed field lines connected to the photosphere — all field lines are drawn out in an enormous spiral by the combined action of solar rotation and solar wind.

The transition from the “flux tube regime” to the “coronal regime” may generally occur in the chromosphere. Here, the field lines bend over from a nearly vertical orientation in the photospheric flux tubes to lie horizontally at the merging level. The slender flux-tube approximation, which may describe small magnetic elements in the photosphere and convection zone, must break down in the chromosphere.

In the low chromosphere, enhanced emission in the cores of the CaII H and K and MgII h and k resonance lines originates in the flux tubes. The observed close correspondence between patches of enhanced CaII H and K emission and patches of magnetic flux (Leighton, 1959; Howard, 1959) suggests that the radiative flux density in the CaII H and K line cores may be regarded as a measure of the magnetic flux density itself (outside sunspots). Indeed, a tight relation between CaII K core brightness and magnetic flux density has been established from observations of unresolved solar network elements by Skumanich, Smythe, and Frazier (1975).

At the merging level the magnetic field may form a canopy arching over the parts of the photosphere that are nearly nonmagnetic (Giovanelli, 1980b). Above the canopy the gas pressure is much smaller than the magnetic pressure ($\beta \ll 1$), and relatively large variations in gas pressure and density can be accommodated by slight changes in the magnetic field. This property may help to explain the existence of fibrils that stand out in solar spectroheliograms obtained in the H α line core.

Many authors assume that these dark fibrils are aligned along the magnetic field, festooning the canopy.

III.B.2. HEATING IN THE PRESENCE OF MAGNETIC FIELDS

Observations of the Sun (see Jordan, 1981, Chapters 4, 5, 6, and 7) show that there is a strong connection between the presence of magnetic fields and enhanced nonradiative heating throughout the chromosphere and corona. The observations described in this volume in Chapters 2, 3, and 4 also provide circumstantial evidence that magnetic fields play an important role in nonradiative heating in most cool stars. Indeed, there is a currently widely held view that electrodynamic heating processes are central to the formation and maintenance of chromospheres, coronae, and winds in all cool stars.

At first sight, the theory of stellar atmospheric heating in the presence of magnetic fields involves a bewildering variety of possible mechanisms which could be acting. This implies that it is difficult to make predictions which can be used as critical tests of hypotheses regarding the mechanisms operating in any particular case. However, much of contemporary solar physics aims at the analysis and validation of magnetic heating theories, and there has been some progress in resolving this problem. Productive cross-fertilization may be expected between this solar work and the wealth of empirical studies of stars.

Because the subject of atmospheric heating in the presence of magnetic fields is of great current interest, there are many up-to-date review articles available (see, e.g., Byrne and Rodono, 1983; Stenflo, 1983; Kuperus et al., 1981), and two comprehensive books have appeared recently (Parker, 1979a; Priest, 1984). In view of these publications, this section is intended as an overview of the problem, serving as a link between earlier material in this book and the general literature. We consider first, as

three distinct processes, the generation, the propagation, and the dissipation of the non-radiative energy in the presence of magnetic fields, and then we attempt to link these parts by means of the concept of "electrodynamic coupling."

An early study of *the generation of nonradiative energy* in the presence of magnetic fields was that of Kulsrud (1955 — see also Kato, 1968), who used Lighthill's method (Chapter 6.IV.D) to investigate the influence of magnetic fields on energy generation by isotropic turbulence. Kulsrud considered two cases, one involving turbulent magnetic fields and the other a constant, uniform field. In both cases, it was found that the magnetic field could enhance the flux of wave energy excited by turbulence. However, just as we have questioned the relevance of applications of Lighthill's method to the generation of purely acoustic waves (cf., Chapter 6.IV.D), we must also question the relevance of Kulsrud's study to the generation of waves in the presence of magnetic fields. Nevertheless, there has been substantial progress in our understanding of magnetic fields and turbulent convection in the atmospheres of cool stars (particularly the Sun), so a re-examination of Kulsrud's study in the light of the new data could be rewarding.

In particular, a thorough analysis of the excitation of waves in an isolated flux tube by interactions with turbulent convection would be valuable; the term "buffeting" has been used frequently to describe this interaction, but existing analyses are rather incomplete (e.g., Hollweg, 1974). The importance of a more complete analysis has been emphasized by the investigation of Heyvaerts and Priest (1984), which suggests that the question of the generation of a nonradiative energy flow cannot be easily separated from questions of propagation and dissipation (see below). A closely related effect is the persistent distortion of atmospheric magnetic fields as a result of "shuffling" or random-walk motions of the photospheric magnetic field (e.g., Parker, 1983). Indeed, we

should recognize that in the conditions encountered in photospheres of cool stars, almost any form of bulk motion of a magnetic region in a direction orthogonal to the field will generate a flow of electrodynamic energy away from the moving region.

The problem of *propagation of magnetohydrodynamic waves* has received a great deal of attention, perhaps because the theory is generally amenable to rather straightforward mathematical analysis. The problem can be developed systematically by starting from the normal-mode analysis of an infinite, uniform, perfectly conducting, fully ionized plasma permeated by a uniform magnetic field. Three kinds of waves exist in this simple case, two magnetosonic waves (fast and slow modes) and the Alfvén wave (e.g., Ferraro and Plumpton, 1966). When additional forces (e.g., gravity, radiation pressure, or Coriolis force) are acting, or when the excited medium is inhomogeneous (in temperature, density, ionization fraction, bulk velocity, or magnetic field), the picture becomes vastly more complicated, with several kinds of waves co-existing in both their fundamental mode and as a large number of overtones. Priest (1984, Chapter 4) provides an introduction to this field of research.

Two properties are of particular importance to stellar atmospheric heating: (i) magnetic fields can channel and focus mechanical energy fluxes (or, equally importantly, disperse and scatter the flux), and (ii) inhomogeneous regions can convert one mode to another. This implies, for example, that a weakly dissipating wave mode may be guided to a remote, inhomogeneous region, where it may be converted to a strongly damped mode, leading to local heating. Despite the large number of theoretical studies of magnetohydrodynamic waves in this field, observations have not as yet provided any clear picture of the nature of MHD waves in the solar atmosphere (except in sunspots — see Thomas, 1981), and there is no

direct evidence at all for MHD waves in other stars.

The *dissipation of an MHD wave* involves the conversion of a part of the mechanical or electromagnetic field energy of the wave into thermal energy. A large number of processes are known to lead to such conversion. For small-amplitude waves, dissipation by viscous damping and Joule heating (Osterbrock, 1961) can be important, although the ion-neutral frictional dissipation mechanism of Piddington (1956) is likely to be more effective in many conditions. The problem of radiative dissipation (e.g., Souffrin, 1966) of MHD waves has not been studied thoroughly, but this dissipation could be important in photospheric layers. Osterbrock's (1961) work suggested that Alfvén (or slow-mode) waves would be heavily damped beneath the photosphere, but would be weakly damped in the chromosphere, and so might carry a substantial energy flow to the corona. Fast-mode waves would dissipate by nonlinear (shock) processes in layers where the Alfvén speed exceeds the sound speed. Osterbrock used weak-shock theory to study this process, while Ulmschneider and Stein (1982) have described a detailed, nonlinear, time-dependent model of the dissipation of fast modes in idealized models of the atmosphere of cool stars.

Alternative dissipative processes in the presence of magnetic fields involve electric current dissipation by classical Ohmic heating or other (nonclassical) means. Up to the present, almost all theoretical studies of these problems in the context of cool stars have been directed towards the interpretation of solar flares (Svestka, 1976; Spicer and Brown, 1981). Far fewer studies (e.g., Levine, 1974; Parker, 1983) have considered similar processes in the context of relatively quiescent solar coronal heating, and only a few tentative steps have been taken to consider the problem in relation to stellar atmospheric heating (e.g., Stencel and Ionson, 1979; Kuperus et al., 1981; Uchida and Sakurai, 1983). The field appears to be ripe for

closer examination, since X-ray and EUV observations (Chapters 2, 3, and 4) now provide some useful constraints on models, although the difficulties that have hindered progress in solar physics (particularly a lack of spatially resolved observations of fundamental properties such as the coronal magnetic field) are even more serious in stellar studies.

A concept which may prove useful in unifying the study of the effects of magnetic fields in stellar atmospheres is that of "electrodynamic coupling." Using ideas which have emerged in studies of the terrestrial ionosphere-magnetosphere (e.g., Spicer, 1981; Volland, 1984), Ionson (1983) has explained the concept as follows (see Figure 7-11): Magnetic fields thread the inner (photospheric) and outer (coronal) parts of a stellar atmosphere. If the parameter β (Expression 7-36) is less than unity in the corona but of order unity or larger in the photosphere and subphotosphere, "mechanical activity" in the inner zone (e.g., convection, differential rotation, oscillation) couples to and energetically maintains the outer atmosphere through various electrodynamic processes, such as Alfvén waves, field-aligned currents, and

coronal resonances. The coupling can be described crudely in terms of an LRC-circuit analogue (Spicer, 1981; Ionson, 1982, 1984), and in a few cases (e.g., Heyvaerts, 1974; Parker, 1983; Heyvaerts and Priest, 1984) rather detailed models have been presented to illustrate specific examples of such coupling. The concept should prove useful in the ongoing systematic study of solar atmospheric heating, and should find increasing application in studies of other stars as well.

III.B.3. MODELS OF CORONAL MAGNETIC LOOPS

It has been recognized for many decades that the form of the solar corona is controlled in large measure by magnetic fields. The *Skylab* mission (1973) provided an abundance of coronal observations made in soft X-rays which reinforce this idea. Moreover, the *Skylab* observations suggest that there are at least two main states in the corona, the one involving bright emitting structures with the appearance of loops, and the other consisting of relatively faint regions, which are termed coronal holes (see Zirker, 1981). The loop-like structures are

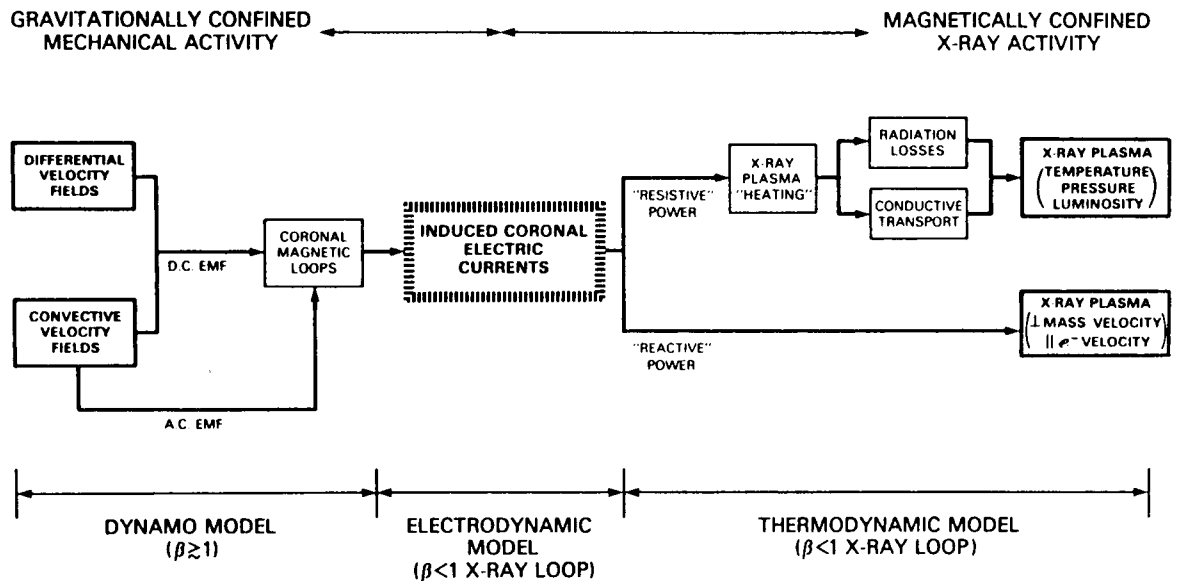


Figure 7-11. Illustrating the global electrodynamic coupling in a stellar atmosphere (Ionson, 1983).

attributed to loop-like configurations in the coronal magnetic field, although direct observational confirmation of this is not yet available. The loops seen in soft X-ray images of the Sun appear to be one of the most important components of the corona, and we may speculate that similar loop-like structures play an important role in the coronae of many other stars. Consequently, there is considerable interest in developing theoretical models for the geometry and energy balance of individual coronal loops.

A simple case involves the study of the energy balance in a static, symmetric loop with a prespecified geometry (Rosner et al., 1978). The energy balance in such a loop arises from the interplay between the (unknown) coronal heating process(es) and the loss of energy by radiation and by conduction parallel to the loop axis. Pressure balance will follow the hydrostatic law (cf., Pye et al., 1978). Rosner et al. (1978) have assumed further that the loop cross-section is constant and that no energy is carried from the ends of the loop by conduction. They have shown that the resulting model is characterized by scaling laws, for example,

$$T_1 \propto (PL)^{1/3} \quad (7-39)$$

and

$$H \propto P^{7/6} L^{-5/6} \quad (7-40)$$

where T_1 is the apex temperature, P the pressure, L the loop length, and H the heating rate.

There is some empirical evidence supporting such scaling laws in the solar corona (Rosner et al., 1978). Related theories have been used to estimate the number of putative loops that could be present in the coronae of other stars observed in soft X-rays (Golub et al., 1982; Golub, 1983). In some cases, however, it is found that the observations can be explained only if the corona is more than 100% filled with loops. Chiuderi et al. (1981) and others have questioned the value of tests of scaling laws,

given the uncertainties in the available data, and other authors (e.g., Foukal, 1976; Hood and Priest, 1979) have suggested that bulk flows and instabilities could play an important role in loop physics. Indeed, observations in $H\alpha$ of cool loops (for which Doppler shifts are readily measured) show that supersonic flows occur widely, and that gross changes in loop visibility can occur in intervals as short as a few minutes.

We conclude, therefore, that while the currently available simple loop models may give some insight into aspects of the structure of coronal loops, more work is required to place the theory on a sound basis. Much of this work should be conducted in the context of solar physics, because there the observational material is more diverse and abundant. However, observations of stellar coronae will be of considerable value in delineating the relationship between coronal structure and other measures of stellar activity, and in providing information on the evolution of global coronal properties on time scales ranging from minutes to billions of years.

III.C. MASS LOSS AND MAGNETIC FIELDS

It is known that there is a close connection between the solar wind and the topology of the magnetic field in and beneath the corona. High-speed streams in the wind (which actually carry less-than-average mass fluxes because of reduced density) appear to emerge from coronal holes, which are relatively cool, low-density parts of the corona characterized by a large-scale unipolar magnetic field (Zirker, 1981). Solar wind also emerges from regions other than holes, but it is believed that the closed, loop-like fields frequently encountered outside holes inhibit the flow of the wind, except when they are evolving rapidly in flares and mass ejections (Wagner, 1984; Axford, 1985). Neugebauer (1983) estimates that the largest fraction of net solar mass loss occurs from

coronal holes. Theoretical studies of the influence of magnetic fields on the solar wind cover such topics as the channelling of flows (Summers, 1983), transfer of energy and momentum in magnetogasdynamic waves (Jacques, 1978), and unidirectional evolution of unstable magnetic fields (Low, 1982).

It is not possible with current technology to detect on stars other than the Sun evidence of any high-velocity, high-temperature, low-density wind which might be present. However, as discussed in Chapters 3 and 4, other kinds of winds are observed on certain stars; they are denser, cooler, and have slower radial velocity than the solar wind. In Chapter 6 it was noted that gasdynamic theories (not involving electrodynamic effects) have not as yet provided a satisfactory explanation of these winds. Models based on thermally driven winds require temperatures higher than have been detected (e.g., Weymann, 1963), models based on radiation pressure face a fundamental problem of the mismatch between the wavelength of the peak of the spectral distribution (near IR) and that of the main absorbers in the wind (UV and EUV spectral lines, and cool dust) (Goldberg, 1979), and models based on shock waves associated with pulsation seem to be relevant only for a subclass of the stars in question (e.g., Mira variables — Willson and Bowen, 1985).

In view of these difficulties, several authors have speculated that magnetic fields may play a key role in the processes which lead to high rates of mass loss in some cool stars. Hartmann and McGregor (1980) presented a crude theory based on the assumption that momentum (and energy) is transferred to the wind by Alfvén waves propagating along radial field lines. They argued that this process would lead to a mass-loss rate of

$$\dot{M} = 10^{-25} M^{-1.5} R^{3.5} (F_5/B_0)^2 M_{\odot} \text{ yr}^{-1} \quad , \quad (7-41)$$

where M and R are the stellar mass and radius in solar units, B_0 is the magnetic field strength

in gauss, and F_5 is the injected wave energy flux in units of $10^5 \text{ erg cm}^{-2} \text{ s}^{-1}$. This theory has been developed further by Hartmann, Dupree, and Raymond (1982), who have constructed model atmospheres and computed line spectra which are similar in several respects to observed spectra of emission lines in cool giant stars. De Campli (1981), Hartmann (1982), and Hartmann, Avrett, and Edwards (1982) have applied a similar theory to the problem of mass loss from T Tauri stars. The speculative nature of these models must be re-emphasized: magnetic fields have not as yet been detected on these stars, and any fields that are present may depart markedly from a radial configuration. Moreover, we have only a rudimentary understanding of the transport and deposition of momentum and energy by hydromagnetic waves in non-equilibrium, strongly inhomogeneous media which characterize these stellar winds.

Mullan (1980) has suggested that instabilities in atmospheric magnetic fields could lead to high rates of mass loss in cool giants. The suggestion is based on a study by Pneuman (1980) of the behavior of fields in bipolar configuration subject to mass outflow. Pneuman showed that the apex of the highest closed field line in a stable system lies at about half the radius of the sonic point in the flow. Mullan suggested that, in stars with atmospheric properties which lead to sonic points lying closer than one stellar radius above the surface, no stable atmospheric field structures can exist. Any magnetic flux emerging into the atmosphere will presumably be ejected, taking with it a substantial mass flux. Again, the speculative character of this proposal should be emphasized. It is possible that some progress might be made on the problem by detailed studies of the “turbulence” and “prominences” seen in 31 Cyg and related stars (see Chapter 3.V.B).

IV. EVOLUTIONARY ASPECTS

During the evolution of a star its main magnetic characteristics are expected to change, because the varying depth of the convective

envelope affects the dynamo action. However, the observations cannot be explained by slow changes on evolutionary time scales only, since stars of similar effective temperature and surface gravity may differ markedly in level of magnetic activity, even if averaged over the activity cycle. Young main-sequence stars tend to be more active than older ones; hence the magnetic structure appears to change on a time scale much shorter than the evolutionary time scale. Moreover, components in close, but well detached, binary systems show a relatively high level of magnetic activity. In this section we discuss how the dynamo action may decrease over times much shorter than the evolutionary time scale because of magnetic braking of stellar rotation, and how a high level of activity may be produced and maintained in binary systems.

IV.A. MAGNETIC BRAKING OF STELLAR ROTATION

The basic idea of magnetic braking was introduced by Schatzman (1962, 1965); for a review we refer to Mestel (1984). Any ionized matter moving out from the star is forced to flow parallel to the magnetic field (see the discussion of Equation 7-7), and so the plasma flow and the magnetic field interact with each other. If the kinetic energy of the flow is less than the magnetic energy (flow velocity $v < v_A$, the Alfvén speed), the magnetic field tends to keep the flow corotating with the star, and thus increases the angular-momentum density as the matter moves outward. This argument applies both to isolated plasma clouds blown away from the star, for instance during a flare, and to the permanent stellar wind.

As the flow carries angular momentum away from the star, the Lorentz force transmits a torque to the stellar envelope in which the magnetic field is anchored, and so brakes the stellar rotation. Beyond the Alfvén radius r_A , where the flow velocity equals the Alfvén speed, the magnetic field has little effect on the stellar wind, which therefore conserves its angular

momentum and winds the magnetic field into a spiral structure. The angular-momentum loss per unit mass transported in a magnetically coupled flow is quite large, because the Alfvén radius is large: in the solar case, r_A amounts to 10 to 20 solar radii.

The rates of loss of mass and angular momentum from stars with convective envelopes depend on the configuration of the magnetic field, particularly on that part of the field which is open to interstellar space, and on the location of the Alfvénic surface. However, the magnetic topology of late-type stars is complicated and, except for the Sun, unknown; and estimates of rates of angular-momentum loss are thus based on simplified models. The study by Weber and Davis (1967) is for a model of a radial field ($B \sim r^{-2}$), which yields a high braking efficiency. Mestel (1968) studied a model with a magnetic dipole aligned with the stellar-rotation axis. Roxburgh (1983) constructed approximate models for multipole fields, which yield rates of angular-momentum loss

$$-\frac{dH}{dt} \approx \frac{8\pi}{3} \rho_o v_o \Omega R^4 (r_A/R)^{2-n} \quad , \quad (7-42)$$

where H is the angular momentum, ρ_o and v_o are the density and the wind velocity at some base level in the corona, R is the stellar radius, n indicates the multipole mode, and r_A is the Alfvénic radius which satisfies

$$\left(\frac{r_A}{R}\right)^{n+2} v_{AS} = \left(\frac{B_o^2}{\mu \rho_o v_o}\right) \quad , \quad (7-43)$$

where v_{AS} is the Alfvén speed at the Alfvénic radius, which in Roxburgh's approximation is defined as the average distance where the wind velocity equals the Alfvén speed. From these equations it follows that the rate dH/dt depends on the characteristic flux density B_o as $(B_o^2/v_{AS})^a$, with $a = (2-n)/(2+n)$. Since v_{AS} depends only weakly on B_o , the angular momentum loss is found to increase with the magnetic flux density only for radial ($n = 0$) and dipole ($n = 1$) fields. For $n > 2$, the loss rate $-dH/dt$ decreases as B_o increases,

because the fraction of the coronal magnetic field that is closed increases for increasing B_0 .

With increasing activity level, not only does the characteristic flux density B_0 increase but the field structure also becomes more complex, so higher multipole components become more important. Hence it is not clear whether the loss of angular momentum increases or decreases with increasing activity level. Even for semi-quantitative investigations the geometry of the coronal magnetic field has to be known in quite some detail.

The magnetic braking acts immediately on the part of the stellar envelope in which the magnetic field is rooted, which probably involves the whole convective envelope. It is not yet clear, however, how the rotation of the radiative core is coupled to the envelope's rotation.

For young, rapidly rotating, main-sequence stars the time scale for magnetic braking may be short — values as low as 10^7 years have been estimated from possible values for stellar parameters.

IV.B. SINGLE STARS: MAGNETIC ACTIVITY — ROTATION — AGE RELATION

There is observational evidence that the level of activity depends on the rotation rate: among stars of similar effective temperature and surface gravity the rapidly rotating stars are more active than slowly rotating stars (Chapter 3.VII.A.2). The dynamo principles sketched in Section II.C may be generalized to an evolutionary dynamo (Kippenhahn, 1973): the dynamo efficiency decreases with decreasing magnitude of differential rotation, and the magnitude of differential rotation is assumed to decrease with decreasing rotation rate. Such an evolutionary dynamo (Figure 7-12) suggests the following history for the magnetic activity of single main-sequence stars with convective envelopes.

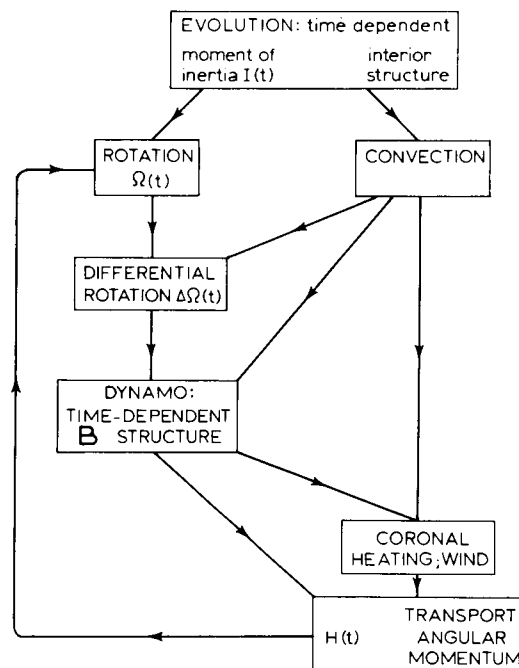


Figure 7-12. Block diagram illustrating the interactions that are incorporated in evolutionary dynamo action.

The star arrives at the zero-age main sequence with a relatively high total angular momentum. There is vigorous dynamo action, and the star is very active. Magnetic braking reduces the angular momentum on a time scale much shorter than the time spent on the main sequence; hence aged main-sequence stars rotate slowly and show a low level of magnetic activity. Skumanich (1972) estimated from scanty observational data that for G-type main-sequence stars the angular rotation rate Ω drops with time as $\Omega \propto t^{-1/2}$. This relation may be derived from ad hoc assumptions on the dependence of the mean magnetic flux density on the rotation rate, the structure of the coronal magnetic field, and the driving of the stellar wind, but the theory is incomplete (see Mestel (1984) for a discussion of these matters).

Stars with masses up to about 1.3 solar mass have relatively deep convective envelopes during the main-sequence phase. Dynamo action and magnetic braking in these stars result in slowly rotating, cool, dwarf stars which evolve

into G- and K-type subgiants and low-mass giants, which rotate very slowly and which have a very low level of activity.

Stars with masses larger than about 1.5 solar mass do not develop a deep convective envelope during the main-sequence stage. Hence there is no dynamo action and no magnetic braking, and these stars leave the main sequence and cross the Hertzsprung gap with rather high angular momentum. Once such a star becomes a G-type giant, a convective envelope is formed and dynamo action starts. Zwaan (1981a) suggested that rapidly rotating and very active G-type giants and bright giants are formed in this way (Chapter 2.V.B). During the evolution to the right in the Hertzsprung-Russell diagram, the stellar radius and the moment of inertia both increase. As a consequence, a rapidly rotating G-type giant becomes a slowly rotating K-type giant of low activity. Rutten and Pylyser (1988) demonstrated that the sharp drop in the level of activity in the transition from G-type to K-type giant is readily explained by the rapid increase in the moment of inertia; magnetic braking is not involved significantly in the drop in activity.

It is interesting to speculate on the fate of a magnetic A star during the giant phase. What happens as the convective envelope develops against the Lorentz forces in the strong and well-ordered magnetic field in the star? What is the further evolution of these stars, most of which are relatively slow rotators?

IV.C. CLOSE BINARY SYSTEMS

Single stars spend only a small fraction of their life as a very active star: F-, G-, and K-type main-sequence stars quickly lose their angular momentum by magnetic braking and more massive stars are active only during the brief phase spent as a G-type giant (see Figure 7-9).

However, binary systems contain much more angular momentum than do single stars. The

orbital angular momentum is much larger than the spin angular momentum in the components, if the angular velocities of the orbital motion (Ω_o) and the spin (Ω_s) are comparable: $\Omega_o \simeq \Omega_s$.

Tidal torques couple the rotation of the components and the orbital motion, tending to make the periods equal. The tidal friction is relatively large in components with extensive convective envelopes. The synchronization time scale is shorter than the evolutionary time scale provided that the orbital period is sufficiently short, and the original difference between the orbital and the spin periods is small (for the pioneering study, see Zahn, 1977; recent developments are reviewed by Savonije and Papaloizou, 1985). There is observational evidence that late-type main-sequence components in binaries tend to be synchronized, provided that the orbital period is shorter than about one week (Middelkoop, 1981, 1982; see also Rutten, 1986). Most of the giants of luminosity class III are synchronized for orbital periods shorter than about 100 days (Middelkoop and Zwaan, 1981; Rutten, 1987).

In synchronized binaries, the spin angular momentum lost by the magnetically coupled stellar wind is replenished by momentum from the orbital motion which is fed into the star by tidal coupling. Hence a component in a synchronized binary has a much larger supply of angular momentum, which can be spent in magnetic braking, than has a single but otherwise similar star. This explains why components in sufficiently close binaries are very active, even in cases in which single counterparts in the same evolutionary stage are quiet. The case of the late F-, G-, and K-type subgiants (luminosity class IV) is particularly striking: these stars are quiet as single stars but they are very active as components in close binaries — the so-called RS CVn binaries (Chapter 3).

Note that loss of angular momentum from a synchronized binary system causes the components to approach each other. Hence the

period decreases, and for components with convective envelopes the level of activity increases. Eventually the components will merge. Huang (1966) suggested that the W UMa-type contact binaries may be formed by such a process.

After an interacting binary is formed, its further evolution depends on the rate of angular momentum loss from the system. In the case of cataclysmic binaries and low-mass X-ray binaries, magnetic braking is more important than losses by gravitational radiation, except perhaps for systems with very light late-type secondaries (Verbunt and Zwaan, 1981; Taam, 1983).

Virtually all main-sequence stars and the majority of the giants in synchronized binaries follow the same relation between chromospheric radiative flux density and angular rotation rate as do single stars (see Rutten, 1986, 1987). However, there are groups of "overactive" stars, i.e., stars that are more active than the rotation rate indicates. Some close binaries with evolved components are overactive (Rutten, 1987), and so are T Tauri stars. Apparently, for the majority of the cool stars the magnetic activity level is determined by the rotation rate itself, and not by age. This result provides support for the hypothesis that dynamo action is responsible for activity in late-type stars.

V. COOL STARS AND STELLAR SYSTEMS: THE MAGNETIC CONNECTION

The outer atmospheres or photospheres of cool stars should not be studied in isolation: the magnetic fields threading the outer atmospheres, photospheres, and convective envelopes connect many of the processes in the three regimes. In this section we summarize some of the links in the "magnetic connection" that have been identified in studies to date, by referring to previous sections in this chapter.

In the convective envelope the interplay between magnetic field and convection leads to the mutual expulsion of magnetic field and turbulent convection (Section II.B). The resulting inhomogeneity of the magnetic field profoundly affects photospheric, chromospheric, and coronal structure. Rotation of the convective envelope leads to dynamo action which produces large-scale order in the magnetic structure, and which determines the time-dependent level of magnetic activity (Section II.C).

In the photosphere, radiative cooling causes "convective collapse" of emerging flux tubes, which intensifies the magnetic field in the tubes to strengths well above the equipartition strength (Section III.A.2). This intensification reaches downward in the convection zone, affecting at least the strongly superadiabatic top layer. The inhomogeneity of the magnetic field in the photosphere is responsible for the intricate structure observed in the solar chromosphere.

Magnetic fields physically connecting the "high- β " convection zone beneath the photosphere to the "low- β " chromospheric-coronal plasma provide a path for electrodynamic coupling between mechanical processes in the subphotosphere and nonthermal processes in the atmosphere. Matter can be transported, and energy can be transported and transformed, as a result of the mechanisms involved in this coupling.

The magnetic structure of the corona controls the coronal heating rate, the stellar mass-loss rate, and the rate of loss of rotational angular momentum from the convective envelope. This in turn determines the evolution of the efficiency of the dynamo (Sections IV.A through IV.C).

Observations of magnetic activity on cool stars indicate that the rotation rate is an important stellar parameter (Chapters 2.V and 3.VII), which suggests the concept of an evolutionary

dynamo (Figure 7-12; Section IV.B). Note that these effects arise despite the fact that the amount of energy contained in stellar rotation is relatively small: for the present Sun, rotating with an equatorial velocity $v_e = 2.0 \text{ km s}^{-1}$, the rotational energy amounts to about $3.0 \times 10^{35} \text{ J}$ (assuming rigid rotation). This is to be compared with the solar thermal energy content of $2.0 \times 10^{41} \text{ J}$ and the solar luminosity of $3.9 \times 10^{26} \text{ W}$ — the present rotational energy equals the energy that the Sun radiates in only 25 years. Even in the case of an extremely rapidly rotating, solar-like star, with $v_e = 200 \text{ km s}^{-1}$, the rotational energy of $3.0 \times 10^{39} \text{ J}$ is still a small fraction of the thermal energy contents.

For single stars the level of magnetic activity as a function of time is determined by the angular momentum at some specific time, say, upon reaching the zero-age main sequence. The evolution of the activity depends on the moment of inertia as it changes with the evolution of the star, on the transfer of angular momentum within the star, and on the rate of angular momentum loss by the magnetically coupled stellar wind.

Cool components in close binary systems may gain rotational angular momentum at the

expense of orbital momentum through tidal interaction. Even without consideration of the loss of angular momentum by magnetic braking there is a bewildering variety of possible evolutionary paths for interacting binaries, depending on the amounts of mass and angular momentum transferred from one component to the other, the mass lost from the system, and when in the evolution of the system these transfers and losses happen. When one of the components is a cool star with a convective envelope, tidal interaction is particularly efficient in the attempt to synchronize rotation and orbital motion, and magnetic braking of rotation may drive the components together.

We conclude that magnetic fields link the physics in various parts of a cool star. In sufficiently close binaries the magnetic braking of the rotation of the cool component effects the evolution of the binary system. The “magnetic connection” within cool stars and stellar systems is a promising field for further endeavor.

We are grateful to G.M.H.J. Habets, P. Hoyng, R.G.M. Rutten, and C.J. Schrijver for scientific commentary on a draft of this chapter.

REFERENCES

- Abt, H.A. 1957, *Astrophys. J.*, **126**, 503.
- Abt, H.A. 1958, *Astrophys. J.*, **127**, 658.
- Abt, H.A., and Chaffee, F.H. 1967, *Astrophys. J.*, **148**, 459.
- Abt, H.A., and Hunter, J.H. 1962, *Astrophys. J.*, **136**, 381.
- Abt, H.A., Meinel, A.B., Morgan, W.W., and Tapscott, J.W. 1968, *An Atlas of Low-dispersion Grating Stellar Spectra* (Tucson: Kitt Peak National Observatory).
- Adam, M.G., Ibbetson, P.A., and Petford, A.D., 1976, *Mon. Not. Roy. Astron. Soc.*, **177**, 687.
- Adams, F.C., and Shu, F.H. 1986, *Astrophys. J.*, **308**, 836.
- Adams, M.T., Strom, K.M., and Strom, S.E. 1983, *Astrophys. J. Supp.*, **53**, 893.
- Adams, W., and Kohlschütter, A. 1914, *Astrophys. J.*, **40**, 385.
- Adelman, S.J. 1974, *Pub. Astron. Soc. Pacific*, **86**, 486.
- Adelman, S.J., and Shore, S. N. 1982, *Astron. J.*, **87**, 665.
- Adrian, R. 1975, *J. Fluid Mech.*, **69**, 753.
- Aiad, A., and 5 others 1983, *Pub. Astron. Soc. Pacific*, **95**, 656.
- Aiad, A., and 7 others, 1984, *Astron. Astrophys.*, **136**, 67
- Albregtsen, F., and Hansen, T.L. 1977, *Solar Phys.*, **54**, 31.
- Alfvén, H. 1967, *Ann. Geophys.*, **24**, 341.
- Allen, C.W. 1949, *Mon. Not. Roy. Astron. Soc.*, **109**, 343.
- Allen, C.W. 1973, *Astrophysical Quantities* (London: Athlone Press), 3rd ed., pp. 204-6.
- Aller, H.D., Rugare, T.J., and Hodge, P.E. 1978, *Astron. J.*, **83**, 1985.
- Aller, L.H. 1963, *The Atmospheres of the Sun and Stars*, 2nd ed. (New York: Ronald Press).
- Aller, L.H., and Greenstein, J.L. 1960, *Astrophys. J. Supp.*, **5**, 139.
- Alschuler, W.R. 1975, *Astrophys. J.*, **195**, 649.
- Altenhoff, W.J., Braes, L.L.E., Olon, F.M., and Wendker, H.J. 1976, *Astron. Astrophys.*, **46**, 1.

- Altenhoff, W.J., Oster, L., and Wendker, H.J. 1979, *Astron. Astrophys.*, **73**, L21.
- Altschuller, M.C., and Newkirk, G. 1969, *Solar Phys.*, **9**, 131.
- Ambartsumyan, V.A. 1958, *Theoretical Astrophysics* (London: Pergamon).
- Anderson, C.M., Stoeckly, R., and Kraft, R.P. 1966, *Astrophys. J.*, **143**, 299.
- Anderson, L., and Kuhi, L.V. 1968, in *Non-Periodic Phenomena in Variable Stars*, ed. L. Detre (Academic Press, Budapest).
- Ando, H. 1976, *Pub. Astron. Soc. Japan*, **28**, 517.
- Ando, H., and Osaki, Y. 1975a, *Pub. Astron. Soc. Japan*, **27**, 581.
- Ando, H., and Osaki, Y. 1975b, *Pub. Astron. Soc. Japan*, **29**, 221.
- André, P., Montmerle, T., and Feigelson, E.D. 1987, *Astron. J.*, **93**, 1182.
- Appenzeller, I., Bertout, C., Mundt, R., and Krautter, J. 1981, *Mitt. Astr. Ges.*, **52**, 15.
- Appenzeller, I., Chavarria, C., Krautter, J., Mundt, R., and Wolf, B. 1980, *Astron. Astrophys.*, **90**, 184.
- Appenzeller, I., and Dearborn, D. 1984, *Astrophys. J.*, **278**, 689.
- Appenzeller, I., Jankovics, I., and Jetter, R. 1985, *Astron. Astrophys. Supp.*, **64**, 65.
- Appenzeller, I., Jankovics, I., and Krautter, J. 1983, *Astron. Astrophys. Supp.*, **53**, 291.
- Appenzeller, I., Jankovics, I., Ostreicher, R. 1984, *Astron. Astrophys.*, **141**, 108.
- Appenzeller, I., and Wolf, B. 1977, *Astron. Astrophys.*, **54**, 713.
- Appenzeller, I., and Wolf, B. 1979, *Astron. Astrophys.*, **75**, 164.
- Athay, R. 1970a, *Astrophys. J.*, **161**, 713.
- Athay, R. 1970b, *Solar Phys.*, **12**, 175.
- Athay, R. 1972, *Radiation Transport in Spectral Lines* (Dordrecht: Reidel).
- Athay, R. 1981, in *The Sun as a Star*, ed. S.D. Jordan, NASA SP-450, p 85.
- Athay, R., and Skumanich, A. 1968, *Astrophys. J.*, **155**, 273.
- Auer, L., and Mihalas, D. 1969, *Astrophys. J.*, **158**, 641.
- Auer, L., and Newell, J. 1978, in *Multicolor Photometry and the Theoretical HR Diagram*, ed. A. Phillip (New York: Dudley Observatory).
- Auvergne, M., Frisch, H., Frisch, U., Froeschle, Ch., and Pouquet, A. 1973, *Astron. Astrophys.*, **29**, 93.
- Avrett, E.H., and Jordan, S.D. 1973, *Stellar Chromospheres*, NASA SP-317.
- Axford, W.I. 1985, *Solar Phys.*, **100**, 575.
- Ayres, T.R. 1979, *Astrophys. J.*, **228**, 509.
- Ayres, T.R. 1984, *Astrophys. J.*, **284**, 784.
- Ayres, T.R., and Johnson, H.R. 1977, *Astrophys. J.*, **214**, 410.
- Ayres, T.R., and Linsky, J.L. 1980, *Astrophys. J.*, **241**, 279.
- Ayres, T.R., and Linksy, J. 1981, *Astrophys. J.*, **247**, 545.
- Ayres, T.R., Linsky, J.L., and Shine, R.A. 1974, *Astrophys. J.*, **192**, 93.

- Ayres, T.R., Linsky, J.L., and Shine, R.A. 1975, *Astrophys. J. Lett.*, **195**, L121.
- Ayres, T.R., Linsky, J.L., Vaiana, G.S., Golub, L., and Rosner R. 1981, *Astrophys. J.*, **250**, 293.
- Ayres, T.R., Linsky, J.L., Basri, G.S., Landsman, W., Henry, R.C., Moos, H.W., and Stencel, R.E. 1982, *Astrophys. J.*, **256**, 550.
- Ayres, T.R., Marstad, N.C., and Linsky, J.L. 1981a, *Astrophys. J.*, **247**, 545.
- Ayres, T.R., Stencel, R.E., Linsky, J.L., Simon, T.R., Jordan, C., Brown, A., and Engvold, O. 1983, *Astrophys. J.*, **274**, 801.
- Ayres, T.R., and Testerman, L. 1981, *Astrophys. J.*, **245**, 1124.
- Babcock, H.W. 1953, *Astrophys. J.*, **118**, 387.
- Babcock, H.W. 1958, *Astrophys. J. Supp.*, **3**, 141.
- Babcock, H.W. 1962, in *Astronomical Techniques*, ed. W. Hiltner (Chicago: Univ. Chicago), Chap. 5.
- Bahcall, J.N., Hueber, N.F., Lubow, S.H., Parker, P.D., and Ulrich, R.K. 1982, *Rev. Mod. Physics*, **54**, 767.
- Balescu, R. 1963, *Statistical Mechanics of Charged Particles* (New York: Academic Press).
- Baliunas, S.L., and Dupree, A.K. 1982, *Astrophys. J.*, **252**, 668.
- Baliunas, S.L., Hartmann, L., and Dupree, A.K. 1983, *Astrophys. J.*, **271**, 672.
- Baliunas, S.L., Hartmann, L., Vaughan, A., Liller, W., and Dupree, A.K. 1981, *Astrophys. J.*, **246**, 473.
- Baliunas, S.L., Vaughan, A. 1985, *Ann. Rev. Astron. Astrophys.*, **23**.
- Baliunas, S.L., Vaughan, A.H., Middelkoop, F., Hartmann, L.W., Mihalas, D., Noyes, R.W., Preston, G.W., Frazer, J., and Lanning, H. 1982, *Astrophys. J.*, **275**, 752.
- Balthasar, H., and Wöhl, H. 1980, *Astron. Astrophys.*, **92**, 111.
- Barambon, C., and Müller, E.A. 1979, *Solar Phys.*, **64**, 201.
- Barker, P.K., and Marlborough, J.M. 1982, *Astrophys. J.*, **254**, 297.
- Basri, G.S., and Linsky, J.L. 1979, *Astrophys. J.*, **234**, 1023.
- Basri, G.S., Linsky, J.L., and Eriksson, K. 1981, *Astrophys. J.*, **251**, 162.
- Bastian, U. 1982, *Astron. Astrophys.*, **109**, 245.
- Bastian, U., Finkenzeller, U., Jäschek, C., and Jäschek, M. 1983, *Astron. Astrophys.*, **126**, 438.
- Bastien, P. 1981, *Astron. Astrophys.*, **94**, 294.
- Bastien, P. 1982, *Astron. Astrophys. Supp.*, **48**, 153 and 164.
- Bastien, P. 1985, *Astrophys. J. Supp.*, **59**, 277.
- Bastien, P., and Landstreet, J.D. 1979, *Astrophys. J. Lett.*, **229**, L137.
- Beall, J.H. 1986, *Astrophys. J.*, **316**, 227.
- Beals, C.S. 1950, *Publ. D.A.O.*, **9**, 1.
- Becker, W. 1967, *Zeit. f. Astrophys.*, **66**, 404.
- Becker, W., and Stock, J. 1954, *Zeit. f. Astrophys.*, **34**, 1.

- Beckers, J.M. 1969, *AFCRL No. 471*.
- Beckers, J.M. 1981, in *The Sun as a Star*, ed. S.D. Jordan (Washington, D.C.: CNRS NASA SP-450), p. 11.
- Beckers, J.M., and Canfield, R.C. 1976, *Physique des Mouvements dans les Atmospheres Stellaires*, eds. R. Cayrel, and M. Steinberg (Paris: Colloques Internationaux d. CNRS No. 250), p. 207.
- Beckman, J.E., and Crivellari, L. 1985 (eds.), *Progress in Stellar Spectral Line Formation Theory*, (Dordrecht: Reidel)
- Beiging, J.H., Cohen, M., and Schwartz, P.R. 1984, *Astrophys. J.*, **282**, 699.
- Belcher, J.W., and MacGregor, K.B. 1976, *Astrophys. J.*, **210**, 498.
- Belvedere, G., and Paterno, L. 1983, *Astrophys. J.*, **268**, 246.
- Belvedere, G., Paterno, L., and Stix, M. 1980, *Astron. Astrophys.*, **88**, 240.
- Bernat, A.P. 1982, *Astrophys. J.*, **252**, 644.
- Bernat, A.P., Hall, D.N.B., Hinkle, K-H., and Ridgway, S.T. 1979, *Astrophys. J. Lett.*, **233**, L135.
- Bernat, A.P., and Lambert, D.L. 1976, *Astrophys. J.*, **210**, 395.
- Bertout, C. 1977, *Astron. Astrophys.*, **58**, 153.
- Bertout, C. 1978, *Mitt. Astr. Ges.*, **43**, 176.
- Bertout, C. 1979, *Astron. Astrophys.*, **80**, 138.
- Bertout, C. 1984, *Rep. Prog. Phys.*, **47**, 111.
- Bertout, C., Basri, G.S., and Bouvier, J. 1987, *Astrophys. J.*
- Bertout, C., Carrasco, L., Mundt, R., and Wolf, B. 1982, *Astron. Astrophys. Supp.*, **47**, 419.
- Bertout, C., and Thum, C. 1982, *Astron. Astrophys.*, **107**, 368.
- Bertout, C., and Yorke, H. 1976, *Physical Studies of Minor Planets*, ed. T. Gehrels (Tucson: Univ. of Arizona Press), p. 648.
- Bessell, M.S. 1979, *Dudley Obs. Rept. No. 14*, p. 279.
- Biermann, L. 1977, *Problems of Stellar Convection*, IAU Coll. No. 38, eds. Spiegel and Zahn (Berlin: Springer-Verlag), p. 4.
- Blaauw, A. 1963, *Basic Astronomical Data*, ed. K. Aa. Strand (Chicago: Univ. Chicago Press), p. 383.
- Blanco, C., Bruca, L., Catalano, S., and Marilli, E. 1982, *Astron. Astrophys.*, **115**, 280.
- Blanco, C., Catalano, S., and Marilli, E. 1976, *Astron. Astrophys.*, **48**, 19.
- Blanco, C., Catalano, S., and Marilli, E. 1979a, *Nature*, **280**, 661.
- Blanco, C., Catalano, S., and Marilli, E. 1979b, *Astron. Astrophys. Supp.*, **36**, 297.
- Bless, R.C., and Code, A.D. 1972, *Ann. Rev. Astron. Astrophys.*, **10**, 197.
- Boesgaard, A.M. 1984, *Astron. J.*, **89**, 1635.
- Boesgaard, A.M., and Herbig, G.H. 1981 (private communication).
- Boesgaard, A.M., and Simon, T. 1981 in *Second Cambridge Workshop on Cool Stars, Stellar Systems and the Sun*, SAO Special Rep. 392, Vol. II, p. 161.
- Bogdan, T.J. 1986, *Solar Phys.*, **103**, 311.

- Böhm-Vitense, E. 1977, *Problems of Stellar Convection*, IAU Coll. No. 38, eds. Spiegel and Zahn (Berlin: Springer-Verlag), p. 63.
- Böhm-Vitense, E. 1980, *Stellar Turbulence* IAU Coll. No. 51, eds. Gray and Linsky (Berlin: Springer-Verlag), p. 300.
- Böhm-Vitense, E. 1981, *Ann. Rev. Astron. Astrophys.*, **19**, 295.
- Böhm-Vitense, E., and Dettmann, T. 1980, *Astrophys. J.*, **236**, 560.
- Bonnet, R., and Dupree, A.K. (eds.) 1981, *Solar Phenomena in Stars and Stellar Systems* (Dordrecht: Reidel).
- Bonsack, W.K., and Culver, R.B. 1966, *Astrophys. J.*, **145**, 767.
- Bopp, B.W. 1983, in *Activity in Red Dwarf Stars* (IAU Coll. No. 71), eds. P.B. Byrne and M. Rodono (Dordrecht: Reidel) p. 363.
- Bopp, B.W., and Espanak, F. 1977, *Astron. J.*, **82**, 916.
- Bopp, B.W., and Evans, D.S. 1973, *Mon. Not. Roy. Astron. Soc.*, **164**, 343.
- Bopp, B.W., and Fekel, F. 1977, *Astron. J.*, **82**, 490.
- Bopp, B.W., and Noah, P.V. 1980, *Pub. Astron. Soc. Pacific*, **92**, 717.
- Bopp, B.W., and Talcott, J.C. 1978, *Astron. J.*, **83**, 1517.
- Botticher, W. 1968, in *Plasma Diagnostics*, ed. W. Lochte-Holtgreven (Amsterdam: North-Holland), p. 650.
- Bouvier, J., Bertout, C., Benz, W., and Mayor, M. 1986a, *Astron. Astrophys.*, **165**, 110.
- Bouvier, J., Bertout, C., and Bouchet, P. 1986b, *Astron. Astrophys.*, **158**, 149.
- Bray, R.J., and Loughhead, R.E. 1964, *Sunspots* (London: Chapman and Hall).
- Bray, R.J., and Loughhead, R.E. 1978, *Pub. Astron. Soc. Pacific*, **90**, 609.
- Bray, R.J., Loughhead, R.E., and Durrant, C.J. 1984, *The Solar Granulation*, 2nd Edition (Cambridge: Cambridge Univ. Press).
- Bray, R.J., Loughhead, R.E., and Tappere, E.J. 1976, *Solar Phys.*, **49**, 3.
- Breger, M. 1976, *Astrophys. J. Supp.*, **32**, 1 and 7.
- Brooks, R.J., Isaak, G., McLeod, C., Van der Raay, J., and Roca Cortes, T. 1978, *Mon. Not. Roy. Astron. Soc.*, **184**, 759.
- Brosius, J.W., Mullan, D.J., and Stencel, R.E. 1985, *Astrophys. J.*, **288**, 310.
- Brown, A. 1985 (private communication).
- Brown, A., and Carpenter, K.G. 1984, *Astrophys. J. Lett.*, **272**, L43.
- Brown, A., and Jordan, C. 1981, *Mon. Not. Roy. Astron. Soc.*, **196**, 757.
- Brown, A., and Jordan, C. 1983, *Activity in Red Dwarf Stars*, IAU Coll. No. 71, eds. Byrne and Rodono (Amsterdam: North-Holland), p. 509.
- Brown, A., Jordan, C., Millar, T.J., Gondhalekar, P., and Wilson, R. 1981, *Nature*, **290**, 34.
- Brown, A., Jordan, C., Stencel, R.E., Linsky, J.L., and Ayres, T.R. 1984, *Astrophys. J.*, **283**, 731.
- Brown, A., Jordan, C., and Wilson, R. 1979, *The First Year of IUE*, ed. A. Willis (London: University College London) p. 232.

- Brown, D.N., and Landstreet, J. 1981, *Astrophys. J.*, **246**, 899.
- Brown, R.L., and Crane, P.C. 1978, *Astron. J.*, **83**, 1504.
- Brueckner, G.E., and Bartoe, J.D.F. 1983, *Astrophys. J.*, **272**, 329.
- Bruning, D.H. 1981, *Astrophys. J.*, **248**, 274.
- Brussard, P., and van de Hulst, H. 1962, *Rev. Mod. Physics*, **34**, 507.
- Bumba, V., and Kleczek, J. 1976 (eds.), *Basic Mechanisms of Solar Activity*, IAU Symp. 71 (Dordrecht: Reidel)
- Burbidge, E., Burbidge, G., Fowler, W., and Hoyle, F. 1957, *Rev. Mod. Physics*, **29**, 547.
- Buser, R. 1978, *Astron. Astrophys.*, **62**, 425.
- Buser, R. 1979, *Dudley Obs. Rept. No. 14*, p. 411.
- Busko, I.C., Quast, G.R., and Torres, C.A.O. 1977, *Astron. Astrophys.*, **60**, L27.
- Byrne, P.B., and Rodono, M. 1983, (eds.), *Activity in Red Dwarf Stars*, IAU Coll. No. 71 (Dordrecht: Reidel)
- Cacciari, C., and Freeman, K.C. 1983, *Astrophys. J.*, **268**, 185.
- Caillault, J.-P., and Helfand, D. 1981, *Bull. Amer. Astron. Soc.*, **13**, 811.
- Calvet, N. 1984, *Rev. Mex. Astron. Astrophys.*, **9**, 49.
- Calvet, N., Basri, G.S., Imhoff, C.L., and Giampapa, M.S. 1985, *Astrophys. J.*, **293**, 575.
- Calvet, N., Basri, G.S., and Kuhl, L.V. 1984, *Astrophys. J.*, **277**, 725.
- Cameron, R.C. 1967, (ed): *The Magnetic and Related Stars*, (Baltimore: Mono Book Corp.)
- Campbell, B. 1977, *Pub. Astron. Soc. Pacific*, **89**, 728.
- Canfield, R.C. 1976, *Solar Phys.*, **50**, 239.
- Canfield, R.C., and Beckers, J.M. 1976, *Physique des Mouvements dans les Atmospheres Stellaires*, eds. R. Cayrel and M. Steinberg (Paris: Colloques Internationaux du CNRS No. 250), p. 291.
- Cannon, C., and Thomas, R. 1976, *Astrophys. J.*, **211**, 910.
- Canto, J., and Mendoza, E.E. 1983 (eds.), *Rev. Mex. Astr. Astron.* **7** (whole issue).
- Carbon, C.F., and Gingerich, O. 1969, in O. Gingerich (ed.) *Theory and Observations of Normal Stellar Atmospheres* (Cambridge: MIT Press), p. 377.
- Carpenter, K.G., Brown, A., and Stencel, R.E. 1985, *Astrophys. J.*, **289**, 676.
- Carrasco, L., Franco, J., and Roth, M. 1980, *Astron. Astrophys.*, **86**, 217.
- Castor, J.I. 1981, in *Physical Processes in Red Giants*, eds. I. Iben and A. Renzini (Dordrecht: Reidel), p. 285.
- Catalano, S. 1983, in *Activity in Red Dwarf Stars* (IAU Coll. No. 71) eds. P.B. Byrne and M. Rodono (Dordrecht: Reidel), p. 343.
- Caterna, R., and Harris H. 1979, *Dudley Obs. Rept. No. 14*, p. 489.
- Cayrel, R. 1963, *Comp. Rend. Acad. Soc.*, **257**, 3309.

- Cayrel, R., and Cayrel, G. 1963, *Astrophys. J.*, **137**, 431.
- Cayrel, G., Cayrel, R., and Foy, R. 1977, *Astron. Astrophys.*, **54**, 797.
- Cayrel de Strobel, G., Foy, R., Hernandez, G., Bentolila, C., and Proust, D. 1981, in *Haute Resolution Spectrale en Astrophysique* (Orsy: Deuxieme Coll. Nat. du Conseil Francais du Telescope Spatial), p. 33.
- Cayrel, R., and Steinberg, M. eds., 1976, *Physique des Mouvements dans les Atmospheres Stellaires* (Paris: Colloques).
- Chaffee, H. 1970, *Astron. Astrophys.*, **4**, 291.
- Chandrasekhar, S. 1933, *Mon. Not. Roy. Astron. Soc.*, **94**, 14.
- Chandrasekhar, S. 1949, *Astrophys. J.*, **110**, 329.
- Chandrasekhar, S. 1960, *Radiation Transfer* (New York: Dover).
- Chandrasekhar, S. 1961, *Hydrodynamic and Hydromagnetic Stability* (Oxford: Oxford Univ. Press)
- Chapman, R.D. 1980, *Nature*, **286**, 580.
- Chapman, R.D. 1981, *Astrophys. J.*, **248**, 1043.
- Chapman, S., and Cowling, T. 1970, *The Mathematical Theory of Non-Uniform Gases* (Cambridge: Cambridge University Press).
- Che, A., and Reimers, D. 1983, *Astron. Astrophys.*, **127**, 227.
- Che, A., Hempe, K., and Reimers, D. 1983, *Astron. Astrophys.*, **126**, 225.
- Che-Bohnenstengel, A. 1984, *Astron. Astrophys.*, **138**, 333.
- Che-Bohnenstengel, A., and Reimers, D. 1985, in *Fourth Cambridge Workshop on Cool Stars, Stellar Systems and the Sun*, eds. M. Zeilik and D. Gibson (Berlin: Springer-Verlag).
- Che-Bohnenstengel, A., Reimers, D. 1986, *Astron. Astrophys.*, **156**, 172.
- Chevallier, R.A. 1983, *Astrophys. J.*, **268**, 753.
- Chiu, H., and 5 others, 1977, *Astrophys. J.*, **211**, 453.
- Chiuderi, C., Einaudi, G., and Torricelli-Ciamponi, G. 1981, *Astron. Astrophys.*, **97**, 27.
- Christensen-Dalsgaard, J. 1982, *Mon. Not. Roy. Astron. Soc.*, **199**, 735.
- Christensen-Dalsgaard, J. 1984, in *Space Research Prospects in Stellar Activity and Variability*, eds. A. Mageny and F. Praderie (Obs. de Paris: Meudon), p. 11.
- Christensen-Dalsgaard, J., and Frandsen, S. 1983, *Solar Phys.*, **82**, 469.
- Christensen-Dalsgaard, J., and Gough, D.O. 1982, *Mon. Not. Roy. Astron. Soc.*, **198**, 141.
- Christy, R. 1962, *Astrophys. J.*, **136**, 887.
- Claverie, A., *Nature*, **282**, 591.
- Claverie, A. 1981, Isaak, G.R., McLeon, C.P., and van der Raay, H.B. 1979, *Nature*, **293**, 443.
- Claverie, A., Isaak, G.R., McLeod, C.P., van der Raay, H.B., and Roca Cortes, T. 1980, *Astron. Astrophys.*, **91**, L9.
- Clements, G.L., and Neff, J.S. 1979, *Astron. Astrophys.*, **75**, 193.
- Cloutman, L.D. 1979, *Astrophys. J.*, **227**, 614.
- Cochran, A. 1981, *Astrophys. J. Supp.*, **45**, 83.

- Cochran, A., and Barnes, T.G. III 1981, *Astrophys. J. Supp.*, **45**, 73.
- Code, A.D. 1960, in *Stellar Atmospheres*, ed. J.L. Greenstein (Chicago: Univ. Chicago Press), Chap. 2.
- Cohen, J. 1976, *Astrophys. J. Lett.*, **203**, L127.
- Cohen, M. 1973a, *Mon. Not. Roy. Astron. Soc.*, **161**, 85.
- Cohen, M. 1973b, *Mon. Not. Roy. Astron. Soc.*, **161**, 97.
- Cohen, M. 1973c, *Mon. Not. Roy. Astron. Soc.*, **161**, 105.
- Cohen, M. 1974, *Mon. Not. Roy. Astron. Soc.*, **169**, 257.
- Cohen, M. 1975, *Mon. Not. Roy. Astron. Soc.*, **173**, 279.
- Cohen, M. 1980, *Mon. Not. Roy. Astron. Soc.*, **191**, 499.
- Cohen, M. 1983, *Astrophys. J. Lett.*, **270**, L69.
- Cohen, M. 1984, *Phys. Rep.*, **116**, 173.
- Cohen, M., Bieging, J.M., and Schwartz, P.R. 1982, *Astrophys. J.*, **253**, 707.
- Cohen, M., and Kuhl, L.V. 1976, *Astrophys. J.*, **210**, 365.
- Cohen, M., and Kuhl, L.V. 1979, *Astrophys. J. Supp.*, **41**, 743.
- Cohen, M., and Schwarz, R.D. 1976, *Mon. Not. Roy. Astron. Soc.*, **174**, 137.
- Cohen, M., and Witteborn, 1984, *Astrophys. J.*, **294**, 345.
- Conti, P., and Deutsch, A.J. 1966, *Astrophys. J.*, **145**, 742.
- Cowley, C.R. 1970, *The Theory of Stellar Spectra* (New York: Gordon and Breach).
- Cowling, T.G. 1934, *Mon. Not. Roy. Astron. Soc.*, **94**, 39.
- Cowling, T.G. 1953, *The Sun*, ed. G.P. Kuiper (Chicago: Univ. Chicago Press), p. 532.
- Cowling, T.G. 1957, *Magnetohydrodynamics* (New York: Wiley-Interscience)
- Cowling, T.G. 1976, *Magnetohydrodynamics* (Bristol: Adam Hilger)
- Cowling, T.G. 1981, *Ann. Rev. Astron. Astrophys.*, **19**, 115
- Cox, J. 1974, *Rep. Prog. Phys.*, **37**, 563.
- Cox, J. 1980, *Theory of Stellar Pulsation* (Princeton: Princeton Univ. Press).
- Cox, J., and Giuli, R. 1968, *Principals of Stellar Structure* (New York: Gordon and Breach).
- Craig, I., and Brown, J. 1976, *Astron. Astrophys.*, **49**, 239.
- Cram, L.E. 1976, *Astron. Astrophys.*, **50**, 263.
- Cram, L.E. 1977, *Astron. Astrophys.*, **59**, 151.
- Cram, L.E. 1978, *Astron. Astrophys.*, **67**, 301.
- Cram, L.E. 1979, *Astrophys. J.*, **234**, 949.
- Cram, L.E. 1981, *Astrophys. J.*, **247**, 239.
- Cram, L.E., Brown, D., and Beckers, J.M. 1977, *Astron. Astrophys.*, **57**, 211.
- Cram, L.E., and Damé, L. 1983, *Astrophys. J.*, **272**, 355.
- Cram, L.E., Durney, B.R., and Guenther, D.B. 1983, *Astrophys. J.*, **267**, 442.

- Cram, L.E., Keil, S., and Ulmschneider, P. 1979, *Astrophys. J.*, **234**, 768.
- Cram, L.E., Giampapa, M.S., and Imhoff, C. 1980, *Astrophys. J.*, **238**, 905.
- Cram, L.E., Krikorian, R., and Jefferies, J.T. 1979, *Astron. Astrophys.*, **71**, 14.
- Cram, L.E., Rutten, R., and Lites, B. 1980, *Astrophys. J.*, **241**, 374.
- Culhane, J., and Acton, L. 1970, *Mon. Not. Roy. Astron. Soc.*, **151**, 141.
- Danielson, R.E. 1964, *Astrophys. J.*, **139**, 45.
- Davidson, J.K., and Neff, J.F. 1977, *Astrophys. J.*, **214**, 140.
- DeCampli, W.N. 1981, *Astrophys. J.*, **244**, 124.
- Deinzer, W. 1965, *Astrophys. J.*, **141**, 548.
- Deinzer, W., Hensler, G., Schussler, M., and Weisshaar, E. 1984, *Astron. Astrophys.*, **139**, p. 426, p. 435.
- de Jager, C. 1959, *Handbuch der Physik* (Berlin: Springer-Verlag) vol. 52, p. 80.
- Deubner, F.-L. 1974, *Solar Phys.*, **39**, 31.
- Deubner, F.-L. 1975, *Astron. Astrophys.*, **44**, 371.
- Deubner, F.-L. 1976a, in *Physique des Mouvements dans les Atmospheres Stellaires*, eds. R. Cayrel and M. Steinberg (Paris: Colloques Internationaux d. CNRS No. 250), p. 259.
- Deubner, F.-L. 1976b, in *Physique des Mouvements dans les Atmospheres Stellaires*, eds. R. Cayrel and M. Steinberg (Paris: Colloques Internationaux d. CNRS No. 250), p. 263.
- Deubner, F.-L. 1976c, *Astron. Astrophys.*, **51**, 189.
- Deubner, F.-L. 1981a, in *The Sun as a Star*, ed. S.D. Jordan (Washington, D.C.: CNRS NASA SP-450), p. 65.
- Deubner, F.-L. 1981b, *Nature*, **290**, 682.
- Deubner, F.-L., Ulrich, R.K., and Rhodes, E.J., Jr. 1979, *Astron. Astrophys.*, **72**, 177.
- Deutsch, A.J. 1956, *Astrophys. J.*, **123**, 210.
- Deutsch, A.J. 1960, in *Stellar Atmospheres*, ed. J.L. Greenstein (Chicago: Univ. of Chicago Press) p. 543.
- Dibai, E.A. 1971, *Soviet Astron.*, **14**, 785.
- Dicke, R.H. 1970, in *Stellar Rotation*, ed. A. Slettebak (Dordrecht: Reidel), p. 289.
- Doazan, V. 1970, *Astron. Astrophys.*, **8**, 148.
- Dorren, J.D., Siah, M.J., Guinan, E.F., and McCook, G.P. 1981, *Astron. J.*, **86**, 572.
- Drake, S.A., and Linsky, J.L. 1983, *Astrophys. J.*, **273**, 299.
- Drake, S.A., and Linsky, J.L. 1984, in *Third Cambridge Workshop on Cool Stars, Stellar Systems and the Sun*, eds. S.L. Baliunas and L. Hartmann (Berlin: Springer-Verlag), p. 350.
- Dravins, D. 1974, *Astron. Astrophys.*, **36**, 143.
- Dravins, D. 1976, in *Physique des Mouvements dans les Atmospheres Stellaires*, eds. R. Cayrel and M. Steinberg (Paris: Colloques Internationaux d. CNRS No. 250), p. 459.
- Dravins, D. 1981a, *Ann. Rev. Astron. Astrophys.*, **19**.
- Dravins, D. 1981b, *Astron. Astrophys.*, **96**, 64.

- Dravins, D. 1982, *Ann. Rev. Astron. Astrophys.*, **20**, 61.
- Dravins, D. 1983, *The ESO Messenger*, No. 32, p. 15.
- Dravins, D., Lindgren, L., and Nordlund, A. 1981, *Astron. Astrophys.*, **96**, 345.
- Drescher, Th., Wohl, H., and Kuveler, G. 1984, *The Hydrodynamics of the Sun*, eds. T.D. Guyenne and J.J. Hunter (Noordwijk: ESTEC) p. 29.
- Dumont, S., Heidmann, N., Kuhi, L.V., and Thomas, R.N. 1973, *Astron. Astrophys.*, **29**, 199.
- Duncan, D.K. 1981, *Astrophys. J.*, **248**, 651.
- Duncan, D.K. 1983, *Pub. Astron. Soc. Pacific*, **95**, 589.
- Duncan, D.K., Baliunas, S.L., Noyes, R.W., Vaughan, A.H., Frazer, J., and Lanning, H. 1984, *Pub. Astron. Soc. Pacific*, **96**, 707.
- Dunn, R.B., and Zirker, J.B. 1973, *Solar Phys.*, **33**, 281.
- Dupree, A.K. 1976, in *Physique de Mouvements dans les Atmospheres Stellaires*, Int. CNRS Coll., Nice, p. 439.
- Dupree, A.K. 1981, in *Solar Phenomena in Stars and Stellar Systems*, eds. R.M. Bonnet and A.K. Dupree (Dordrecht: Reidel), p. 407.
- Dupree, A.K. 1982, in *Advances in Ultraviolet Astronomy*, eds. Y. Kondo, J. Mead, and R. Chapman (NASA CP-2238), p. 3.
- Dupree, A.K., and Baliunas, S.L. 1979, *IAU Circular*, 3435.
- Dupree, A.K., Hartmann, L., Avrett, E.H., and Smith, G. 1984, *ESA SP-218*, 191.
- Durant, W., and Durant, A. 1961, *The Age of Reason Begins* (New York: Simon and Schuster), p. 605.
- Durney, B.R. 1973, *Stellar Chromospheres* NASA SP-137, eds. Avrett and Jordan, p. 282.
- Durney, B.R., Keil, S.L., and Lytle, D.M. 1984, *Astrophys. J.*, **281**, 455.
- Durney, B.R., and Latour, J. 1978, *Geophys. Astrophys. Fluid Dyn.*, **9**, 241.
- Durrant, C.J. 1979, *Astron. Astrophys.*, **73**, 37.
- Durrant, C.J. 1980, *Astron. Astrophys.*, **89**, 80.
- Durrant, C.J., Mattig, W., Nesis, A., Reiss, L., and Schmidt, W. 1979, *Solar Phys.*, **61**, 251.
- Duvall, T.L., and Harvey, J.W. 1983, *Nature*, **302**, 24.
- Duvall, T.L., and Harvey, J.W. 1984, *Nature*, **310**, 19.
- Duvall, T.L., Harvey, J.W., and Pomerantz, M.A. 1986, *Nature*, **321**, 500.
- Dyck, H.M., Simon, T., and Zuckerman, B. 1982, *Astrophys. J. Lett.*, **255**, L103.
- Eaton, J.A., and Hall, D.S. 1979, *Astrophys. J.*, **227**, 907.
- Ebbets, D. 1978, *Astrophys. J.*, **224**, 185.
- Eddington, A. 1917, *Observatory*, **40**, 209.
- Eddington, A. 1926, *The Internal Constitution of the Stars* (Cambridge: Cambridge University Press).
- Eddington, A. 1927, *Stars and Atoms* (New Haven: Yale University Press).

- Edmunds, M.G. 1978, *Astron. Astrophys.*, **64**, 103.
- Edwards, S., Hartmann, L., and Avrett, E.H. 1981, in *Second Cambridge Workshop on Cool Stars*, eds. M.S. Giampapa and L. Golub (Smithsonian Spec. Report 392), p. 191.
- Edwards, S., and 5 others 1987, *Astrophys. J.*, **321**, 473.
- Eggen, O. 1960, *Vistas in Astron.*, **3**, 258.
- Endal, A.S., and Sofia, S. 1979, *Astrophys. J.*, **232**, 531.
- Epstein, E.E., and Briggs, F.H. 1978, *Astron. J.*, **83**, 1487.
- Feigelson, E.D., and Kriss, G.A. 1981, *Astrophys. J. Lett.*, **248**, L35.
- Feigelson, E.D., and Montmerle, T. 1985, *Astrophys. J.*, **289**, L19.
- Fekel, F. 1983, *Astrophys. J.*, **268**, 274.
- Feldman, P.A. 1983, in *Activity in Red-Dwarf Stars*, eds. P.B. Byrne and M. Rodono (Dordrecht: Reidel), p. 429.
- Feldman, P.A., Taylor, A.R., Gregory, P.C., Seaquist, E.R., Balonek, T.J., and Cohen, N.L. 1978, *Astron. J.*, **83**, 1471.
- Felli, M., Gahm, G.F., Harten, R.H., Liseau, R., and Panagia, N. 1982, *Astron. Astrophys.*, **107**, 354.
- Ferraro, V.C.A., and Plumpton, C. 1966, *An Introduction to Magneto-Fluid Mechanics* (Oxford: Clarendon).
- FitzGerald, M. 1970, *Astron. Astrophys.*, **4**, 234.
- Flower, P.J. 1977, *Astron. Astrophys.*, **54**, 31.
- Fossat, E. 1984, *Space Research Prospects in Stellar Activity and Variability*, eds. A. Mangeney and F. Praderie (Paris: Observ. Paris-Meudon), p. 77.
- Fossat, E., Grec, G., Gelly, B., and Decanini, Y. 1984, *Comptes Rendus de l'Academie des Sciences*, **229**, 17.
- Foukal, P. 1976, *Astrophys. J.*, **210**, 575.
- Foukal, P., Fowler, L.A., and Livshitz, M. 1983, *Astrophys. J.*, **267**, 863.
- Foy, R. 1972, *Astron. Astrophys.*, **18**, 26.
- Foy, R. 1978, *Astron. Astrophys.*, **67**, 311.
- Foy, R. 1980, in *Stellar Turbulence*, IAU Coll. No. 51, eds., D.F. Gray and J.L. Linsky (Heidelberg: Springer-Verlag), p. 164.
- Foy, R. 1981, *Astron. Astrophys.*, **93**, 315.
- Fraquelli, D.A. 1978, *Astron. J.*, **83**, 1535.
- Fraquelli, D.A. 1982, *Astrophys. J. Lett.*, **254**, L41.
- Frazier, E.N. 1968, *Zeit. f. Astrophys.*, **68**, 345.
- Freidman, C., and Gurtler, J. 1975, *Astron. Nachr.*, **296**, 125.
- Fredga, K. 1971, *Solar Phys.*, **21**, 60.
- Frisch, H. 1975, *Astron. Astrophys.*, **40**, 267.
- Frisch, H., and Frisch, U. 1976, *Mon. Not. Roy. Astron. Soc.*, **175**, 157.
- Fröhlich, C. 1977, in *The Solar Output and Its Variations*, ed. O.R. White (Boulder: Colorado Assoc. Univ. Press), p. 93.
- Fukuda, I. 1982, *Pub. Astron. Soc. Pacific*, **94**, 271.

- Furenlid, I., and Young, A. 1978, *Astron. J.*, **83**, 1527.
- Gahm, G.F. 1980, *Astrophys. J.*, **242**, L163.
- Gahm, G.F. 1981, *Astrophys. J. Lett.*, **242**, L163.
- Gahm, G.F. 1986, in *Flares: Solar and Stellar*, ed. P.M. Gondhalekar (Rutherford-Appleton Lab. RAL-86-085).
- Gahm, G.F., Fredga, K., Liseau, R., and Dravins, D. 1979, *Astron. Astrophys.*, **73**, L4.
- Gahm, G.F., and Hultquist, L. 1972, *Astron. Astrophys.*, **16**, 329.
- Gahm, G.F., and Krautter, J. 1982, *Astron. Astrophys.*, **106**, 25.
- Gahm, G.F., Nordh, H.L., Olofsson, S.G., and Carlborg, N.C. 1974, *Astron. Astrophys.*, **33**, 399.
- Gail, H.-P., and 4 others, 1974, *Astron. Astrophys.*, **32**, 65.
- Gail, H.-P., and Sedlmayr, E. 1974, *Astron. Astrophys.*, **36**, 17.
- Galloway, D.J., and Moore, D.R. 1979, *Geophys. Astr. Fluid Dyn.*, **12**, 73.
- Garcia-Alegre, M.C., Vazquez, M., and Wöhl, H. 1982, *Astron. Astrophys.*, **45**, 410.
- Garcia-Colin, L., Robles-Dominguez, J., Fuentes-Martinez, G. 1981, *Phys. Rev. Lett.*, **84A**, 169.
- Garrison, R.F. 1979, in *Spectral Classification of the Future*, IAU Coll. No. 47, eds. M.F. McCarthy, A.G.D. Philip, and G.V. Coyne (Vatican City: Vatican Obs.), p. 23.
- Gary, D.E., and Linsky, J.L. 1982, *Astrophys. J.*, **250**, 284.
- Gebbie, K.B., and Thomas, R. 1968, *Astrophys. J.*, **154**, 271.
- Gebbie, K.B., and Thomas R. 1970, *Astrophys. J.*, **161**, 229.
- Gebbie, K.B., and Thomas, R. 1971, *Astrophys. J.*, **168**, 461.
- Gehrels, T. 1978 (ed.), *Protostars and Planets* (Tucson: University of Arizona Press).
- Gehren, P. 1975, *Astron. Astrophys.*, **38**, 289.
- Gehren, T. 1980, in *Stellar Turbulence*, eds. D.F. Gray and J.L. Linsky (Heidelberg: Springer), p. 103.
- Gehren, T. 1981, *Astron. Astrophys.*, **100**, 97.
- Giampapa, M.S., Calvet, N., Imhoff, C.L., and Kuhl, L.V. 1981, *Astrophys. J.*, **251**, 113.
- Giampapa, M.S., Golub, L., and Worden, S.P. 1983, *Astrophys. J. Lett.*, **268**, L121.
- Giampapa, M.S., Worden, S., and Gilliam, L. 1979, *Astrophys. J.*, **229**, 1143.
- Gibson, D.M. 1984, *Workshop on Stellar Continuum Radio Astronomy*, Boulder.
- Gibson, D.M., Hicks, P.D., and Owen, F.N. 1978, *Astron. J.*, **83**, 1495.
- Gilman, P.A. 1980, in *Stellar Turbulence*, eds. D.F. Gray and J.L. Linsky (Heidelberg: Springer), p. 19.
- Gilman, P.A. 1981, in *The Sun as a Star*, ed. S.D. Jordan (Washington, D.C.: CNRS/NASA, SP-450), p. 231.
- Gilman, P.A. 1983, in *Solar and Stellar Magnetic Fields*, ed. J.O. Stenflo (Dordrecht: Reidel), p. 247.
- Giovanelli, R.G. 1977, *Solar Phys.*, **52**, 315.

- Giovanelli, R.G. 1978, *Solar Phys.*, **59**, 293.
- Giovanelli, R.G. 1980a, *Solar Phys.*, **67**, 211.
- Giovanelli, R.G. 1980b, *Solar Phys.*, **68**, 49.
- Glandsdorff, P., and Prigogine, J. 1971, *Thermodynamic Theory of Structure, Stability, and Fluctuations* (New York: Wiley-Interscience).
- Glasby, J.S. 1968, *Variable Stars* (London: Constable).
- Glatzmaier, G., and Gilmore, P. 1981, *Solar Phenomena in Stars and Stellar Systems*, eds. Bonnet and Dupree (Dordrecht: Reidel), p. 145.
- Glebocki, R., and Stawikowski, A. 1980, in *Stellar Turbulence*, eds. D.F. Gray and J.L. Linsky (Heidelberg: Springer-Verlag), p. 55.
- Glushneva, I.N. 1964, *Soviet Astron.*, **8**, 163.
- Golant, V., Zhilinsky, A., and Sakharov, I. 1977, *Fundamentals of Plasma Physics* (New York: Wiley).
- Golay, M. 1979, *Dudley Obs. Rept. No. 14*, p. 477.
- Goldberg, L. 1979, *Quart. J. Roy. Astron. Soc.*, **20**, 361.
- Goldberg, L., Hege, E.K., Hubbard, E.N., Strittmatter, P.A., and Cocke, W.J. 1981, *SAO Spec. Rep.*, **392**, 131.
- Goldreich, P., and Keeley, D. 1977, *Astrophys. J.*, **211**, 934.
- Golub, L. 1983, *Activity in Red Dwarf Stars*, IAU Coll. No. 71, eds. Byrne and Rodono (Amsterdam: North-Holland), p. 83.
- Golub, L., Harnden, F.R. Jr., Maxson, C.W., Rosner, R., Vaiana, G.S., Cash W., Jr., and Snow, T.P., Jr. 1983, *Astrophys. J.*, **271**, 264.
- Golub, L., Harnden, F.R., Pallavacini, R.P., Rosner, R., and Vaiana, G.S. 1982, *Astrophys. J.*, **253**, 242.
- Gonczy, G., and Roddier, F. 1971, *Astron. Astrophys.*, **11**, 28.
- Gondhalekar, P., Penston, M.V., and Wilson, R. 1979, *The First Year of IUE*, ed. A. Willis (London: SRC), p. 109.
- Gough, D.O., and Spiegel, E. 1977, *Solar and Stellar Magnetic Fields*, eds. Spiegel and Zahn, p. 15.
- Gough, D.O., and Weiss, N. 1976, *Mon. Not. Roy. Astron. Soc.*, **176**, 589.
- Grad, H. 1958, *Handbuch der Physik*, Vol. XII, 205.
- Grasdalen, G.L., and 5 others, 1984, *Astrophys. J.*, **283**, L57.
- Gray, D.F. 1973, *Astrophys. J.*, **184**, 461.
- Gray, D.F. 1975, *Astrophys. J.*, **202**, 148.
- Gray, D.F. 1976, *The Observation and Analysis of Stellar Photospheres* (New York: Wiley).
- Gray, D.F. 1977a, *Astrophys. J.*, **211**, 198.
- Gray, D.F. 1977b, *Astrophys. J.*, **218**, 530.
- Gray, D.F. 1978, *Solar Phys.*, **59**, 193.
- Gray, D.F. 1980a, in *Stellar Turbulence*, IAU Coll. No. 51, eds. D.F. Gray and J.L. Linsky (Heidelberg: Springer-Verlag), p. 75.
- Gray, D.F. 1980b, *Astrophys. J.*, **235**, 508.
- Gray, D.F. 1981a, *Astrophys. J.*, **245**, 992.
- Gray, D.F. 1981b, *Astrophys. J.*, **251**, 152.
- Gray, D.F. 1981c, *Astrophys. J.*, **251**, 155.
- Gray, D.F. 1981d, *Astrophys. J.*, **251**, 583.

- Gray, D.F. 1982a, *Astrophys. J.*, **255**, 200.
- Gray, D.F. 1982b, *Astrophys. J.*, **258**, 201.
- Gray, D.F. 1982c, *Astrophys. J.*, **261**, 259.
- Gray, D.F. 1982d, *Astrophys. J.*, **262**, 682.
- Gray, D.F. 1984a, *Astrophys. J.*, **277**, 640.
- Gray, D.F. 1984b, *Astrophys. J.*, **281**, 719.
- Gray, D.F. 1985, *Pub. Astron. Soc. Pacific*, in press.
- Gray, D.F., and Endal, A.S. 1982, *Astrophys. J.*, **254**, 162.
- Gray, D.F., and Evans, J.C. 1973, *J. Roy. Astron. Soc. Canada*, **67**, 241.
- Gray, D.F., and Linsky, J.L., (eds.) 1980, *Stellar Turbulence*, IAU Coll. No. 51 (Heidelberg: Springer-Verlag).
- Gray, D.F., and Martin, B.E. 1978, *Astrophys. J.*, **226**, 907.
- Gray, D.F., and Nagar, P. 1985, *Astrophys. J.*, in press.
- Gray, D.F., and Toner, C.G. 1985, *Pub. Astron. Soc. Pacific*, in press.
- Greaves, W. 1956, *Vistas in Astronomy*, **3**, 1309.
- Grec, G., and Fossat, E. 1977, *Astron. Astrophys.*, **55**, 411.
- Grec, G., Fossat, E., and Pomerantz, M.A. 1980, *Nature*, **288**, 541.
- Grec, G., Fossat, E., and Pomerantz, M.A. 1983, *Solar Phys.*, **82**, 55.
- Gredin, Yu. N., and Red'kina, N. 1984, *Soviet Astron. Lett.*, **10**, 255.
- Greenstein, J.L., ed. 1960, *Stellar Atmospheres* (Chicago: Univ. Chicago Press).
- Griffin, R.F. 1963, *Observatory*, **83**, 255.
- Grinin, V.P., Mitskevich, A., and Timoshenko, L. 1985, *Astrophysics*, **22**, 24.
- Grinin, V.P., Petrov, P.P., and Shakhovskaya, N.I. 1983, *Activity in Red Dwarf Stars*, IAU Coll. No. 71, eds. Byrne and Rodono, p. 513.
- Groth, H.G. 1957, *Zeit. f. Astrophys.*, **43**, 185.
- Gurtovenko, E.A., de Jager, C., Lindenbergh, A., and Rutten, R.J. 1976, in *Physique des Mouvements dans les Atmospheres Stellaire*, eds., R. Cayrel and M. Steinberg (Paris: Colloques Internationaux du CNRS No. 250), p. 331.
- Gustaffson, B., Bell, R.A., Eriksson, K., and Nordlund, A. 1975, *Astron. Astrophys.*, **42**, 407.
- Gustaffson, B., Kjaeraard, P., and Andersen, S. 1974, *Astron. Astrophys.*, **34**, 99.
- Hack, M., and Struve, O. 1969, *Stellar Spectroscopy: Normal Stars* (Trieste: Osservatorio Astronomico).
- Hagen, H.J. 1984, *Diplom-Thesis*, Univ. of Hamburg.
- Hagen, H.J., Hempe, K., and Reimers, D. 1986, *Astron. Astrophys.* submitted.
- Hagen, H.J., Hempe, K., and Reimers, D. 1987, *Astron. Astrophys.*, **184**, 256.
- Hagen, W., Humphreys, R.M., and Stencel, R.E. 1981, *Pub. Astron. Soc. Pacific*, **93**, 567.
- Haisch, B.M., Linsky, J., and Basri, G.S. 1980, *Astrophys. J.*, **235**, 519.
- Haisch, B.M., and 12 others, 1981, *Astrophys. J.*, **245**, 1009.

- Hall, D.S. 1976, in *Multiple Periodic Variable Stars*, IAU Coll. No. 29, ed. W.S. Fitch (Dordrecht: Reidel).
- Hall, D.S. 1978, *Astron. J.*, **83**, 1469.
- Hall, D.S. 1981, in *Solar Phenomena in Stars and Stellar Systems*, eds. R.M. Bonnet and A.K. Dupree (Dordrecht: Reidel), p. 431.
- Hallum, K.L., and Wolf, C.L. 1981, *Astrophys. J. Lett.*, **248**, L73.
- Hanson, R.B., Jones, B.F., and Lin, D. 1983, *Astrophys. J.*, **270**, L27.
- Haro, G. 1976, *Bol. inst. Tonantzintla*, **2**, 3.
- Haro, G., and Herbig, G. 1954, *Bol. obs. Tonant. y Tac.*, **2**, 33.
- Haro, G., Iriarte, B., and Chavira, E. 1953, *Bol. obs. Tonant. y Tac.*, **8**, 3.
- Harris, D.L., III, Strand, K. Aa., and Worley, C.E. 1963, in *Basic Astronomical Data*, ed. K. Aa. Strand (Chicago: Univ. Chicago Press), p. 273.
- Hartmann, L. 1981, *Solar Phenomena in Stars and Stellar Systems*, eds. Bonnet and Dupree (Dordrecht: Reidel), p. 487.
- Hartmann, L. 1982, *Astrophys. J. Supp.*, **48**, 109.
- Hartmann, L., and Avrett, E.H. 1984, *Astrophys. J.*, **284**, 238.
- Hartmann, L., Avrett, E.H., and Edwards, S. 1982, *Astrophys. J.*, **261**, 279.
- Hartmann, L., Bopp, B.W., Dussault, M., Noah, P.V., and Klimke, A. 1981, *Astrophys. J.*, **249**, 662.
- Hartmann, L., Dupree, A.K., and Raymond, J.C. 1980, *Astrophys. J. Lett.*, **236**, L143.
- Hartmann, L., Dupree, A.K., and Raymond, J.C. 1981, *Astrophys. J.*, **246**, 193.
- Hartmann, L., Dupree, A.K., and Raymond, J.C. 1982, *Astrophys. J.*, **252**, 214.
- Hartmann, L., Edwards, S., and Avrett, E.H. 1981, *Astrophys. J.*, **261**, 279.
- Hartmann, L., Jordan, C., Brown, A., and Dupree, A.K. 1985, *Astrophys. J.*, **296**, 576.
- Hartmann, L., and Kenyon, S.J. 1985, *Astrophys. J.*, **299**, 462.
- Hartmann, L., Londono, C., and Phillips, M.J. 1979, *Astrophys. J.*, **229**, 183.
- Hartmann, L., and MacGregor, K. 1980, *Astrophys. J.*, **242**, 260.
- Hartmann, L., and Noyes, R. 1987, *Ann. Rev. Astron. Astrophys.*, **25**, 271.
- Hartmann, L., and Rosner, R. 1979, *Astrophys. J.*, **230**, 802.
- Harvey, P.M., Thronson, H.A., and Gatley, I. 1979, *Astrophys. J.*, **231**, 115.
- Hayes, D.S. 1970, *Astrophys. J.*, **159**, 165.
- Hayes, D.S. 1978, in *The HR Diagram*, IAU Symp. No. 80, eds. A.G.D. Philip and D.S. Hayes (Dordrecht: Reidel), p. 65.
- Hayes, D.S. 1979, *Dudley Obs. Rept. No. 14*, p. 223.
- Hayes, D.S. 1981, *Pub. Astron. Soc. Pacific*, **93**, 752.
- Hayes, D.S., and Latham, D. 1975, *Astrophys. J.*, **197**, 593.
- Hayes, D.S., Latham, D., and Hayes, S.N. 1975, *Astrophys. J.*, **197**, 587.
- Hearn, A. 1975, *Astron. Astrophys.*, **40**, 355.

- Hearnshaw, J.B. 1976a, *Astron. Astrophys.*, **51**, 85.
- Hearnshaw, J.B. 1976b, *Astron. Astrophys.*, **51**, 85.
- Hearnshaw, J.B. 1978, *Astron. J.*, **83**, 1531.
- Heidmann, N., and Thomas, R.N. 1981, *Astron. Astrophys.*, **87**, 36.
- Hempe, K. 1982, *Astron. Astrophys.*, **115**, 133.
- Hempe, K. 1983, *Astron. Astrophys. Supp. Ser.*, **53**, 339.
- Hempe, K. 1984, *Astron. Astrophys. Supp. Ser.*, **56**, 115.
- Hempe, K., and Reimers, D. 1982a, *Astron. Astrophys.*, **107**, 36.
- Hempe, K., and Reimers, D. 1982b, *Third European IUE Conference ESA SP-176*, p. 339.
- Herbig, G.H. 1954, *Astrophys. J.*, **119**, 483.
- Herbig, G.H. 1957, *Astrophys. J.*, **128**, 259.
- Herbig, G.H. 1958, *Mem. Roy. Soc. Soc. Liege*, (4), **20**, 251.
- Herbig, G.H. 1962, *Adv. Astron. Astrophys. I*, ed. Z. Kopal (New York: Academic Press), p. 47.
- Herbig, G.H. 1970, *Mem. Roy. Soc. Soc. Liege, Ser. 5*, **9**, 13.
- Herbig, G.H. 1977a, *Astrophys. J.*, **214**, 747.
- Herbig, G.H. 1977b, *Astrophys. J.*, **217**, 693.
- Herbig, G.H. 1985, *Naissance et enfance des étoiles*, eds. Lucas et al. (Amsterdam: North-Holland), p. 535.
- Herbig, G.H., and Goodrich, R.W. 1986, *Astrophys. J.*, **309**, 294.
- Herbig, G.H., and Jones, B.F. 1981, *Astron. J.*, **86**, 1232.
- Herbig, G.H., and Kuhl, L.V. 1963, *Astrophys. J.*, **137**, 398.
- Herbig, G.H., and Rao, N.K. 1972, *Astrophys. J.*, **174**, 401.
- Herbig, G.H., and Soderblom, D.B. 1980, *Astrophys. J.*, **242**, 628.
- Herbig, G.H., and Spalding, J.F., Jr. 1955, *Astrophys. J.*, **121**, 118.
- Herbig, G.H., Vrba, F.J., and Rydgren, A. 1986, *Astron. J.*, **91**, 575.
- Herbst, W., *Pub. Astron. Soc. Pacific*, **98**, 1088.
- Herbst, W., Holtzman, J., and Klasky, R. 1983, *Astron. J.*, **88**, 1648.
- Herbst, W., and Stine, P.C. 1984, *Astron. J.*, **89**, 1716.
- Herbst, W., and 8 others, 1986, *Astrophys. J.*, **310**, L71.
- Heyvaerts, J. 1974, *Astron. Astrophys.*, **37**, 65.
- Heyvaerts, J., and Priest, E. 1984, *Astron. Astrophys.*, **137**, 63.
- Hill, H., Bos, R.J., and Goode, P.R. 1982, *Phys. Rev. Lett.*, **49**, 1794.
- Hill, H., and Dziembowski, W. 1980, *Non-radial and Non-linear Stellar Pulsation* (New York: Springer).
- Hiltner, W.A., and Iriarte, B. 1958, *Astrophys. J.*, **127**, 510.
- Hobbs, R.W., Kondo, Y., and Feibelman, W.A. 1978, *Astron. J.*, **83**, 1525.

- Hoffmeister, C. 1957, in *Non-Stable Stars*, ed. G.H. Herbig (Cambridge: Cambridge Univ. Press), p. 22.
- Hoffmeister, C. 1958, *Veroff. Sonneberg*, **3**, 339.
- Hollars, D., and Beebe, H. 1976, *Pub. Astron. Soc. Pacific*, **88**, 934.
- Hollweg, J.V. 1974, *J. Geophys. Res.*, **79**, 1539.
- Holtzmann, J.A., Herbst, W., and Booth, J. 1986, *Astron. J.*, **92**, 1387.
- Holweger, H., Gehlsen, M., and Ruland, F. 1978, *Astron. Astrophys.*, **70**, 537.
- Honeycutt, R.K., Bernat, A.P., Kephart, J.E., Gow, C.E., Sanford, M.P., and Lambert, D.L. 1980, *Astrophys. J.*, **239**, 565.
- Hood, A.W., Priest, E. 1979, *Astron. Astrophys.*, **77**, 233.
- Houk, N., Irvine, N.J., and Rosenbush, D. 1974, *An Atlas of Objective-Prism Spectra* (Ann Arbor: Univ. Michigan).
- Howard, R.F. 1959, *Astrophys. J.*, **130**, 193.
- Howard, R.F. 1971, (ed): *Solar Magnetic Fields*, IAU Symp. 43 (Dordrecht: Reidel).
- Howard, R.F. 1975, *Sci. Am.*, 232, No. 4, 106.
- Howard, R.F. 1978, *Rev. Geophys. Space Phys.*, **16**, 721.
- Howard, R.F., and Harvey, J. 1970, *Solar Phys.*, **12**, 23.
- Howard, R.F., and LaBonte, B.J. 1983, IAU Symp. No. 102, *Solar and Stellar Magnetic Fields: Origins and Coronal Effects*, ed. J.O. Stenflo (Dordrecht: Reidel), p. 101.
- Hoyle, F., and Schwarzschild, M. 1955, *Astrophys. J. Supp.*, **2**, 1.
- Hoyle, F., and Wilson, O. 1958, *Astrophys. J.*, **128**, 604.
- Huang, S.-S. 1953, *Astrophys. J.*, **118**, 285.
- Huang, S.-S. 1966, *Ann. Rev. Astron. Astrophys.*, **4**, 35.
- Huang, S.-S. 1967a, *Astrophys. J.*, **150**, 229.
- Huang, S.-S. 1967b, *Astron. J.*, **72**, 804.
- Huang, S.-S., and Struve, O. 1953, *Astrophys. J.*, **118**, 463.
- Huang, S.-S., and Struve, O. 1954, *Ann. d'Ap.*, **17**, 85.
- Huang, S.-S., and Struve, O. 1960, in *Stellar Atmospheres*, ed. J.L. Greenstein (Chicago: Univ. Chicago Press), p. 321.
- Hubený, I. 1981a, *Bull. Astron. Inst. Czechoslovakia*, **32**, 271.
- Hubený, I. 1981b, *Astron. Astrophys.*, **100**, 314.
- Hudson, H.S., and Willson, R.C. 1981, in *The Physics of Sunspots*, eds. L.E. Cram and J.H. Thomas (Sacramento: Sacramento Peak Obs.), p. 434.
- Hundt, E. 1973, *Astron. Astrophys.*, **29**, 17.
- Hunger, K., and Kron, G.E. 1957, *Pub. Astron. Soc. Pacific*, **69**, 347.
- Iben, I. 1965, *Astrophys. J.*, **144**, 968.
- Imhoff, C.L. 1977, *Astrophys. J.*, **214**, 773.
- Imhoff, C.L., and Giampapa, M.S. 1980a, in *The Universe in Ultraviolet Wavelengths: The First Two Years of IUE*, ed. R.D. Chapman (NASA), p. 185.
- Imhoff, C.L., and Giampapa, M.S. 1980b, *Astrophys. J. Lett.*, **239**, L115.

- Imhoff, C.L., and Mendoza, E.E. 1974, *Rev. Mex. Astron. Astrof.*, **1**, 25.
- Ionson, J.A. 1982, *Astrophys. J.*, **254**, 318.
- Ionson, J.A. 1983, *Astrophys. J.*, **271**, 778.
- Ionson, J.A. 1984, *Astrophys. J.*, **276**, 357.
- Iriarte, B., Johnson, H.L., Mitchell, R.I., and Wisniewski, W.K. 1965, *Sky and Telescope*, **30**, 21.
- Ishchenko, I.M. 1937, *Variable Stars*, **16**, 157.
- Jacques, S.A. 1977, *Astrophys. J.*, **215**, 942.
- Jacques, S.A. 1978, *Astrophys. J.*, **226**, 632.
- Jebsen, D.E., and Mitchell, W.E. 1978, *Solar Phys.*, **57**, 309.
- Jefferies, J. 1968, *Spectral Line Formation* (Waltham: Blaisdel).
- Johnson, H.L., and Harris, D.L., III, 1954, *Astrophys. J.*, **120**, 196.
- Johnson, H.L., and Morgan, W.W. 1953, *Astrophys. J.*, **117**, 313.
- Johnson, H.M. and 16 others 1981, *Astrophys. J.*, **245**, 163.
- Johnson, M. 1953, *Observatory*, **73**, 109.
- Johnstone, R.M., and Penston, M. 1986, *Mon. Not. Roy. Astron. Soc.*, **219**, 927.
- Jordan, C., and Brown, A. 1981, *Solar Phenomena in Stars and Stellar Systems*, eds. Bonnet and Dupree (Dordrecht: Reidel), p. 199.
- Jordan, C., de Ferraz, N.C., and Brown, A. 1982, *Proc. 3rd European IUE Conf.*, ESA Publ. ESA-SP 176, p. 83.
- Jordan, S.D. 1969, *The Temperature Distribution in the Solar Chromosphere*, NASA TR R-291.
- Jordan, S.D. 1981, *The Sun as a Star*, ed. S.D. Jordan, NASA SP-450.
- Joy, A.H. 1942, *Pub. Astron. Soc. Pacific*, **54**, 15.
- Joy, A.H. 1945, *Astrophys. J.*, **102**, 168.
- Joy, A.H. 1949, *Astrophys. J.*, **110**, 424.
- Karp, A.H., and Fillmore, J.A. 1980, *Astrophys. J.*, **236**, 294.
- Kato, S. 1968, *Pub. Astron. Soc. Japan*, **20**, 59.
- Kearns, M. 1979, *Solar Phys.*, **62**, 393.
- Keenan, P.C. 1963, in *Basic Astronomical Data* (Chicago: Univ. Chicago Press), p. 78.
- Keil, S.L. 1980, *Astrophys. J.*, **237**, 1024.
- Keil, S.L., and Canfield, R.C. 1978, *Astron. Astrophys.*, **70**, 169.
- Keil, S.L., and Cram, L.E. 1978, *Bull. American Astron. Soc.*, **10**, 638.
- Keil, S.L., and Yackovich, F.H. 1981, *Solar Phys.*, **69**, 213.
- Kelch, W.L., Linsky, J.L., Basri, G.S., Chin, H.-Y., Chang, S.-H., Maran, S.P., and Furenlid, I. 1978, *Astrophys. J.*, **220**, 962.
- Kelch, W.L., Linsky, J., and Worden, S. 1979, *Astrophys. J.*, **229**, 700.
- Kenyon, S., and Hartmann, L. 1987, *Astrophys. J.*, **312**, 243.
- Kharitonov, A.V. 1963, *Soviet Astron.*, **7**, 258.

- Kimble, R.A., Kahn, S.M., and Bowyer, S. 1981, *Astrophys. J.*, **251**, 585.
- Kippenhahn, R. 1973, in *Stellar Chromospheres*, eds. S.D. Jordan and E. Avrett, NASA SP 317, p. 265.
- Kiuper, G. 1953, (ed.) *The Sun* (Chicago: Chicago University Press).
- Klyachkov, L.L., and Shevaschenko, V.S. 1976, *Pisma Astron. Zur.*, **2**, 494.
- Klyees, I.A., and Lobaser, I.I. 1975, *Variable Stars*, **20**, 13.
- Kolotilov, A.E. 1986, *Soviet Astron.*, **30**, 398.
- Kondo, Y., Modisette, J.L., and Wolf, J.G. 1975, *Astrophys. J.*, **199**, 110.
- Korotin, S.A., and Krasnobabtsev, V.I. 1986, *Bull. Crim. Astr. Obs.*, **75**, 166.
- Kostyk, R.I., and Gerbil'skaya, I.M. 1976, *Astron. Zh.*, **53**, 1244 *Soviet Astron. AJ*, **20**, 704.
- Kraft, R.P. 1965, *Astrophys. J.*, **142**, 681.
- Kraft, R.P. 1967, *Astrophys. J.*, **150**, 551.
- Kraft, R.P. 1968, in *Stellar Astronomy*, eds. H.U. Chiu, R. Narasila, and J. Remo (New York: Gordon and Breach), Chap. IV-1.
- Kraft, R.P. 1970, in *Spectroscopic Astrophysics*, ed. G.H. Herbig (Berkeley: Univ. Calif. Press), p. 385.
- Kraft, R.P., Preston, G.W., and Woolf, S.C. 1964, *Astrophys. J.*, **140**, 235.
- Krause, F., and Rädler, K.H. 1980, *Mean-field Magnetohydrodynamics and Dynamo Theory* (Pergamon: Oxford).
- Krautter, J., and Bastian, U. 1980, *Astron. Astrophys.*, **88**, L6.
- Kron, G.E. 1950, *Astron. J.*, **55**, 69.
- Krzeminski, W. 1968, in *Low Luminosity Stars*, ed. S.S. Kumar (London: Gordon and Breach), p. 57.
- Ku, W., and Chanan, G. 1979, *Astrophys. J. Lett.*, **234**, 159.
- Kuan, P. 1975, *Astrophys. J.*, **202**, 425.
- Kuan, P. 1976, *Astrophys. J.*, **210**, 120.
- Kudritzki, R., and Reimers, D. 1978, *Astron. Astrophys.*, **70**, 227.
- Kuhi, L.V. 1964a, *Astron. Astrophys. Supp.*, **15**, 47.
- Kuhi, L.V. 1964b, *Astrophys. J.*, **140**, 1409.
- Kuhi, L.V. 1970, in *Evolution Stellaire avant la Sequence Principale* (Universite de Liege), 295.
- Kuhi, L.V. 1974, *Astron. Astrophys. Supp.*, **15**, 47.
- Kuhi, L.V. 1983, *Pub. Astron. Soc. Pacific*, **95**, 591.
- Kulsrud, R. 1955, *Astrophys. J.*, **121**, 461.
- Kuperus, M., Ionson, J.A., and Spicer, D.S. 1981, *Ann. Rev. Astron. Astrophys.*, **19**, 7.
- Kurucz, R. 1979, *Astrophys. J. Supp.*, **40**, 1.
- Kurucz, R., and Avrett, E.H. 1981, *SAO Special Report No. 391*.
- Kurucz, R., and Peyremann, E. 1975, *Smithsonian Astrophys. Obs. Spec. Rep.*, **387**, 1.
- Labeyrie, A. 1982, *Sky and Telescope*, **63**, 334.

- LaBonte, B. 1982, *Astrophys. J.*, **260**, 647.
- Lada, C.J. 1985, *Ann. Rev. Astron. Astrophys.*, **23**, 267.
- Lago, M.T.V.T., Penston, M., and Johnstone, R. 1985, *Mon. Not. Roy. Astron. Soc.*, **212**, 151.
- Lambert, D., Hall, D., and Hinkle, K. 1981, *Astrophys. J.*, **248**, 638.
- Lambert, D., and Luck, R.E. 1978, *Mon. Not. Roy. Astron. Soc.*, **184**, 405.
- Lamzin, S.A. 1985, *Soviet Astron.*, **29**, 176.
- Landstreet, J.D. 1969, *Pub. Astron. Soc. Pacific*, **81**, 896.
- Layzer, D., Rosner, R., and Doyle, H.T. 1979, *Astrophys. J.*, **229**, 1126.
- Ledoux, P., and Walraven, T. 1958, *Handbuch der Physik*, Vol. 51, 353.
- Leibacher, J., Gouttebroze, P., and Stein, R. 1982, *Astrophys. J.*, **258**, 393.
- Leibacher, J., and Stein, R. 1971, *Astrophys. J. Lett.*, **7**, 191.
- Leibacher, J., and Stein, R. 1981, *The Sun as a Star*, NASA SP-450, ed. S.D. Jordan, p. 263.
- Leighton, R.B. 1959, *Astrophys. J.*, **130**, 366.
- Leighton, R.B. 1961, in *Aerodynamic Phenomena in Stellar Atmospheres*, IAU Symp. No. 12, ed., R.N. Thomas (Nuovo Cimento Supp. 22, Ser. 10, No. 1), p. 321.
- Leighton, R.B. 1969, *Astrophys. J.*, **156**, 1.
- Leighton, R.B., Noyes, R.W., and Simon, G.W. 1962, *Astrophys. J.*, **135**, 474.
- Levine, R. 1974, *Astrophys. J.*, **190**, 457.
- Levine, R. and Altschuller, M.D. 1974, *Solar Phys.*, **36**, 345.
- Lighthill, M. 1952, *Proc. Roy. Soc. London*, **A211**, 564.
- Liller, W. 1968, *Astrophys. J.*, **151**, 589.
- Linsky, J.L. 1980, *Ann. Rev. Astron. Astrophys.*, **18**, 439.
- Linsky, J.L. 1981a, *Ann. Rev. Astron. Astrophys.*, **18**, 439.
- Linsky, J.L. 1981b, in *X-ray Astronomy in the 1980's*, ed. S.S. Holt, NASA TR 83848, p. 13.
- Linsky, J.L. 1983, in *Activity in Red Dwarf Stars*, eds. P. Byrne and M. Rodono (Dordrecht: Reidel), p. 33.
- Linsky, J.L. 1984a, in *Cool Stars, Stellar Systems and the Sun*, eds. S. Baliunas and L. Hartmann (Berlin: Springer-Verlag), p. 244.
- Linsky, J.L. 1984b, in *Third Trieste Meeting: Relations Between Chromospheric Heating and Mass Loss in Stars*, eds. R. Stalio and J. Zirker (Sunspot: National Solar Observatory).
- Linsky, J.L., and Ayres, T.R. 1978, *Astrophys. J.*, **220**, 619.
- Linsky, J.L., and Haisch, B.M. 1979, *Astrophys. J. Lett.*, **229**, L27.
- Linsky, J.L., Hunten, D.M., Sowell, R., Glackin, D.L., and Kelch, W.L. 1979b, *Astrophys. J. Supp.*, **41**, 481.
- Linsky, J.L., and Marstad, N. 1981 in *The Universe at Ultraviolet Wavelengths*, NASA CP-2171, p. 287.

- Linsky, J.L. et al., 1978, *Nature*, **275**, 389.
- Linsky, J.L., Worden, S.P., McClintock, W., and Robertson, R.M. 1979a, *Astrophys. J. Supp.*, **41**, 47.
- Lites, B. 1973, *Solar Phys.*, **32**, 283.
- Lites, B., and Cowley, C. 1974, *Astron. Astrophys.*, **31**, 361.
- Livingston, W.C. 1982, *Nature*, **297**, 208.
- Livingston, W.C. 1983, in IAU Symp. No. 102, *Solar and Stellar Magnetic Fields: Origins and Coronal Effects*, ed. J.O. Stenflo (Dordrecht: Reidel), p. 149.
- Low, B.C. 1982, *Astrophys. J.*, **254**, 796.
- Low, F.J., and Smith, F. 1966, *Nature*, **212**, 675.
- Lub, J., and Pel, J.W. 1979, *Dudley Obs. Rept. No. 14*, p. 481.
- Lucas, R., Omont, A., and Stora, R. 1985, *Birth and Infancy of Stars* (North Holland).
- Luck, R.E. 1977, *Astrophys. J.*, **218**, 752.
- Luck, R.E. 1982, *Astrophys. J.*, **256**, 177.
- Lüst, R. 1965, *Stellar and Solar Magnetic Fields*, IAU Symp. 22 (North Holland: Amsterdam).
- Lutz, P.E., and Pagel, B.E.J. 1982, *Mon. Not. Roy. Astron. Soc.*, **199**, 1101.
- Lynds, C.R., Worden, S.P., and Harvey, J.W. 1976, *Astrophys. J.*, **207**, 174.
- MacGregor, K.B., and Pizzo, V.J. 1983, *Astrophys. J.*, **267**, 340.
- Mackle, R., Holweger, H., Griffin, R., and Griffin, R., 1975, *Astron. Astrophys.*, **38**, 239.
- Magnan, C. 1979, *Astron. Astrophys.*, **72**, 18.
- Mandy, K., and Pratt, N. 1972, *Astrophys. and Space Sci.*, **1**.
- Marcy, G.W. 1980, *Bull. American Astron. Soc.*, **12**, 834.
- Marcy, G.W. 1981, *Astrophys. J.*, **245**, 624.
- Marcy, G.W. 1982, *Pub. Astron. Soc. Pacific*, **94**, 989.
- Marcy, G.W. 1984, *Astrophys. J.*, **276**, 286.
- Marcy, G.W., and Bruning, D.H. 1984, *Astrophys. J.*, **281**, 286.
- Marcy, G.W., Duncan, D.K., and Cohen, R.D. 1985, *Astrophys. J.*, **288**, 259.
- Marstad, N. 1983, unpublished MSC thesis, University of Colorado.
- Marstad, N., Linsky, J.L., Simon, T., Rodono, M., Blanco, C., Catalano, S., Marilli, E., Andrews, A.D., Butler, C.J., and Byrne, P.B. 1982, in *Advances in Ultraviolet Astronomy: Four Years of IUE Research*, NASA CP-2238, p. 544.
- Martin, P. 1977, *Astron. Astrophys.*, **61**, 591.
- Mattig, W. 1980, *Astron. Astrophys.*, **83**, 129.
- Mattig, W., and Schlebbe, H. 1974, *Solar Phys.*, **34**, 299.
- Mauron, N., Fort, B., Querci, F., Dreux, M., Fauconnier, T., and Larry, P. 1984, *Astron. Astrophys.*, **130**, 341.
- McClintock, W., Henry, R.C., Moos, H.W., and Linsky, J.L. 1975, *Astrophys. J.*, **202**, 733.

- McClure, R.D. 1976, *Astron. J.*, **81**, 182.
- McClure, R.D., and Forrester, W.T. 1981, *Pub. Dominion Ap. Obs., Victoria*, **15**, 439.
- McClure, R.D., and van den Bergh, S. 1968, *Astron. J.*, **73**, 313.
- McCrea, W. 1929, *Mon. Not. Roy. Astron. Soc.*, **89**, 483, and 718.
- McLaughlin, D.B. 1924, *Astrophys. J.*, **60**, 22.
- McMath, R., Mohler, O., Pierce, A., and Goldberg, L. 1956, *Astrophys. J.*, **124**, 1.
- McNally, D. 1966, *Observatory*, **85**, 166.
- Meadows, A.J. 1966, *Early Solar Physics* (New York: Pergamon), p. 32.
- Meggers, W.F. 1953, *Encyclopedia Britannica*, **23**, 940.
- Melrose, D. 1980, *Plasma Astrophysics: Non-thermal Processes in Diffuse Magnetized Plasmas*, in 2 volumes (New York: Gordon and Breach).
- Mendoza, E.E. 1966, *Astrophys. J.*, **143**, 1010.
- Mendoza, E.E. 1968, *Astrophys. J.*, **151**, 977.
- Mendoza, E.E., Firmani, C., and Haro, G. 1985, *Inf. Bull. Var. Stars*, No. 2817.
- Menzel, D.H. 1939, *Proc. American Phil. Soc.*, **81**, 107.
- Mestel, L. 1968, *Mon. Not. Roy. Astron. Soc.*, **138**, 359.
- Mestel, L. 1984, in *Cool Stars, Stellar Systems and the Sun*, eds. S.L. Baliunas and L. Hartmann (Berlin: Springer-Verlag), p. 49.
- Mew, R., Schrijver, C.J., Zwaan, C. 1981, *Space Sci. Rev.*, **30**, 191.
- Mew, R. 1979, *Space Sci. Rev.*, **24**, 101.
- Micela, G., Serio, S., Vaiana, G.S., and Golub, L. 1982, *Bull. American Astron. Soc.*, **14**, 891.
- Middelkoop, F. 1981, *Astron. Astrophys.*, **101**, 295.
- Middelkoop, F. 1982, *Astron. Astrophys.*, **107**, 31.
- Middelkoop, F., and Zwaan, C. 1981, *Astron. Astrophys.*, **101**, 26.
- Mielbrecht, R.A., and Young, A. 1981, *Pub. Astron. Soc. Pacific*, **93**, 549.
- Mihalas, B. 1981, unpublished Ph.D. Thesis (Boulder: Univ. Colorado).
- Mihalas, D. 1974, *Astron. J.*, **79**, 1111.
- Mihalas, D. 1978, *Stellar Atmospheres*, 2nd. ed. (San Francisco: W.H. Freeman).
- Milne, E. 1922, *Phil. Trans. Roy. Soc. London*, **A223**, 201.
- Milne, E. 1924, *Mon. Not. Roy. Astron. Soc.*, **85**, 111.
- Minnaert, M. 1953, in *The Sun*, ed. Kuiper (Chicago: Univ. of Chicago Press), p. 88.
- Moffat, H.K. 1978, *Magnetic Field Generation in Electrically Conducting Fluids* (Cambridge: Cambridge Univ. Press).
- Moffett, T.J., and Barnes, T.G., III 1979, *Pub. Astron. Soc. Pacific*, **91**, 180.
- Molchanov, S.A., Ruzmaikin, A.A., and Sokolov, D.D. 1985, *Soviet Phys. Usp.*, **28**, 307.

- Montgomery, D., and Tidman, D. 1964, *Plasma Kinetic Theory* (New York: McGraw-Hill).
- Montmerle, T., Koch, L., Falgarone, E., and Grindlay, J.E. 1984, *Phys. Scr.*, **T7**, 59.
- Montmerle, T., Koch-Miramond, L., Falgarone, E., and Grindlay, J.E. 1983, *Astrophys. J.*, **269**, 182.
- Moore, D. 1981, *The Sun as a Star*, ed. S.D. Jordan, NASA SP-450, p. 253.
- Morgan, W.W., Abt, H.A., and Tapscott, J.W. 1978, *Revised MK Spectral Atlas for Stars Earlier Than the Sun* (Chicago: Univ. Chicago Press and Tucson: Kitt Peak National Obs.).
- Morgan, W.W., and Keenan, P.C. 1973, *Ann. Rev. Astron. Astrophys.*, **11**, 29.
- Morgan, W.W., Keenan, P.C., and Kellman, E. 1943, *An Atlas of Stellar Spectra* (Chicago: Univ. Chicago Press).
- Moss, D., and Vilhu, O. 1983, *Astron. Astrophys.*, **119**, 47.
- Mould, J.R., and Wallis, R.E. 1977, *Mon. Not. Roy. Astron. Soc.*, **181**, 625.
- Mullan, D.J. 1975, *Astrophys. J.*, **198**, 563.
- Mullan, D.J. 1976, *Irish Astron. J.*, **12**, 161.
- Mullan, D.J. 1978, *Astrophys. J.*, **226**, 151.
- Mullan, D.J. 1980, in *Cool Stars, Stellar Systems and the Sun*, ed. A.K. Dupree, SAO Rep. No. 389, p. 189.
- Mullan, D.J., and Stencel, R.E. 1982, *Astrophys. J.*, **253**, 716.
- Müller, R., and Roudier, T. 1984, *The Hydro-magnetics of the Sun*, eds. T.D. Guyenne and J.J. Hunter (ESOTEC: Noordwijk), p. 51.
- Münch, G., Roesler, A., and Trauger, J. 1976, *Carnegie Yearbook 1975*, p. 283.
- Mundt, R. 1982, *Workshop on Cool Stars, Stellar Systems and the Sun*, eds. M.S. Giampapa and L. Golub, SAO Special Rep., **392**, 181.
- Mundt, R. 1984, *Astrophys. J.*, **280**, 749.
- Mundt, R., Appenzeller, I., Bertout, C., Chavarria, C., and Krautter, J. 1981, *Astron. Astrophys.*, **93**, 412.
- Mundt, R., Brugel, E., and Buhrki, T. 1987, *Astrophys. J.*, **319**, 275.
- Mundt, R., and Fried, J.W. 1983, *Astrophys. J. Lett.*, **274**, L83.
- Mundt, R., and Giampapa, M.S. 1982, *Astrophys. J.*, **256**, 156.
- Mundt, R., Walter, R.M., Feigelson, E.D., Finkenzeller, U., Herbig, C.H., and Odell, A.P. 1983, *Astrophys. J.*, **269**, 229.
- Mutel, R.L., and Weisberg, J.M. 1978, *Astron. J.*, **83**, 1499.
- Nadeau R., and Bastien, P. 1986, *Astrophys. J.*, **307**, L5.
- Nairai, K. 1969, *Astr. Space Sci.*, **3**, 150.
- Nakada, M. 1970, *Solar. Phys.*, **14**, 457.
- Neckel, H., and Labs, D. 1973, in *Problems of Calibration of Absolute Magnitudes and Temperatures of Stars*, IAU Symp. No. 54, eds. B. Hauck and B.E. Westerlund (Dordrecht: Reidel), p. 149.
- Neidig, D.F. 1983, *Solar Phys.*, **85**, 285.

- Nelson, G. 1980, *Astrophys. J.*, **238**, 659.
- Nelson, G., and Musman, S. 1977, *Astrophys. J.*, **214**, 912.
- Nelson, G., and Musman, S. 1978, *Astrophys. J. Lett.*, **222**, L69.
- Neugebauer, M. 1983, in *Solar Wind Five*, NASA CP-2280, p. 135.
- Nha, I.-S., and Kang, Y.-W. 1982, *Pub. Astron. Soc. Pacific*, **94**, 496.
- Nissen, P.E., and Gustafson, B. 1978, in *Important Advances in Twentieth Century Astronomy* (Copenhagen: Strömrgren Symposium), p. 43.
- Nordlund, A. 1976, *Astron. Astrophys.*, **50**, 23.
- Nordlund, A. 1978, in *Astronomical Papers Dedicated to Bengt Strömrgren*, eds. A. Reiz and T. Andersen (Copenhagen: Copenhagen Univ. Obs.), p. 95.
- Nordlund, A. 1980, in *Stellar Turbulence*, IAU Coll. No. 51, eds. D.F. Gray and J.L. Linsky (Heidelberg: Springer-Verlag), p. 213.
- Nordlund, A. 1982, *Astron. Astrophys.*, **107**, 1.
- Nordlund, A. 1983, *Solar and Stellar Magnetic Fields*, ed. J.O. Stenflo (Dordrecht: Reidel), p. 79.
- November, L.J., Toomre, J., and Gebbie, K.B. 1981, *Astrophys. J. Lett.*, **245**, L123.
- Noyes, R.W. 1982, in *Second Cambridge Workshop on Cool Stars, Stellar Systems, and the Sun*, eds. M.S. Giampapa and L. Golub, SAO Special Report 392, Vol. II.
- Noyes, R.W. 1984 in *Advances in Space Research*, Cospar XXV Meeting.
- Noyes, R.W., Baliunas, S.L., Belserene, E., Duncan, D.K., Horne, J., and Widrow, L. 1984, *Astrophys. J. Lett.*, **285**, L23.
- Noyes, R.W., Hartmann, L.W., Baliunas, S.L., Duncan, D.K., and Vaughan, A.H. 1984, *Astrophys. J.*, **279**, 763.
- Noyes, R.W., and Kalkofen, W. 1970, *Solar Phys.*, **15**, 120.
- O'Brien, G.T., and Lambert, D. 1979, *Astrophys. J. Lett.*, **229**, L33.
- O'Brien, G.T. 1980, *Ph.D. Thesis*, University of Texas, Austin.
- Oinas, V. 1974, *Astrophys. J. Supp.*, **27**, 405.
- Oinas, V. 1977, *Astron. Astrophys.*, **61**, 17.
- Oke, J.B. 1964, *Astrophys. J.*, **140**, 889.
- Oke, J.B. 1965, *Ann. Rev. Astron. Astrophys.*, **3**, 23.
- Oke, J.B., and Greenstein, J.L. 1954, *Astrophys. J.*, **120**, 384.
- Oke, J.B., and Schild, R.E. 1970, *Astrophys. J.*, **161**, 1015.
- Osborne, W. 1979, *Dudley Obs. Rept. No. 14*, p. 115.
- Osherovich, V. 1982, *Solar Phys.*, **77**, 63.
- Oskanyan, V.S., Evans, D.S., Lacy, C., and McMillan, R.S. 1977, *Astrophys. J.*, **214**, 430.
- Osmer, P. 1972, *Astrophys. J. Supp.*, **24**, 255.
- Osterbrock, D.E. 1961, *Astrophys. J.*, **134**, 347.
- Owen, F.N., Jones, T.W., and Gibson, D.M. 1976, *Astrophys. J. Lett.*, **210**, L27.

- Oxenius, J. 1965, *J. Quant. Spec. Rad. Trans.*, **5**, 771.
- Pallavicini, R., Golub, L., Rosner, R., Vaiana, G.S., Ayres, T.K., and Linsky, J.L. 1981, *Astrophys. J.*, **248**, 279.
- Parenago, P.P. 1933, *Variable Stars*, **4**, 222.
- Parker, E.N. 1955, *Astrophys. J.*, **122**, 293.
- Parker, E.N. 1958, *Astrophys. J.*, **128**, 664.
- Parker, E.N. 1963a, *Interplanetary Dynamical Processes* (New York: Interscience).
- Parker, E.N. 1963b, *Astrophys. J.*, **138**, 552.
- Parker, E.N. 1975, *Astrophys. J.*, **198**, 205.
- Parker, E.N. 1979a, *Cosmical Magnetic Fields* (Oxford: Clarendon Press).
- Parker, E.N. 1979b, *Astrophys. J.*, **230**, 905.
- Parker, E.N. 1981, *Astrophys. J.*, **251**, 266.
- Parker, E.N. 1983, *Geophys. Astr. Fluid Dyn.*, **23**, 85.
- Parker, E.N., 1985, *Astrophys. J.*, **294**, 47.
- Payne, C. 1925, *Stellar Atmospheres* (Cambridge, Mass.: Harvard University Press).
- Payne-Gaposchkin, C. 1979, *Stars and Clusters* (Cambridge, Mass.: Harvard Univ. Press).
- Payne-Gaposchkin, C., and Gaposchkin, S. 1938, *Variable Stars* (Cambridge, Mass.: Harvard University Press).
- Pecker, J.C. 1965, *Ann. Rev. Astron. Astrophys.*, **3**, 135.
- Pecker, J.C., Praderie, F., and Thomas, R.N. 1973, *Astron. Astrophys.*, **29**, 289.
- Penston, M.V., and Lago, M.T.V.T. 1983, *Mon. Not. Roy. Astron. Soc.*, **202**, 77.
- Perrin, M.-N. 1975a, *Astron. Astrophys.*, **39**, 97.
- Perrin, M.-N. 1975b, *Astron. Astrophys.*, **44**, 9.
- Perrin, M.-N., Hejlesen, P.M., Cayrel de Strobel, G., and Cayrel, R. 1977, *Astron. Astrophys.*, **54**, 779.
- Peterson, R.C. 1981, *Astrophys. J. Lett.*, **248**, L31.
- Peterson, R.C., Tarbell, T.D., and Carney, B.W. 1983, *Astrophys. J.*, **265**, 972.
- Phillips, M.J., and Hartmann, L. 1978a, *Astrophys. J.*, **224**, 182.
- Phillips, M.J., and Hartmann, L. 1978b, *Astrophys. J.*, **250**, 327.
- Piddington, T.H. 1956, *Mon. Not. Roy. Astron. Soc.*, **116**, 314.
- Piddington, T.H. 1976, *Basic Mechanisms of Solar Activity*, eds. Bumba and Kleczek (Dordrecht: Reidel), p. 389.
- Plagemann, S. 1960, *Liege Colloq.*, **19**, 331.
- Plaskett, H. 1936, *Mon. Not. Roy. Astron. Soc.*, **96**, 402.
- Pneuman, G.W. 1980, *Solar Physics*, **65**, 369.
- Pneuman, G.W. and Kopp, R. 1977, *Astron. Astrophys.*, **55**, 305.
- Popper, D.M. 1947, *Astrophys. J.*, **105**, 204.
- Popper, D.M. 1978, *Astron. J.*, **83**, 1522.
- Popper, D.M. 1980, *Ann. Rev. Astron. Astrophys.*, **18**, 115.

- Poveda, A. 1967, *Astron. J.*, **72**, 824.
- Praderie, F. 1973, in *Stellar Chromospheres*, eds. S.D. Jordan and E.H. Avrett, NASA SP-317.
- Pravdjuk, L.M., Karpinsky, V.N., and Andreiko, A.V. 1974, *Solnechnye Dannye Bjulleten*, **2**, 70.
- Preston, G.W. 1971, *Astrophys. J.*, **164**, 309.
- Priest, E.R. 1984, *Solar Magnetohydrodynamics* (Dordrecht: Reidel)
- Pye, J.P., Evans, K.D., and 5 others, 1978, *Astron. Astrophys.*, **65**, 123.
- Radick, R.R., Hartmann, L., Mihalas, D., Worden, S.P., Africano, J.L., Klimke, A., and Tyson, E.T. 1982, *Pub. Astron. Soc. Pacific*, **94**, 934.
- Rajamohan, R. 1978, *Mon. Not. Roy. Astron. Soc.*, **184**, 743.
- Ramsey, L.W., and Nations, H.L. 1980, *Astrophys. J. Lett.*, **239**, L121.
- Reimers, D. 1973, *Astron. Astrophys.*, **24**, 79.
- Reimers, D. 1975a, *Mem. Roy. Soc. Sci. Liege*, 6th Ser., **8**, 369.
- Reimers, D. 1975b, in *Problems in Stellar Atmospheres and Envelopes*, eds. B. Baschek, W.H. Kegel, G. Traving, (Berlin: Springer-Verlag), p. 229.
- Reimers, D. 1976, in *Physique Du Mouvement Dans Les Atmospheres Stellaires*, International CNRS Colloq., Nice, p. 421.
- Reimers, D. 1977a, *Astron. Astrophys.*, **57**, 395.
- Reimers, D. 1977b, *Astron. Astrophys.*, **61**, 217 (Erratum 67, 161).
- Reimers, D. 1981, in *Physical Processes in Red Giants*, eds. I. Iben and A. Renzini (Dordrecht: Reidel), p. 269.
- Reimers, D. 1982, *Astron. Astrophys.*, **107**, 292.
- Reimers, D. 1984, *Astron. Astrophys.*, **136**, L5.
- Reimers, D. 1985, *Astron. Astrophys.*, **142**, L16.
- Reimers, D. 1987, in *Circumstellar Matter*, eds. I. Appenzeller and C. Jordan (Dordrecht: Reidel), p. 307-318.
- Reimers, D., Baade, R., Schröder, K.-P. 1989, *Astron. Astrophys.*, in press.
- Reimers, D., and Cassatella, A. 1985, *Astrophys. J.*, **297**, 275.
- Reimers, D., Che, A., and Hempe, K. 1981, in *Second Cambridge Workshop on Cool Stars, Stellar Systems and the Sun*, eds. M.S. Giampapa and L. Golub, SAO Special Report 392, Vol. I, p. 245.
- Reimers, D., Che-Bohnenstengel, A. 1986b, *Astron. Astrophys.*, **166**, 252.
- Reimers, D., and Kudritzki, R.P. 1980, *Second European IUE Conference*, ESA SP-157, p. 229.
- Reimers, D., and Schröder, K.P. 1983, *Astron. Astrophys.*, **124**, 241.
- Reipurth, B. 1985, *Astron. Astrophys.*, **143**, 435.
- Relyea, L.J., and Kurucz, R.L. 1978, *Astrophys. J. Supp.*, **37**, 45.
- Rengarajan, T.N. 1984, *Astrophys. J. Lett.*, **283**, L63.

- Renzini, A., Cacciari, C., Ulmschneider, R., and Schmitz, F. 1977, *Astron. Astrophys.*, **61**, 39.
- Rhodes, E.J., Jr., Ulrich, R.K., and Simon, G.W. 1977, *Astrophys. J.*, **218**, 901.
- Rhodes, E.J., Jr., Deubner, F.-L., Ulrich, R.K. 1979, *Astrophys. J.*, **227**, 629.
- Ridgway, S.T., and Friel, E.D. 1981, in *Effects of Mass Loss on Stellar Evolution*, eds. C. Chiosi and R. Stalio (Dordrecht: Reidel), p. 119.
- Ridgway, S.T., Joyce, R.R., White, N.M., and Wing, R.F. 1980, *Astrophys. J.*, **283**, 126.
- Roberts, P.H. 1967, *An Introduction to Magnetohydrodynamics* (London: Longmans)
- Roberts, P.H., and Soward, A. 1972, *Proc. Roy. Soc. London*, **A328**, 185.
- Robinson, R.D., Jr. 1980, *Astrophys. J.*, **239**, 961.
- Robinson, R.D., Worden, S.P., and Harvey, J.W. 1980, *Astrophys. J. Lett.*, **236**, L155.
- Roddiar, F. 1965, *Ann. d'Ap.*, **28**, 478.
- Rodono, M. 1983, in *Advances of Space Research*, 2, No. 9, p. 225.
- Rosendahl, J. 1970, *Astrophys. J.*, **160**, 627.
- Rosenwald, R., and Hill, H. 1980, in *Nonradial and Nonlinear Stellar Pulsation*, eds. Hill and Dziembowski (Berlin: Springer-Verlag), p. 404.
- Rosner, R., Tucker, W.H., and Vaiana, G.S. 1978, *Astrophys. J.*, **220**, 643.
- Ross, J., and Aller, L.H. 1968, *Astrophys. J.*, **153**, 235.
- Rosseland, S. 1936, *Theoretical Astrophysics* (Oxford: Clarendon Press).
- Rosseland, S. 1949, *The Pulsation Theory of Variable Stars* (Oxford: Clarendon Press).
- Rossiter, R.A. 1924, *Astrophys. J.*, **60**, 15.
- Roxburgh, I. 1983, *Solar and Stellar Magnetic Fields*, ed. J.O. Stenflo (Dordrecht: Reidel), p. 449.
- Rucinski, S.M. 1977, *Pub. Astron. Soc. Pacific*, **89**, 280.
- Rucinski, S.M. 1979, *Acta Astron.*, **29**, 203.
- Rucinski, S.M. 1980, *Acta Astron.*, **30**, 323.
- Rucinski, S.M. 1985, *Astron. J.*, **90**, 2321.
- Rufener, F. 1979, *Dudley Obs. Rept. No. 14*, p. 443.
- Rufener, F., and Maeder, A. 1971, *Astron. Astrophys. Supp.*, **4**, 43.
- Ruland, F., Holweger, H., Griffin, R., Griffin, R., and Biehl, D. 1980, *Astron. Astrophys.*, **92**, 70.
- Russell, H. 1933, *The Composition of the Stars* (Oxford: Clarendon Press).
- Russell, H., Payne-Gaposchkin, C., and Menzel, D. 1935, *Astrophys. J.*, **81**, 107.
- Rutten, R.G.M. 1986, *Astron. Astrophys.*, **159**, 291.
- Rutten, R.G.M. 1987, *Astron. Astrophys.*, **177**, 131.
- Rutten, R.G.M. and Pylyser, E. 1988, *Astron. Astrophys.*, **191**, 227.
- Rutten, R.J., Hoynig, P., and de Jager, C. 1974, *Solar Phys.*, **38**, 321.
- Rydgren, A.E., Schmelz, J.T., and Vrba, F.J. 1982, *Astrophys. J.*, **256**, 168.

- Rydgren, A.E., Schmelz, J.T., Zak, D., and Vrba, F. 1984a, *Publ. U.S. Naval Obs.*, **25**, Part 1.
- Rydgren, A.E., Strom, S.E., and Strom, K.M. 1976, *Astrophys. J. Supp.*, **30**, 307.
- Rydgren, A.E., and Vrba, F.J. 1981, *Astron. J.*, **86**, 1069.
- Rydgren, A.E., and Vrba, F.J. 1983a, *Astron. J.*, **88**, 1017.
- Rydgren, A.E., and Vrba, F.J. 1983b, *Astrophys. J.*, **267**, 191.
- Rydgren, A.E., Zak, D.S., Vrba, F.J., Chugainov, P.F., and Zajtseva, G.V. 1984b, *Astron. J.*, **89**, 1015.
- Sá, C., Penston, M.V., and Lago, L. 1986, *Mon. Not. Roy. Astron. Soc.*, **222**, 213.
- Saar, S.H., and Linsky, J.F. 1985, *Astrophys. J.*, **299**, L47.
- Sack, N. 1966, *Ann. d'Ap.*, **29**, 633.
- Sacotte, D., and Bonnet, R. 1972, *Astron. Astrophys.*, **17**, 60.
- Saijo, K., Saito, M. 1977, *Pub. Astron. Soc. Japan*, **29**, 739.
- Sampson, D. 1965, *Radiative Contributions to Energy and Momentum Transport in a Gas* (New York: Interscience).
- Sargent, W.L.W. 1961, *Astrophys. J.*, **134**, 142.
- Savonije, G.J., and Papaloizou, J.C.B. 1985, in *Interacting Binaries*, eds. P.P. Eggleton and J.E. Pringle (Dordrecht: Reidel), p. 83.
- Scalo, J.M., Dominy, J.F., and Pumphrey, W.A. 1978, *Astrophys. J.*, **221**, 616.
- Schaefer, B.E. 1983, *Astrophys. J. Lett.*, **266**, L45.
- Schatzman, E. 1949, *Ann. d'Ap.*, **12**, 203.
- Schatzman, E. 1962, *Ann. d'Ap.*, **25**, 18.
- Schatzman, E. 1965, in *Stellar and Solar Magnetic Fields*, ed. R. Lüst, IAU Symp. No. 22, p. 153.
- Scherrer P.H., Wilcox, J.M., and Svalgaard, L. 1980, *Astrophys. J.*, **241**, 811.
- Schlüter, A., and Temesvary, S. 1958, in *Electromagnetic Phenomena In Cosmical Physics*, ed. B. Lehnert, IAU Symp., **6**, 263.
- Schmelz, J.T. 1984, *Astron. J.*, **89**, 108.
- Schmitt, J.H.M.M., Golub, L., Harndon, K.F., Maxon, C., and Vaiana, G. 1983, *Bull. American Astron. Soc.*, **15**, 673.
- Schröder, K.P. 1983, *Astron. Astrophys.*, **124**, L16.
- Schröder, K.P. 1985a, *Astron. Astrophys.*, **147**, 103.
- Schröder, K.P. 1985b, *Ph.D. Thesis*, Univ. of Hamburg.
- Schröder, K.P., and Che-Bohnenstengel, A. 1985, *Astron. Astrophys.*, **151**.
- Schröter, E.H. 1957, *Zeit. f. Astrophys.*, **41**, 141.
- Schröter, E.H., and Wöhl, H. 1978, in *Workshop on Solar Rotation*, eds. G. Belvedere and L. Paterno (Catania: Osservatorio Astron. Catania), Publ. No. 162, p. 35.
- Schulte-Ladback, R. 1983, *Astron. Astrophys.*, **120**, 230.

- Schüssler, M. 1983, *Solar and Stellar Magnetic Fields*, ed. J.O. Stenflo (Dordrecht: Reidel), p. 213.
- Schüssler, M. 1984, in *The Hydromagnetics of the Sun*, Proc. 4th Eur. Meeting on Solar Physics, ESA SP-220, p. 67.
- Schwartz, P.R., and Spencer, J.H. 1977, *Mon. Not. Roy. Astron. Soc.*, **180**, 297.
- Schwartz, P.A., Simon, T., and Campbell, R. 1986, *Astrophys. J.*, **303**, 233.
- Schwarzschild, K. 1906, *Göttinger Nach.*, 195, 41: English translation available in *Selected Papers on the Transfer of Radiation*, ed. D.H. Menzel, 1966 (New York: Dover).
- Schwarzschild, M. 1958, *Structure and Evolution of the Stars* (Princeton).
- Schwarzschild, M. 1961, *Astrophys. J.*, **134**, 1.
- Schwarzschild, M. 1975, *Astrophys. J.*, **195**, 137.
- Schwarzschild, M., Schwarzschild, B., and Adams, W. 1948, *Astrophys. J.*, **108**, 225.
- Seares, F.H. 1913, *Astrophys. J.*, **38**, 99.
- Serkowski, K. 1969, *Astrophys. J. Lett.*, **156**, L55.
- Shajn, G., and Struve, O. 1929, *Mon. Not. Roy. Astron. Soc.*, **89**, 222.
- Shine, R.A. 1975, *Astrophys. J.*, **202**, 543.
- Shklovskii, I. 1965, *Physics of the Solar Corona* (Oxford: Pergamon Press).
- Shore, B., and Menzel, D.H. 1968, *Principles of Atomic Spectra* (New York: Wiley).
- Shu, F.H., Adams, F.C., and Lizano, S. 1987, *Ann. Rev. Astron. Astrophys.*, **25**, 23.
- Simon, R. 1963, *J. Quant. Spec. Rad. Trans.*, **3**, 1.
- Simon, T. 1984, *Astrophys. J.*, **279**, 738.
- Simon, T., Linsky, J.L., and Stencel, R.E. 1982, *Astrophys. J.*, **257**, 225.
- Sistla, G., and Harvey, J.W. 1970, *Solar Phys.*, **12**, 66.
- Skumanich, A. 1972, *Astrophys. J.*, **171**, 565.
- Skumanich, A., Smythe, C., and Frazier, E.N. 1975, *Astrophys. J.*, **200**, 747.
- Slettebak, A. 1949, *Astrophys. J.*, **110**, 498.
- Slettebak, A. 1954, *Astrophys. J.*, **119**, 146.
- Slettebak, A. 1955, *Astrophys. J.*, **121**, 653.
- Slettebak, A. 1956, *Astrophys. J.*, **124**, 173.
- Slettebak, A. 1968, *Astrophys. J.*, **154**, 933.
- Slettebak, A. 1970, *Stellar Rotation* (Dordrecht: Reidel).
- Slettebak, A., Collins, G.W., Boyce, P.B., White, N.M., and Parkinson, T.D. 1975, *Astrophys. J. Supp.*, **29**, 137.
- Slovak, M.H. 1982, *Astrophys. J.*, **262**, 282.
- Smak, J. 1964, *Astrophys. J.*, **139**, 1095.
- Smith, M.A. 1975, *Astrophys. J.*, **203**, 603.
- Smith, M.A. 1976, *Astrophys. J.*, **208**, 487.
- Smith, M.A. 1978, *Astrophys. J.*, **224**, 584.
- Smith, M.A. 1980a, *Astrophys. J. Lett.*, **242**, L115.
- Smith, M.A. 1980b, *Pub. Astron. Soc. Pacific*, **91**, 737.

- Smith, M.A. 1980c, *Highlights in Astron.*, **5**, 827.
- Smith, M.A. 1982a, *Astrophys. J.*, **253**, 727.
- Smith, M.A. 1982b, *Astrophys. J.*, **265**, 325.
- Smith, M.A., and Dominy, J.F. 1979, *Astrophys. J.*, **231**, 477.
- Smith, M.A., and Frisch, H. 1976, *Solar Phys.*, **47**, 461.
- Smolinski, J., Feldman, P.A., Higgs, L.A. 1977, *Astron. Astrophys.*, **60**, 277.
- Snodgrass, H.B. 1983, *Astrophys. J.*, **270**, 288.
- Sobolev, V.V. 1960, *Moving Envelopes of Stars* (Cambridge, Mass.: Harvard University Press).
- Sobolev, V.V. (ed.) 1966, *Theory of Stellar Spectra*, NASA TTF-457.
- Soderblom, D.R. 1982, *Astrophys. J.*, **263**, 239.
- Soderblom, D.R. 1983, *Astrophys. J. Supp.*, **53**, 1.
- Souffrin, P. 1966, *Ann. d'Ap.*, **29**, 55.
- Spangler, S., Owen F., and Hulse, R. 1977, *Astron. J.*, **82**, 989.
- Spencer, J.H., and Schwartz, P.R. 1974, *Astrophys. J. Lett.*, **188**, L105.
- Spicer, D.S. 1978, *Solar Phys.*, **62**, 269.
- Spicer, D.S. 1981, *Magnetic Energy Storage and Conversion in the Solar Atmosphere*, NRL Mem. Rep. 4550.
- Spicer, D.S. and Brown, J.C. 1981, in *The Sun as a Star*, ed. S.D. Jordan, NASA SP-450, p. 413.
- Spiegel, E. 1971, *Ann. Rev. Astron. Astrophys.*, **9**, 323.
- Spiegel, E., and Zahn, J.-P. (eds.) 1977, *Problems of Stellar Convection* (New York: Springer-Verlag).
- Spite, M., and Martin, P. 1981, *Astron. Astrophys.*, **101**, 265.
- Spitzer, L. 1939, *Astrophys. J.*, **90**, 494.
- Spitzer, L. 1962, *Physics of Fully Ionized Gases* (New York: Interscience).
- Spruit, H.C. 1976, *Solar Phys.*, **50**, 269.
- Spruit, H.C. 1977, *Solar Phys.*, **55**, 3.
- Spruit, H.C. 1979, *Solar Phys.*, **61**, 363.
- Spruit, H.C. 1981, in *The Sun as a Star*, ed. S.D. Jordan (Washington: CNRS/NASA SP-450), p. 385.
- Spruit, H.C. 1982, *Astron. Astrophys.*, **108**, 348.
- Spruit, H.C. 1983, in *Solar and Stellar Magnetic Fields*, ed. J.O. Stenflo (Dordrecht: Reidel), p. 41.
- Stahler, S.W. 1983, *Astrophys. J.*, **274**, 822.
- Stauffer, J.R., Hartmann, L., Soderblom, D.R., and Burnham, N. 1984, *Astrophys. J.*, **280**, 202.
- Stauffer, J.R. 1985a, preprint.
- Stauffer, J.R., Hartmann, L.W., Burnham, J.N., and Jones, B.F. 1985b, preprint.
- Stawikowski, A. 1976, *Thesis*, Torun Univ.
- Stebbins, J. 1945, *Astrophys. J.*, **102**, 318.

- Stebbins, J., and Whitford, A.E. 1943, *Astrophys. J.*, **98**, 20.
- Steenbock, W., and Holweger, H. 1981, *Astron. Astrophys.*, **99**, 192.
- Stein, R.F. 1967, *Solar Phys.*, **2**, 385.
- Stein, R.F. 1981, *Astrophys. J.*, **246**, 966.
- Stein, R.F. and Schwartz, R. 1972, *Astrophys. J.*, **177**, 807.
- Steinlin, U.W. 1968, *Zeit. f. Astrophys.*, **69**, 276.
- Stencel, R.E. 1977, *Astrophys. J.*, **215**, 175.
- Stencel, R.E. 1978, *Astrophys. J. Lett.*, **223**, L37.
- Stencel, R.E. 1982, *Smithsonian Astrophys. Obs. Spec. Rep. No. 392*, p. 137.
- Stencel, R.E., and Ionson, J.A. 1979, *Pub. Astron. Soc. Pacific*, **91**, 452.
- Stencel, R.E., Kondo, Y., Bernat, A.P., and McCluskey, G.E. 1979, *Astrophys. J.*, **233**, 621.
- Stencel, R.E., and Mullan, D.J. 1980, *Astrophys. J.*, **238**, 221.
- Stencel, R.E., and 6 others, 1981, *Mon. Not. Roy. Astron. Soc.*, **196**, 47.
- Stenflo, J.O. (ed.) 1983, *Solar and Stellar Magnetic Fields* (Dordrecht: Reidel).
- Stenholm, L. 1977a, *Astron. Astrophys.*, **54**, 127.
- Stenholm, L. 1977b, *Astron. Astrophys.*, **61**, 155.
- Stephenson, C.B. 1960, *Astron. J.*, **65**, 60.
- Stephenson, C.B., and Sanwall, N.B. 1969, *Astron. J.*, **74**, 689.
- Sterne, R.A., Zolcinski, M.-C., Antiochos, S.K., and Underwood, J.H. 1981, *Astrophys. J.*, **249**, 647.
- Stickland, D.J., and Harmer, D.L. 1978, *Astron. Astrophys.*, **70**, L53.
- Stilley, J. and Calaway, J. 1970, *Astrophys. J.*, **160**, 245.
- Stimets, R.V., and Giles, R.H. 1980, *Astrophys. J. Lett.*, **242**, L37.
- Stix, M. 1981, *Solar Phys.*, **74**, 79.
- Stone, R.P.S. 1977, *Astrophys. J.*, **218**, 767.
- Straizys, V. 1979, *Dudley Obs. Rept. No. 14*, p. 485.
- Strazzulla, G., Pirronello, V. and Foti, G. 1983, *Astrophys. J.*, **271**, 255.
- Strom, K., Strom, S.E., Kenyon, S., and Hartmann, L. 1987, *Astron. J.* (submitted).
- Strom, S.E. 1968, *Pub. Astron. Soc. Pacific*, **80**, 269.
- Strom, S.E., Strom, K.M., Yost, J., Carasco, L., and Grasdalen, G.L. 1972, *Astrophys. J.*, **173**, 353.
- Strömgren, B. 1963, in *Basic Astronomical Data*, ed. K.A. Strand (Chicago: Univ. Chicago Press), p. 123.
- Strömgren, B. 1966, *Ann. Rev. Astron. Astrophys.*, **4**, 433.
- Struve, O. 1930, *Astrophys. J.*, **72**, 1.
- Struve, O. 1933, *Astrophys. J.*, **78**, 73.
- Struve, O. 1942, *Astrophys. J.*, **95**, 134.

- Struve, O. 1943, *Astrophys. J.*, **98**, 134.
- Struve, O. 1945a, *Pop. Astron.*, **53**, 201.
- Struve, O. 1945b, *Pop. Astron.*, **53**, 259.
- Struve, O. 1946, *Astrophys. J.*, **104**, 138.
- Struve, O., and Elvey, C. 1934, *Astrophys. J.*, **79**, 409.
- Summers, D. 1983, *Solar Phys.*, **85**, 93.
- Svestka, Z. 1976, *Solar Flares* (Dordrecht: Reidel).
- Swank, J.H., White, J.L., Holt, S.S., and Becker, R.H. 1981, *Astrophys. J.*, **246**, 208.
- Taam, R.E. 1983, *Astrophys. J.*, **268**, 361.
- Tassoul, J.L. 1978, *Theory of Rotating Stars* (Princeton Univ. Press).
- Taylor, B.J. 1978, *Astron. J.*, **83**, 1377.
- Thomas, J.H. 1981, in *The Physics of Sunspots*, eds. L.E. Cram and J.H. Thomas (Sunspot: Sacramento Peak Observatory).
- Thomas, R.N. 1957, *Astrophys. J.*, **123**, 260.
- Thomas, R.N. 1961 (ed.), *Aerodynamic Phenomena in Stellar Atmospheres*, IAU Symp. No. 12 (Nuovo Cimento Supp. 22, Ser. 10, No. 1).
- Thomas, R.N. 1965, *Some Aspects of Non-equilibrium Thermodynamics in the Presence of a Radiation Field* (Boulder: University of Colorado Press).
- Thomas, R.N. 1967, Fifth Symp. Cosmical Gas Dynamics, *Aerodynamical Phenomena in Stellar Atmospheres*, IAU Symp. No. 28 (New York: Academic).
- Thomas, R.N. 1973, *Astron. Astrophys.*, **29**, 297.
- Thomas, R.N. 1976, *Found. Phys.*, **7**, 137.
- Thomas, R.N. 1983, *Stellar Atmospheric Structural Patterns*, NASA SP-471.
- Thomas, R.N., and Athay, R. 1961, *Physics of the Solar Chromosphere* (New York: Interscience).
- Tinbergen, J., and Zwaan, C. 1981, *Astron. Astrophys.*, **101**, 223.
- Tomkin, J., Lambert, D.L., and Luck, R.E. 1975, *Astrophys. J.*, **199**, 436.
- Toomre, J., Zahn, J.P., Latour, J., and Spiegel, E. 1976, *Astrophys. J.*, **207**, 545.
- Torres, C.A.O., and Ferraz Mello, S. 1973, *Astron. Astrophys.*, **27**, 231.
- Traub, W.A., Mariska, J.T., and Carleton, N.P. 1978, *Astrophys. J.*, **223**, 583.
- Traving, G. 1975, in *Problems in Stellar Atmospheres and Envelopes*, eds., B. Baschek, W.H. Kegel, and G. Traving (New York: Springer-Verlag), p. 325.
- Tug, H. 1980a, *Astron. Astrophys.*, **82**, 195.
- Tug, H. 1980b, *Astron. Astrophys. Supp.*, **39**, 67.
- Tug, H., and Schmidt-Kaler, T. 1982, *Astron. Astrophys.*, **105**, 400.
- Tug, H., White, N.M., and Lockwood, G.W. 1977, *Astron. Astrophys.*, **61**, 679.
- Uchida, Y., and Sakurai, T. 1983, *Activity in Red Dwarf Stars*, eds. Byrne and Rodono, IAU Coll. No. 71 (Amsterdam: North-Holland), p. 629.

- Uesugi, A. 1976, *Revised Catalogue of Stellar Rotational Velocities* (Kyoto: Univ. of Kyoto).
- Ulmschneider, P. 1976, *Solar Phys.*, **49**, 249.
- Ulmschneider, P. 1979, *Space. Sci. Rev.*, **24**, 71.
- Ulmschneider, P., Schmitz, F., Kalfogen, W., and Bohn, H. 1978, *Astron. Astrophys.*, **70**, 487.
- Ulmschneider, P., and Stein, R. 1982, *Astron. Astrophys.*, **106**, 9.
- Ulrich, R.K. 1970a, *Astrophys. Space. Sci.*, **7**, 71.
- Ulrich, R.K. 1970b, *Astrophys. J.*, **162**, 993.
- Ulrich, R.K. 1976, *Astrophys. J.*, **210**, 377.
- Ulrich, R.K., and Knapp, G.R. 1979, *Astrophys. J. Lett.*, **230**, L99.
- Ulrich, R.K., and Rhodes, E.J., Jr. 1977, *Astrophys. J.*, **218**, 521.
- Ulrich, R.K., Rhodes, E.J., Jr., and Deubner, F.-L. 1979, *Astrophys. J.*, **227**, 638.
- Ulrich, R.K., Shafter, A.W., and Hawkins, G. 1983, *Astrophys. J.*, **267**, 199.
- Ulrich, R.K., and Wood, B.C. 1981, *Astrophys. J.*, **244**, 147.
- Underhill, A., and Doazan, V. 1982, *Be Stars With and Without Emission Lines*, NASA SP-456.
- Unno, W., Osaki, W., Ando, H., and Shibahashi, H. 1979, *Nonradial Oscillations of Stars* (Tokyo: University of Tokyo Press).
- Unsöld, A. 1930, *Zeit. f. Astrophys.*, **1**, 138.
- Unsöld, A. 1931, *Zeit. f. Astrophys.*, **1**, 138, and **2**, 209.
- Unsöld, A. 1955, *Physik der Sternatmosphären* (Berlin: Springer-Verlag).
- Vaiana, G.S., Cassinelli, J.P., Fabbiano, G., Giacconi, R., Golub, L., Gorenstein, P., Haisch, B.M., Harnden, F.R., Jr., Johnson, H.M., Linsky, J.L., Maxson, C.W., Mewe, R., Rosner, R., Seward, F., Topka, K., and Zwaan, C. 1981, *Astrophys. J.*, **245**, 163.
- Vaiana, G.S., and Rosner, R. 1978, *Ann. Rev. Astron. Astrophys.*, **16**, 393.
- Vainshtein, S.I., Zel'dovich, Ya. B., and Ruzmaikin, A.A. 1980, *Turbulent Dynamo in Astrophysics* (Moscow) (in Russian).
- van Ballegooijen, A.A. 1982, *Thesis*, Utrecht.
- van Ballegooijen, A.A. 1984, in *Small-Scale Dynamical Processes in Quiet Stellar Atmospheres*, ed. S.L. Keil (Sunspot: Sacramento Peak Observatory) p. 260.
- van Ballegooijen, A.A. 1985, *Astrophys. J.*, **298**, 421.
- van den Bösch, J.C. 1957, *Handbuch der Physik*, **28**, 296.
- van der Hucht, K., Bernat, A.P., and Kondo, Y. 1980, *Astron. Astrophys.*, **82**, 14.
- van Dien, E. 1948, *Pub. Roy. Astron. Soc. Canada*, **42**, 249.
- van Leeuwen, F. 1983, *Ph.D. Thesis*, Leiden.
- van Leeuwen, F., and Alphenaar, P. 1982, *ESO Messenger*, No. 28, 15.
- van Paradijs, J. 1973, *Astron. Astrophys.*, **23**, 369.

- van Paradijs, J., and Meurs, E.J.A. 1974, *Astron. Astrophys.*, **35**, 225.
- van Paradijs, J., and Ruiter, H. 1972, *Astron. Astrophys.*, **20**, 169.
- Vardanian, R.A. 1964, *Sooschch. Bjurak. Obs.*, **35**, 3.
- Varsavsky, C.M. 1959, *Astrophys. J.*, **132**, 354.
- Vauclair, G., Vauclair, S., and Michaud, G. 1978, *Astrophys. J.*, **223**, 920.
- Vaughan, A.H. 1980, *Pub. Astron. Soc. Pacific*, **92**, 392.
- Vaughan, A.H., Baliunas, S.L., Middelkoop, F., Hartmann, L.W., Mihalas, D., Noyes, R.W., and Preston, G.W. 1981, *Astrophys. J.*, **250**, 276.
- Vaughan, A.H., and Preston, G.W. 1980, *Pub. Astron. Soc. Pacific*, **92**, 385.
- Vaughan, A.H., and Zirin, H. 1968, *Astrophys. J.*, **152**, 132.
- Verbunt, F., and Zwaan, C. 1981, *Astron. Astrophys.*, **100**, L7.
- Vernazza, J., Avrett, E.H., and Loeser, R. 1973, *Astrophys. J.*, **184**, 605.
- Vernazza, J., Avrett, E.H., and Loeser, R. 1976, *Astrophys. J. Supp.*, **30**, 1.
- Vernazza, J., Avrett, E.H., and Loeser, R. 1981a, *Astrophys. J. Supp.*, **41**, 634.
- Vernazza, J., Avrett, E.H., and Loeser, R. 1981b, *Astrophys. J. Supp.*, **45**, 619.
- Vitense, E. 1953, *Zeit. f. Astrophys.*, **32**, 135.
- Vogel, S.N., and Kuhl, L.V. 1981, *Astrophys. J.*, **245**, 960.
- Vogt, S.S. 1975, *Astrophys. J.*, **199**, 418.
- Vogt, S.S. 1979, *Pub. Astron. Soc. Pacific*, **91**, 616.
- Vogt, S.S. 1980, *Astrophys. J.*, **240**, 567.
- Vogt, S.S. 1981a, *Astrophys. J.*, **247**, 975.
- Vogt, S.S. 1981b, *Astrophys. J.*, **250**, 327.
- Vogt, S.S. 1982, in *The Physics of Sunspots*, eds. L. Cram and J. Thomas (Sunspot: Sacramento Peak Obs.), p. 455.
- Vogt, S.S., and Fekel, F. 1979, *Astrophys. J.*, **234**, 958.
- Vogt, S.S., and Penrod, G.D. 1983, *Pub. Astron. Soc. Pacific*, **95**, 565.
- Voigt, H.H. 1956, *Zeit. f. Astrophys.*, **40**, 157.
- Voigt, H.H. 1959, *Zeit. f. Astrophys.*, **47**, 144.
- Volland, H. 1984, *Atmospheric Electrodynamics* (Berlin: Springer-Verlag).
- Vrabc, D. 1973, in *Chromospheric Fine Structure*, ed. R.G. Athay, IAU Symp. 56 (Dordrecht: Reidel), p. 201.
- Vrba, F.J., Rydgren, A.E., Chugainov, P.F., Shakhavskaya, N., and Dak, D. 1986, *Astrophys. J.*, **306**, 199.
- Vrba, F.J., Rydgren, A.E., Zak, D., and Schmelz, J. 1985, *Astron. J.*, **90**, 326.
- Wagenblast, R., Bertout, C., and Bastian, U. 1983, *Astron. Astrophys.*, **120**, 6.
- Wagner, W.J. 1984, *Ann. Rev. Astron. Astrophys.*, **22**, 267.
- Walker, M.F. 1956, *Astrophys. J. Supp.*, **2**, 365.
- Walker, M.F. 1972, *Astrophys. J.*, **175**, 89.
- Walker, M.F. 1978, *Astrophys. J.*, **224**, 546.

- Walker, M.F. 1980, *Pub. Astron. Soc. Pacific*, **92**, 66.
- Wallenhorst, S. 1980, *Astrophys. J.*, **241**, 229.
- Walter, F.M. 1981, *Astrophys. J.*, **245**, 677.
- Walter, F.M. 1982, *Astrophys. J.*, **253**, 75.
- Walter, F.M. 1983, *Astrophys. J.*, **274**, 794.
- Walter, F.M. 1986, *Astrophys. J.*, **306**, 573.
- Walter, F.M., and Bowyer, S. 1981, *Astrophys. J.*, **245**, 671.
- Walter, F.M., Gibson, D.M., and Basri, G.S. 1983, *Astrophys. J.*, **267**, 665.
- Walter, F.M., and Kuhi, L.V. 1981, *Astrophys. J.*, **250**, 253.
- Walter, F.M., and Kuhi, L.V. 1984, *Astrophys. J.*, **284**, 194.
- Walter, F.M., Linsky, J.L., Simon, T., Golub, L., and Vaiana, G.S. 1984, *Astrophys. J.*, **281**, 815.
- Warner, B. 1968, *Observatory*, **88**, 217.
- Weaver, W.B. 1984, *Astrophys. J.*, **282**, 688.
- Weber, E.J., and Davis, L., Jr. 1967, *Astrophys. J.*, **148**, 217.
- Weiler, E.J. 1978, *Astron. J.*, **83**, 795.
- Weis, E.W. 1974, *Astrophys. J.*, **190**, 331.
- Weiss, N.O. 1966, *Proc. Roy. Soc. London Ser. A*, **293**, 310.
- Weiss, N.O. 1983, in *Activity in Red Dwarf Stars*, eds. P. Byrne and M. Rodono (Dordrecht: Reidel), p. 639.
- Welin, G. 1971, *Astron. Astrophys.*, **12**, 312.
- Wenzel, W. 1968, *Non-Periodic Phenomena in Variable Stars*, ed. L. Detre (Budapest: Academic Press).
- Westgate, C. 1933a, *Astrophys. J.*, **77**, 141.
- Westgate, C. 1933b, *Astrophys. J.*, **78**, 46.
- Westgate, C. 1934, *Astrophys. J.*, **79**, 357.
- Weymann, R. 1962, *Astrophys. J.*, **136**, 844.
- Weyman, R. 1963, *Ann. Rev. Astron. Astrophys.*, **1**, 97.
- Whitaker, W. 1963, *Astrophys. J.*, **137**, 914.
- White, N.M., Kreidl, T.J., and Goldberg, L. 1981, *Astrophys. J.*, **254**, 670.
- White, O.R., and Cha, M.Y. 1973, *Solar Phys.*, **31**, 23.
- White, O.R., and Livingston, W.C. 1981, *Astrophys. J.*, **249**, 798.
- Wilcox, J.M., and Howard, R. 1970, *Solar Phys.*, **13**, 251.
- Wildt, R. 1939, *Astrophys. J.*, **90**, 611.
- Wilkerson, M.S., and Worden, S.P. 1977, *Astron. J.*, **82**, 642.
- Willson, L.A. 1974, *Astrophys. J.*, **191**, 143.
- Willson, L.A. 1975, *Astrophys. J.*, **197**, 365.
- Willson, L.A., and Bowen, G.W. 1985, in *Relations Between Chromospheric-Coronal Heating and Mass Loss in Stars*, eds. R. Stalio and J.B. Zirker (Osservatorio Astronomico di Trieste).
- Willson, R.C., and Hickey, J.R. 1977, *The Solar Output and Its Variations*, ed. O.R. White (Boulder: Colorado Assoc. Univ. Press), p. 111.

- Willstrop, R.V. 1965, *Mem. Roy. Astron. Soc. London*, **69**, 83.
- Wilson, O.C. 1957, *Astrophys. J.*, **126**, 46.
- Wilson, O.C. 1960a, *Astrophys. J.*, **132**, 136.
- Wilson, O.C. 1960b, in *Stellar Atmospheres*, ed. J.L. Greenstein (Chicago: Univ. of Chicago Press).
- Wilson, O.C. 1963, *Astrophys. J.*, **138**, 832.
- Wilson, O.C. 1966a, *Science*, **151**, 1487.
- Wilson, O.C. 1966b, *Astrophys. J.*, **144**, 695.
- Wilson, O.C. 1967, *Pub. Astron. Soc. Pacific*, **79**, 46.
- Wilson, O.C. 1970, *Pub. Astron. Soc. Pacific*, **82**, 865.
- Wilson, O.C. 1978, *Astrophys. J.*, **226**, 379.
- Wilson, O.C. 1982, *Astrophys. J.*, **257**, 179.
- Wilson, O.C., and Abt, H.A. 1954, *Astrophys. J. Supp.*, **1**, 1.
- Wilson, O.C., and Bappu, M.K.V. 1957, *Astrophys. J.*, **125**, 661.
- Wilson, O.C., and Hoyle, F. 1958, *Astrophys. J.*, **128**, 604.
- Wilson, O.C., and Skumanich, A. 1964, *Astrophys. J.*, **140**, 1401.
- Wilson, O.C., and Woolley, R. 1970, *Mon. Not. Roy. Astron. Soc.*, **148**, 463.
- Wing, R.F. 1979, *Dudley Obs. Report No. 14*, 499.
- Wischnewski, E., and Wendker, H.J. 1981, *Astron. Astrophys.*, **96**, 102.
- Wöhl, H. 1983, in IAU Symp. No. 102, *Solar and Stellar Magnetic Fields: Origins and Coronal Effects*, ed. J.O. Stenflo, (Dordrecht: Reidel), p. 155.
- Wolf, B., Appenzeller, I., and Bertout, C. 1977, *Astron. Astrophys.*, **58**, 163.
- Wolff, C.L. 1972a, *Astrophys. J.*, **176**, 833.
- Wolff, C.L. 1972b, *Astrophys. J. Lett.*, **177**, L87.
- Wolff, C.L. 1973, *Solar Phys.*, **32**, 31.
- Wolff, S.C. 1983, *The A-Stars: Problems and Perspectives* (NASA-CNRS), NASA SP-463.
- Woodward, M., and Hudson, H. 1983a, *Solar Phys.*, **82**, 67.
- Woolley, R. 1941, *Mon. Not. Roy. Astron. Soc.*, **101**, 59.
- Woolley, R., and Stibbs, D. 1953, *The Outer Layers of a Star* (Oxford: Clarendon Press).
- Worden, S.P., and Keil, S.L. 1983b, *Nature*, **305**, 589.
- Worden, S.P., and Keil, S.L. 1984, *Bull. American Astron. Soc.*, **16**, 1075.
- Worden, S.P., Schneeberger, T.J., Kuhn, J.R., and Africano, J.L. 1981, *Astrophys. J.*, **244**, 520.
- Worrall, G., and Wilson, A.M. 1973, in *Vistas in Astronomy*, **15**, 39.
- Wright, A., and Barlow, M. 1975, *Mon. Not. Roy. Astron. Soc.*, **170**, 41.
- Wright, K.O. 1955, *Transactions IAU*, **9**, 739.
- Wynne-Jones, I., Ring, J., and Wayte, R.C. 1978, in *High Resolution Spectrometry*, ed. M. Hack (Trieste: Osservatorio Astron. d. Trieste), p. 519.

- Yi Li Sun, Jaschek, M., Andrillat, Y., and Jaschek, C. 1985, *Astron. Astrophys. Supp.*, **62**, 309.
- Yoshimura, H. 1982, in *Reports on Astronomy*, IAU Trans. 28 A, p. 55.
- Yoss, K.M. 1977, *Astron. J.*, **82**, 832.
- Yun, H.S. 1970, *Astrophys. J.*, **162**, 975.
- Zahn, J.-P. 1977, *Astron. Astrophys.*, **57**, 383.
- Zajtscva, G.V., and Lyuty, V.M. 1976, *Variable Stars*, **20**, 255.
- Zappala, R.R. 1972, *Astrophys. J.*, **172**, 57.
- Zirin, H. 1976, *Astrophys. J.*, **208**, 414.
- Zirker, J.B. 1977 (ed.), *Coronal Holes and High Speed Streams* (Boulder: Colo. Assoc. Univ. Press).
- Zirker, J.B. 1981, in *The Sun as a Star*, ed. S.D. Jordan (Washington: CNRS/NASA SP-450), p. 135.
- Zolcinski, M.-C., Antiochos, S.K., Stern, R., and Walker, A.B.C. 1982, *Astrophys. J.*, **258**, 177.
- Zwaan, C. 1977, *Mem. Soc. Astr. Italy*, **48**, 525.
- Zwaan, C. 1978, *Solar Phys.*, **60**, 213.
- Zwaan, C. 1981a, *Solar Phenomena in Stars and Stellar Systems*, eds. R. Bonnet and A.K. Dupree (Dordrecht: Reidel), p. 463.
- Zwaan, C. 1981b, in *The Sun as a Star*, ed. S.D. Jordan (Washington: CNRS/NASA SP-450), p. 163.
- Zwaan, C. 1983, in *Solar and Stellar Magnetic Fields: Origins and Coronal Effects*, ed. J.O. Stenflo, IAU Symp. No. 102, (Dordrecht: Reidel), p. 85.
- Zwaan, C. 1985, *Solar Phys.*, **100**, 397.

SUBJECT INDEX

- abundances 166
- acoustic emission 198-199, 204, 242
- activity, stellar 215-216
 - complexes (nests) 227
 - cycles 89, 226-227
 - T Tauri stars 104
- ages, stellar 91
- Alfvén waves 133, 211-212, 243
 - dissipation of 243
- angular momentum 247
- asymmetric lines
 - absorption 8, 18, 21, 169, 175-176, 195
 - CaII H and K 174-175
 - emission 120-124, 174-175
- atmosphere
 - extended 144, 149, 176, 179-180, 187
 - inhomogeneous 149-151, 163, 175, 180, 188
 - radial structure 149-151, 183-185, 186
- binary stars 49, 80-84, 96-98, 251
- bipolar flow 133
- black body radiation 141, 191
- Boltzmann equation 188-190
- Boltzmann number 147
- buoyancy, flux tube 220, 221-222, 226, 229
- canopy, magnetic 241
- Chapman-Enskog method 193
- chromospheres 78, 184
 - extended 66, 80, 84, 208, 213
 - semi-empirical 175-178
 - solar 146
 - T Tauri stars 106, 135-137
 - waves 206
- classical model
 - critique 167-168
 - computation of 162-163
 - definition 139
- convection 142, 194-198
 - acoustic emission 198, 204
 - cyclonic 224, 226
 - lateral scale 197-198
 - magnetic fields 218-222, 229-230
 - mixing length theory 161-162
 - overshooting 170, 195-196, 203-204
 - solar granulation 196
 - thermal time scale 232-233
 - velocity of 196-197
- coronae
 - extension 179
 - magnetic heating 243-245

magnetic structure 239-242
 smothered 209
 solar 146, 207, 208
 T Tauri stars 112
 X-rays 57

coronal holes 209, 241

Cowling's theorem 223

critical point 211

curve of growth 11, 166, 169

disks 134-135

dividing lines 68, 86, 87, 176, 179, 208, 211

dust 65, 108, 113

dynamo

- α -effect 224-226
- axisymmetric 223
- episodic 202
- evolution of 248
- mean-field theory 226

dynamo number 225-226

eclipsing binaries 71

electrodynamic coupling 242, 244

electron scattering 114, 151

escape velocities 67

Euler equations 192, 210

evolution, stellar 130, 165, 202, 248

faculae 233, 234-238

filling factor 237, 239

fine analysis 166

flares 104, 107-108

fluorescent spectral lines 114, 125

Fokker-Planck equation 188, 193

forbidden spectral lines 114, 125

Fourier analysis 13-14, 117

free-free emission

- theory 151-152
- T Tauri stars 110

FU Orionis stars 103, 186, 202

gas dynamic equations 191

Goldberg-Unno method 170

granulation

- solar 17, 19-20, 196-197, 203, 231
- stellar 17, 20-23

gravities, stellar 50-51

H^- absorption 142-143, 152, 159

Herbig-Haro objects 109, 137

Hertzprung-Russell (HR) diagram 141, 168

- T Tauri stars 102, 129-130

hybrid stars 68, 95

hydrostatic equilibrium 156

infrared

- excess 110
- T Tauri stars 108-111

interstellar medium 182

line blanketing

- LTE 160
- non-LTE 160, 161

picket-fence model 142
 solar 164

line broadening
 macroturbulence 10, 169, 172-173
 mesoturbulence 169
 microturbulence 10, 16, 169, 170-172
 rotation 13, 25-26, 169, 173-174

lithium 165

local stellar environment 188

Lorentz force 216, 219, 220

luminosity variation 233-234

macroturbulence 10-12, 14-16, 169, 172-173

magnetic Ap stars 238-239

magnetic braking 247-249

magnetic fields
 concentration of 219, 231
 convection 218-222
 diffusivity 217
 equipartition field strength 219, 222, 229, 234
 force free 239
 frozen-in 217
 gyrosynchrotron radiation 155-156
 observations 40-41
 mass loss 133, 246
 primordial 222
 solar 146
 topology of 241
 T Tauri stars 106, 116
 Zeeman effect 36, 116

magnetic flux tubes 218, 219-222, 234, 240-241
 collapse of 230
 formation of 229-230
 heat flow in 227-228, 229
 magnetostatic 227-229
 merging of 239, 241
 thermally insulated 222

magnetic pressure 219, 228, 239

magnetic Reynolds number 217, 218

magnetic tension 219

magnetohydrodynamics
 equations 216
 waves 243

masses, stellar 49-50

mass flux 184, 212-213

mass loss
 magnetically driven 246
 rates 69, 70
 red giants 63
 theory 210-211
 T Tauri stars 131, 133-134
 V/R ratio 175

Maxwell's equations in stellar media 216

microturbulence 10, 11, 16-17, 169-172

minimum flux corona 213

mixing length theory 161-162, 197-198, 221

monolithic group 2

naked T Tauri stars 113, 119

nebulae, cometary 109

nebular variables 100

net radiative bracket 157

non-LTE 147
 continua 152
 line blanketing 160-161
 line formation 143, 154-155
 T Tauri chromospheres 136, 137

- nonradiative heating 176-179
 - diagnosis 176
 - shock waves 205
- nonthermal phenomena 8, 9, 155-156, 168-176
- optical depth 149, 158, 159, 234
- Orion population 100
- oscillations and waves
 - solar 42-43
 - stellar 43
- photometry
 - systems 46
 - T Tauri stars 102-111
- photospheres
 - dynamics 203-205
 - quasi-thermal 184
 - T Tauri stars 114, 116
 - turbulence 10-25
- plasma loops 240-241, 244-245
- polarization
 - free electron scattering 114
 - linear, T Tauri stars 113-114
 - Zeeman effect 8, 116
- polythetic group 2
- pores, magnetic 227, 228, 236
- postcoronae 185, 187, 209-213
- post-T Tauri stars 112, 119
- prominence 83-84, 180
- pulsation
 - amplitudes 200
 - nonradial 199-200
 - photospheric 204-205
 - theory 199-201
- radiation pressure 190, 211
- radiation transfer equation 148, 189-190, 191
- radiative equilibrium 155, 156
 - gray absorption 142, 158-159
 - non-gray absorption 159-162
- radio emission
 - non-thermal 111, 155-156
 - thermal 65-66, 86, 111, 152
 - T Tauri stars 111
- reddening 110
- rotation 201
 - activity 91, 248-249
 - decay of 247-248
 - differential 31-33, 223, 224, 225-226, 248
 - dwarfs 29, 174
 - giants 26-28, 174
 - magnetic braking 247-248
 - measurement 173-174
 - modulation 186
 - subgiants 28-29
 - T Tauri stars 116-118
- RS CVn stars 96-98, 249
- scale height 179
- semi-empirical construct 168
- shock waves 205-207, 209, 213
- spectral classification 2-3, 143-144, 182-183
 - absolute magnitudes 142
 - T Tauri stars 99-100, 116
- spectral lines
 - calcium 54, 65, 91-93, 95, 176-177
 - circumstellar 64
 - EUUV 56, 62, 97, 126-129, 144

- helium 56, 65, 95, 124
 - hydrogen 53-54, 65, 119-122
 - magnesium 55
 - sodium 53, 120-123
 - theory 143-144, 153-155
- spectrophotometric standards 45
- spectroscopic diagnostics 147-148
- star formation 102-103, 130, 182-183
- starspots 236-238
 - blocking by 231-232
 - magnetic fields 35
 - missing heat flux 231
 - photometry 33-34, 96
- stellar winds
 - coronal holes 241
 - energy loss 75-76
 - magnetic fields 248
 - temperatures 67-68
 - theory 210
 - T Tauri stars 131, 133-134
 - variable 74
 - velocities 67
 - wave driven 133-134, 212
- Sun
 - chromosphere 146
 - classical model 164-165
 - corona 146, 207-208
 - oscillations 199-200
 - sunspots 146, 227, 230
 - transition region 207

temperature control bracket 157, 160-161

thermal diffusion 228, 232

transition regions
 - emission measure 77-78, 128
 - solar 207-208
 - T Tauri stars 128
 - UV emission lines 62-63, 126-129

transonic flow 207

T Tauri stars
 - absorption lines 115-116
 - birth of 130

coronae 111-112, 125-126, 208
 - chromospheres 135-137
 - disks 134-135
 - emission lines 119-126
 - extreme 101
 - infrared observations 108-111
 - infall models 131-133, 180
 - magnetic fields 116
 - mass loss 131, 133-134, 180
 - photometry 102-106
 - rotation 116-118
 - T associations 102
 - taxonomy 99-102, 186
 - variability 100, 103-106, 109-110, 201-202
 - winds 133-134
 - X-rays 111-113, 209

turbulence 169, 219

turbulent diffusion 224

variability 183, 186-188
 - classification 100, 144-145
 - episodic 201-202
 - giants 95
 - T Tauri stars 103-106, 109-110

veiling 106, 114, 116, 133, 136

velocity distribution function 188-189, 193
 - Maxwellian 191

waves (*see pulsation*)

Wilson-Bappu effect 87, 178

Wilson depression 228, 235

X-rays 57, 59, 145, 179
continuum 152
hard 155

loops 244-245
RS CVn stars 97-98
T Tauri stars 111-113

LIST OF CONTRIBUTING AUTHORS

Lawrence E. Cram

*School of Physics
University of Sydney
Sydney, NSW 2006
Australia*

David F. Gray

*Department of Astronomy
University of Western Ontario
London, ON N6A 3K7
Canada*

Leonard V. Kuhi

*Astronomy Department
University of California
Berkeley, CA 94720
USA*

Dieter Reimers

*Hamburger Sternwarte
Universität Hamburg
Gojenbergsweg 112
D-2050 Hamburg 80
Federal Republic of Germany*

Cornelis Zwaan

*Sterrekundig Institute
Postbus 80000
3508 TA Utrecht
Netherlands*